Doctor Thesis

Shibaura Institute of Technology

Design and Evaluation of AIRGAIT Exoskeleton's Leg Orthosis: Development of a Control Scheme and Strategy for a Noble Control of Antagonistic Mono- and Bi-Articular Actuators

Date 2014/September

Mohd Azuwan Mat Dzahir

Shibaura Institute of Technology
Graduate School of Engineering and Science

2014 September

Doctoral Dissertation

Design and Evaluation of AIRGAIT Exoskeleton's Leg Orthosis: Development of a Control Scheme and Strategy for a Noble Control of Antagonistic Mono- and Bi-Articular Actuators

Name	Mohd Azuwan Mat Dzahir
Student ID	NB11503
Major	Functional Control System
Department	Graduate School of Engineering and Science
Supervisor	Prof. Shin-ichiroh Yamamoto

TABLE OF CONTENTS

LIST OF FIGURES

LIST OF TABLES

LIST OF PUBLICATIONS

ABSTRACT

This research thesis introduces the development of body weight support gait training system known as the AIRGAIT exoskeleton and delves into the design and evaluation of its leg orthosis control paradigm. The implementation of the antagonistic mono- and bi-articular actuators using pneumatic muscle actuator (PMA) as the actuation system were initiated to generate more power and precisely control the leg orthosis. This research proposes a simple paradigm for controlling the antagonistic mono- and bi-articular actuators movements co-contractively by introducing a co-contraction model. Three tests were performed. The first test involved control of the orthosis with mono-articular actuators alone without a subject (WO/S); the second involved control of the orthosis with mono- and bi-articular actuators tested WO/S; and the third test involved control of the orthosis with mono- and bi-articular actuators tested with a subject (W/S). It comprises of five comparisons for evaluating the performance of the design controller scheme. The first assessment involved comparison between simulated co-contraction model control scheme, and derived co-contraction model control scheme test WO/S; the second assessment involved comparison between the mono-articular actuators acting on their own (i.e., hip and knee joints), and with the addition of bi-articular actuators; the third assessment involved comparison between the position (P) controller based on co-contraction model control scheme, and the position-pressure (PP) controllers based on co-contraction model control scheme; the fourth assessment involved comparison between the control of the leg orthosis WO/S and control of the leg orthosis W/S; and the fifth assessment involved comparison between the conventional PID based control schemes, and co-contraction model based control schemes tested WO/S. Full body weight support (BWS) was implemented in this study during the test W/S as the load supported by the orthosis was at its maximum capacity. This assessment will optimize the control system strategy so that the system

operates to its full capacity. The evaluation was based on the gait cycle (GC), trajectory of the hip and knee joints, maximum angle extension of the joints, foot trajectory, effective work, inertia, gravitational effect, and time shift. The results revealed that the proposed co-contraction model control scheme and strategy were able to co-contractively actuate the mono- and bi-articular actuators simultaneously as well as increase stiffness and stability at both hip and knee joints.

Keywords: AIRGAIT exoskeleton, antagonistic mono- and bi-articular actuators, pneumatic muscle actuator (PMA), and co-contraction model.

ACKNOWLEDGMENTS

In preparation of this thesis, various parties have contributed directly or indirectly in many ways during the execution of the project. First and foremost, I wish to express my sincere appreciation to my doctoral project supervisor, Prof. Shin-Ichiroh Yamamoto for his continuous guidance, encouragement and advice. Without his constant support and assistance, this project would not have been the same as presented here. The sharing of his invaluable knowledge and constructive ideas was the key way to success in this project.

Special thanks to my wife for her untiring efforts and practical suggestions which had been contributed significantly toward the success of this project were greatly appreciated.

Last but not least, I would also like to extend my gratefulness to my fellow course mates, friends and seniors for their help and assistance on various matters. Their support was indeed very valuable for me. Thank you.

This work was supported by the Brain Science and Life Technology Research Center and KAKENHI: Grant-in-Aid for Scientific Research (B) 21300202.

CHAPTER 1

INTRODUCTION

Early work of this research thesis presents a survey on existing lower-limb leg orthosis for rehabilitation which implemented pneumatic muscle types of actuators such as McKibben artificial muscle, rubbertuators, air muscle, pneumatic artificial muscle (PAM) or pneumatic muscle actuator (PMA). It is a general assumption that pneumatic muscle types of actuators will play an important role in development of assistive rehabilitation robotics system. In the last decade, the development of pneumatic muscle actuated lower-limb leg orthosis was rather slow compared to the other types of actuated leg orthosis using ac-motor, dc-motor, pneumatic cylinder, linear actuator, series elastic actuator (SEA), and brushless servomotor. However, in recent years, the interest in this field has grown exponentially mainly due to the demand on much compliant and interactive human-robotics system. The exponentially growth of these systems might also be due to the advantageous attributes of the pneumatic muscle actuator as well as its nonlinear dynamics behaviours. However, according to its evaluations, it could be understood that the suitable control schemes and strategies have yet to be found. Albeit that, this only suggested the space available for the device orthosis improvement and enhancement in either mechanical design or control scheme and strategy are still boundless. This opportunity will attracts the researcher's interest in coming up with different ideas and strategies to rectify previous methods or to discover a new methods for the control system. Even though lots of different robotic system types for lower-limb rehabilitation orthosis had been developed, most of the prototypes were only implemented the use of mono-articular muscles alone either for hip, knee, or ankle

joints (i.e., flexion, extension, abduction, adduction, dorsiflexion, plantar-flexion, inversion, eversion, etc). However, the implementation of bi-articular muscle actuators either to compensate the lack of force/torque at the joints or to improve the control scheme and strategy of the lower-limb rehabilitation orthosis have yet to be extensively investigated and made commercially available.

For understanding the coordination of muscles in complex movements, it is of particular interest to know the potential actions of all types of muscles involved. At the present the action of muscles that pass over more than one joint is mainly described with respect to movements in the joints that are crossed. However, Elfman et al., in 1939-1940 hypothesized that bi-articular muscles might play a role in saving energy expenditure. Bi-articular muscles is the muscles that cross two joints rather than just one joint such as 'hamstring' and 'rectus femoris' which cross both hip and knee joint. The function of these muscles is complex and often depends upon their anatomy and the activity of their other muscles at the joints. Bi-articular muscles can play a unique role in the transformation of rotation in the knee joint into the translation of the body centre of gravity in such a way that this centre of gravity is continuously accelerate during push-off, thus these results made it a likely assumption for understanding the co-ordination of muscles in complex movements. The literature of this thesis will reviews all the current lower-limb rehabilitation orthosis systems then make a comparison in terms of its evaluation, design, as well as its control scheme and strategy, with the aim to clarify the current and ongoing research in this lower-limb robotic rehabilitation field.

1.1 Problem Statements

This research thesis introduces the development of body weight support gait training system also known as an AIRGAIT system for lower limb disability patients such as stroke and spinal cord injury (SCI) patients. Based on the assessments and its evaluations, it is suggested that the implementation of antagonistic bi-articular actuators with the presence of mono-articular actuators was a key to achieve high muscle moment (flexion and extension) at hip joint and a wider range of motion (flexion) at knee joint. To the authors' best knowledge, assistive leg orthosis that emphasizes on the control of antagonistic bi-articular actuators using PMA in the gait

rehabilitation field is yet to be extensively investigated and made commercially available. This then provides the motivation and purpose to investigate a noble control for the antagonistic bi-articular actuators using a suitable model paradigm. In addition, even though lots of researches had been investigated regarding the co-contraction movements of human antagonistic muscles. However, their model implementation in controlling the antagonistic muscle actuators of lower-limb orthosis is not extensively discovered. This research thesis focuses on the implementation of the antagonistic mono- and bi-articular actuators using pneumatic muscles to drive the lower-limb orthosis. Thus, simply actuating the actuators might not give a good result on the joint's stiffness and stability of the lower-limb leg orthosis and its position trajectory. Therefore, the simultaneous co-contraction movements between the agonist and antagonist muscle actuators should also be considered during the control system scheme and strategy.

1.2 Objectives

This research thesis embarks on the following objectives:

i. To optimize the body weight support gait training system (AIRGAIT) by implementing antagonistic mono- and bi-articular actuators using pneumatic artificial muscles.
ii. To derive and design a model control scheme and strategy for the AIRGAIT exoskeleton's leg orthosis system.
iii. To develop and evaluate the controllers for the AIRGAIT exoskeleton's leg orthosis using real time control system.

1.3 New Findings/Knowledge

This research will result in new potential towards application of lower-limb pneumatic muscles actuated rehabilitation orthosis system. Some of the concepts and novel knowledge acquired from this research will lead to a new exploration as follows:

i. Exploration of the lower-limb orthosis which implements antagonistic mono-

and bi-articular actuators using pneumatic muscles similar to human musculoskeletal system as an alternative for human compliance rehabilitation robotics system.

ii. Derivation of the model paradigm for estimating the co-contraction patterns of the antagonistic mono-and bi-articular actuators based on angular positional data.

iii. Derivation of the control strategy that able to reduce the nonlinearity effects of the pneumatic muscles using simple approach.

iv. The therapists' perception in using the body weight support gait training system of AIRGAIT exoskeleton as alternative for clinical rehabilitation training can be evaluated.

1.4 Significance of Research

People suffering from walking deficiencies have better recovery expectancies if they undergo intensive rehabilitation programs. However, standard rehabilitation programs necessitate intensive efforts of one, two, or even three physiotherapists to move the patient, this being potentially painful for the therapists as well. Rehabilitation robotics is a promising research avenue to take over some of this time- and energy-consuming workload. There is argument that robots should be developed to assist with therapeutic activities that are difficult or impossible for the therapist to administer alone. For instance, attempting overground gait and balance training in a patient with both heavy weight and low function is difficult and unsafe for the average therapist. Therefore, the goal is not to replace the physiotherapist, but to relieve him of the most painful aspects of his task, eventually leading to longer and/or more frequent training sessions. The goals of such devices are to assist the therapist so that they may safely train patients in standing, walking, and performing balance activities early after injuries. These tasks are difficult for therapists; however, with robotic technologies, they are possible.

Lately, the rehabilitation robotics has been used in training medicine, surgery, remote surgery and other things, but there have been too many complaints about the robot not being controlled by a remote. Many people would think that using an industrial robot as a rehabilitation robot would be the same thing, but this is not true.

Rehabilitation robots need to be adjustable and programmable, because the robot can be used for multi reasons. Meanwhile, an industrial robot is always the same; there is no need to change the robot unless the product it is working with is bigger or smaller. This development is capable of solving the problem of the lack of the doctors, enhances the efficacy of clinician's therapies; and increasing the ease of activities in the daily lives of patients. The operations can be conducted remotely, creating medical teamwork while in different places and relieve the psychological stress of doctors. For the developing country or places that not have enough medical structure, remote-control system giving hope for them to have better medication treatment. In addition, this could also be served as a reinforcement of emergency medical care.

In parallel, developing autonomous rehabilitation robots might also be useful to extend the therapy at home. If patients could begin therapy sessions quickly, this would translate into more time for repetitions and activities and thus, greater functional outcomes. Unfortunately, easy-to-use does not necessarily translate into low cost. In fact, sometimes being able to deliver an easy-to-use and highly flexible systems were results in substantial costs. In the end, for devices to gain widespread acceptance in small rehabilitation clinics, the costs for providing and using these systems must first come down.

This research will result in a highly compliance body weight support gait training system for lower-limb disability of stroke and SCI patients. The AIRGAIT system allows the gait motion training with different body weight support (BWS) on a treadmill. Furthermore, it also allows patients to train their disabled legs for a repetitive gait motion training at different gait cycle (GC) speed. The measurement system which identifies the subject’s center of mass (CoM) and center of pressure (CoP) was also developed together with the AIRGAIT system. This allows the therapists to analyze the condition of the subject and identify the level of training to be practice. Finally, it is also expect that some design methodologies developed for rehabilitation robotics might also be adapted to active prosthesis design.

1.5 State of Art

The goal of the research was to describe past and current developments and, on the basis of this, formulate future challenges for the field. This research reviews the

state-of-the-art of lower-limb exoskeleton robots that are applied in the areas of rehabilitation and assistive robotics. In general, the development of rehabilitation robotics application is motivated by the promise that people with severe impairments will benefit from these developments. Although, over the decades, there has been continuous progress in technological developments, only few systems have become commercially available, and even fewer were accepted for provision. Based on the literature review, the lower-limb rehabilitation orthosis which implemented antagonistic mono- and bi-articular actuators using pneumatic muscle has yet to be extensively investigated and commercially available. However, the development of this technology itself is obviously an essential element of progress in the domain of rehabilitation robotics. In addition, the main requirements of the lower-limb exoskeleton robot are identified and the mechanical designs of existing lower-limb exoskeleton robot are classified. The design difficulties of a lower-limb exoskeleton robot are discussed.

1.6 Scopes and Limitations

i. The model derivation is based on the antagonistic mono-articular (i.e., hip and knee joints) and bi-articular actuators of the AIRGAIT exoskeleton's leg orthosis system.
ii. All the measurements, control system, experimental tests, and design will be based on the developed body weight support gait training system of AIRGAIT exoskeleton.
iii. The simulation program and control paradigm are coded in MATLAB language, while the control system will be modelled using SIMULINK and xPC Target toolbox.

1.7 Outline of the Thesis

The research title is "Design and Evaluation of the AIRGAIT Exoskeleton's Leg Orthosis: Development of a Control Scheme and Strategy for a Noble Control of Antagonistic Mono and Bi-Articular Actuators". This section briefly describes the

content of the research thesis which consists of seven different chapters including introduction, literature review, design system, methodology, control system, results and discussion, and conclusions.

Chapter 1: The first chapter provides a general introduction and background of the whole research including the problem of statement, specific objectives, scopes and limitation, and outline of the thesis.

Chapter 2: The second is the literature review section which provides detailed descriptions on a few topics related to this project. At the beginning of this chapter, an introduction on human motion research is included. General knowledge on stroke, including rehabilitation therapy, mechanical system and laws of robotic, is also discussed with greater detail in this chapter. Finally, some of the existing assistive robotic leg orthosis researches including their descriptions are included.

Chapter 3: The third chapter is the design system and evaluation section for the AIRGAIT exoskeleton's leg orthosis. All of the mechanical structure of leg orthosis, antagonistic mono-articular (i.e., hip and knee joints) and bi-articular actuators, AIRGAIT's prototype, mechanical system, and safety features were described thoroughly in this section.

Chapter 4: The fourth chapter describes about the materials and methods used in the execution of this project. MATLAB, Simulink, and xPC Target toolbox which were used extensively in this project, is briefly discussed as an introduction to this chapter. Subsequently, the procedures and experimental tests for the controller schemes evaluation were discussed in details.

Chapter 5: The fifth chapter describes about the control system development for the antagonistic mono- and bi-articular actuators of the AIRGAIT exoskeleton's leg orthosis. In this section, co-contraction model control scheme and strategy were introduced. All the kinematics analysis and the mathematical derivation of the co-contraction model that generates the input patterns for the antagonistic actuators were described in details. Furthermore, the control system strategy on how the controller scheme works was also included.

Chapter 6: The sixth chapter consists of the results and discussion of this research project which delves into several sub-topics based on the assessments evaluation, control tests, and analysis. This section describes the evaluation on the antagonistic actuators' settings, limitation and performance of the antagonistic mono- and bi-articular actuators in manipulating the leg orthosis when tested without a subject (WO/S) and with a subject (W/S). Full BWS was implemented during the test W/S where the load supported by the leg orthosis was at its maximum capacity. This assessment will optimize the control scheme and strategy so that it will operate at its maximum capability. The options for the subject were not really critical as the focus of the research is on the design controller. As such, the subject chosen was young, healthy, and not bearing any neurological disorder.

Chapter 7: The last chapter includes the conclusion of the whole research's assessments and recommendations for upcoming project improvements in design, control system, control scheme and strategy, methods, and analysis were also stated here for obtaining a better result.

CHAPTER 2

LITERATURE REVIEW

The outcomes of rehabilitation therapy, which implemented body weight support treadmill training for incomplete spinal cord injuries (SCI) and stroke patients, were reported in several previous studies since the 1990s. SCI involves damage to any component of nerves or spinal cords located at the end of the spinal canal, which is either complete or incomplete. However, it often causes permanent changes in strength, sensation and other body functions below the side of the injury. The symptoms vary widely, beginning with pain to paralysis and then to incontinence. The paralysis could be identified as a weakness which might occur with abnormal tone (e.g., spasticity or rigidity). During the stance phase, leg instability (i.e., hyperextension or knee buckling) may result in unsafe walking, pain and inefficient energy. Moreover, inadequate limb clearance, impaired balance, sensory deficits and pain during the swing phase may contribute to falls, loss of balance and increased nervousness associated with walking. Furthermore, a loss of motor control prevents a patient from performing a precise movement in coordination with timing and intensity of muscle action.

Previously, a patient's paralyzed legs were physically operated by two therapists in manual training. In accordance with the treadmill training therapy, based on rules of spinal locomotion, research carried out by Wernig et al., for incomplete paralysation of paraplegic and tetraplegic patients, confirmed that the training was able to improve most of the patient's walking capability [1-2]. The patients involved in this training were provided with a motor driven treadmill training therapy, along with a body weight support (BWS) and assisted limb movements by therapists, for a

daily upright walking training. Based on the rehabilitation sessions, nearly 80% of patients with incomplete spinal cord injuries (a total of 33 individuals) were capable of walking independently after the treadmill training, with partial body weight support. In addition, the clinical evaluation on complete paraplegic and tetraplegic patients was carried out by Dietz et al., to differentiate the effects of BWS and joint movements on the leg muscle activity pattern during assisted locomotion in SCI patients [3 – 4]. However, this training procedure was physically difficult for therapists to execute for long durations of time. Recently, robot-assisted therapy devices became increasingly used in SCI rehabilitation therapy. This assistive robot either compensates the functionalities that a patient does not have, or tries to recover the impaired functionalities. Even though it may not be able to fully compensate impairments, or even provide a cure, it should be able to enhance or extend certain impaired functions; sequentially, raising the quality of life, encouraging independent living, as well as, supporting the need for social interactions and communications. Depending on the degree and location of the injury, the actual rehabilitation or treatment can vary widely. In many cases, substantial rehabilitation and physical therapy are required for spinal cord injuries, particularly if the patient's injuries interfere with daily life activities.

Since SCI patients frequently have difficulties with daily functional movements and activities, it is possible to decrease their loss of function through rehabilitation therapy during the critical stage. This rehabilitation therapy engages carefully designed repetitive exercises, which are either passive or active. In a passive exercise, the therapist or a robot will actively assist the patient to move the affected lower-limb repetitively as prescribed. In an active exercise, the patients themselves will put effort to move their legs, with no physical assistance. With the contribution of therapists, assistive robotic technology had a significant ability to provide novel means for motivating, monitoring and coaching. In addition, many lower-limb leg orthoses for rehabilitation have been developed to assist in human locomotion training; they can be used for a long time, for varying degrees of spasticity or paresis [9 - 21]. According to Dietz et al., who performed the lower-limb assisted gait training using a developed orthosis system with BWS and treadmill training on patients with incomplete SCI, advocated that the afferent participation from the lower limbs and hip joints' movements are essential for the activation of the central pattern generator for locomotion rehabilitation training in SCI patients [3 - 4].

In addition, the clinical study on the developed robotic gait training such as LOKOMAT, LokoHelp, ReoAmbulator, and Alex had been evaluated [9, 12, 13, 17, and 18]. The tests were performed on patients suffered with incomplete or/and complete SCI. The results proved that robotic assisted gait training not only able to improve the gait ability of the patients. However, the requirement for therapeutic assistance was also reduced. Additionally, the burden of the physiotherapist in managing time-consuming rehabilitation training also could be solved.

Consequently, the interest in this field has grown exponentially in recent years, mainly due to the demand for a much more compliant and interactive human-robotics system. Therefore, this work will appraise all the current existing lower-limb rehabilitation orthoses, based on compliant actuator systems, in terms of evaluation, design, control scheme and strategy. They will then be compared between one another, with the intent of clarifying current and on-going research in the lower-limb robotic rehabilitation field.

2.1 Existed Lower Limb Gait Rehabilitation Orthosis and Evaluations.

Numerous assistive orthosis systems for gait rehabilitation have been developed, delving into several types of lower-limb rehabilitations, such as: treadmill gait trainers, over-ground gait trainers, stationary gait and ankle trainers, foot-plate-based gait trainers and active foot orthoses for the neurologically impaired (including stroke and Spinal Cord Injury (SCI) patients) [5 - 8]. These systems implemented very unique mechanical structures, designs, actuators, methods, control schemes and rehabilitation strategies; as well as, various procedures to ensure the reliability and robustness of the systems when compared to others. The rapid development of rehabilitation robotics over the last decade is to fully restore or improve the mobility of affected limb functions, and to help patients achieve a better life.

2.2 Motorized Lower-Limb Rehabilitation Orthosis System.

The Driven Gait Orthosis (DGO), also known as LOKOMAT (Hocoma AG, Volketswill Switzerland), is currently available in the market and is extensively

researched in many rehabilitation centres as one of the best examples for gait orthosis that can be used for lower-limb disabilities [9 - 11]. This orthosis system is shown in Figure 1(a). It consists of three main parts: body weight support, treadmill and powered leg orthosis. The Direct Current (DC) motor, with helical gears, was used for the actuation power of the system to precisely control the trajectory of the hip and knee joints. Considerable control algorithms have been implemented into this system to improve its performance, such as position, adaptability, impedance controllers, etc. To stimulate the locomotor function of the spinal cord and activate leg muscles that have lost the capacity to actuate voluntary movement, it is important to provide adequate afferent input to the affected lower-limb. It could be anticipated that the afferent input produced using the automatically based training, is at least as efficient as that generated using the manual training.

Figure 1(b) shows the treadmill gait trainer system which incorporated the electromechanical gait device with the treadmill/gait training, known as the LokoHelp (LokoHelp Group, Germany). The LokoHelp used a different mechanical system compared to the LOKOMAT, which implemented the powered leg orthosis. The foot powered orthosis, known as "Pedago", used an electromechanical gait device that was designed to provide a gait motion during training session [12]. The control device helps to move the patients' foot trajectory with a fixed step length of 400mm, in which the gait cycle (GC) speed can be varied from 0 up to 5 km/h. Based on the research findings, it was proven that walking ability could be improved by incorporating the task oriented gait training with mechanical gait training devices or with treadmill training.

The ReoAmbulator robotic system (Motorika Ltd, USA), which is also known as "AutoAmbulator", is another example of existing treadmill gait trainers for lower-limb rehabilitation therapy, as shown in Figure 1(c). This system has been used in research centres and medical hospitals for rehabilitation therapies and educational research studies [13 - 14]. This system also implemented powered leg orthosis, "robotic arms", which enables patients to contribute during the gait motion but also provide remaining force necessary for walking. The robotic arms are attached to the thigh and ankle of the patient's leg before a stepping pattern is performed using the implemented control scheme and strategy. In previous research on this system, it was concluded that robot assisted gait training was able to provide

the improvements in balance and gait, which is comparable to conventional/manual physical rehabilitation therapies.

(a) 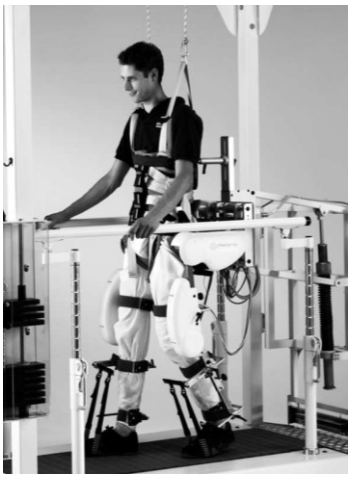 (b) 

(c)

Figure 1 (a) LOKOMAT; (b) LokoHelp; and (c) ReoAmbulator

Apart from the available commercialized rehabilitation orthosis systems, the growth of the ReoAmbulator system is rather immense with the development of different prototypes. The development of LOPES increased researchers' interest in developing a humanlike musculoskeletal assistive orthosis system. This gait rehabilitation orthosis employs the Bowden-cable driven series of elastic actuators (SEA), with the servomotors as the actuation system, to implement low weight (pure) force sources at both posterior and anterior sides of the leg orthosis, as illustrated in Figure 2(a) [15 - 16]. It implemented impedance control (opposed to admittance control), which is based on a combination of position sensing with force actuation to operate the lower-limb leg orthosis. The training effect of this orthosis was enhanced by emphasizing the implementation of an Assist as Needed (AAN) control algorithm. This enabled an increment of the active voluntary participation of the patients.

Moreover, it is also possible to imply unhindered walking practice in the orthosis device where the required forces/torques for imposing a gait pattern are determine based on the system's evaluation.

(a) 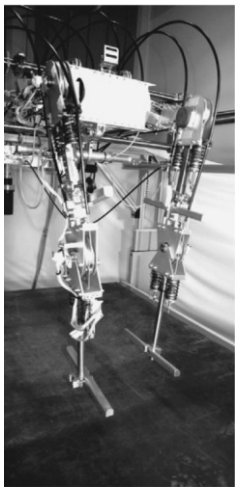 (b) 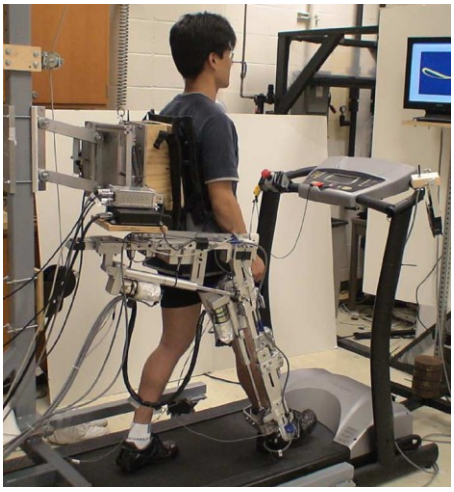

(c) 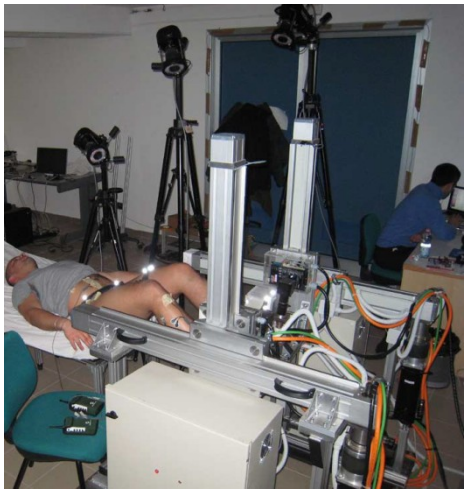

Figure 2 (a) LOPES; (b) ALEX; and (c) NEUROBike

In the following years, the developed robot assisted gait training (RAGT) with an active leg exoskeleton (ALEX) also integrated the AAN rehabilitation strategy into the orthosis system. Compared to other existing robotic training methods, this strategy allows the patient to actively contribute during the retraining process of the gait locomotion. This gait rehabilitation device is shown in Figure 2(b). It implemented the use of linear actuators to actuate the hip joint thigh device and knee joint shank device of the leg orthosis [17 - 18]. It has been proven that an intensive gait retraining process has great potential to significantly provide benefits for the patients, including chronic stroke survivors. This can be achieved by effectively applying enough forces on the ankle of the subject through actuators

placed at the hip and knee joints of the exoskeleton's leg orthosis, by means of a force-field controller.

Later, a stationary gait and ankle trainers system was developed to provide neural-rehabilitative treatments aimed at recovering walking abilities in post-stroke patients. This orthosis system employed the use of brushless servomotors and pulleys to actively control the angular excursions of the gait orthosis, known as the neural-rehabilitative platform for bedridden post-stroke patients (NEUROBike) [19]. The prototype of this system is shown in Figure 2(c). The passive and active exercises were emphasized in this system by implementing the kinematic models of leg-joint angular excursions during both 'sit-to-stand' and 'walking' into the control algorithms. To summarize, providing a number of exercises at an early phase based on the intensity and the severity of the pathology is required by the programmed therapy. In addition, customized treatment adapted by this system may facilitate patients to increase flexibility in lower limb control, which leads to significant improvements in motor control performance during locomotion.

In addition, the Robotic Gait Rehabilitation (RGR) trainer's prototype was also invented within the same year as the NEUROBike system, to assist treadmill gait retraining for patients with unusual gait patterns that were associated with exaggerated pelvis obliquity, illustrated in Figure 3(a). This orthosis is composed of three subsystems: stationary frame, Human-Robot Interface (HRI) and treadmill training. Servo-tube linear electromagnetic actuators were used to generate the power source for the exoskeleton [20]. Based on a hypothesis, the correction of a stiff-legged gait pattern entails addressing both the primary and secondary gait deviations to restore a physiological gait pattern. Therefore, an expanded impedance control strategy was used to generate the corrective moments, only when the leg is in swing motion, by switching the force field that affects the obliquity of the pelvis. It has been demonstrated that this system can be effective in guiding the pelvis to frontal plane via force fields used for altering pelvic obliquity.

Recently, a new gait training robotic device, (LOKOIRAN), was suitably designed for patients with various diagnoses such as SCI, stroke, multiple sclerosis (MS), sport injury cases, aging and people with balance and locomotion disorders. Figure 3(b) illustrates the system's prototype. This gait training device delved into several subsystems, consisting of: body weight support, leg exoskeleton, driving system and transmission system. It employed alternating current (AC) motors

connected to a slide-crank mechanism via belts and pulleys to provide the energy for the system [21]. The implemented control system enables flexibility in motion and permits subjects to change the speed of the foot plates by engaging the speed control mode and the admittance control mode.

(a)  (b) 

Figure 3 (a) robotic gait rehabilitation (RGR) trainer; and (b) LOKOIRAN

The evaluated motorized lower-limb gait rehabilitation orthosis systems mentioned above are only represented a fraction of the currently existing rehabilitation orthoses. However, it could be summarized from these examples that its development has reached an advanced level; whereby, many of the lower-limb gait rehabilitation orthoses, based on electrical motors, have already been commercialized. With its growth speed in the mechanical design, as well as, the implementation of advanced control schemes and strategies, the space available for enhancements might closely reach its peak.

2.3 Pneumatic Muscle Actuators Attributes.

The implementation of pneumatic muscle enabled pneumatic power to be transferred into mechanical power. This actuator will be shortened in the longitudinal direction and enlarged in the radial direction during the contraction stage when it is being inflated; when being deflated, it will turn back to its original form. The pneumatic muscle is able to employ a tensile force to an attached load during contraction stage. This force is unidirectional, whereby, the original length of a certain designed diameter and the internal pressure will determine its value. Moreover, this actuator

also inhibits nonlinear behaviours such as hysteresis, compressibility and time variance. However, in exchange, this pneumatic muscle also has an inherently compliant attribute which is suitable for a human-robotics system. This type of actuator is similar to the human muscle principle; shorter muscle length produces smaller contracting force and vice versa. Furthermore, it is comparable to electric actuators due to the direct coupling to the load and structural optimization. In addition it also has a high power to weight ratio.

In addition to the abovementioned attributes, there exist two main weaknesses that limit the application of pneumatic muscle. The first weakness is the nonlinear behaviour of pressure build-up, and the second weakness is the hysteresis effect due to its geometric structure. These drawbacks cause complexity when scheming high-performance control systems. Therefore, this research is dedicated to solve these problems, using a simple paradigm and control strategy for handling the sudden increase in pressure and hysteresis behaviour of the PMA. Based on the proposed empirical-based static force mathematical model, which consist of a correction factor caused by the effect of the end caps, it showed an inconsistency of high contracting ratios derived by the famous researcher Tondu et al., [22]. The extreme difficulty in constructing an accurate mathematical model was established by the fact that nearly all of the present models proposed were approximations. This model was later modified through various methods, used by other researches, to further improve the mathematical model [23 - 30].

2.4 Pneumatic Muscle Actuated Lower-Limb Rehabilitation Orthosis System.

Compared to the motorized lower-limb rehabilitation orthosis systems (i.e., DC-motors, AC-motors, linear actuators, SEA, servomotors, brushless motors, and pneumatic cylinders), the growth of the pneumatic muscle actuated rehabilitation orthosis system was rather poor. This was also the description based on the development of the control system for the pneumatic muscle. However, numerous research studies in the last 10 years have tried to introduce these types of actuation systems into the lower-limb rehabilitation robotics field. This may indicate a significant shift of researchers' interests towards the implementation of the pneumatic muscle actuated lower-limb rehabilitation orthosis.

The development of the hip orthosis exoskeleton powered by pneumatic artificial muscle (PAM) was invented by Vimieiro et al., at Bioengineering Laboratory in 2004, as shown in Figure 4(a) [31 - 32]. This exoskeleton system was designed and modelled for patients with a motor deficit, a resultant of Poliomyelitis. It consisted of two main parts: the first is polyethylene pelvic brace to provide the stability for the orthosis system, and the second is polyethylene support for the thigh. This orthosis system implemented the position control using the potentiometers for activating the control valves, either to pressurize the PAM or to return it to neutral status. Based on clinical tests, it was proven that the rehabilitation engineering was able to provide equipment and devices for aiding patients to recover their movements or improve their quality of life. A better gait pattern and an improvement of the left step transposition in the toe-off phase were reported by patients.

Later came the Robotic Gait Trainer (RGT) for stroke rehabilitation, which is an ankle rehabilitation device powered by lightweight Springs Over Muscle (SOM), proposed by Kartik et al. It was developed in 2006, as shown in Figure 4(b) [33]. The design was structurally based on a tripod mechanism with one fixed link. This orthosis device was able to provide the dorsiflexion and plantar-flexion, as well as, the inversion and eversion when moving the foot about the ankle joint. It implemented an angular position for the control system and used two types of sensors (i.e., potentiometer and pressure sensor). In this study, Kartik et al. suggested that the range and position of motion (ROM) are necessary for safe dorsiflexion/plantar-flexion and inversion/eversion movements. This was proven by the results from their analysis which demonstrated that the tripod structure was able to generate a ROM that matches the safe anatomical range of the ankle joint during the gait cycle training.

In contrast, the prototype of an Ankle-Foot Orthosis (AFO) powered by artificial pneumatic muscle was also introduced by Ferris et al. in 2006. The prototype was of the human lower-limb that could comfortably provide dorsiflexion and plantar flexion torque during walking motion training, as illustrated in Figure 4(c) [34 - 36]. This orthosis is composed of a hinge joint, carbon fibre shell and two pneumatic artificial muscles. The proportional myoelectric control, using a PC-based controller (real time control), had been implemented into the control system. The performance of the novel controller enables the naive wearers to promptly become accustomed to the orthosis, without the pneumatic muscle co-contraction. It is

believed that this orthosis design will be useful in learning human walking biomechanics and providing assistance in the neurological injuries of patients during the rehabilitation training.

(a)

(b)

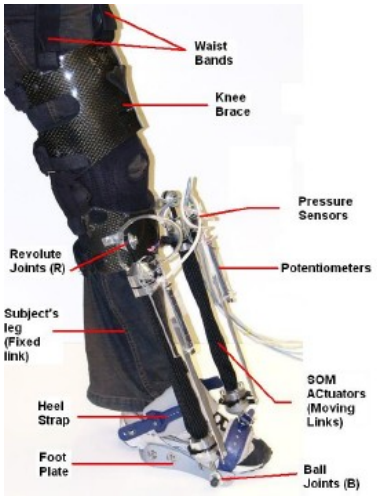

(c)

Figure 4 (a) hip orthosis; (b) robotic gait trainer (RGT); and (c) ankle-foot orthosis (AFO)

Conversely, by focusing on the development of "human friendly" exoskeleton orthosis systems, Costa et al. in 2006, proposed a powered lower-limb orthosis which can produce powerful, yet naturally safe, operations for paraplegic patients; as illustrated in Figure 5(a) [37]. This was realized by combining a highly compliant actuator (PMA) with an embedded intelligent control system (a three level PID joint torque control scheme) to manipulate the antagonistic actuators of the exoskeleton. It is difficult to provide a system with dependability and inherent safety while utilizing a highly compliant actuator, using conventional designs alone. However, the design philosophy of this system may provide a significant insight into

the development of rehabilitation orthosis systems and improve the rehabilitative procedures for paraplegic patients.

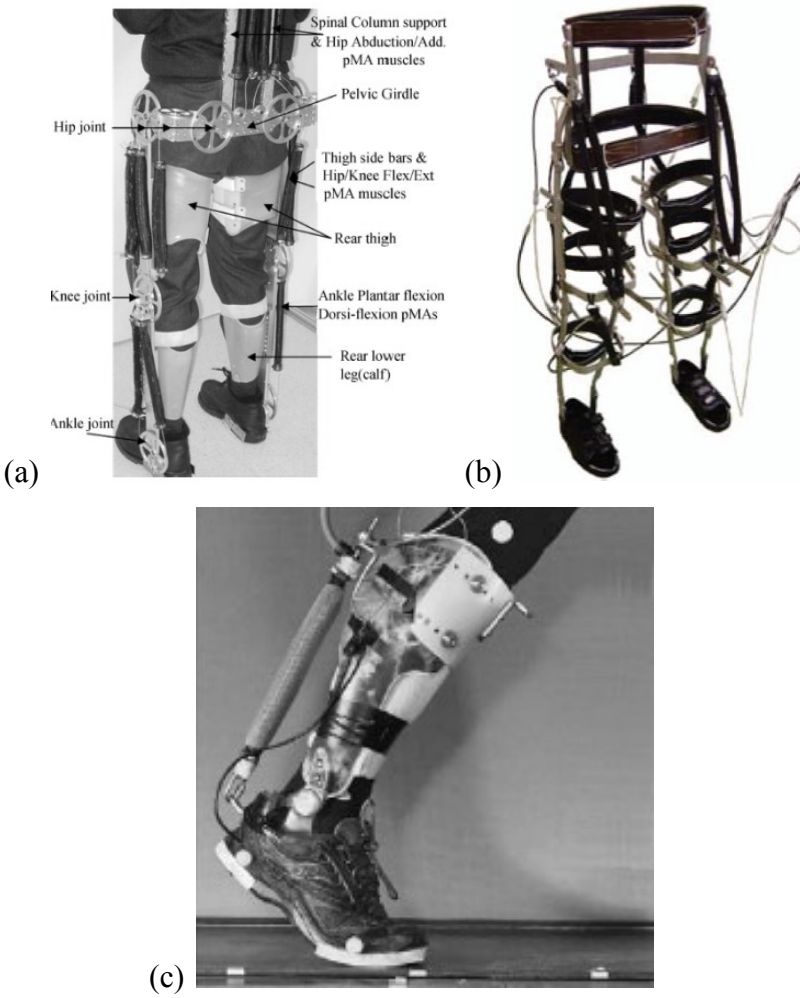

Figure 5 (a) powered lower-limb orthosis; (b) RGTW; and (c) powered ankle-foot exoskeleton

Contrastingly, Figure 5(b) shows the Robotic Gait Trainer in Water (RGTW). This system was designed for a development of an underwater gait training orthosis by Miyoshi et al. in 2008 [38]. The RGTW is a hip-knee-ankle-foot orthosis with pneumatic McKibben actuators as the actuation system. The basis of the angular motion for the control system was determined by a healthy subject walking under water. The aim for this study was to achieve repetitive physiological gait patterns to improve movement dysfunctions. By implementing this orthosis system device, it is not only the effect of hydrotherapy that should be expected; standard treadmill training is also included. This could also be sufficiently effective for patients undergoing hip-joint movement dysfunction treatments.

In 2009, Malcom et al., developed the powered ankle-foot exoskeleton, which investigated the role of the tibialis anterior (TA) in the walk-to-run condition (WRT), as shown in Figure 5(c) [39 - 42]. The pneumatic muscles were used to provide the dorsiflexion and plantar-flexion torques through the assisting orthosis for incomplete SCI patients during assist and resist conditions. This orthosis device implemented an electromyography (EMG) control with a feed-forward algorithm; whereby a set of rotary encoders and load cells were used to measure the treadmill belt speed, ankle angle, dorsiflexion and plantar-flexion torques. Through the hypothesis from gait transitions and research evaluations, it was demonstrated that the powered exoskeleton had great potential in fundamental gait studies.

After the introduction of AFO by Ferris et al., the development of this system was later continued by Sawicki et al., a few years later. In 2009, the pneumatically powered Knee-Ankle-Foot Orthosis (KAFO) was proposed through the study of human motor adaptation, gait rehabilitation and locomotion energetics; as shown in Figure 6(a) [43]. Compared to the AFO control system, this system implemented a physiological-inspired controller that utilised the patient's muscle information; which is determined using electromyography to measure the timing and amount of the artificial muscle forces. Based on several research findings, it is believed that powered knee-ankle-foot orthoses are promising for basic science and clinical applications; since they had successfully assisted individuals with incomplete SCI during locomotor training, metabolic energy consumption and neural adaptation for neurologically intact human walkers.

New high performance devices are required for applying continuous passive rehabilitation training for post-traumatic disabilities regarding the bearing joints of the inferior limbs; therefore, the introduction of a stationary gait and ankle trainers, known as Continuous Passive Motion (CPM), were based on the rehabilitation system illustrated in Figure 6(b) [44]. This system was invented by Tudor et al. in 2009, using the pneumatic muscles as the actuation system for providing a low cost rehabilitation system. With the lower limb being immobilized during the rehabilitation (patient lying on a bed), it allows for the hip and knee joints to perform recovery exercises. When compared to the electro-mechanically actuated rehabilitation system that causes discomfort to the users due to the introduction of shocks upon the reversion of sense of motion, this system utilises a source of energy, namely air, which enables the occurring shocks to be completely absorbed.

Figure 6(c) shows a power-assist lower-limb orthosis, proposed by Yeh et al., in 2010, for assisting the elderly and individuals suffering from sport injuries such as inability to walk or climb stairs using McKibben pneumatic muscles as the actuation system [45]. For achieving a better tracking performance, an inverse control for the feed-forward compensation was constructed using the hysteresis model, which was then combined with the Loop Transfer Recovery (LTR) feedback control. In addition, to ensure smooth switching between different phases during operation, bump-less switching compensators were implemented into the combine control system. Based on the research findings, it was demonstrated that the orthosis was able to effectively accomplish the assistive function of human locomotion during walking and climbing stairs.

(a)  (b) 

(c) 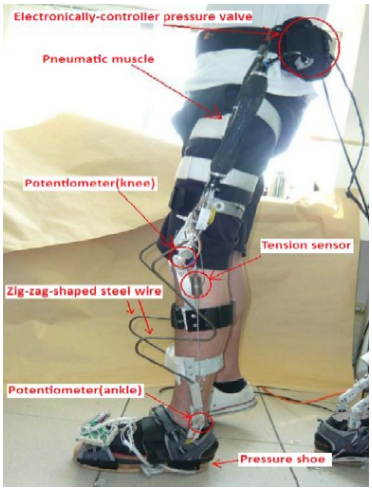

Figure 6 (a) KAFO; CPM; and power-assist lower-limb orthosis

Moreover, a two degree of freedom Active Ankle-Foot Orthosis (AAFO) was designed and manufactured in 2011 by Carberry et al. for post stroke rehabilitation, exemplified in Figure 7(a) [46]. By implementing a novel actuator linkage using air

muscle, a lightweight and discrete orthosis system was achieved. This design enabled the entire actuation system to be placed behind the leg of the orthosis. A feedback control that utilised a fuzzy logic gait phase detection system was implemented with the use of two types of sensory devices: the first is Force Sensitive Resistors (FSRs), located under the insole of the shoe; the second is the rotary encoder for measuring the angular displacement of the ankle joint. However, it is unlikely that suitable methods of supplying air pressure to the device can be found, even though this system exhibits many desirable features. This system may well be beneficial to after-stroke patients, as it allows a more complete rehabilitation of the ankle joint.

In 2011, bio-inspired active soft orthotic device for ankle foot pathology was developed by Park et al. for treating gait pathologies associated with neuromuscular disorders, as shown in Figure 7(b) [47]. By utilizing the advantages of the pneumatic artificial muscle actuators, an inspired biological musculoskeletal system with muscle-tendon-ligament structure had been introduced as the design of the orthosis system. Three types of sensors were used for the control system: the first is strain sensor for measuring ankle joint angle changes; the second is internal measurement unit (IMU) to measure the orientations of the lower leg and the foot; and the third is pressure sensor to identify the foot ground contacts and gait cycle events. The implemented feed-forward and feedback controllers were able to demonstrate a good repeatability of the ankle joint angle control, respectively. Based on the outcomes of the result, this research is believed to be capable of providing rich spaces for the rehabilitation techniques for ankle pathologies in the near future.

Furthermore, in 2012, Park et al. had also developed another lower-limb rehabilitation orthosis known as the active modular elastomer sleeve for soft wearable assistance robots; to support and monitor human joint motions, as illustrated in Figure 7(c) [48]. With a different system design proposal, this orthosis device implemented a series of miniaturized pneumatically-powered McKibben-type of actuators. These actuators were wrapped in between monolithic elastomer sheets so as to exert tension. Through shape and rigidity control, the simultaneous motion sensing and active force response were allowed by wrapping the material around the joint. The muscle contractions for the actuators are measured by placing the hyper-elastic strain sensor perpendicularly to the axial direction of each corresponding actuators. This strain sensor will detect the radial expansion of each actuator, which is then transformed to the contraction length of the muscle actuator. Based on the

preliminary study of this device system, few improvements should still be made within the design structure and control system.

(a)  (b) 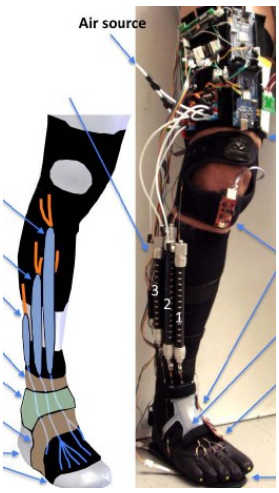

(c) 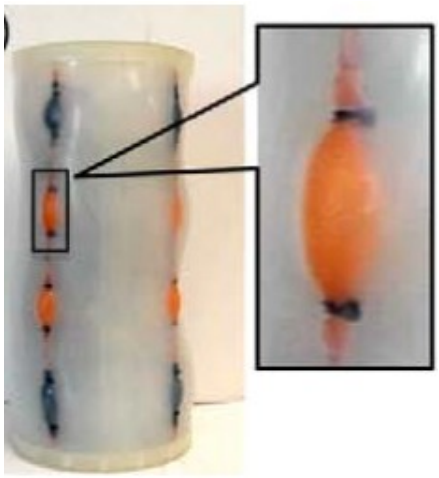

Figure 7 (a) AAFO; (b) bio-inspired active soft orthotic for ankle-foot pathologies; and (c) active modular elastomer for soft wearable assistance robots

Figure 8(a) presents a developed inexpensive pneumatically powered assisted knee-ankle-foot orthosis (KAFO), using McKibben actuators, for providing assistance during gait training; proposed by Teng et al., in 2012 [49]. To determine the relationship between the inclination angles of each joint with pneumatic muscle displacement, the equation was expressed by using a trigonometry method; employed into the control system algorithm and strategy. However, this lower-limb orthosis system is still in the early development stage of design improvement, therefore, further evaluation on system performance has yet to be concluded.

In 2013, Kawamura et al. initiated the development of an orthosis for walking assistance. It was designed using straight fibre pneumatic artificial muscles in assisting the forward swing of the leg and increasing the step length to further

recuperate patients' walking abilities, as illustrated in Figure 8(b) [50]. The pressure control unit was implemented using the developed Dual Pneumatic Control System (DPCS) by manipulating the Pulse-Width Modulation (PWM) signal to control the valve. This orthosis system has yet to reach its completion and require further improvements in its control scheme and strategy when handling the nonlinearity behaviour of the actuator. The assistant force generated by the orthosis system is not adequate enough for driving the intended task.

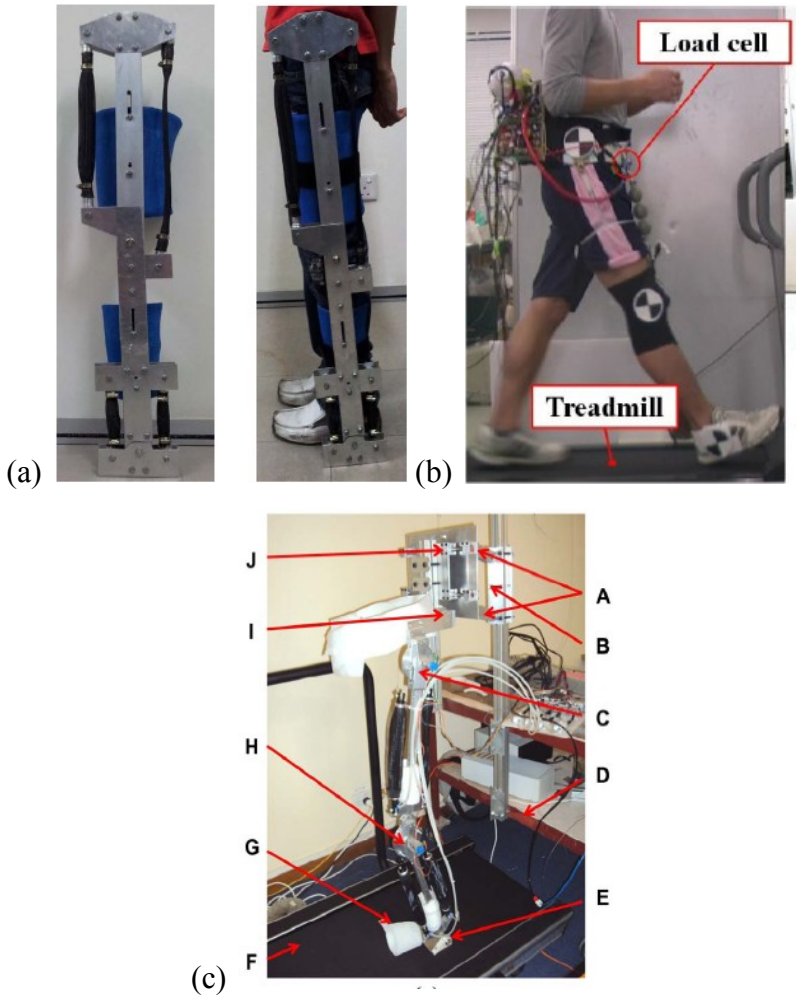

Figure 8 (a) inexpensive KAFO; (b) orthosis for walking assistant; and (c) 6 DOF robotic orthosis for rehabilitation

Recently, in 2013, Hussain et al., invented a six degree of freedom robotic orthosis for gait rehabilitation to encourage patient voluntary contribution in the robotic gait training process, as shown in Figure 8(c) [51-52]. It implemented four pneumatic muscle actuators which were arranged as two pairs of antagonistic mono-articular muscles at hip and knee joint angles. This system integrated the AAN gait training algorithm based on the adaptive impedance control, employing a Boundary-

layer-Augmented Sliding Mode Control (BASMC)-based position controller, to afford an interactive robotic gait training system. It was proven that the implementation of the adaptive impedance control scheme was able to provide the gait motion training, which is comparable to the one provided by physical therapists. Additionally, the result findings demonstrated that an increase/decrease in a human's voluntary participation during the gait training will result in a decrease/increase of robotic assistance.

Table 1 shows the comparison of existing pneumatic muscle actuated lower-limb rehabilitation orthosis systems. Based on the evaluations of these systems for the past 10 years, it can be concluded that researchers' interests shifted to the implementation of the natural compliant type of actuators (i.e., McKibben muscle, rubbertuators, air muscle, PAM, PMA, etc.). This was proven by the development of different types of assistive gait rehabilitation orthoses system prototypes, including foot orthoses, hip orthoses, knee-foot orthoses, stationary gait and ankle trainers, over-ground gait trainers with orthoses, mobile over-ground gait trainers and treadmill gait trainers [31-52]. In addition, the improvement of the control system implementation, since the year 2004 up until 2013, showed that researchers were gradually trying to improve the control of pneumatic muscle actuated lower-limb orthoses, as illustrated in Table 1. In the beginning, only a simple angular position control was proposed to activate the control valves. Later, it was shifted to the implementation of proportional myoelectric control, intelligent embedded control, inverse control, feedback control (which utilised a fuzzy logic), rigidity control, and subsequently, the adaptive impedance control.

The exponential growth of these systems might also be due to the advantageous attributes of the pneumatic muscle actuator, as well as its nonlinear dynamic behaviour. However, according to the evaluations of currently existing systems, it could be understood that suitable control schemes and strategies have yet to be found. Regardless, this only suggests that the space available for orthoses device improvements and enhancements, in either mechanical design or control scheme and strategy, are still boundless. This opportunity will attract researchers' interest in devising distinctive ideas and strategies to rectify previous methods, or to discover new methods for the control system. Even though many different robotic system types for lower-limb rehabilitation orthoses have been developed, each prototype only implemented the use of mono-articular muscles alone, either for hip,

knee or ankle joints (i.e., flexion, extension, abduction, adduction, plantar-flexion, dorsiflexion, inversion, eversion, etc.). However, no attempt was made to introduce the implementation of bi-articular muscles, either to compensate the lack of force/torque at the joints, or to improve the performance of the implemented control scheme and strategy.

Table 1 Comparison of existing pneumatic muscle actuated lower-limb rehabilitation orthosis systems

Comparison for existed pneumatic muscle actuated lower-limb rehabilitation orthosis systems						
Orthosis system	Time scale	Robotic system types	Actuators	Antagonistic actuators	Control system	References
Hip orthosis exoskeleton	2004	Hip orthoses	McKibben pneumatic muscle	Mono-articular for hip joint (flexion)	Position control using the potentiometers for activating the control valves	[31 - 32]
Robotic gait trainer (RGT)	2006	Foot orthoses	Lightweight spring over muscle (SOM)	Mono-articular for ankle joint (dorsiflexion)	Angular position control system	[33]
Ankle-foot orthosis (AFO)	2006	Foot orthoses	McKibben pneumatic muscle	Mono-articular for ankle joint (dorsiflexion and plantar-flexion)	Proportional myoelectric control using a PC-based controller	[34 - 36]
Powered lower-limb orthosis	2006	Treadmill gait trainers	Pneumatic muscle actuators (PMA)	Mono-articular for hip joint (flexion, extension, abduction, and adduction), knee joint (flexion and extension), and ankle joint (dorsiflexion and plantar-flexion)	Intelligent embedded control mechanism (a three level PID joint torque control scheme)	[37]

Robotic gait trainer in water (RGTW)	2008	Over-ground gait trainers with orthosis	McKibben pneumatic muscle	Mono-articular for hip joint (flexion and extension), and knee joint (flexion and extension)	Position control system	[38]
Powered ankle-foot exoskeleton	2009	Foot orthoses	Pneumatic artificial muscle (PAM)	Mono-articular for ankle joint (dorsiflexion and plantar-flexion)	Electromyography (EMG) control with feed-forward algorithm	[39 - 42]
Powered knee-ankle-foot orthosis (KAFO)	2009	Knee and foot orthoses	McKibben pneumatic muscle	Mono-articular for knee joint (flexion and extension), and ankle joint (dorsiflexion and plantar-flexion)	Physiological-inspired controller using electromyography	[43]
Continuous passive motion (CPM)	2009	Stationary gait and ankle trainers	Pneumatic artificial muscle (PAM)	_	_	[44]
Power-assist lower-limb orthosis	2010	Over-ground gait trainers (mobile)	McKibben pneumatic muscle	Mono-articular for knee joint (extension)	Inverse control and loop transfer recovery (LTR) feedback control	[45]
Active ankle-foot orthosis (AAFO)	2011	Foot orthoses	McKibben pneumatic muscle	Mono-articular for ankle joint (plantar-flexion)	Feedback control which utilized a fuzzy logic gait phase detection system	[46]

Bio-inspired active soft orthotic device	2011	Foot orthoses	Pneumatic artificial muscle (PAM)	Mono-articular for ankle joint (dorsiflexion, inversion, and eversion)	Feed-forward and feedback controllers	[47]
Active modular elastomer sleeve for soft wearable assistance robots	2012	Knee orthoses	Miniaturized McKibben pneumatic muscle	Mono-articular for knee joint (flexion and extension)	Through shape and rigidity control	[48]
Knee-ankle-foot orthosis (KAFO)	2012	Knee and foot orthoses	Pneumatic artificial muscle (PAM)	Mono-articular for hip joint (flexion and extension), and knee joint (flexion and extension)	_	[49]
Orthosis for walking assistant	2013	Hip orthoses	Straight fiber pneumatic artificial muscle (PMA)	Mono-articular for hip joint (flexion)	Dual pneumatic control system (DPCS) with pulse-width modulation (PWM) signal	[50]
Six degree of freedom robotic orthosis for gait rehabilitation	2013	Treadmill gait trainers	McKibben pneumatic muscle	Mono-articular for hip joint (flexion and extension), and knee joint (flexion and extension)	Adaptive impedance control using boundary-layer-augmented sliding mode control (BASMC)	[51 - 52]

2.5 Control Scheme and Strategy

The need for improved control strategies in handling the antagonistic actuator of pneumatic muscles will determine the progression of growth in lower-limb rehabilitation orthosis systems. Based on previous research, it is possible to utilize a standard PID controller in a feedback loop to control the joint's angle of the assistive robotic towards desired values. Nevertheless, without additional model paradigms or integrated controllers, it may not be able to accurately control the compliant robotic system due to the complex and highly nonlinear dynamics of the pneumatic muscle. Thus, the resulting position control would be rather poor. For that reason, the implementation of conventional PID controllers should come with additional control strategies, such as: additional model paradigm, auto-tuning, nonlinear system, adaptive control, intelligent control (i.e., neural network, fuzzy logic, genetic algorithm, etc.), robust control and stochastic control. An existing control scheme and strategy which enables a much simpler approach for the control system implementation on the orthotics' rehabilitation robotics is strongly desired. Therefore, in this review article, the implementation of co-contraction controls in manipulating the antagonistic actuators and its advantages will be discussed and elaborated thoroughly.

2.6 Pneumatic Muscle Actuators Control System.

Even though numerous control systems have been established for the pneumatic actuators, especially pneumatic cylinders, only a fraction were for the artificial pneumatic muscles. From 1993-1995, some examples of well-known controllers that could be implemented, adopted by Caldwell et al., were tested on a feed forward PID regulator to develop an adaptive controller for the pneumatic artificial muscle (PAM) manipulator [53 - 55]. Likewise, in 1995, Gustavo et al. developed an adaptive position control for antagonistic pneumatic muscle actuators via adaptive pole-placement [56]. Also in 1995, Hamerlain et al. introduced a variable structure control that included a high robust performance, with respect to model errors, parameter variations and quick responses [57]. Within the same year, Iskarous et al. proposed intelligent control using the neuro-fuzzy network to control the complex dynamic

properties of muscle actuators [58]. In 1996, P. van der Smagt et al., introduced a neural network based controller to a pneumatic robot arm; with complex, highly nonlinear, dynamics that change in time due to internal influences [59]. Additionally, in 1996, Cai and Yamaura presented a robust tracking control approach by implementing a sliding mode controller [60]. Within the same year, Colin et al. proposed the position and PID controllers for force manipulation using adaptive pole-placement techniques [61].

Afterwards, in 1999, Repperger et al. handled the nonlinear factor with a nonlinear feedback controller, using a gain scheduling method [62]. Tondu and Lopez also employed a sliding-mode control approach in the year 2000 [22]. Contrarily, Carbonell et al. introduced the nonlinear control of a pneumatic muscle actuator by using adaptive back-stepping and sliding-mode tracking controllers in 2001 [63 - 64]. In 2003, Folgheraiter et al. developed an adaptive controller based on the neural network for the artificial hand [65]. In the same year, Balasubramanian and Rattan proposed the feed forward control of a nonlinear pneumatic muscle system using fuzzy logic [66]. From 2004 to 2006, Ahn and Tu proposed an intelligent switching control scheme by utilizing a learning vector quantization neural network and a nonlinear PID control to improve the control performance of PAM manipulator using Neural Network (NN) [67-68]. In 2008, Harald et al., developed the cascade sliding mode (SM) control scheme for a high speed linear axis pneumatic muscle [69]. Moreover, Seung et al. proposed a trajectory tracking control using a neural network based on PID control in 2009 [70]. In 2010, Xing et al. introduced the tracking control of pneumatic artificial muscle actuators based on the sliding-mode and non-linear disturbance observer (SMCBNDO) in order to improve the robustness and performance of the trajectory tracking control [71].

Unfortunately, applying a complicated control algorithm does not always indicate the best solution used to control pneumatic muscles. There is an argument in the field of rehabilitation robotics regarding what is the best control system to the orthotic problem for rehabilitation. It is preferred that control systems are simplified as much as possible; multiple sensors and impedances only increase the complexity of control systems. Rather than using a very complicated algorithm for a system, a much simpler approach may be proposed.

2.7 Co-Contraction of Antagonistic Muscle Control.

The early study of the co-contraction of antagonist muscle control was carried out by Neville Hogan in 1984, which introduced adaptive control of mechanical impedance by co-activation of antagonist muscles [72]. This research study focused on biomechanical modelling and analysis of simultaneous co-activation of antagonist muscles by controlling the mechanical impedance. A dynamic optimization theory was used to obtain a prediction of antagonist co-activation, thus enabling a criterion function minimization which represented the task of maintaining upright posture. Based on the research findings, it concluded that under the normal psychological conditions, the significant levels of simultaneous activation of antagonist muscles were observed. In addition, the levels of antagonist muscles co-activation were also increased with the increment of gravitational torques. The modelled isometric muscle torque was represented in the following:

$$T_{biceps} = \left(T_o - K_{QS}\theta\right)u_{biceps}$$

$$T_{triceps} = -(T_o + K_{QS}\theta)u_{triceps}$$

(u) is the neural control $\begin{cases} 0 \le u_{biceps} \le 1 \\ 0 \le u_{triceps} \le 1 \end{cases}$

Joint stiffness at maximum activation is $\left(0 \le K_{QS} \le {}^{2T_o}/_{\pi}\right)$ where (T_o) is maximum isometric muscle torque.

Subsequently, in 1988, William R. Murray et al. carried on this research by implementing a simple model demonstrating the quasi-static behaviour of skeletal muscles, in which the force generated by the muscle was the neural activation of the muscle and the bilinear function of muscle length [73 - 74]. This muscle activation could be defined as the synchronized activation of agonist and antagonist muscle groups, acting in the same plane and crossing at the same joint. It was verified that the relationship between antagonistic actuators (i.e., agonist and antagonist) could be linearly related in the occurrence of various fixed levels of co-contractions. In other words, the plane of agonist and antagonist muscle activity, the ‘equilibrium line’ or

the locus of all feasible levels of muscular activation, will be a straight line for which a particular equilibrium position is sustained. In addition, the intercepts and slopes of these equilibrium lines are such that the expected levels of muscular activation are counterintuitive. This explained why the anterior muscle activation levels were higher than posterior activation levels for all, regardless of how low the levels of muscular activity.

Since then, numerous research studies were implemented on the co-contraction of antagonistic muscle control, which proved its ability to increase the stiffness and stability at the joints during volitional movements [75 - 86]. Based on these research studies, it showed that by utilizing information from the antagonistic muscle co-contraction, muscular activation levels could be manipulated to control the movements of the joints. Recently in 2013, Klauer et al. introduced the nonlinear joint-angle feedback control of electrical stimulated and λ-controlled antagonistic muscle pairs, in order to control the human limb movements in neural-prosthetic systems [87 - 88]. The desired recruitment levels λ of both muscles were estimated using the electrical stimulation evoked electromyography (EMG) measurements. The proposed controller enabled the tracking of reference joint torques and predefined muscular co-contraction using exact linearization methods. Based on the outcomes of the result, the control system was able to rapidly compensate the muscle fatigue and then change the muscular thresholds. It could be said that this is a prerequisite of neural-prosthetic system's practical application within clinical environments. The asymptotically stable system for the torques was depicted in the following:

$$T_i(k) = k_{s,i}\big(\theta_{max,i} - \theta(k)\big)\left(\frac{q^{-2}(1-a)}{1-aq^{-1}}\right)\left(\frac{1-b_i}{1-b_i q^{-1}}\right) r_{\lambda_i}$$

where (λ_i) is the muscular recruitment levels; (r_{λ_i}) is the desired recruitment levels; (q^{-1}) is the backward shift operator; (q^{-2}) is the delay of two sampling steps; (k) is the sampling index;

$$\theta \in \left[\theta_{max,1}, \theta_{max,2}\right];$$

$$a \in [0, 1];$$

$$b_i \in [0, 1]$$

2.8 Simulation of Co-Contraction Model for Antagonistic Muscles.

In recent years, plenty of research studies were carried out on assistive robotics for rehabilitation, either using motors or pneumatic muscle actuators for the robotic system's source of power [5-8]. Consequently, these studies became the basis for many findings. Famous researchers in this field, such as Daniel Ferris, have mentioned that powered orthosis could assist the task-specific practice of gait, with a long-term goal of improving patient's inherent locomotor capabilities [89]. According to Kalyan K. Mankala and Sunil K. Agrawal et al., passive swing assistance was able to assist patients, with less than ordinary muscle strength, to attain better gait trajectories [90]. Furthermore, analyses on the implementation of the mono- and bi-articular actuators for achieving high muscle moment required at joints and better gait trajectories, were also taken into consideration in real practices [91-95]. The study of antagonistic muscle co-contraction had suggested that the control of orthosis, which implemented these mono- and bi-articular actuators, could achieve good joint stiffness and stability [75-86]. The design was biologically inspired (by human muscles), as it employed two compliant elements to manipulate the joints. Usually, this type of orthosis system, implemented antagonistically, actuated joints using pneumatic type of muscle actuators. In addition, the co-contraction activations were also able to reduce a kinematic variability; whereby, through the increment of co-contraction activations, the kinematic variability could be reduced with the exception of low co-contraction activation levels [96]. Therefore, it could be concluded that the modelling of co-contraction models to represent the movement of antagonistic actuators may be beneficial.

The early study of the co-contraction model was proposed by William K. Durfee et al. in 1989. They developed task-based methods for evaluating electrically simulated antagonist muscle controllers in a novel animal model [97]. The stimulus activation levels of two antagonist muscles, that manipulated an anesthetized cat's intact ankle joint, were determined by the controller output. In this study, three types of controllers were evaluated: the first was open loop reciprocal control, the second was P-D closed loop reciprocal control and the third was open loop co-contraction control (Figure 9). Based on the results of the analysis, it showed that in the visual feedback, the performance of the open loop co-contraction control was comparable to the performance of P-D closed loop control. This suggested that in some cases of

clinical neural prostheses implementation, the feedback controller may not be required for good control system performance. In addition, these results also suggested the importance of co-contraction for position control tasks in neural prostheses. However, the disadvantages of this control scheme was that it required more than one input command for each degree of freedom of motion, which could cause premature muscle fatigue.

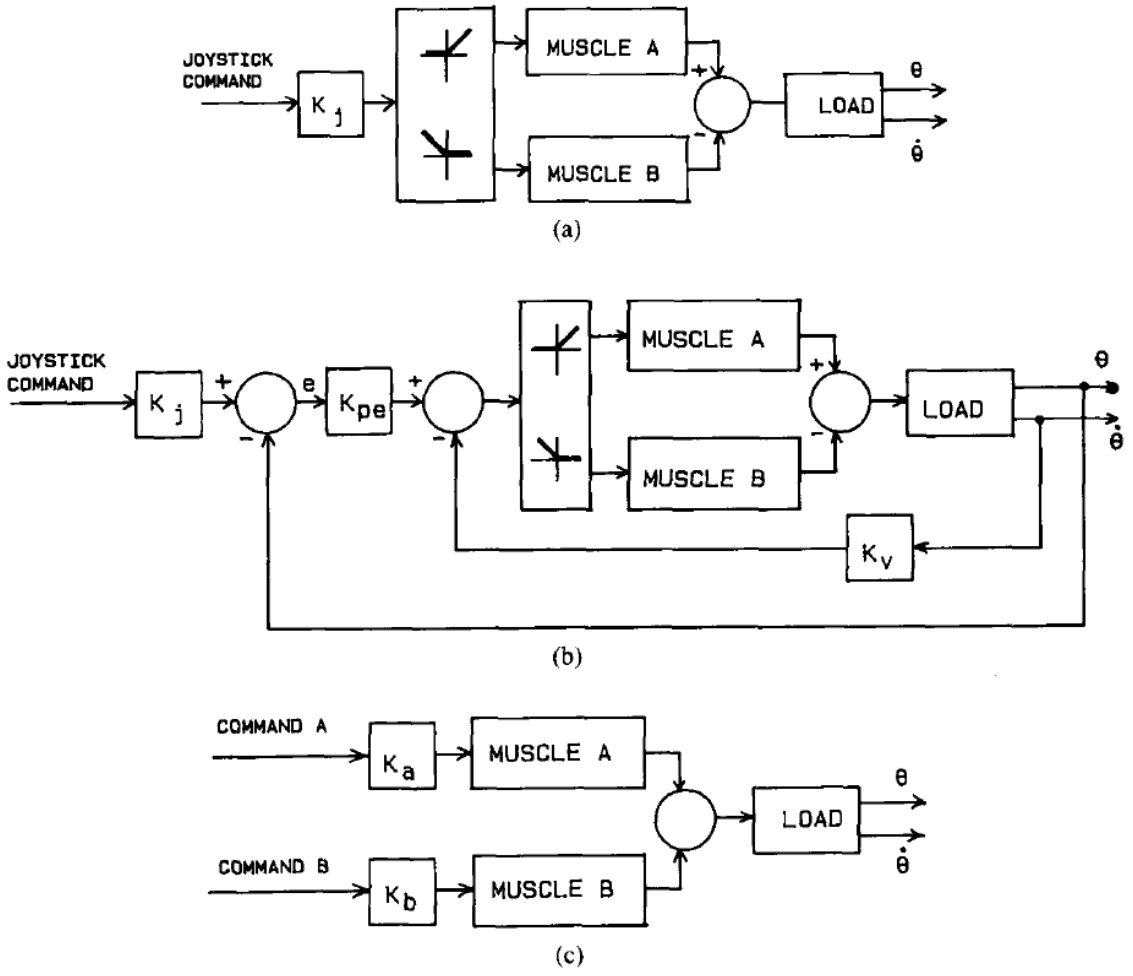

Figure 9 (a) is open loop reciprocal control; (b) is P-D closed loop reciprocal control; and (c) open loop co-contraction control [97].

The simulation study of the co-contraction model control scheme for simultaneously manipulating antagonistic actuators was reinitiated by Mohammed et al. in 2005. It was mentioned in their study of co-contraction muscle control strategy for paraplegics, that co-contraction of antagonistic muscle functions (basically quadriceps and hamstrings) are not necessarily restricted to oppose motion, but may

yield to increasing joint stiffness and stable movements [98]. The magnitude of antagonistic muscle co-contractions were first determined based on the optimization of static linear constraints of muscle forces acting on the joint; whereby, the redundancy of two muscles in co-contraction (i.e., agonist and antagonist) spanning the joint was resolved using linear minimization of the total stress in antagonistic muscles. Afterwards, the relationship between the amounts of muscle co-contractions and maximum force for the antagonistic muscle actuators were computed by implementing weight factors. However, to ensure the robustness and the safety movement of the orthosis, due to the nonlinearity and presence of 2nd order system, a High Order Sliding Mode (HOSM) controller was implemented. In addition, Mohammed et al. continued their research in 2010 by introducing an inverse model that considered the muscular dynamic contraction of muscle actuators [99]. This dynamic contraction consisted of two main components: the first was activation dynamics, and the second was contraction dynamics (i.e., force-length and force-velocity relationships). However, the activation dynamics was neglected as its role was assumed to not be essential during the optimization. The inability of most optimization models to compute muscle co-contractions may be caused by the utilization of monotonous increment objective functions that will penalize every additional increment of muscle force. The amount of co-contraction muscle forces (i.e., quadriceps and hamstrings) was derived as follows:

$$F_q = \xi_q F_{max,q} + r_q {F^2}_{max,q} \left(\frac{M - \xi_q \sum_q \left(r_q F_{max,q} \right)}{\sum_q \left(r_q F_{max,q} \right)^2} \right)$$

$$F_h = \xi_h F_{max,h} + r_h {F^2}_{max,h} \left(\frac{M - \xi_h \sum_h \left(r_h F_{max,h} \right)}{\sum_h \left(r_h F_{max,h} \right)^2} \right)$$

$$\text{The constrains are } \begin{cases} 0 \le F_i \le F_{max,i} \\ \sum_i r_i F_i = M \end{cases} (i = q, h)$$

where (ξ_q) and (ξ_h) are the weight factors; (F_{max}) is the maximum isometric muscle forces; (r) is the radius;

Subsequently, a simulation research study was instigated by Heitmann et al. in 2012 on muscle co-contraction of a three-link biomechanical limb that modulates

the damping and stability of the joints. This study was conducted for replicating the natural relationship, without the information of anatomical detail, between the muscle activation and joint dynamics [100]. It was proven that the muscle co-contraction was able to alter the damping and the stiffness of the limb joint without altering the net joint torque, and its effect was incorporated into the model by attaching each manipulator joint with a pair of antagonist muscles. These muscles could be activated individually with each other using ideal mathematical forms of muscle co-contraction. This mathematical equation was derived from natural force-length-velocity relationships of contractile muscle tissue. From the simulation result and numerical stability analysis, it was proven that the damping in biomechanical limb had increased consistently with the human motor control observation. Moreover, it was also revealed that under identical levels of muscle co-contraction, the bi-stable equilibrium positions could co-exist when the opponent muscles were configured with asymmetric contractile element force-length properties. There were two implications of these result findings: the first was practical implications for the nonlinear bio-mimetic actuator design, and the second was theoretical implications of biological motor control that presumes antagonist muscle systems are universally mono-stable.

In 2011, H. Kawai et al. had also instigated a simulation study for manipulating the antagonistic mono- and bi-articular muscle actuators using a co-contraction based model [101]. The purpose of this simulation study was to verify the proposed passivity-based control for two degrees of freedom (2DOF) for human arm manipulators. The termed bi-articular manipulator dynamics for three muscle torques (i.e., two pairs of mono-articular and a pair of bi-articular actuators) were constructed in order to design the control inputs for the system. The important property of the passivity was used to examine stability analysis of the proposed control law, even though the bi-articular manipulator dynamics passivity could not be determined based on antagonistic bi-articular muscles. Afterwards, in 2012, K. Sano, H. Kawai et al. proposed a simulation study of the same 2DOF manipulator systems using open loop control [102]. Compared to their previous simulation study, the Lyapunov method was used to examine the stability analysis of the proposed control law. However, the anticipated approach did not pact with the bi-articular manipulator dynamic's uncertainties. This simulation study was then extended to a robust control method that enabled semi global asymptotic tracking, using RISE

control due to uncertain nonlinear model of the lower limb of the human body in 2013 [103]. The results showed that the lower limb was able to position to the desired trajectories in the presence of un-modelled bounded disturbances. However, the torque generated at knee joint was less when compared to their previous method due to the antagonistic bi-articular muscles. The contractile force of the flexor muscle (u_{fi}) and extensor muscle (u_{ei}) was derived as follows:

$$T_i = (u_{ei} - u_{fi})l_p - (u_{ei} + u_{fi})k_i {l_p}^2 q_i + (u_{e3} - u_{f3})l_p - (u_{e3} + u_{f3})k_3 {l_p}^2 (q_1 + q_2)$$

where ($i = 1, 2$); (l_p) and (k_i) are the radius of the joints;

(q_1) and (q_2) are the hip and knee joint angles;

(u_{e1}) and (u_{f1}) are the antagonistic mono-articular muscle for hip joint;

(u_{e2}) and (u_{f2}) are the antagonistic mono-articular muscle for knee joint;

(u_{e3}) and (u_{f3}) are the antagonistic bi-articular muscle;

Within the same year of 2013, H. Kawai et al. also proposed a design of co-contraction level of antagonistic muscles with muscle contraction dynamics for tracking the control of human lower limbs [104-105]. The manipulation of antagonistic muscle's co-contraction level was dependant on the angular velocity of human lower limbs. Based on the research findings, it could be verified that the co-contraction of antagonist muscles were playing an important role for the joint's stiffness and stability. In addition, the muscle co-contraction was not only useful for compensating the joint's stiffness and stability, it was also able to manoeuvre the direction of output force.

2.9 Co-Contraction Model for Antagonistic Actuators.

Numerous studies have been investigated regarding the co-contraction movements of human antagonistic muscles. However, their model implementations in controlling

the antagonistic muscle actuators of lower-limb orthosis were not completely discovered. In addition, the research paper that focuses on the implementation of mono-articular and bi-articular muscle actuators using pneumatic muscles for the lower-limb rehabilitation orthosis has yet to be extensively investigated; thus, simply actuating the actuators may not give a good result on the joint's stiffness and stability of the lower-limb leg orthosis and its position trajectory. Therefore, based on the evaluation and suggestion of the related research findings, the simultaneous co-contraction movements between the agonist and antagonist muscle actuators should be considered during the control system.

In this review article, the evaluation and comparison of the developed lower-limb rehabilitation orthosis using pneumatic muscle-type of actuators, including its control algorithms and strategies intended to provide stiffness and stability during the control system, were reviewed. Although a considerable amount of work is now complete, the field is still rapidly evolving. The issue of which is the most effective control algorithm is still widely open. However, the randomized controlled trials are necessary for identifying suitable control algorithms, even though it is expensive and time-consuming. In conclusion, a few remarks to be suggested for future research of pneumatic muscle actuated gait trainers system are: firstly, the pneumatic muscle actuators' arrangement of the lower-limb orthosis should be antagonistic; secondly, the co-contractive movement of the antagonistic pneumatic muscles should provide a good stiffness and stability for the leg orthosis system; thirdly, a model paradigm is essential to generate adequate co-contractive input data for manipulating the antagonistic muscle actuators; and finally, the developed model should be managed by controllers to deal with the presence of dynamic properties and nonlinearity behaviour of the system.

CHAPTER 3

SYSTEM DESIGN

Figure 10(a) shows the schematic diagram for the AIRGAIT exoskeleton. The design of this system and the mechanical structures involved were thoroughly evaluated in previously published papers [106 - 107]. Currently the AIRGAIT exoskeleton employs the PC-based control which utilizes the xPC-Target toolbox and MATLAB/Simulink software as the operating system. The input data is generated within the host-PC and then transferred to the target-PC using the D/A converter to operate the electro-pneumatic regulators. To realize the co-contraction movements between the antagonistic mono- and bi-articular actuators, one regulator for each actuator was used. Then, measurements by the system (i.e. joints' angle and PMAs' pressure) provide feedback to the host-PC through the A/D converter. The rotary potentiometer (contactless Hall-IC angle sensor CP-20H series, MIDORI PRECISIONS) was used to determine the trajectory of the hip and knee joints, and then manage the PMAs' contraction parameters using a position controller. The compact pressure sensor for pneumatic actuators (PSE540-R06, SMC) was used to read the pressure level in each PMA and the input patterns of the PMAs were managed with the utilisation of a pressure controller. This system will change to the Lab-View system for the implementation of real-time control of gait rehabilitation.

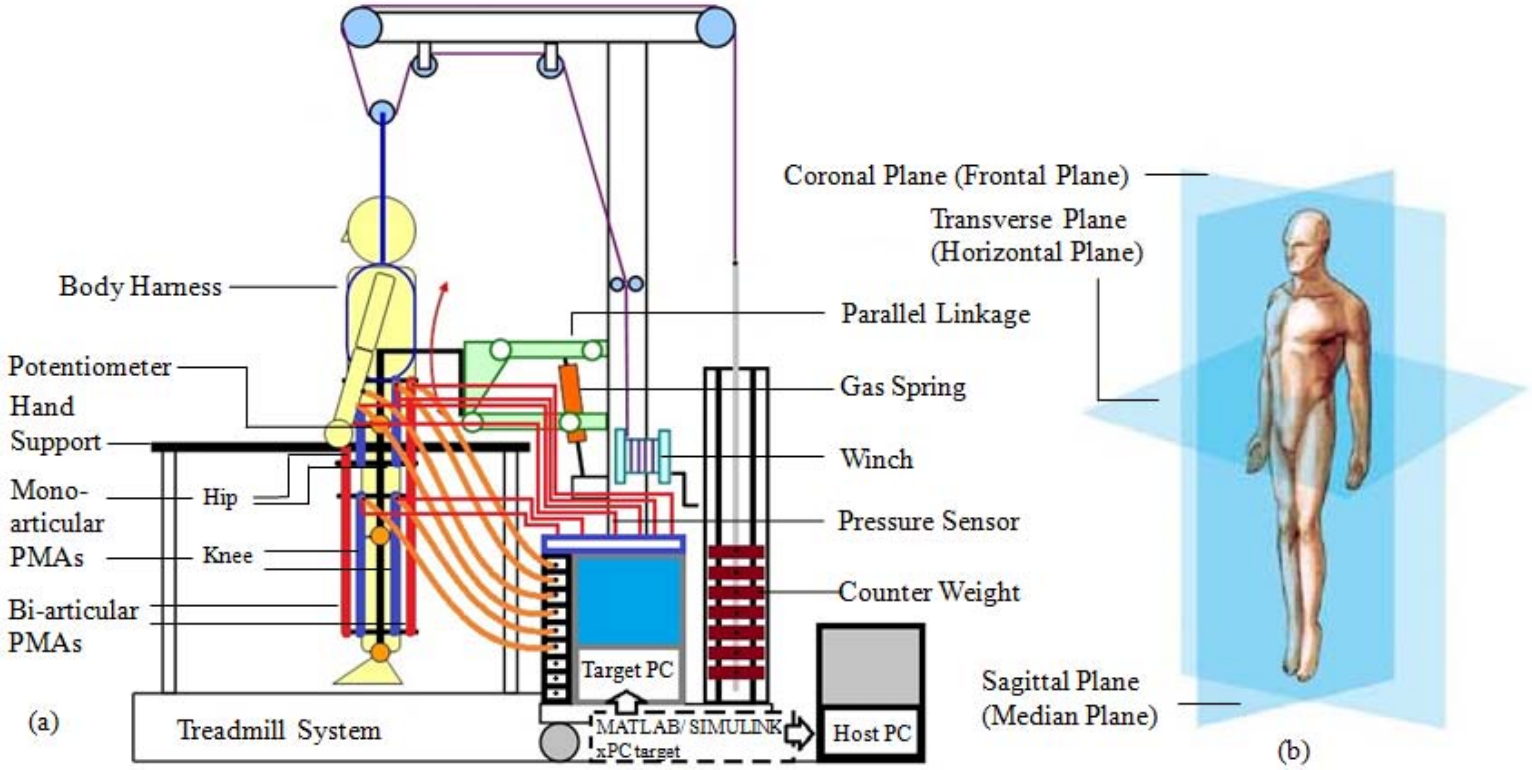

FIGURE 10 Schematic diagrams for body weight support gait training system (AIRGAIT).

3.1 Mechanical Structure of the Leg Orthosis

The structure of the leg orthosis covers the thigh at the lower end of hip joint, and shank at the lower end of the knee joint. The ankle joint orthosis was not included as the foot clearance during swing can be realized by implementing elastic straps, a passive foot lifter, or passive orthosis [9, 10, 11, and 15]. However, for the implementation of the passive orthosis, the research on the ankle orthosis of the AIRGAIT exoskeleton was conducted separately. This leg orthosis was fixed in a sagittal plane at the pelvis rotation to facilitate gait motion training for the hip and knee joints [9, 15, 17, 21 and 51]. The sagittal plane is a vertical plane which passes from ventral (front) to dorsal (rear) which dividing the body into the right and left halves as shown in Figure 10(b). Weight compensation for leg orthosis is provided for by the parallel linkage and gas spring mechanisms. This limits vertical motion during the training session [9, 15, 17, 21 and 51]. The upper and lower parts of the leg orthosis (i.e., thigh and shank) can be adjusted to agree with the height of the subject. Parallel bars were used to attach the end connectors of the mono- and bi-articular actuators (PMAs) at the anterior and posterior sides of the leg orthosis. By using the slider, these parallel bars can be adjusted accordingly to maximise the outcome of the joints angle trajectory.

3.2 Mono- and Bi-Articular Muscle Actuators

In this research study, the implementation of antagonistic mono-articular and bi-articular actuators to actuate the AIRGAIT exoskeleton's leg orthosis are based on the McKibben muscle actuator. These actuators were fabricated within our laboratory using special clamping tools which were designed to assemble the parts of the actuator (i.e., rubber tube, braided fabric, copper ring, end connector, and input connector). The implementation of these mono- and bi-articular actuators is based on the various human muscles (i.e., Gluteus Maximus, Gluteus Minimus, Gluteus Medius, Vastii Lateralis, Gastrocnemius, Rectus Femoris, and Hamstring) and antagonistically (i.e. anterior and posterior) attached to the leg orthosis. Compared to mono-articular actuators, bi-articular actuators require accurate input patterns to

simultaneously actuate the antagonistic actuators which control two of the leg orthosis joint angles [106 – 107].

Even though the bi-articular actuators may be considered as a redundancy in the actuation system, the strong force they generate will improve the maximum angle extension, provide precise movements, and ensure balance between antagonistic actuators and stiffness at the joints [91 – 95]. The position setting of the antagonistic actuators is illustrated in the Figure 11, where the position of the antagonistic mono-articular actuators both for the hip and knee joints is placed in between the antagonistic bi-articular actuators. This then provides the antagonistic bi-articular actuators with an extra length which helps in achieving much wider movement at the joints. The detail on the best setting position of the antagonistic actuators was recorded earlier and can be referred to in [109].

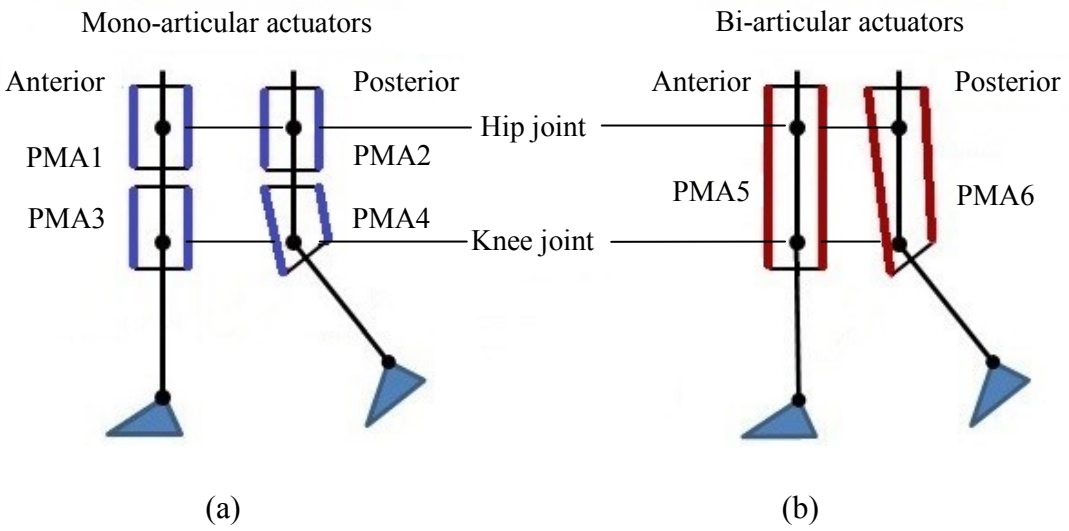

FIGURE 11 PMA positions for leg orthosis; (a) antagonistic mono-articular actuators for hip and knee joints; and (b) bi-articular actuators.

3.3 PMA Settings

The required software and hardware for this gait training system experiment is showed in the previous section (see Figure 10). There are two tests for this experiment which is with the antagonistic mono-articular PAMs alone, and with the addition of antagonistic bi-articular PAMs. Each test is performed with gait cycles of 3, 4, and 5 seconds for five cycles of the human walking motion. The hip and knee

joint angles data of the leg orthosis are collected for the performance analysis. There are two PAM position settings which are considered for the test as can be seen in Figure 12, and the best position setting is determined based on the gait cycle performance. The tests was performed using four different settings; first, mono-articular setting (PAM setting 1); second, mono-articular setting (PAM setting 2); third, mono- and bi-articular setting (PAM setting 1); and fourth, mono- and bi-articular setting (PAM setting 2). The setting that produces the most accurate joints' angle trajectory will be used as the PMAs setting for the AIRGAIT exoskeleton leg orthosis system.

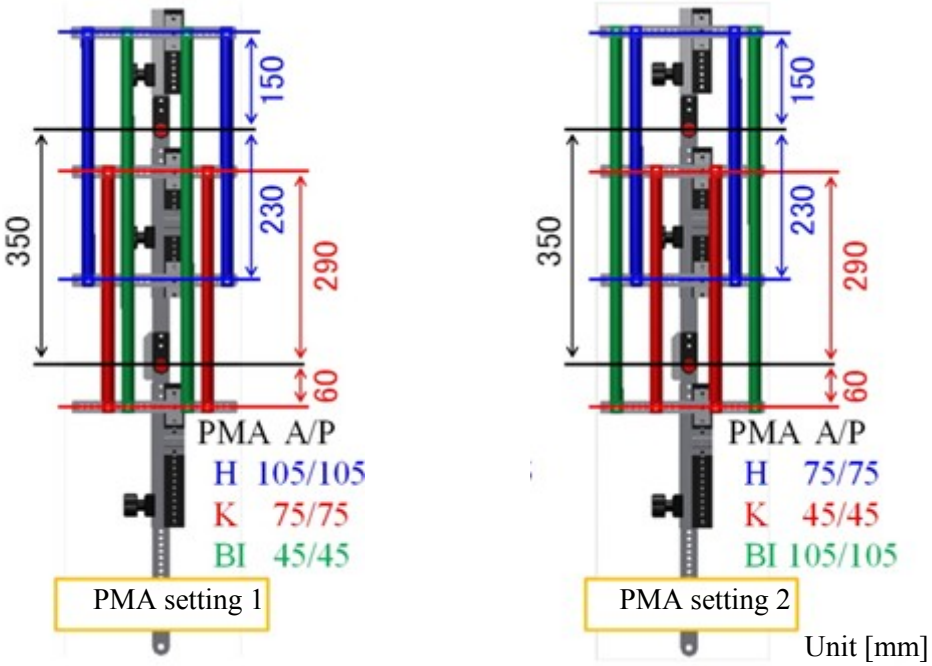

(a) (b)

FIGURE 12 PMA settings for the leg orthosis system; (a) PMA setting 1; and (b) PMA setting 2.

3.4 PMA Measurement Setup

The pneumatic muscle actuator (McKibben) with diameter of 1.0 inch is used as the sample to evaluate the PMA's contraction percentage with the input pressure as the variable. This actuator was also known as air muscle. It is manufactured by Kanda Tsushin Kogyo Co. The core is made from a rubber tube and then it is wrapped in a

tough plastic weave. It have several advantages, but most of all it is their power-weight ratio and usage in rough environments. The implementation of this air muscle could avoided the odds of accidents happened because of short circuit due to its working uniqueness. There is also no oil leakage trouble for using pneumatic drive, thus air pressure is considered safer than hydraulic pressure.

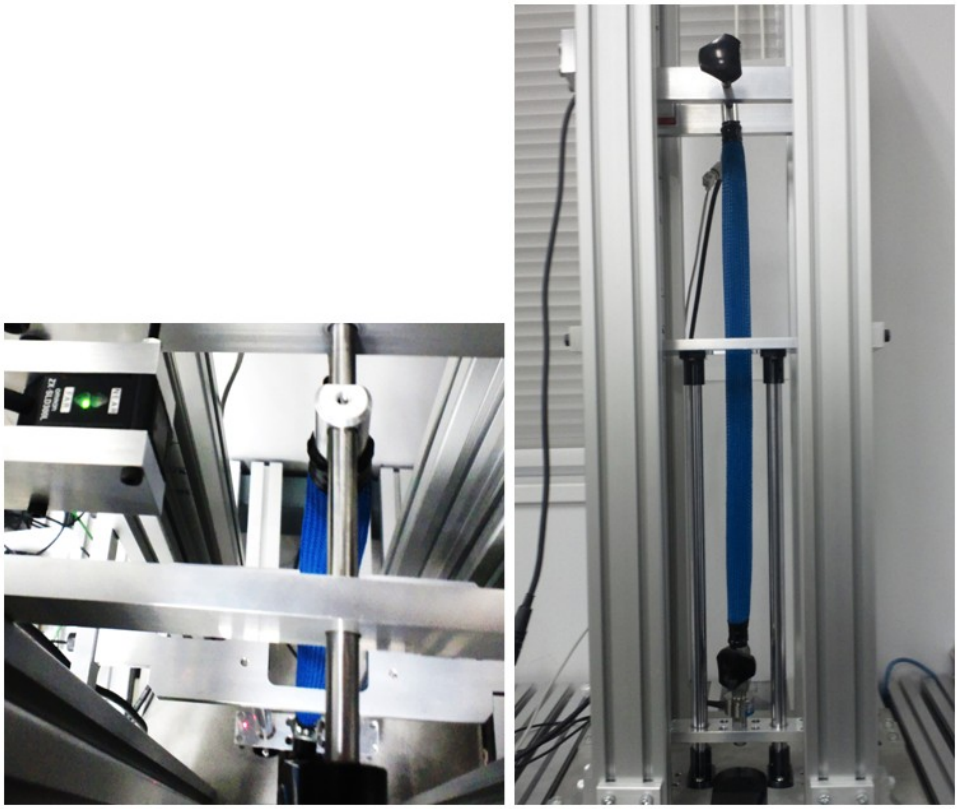

FIGURE 13 Experiment setup for measuring the characteristic of pneumatic muscle actuator.

Similar to a human muscle, the air muscle contracts when activated with maximum contraction over the nominal length is 30%. The air muscle is expanded 1.0 inch across it is pressurized, and maximum force of approximately 800 N at 0.5 MPa can be generated from this muscle actuator without load condition. The problems with the time variance, compliance, nonlinear behavior and large hysteresis made it difficult to realize precise position control with high speed. The behavior of PMA with regards to its shape, contraction and tensile force when inflated depends on the geometry of the inner elastic part and the braid at rest and on the materials used [22]. Figure 13 shows the experimental setup used for the measurements. Three samples of the PMAs with different initial lengths, L of 300, 450, and 600 [mm] are used for the measurements. These PMAs' actuator are evaluated at different pressure

inputs of 0.1, 0.2, 0.3, 0.4, and 0.5MPa for the unloading condition to determine its' contraction characteristics. Further measurement is also conducted for a pressure under 0.1MPa.

3.5 AIRGAIT's Prototype

The prototype of the AIRGAIT exoskeleton was developed in 2010 and extensively researched for improvement. However, it is yet to be commercialized. The research on gait training is progressing rapidly towards enhancement in design structures and control algorithms. A lone operator is sufficient for the running of this system. The process involves providing the subject with information on the training procedures and experiment protocols, putting on of the body harness, attaching the assisted leg orthosis to the lower limb of the subject, and finally, proceeding with the gait training or experiment. Figure 14 shows the prototype of the AIRGAIT exoskeleton.

FIGURE 14 Body weight support gait training system (AIRGAIT) prototype.

3.6 Mechanical System

The mechanical structure of the AIRGAIT exoskeleton is made up of three main parts which are (a) the BWS system which consists of the body harness and counter

weight, (b) the treadmill training which involves the treadmill and hand support, and (c) the assistive gait training which comprises the lower limb powered orthosis, spring, and parallel linkage (parallelogram). The spring and parallel linkage were fixed in a sagittal plane so that the gait motion training at hip and knee joints can be realized. The sagittal plane also compensates for the vertical weight load from the system [11, 15, 21 and 51]. The subject is provided with the BWS so that he/she will be able to maintain his/her balance during the gait training or experimental tests [20, 113 and 115]. A variable speed treadmill is also provided for the assisted leg orthosis gait training and the body weight support gait training [114 - 115].

3.7 Safety Features

To ensure the safety of the subject during the assisted gait rehabilitation and experimental tests, several safety features were included in the AIRGAIT exoskeleton design. The implementation of the PMA as the actuation system is in itself a safety feature due to its naturally compliant mechanism [22]. Also, the exclusion of the possibility of short-circuits in the actuation system during operation makes it suitable for the human-robot interaction. Moreover, as the system involves compressed air and the expansion and contraction of the braided rubber tube, it is possible to perform the orthosis in an underwater rehabilitation training scenario. Our earlier laboratory study of the robotic gait trainer (RGTW) indicated that that hydrotherapy may be particularly effective in the treatment of individuals with hip joint movement dysfunction [38]. Since the PMA characteristics are based on its model parameters such as dimension (i.e. length and contraction) and pressure, the maximum contraction of PMA will prevent the exoskeleton of the AIRGAIT leg orthosis from exceeding the limitation of the joints [112]. However, as a further precaution, a stopper was positioned at the hip and knee joints of the leg orthosis to avoid the unexpected and provide another safety feature. Additionally, the implementation of the BWS system ensures that the subject is able to maintain his/her balance and not fall over while on the treadmill [113 - 115].

CHAPTER 4

METHODOLOGY

For the experimental test setup; a Simulink block and xPC target toolbox of the MATLAB software are used for the real time control system development of the AIRGAIT exoskeleton's leg orthosis. The pneumatic muscles used for this gait training system is a McKibben type muscle actuator with initial diameter of 25mm and initial length of 300mm, 450mm and 600mm. These actuators were first analyzed using the measurement setup for determining its characteristic and form an *n*th order polynomial equation. Six electro-pneumatic regulators are used to regulate the pressure input of the antagonistic mono- and bi-articular actuators for each side of the leg orthosis. The pressure is regulated from 0MPa to 0.5MPa. Before the implementation of the real time control, preliminary studies were first carried out to achieve the best outcome of the research studies. These include the antagonistic actuators position settings, kinematics analysis, dynamics analysis, model derivation, and model simulation.

4.1 Control Model

The implementation of pneumatic muscle enabled pneumatic power to be transferred into mechanical power. This actuator will be shortened in the longitudinal direction and enlarged in the radial direction during the contraction stage when it is being inflated; when being deflated, it will turn back to its original form. The pneumatic muscle is able to employ a tensile force to an attached load during contraction stage.

This force is unidirectional, whereby, the original length of a certain designed diameter and the internal pressure will determine its value. Moreover, this actuator also inhibits nonlinear behaviours such as hysteresis, compressibility and time variance. However, in exchange, this pneumatic muscle also has an inherently compliant attribute which is suitable for a human-robotics system. This type of actuator is similar to the human muscle principle; shorter muscle length produces smaller contracting force and vice versa. Furthermore, it is comparable to electric actuators due to the direct coupling to the load, structural optimization and power/weight ratio. In addition to the abovementioned attributes, there exist two main weaknesses that limit the application of pneumatic muscle. The first weakness is the nonlinear behaviour of pressure build-up, and the second weakness is the hysteresis effect due to its geometric structure. These drawbacks cause complexity when scheming high-performance control systems. Therefore, this research is dedicated to solve these problems, using a simple paradigm and control strategy for handling the sudden increase in pressure and hysteresis behaviour of the PMA. Based on the proposed empirical-based static force mathematical model, which consist of a correction factor caused by the effect of the end caps, it showed an inconsistency of high contracting ratios derived by the famous researcher Tondu et al., [25]. The extreme difficulty in constructing an accurate mathematical model was established by the fact that nearly all of the present models proposed were approximations. This model was later modified through various methods, used by other researches, to further improve the mathematical model [35 - 42].

$$F(P,\varepsilon) = (\pi {r_0}^2)P(a(1-k\varepsilon)^2 - b) \quad \dots(1)$$

$$a = \frac{3}{tan^2(\alpha_0)}, \qquad b = \frac{1}{sin^2(\alpha_0)}$$

There are in literature a lot of control models, they can be divided into two main groups; position and couple controls. The last one requires a completely description of the system and, if it has a high number of degree of freedom (DOF), the formulation of the couple joints expression become difficult. For this reason, many of the controllers used in industry are based on empirical approach as the fuzzy or the PID controls. It could be concluded that there are three main parameters that affect the pneumatic muscle dynamics and nonlinearity such as force (*F*), contraction

(ε), and pressure (P). The main idea of the proposed model is based on the control of the position of the joints by controlling the contraction and the pressure of the antagonistic pneumatic muscles. The stiffness of the system is determined based on magnitude of the muscle activation levels of the antagonistic actuators. The model is composed of a part that describes the geometric configuration between the pneumatic muscles and the joints known as the co-contraction model. This co-contraction model represents or generates contraction patterns for the antagonistic actuators. Furthermore, muscle activation levels are introduced into the derived co-contraction model to increase the stiffness and stability of the system. In addition, it also transformed the derived model into dynamic model. The second part is to develop a control strategy to represent or handle the pressure build up and hysteresis due to the dynamic behavior. Thus, the PMA model control strategy is introduced.

4.2 Muscle Activation Levels (i.e., α and β)

In order to implement the proposed controller scheme, the co-contraction model was developed. The anterior and posterior muscle activation levels (i.e., α and β) are introduced to manipulate the gain of the antagonistic mono- and bi-articular actuator contractions, where the muscle activation level is ranged from ($0 < \alpha \leq \alpha_{max}$ and $0 < \beta \leq \beta_{max}$). By introducing these muscle activation levels, the contraction of the pneumatic muscle was set as a control variable. Thus, enable the static model of the pneumatic muscle was able to be transformed into dynamic model. This is because; all three variables (i.e., pressure, force and contraction) were been taking into consideration during the control system. Where, the pressure is the desired variable, contraction is the control variable, and the change in force (i.e., inertia, hysteresis, etc) will cause the sudden change in pressure and provide the deviation of hip and knee joints. These deviations will then be used to manipulate the control variable gains (i.e., α and β). Table 2 shows the trajectory data of the co-contraction model. Based on these data, saturation value of the muscle activation levels of the antagonistic mono- and bi-articular actuators were determined as shown using the equations (2) - (7). These saturation values will be used as a limitation on the muscle activation levels to prevent a failure during the control of the leg orthosis. The controlled values of the muscle activation levels were shown in Figure 38.

$$\alpha_{h(max)} = 0.3\left[\frac{l_{o_{hip}}}{r.|\theta_{ha}(t)|_{max}}\right] \quad \ldots(2)$$

$$\beta_{h(max)} = 0.3\left[\frac{l_{o_{hip}}}{r.|\theta_{hp}(t)|_{max}}\right] \quad \ldots(3)$$

$$0 < \alpha_h, \beta_h \leq 2.9466$$

$$\alpha_{k(max)} = 0.3\left[\frac{l_{o_{knee}}}{r.|\theta_{ka}(t)|_{max}}\right] \quad \ldots(4)$$

$$\beta_{k(max)} = 0.3\left[\frac{l_{o_{knee}}}{r.|\theta_{kp}(t)|_{max}}\right] \quad \ldots(5)$$

$$0 < \alpha_k, \beta_k \leq 2.4555$$

$$\alpha_{bi(max)} = 0.3\left[\frac{l_{o_{bi}}}{r.|(\theta_h(t) + \theta_k(t))_a|_{max}}\right] \quad \ldots(6)$$

$$\beta_{bi(max)} = 0.3\left[\frac{l_{o_{bi}}}{r.|(\theta_h(t) + \theta_k(t))_p|_{max}}\right] \quad \ldots(7)$$

$$0 < \alpha_{bi}, \beta_{bi} \leq 2.7505$$

TABLE 2 Trajectory data of the co-contraction model.

Actuators	Muscles	Reference joints		Positional data		Length ~ lo	Radius ~ r
		Variables	Range	Variables	$\lvert\theta_{h/k}(t)\rvert_{max}$		
Mono-articular actuator (hip joint)	Anterior	θ_h	$-12 \leq \theta_h \leq 23$	$\theta_{ha}(t)$	35°	0.30m	0.05m
	Posterior	θ_h	$-12 \leq \theta_h \leq 23$	$\theta_{hp}(t)$	35°	0.30m	0.05m
Mono-articular actuator (knee joint)	Anterior	θ_k	$0 \leq \theta_k \leq 63$	$\theta_{ka}(t)$	63°	0.45m	0.05m
	Posterior	θ_k	$0 \leq \theta_h \leq 63$	$\theta_{kp}(t)$	63°	0.45m	0.05m
Bi-articular actuators	Anterior	$\theta_h + \theta_k$	$-55 \leq \theta h + \theta k \leq 20$	$(\theta_h + \theta_k)_a(t)$	75°	0.60m	0.05m
	Posterior	$\theta_h + \theta_k$	$-55 \leq \theta h + \theta k \leq 20$	$(\theta_h + \theta_k)_p(t)$	75°	0.60m	0.05m

4.3 PID Gains

The control strategy was to execute the co-contraction model which implemented position-pressure controller scheme. The PID based-position controller was used to tune the co-contraction model parameters (activation levels) while the PID based-pressure controller was used to control the input patterns of the antagonistic mono- and bi-articular actuators. The derived co-contraction model provides the input patterns for the mono- and bi-articular actuators and simultaneously actuates the antagonistic actuators co-contractively, while the PMA model was determined in order to consider the characteristics of the PMA that were to be introduced into the controller design. This dynamic model was evaluated in an experimental study and represented in an equation. The proposed controller scheme was specifically designed for simplifying the control of antagonistic bi-articular actuators so as to enhance the stiffness at both hip and knee joints. It is an arduous task to construct the plant model of leg orthosis (with antagonistic mono- and bi-articular PMAs) for the implementation of the Stochastic Optimization method to determine the control parameters of the design controller. As such, the heuristic method was first implemented to determine the PID gains of the control system. Table 3 shows the PID parameters and muscle activation levels of the previous system (MATLAB Simulink and xPC target). Table 4 shows the PID parameters and muscle activation levels of the new system (Lab-View).

4.4 Procedures

The exoskeleton of the AIRGAIT leg orthosis is first adjusted to correspond with the position of the hip and knee joints of the subject to obtain precise data during the experimental tests. Then, the controller parameters for the antagonistic mono-articular actuators (i.e., hip and knee joints) are tuned until good joint trajectory is attained. This is followed by the tuning of antagonistic bi-articular actuator controller parameters. The controls for the leg orthosis WO/S is then set for different Gait Cycle (GC) speeds and data for the trajectory of the hip and knee joints are gathered. The steps taken for testing W/S are (a) the subject is provided with sufficient information regarding the tests and procedures, (b) the subject is fitted with a body

harness and a passive foot lifter was secured at the ankle joint before the leg orthosis was attached to the subject, and (c) the subject is provided with the full BWS before the controls of leg orthosis were performed for different GC speeds including that of an average human. Table 6 shows the comparison of existed lower limb gait rehabilitation orthosis system such as LOKOMAT, LOPES, ALEX, Robotic Orthosis for Gait Rehabilitation, and our research AIRGAIT in terms of; (1) type of actuator uses as the actuation system; (2) number of joint manipulators; (3) plane of actuated DOFs; and (4) GC operating speed.

TABLE 3 PID parameters and muscle activation levels of the previous system using Heuristic method.

Actuators	Muscles	PID gains						Muscle activation levels	
		Position control			Pressure control				
		Kp	Ki	Kd	Kp	Ki	Kd		
Mono-articular actuators (hip joint)	Anterior	0.1	0.02	0	0.25	0	0	α	0.9
	Posterior	0.1	0.02	0	0.25	0	0	β	1
Mono-articular actuators (Knee joint)	Anterior	0.03	0.02	0	0.15	0	0	α	0.6
	Posterior	0.03	0.02	0	0.25	0	0	β	0.8
Bi-articular actuators	Anterior	0.03	0.02	0	0.2	0	0	α	0.6
	Posterior	0.03	0.02	0	0.3	0	0	β	0.9

TABLE 4 PID parameters and muscle activation levels of the new system using Heuristic method.

Actuators	Muscles	PID gains						Muscle activation levels	
		Position			Pressure				
		Kp	Ki	Kd	Kp	Ki	Kd		
Mono-articular actuators (hip joint)	Anterior	0.011	0.002	0	0.12	0.02	0	α	1
	Posterior	0.01	0.002	0	0.1	0.02	0	β	1
Mono-articular actuators (Knee joint)	Anterior	0.011	0.002	0	0.14	0.02	0	α	0.8
	Posterior	0.02	0.002	0	0.22	0.02	0	β	1
Bi-articular actuators	Anterior	0.014	0.002	0	0.18	0.02	0	α	0.8
	Posterior	0.025	0.002	0	0.22	0.02	0	β	0.8

TABLE 5 PID parameters and muscle activation levels of the new system using Ziegler-Nichols method (P and PI controllers).

(a)

Actuators	Muscles	PID gains						Muscle activation levels	
		Position			Pressure				
		Kp	Ki	Kd	Kp	Ki	Kd		
Mono-articular actuators (hip joint)	Anterior	0.012	0	0	0.15	0	0	α	1
	Posterior	0.01	0	0	0.1	0	0	β	1
Mono-articular actuators (Knee joint)	Anterior	0.012	0	0	0.15	0	0	α	0.8
	Posterior	0.02	0	0	0.25	0	0	β	1
Bi-articular actuators	Anterior	0.015	0	0	0.2	0	0	α	0.8
	Posterior	0.025	0	0	0.25	0	0	β	0.8

(b)

Actuators	Muscles	PID gains						Muscle activation levels	
		Position			Pressure				
		Kp	Ki	Kd	Kp	Ki	Kd		
Mono-articular actuators (hip joint)	Anterior	0.0108	0.0026	0	0.15	0	0	α	1
	Posterior	0.009	0.0022	0	0.1	0	0	β	1
Mono-articular actuators (Knee joint)	Anterior	0.0108	0.0026	0	0.15	0	0	α	0.8
	Posterior	0.018	0.0043	0	0.25	0	0	β	1
Bi-articular actuators	Anterior	0.0135	0.0032	0	0.2	0	0	α	0.8
	Posterior	0.0225	0.0054	0	0.25	0	0	β	0.8

(c)

Actuators	Muscles	PID gains						Muscle activation levels	
		Position			Pressure				
		Kp	Ki	Kd	Kp	Ki	Kd		
Mono-articular actuators (hip joint)	Anterior	0.0108	0.0026	0	0.135	0.0324	0	α	1
	Posterior	0.009	0.0022	0	0.09	0.0216	0	β	1
Mono-articular actuators (Knee joint)	Anterior	0.0108	0.0026	0	0.135	0.0324	0	α	0.8
	Posterior	0.018	0.0043	0	0.225	0.054	0	β	1
Bi-articular actuators	Anterior	0.0135	0.0032	0	0.18	0.0432	0	α	0.8
	Posterior	0.0225	0.0054	0	0.225	0.054	0	β	0.8

TABLE 6 Existed lower limb gait rehabilitation orthosis system comparison.

Comparison between existed lower limb gait rehabilitation orthosis system					
Orthosis system	Type of actuator	Number of joints	Actuated DOFs	Operating speed	References
LOKOMAT	DC motors	Hip and knee joints, passive foot lifter was applied at ankle Joint	Sagittal plane	0.56m/s	[9-11]
Lower Extremity Powered Exoskeleton (LOPES)	Bowden cable series elastic actuators (SEA) and servomotors	Hip and knee joints, elastic straps was applied at ankle joint	Sagittal plane	0.75m/s	[15, 16]
Active Leg Exoskeleton (ALEX)	Linear actuators	Hip, knee, and ankle joints	Sagittal plane	0.40m/s up to 0.85m/s	[17, 18]
Robotic Orthosis for Gait Rehabilitation	Pneumatic muscle actuators (mono-articular actuators)	Hip, and knee joints, foot lifter was used at ankle joint	Sagittal plane	0.60m/s	[51, 52]
Body Weight Support Gait Training System (AIRGAIT)	Pneumatic muscle actuators (mono- and bi-articular actuators)	Hip, and knee joints, foot lifter was used at ankle joint	Sagittal plane	0.35m/s, 0.47m/s, 0.70m/s), and 1.40m/s	

4.5 Experimental Tests

Three tests were conducted for the experimental study. These tests were performed on one side of the exoskeleton of the AIRGAIT leg orthosis. The first test was conducted using two sets of antagonistic mono-articular actuators (i.e., hip and knee joints) tested WO/S; the second with the addition of one set of antagonistic bi-articular actuators tested WO/S; and the third with the addition of one set of antagonistic bi-articular actuators tested W/S. Full BWS was implemented in this study during the test W/S as the load supported by the orthosis was at its maximum capacity. This assessment will optimize the control system strategy so that it operates at its maximum capability.

The options for the subject were not really critical as the focus of the research is on the design controller. As such, the subject chosen was young, healthy, and not bearing any neurological disorder. With this, we were able to instruct the subject to be passive during the experimental tests. To achieve the natural posture of human walking gait motion during training, the passive foot lifter was used to ensure enough foot clearance was achieved during the swing phase [1, 4]. The controls of the leg orthosis WO/S and W/S are displayed in Figures 15 and 16. For the first and second tests (WO/S), GC speeds of 4 seconds, 3 seconds, 2 seconds, and 1 second were evaluated for the design controller scheme. Four GC speeds were also evaluated for the third test (W/S). Five trials were performed for each GC speed, and each trial consisted of five cycles including the initial cycle position. The total GCs performed for each GC speed was around 25 cycles. The average GC was then calculated and represented in a graph.

Based on these data, five comparative evaluations were analysed to determine the design controller scheme and strategy performance. These were (a) between the simulated co-contraction model control scheme, and derived co-contraction model control scheme test WO/S, (b) between the mono-articular actuators alone (i.e., hip and knee joints), and with bi-articular actuators, (c) between the position (P) controller based on co-contraction model control scheme, and the position-pressure (PP) controllers based on co-contraction model control scheme tested WO/S, (d) between the P controller based on co-contraction model control scheme, and the PP controllers based on co-contraction model control scheme tested W/S, (e) between the conventional PID based control schemes, and co-contraction model based control

schemes tested WO/S. The design controller scheme and strategy performance were evaluated based on the GC, movement of hip and knee joint trajectory, maximum joint angle extension, inertia, gravitational effect, and time shift.

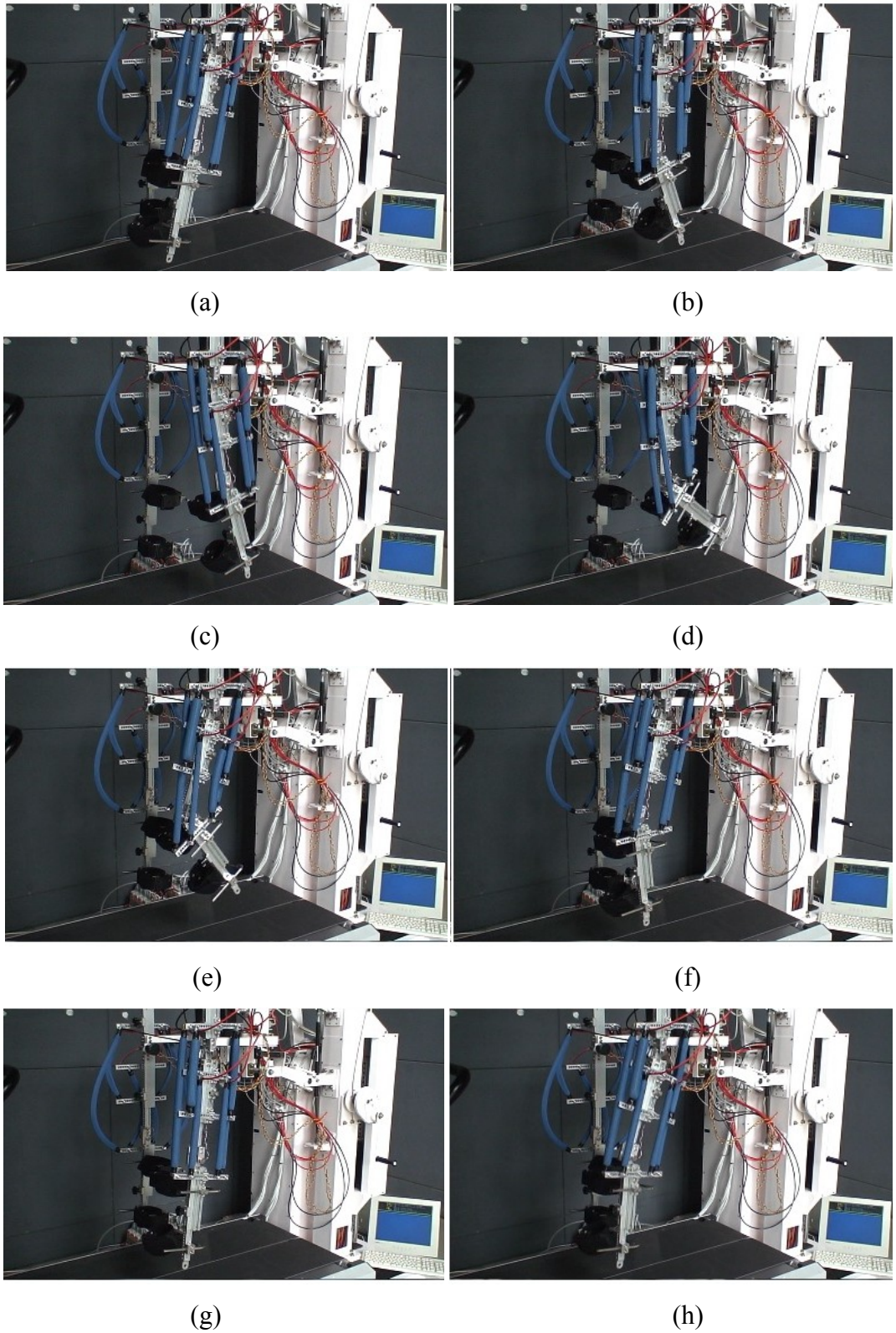

(a) (b) (c) (d) (e) (f) (g) (h)

FIGURE 15 Control of leg orthosis without a subject (WO/S).

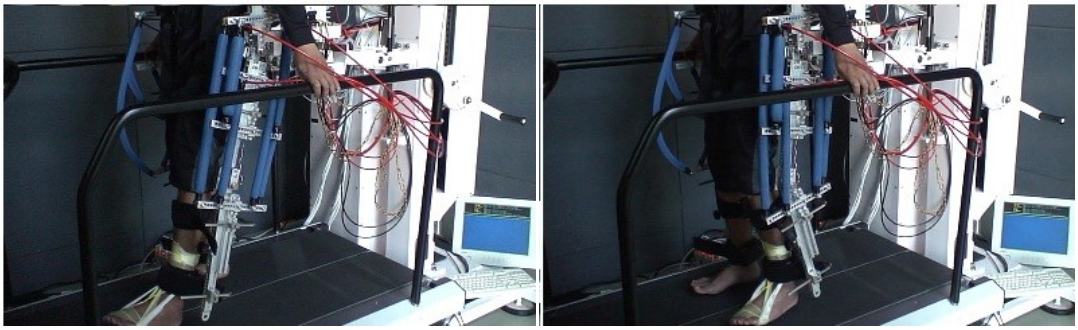

(a) (b)

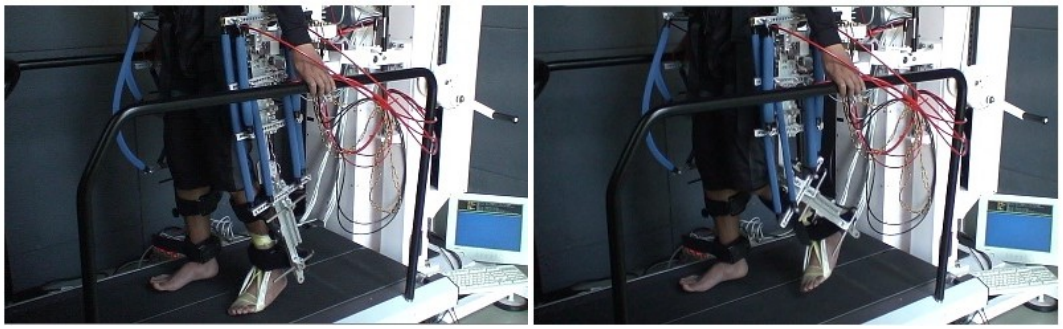

(c) (d)

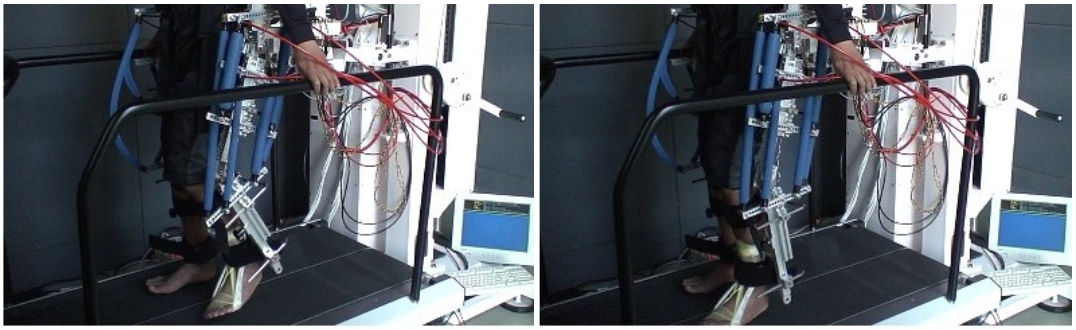

(e) (f)

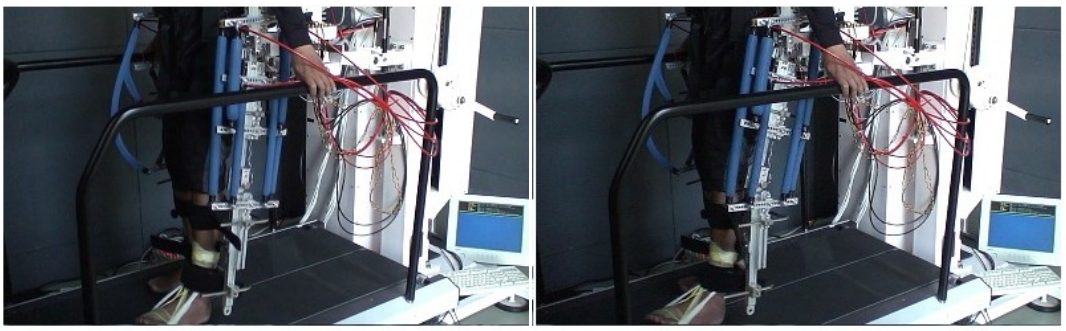

(g) (h)

FIGURE 16 Control of leg orthosis with a subject (W/S).

4.6 Flow of the Research

In this section, the methodology is divided into several parts based on the assessments tests. Part (1) is to derive a contraction model to determine the contraction patterns of antagonistic mono- and bi-articular actuators from positional data. Then, the model is implemented into the control system using the mathematical formulation. Part (2) is carried out to determine the reliability of the derived control scheme and strategy using the simulation analysis. The plant model for the AIRGAIT exoskeleton's leg orthosis was derived using the pendulum model of the two link leg manipulators model. The particle swarm optimization (PSO) method was used to determine the functionality of control parameters (i.e., α, and β muscle activation levels) for each antagonistic actuator which was coded using MATLAB language and Simulink block.

Part (3) is performed to determine the best arrangement PMAs settings for the AIRGAIT exoskeleton's leg orthosis. Two tests were performed in this experiment; first, with the antagonistic mono-articular PAMs alone; and second, is with the addition of antagonistic bi-articular PAMs. These tests are evaluated at different gait cycles of 5, 4, and 3 seconds for five cycles of the human's natural gait trajectory. Moreover, two position settings of the PAMs are performed for both tests as can be seen in Figure 12. In total, we performed four tests for the control system; first, mono-articular setting (PAM setting 1); second, mono-articular setting (PAM setting 2); third, mono- and bi-articular setting (PAM setting 1); and fourth, mono- and bi-articular setting (PAM setting 2). The control system is evaluated using the percentage [%] of gait cycle, joint excursions, and time shift.

Part (4) is carried out to put into practice the proposed co-contraction model control scheme and controls the AIRGAIT exoskeleton's leg orthosis system. Two models will be tested; the first is using the simulated co-contraction model; and the second is using the derived co-contraction model. Both co-contraction model control schemes are tested at different gait cycle speed of 5, 4, and 3 seconds for five cycles including the initial position cycle. The joint excursions of the leg orthosis is collected for a control system tested WO/S using both antagonistic mono- and bi-articular actuators. Results are evaluated based on the maximum muscle moment (flexion and extension), output pattern, time shift, gait cycle, coefficient of determination (r^2), inertia, and effective work.

Part (5) is to determine the limitation of the leg orthosis controls when implementing antagonistic mono-articular actuators (i.e., hip and knee joints) alone, and when implementing both mono- and bi-articular actuators. The tests are performed W/S to increase inertia effect during the control system and evaluated at different GC speed of 5, 4, 3, 2, and 1 seconds. The performance of both tests is compared based on maximum operating GC speed the antagonistic mono-articular actuators alone and with addition of bi-articular actuators are able to withstand. The evaluation also includes the accuracy of the leg orthosis joint excursions in terms of angle deviation and time shift.

Part (6) is performed to implement the contraction model control scheme and strategy when tested WO/S. There are two tests for the control system using antagonistic mono-articular actuators alone and with the addition of antagonistic bi-articular actuators. The controller is tested for different gait cycle times of 5, 4, 3, 2, and 1 second for five cycles including the initial position cycle. The contraction model control scheme was performed on the AIRGAIT exoskeleton's leg orthosis and from that the performance is obtained. The results are evaluated based on maximum flexion/extension of joints (i.e., hip and knee), output pattern, gait cycle, time shift, inertia, effective work, and the coefficient of determination (r^2).

Part (7) is conducted to execute the contraction model control scheme and strategy with the full body weight tests W/S. There are two tests for the control system using antagonistic mono-articular actuators alone and with the addition of antagonistic bi-articular actuators. The controller is tested for different gait cycle times of 5, 4, 3, 2, and 1 second for five cycles including the initial position cycle. The contraction model control scheme was performed on a healthy subject with full body weight support (BWS) during robot assisted walk and from that the performance is obtained. The results are evaluated based on maximum flexion/extension of joints (i.e., hip and knee), output pattern, gait cycle, time shift, inertia, effective work, and the coefficient of determination (r^2).

Part (8) is carried out to improve the previous system of the AITGAIT exoskeleton's leg orthosis by replacing the MATLAB Simulink and xPC-Target system into the Lab-View system with Rio module. In the previous system, we were only able to read and manipulate a discrete data which limiting the choice of the control system that can be used. However, by introducing this new system, much advanced control system that read continuous data could be implemented. In

addition, the design improvement of the leg orthosis was also been instigated to increase the accuracy of the joints of the orthosis. Furthermore, the implementation of couple control model using computed torque method was proposed to improve the control system of the AIRGAIT exoskeleton's leg orthosis. Two tests were performed; the first is without a subject (WO/S), and the second is with a subject (W/S). The tests were evaluated at different frequencies of 0.05 Hz, 0.1 Hz, 0.5 Hz, and 1 Hz. We can say that at the frequency of 1 Hz corresponds a walking speed of 1.40 m/s that is the speed of a healthy person [133]. Instead for a person that needs of rehabilitation we can consider a speed less or equal to 0.7 m/s at which corresponds a frequency of 0.5 Hz.

Part (9) is performed to determine the comparison of the proposed co-contraction model control scheme with the actual human muscles contraction patterns at the leg joints. This is because, it is important to accurately activate human antagonistic muscles (i.e., agonist and antagonist) during the rehabilitation training with the assisted leg orthosis. One of the purposes of this study was to develop a leg orthosis system which is similar to the human muscles. Therefore, we proposed to use both antagonistic mono- and bi-articular actuators to drive the leg orthosis. Three tests were conducted to determine the EMG signals of the muscles (i.e., RF, BF, MGAS, SOL, and TA); the first is normal walking on the treadmill without orthosis, the second is normal walking on the treadmill with attached orthosis, and the third is normal walking on the treadmill with assisted orthosis. The results are evaluated based on the co-contraction activation of the EMG signals of the human muscles.

Part (10) is conducted to improve the control system of the AIRGAIT exoskeleton's leg orthosis by introducing the couple control model using computed torque method. In the previous control system, it is realized that the inertia of the assisted leg orthosis was also affecting the performance of the control system especially when tested with a subject. Therefore, in this section we are trying to implement the couple control model into the system. At first, only the couple control model was tested to determine it reliability in handling the inertia of the leg orthosis. Then in the future research, we are going to introduce a combination of the co-contraction model control scheme and couple control model to control the leg orthosis. The test without a subject was performed at different frequencies of 0.05 Hz, 0.1 Hz, 0.5 Hz and 1 Hz. However, the test with a subject was performed at high frequencies of 0.5 Hz and 1 Hz.

CHAPTER 5

CONTROL SYSTEM

This section shows how xPC Target facilitates embedded control system design by turning general-purpose personal computer (PC) hardware into a rapid prototyping platform. The PC-based platform used is the Math-Works xPC TargetBox. xPC Target is integrated in Simulink, enabling the use of Simulink as a graphical front-end with Math-Works tools for parameter estimation, response optimization, and linearization throughout the design cycle. A control system is an implemented strategy used to cause a physical system, or plant, to behave in a desired manner. There are two types of control strategies; the first is closed-loop control uses feedback measurements to correct error between the plant output and a reference input, i.e., the desired behavior; and the second is reactive control is event driven and interacts with the plant via state transition behavior. As the feedback control strategy increases in complexity, it becomes more difficult to apply analog components for its implementation. Dynamics in an analog feedback control loop always interact, making it more difficult to match desired controller characteristics. For example, an analog system always has a limited filter quality factor, Q, due to parasitic impedances and other limitations. Conversely, it is easy to create an extremely sharp digital filter with very large Q.

Another complication is that analog integrators are always limited by capacitor leakage, yet digital integrators can be nearly perfect. A processor-based approach usually works best for reactive control as well. In modern control systems, the control strategy is thus typically implemented in software. A microprocessor determines the input to manipulate the plant and this requires facilities to apply this

input to the physical world. In addition, the control strategy typically relies on measured values of the plant behavior that have to be made available to the computing resources. The immersion of computing power into the physical world is one characteristic of an embedded control system. The other characteristic is that the software that implements the control strategy is stored in read-only memory. Thus, unlike a general-purpose computer, an embedded control system is not independently programmable. In other words, an embedded control system is expected to function without user intervention, although it may require user interaction.

The general configuration of an embedded control system is shown in Figure 17. Because the controller operates in the low-power electronics domain and the plant operates in high-power hydraulics, mechanics, thermal, and other physical domains, transducers are needed to convert between controller and plant. These transducers are used either by actuators, to drive the plant with controller-computed values, or by sensors, to provide measurements to the low-power electronics domain. In embedded systems, the low-power computational electronics of the controller has to interact with high-power physical domains of many types.

5.1 Drivers

A key step in transforming software into a real-time system is the requirement to have device drivers that communicate between the I/O devices on the target PC and the application code running on this target. These drivers thus enable interaction between the real-time application and the real physical system. The device driver contains the code that runs on the target hardware for interfacing to I/O devices such as (A/D) converters, encoders, digital signals, and communication ports.

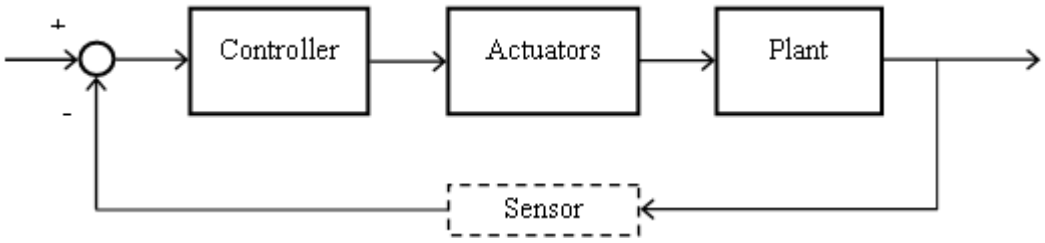

FIGURE 17 Embedded control systems

5.2 xPC Target

A rapid prototyping platform needs to be more powerful and flexible than the eventual target processor. For example, if the software has not yet been optimized, it will not run as efficiently. To achieve real-time behavior, a more powerful microprocessor is necessary. Furthermore, additional measurements may need to be made to obtain insight in the functioning of the controller. The necessary flexibility, computing power, and memory capacity may make rapid prototyping platforms much more expensive than the hardware that is ultimately used in production. Because of the fabrication cost, rapid prototyping platforms are often used for more than one project. It is an approach that is supported by the inherent flexible nature of such platforms.

This xPC Target provides the means to turn general-purpose PC hardware into a prototyping environment that can be used for signal acquisition, rapid prototyping, and hardware-in-the-loop simulation. The xPC Target kernel provides a real-time operating system that supports both interrupt handling and polling and is tuned to provide maximum performance with minimal overhead. High-performance hardware allows sample rates that approach 100 kHz. xPC Target also supports the modification of parameters in the Simulink blocks while the application is running. The parameter changes are immediately reflected in the real-time application. The tight integration between MATLAB, Simulink, Real-Time Workshop, and xPC Target makes it possible to write a script that incrementally changes a parameter and monitors a signal output. The script can then be run on the host PC to optimize the value of the parameter.

5.3 xPC Target Configuration

The xPC Target host-target arrangement is shown schematically in Figure 18. On the host PC (which runs MATLAB, Simulink, Real-Time Workshop, and xPC Target), xPC Target works with the code generated from the Simulink application and a C compiler to build the real-time target application. The target application can run in real time on a target PC once it is downloaded to the target PC from the host PC. The target hardware is booted from a real-time kernel in xPC Target. However, the xPC

Target kernel needs the PC basic input/output system (BIOS) because when the target PC boots and the BIOS is loaded, the BIOS prepares the target PC environment for running the kernel and then starts the kernel.

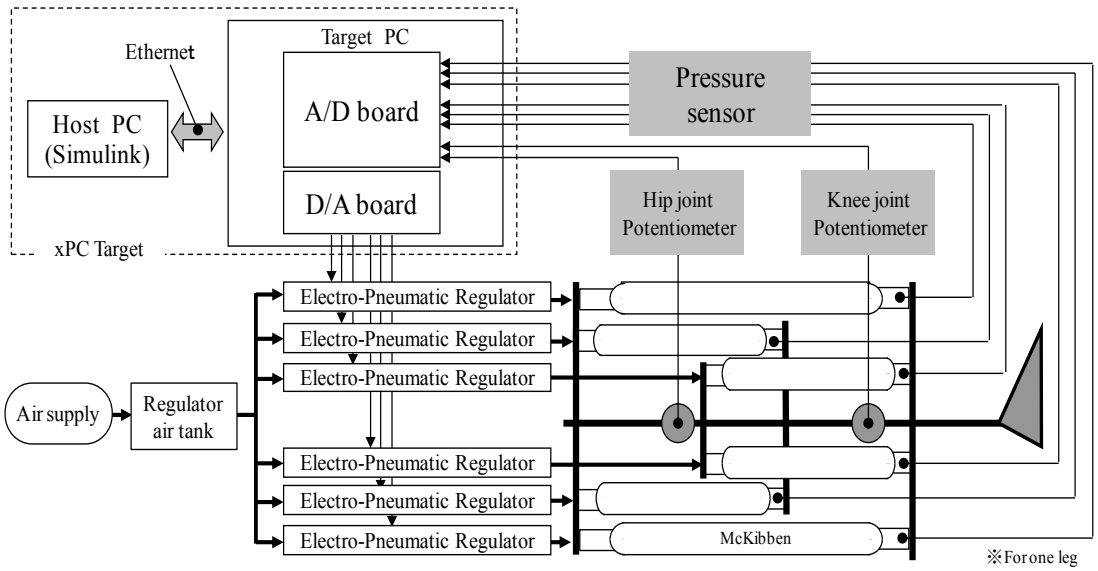

FIGURE 18 xPC Target systems for the AIRGAIT exoskeleton.

The kernel initiates the host-target communication, activates the application loader, and waits for the target application to be downloaded from the host PC. The host-target communication can occur through either serial or TCP/IP communication protocols. Once the target application has been downloaded to the target PC, it can be controlled and modified from the host PC. It is frequently necessary to interact with the real-time application to either observe signals or change parameters of the control system.

5.4 Simulink Simulation

A typical Simulink block consists of inputs, states, and outputs, where the outputs are a function of the sample time, the inputs, and the block states. During simulation, the model execution follows a series of steps. The first step is the initialization of the model, where Simulink incorporates library blocks into the model; propagates signal widths, data types, and sample times; evaluates block parameters; determines block execution order; and allocates memory. Simulink then enters a simulation loop. Each

pass through the loop is referred to as a simulation step. During each simulation step, Simulink executes each of the model blocks in the order determined during initialization. For each block, Simulink invokes functions that compute the values of the block states, the derivatives, and the outputs for the current sample time. The simulation is then incremented to the next step. This process continues until the simulation is stopped.

Using Simulink as a graphical front end to the embedded software combined with automatic code generation technology makes it easy to modify the controller. It is easier to change the model than to change the code (code changes have a higher probability of introducing new defects). The controller can be analyzed in terms of the Simulink model, which is more intuitive than the embedded software code, and sophisticated data analysis tools are immediately available to study and tune the controller performance.

5.5 Feedback Control Model (Co-Contraction Control Scheme)

5.5.1 Controller Algorithm

At first, the antagonistic mono- and bi-articular actuators' contraction of the lower limb orthosis is determined using MATLAB simulation of the coordinates system. The control system which estimates the antagonistic PMA length (contraction) from the hip and knee joints' angle is constructed. Based on the antagonistic actuators' contraction formulation, the pressure input pattern for each actuator was determined. In order to reduce the moment of inertia, the orthosis was set symmetrically in the longitudinal direction. The PMA's location in the coordinate system is obtained from the model simulation which was programmed using the MATLAB. This model is actuated based on the reference input angle of hip and knee joints. The changes in length of the PMAs from the simulation provided the co-contraction data for the mono- and bi-articular actuators. These data is obtained using the coordinate's equation as can be seen in Figure 22 (d). By using this equation, the PMAs' contraction data were converted into input pressures for each of antagonistic mono- and bi-articular actuators. Based on this method, the inputs for manipulating the lower extremity orthosis were determined. In addition, PID feedback controller is

used for correcting the required input pressure for each actuator as can be seen in schematic diagram in Figure 19.

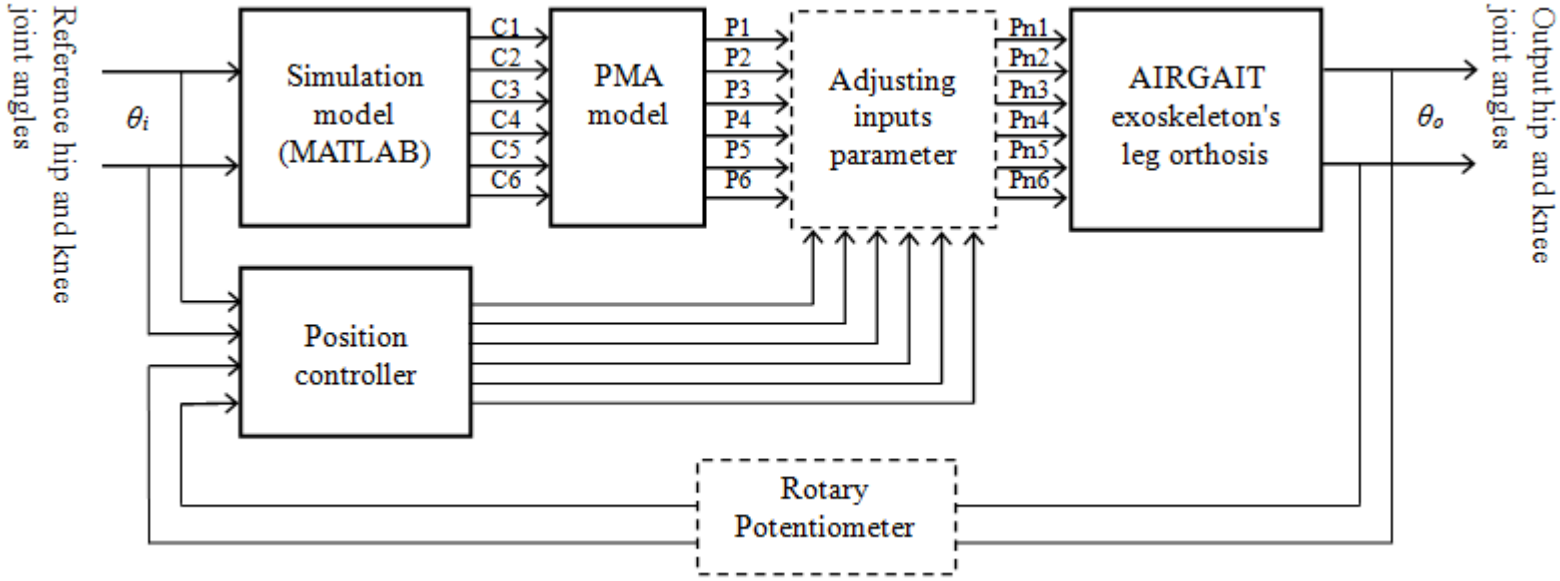

FIGURE 19 Schematic diagram of the exoskeleton of the AIRGAIT leg orthosis controller schemes using MATLAB simulation of co-contraction model based P controller. Where (*C1 – C6*) are the contraction input patterns, (*P1 – P6*) are the pressure input patterns, (*Pn1 – Pn6*) are the corrected pressure input patterns.

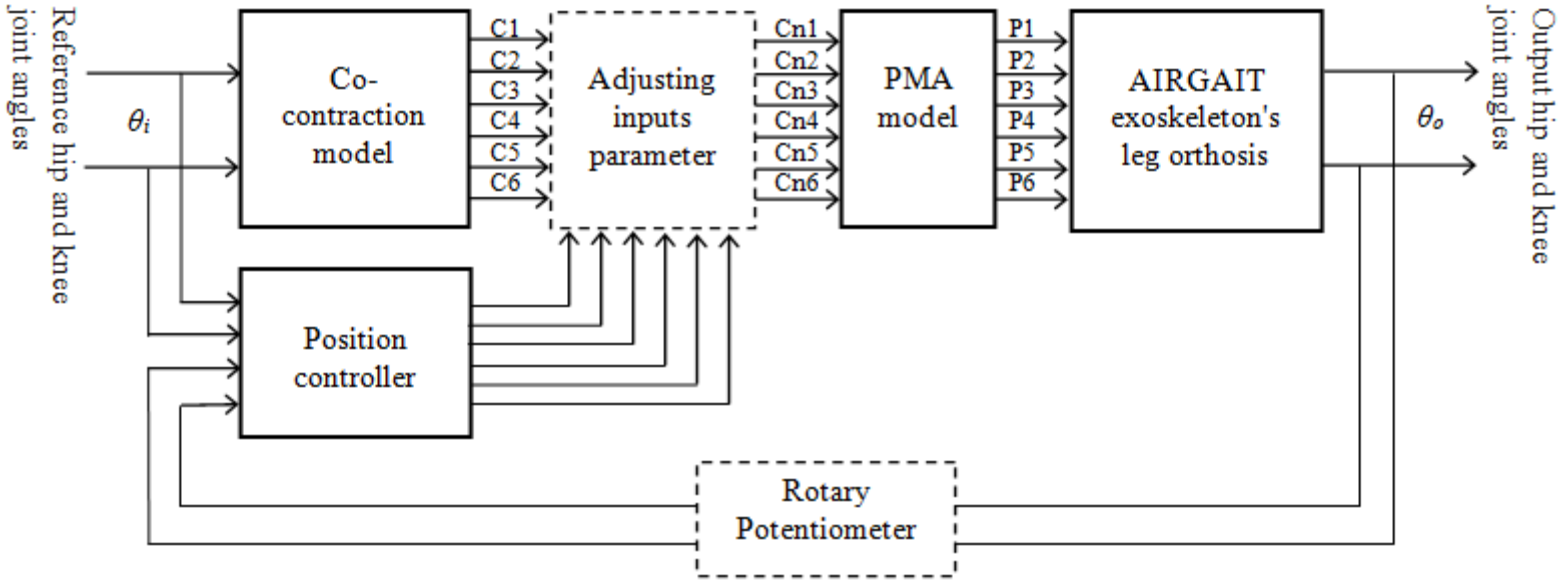

FIGURE 20 Schematic diagram of the exoskeleton of the AIRGAIT leg orthosis controller scheme; co-contraction model based P controller. Where (*C1 – C6*) are the contraction input patterns, (*Cn1 – Cn6*) are the corrected contraction input patterns, and (*P1 – P6*) are the pressure input patterns.

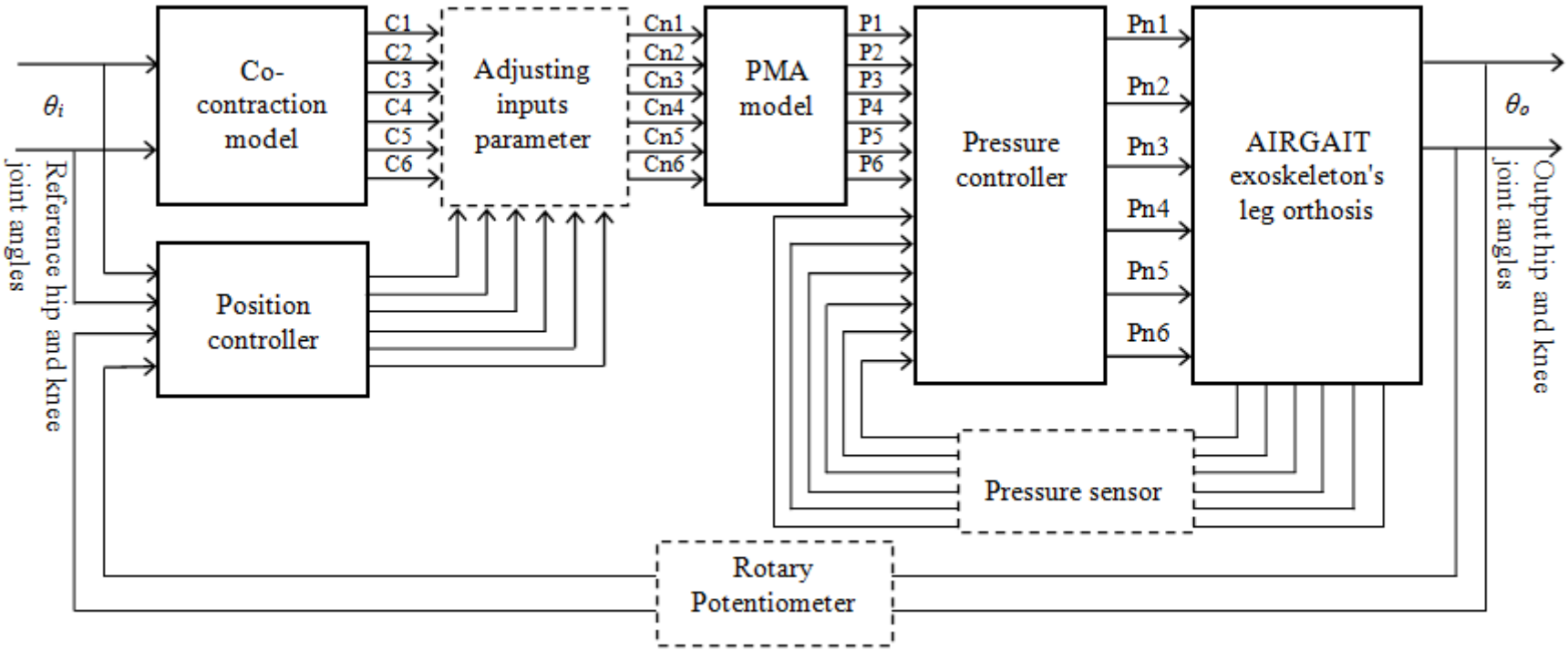

FIGURE 21 Schematic diagram of the exoskeleton of the AIRGAIT leg orthosis controller scheme; co-contraction model based PP controller. Where (*C1 – C6*) are the contraction input patterns, (*Cn1 – Cn6*) are the corrected contraction input patterns, (*P1 – P6*) are the pressure input patterns, and (*Pn1 – Pn6*) are the corrected pressure input patterns.

In the latter half of the research, a contraction model which determines the contraction patterns of antagonistic mono- and bi-articular actuators from positional data is derived and implemented into the control system. Figure 20 and 21 show the schematic diagram of the exoskeleton of the AIRGAIT leg orthosis controller schemes. Figure 20 shows the co-contraction model based P controller, and Figure 21 shows the co-contraction model based PP controller. Unlike other control algorithms for PMA, the designed controller scheme does not predict or measure the required torque at the joints [22, 57, 116 and 117]. Rather, it correlates the angle information of the joints with the dynamic characteristics of the PMA (i.e., contraction and pressure) and then realizes the position and pressure controls.

In order to implement this controller scheme, the co-contraction model was developed. The control strategy was to execute the co-contraction model which implemented position-pressure controller scheme. The PID based-position controller was used to tune the co-contraction model parameters (activation levels) while the PID based-pressure controller was used to control the input patterns of the antagonistic mono- and bi-articular actuators. The derived co-contraction model provides the input patterns for the mono- and bi-articular actuators and simultaneously actuates the antagonistic actuators co-contractively, while the PMA model was determined in order to consider the characteristics of the PMA that were to be introduced into the controller design. This dynamic model was evaluated in an experimental study and represented in an equation. The proposed controller scheme was specifically designed for simplifying the control of antagonistic bi-articular actuators so as to enhance the stiffness at both hip and knee joints. It is an arduous task to construct the plant model of leg orthosis (with antagonistic mono- and bi-articular PMAs) for the implementation of the Stochastic Optimization method to determine the control parameters of the design controller. As such, the heuristic method was implemented.

5.5.2 Kinematic Analysis (Simulated Co-Contraction Model)

Sample data of ideal hip and knee angles were used as an input data for the kinematics simulation of the leg orthosis. The purpose of this simulation was to generate the contraction input patterns for the antagonistic mono- and bi-articular

actuators. Sampling time (frequency) uses for this analysis is 0.001seconds for approximately 5.0 seconds to complete one cycle of human walking motion. The kinematic analyses of the antagonistic mono- and bi-articular actuator models were performed by formulating the actuator's length as a function of hip and knee joint angles. In other words, by plotting the coordinates of antagonistic actuators' end point, the actuators length and contraction for one complete cycle of walking motion can be determined. The obtained contraction data were then used to determine the required input pressures for the antagonistic mono- and bi- articular actuators. Figure 22, 23, 24 and 25 show the co-contraction model using MATLAB simulation for manipulating the antagonistic mono- and bi-articular actuators.

Based on this data, a static data of antagonistic mono-and bi-articular actuators could be determined. These data include the co-contraction patterns and cycles of the antagonistic actuators. However, a static co-contraction data could not efficiently control the leg orthosis by manipulating the antagonistic actuators due to the presence of nonlinear behaviour of the pneumatic muscle and orthosis system. Therefore, this data need to be tuned using the implementation of feedback control system to manipulate the gain of the co-contraction patterns. In addition, the antagonistic actuators muscle activation levels (α and β) also have been introduced into the derived co-contraction model to increase the adaptability of the control scheme to the presence of nonlinearity behaviours. This model was first verified by using the Least Squares (LS) and Recursive Least Squares (RLS) prediction methods between the inputs patterns and the joint angles as can be seen in Table 7. The coding was programmed in MATLAB language. Based on the predetermine Transfer Function (TF), the contraction of antagonistic mono-articular actuators can be differentiated as proportional and inversely proportional (1^{st} order system) to the angle of the joint. However, the model for the antagonistic bi-articular actuators cannot be verified by using the LS and RLS prediction methods, as it requires much higher order and complex system. This could be verified by using Nonlinear ARX model or Genetic Algorithm (GA).

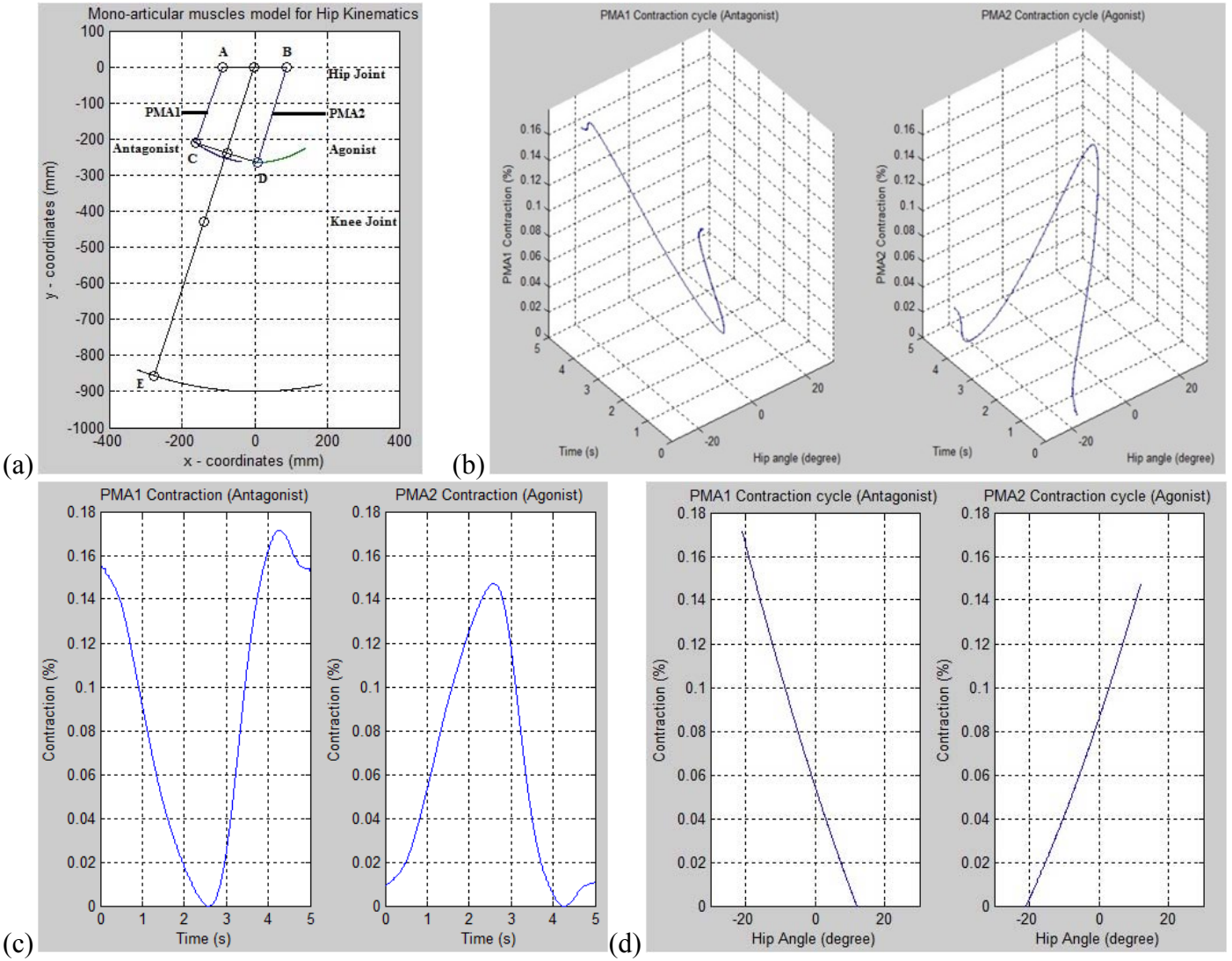

FIGURE 22 Co-contraction model using MATLAB simulations for antagonistic mono-articular actuators at hip joint.

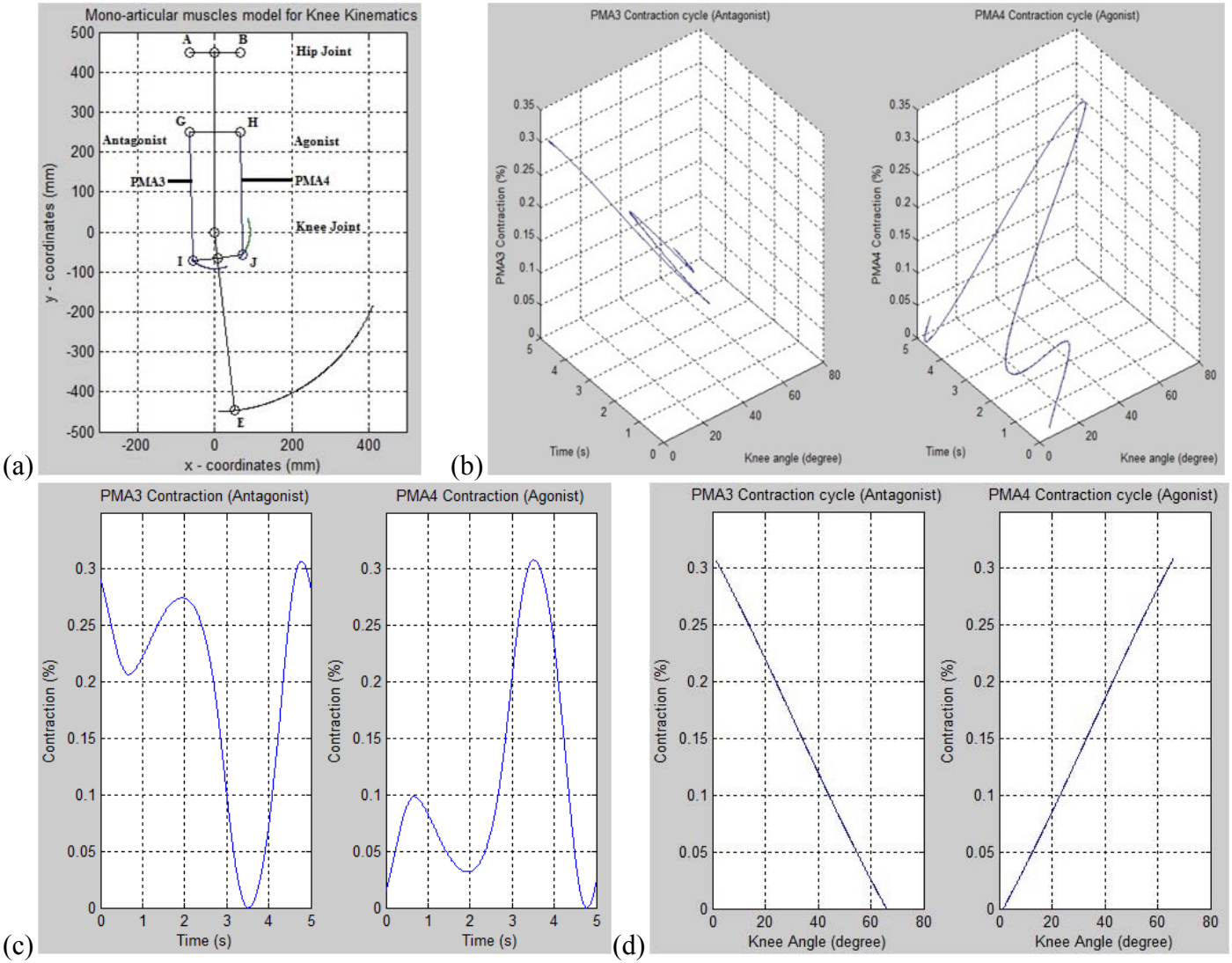

FIGURE 23 Co-contraction model using MATLAB simulations for antagonistic mono-articular actuators at knee joint

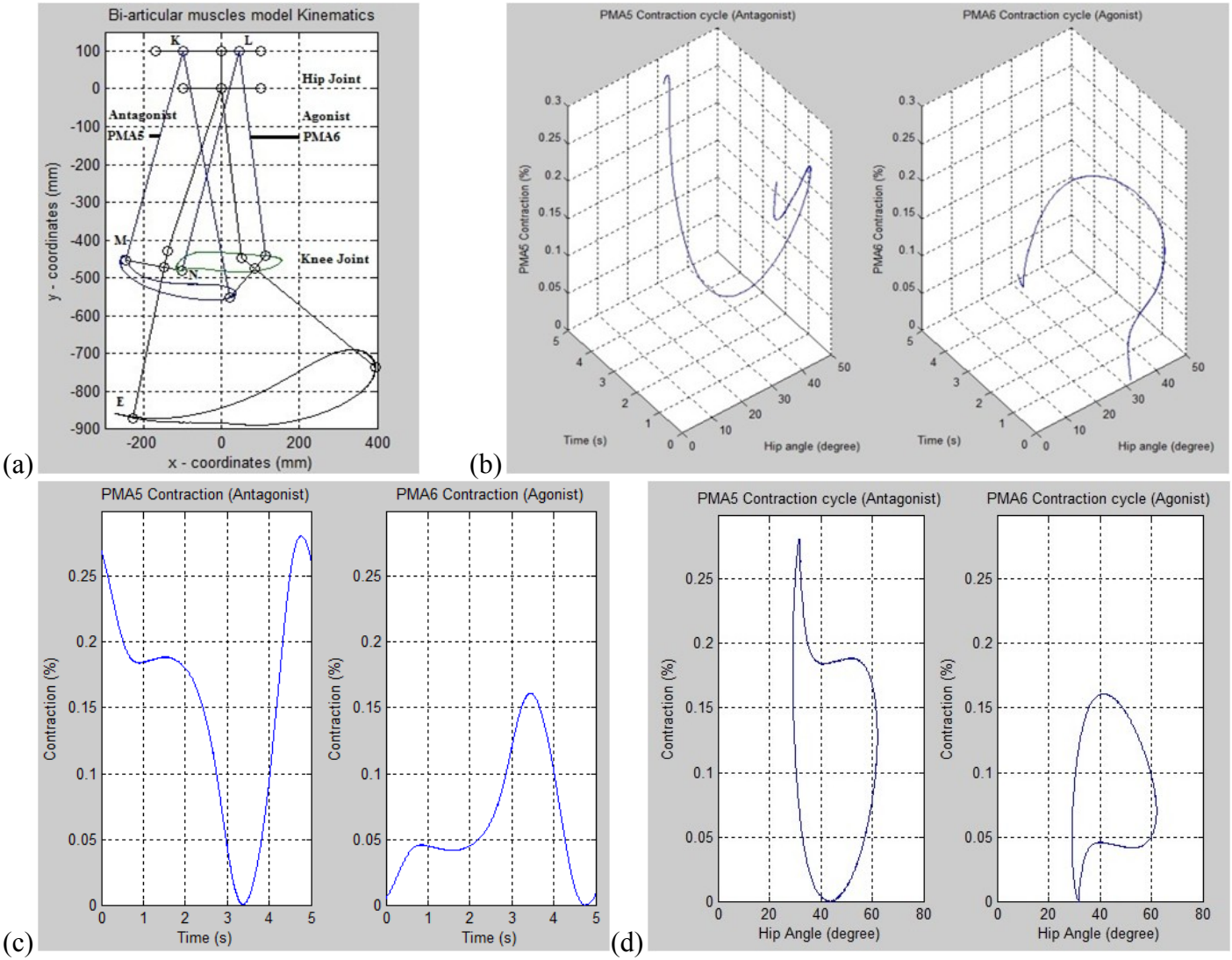

FIGURE 24 Co-contraction model using MATLAB simulations for antagonistic bi-articular actuators based on hip joint.

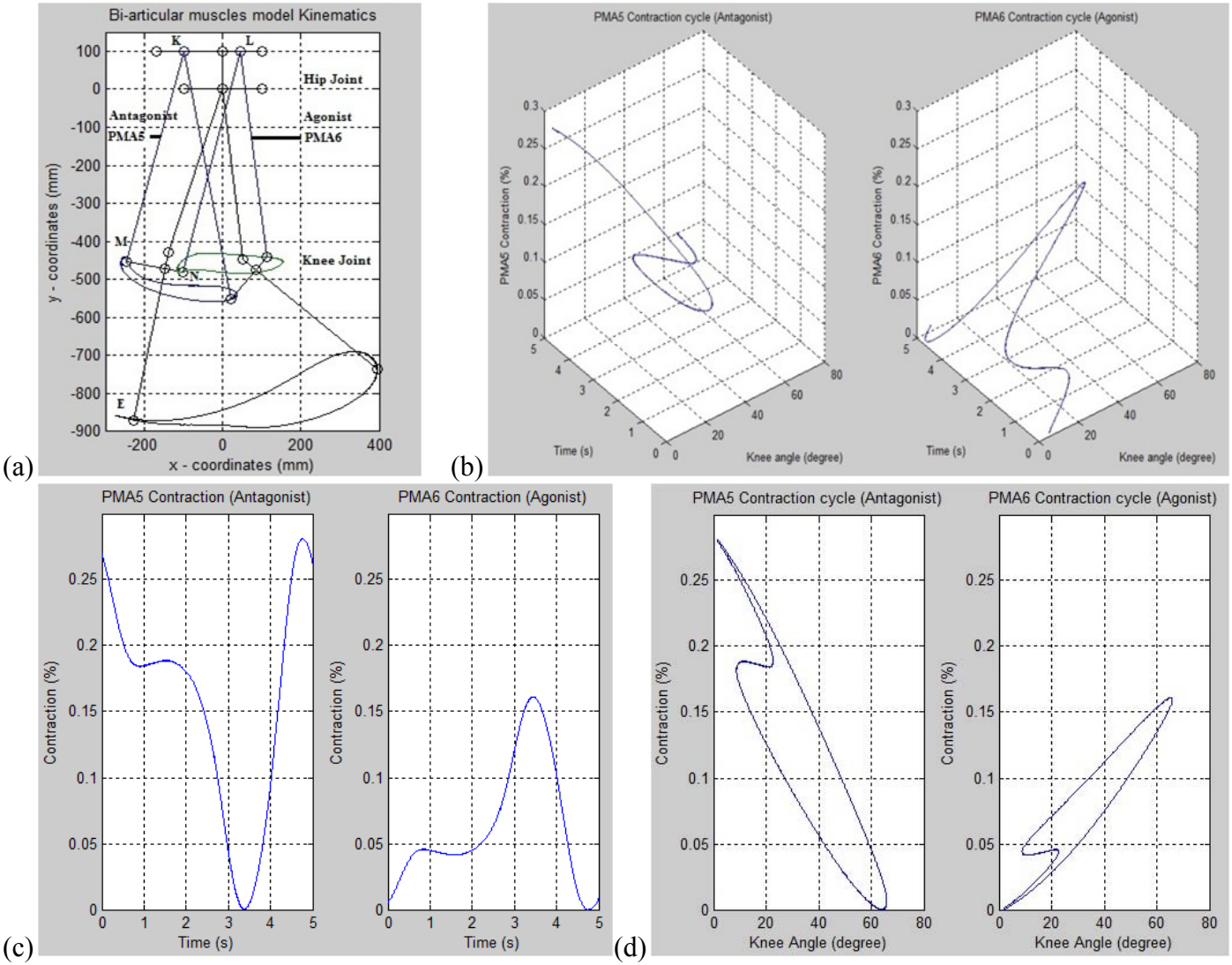

FIGURE 25 Co-contraction model using MATLAB simulations for antagonistic bi-articular actuators based on knee joint.

5.5.3 Derived Co-Contraction Model

The co-contraction model generates the input patterns for the antagonistic mono- and bi-articular actuators (i.e., anterior and posterior) in order to realize the method for implementing the position-pressure controller scheme. This model correlates information on the joints with the dynamic characteristics of the PMA (i.e., contraction and pressure). Based on the derived mathematical model, the contraction of antagonistic mono-articular actuators can be characterized as proportional and inversely proportional (1^{st} order system) to the angle of the joint. As for the bi-articular actuators, a much higher order system is required to enable these actuators to manage two joints simultaneously. To control these joints effectively, the input patterns for the antagonistic bi-articular actuators should be sufficiently accurate as this will ensure the efficient performance of the antagonistic mono-articular actuators and facilitate co-contractive movements between the antagonistic actuators. Determination of the co-contractive input for the bi-articular actuators is insufficient to achieve complete gait motion of the leg orthosis without the inclusion of mono-articular actuators. Thus, the role played by the controls of the mono-articular actuators is crucial in the successful implementation of the bi-articular actuators.

Figure 26 shows the model for leg orthosis system which consists of antagonistic mono-articular PMA model for hip joint, antagonistic mono-articular PMA model for knee joint and antagonistic bi-articular PMA model. According to S. Balasubramanian et al., it is defined that PMAs are based on its model parameters such as relative muscle contraction and rise natural frequency which are affected more by PMA dimensions [112]. In this study, we focus on the mathematical design for contraction model (change in length) of the PMA that is to be implemented into the control system. The general idea for this mathematical model was formed based on the information gained from the reference input data analysis. From the positional input data of hip and knee angles, the locations of minimum (ε_{min}) and maximum (ε_{max}) value for the PMA contractions were determined.

For example, point (A) in Figures 27 (a) and 28 (a) show minimum value for posterior muscle contraction (PMA), but maximum value for anterior muscle contraction (PMA). On the contrary, point (B) shows minimum value for anterior muscle contraction (PMA), but maximum value for posterior muscle contraction (PMA). For a better representation of maximum and minimum antagonistic PMA

contractions, these data were illustrated as positive values to represent the muscle contraction patterns as can be seen in Figure 27(b), 27(c), 28(b) and 28(c). These figures show PMA contraction patterns of antagonistic mono-articular actuators for hip and knee joints. In this mathematical model, a condition for maximum muscle contraction was set, where; $\varepsilon_{p(max)} = \varepsilon_{a(max)} \leq 0.3$.

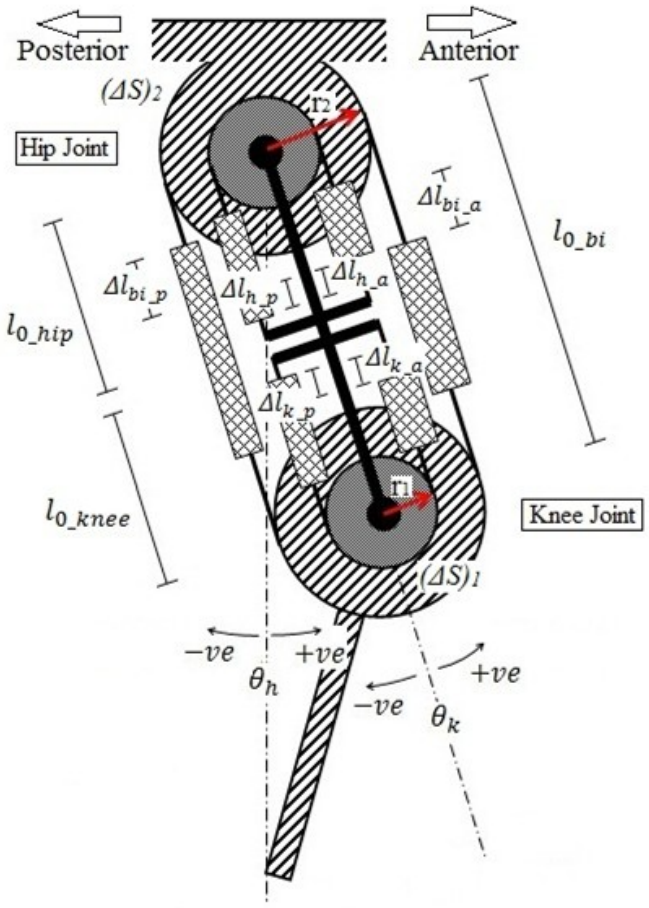

FIGURE 26 AIRGAIT Exoskeleton leg orthosis design kinematics for the antagonistic mono- and bi-articular actuators.

By referring to Figure 26, the change in arc length (ΔS) at the hip and knee joints are defined based on the change in the length (Δl) of PMA to correlate the PMA's contraction with the positional data. Based on this positional data information, the contraction patterns (i.e., *C1 – C6*) of the mono- and bi-articular actuators were then determined using the mathematical derivation as follow. Antagonistic mono-articular actuator contractions (*C1* and *C2*) for hip joint are:

$$\Delta l = \Delta S = \theta . r \quad \ldots (8)$$

$$\Delta l_{h\_p} = \theta_{hp} . r$$

$$\varepsilon_{hp} = \frac{\Delta l_{h\_p}}{l_o} = \beta_h . \left(\frac{\theta_{hp} . r}{l_o}\right) \quad \ldots (9)$$

$$\Delta l_{h\_a} = \theta_{ha} . r$$

$$\varepsilon_{ha} = \frac{\Delta l_{h\_a}}{l_o} = \alpha_h . \left(\frac{\theta_{ha} . r}{l_o}\right) \quad \ldots (10)$$

Equation (9) and (10) can be defined as a time function as follows:

$$C1 = \varepsilon_{hp}(t) = \left(\frac{r}{l_o}\right) . \beta_h . \theta_{hp}(t) \leq 0.3 \quad \ldots (11)$$

$$\varepsilon_{hp(\max)} = \left(\frac{r}{l_o}\right) \beta_{h(max)} . \left|\theta_{hp}(t)\right|_{max} = 0.3$$

$$\beta_{h(max)} = 0.3 \left[\frac{l_o}{r . \left|\theta_{hp}(t)\right|_{max}}\right]$$

$$C2 = \varepsilon_{ha}(t) = \left(\frac{r}{l_o}\right) . \alpha_h . \theta_{ha}(t) \leq 0.3 \quad \ldots (12)$$

$$\varepsilon_{ha(max)} = \left(\frac{r}{l_o}\right) \alpha_{h(max)} . \left|\theta_{ha}(t)\right|_{max} = 0.3$$

$$\alpha_{h(max)} = 0.3 \left[\frac{l_o}{r . \left|\theta_{ha}(t)\right|_{max}}\right]$$

These equations are similar to the antagonistic mono-articular actuators contraction (C3 and C4) for the knee joint:

$$C3 = \varepsilon_{kp}(t) = \left(\frac{r}{l_o}\right) . \beta_k . \theta_{kp}(t) \leq 0.3 \quad \ldots (13)$$

$$\varepsilon_{kp(\max)} = \left(\frac{r}{l_o}\right) \beta_{k(max)} . \left|\theta_{kp}(t)\right|_{max} = 0.3$$

$$\beta_{k(max)} = 0.3\left[\frac{l_o}{r.\left|\theta_{kp}(t)\right|_{max}}\right]$$

$$C4 = \varepsilon_{ka}(t) = \left(\frac{r}{l_o}\right).\alpha_k.\theta_{ka}(t) \leq 0.3 \quad \ldots(14)$$

$$\varepsilon_{ka(max)} = \left(\frac{r}{l_o}\right)\alpha_{k(max)}.\left|\theta_{ka}(t)\right|_{max} = 0.3$$

$$\alpha_{k(max)} = 0.3\left[\frac{l_o}{r.\left|\theta_{ka}(t)\right|_{max}}\right]$$

For the mathematical design's implementation into the system, another condition was set; when the anterior side is in a contraction mode, both the anterior mono- and bi-articular actuators will be in a contraction mode. On the contrary, when the posterior side is in an expansion mode, both the posterior mono- and bi-articular actuators will be in an expansion mode, and, vise versa. Noted that θ_{hp} (hip posterior) and θ_{ha} (hip anterior) have the same magnitude but different signs between muscle contraction (+) or expansion (-). These variables were determined as pattern (positional based data) with a positive value to measure the contraction of the antagonistic mono- and bi-articular actuators, which is also applied for the θ_{kp} (knee posterior) and θ_{ka} (knee anterior). Where; l_o is the initial length for PMA, r is the distance from the PMA endpoint to the attached joint, ε_{hp} is the posterior muscle contraction of mono-articular PMA for hip joint, ε_{ha} is the anterior muscle contraction of mono-articular PMA for hip joint, β_h is the activation level of posterior muscle contraction for hip joint, and α_h is the activation level of anterior muscle contraction for hip joint. Maximum contraction for the posterior and anterior PMAs are $\varepsilon_{p(max)} = \varepsilon_{a(max)} \leq 0.3$. The posterior and anterior muscle activation levels (β and α) are introduced to manipulate the gain of the antagonistic mono- and bi-articular actuator contractions, where the muscle activation level is ranged from ($0 < \beta \leq \beta_{max}$ and $0 < \alpha \leq \alpha_{max}$). These parameters are similar for the antagonistic mono-articular actuators for knee joint and bi-articular actuators.

The interesting part that found in this study was on the bi-articular actuator contraction patterns. It can be defined that, the muscle contraction pattern for the antagonistic bi-articular actuators can be represent as a pattern of the total hip and

knee joint angles. Figure 29(a) shows the positional based data for bi-articular actuators which is defined as a pattern of the total hip and knee angles ($\theta_h + \theta_k$), while Figures 29 (b) and 29 (c) show the muscle contraction patterns of the antagonistic bi-articular actuators. The activation levels for bi-articular actuator muscle contractions are defined as (β_{bi} and α_{bi}). Antagonistic bi-articular actuator muscle contractions (*C5* and *C6*) are:

$$\Delta l_{bi\_p} = (\Delta l_h + \Delta l_k)_p = r.(\theta_h + \theta_k)_p$$

$$\varepsilon_p = \frac{\Delta l_{bi\_p}}{l_o} = \beta_{bi}.\left[\frac{r.(\theta_h + \theta_k)_p}{l_o}\right] \quad \dots(15)$$

$$\Delta l_{bi_a} = (\Delta l_h + \Delta l_k)_a = r.(\theta_h + \theta_k)_a$$

$$\varepsilon_a = \frac{\Delta l_{bi\_a}}{l_o} = \alpha_{bi}.\left[\frac{r.(\theta_h + \theta_k)_a}{l_o}\right] \quad \dots(16)$$

Equation (15) and (16) can be defined as a time function as follows:

$$C5 = \varepsilon_p(t) = \left(\frac{r}{l_o}\right).\beta_{bi}.(\theta_h(t) + \theta_k(t))_p \leq 0.3 \quad \dots(17)$$

$$\varepsilon_{p(max)} = \left(\frac{r}{l_o}\right).\beta_{bi(max)}.\left|(\theta_h(t) + \theta_k(t))_p\right|_{max} = 0.3$$

$$\beta_{bi(max)} = 0.3\left[\frac{l_o}{r.\left|(\theta_h(t) + \theta_k(t))_p\right|_{max}}\right]$$

$$C6 = \varepsilon_a(t) = \left(\frac{r}{l_o}\right).\alpha_{bi}.(\theta_h(t) + \theta_k(t))_a \leq 0.3 \quad \dots(18)$$

$$\varepsilon_{a(max)} = \left(\frac{r}{l_o}\right).\alpha_{bi(max)}.|(\theta_h(t) + \theta_k(t))_a|_{max} = 0.3$$

$$\alpha_{bi(max)} = 0.3\left[\frac{l_o}{r.|(\theta_h(t) + \theta_k(t))_a|_{max}}\right]$$

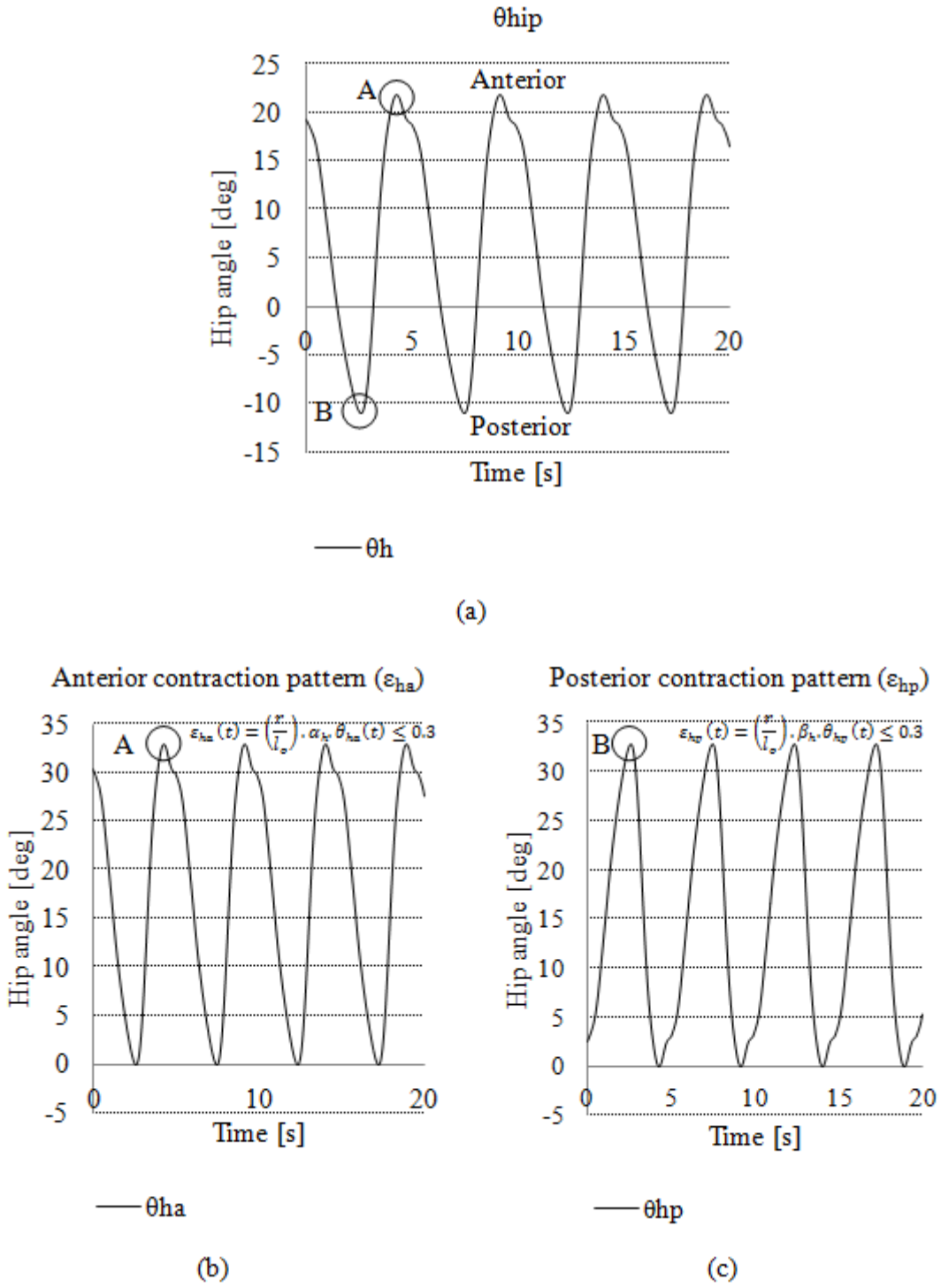

FIGURE 27 Antagonistic mono-articular actuator contraction patterns for the hip joint; (a) reference hip joint angle; (b) anterior contraction pattern; and (c) posterior contraction pattern.

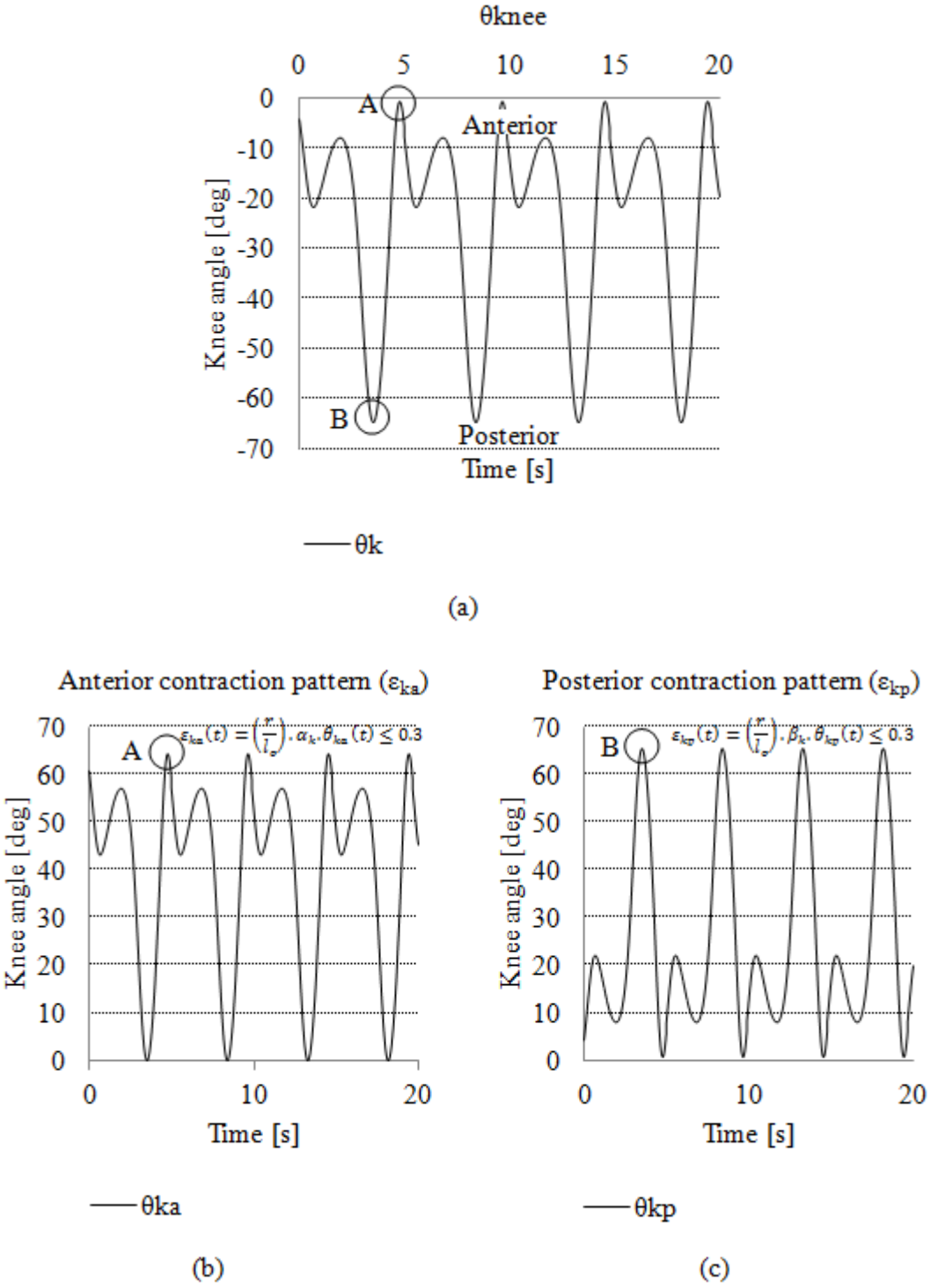

FIGURE 28 Antagonistic mono-articular actuator contraction patterns for the knee joint: (a) reference hip joint angle; (b) anterior contraction pattern; and (c) posterior contraction pattern.

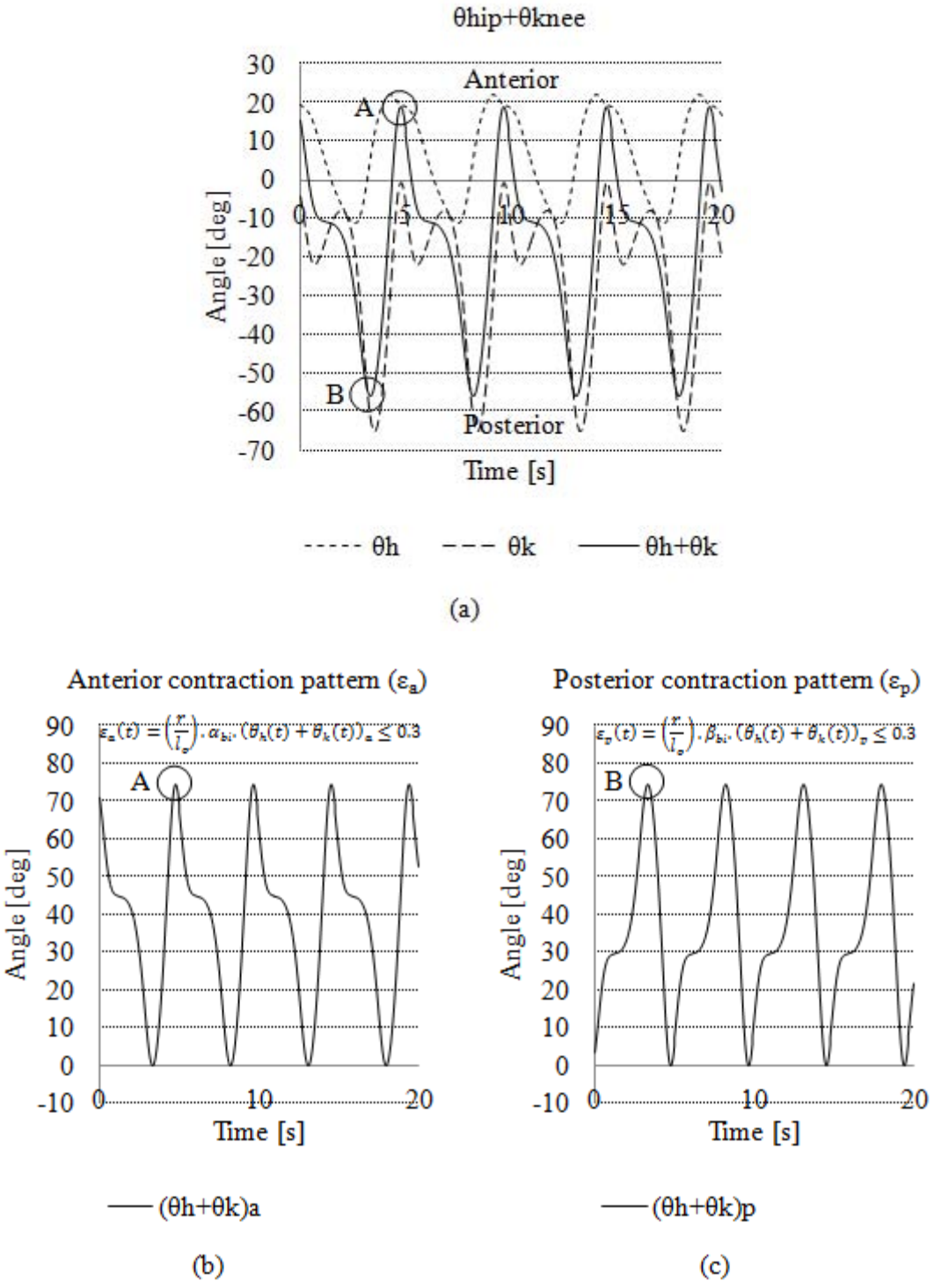

FIGURE 29 Antagonistic bi-articular actuator contraction patterns (positional based data): (a) reference joint angle; (b) anterior contraction pattern; and (c) posterior contraction pattern.

TABLE 7 Models verification using the LS and RLS prediction methods.

LS and RLS Prediction between the Input Patterns and the Joint Angles				
PMA Actuators	LS method		RLS method	
	1st order	*n*th order	1st order	*n*th order
Mono-articular (hip)-anterior PMA	Yes (proportional)	_	Yes (proportional)	_
Mono-articular (hip)-posterior PMA	Yes (inversely proportional)	–	Yes (inversely proportional)	–
Mono-articular (knee)-anterior PMA	Yes (proportional)	_	Yes (proportional)	_
Mono-articular (knee)-posterior PMA	Yes (inversely proportional)	–	Yes (inversely proportional)	–
Bi-articular (hip)-anterior PMA	No	No	No	No
Bi-articular (hip)-posterior PMA	No	No	No	No

TABLE 8 Particle swarm optimization (PSO) control parameters.

Control parameters		
Population size	NP	50
Acceleration constant	C1	2
	C2	2
Inertia weight	w	0.8
Low boundary for kP	L1	3
High boundary for kP	H1	0
Low boundary for kI	L2	3
High boundary for kI	H2	0
Low boundary for kD	L3	3
High boundary for kD	H3	0

5.5.4 Rotational Dynamics

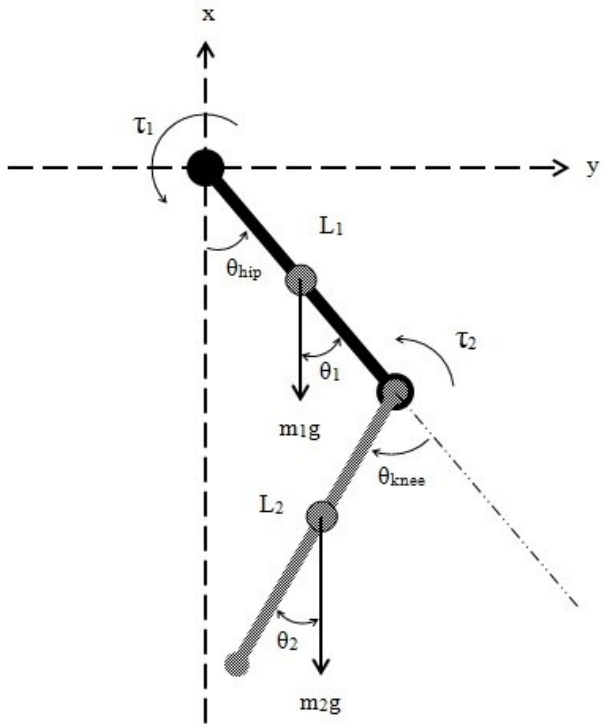

FIGURE 30 Two link leg manipulators model.

The mass of the leg orthosis (m_1 and m_2) as well as the frictions (T_{f1} and T_{f2}) occurs during the gait motion were considered within the rotational dynamics analysis by implementing the equation of motion or Newton's second law of rotation. The torque (τ_1 and τ_2) is calculated by using the equations below. Where the rotational dynamics for the leg orthosis was evaluated based on the simple double pendulum model of two links leg manipulators as can be seen in Figure 30. In this section, a design methodology is proposed to achieve a simple two link leg manipulators model for the simulation analysis. It is well known that the equations of motion for an *n* degree of freedom can be written as:

$$D(\theta)\ddot{\theta} + C(\theta,\dot{\theta})\dot{\theta} + G(\theta) = \tau \quad \ldots(19)$$

where $D(\theta)$ is the $(n \times n)$ inertia matrix, $C(\theta,\dot{\theta})$ is the $(n \times n)$ matrix with centripetal and coriolis terms, $G(\theta)$ is the $(n \times 1)$ gravity torque vector, and τ is the $(n \times 1)$ external actuator inputs;

The inertia matrix $D(\theta)$ is a function of the configuration of the system and elements of $C(\theta, \dot{\theta})$ are partial derivatives of the elements of the inertia matrix given by:

$$c_{kj} = \sum_{i=1}^{n} \frac{1}{2}\left(\frac{\partial d_{kj}}{\partial \theta_i} + \frac{\partial d_{ki}}{\partial \theta_j} - \frac{\partial d_{ij}}{\partial \theta_k}\right)\dot{\theta} \quad \ldots(20)$$

where c_{kj} represents the kj elements of the matrix $C(\theta, \dot{\theta})$, and $d_{ij}(\theta)$ represents the elements of matrix $D(\theta)$;

If the inertia matrix $D(\theta)$ is a constant, i.e., kinetic energy of the system is invariant with configuration of the system, then the matrix $C(\theta, \dot{\theta})$ with nonlinearities becomes a null matrix, since the elements of $C(\theta, \dot{\theta})$ are differentials of elements of $D(\theta)$ matrix. Then, the new system equations can be represented as:

$$D(\theta)\ddot{\theta} + G(\theta) = \tau \quad \ldots(21)$$

This also could be solved by implementing the Newton's second law of rotation which can be described as:

$$\Sigma\tau_o = I_o\alpha \quad \ldots(22)$$

The mass of inertia (I_o) for the slender rod is assumed to be constant, thus neglecting the Coriolis terms. It can be defined using the following equation:

$$I_o = \frac{1}{3}ml^2 \quad \ldots(23)$$

The torques generated at the joints is:

$$\tau_2 = m_2 g sin\theta_2 \left(\frac{l_2}{2}\right) + T_{f2} + I_2\ddot{\theta}_2 \quad \ldots(24)$$

$$\tau_2 - m_2 g sin\theta_2 \left(\frac{l_2}{2}\right) - T_{f2} = I_2\ddot{\theta}_2$$

$$\tau_2 - \left(\frac{m_2 g l_2}{2}\right) sin\theta_2 - T_{f2} = \frac{1}{3}m_2 {l_2}^2 s^2\theta_2$$

$$\left[\tau_2 - \left(\frac{m_2 g l_2}{2}\right) sin\theta_2 - T_{f2}\right]\frac{3}{m_2 {l_2}^2 s^2} = \theta_2 \quad \ldots(25)$$

$$\tau_1 = m_1 g sin\theta_1 \left(\frac{l_1}{2}\right) + m_2 g sin\theta_1 (l_1) + T_{f1} + \tau_2 + I_1 \ddot{\theta}_1 \quad \ldots(26)$$

$$\tau_1 - m_1 g sin\theta_1 \left(\frac{l_1}{2}\right) - m_2 g sin\theta_1 (l_1) - T_{f1} - \tau_2 = I_1 \ddot{\theta}_1$$

$$\tau_1 - m_1 g sin\theta_1 \left(\frac{l_1}{2}\right) - m_2 g sin\theta_1 (l_1) - T_{f1} - \tau_2 = \frac{1}{3} m_1 {l_1}^2 s^2 \theta_1$$

$$\left[\tau_1 - m_1 g sin\theta_1 \left(\frac{l_1}{2}\right) - m_2 g sin\theta_1 (l_1) - T_{f1} - \tau_2\right] \frac{3}{m_1 {l_1}^2 s^2} = \theta_1 \quad \ldots(27)$$

5.5.5 Simulation for Co-Contraction Model Control Scheme

To evaluate the controllability of the derived co-contraction model control scheme, a simulation study was carried out. The particle swarm optimization (PSO) optimization method was used to evaluate the developed control paradigm and strategy, and to determine the reliability of control parameters (i.e., α, and β muscle activation levels). The simulation was performed to determine the functionality and reliability of the designed controller scheme, where the simultaneous and co-contractively movements of the antagonistic actuators to be achieved. Furthermore, the implementation of the position control using PID controller was to manipulate the muscle activation levels of antagonistic actuators. The manipulation of these muscle activation levels will enable the control system to adapt to the presence of the disturbances such as inertia and nonlinearity behaviours of pneumatic muscle. The design co-contractively like movement of the antagonistic actuators should be able to support each other during the control of the leg orthosis and tackling the nonlinearity behaviour of the pneumatic muscle actuators. The control parameters for the PSO are shown in Table 8. Figure 31 shows the schematic diagram of the simulation control model for the leg orthosis system. The derivation of the co-contraction model was recorded earlier and can be referred to in [108]. In addition, a simplified model for the leg orthosis was implemented by using the pendulum model of two-link leg manipulators. This model was the modelled using the Simulink blocks.

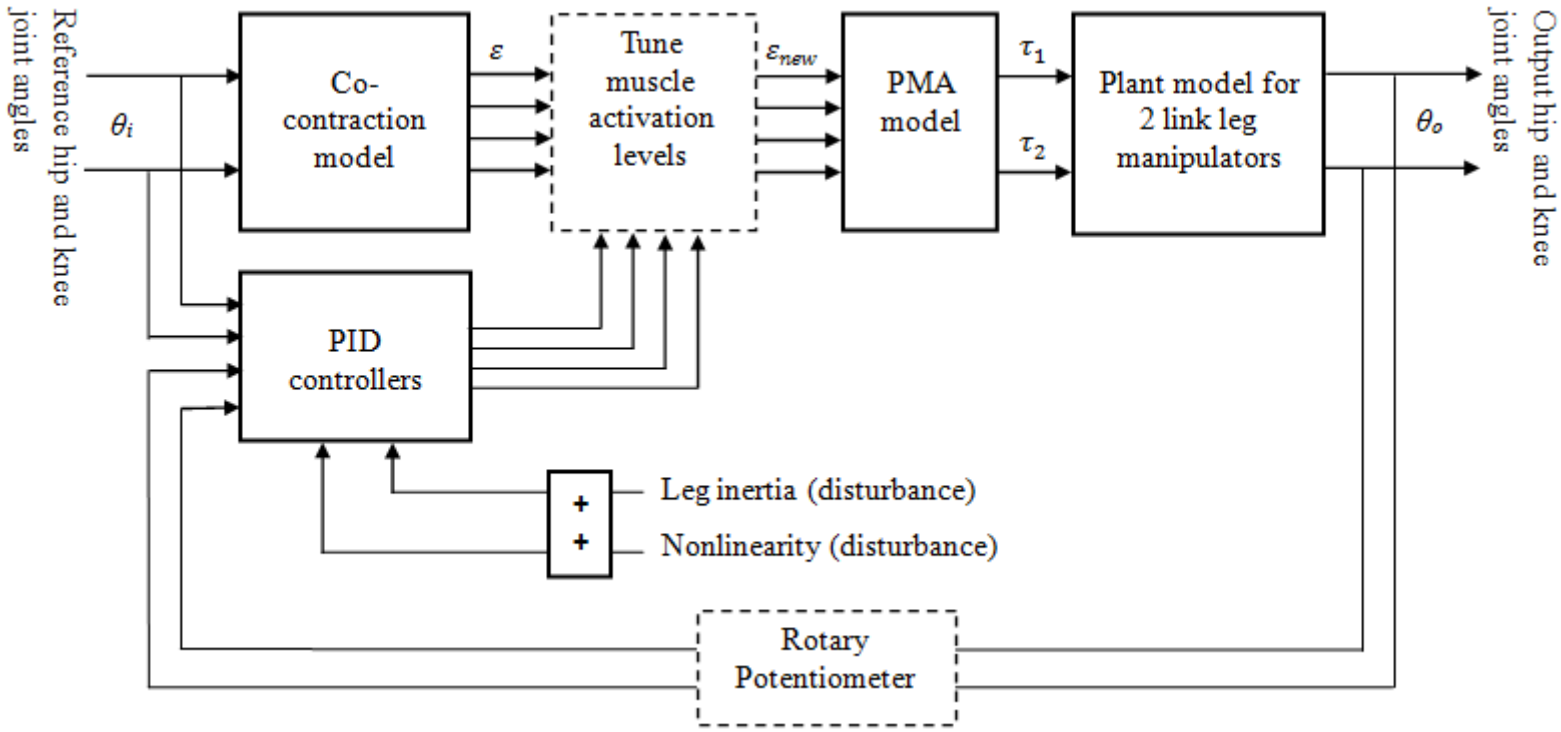

FIGURE 31 Control paradigm's schematic diagram for the system using PSO optimization method. Where (ε) are the contraction input patterns, (ε) are the corrected contraction input patterns, and (τ_1 *a*nd τ_2) are the input torque for the hip and knee joints of the two link leg manipulators.

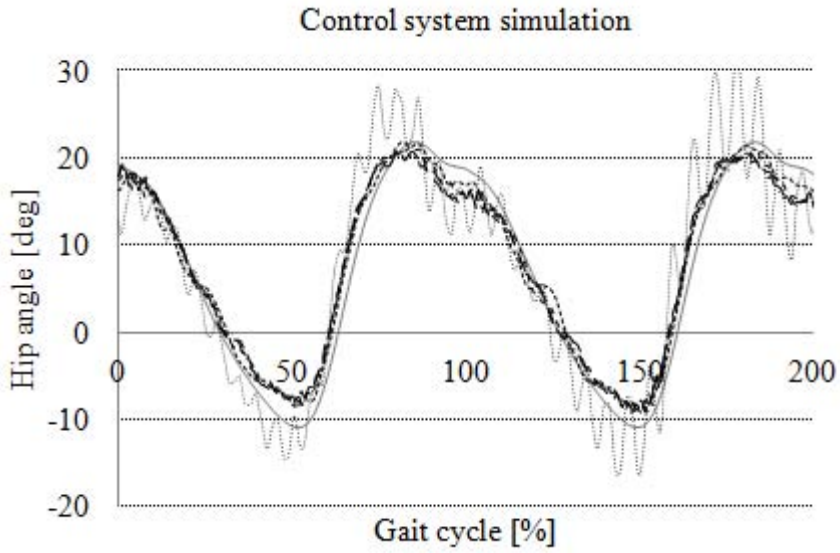

(a)

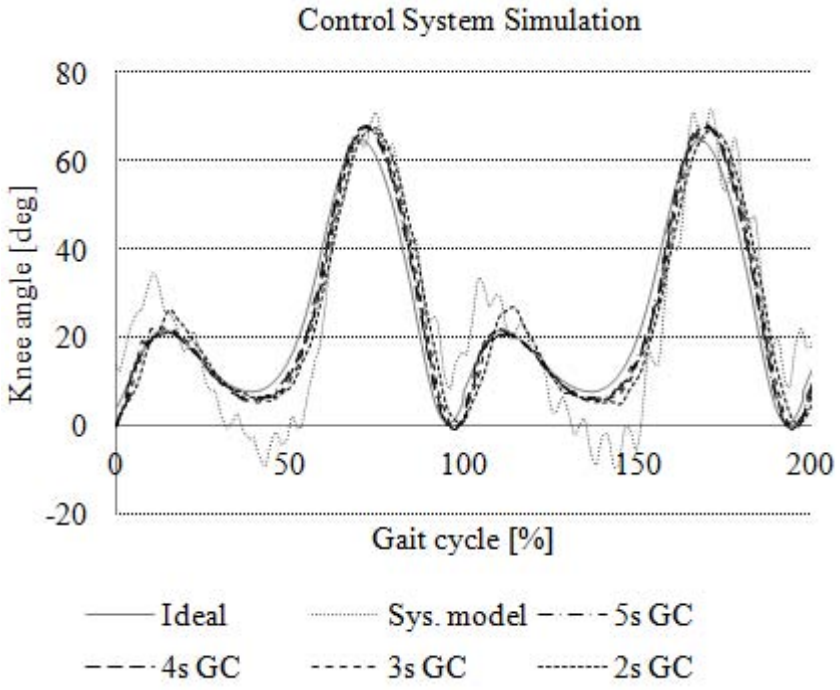

(b)

FIGURE 32 Control system simulation outputs; (a) hip joint excursion; and (b) knee joint excursion.

Figure 32(a) shows the control system simulation for the hip joint excursions at different GC speed of 5, 4, 3, and 2 seconds; and Figure 32 (b) shows the control system simulation for the knee joint excursions at different GC speed of 5, 4, 3, and 2 seconds. The results showed that, the proposed co-contraction model control scheme was able to sufficiently adapt with the introduced disturbances (i.e., inertia and

nonlinearity behaviour of pneumatic muscle) and performed a good controls of hip and knee joint excursions at different GC speed of 5, 4, 3, and 2 seconds. However, the pneumatic muscle's dynamic behaviour due to the time variance was not introduced during the simulation model analysis of the control system.

5.5.6 Hysteresis Characteristic of Pneumatic McKibben Actuator

The characteristic evaluation of pneumatic muscle is conducted to determine the hysteresis at different pressure and load. The experimental setup for this hysteresis characterization is shown in Figure 13. There are two tests performed; the first test is to evaluate the hysteresis model at a zero load condition; and the second test is to evaluate the hysteresis model when test with different load of 100N, 200N and 300N. Both tests are evaluated at different input pressures of 0.1, 0.2, 0.3, 0.4, and 0.5MPa to analyse the behaviours during the contraction and expansion of the pneumatic muscle. The time cycle used to complete one cycle of the contraction and expansion of the pneumatic muscle are 5 seconds, 10 seconds, and 20 seconds.

Figure 33, 34, and 35 show the hysteresis model at different time cycles of 5 seconds, 10 seconds, and 20 seconds for the tests without a load. The results showed that, hysteresis effect were materialized during the contraction and expansion phases when provided with a same input pressure at all evaluated time cycles. This could be explained because of the compressibility of the pneumatic muscle. Due to the compressibility, the contraction of the pneumatic muscle required less input pressure to achieve maximum contraction and to sustain its form compared to the expansion of the pneumatic muscle. Moreover, the shape of the hysteresis was found out to be bigger at a much faster time cycles when compared to the slower time cycle. However, the maximum contraction achieved at all evaluated time cycles was unchanged. In addition, an ability of the pneumatic muscle to accurately return to its initial position was much better at the lower speed of time cycle. Figure 36 shows the hysteresis model at different loads of 0N, 100N, 200N, and 300N evaluated at a time cycle of 20 seconds. The result showed that, the hysteresis model of the pneumatic muscle was different at all evaluated weight loads. Where, the maximum contraction of the pneumatic muscle able to be achieved was decreased with an increase of weight load. In addition, the input pressure required to raise the contraction of pneumatic muscle was also increased.

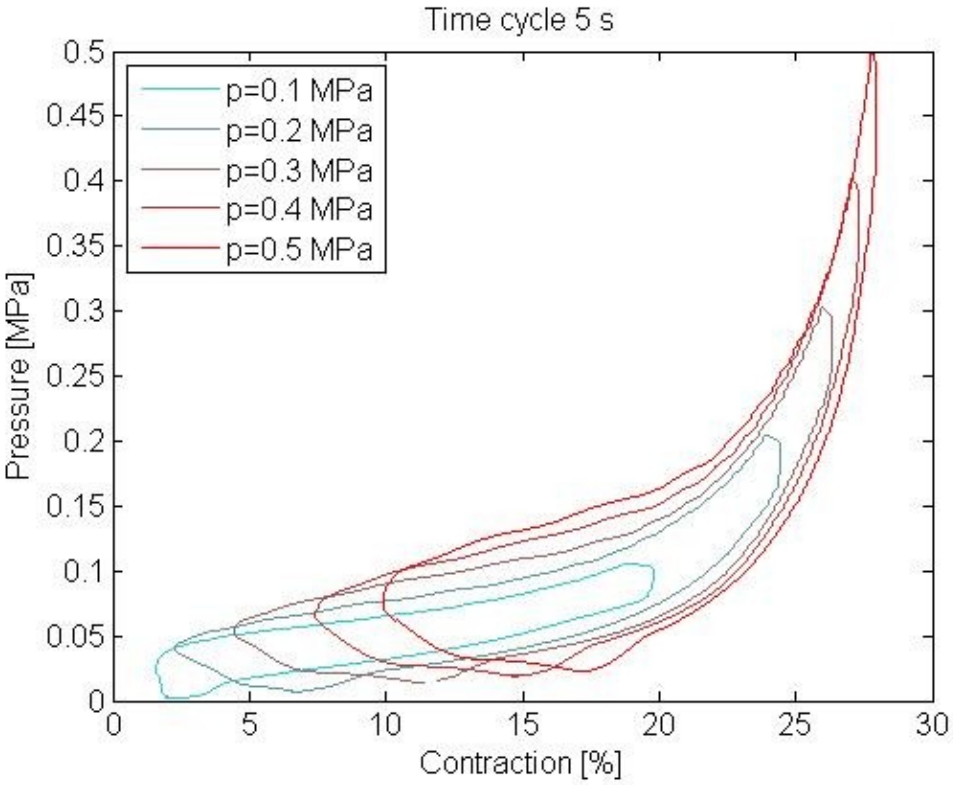

FIGURE 33 Hysteresis model for time cycle of 5 seconds tested without a load.

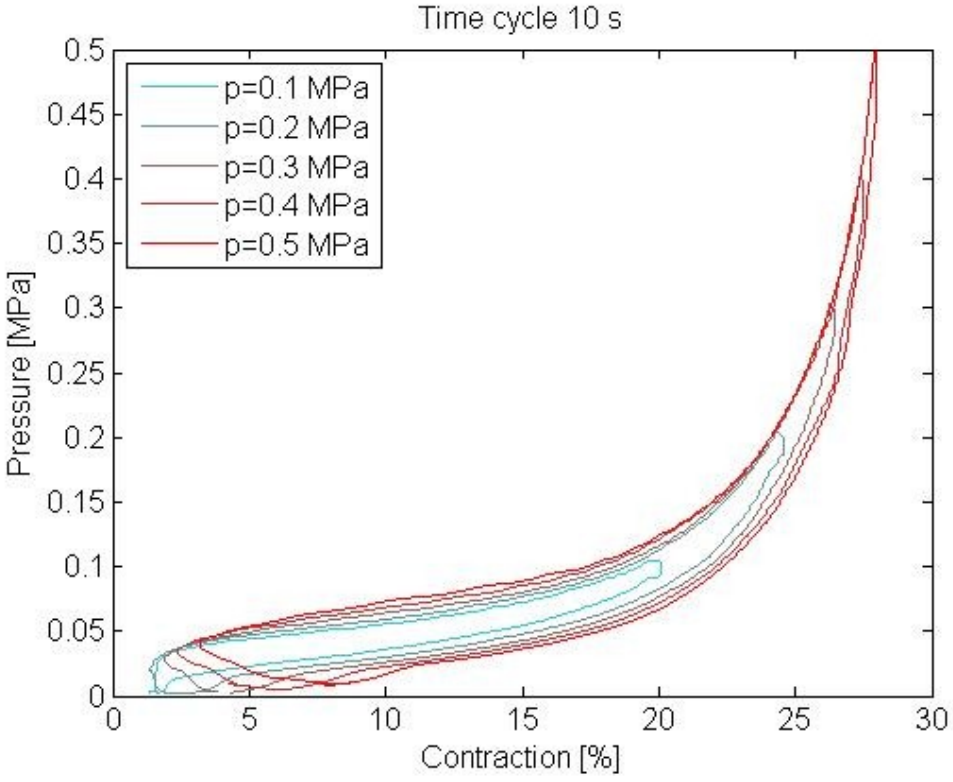

FIGURE 34 Hysteresis model for time cycle of 10 seconds tested without a load.

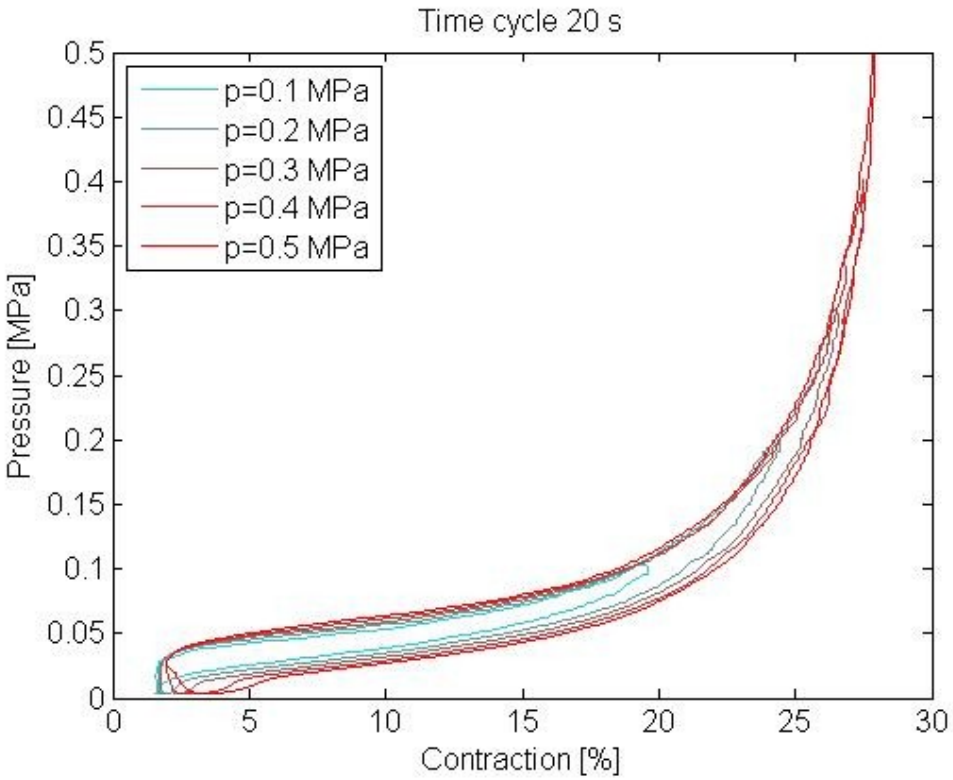

FIGURE 35 Hysteresis model for time cycle of 20 seconds tested without a load.

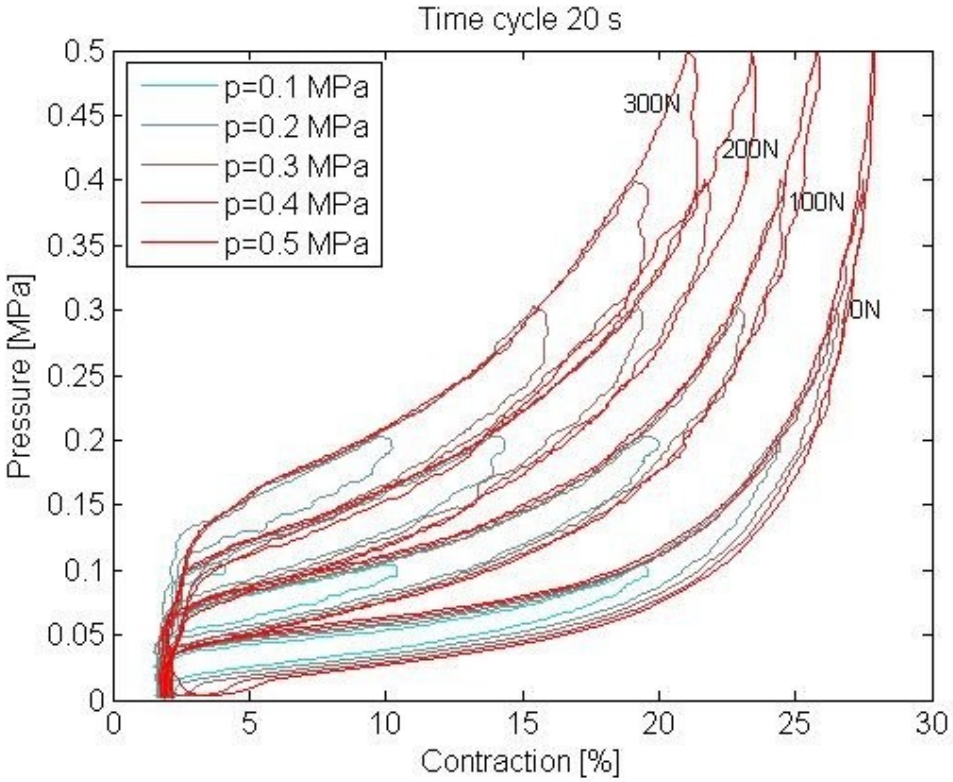

FIGURE 36 Hysteresis model for time cycle of 20 seconds tested with 0N, 100N, 200N, and 300N loads.

Form the evaluation, it could be concluded that the presence of shape of the hysteresis model was different at different time cycle. Moreover, the hysteresis model was also different with an increase in the weight load. Due to this inherent hysteresis of pneumatic muscle, it is almost impossible to derive a precise model to represent this kind dynamic behaviour. For that reason, the control of the antagonistic mono- and bi-articular actuators will be difficult without a suitable control strategy to sufficiently reduce the effect of this nonlinearity. In addition, it could be expensive and time consuming to introduce a complicated model and strategy in precisely control the pneumatic muscle. Therefore, to reduce the hysteresis effect of the pneumatic muscle when manipulating the leg orthosis, an antagonistically arrangement (i.e., anterior and posterior) of the pneumatic muscles on the leg orthosis was introduced. In addition, the co-contractively like movements control of these antagonistic actuators was proposed. It is also believed that the co-contraction of antagonistic actuators was able to increase the stiffness and stability of the leg orthosis. Furthermore, the PMA model was introduce to improve the adaptability of the system with the presence of the nonlinearity behaviours.

5.5.7 PMA Model

The development of the PMA model is for the purpose of increasing the effectiveness of the co-contraction model. While the co-contraction model provides the antagonistic actuators with the contractive data, this model translated that data into pressure patterns [in Volts] for activating the electro-pneumatic regulators. The dynamic characteristics of the PMA such as dimension (i.e., length and muscle contraction), pressure, and force data were determined in an experimental study. A model equation was then formulated to represent the PMA characteristics data with the high accuracy of 6^{th} order polynomial. This will be used as the reference model for the control strategy as can be seen in Figure 37. The co-contraction model control scheme considers the nonlinearity behaviour of the PMA by controlling the muscle activation level of the PMA. The PMA static model at zero load condition was defined as the minimum boundary to determine the nonlinearity area of the PMA. As the critical muscle activity with regard to the PMA is during its contraction, only the contraction mode was considered to realize the co-contraction movements between

the antagonistic mono- and bi-articular actuators. The evaluation and derivation of this PMA model has been recorded earlier and can be observed in [109]. Figure 38 shows the controlled value of the muscle activation levels during a control system.

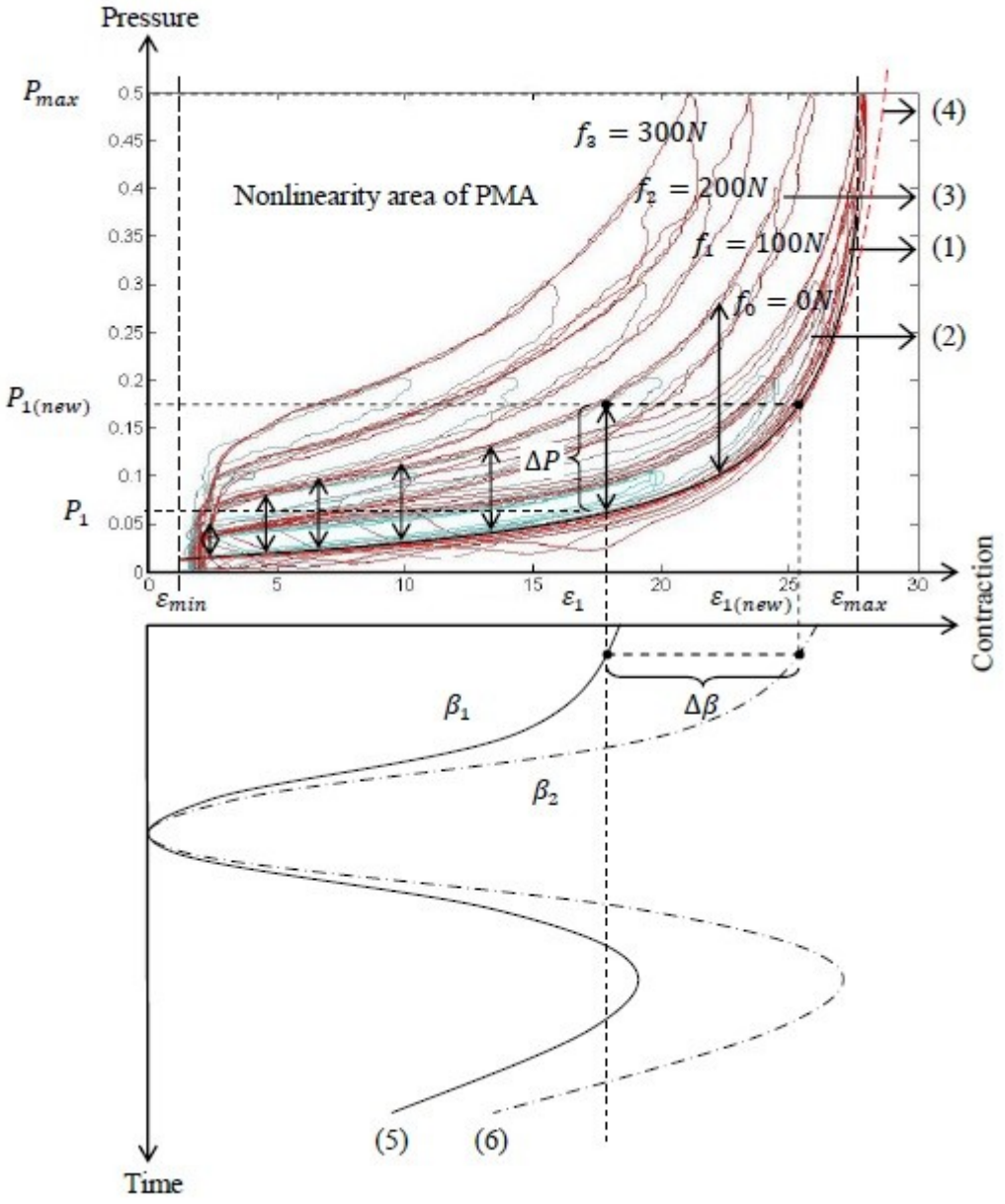

FIGURE 37 Co-contraction model control scheme's strategy; where (1) PMA static model of Pressure vs. Contraction at zero load condition; (2) PMA hysteresis model at zero load (f_0) condition; (3) PMA hysteresis model at load (f_1, f_2, f_3,…) condition; (4) PMA model using 6th order polynomial equation (5) Contraction input pattern for the antagonistic mono- and bi-articular actuators (6) Controlled contraction input patterns after the controls of the muscle activation level (β). ΔP is the sudden increase in pressure due to the PMA nonlinearity. Δβ is the increase in muscle activation level.

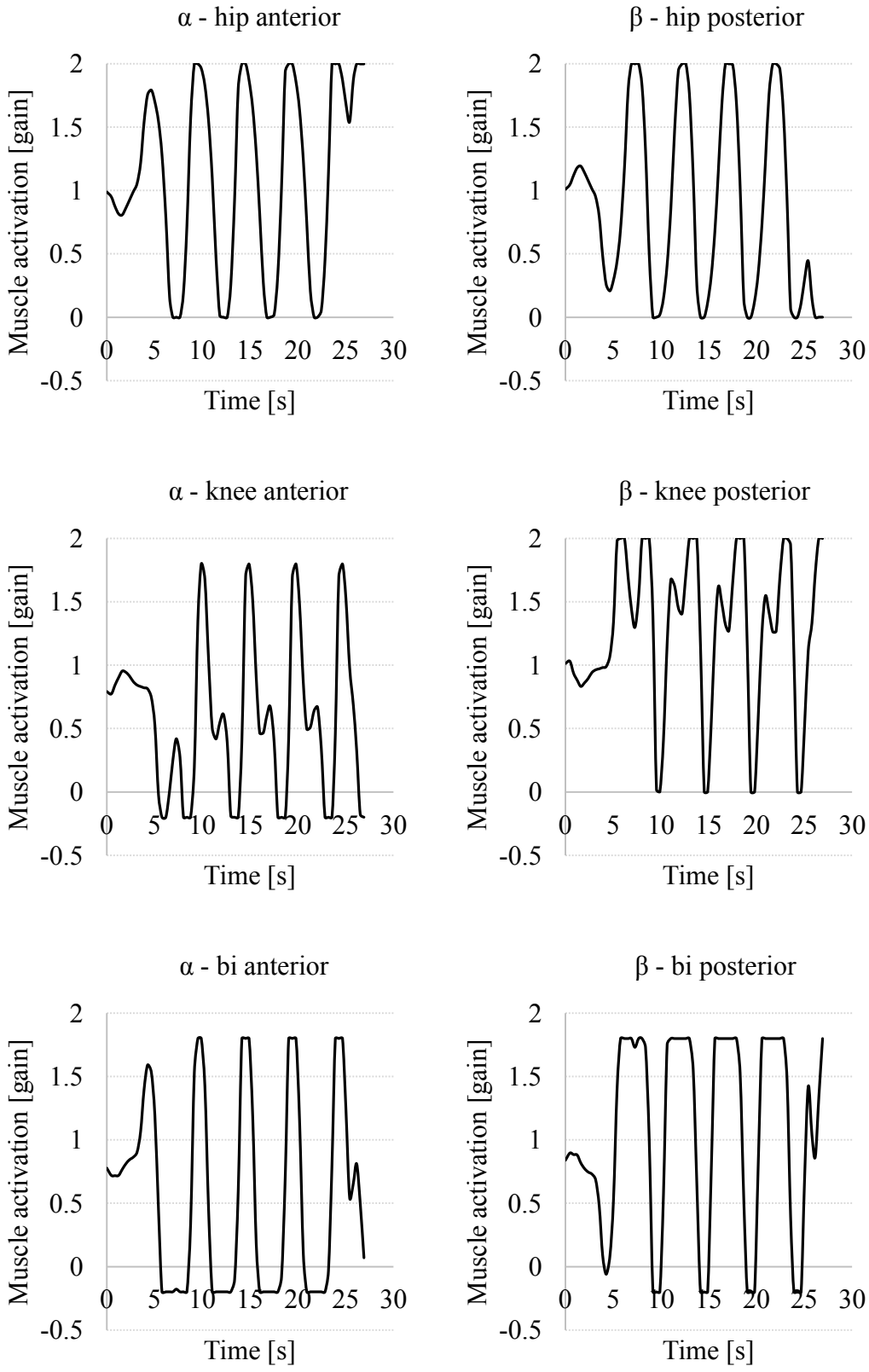

FIGURE 38 Controlled values of the muscle activation levels for the antagonistic mono- and bi-articular actuators.

5.6 Couple Control Model (Computed Torque Method)

5.6.1 Introduction

Pneumatic artificial muscles (PMAs) are often used for the actuation of rehabilitation devices or, more generally, in most application where there is the interaction between machines and humans [119 - 121]. In these devices, when the motion is not managed by the human, a control model is needed. In literature there are a lot of models for this purpose and applied to PMAs based actuations. The different approaches can be divided into two main groups: feedback linearization and computed-torque method [122]. In the first class can be group all the control models that work on the feedback of the measured control variable such as fuzzy [121], PID, Neural Network [123] or other models [124, 125]. Many of these control models were tested on 1 degree of freedom systems [124, 126] but in the last years many authors are working on more complex systems that can simulate well the human morphology of the arms or of the legs, then with 2 degrees of freedom, see [123, 125, 127].

The computed-torque method, instead, requires a completely description of the system and, if it has a high number of degrees of freedom, the formulation of the couple joint expression can become very difficult. On the contrary, if the analytical description of the system is well-made, it will be very faster on follow the inputs with respect to the other main control model class. In this paper we propose and use a model control based on the computed-torque method for the managing of our AIRGAIT orthosis for the rehabilitation of the lower limb [110, 111, and 128]. The paper is organized as follow. In section 2 we give an overview on the AIRGAIT system. In section 3 we show the main characterization of our self-made PMAs. The control model with all its parts is described in section 4. Section 5 contains all the validation tests made on the system in order to verify the goodness of the control model. At last, in section 6 we give some concluding remarks.

5.6.2 Overview of the AITGAIT Exoskeleton's Leg Orthosis New System

Figure 39 shows the AIRGAIT exoskeletons leg orthosis of the developed body weight support gait training system used for this research. The leg orthosis system

implemented six PMA which antagonistically arranged based on the human musculoskeletal system (i.e., mono- and bi-articular muscles). The PMA used in this research is a self fabricated McKibben artificial muscle actuator. The input pressure of the PMA is regulated by electro-pneumatic regulator separately for each actuator. The special characteristic of PMA will cause it to contract when the air pressure is supplied, and expand when the air pressure is removed. In other words, the PMA is able to emulate the force and muscle contraction of humans muscle. In addition, it is also might be able to perform similar contractions and expansions, where their movement is almost similar to the movements of the humans muscles. The measurement of the joint excursions (i.e., hip and knee) is made using potentiometer. This system uses the Lab-View software and RIO module to provide the input signals and to read the output data of the leg orthosis.

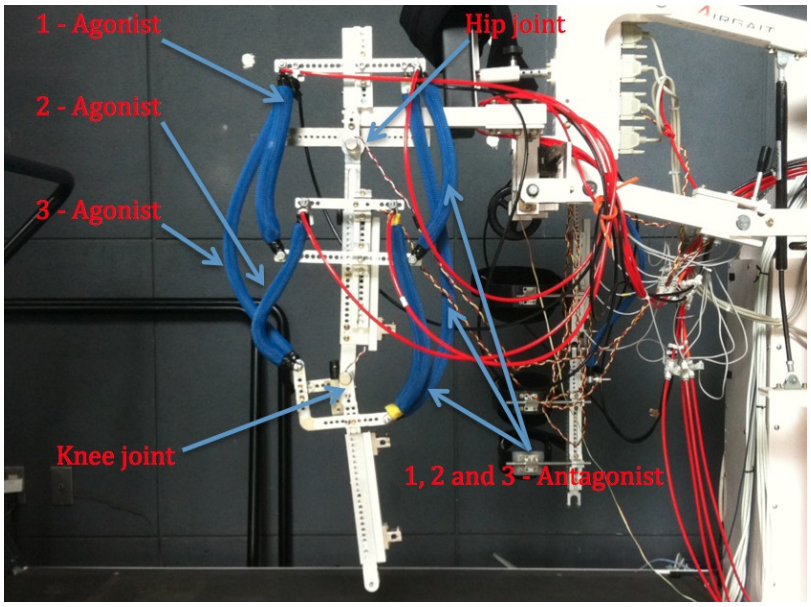

FIGURE 39 AIRGAIT exoskeleton's leg orthosis antagonistic actuators.

5.6.3 Pneumatic Muscle Characterization

The McKibben PMA used for this study is built in our laboratory using commercial parts. For this reason we have to characterize them in order to understand and fix their properties and behaviours. We conducted two main kinds of characterizations, one static and another dynamic. With the data collected by the first one we are able to model the non-linearity of the PMA by fitting the data with a polynomial function. With the dynamic characterization instead, we can estimate a priori the error in

position due to the hysteresis. The static characterization is conducted by setting the ends of the PMA at given positions in order to have a variation from 0 to the 30% of the contraction.

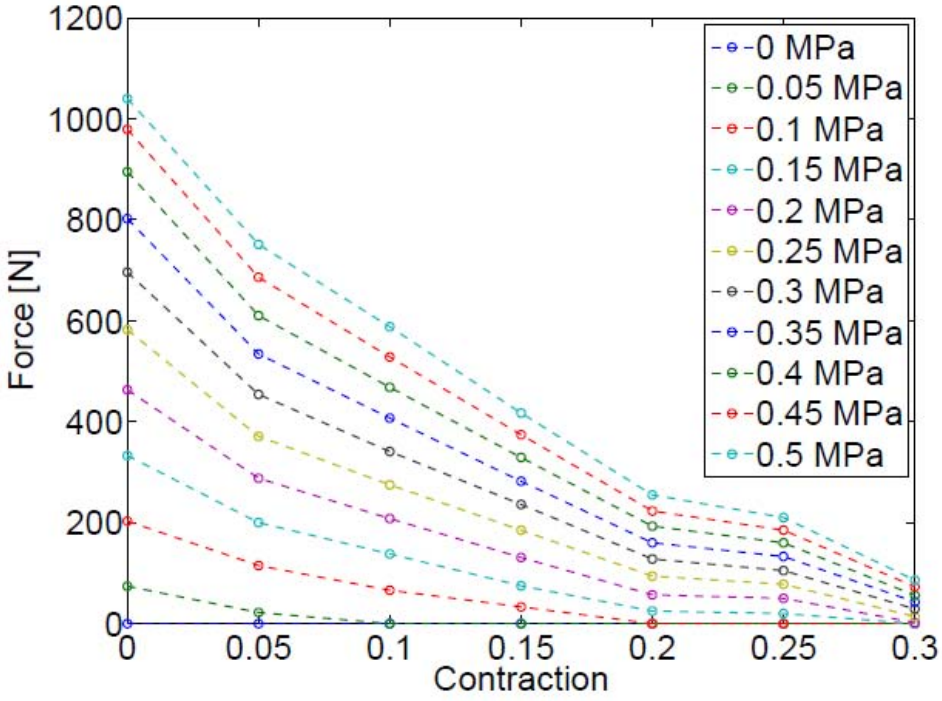

FIGURE 40 Static characterization of pneumatic muscle.

This parameter is determined as the difference between the length of the muscle and the given position, divided by the length of the muscle, then:

$$k = \frac{l_m - l}{l_m} \quad \ldots (28)$$

Once the distance between the ends is fixed, we vary the supply pressure inside the PMA from 0 to 0.5 MPa and we record, through a load cell, the reaction force. The results of the described experiment are show in Figure 40. It is possible to note in this figure that the main static properties of the PMA are very similar to those of the commercial PMA. The dynamic characterization was enabled us to check the ability of the artificial muscle to follow dynamic signals. We conducted two dynamic experiments one without and one with loads. To conduct these experiments we fix the PMA only on one side, maintaining the other free or putting on a weight. We supply the muscle with a pressure signal going from zero to a set value and once again to zero. The set value is varied to be 0.1, 0.2, 0.3, 0.4 and 0.5 MPa. The results

of the experiment without loads are presented in Figure 33, 34 and 35. It shows the hysteresis behaviours with a time cycle of 5 seconds, 10 seconds, and 20 seconds. As it is possible to note, for high values of the pressure 5 and 10 seconds are not enough to complete the loading-unloading cycle. Instead, there are the hysteresis trends for a time cycle of 20 seconds. In this case, with all the values of the pressure the cycle is completed. Fixing the time cycle to 20 seconds, we conducted the same hysteresis characterization, then loading and unloading cycle, with different maximum pressures, but including a load on the muscle. We test it with 10 kg, 20 kg, and 30 kg, which can be considered very high in comparison with the real loads that the system could be stressed. Figure 36 shows the hysteresis behaviour with a different load of 10, 20, and 30 kg. The main interesting consideration can be made by comparing the results of Figure 33, 34, and 35 with those of Figure 36 in terms of distance between the loading and unloading curves. Also with the presence of great load this distance remains almost constant which conforming the goodness of this kind of actuation.

5.6.4 Control Model and Application to the Orthosis

The control model, proposed in this paper, is based on the analytical description of the system and on the use of the so called computed-torque method. In this section we will show all the main components of the entire control model and the main idea at its basis.

5.6.4.1 Fitting Model of the Non-Linear Behaviour PMA

One of the most difficult problems to solve when we work with PAMs is the non-linear behaviour of the PMAs. The main task is to find, as made by [129], the force that the PMA can apply as a function of the supply pressure and of its contraction. The data collected into the static characterization (see Figure 40) will be here fit with a surface. We choose to fit the surface with a two variables polynomial function. We need to express the supply pressure as a function of the force and the contraction. To do this, the fitting equation must be solvable in the term of the pressure, and then the term of the pressure must have a degree equal or less to two (different approach used

in [129] in which the equation is fifth degree in both variables, then needs to solve numerically with long time of computing). We then conduct a sensibility analysis on the degree of the fitting equation. Particularly we compute the Root Mean Square Error (RMSE) between the experimental point of Figure 40 and the fitting surface and we express the results as a function of the of the degrees of the two variables *x* and *y* (pressure and contraction). The results are summarized in the Table 9. As it is possible to note we have a great reduction of the RMSE from first to second degree in x and, at the same time, we choose to have third degree in y. This choice is due to the fact that we do not have a great reduction of the RMSE between third and fourth degree in y and then we decide to reduce the number of the parameters to increase the computational speed. The resulting fitting equation is the follow:

$$f(x,y) = a_1 + a_2x + a_3y + a_4x^2 + a_5xy + a_6y^2 + a_7x^2y$$

$$+a_8xy^2 + a_9y^3 \quad \ldots(29)$$

Where, as mentioned before, *x* represents the supply pressure, *y* is the contraction and *f(x; y)* is the force. The numeric values of the parameters of this equation are shown in the Table 10. At last, we show in Figure 41 the equivalent polynomial surface with the experimental points coming from the characterization. As it is possible to note from this figure, the equation fit well the real data.

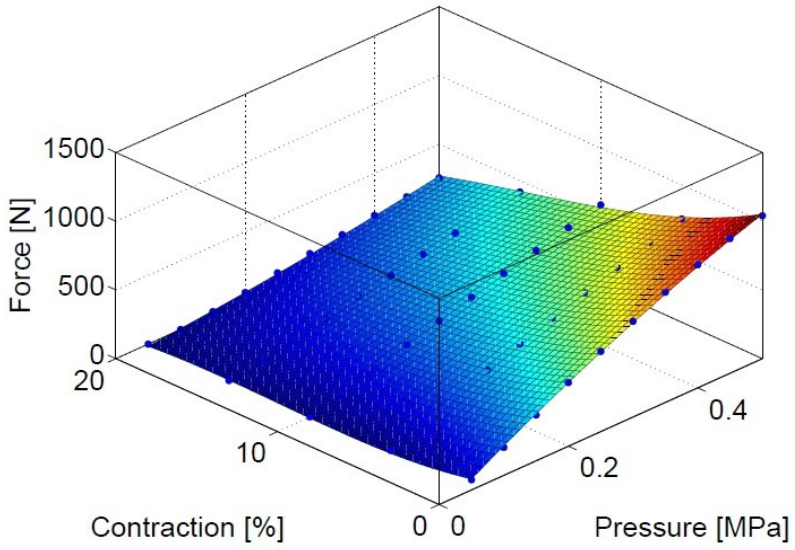

FIGURE 41 Graphical visualization of the fitting polynomial equation (blue dot are the experimental points).

TABLE 9 Sensibility analysis of the fitting curve of the experimental data as a function of the degrees of the polynomial surface.

Degree of x	Degree of y	RMSE
1	1	88.2
2	1	36.7
2	2	23.2
2	3	11.6
2	4	7.4
1	2	24.3
1	3	18.4
1	4	17.2

TABLE 10 Numeric values of the parameters of the fitting polynomial equation.

Parameter	Value
a_1	-7
a_2	2384
a_3	-1135
a_4	-467
a_5	-12480
a_6	8682
a_7	4160
a_8	13290
a_9	-15960

5.6.4.2 Newton Euler's Equation Model

The crucial part of the proposed model is based on the computation of the couples for every angles assumed by the two joints. Here we follow the Newton-Euler approach in order to obtain an analytical formulation of the two couples. Just to remind and using a simplified formulation, we can model the dynamics of a robot with revolution joints by the follow equation:

$$M(q)\ddot{q} + C(q,\dot{q}) + g(q) = \tau \quad \dots(30)$$

where $\ddot{q}$, $\dot{q}$ and q are respectively the vectors of the joint positions, velocities and acceleration, *M(q)* is the articulated robot inertia matrix, *C(q, $\dot{q}$)* is the vector of centripetal and Coriolis force, *g(q)* is the vector of gravitational forces and τ is the vector of joint torque [122];

In Figure 41 we give a schematic representation of the orthosis. In this figure d_1 and d_2 denote the distances between the joints and the centers of mass of the two links instead; d_{12} and d_{T2} are the lengths of the two links. Referring to Figure 42, we can solve the equation 24, in order to find the couples of the two joints:

$$C_1 = I_{11}\ddot{\theta}_1 + I_{22}\ddot{\theta}_1 + I_{22}\ddot{\theta}_2 + \ddot{\theta}_1 d_1^2 m_1 + \ddot{\theta}_1 d_2^2 m_2 + \ddot{\theta}_2 d_2^2 m_2 + \ddot{\theta}_1 d_{21}^2 m_2$$

$$+d_2 g m_2 cos(\theta_1 + \theta_2) + d_1 g m_1 cos(\theta_1) + d_{21} g m_2 cos(\theta_1)$$

$$-\dot{\theta}_2^2 d_2 d_{21} m_2 sin(\theta_2) + 2\dot{\theta}_1^2 d_2 d_{21} m_2 cos(\theta_2) + \dot{\theta}_2^2 d_2 d_{21} m_2 cos(\theta_2)$$
$$- 2\dot{\theta}_1 \dot{\theta}_2 d_2 d_{21} m_2 sin(\theta_2) \quad \dots (31)$$

$$C_2 = I_{22}\left(\ddot{\theta}_1 + \ddot{\theta}_2\right) + d_2 m_2 \begin{pmatrix} d_{21} sin(\theta_2)\dot{\theta}_1^2 \\ +g cos(\theta_1 + \theta_2) \\ +d_2\left(\ddot{\theta}_1 + \ddot{\theta}_2\right) \\ +\ddot{\theta}_1 d_{21} cos(\theta_2) \end{pmatrix} \quad \dots (32)$$

where I is the inertia, m is the mass and g is the gravity acceleration;

The equations of the two couples are obtained by a symbolic generation of large multi-body system dynamic equations proposed in [122] and in [123]. In the Table 11 are summarized the numerical data of the orthosis geometry.

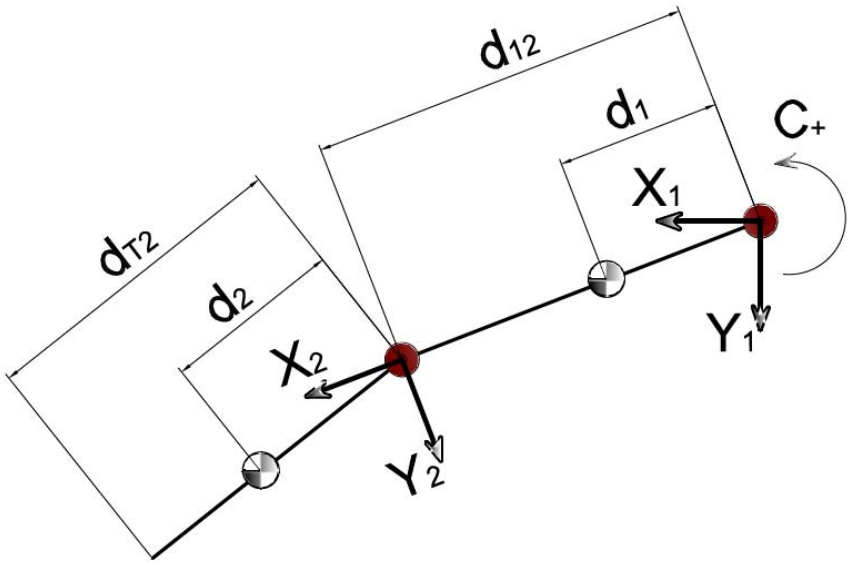

FIGURE 42 Schematic representations of the AIRGAIT exoskeleton's leg orthosis two-link model.

TABLE 11 Numerical data of the orthosis geometry.

Parameter	Value
I_{11}	$0.052\ kgm^2$
I_{22}	$0.032\ kgm^2$
m_1	$1.34\ kg$
m_2	$0.97\ kg$
d_1	$0.2\ m$
d_2	$0.15\ m$
d_{21}	$0.4\ m$
d_{T2}	$0.37\ m$

5.6.4.3 Geometric Description Model

Figure 43 and 44 show the mono- and bi-articular actuators model's contraction. Based on the information gained from the AIRGAIT exoskeleton's leg orthosis, the contraction of the antagonistic mono- and bi-articular actuators are derived using the trigonometric function. The antagonistic mono-articular actuator's contraction for the hip joint (θ_1) is:

$$AB = \sqrt{\overline{AC}^2 + \overline{BC}^2 - 2\overline{AC}.\overline{BC}cos(\alpha)} \quad \dots(33)$$

$$\theta_0 = \alpha|_{\theta_1=0}$$

$$Antagonist: \ \alpha = \theta_1 - \theta_0 = \alpha(\theta_1)$$

$$Agonist: \ \alpha = \theta_1 + \theta_0 = \alpha(\theta_1)$$

$$k(\theta_1) = k_1^{ant.} = k_1^{ag.} = \frac{l_m - AB}{l_m} \quad \dots(34)$$

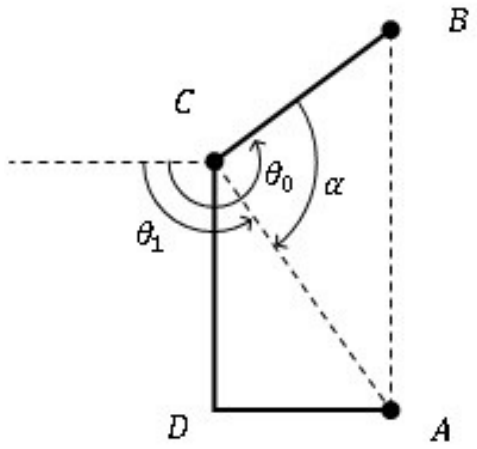

FIGURE 43 Schematic representations of the mono-articular actuators.

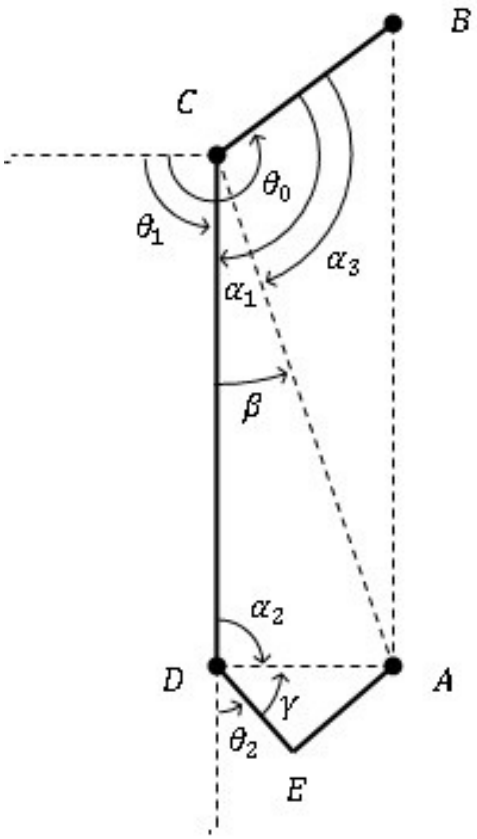

FIGURE 44 Schematic representations of the bi-articular actuators.

The implementation is also similar for the antagonistic mono-articular actuators for the knee joint (θ_2). However, the axis for the knee joint motion is based on the line formed between the hip and knee joints. The antagonistic bi-articular actuator's contraction is derived as follows:

$$AC = \sqrt{\overline{AD}^2 + \overline{CD}^2 - 2\overline{AD}.\overline{CD}cos(\alpha_2)} \quad \dots(35)$$

$$\alpha_2 = 180 - \gamma - \theta_2$$

$$AB = \sqrt{\overline{AC}^2 + \overline{CB}^2 - 2\overline{AC}.\overline{CB}cos(\alpha_3)} \quad \dots(36)$$

$$\alpha_3 = \alpha_1 - \beta, \qquad \alpha_1(\theta_1) = \theta_0 - \theta_1$$

$$\beta = acos\left(\frac{\overline{CD}^2 + \overline{AC}^2 - \overline{DA}^2}{2.\overline{CD}.\overline{AC}}\right) \quad \dots(37)$$

$$k(\theta_1, \theta_2) = \frac{l_m - AB}{l_m} \quad \dots(38)$$

5.6.4.4 Control model

There are in literature a lot of control model, they can be divided into two main groups: position and couple control. The last one requires a completely description of the system and, if it has a high number of degree of freedom, the formulation of the couple joint expression become difficult. For this reason many of the controllers used in industry are based on empirical approach as the fuzzy or the PID controls. The main idea of the proposed model is based on the control of the position by controlling the couples of the joints and varying the stiffness of the system as a function of the degree of precision required and of moving masses. The model is composed of a part that describe the geometric configuration between the pneumatic muscles and the joints, another part for the computing of the joints couple based on the Newton-Euler equations and the last part that able us to compute the needed supply pressure knowing the equivalent forces and the contractions. First of all, we can define the stiffness of a system as the measure of the resistance to the deformations. For our system this concept of stiffness translates itself into the level of the force of the antagonist muscle that we can call the "base force" (following a

similar nomenclature proposed by [120]). In order to describe the control model we can set and define, for the moment, as R = cost the stiffness of the system that represent the force of the antagonist pneumatic muscle. From the geometrical model we can find the percentage contraction of the two muscles as a function of the angle θ, then:

$$k_1^{ag.} = f(\theta_1) \; and \; k_1^{ant.} = f(\theta_1) \quad \dots (39)$$

$$k_2^{ag.} = f(\theta_2) \; and \; k_1^{ant.} = f(\theta_2) \quad \dots (40)$$

$$k_3^{ag.} = f(\theta_1, \theta_2) \; and \; k_3^{ant.} = f(\theta_1, \theta_2) \quad \dots (41)$$

where k_1^{ag} represents the contraction of the agonist muscle of the joint 1, instead k_2^{ant} is the contraction of the antagonist muscle of the joint 2;

From the NE equations we can compute the couples *C1* and *C2* as follow:

$$C_1 = f\left(m_1, m_2, I_{11}, I_{22}, \theta_1, \theta_2, \dot{\theta}_1, \dot{\theta}_2, \ddot{\theta}_1, \ddot{\theta}_2\right) \quad \dots (42)$$

$$C_2 = f\left(m_2, I_{22}, \theta_1, \theta_2, \dot{\theta}_1, \dot{\theta}_2, \ddot{\theta}_1, \ddot{\theta}_2\right) \quad \dots (43)$$

But geometrically the couples *C1* and *C2* can be also computed as:

$$C_1 = \left(F_1^{ag.} - F_1^{ant.}\right).l_1, \qquad C_2 = \left(F_2^{ag.} - F_2^{ant.}\right).l_2 \quad \dots (44)$$

Being F_1^{ant}, and F_2^{ant}, equal to R, from the last equations we can compute the forces F_1^{ag}, and F_2^{ag}:

$$F_1^{ag.} = \frac{C_1}{l} + R, \qquad F_2^{ag.} = \frac{C_2}{l} + R \quad \dots (45)$$

Now we have to find the pressures that correspond to the forces F_1^{ag} and F_2^{ag}. To do this it is necessary to invert the equation of the fit of the pneumatic muscle characterization. The equation showed in the previous section is of the second degree in x and then we can solve it easily:

$$A = a_4 + a_7 y \quad \dots (46)$$

$$B = a_2 + a_5 y + a_8 y^2 \quad \ldots (47)$$

$$C = a_1 + a_3 y + a_6 y^2 + a_9 y^3 - f(x, y) \quad \ldots (48)$$

$$x = \frac{-B}{2A} \pm \frac{\sqrt{B^2 - 4AC}}{2A} \quad \ldots (49)$$

Then considering the physical meaning of *x*, *y* and *f(x; y)*, the equation can be summarize as *P = f(F;K)*. Then, known the force and the percentage contraction of the muscle we can compute the pressure. In the Figure 45 we give the schematic idea of the proposed control model.

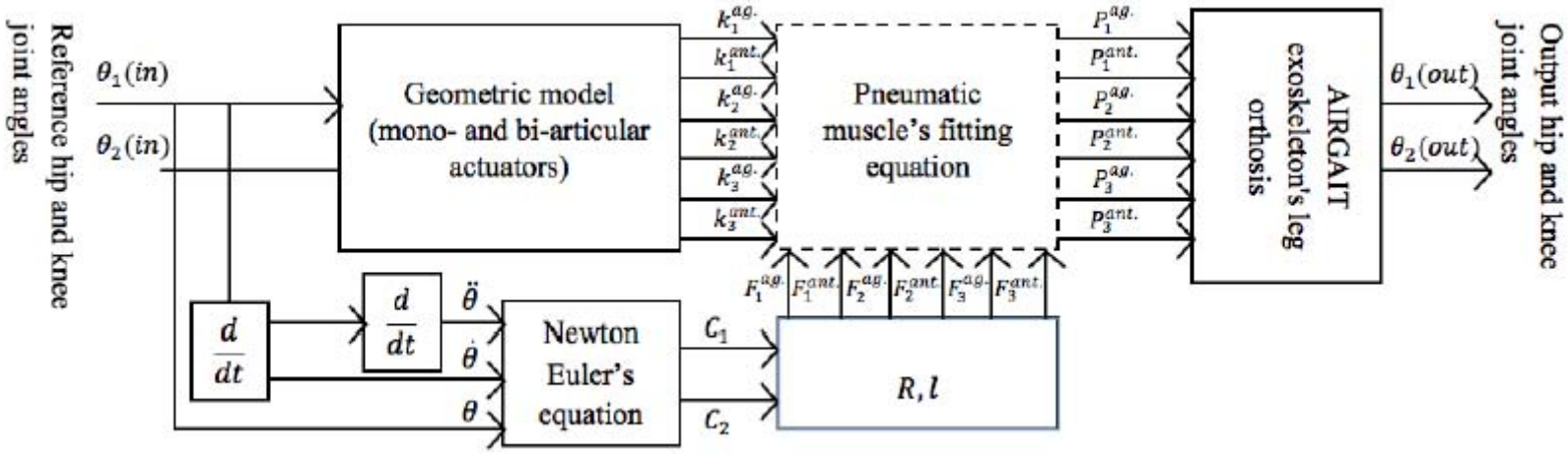

FIGURE 45 Block diagram of the couple control model.

CHAPTER 6

RESULTS AND DISCUSSION

In this section, findings for the designed controller scheme tests and strategy were evaluated and discussed. The modus operandi from the early stage until the final stage was appropriately modelled to optimize the flow of this research. The discussion and evaluation of the findings were divided into several parts to explain each stage of the study. It comprises of several assessments for evaluating the performance of the design control scheme and strategy. These assessments are including the evaluation of pressure and position-pressure controls using conventional PID and the proposed co-contraction model control scheme. Then, the comparison were made between (a) mono-articular actuators acting on their own (i.e., hip and knee joints), and with the addition of bi-articular actuators; (b) co-contraction model based position (P) controller, and the co-contraction model based position-pressure (PP) controller; and (c) comparison between the control of the leg orthosis WO/S and control of the leg orthosis W/S. The evaluation was based on the GC, movement of the trajectory of the hip and knee joints, maximum angle extension of the joints, inertia, gravitational effect, and time shift.

6.1 Control of the Leg Orthosis WO/S and W/S: Pressure and Position-Pressure Control based on Conventional PID Controller

The focus in this assessment is on the control of leg orthosis using conventional PID controller. The tests were performed with mono-articular actuators alone, and with

addition of bi-articular actuators. The bi-articular actuators only provided with a constant input pressure of 0.25MPa to investigate the contribution of this actuators during leg orthosis controls. Two control schemes (i.e., pressure and position-pressure controls) based on conventional PID controller were evaluated during the control system. Both tests were conducted without a subject and with a subject at a GC speed of 5 seconds. Figure 46 shows the schematic diagram for the pressure and position-pressure controls using conventional PID.

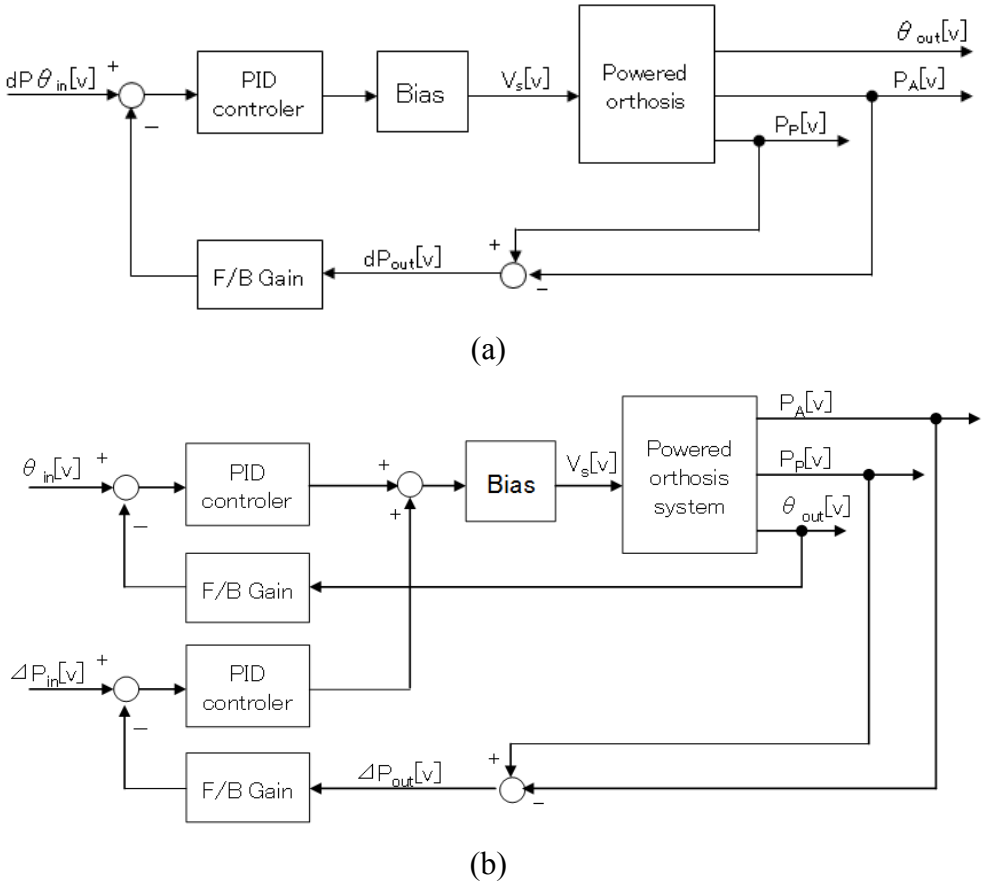

Figure 46 (a) Pressure control using conventional PID controller; and (b) position-pressure control using conventional PID controller.

Figure 47 shows the result of joint excursions for the pressure and position-pressure control using conventional PID tested WO/S. Both control schemes were only implemented mono-articular actuators to manipulate the leg orthosis. The result showed that, the leg orthosis was able to perform human walking gait motion by implementing the pressure control alone. However, the resultant hip and knee joint trajectories when tested without a subject were rather poor. Moreover, large angle deviation and time shift were also occurred during the control system. This might be due to the nonlinearity behavior of the pneumatic muscles which include of

hysteresis effects and time variances. In addition, the implementation of both position-pressure controls was also unable to improve the joint excursions of the leg orthosis due to the similar nonlinearity problems.

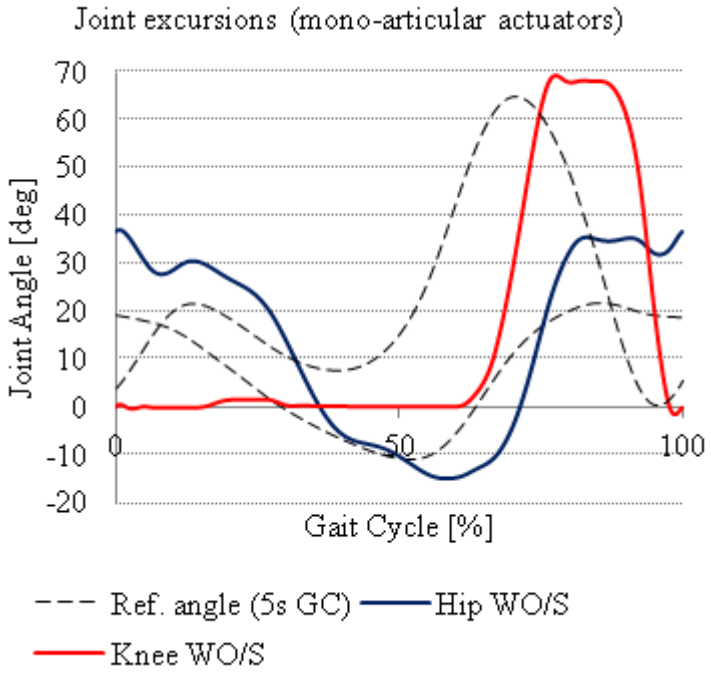

(a)

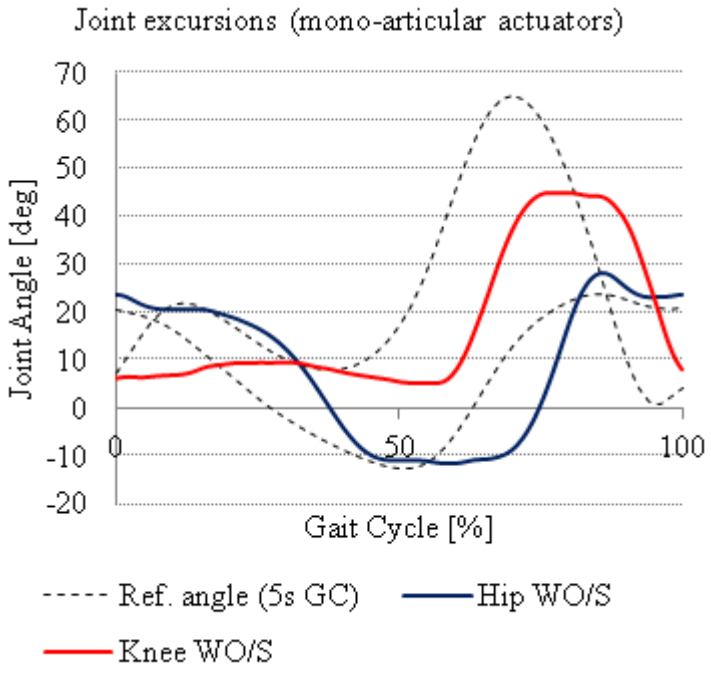

(b)

FIGURE 47 Joint excursions for; (a) pressure control; and (b) position-pressure control using conventional PID controller tested WO/S.

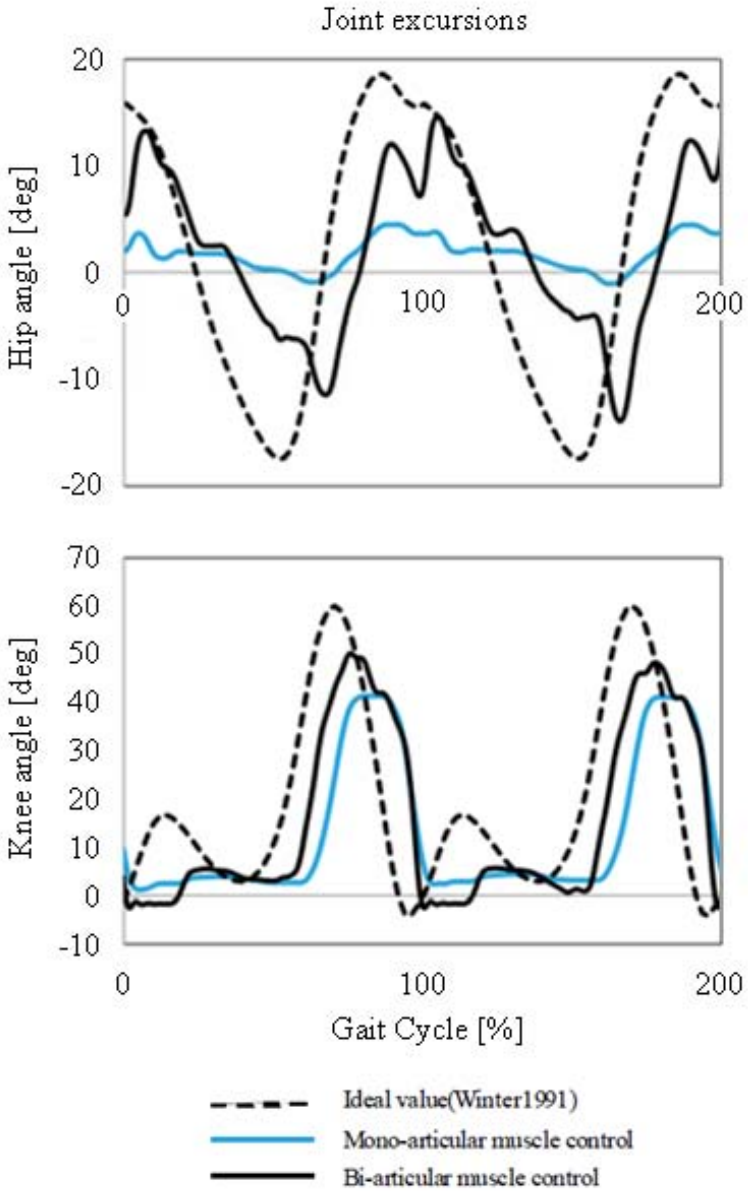

FIGURE 48 Hip and knee joint excursions for pressure control using conventional PID controller tested W/S.

Figure 48 shows the result of hip and knee joint excursions for pressure control using conventional PID controller tested W/S. There were two tests performed; the first is with mono-articular actuators; and the second is with an additional of bi-articular actuators. When the leg orthosis with a subject was driven by using the mono-articular actuators alone, the range of motion at the hip joint was decreased as compared to that of the human natural gait angle pattern. This indicated that the flexion and extension forces of the hip joint were not achieved. However, when implementing both the mono- and bi-articular actuators, the result was not as decreased compared to the mono-articular actuators alone. It seemed that addition of

the bi-articular actuators increased the range of motion by the high muscle moment, especially the hip joint moment. In this study, we tried to increase the stiffness of both the hip and knee joints by the co-contraction of agonistic and antagonistic mono-articular muscle models and to compensate for the lack of muscle moment by applying an agonistic and antagonistic bi-articular muscle model. At this point, the results of the preliminary experiment almost achieved the aim of the study. However, the timing of the angle changes for both the hip and knee angles were delayed when compared to the input data of the natural gait angle pattern. It seemed that this delay was caused by the mechanical property of the pneumatic actuator. Therefore, it is necessary to improve the control system and/or to reform the structure of the pneumatic McKibben actuator.

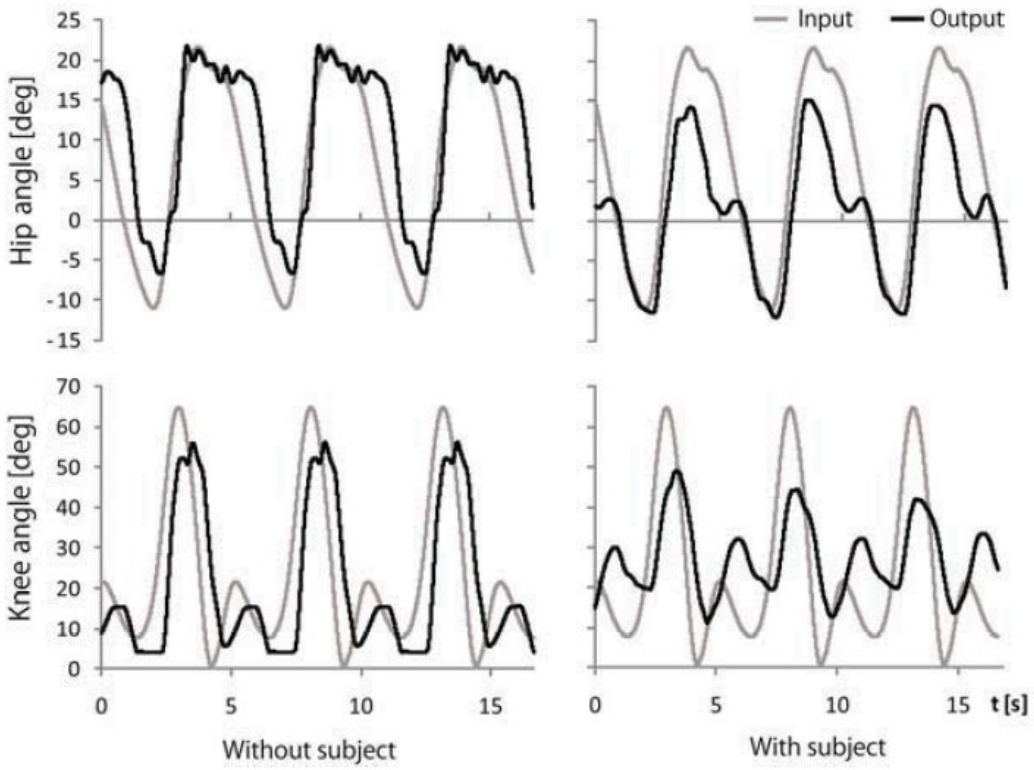

(a) (b)

FIGURE 49 Hip and knee joint excursions for position-pressure control using conventional PID controller tested WO/S and W/S.

Figure 49 (a) shows the hip and knee joint excursions data for position-pressure control using conventional PID tests without a subject. In this test, both mono- and bi-articular actuators were implemented. The result showed a pretty good gait motion was achieved when compared to the human natural gait. However, when the orthosis was driven with a subject, range of motion was decreased as illustrated

in Figure 49 (b). It seemed that flexion force of hip joint and extension force of knee joints were not satisfied. It is necessary to change McKibben actuator to larger size than the current one or tune a gain of proportional directional control valve. In this study, we have tried to increase stiffness of both hip and knee joints by co-contraction of antagonistic bi-articular muscle model. It results high stability of walking of the powered orthosis. However, the bi-articular muscles are muscles that work on two joints such as the rectus femoris and the hamstring. These bi-articular muscles drive both knee and hip joints by single command. If the bi-articular actuator is to be controlled properly, the range of motion of the orthosis might be increased when test with a subject.

Therefore, it could be concluded that by using the conventional PID based control schemes, the nonlinearity behaviors of the pneumatic muscles could not be solved. This will be required for the implementation of a suitable control system to deal with the dynamic characteristics of the pneumatic muscle. In addition, a better control strategy will also be needed in controlling the antagonistic actuators (i.e., anterior and posterior) precisely and simultaneously. In this system, the implementation of electro-pneumatic servo valve was being used to control the input pressure into the antagonistic actuators. However, due to the mechanical properties of the valve, the input pressure was controlled alternately between the anterior and posterior actuators. Thus unable to simultaneously manipulated the antagonistic actuators which leads to a poor control system performance.

6.2 Control of the Leg Orthosis WO/S: Evaluation on Mono- and Bi-Articular Actuators Position Settings using Simulated Co-Contraction Model Control Scheme

The focus of this second assessment is on the PMA settings evaluation as to determine the suitable arrangement for the antagonistic mono-and bi-articular actuators. Two tests were performed; first, with the antagonistic mono-articular actuators alone; and second, with the addition of antagonistic bi-articular actuators. The tests were evaluated at three GC speeds of 5 seconds, 4 seconds, and 3 seconds of the human walking motion. Two PMAs arrangements were considered, where the tests were performed using four different settings as can be seen in Figure 12; first, mono-articular setting (PMA setting 1); second, mono-articular setting (PMA setting

2); third, mono- and bi-articular setting (PMA setting 1); and fourth, mono- and bi-articular setting (PMA setting 2). A total of eight PMAs GCs were performed for the tests and data related to the trajectory of the joints were then gathered. The average GC for each GC speed was measured and represented in a graph.

Figure 50 shows the hip angle control for the tests with mono-articular actuators alone, and with the addition of bi-articular actuators, both for PAM settings 1 and 2. In addition, Figure 51 shows the knee angle control with the same PAM settings. For the hip angle control performance (Figure 50), the result shows that, we are not able to achieve the maximum muscle moment (flexion) by using the mono-articular PMA actuators alone. However, when we tested the control system with the addition of bi-articular PMA actuators, there is an improvement in hip angle control for both of the tests with PMA settings 1 and 2. Moreover, the performance for the knee angle control also shows an improvement as can be seen in Figure 51. The result shows that we are not able to achieve the maximum muscle moment (flexion) and unable to get smooth heel contact movement at knee joint by using the mono-articular PMA actuators alone. However, when we implement the gait training system with the addition of bi-articular PMA actuators, we were able to achieve the maximum knee angle extension as well as smoother movement during the heel contact position for both PMA settings.

The evaluation of range of motion of the joint angles between the antagonistic mono- and bi-articular actuators showed that, bi-articular pneumatic muscle has a wider range of motion and are able to generate a greater force. As a result, this enables the orthosis system to achieve the high muscle moment which cannot be obtained by using mono-articular actuators alone. The addition of bi-articular actuators works as a muscle support system that provides the orthosis system with greater actuation power and smoother movement at the joints including the heel contact position. When we consider the result of the hip and knee angles (with addition of bi-articular PMA s), its range of motion is sufficient to simulate the human's walking motion with little time delay. In the single support phase of the gait cycle 10-30 [%], sufficient bending at the knee joint was achieved during the heel contact movement which is difficult to obtain using mono-articular PMA actuators alone for both PMA settings. However, if we try to shorten the gait cycle and time delay, the inertia effect becomes evident. In addition, if we compared the results of the leg orthosis controls based on simulated co-contraction model, it could be said

that its performance was far exceeded than the performance of the leg orthosis controls using conventional PID. This could be concluded that, the co-contraction control strategy was effective in handling the nonlinearity of the system.

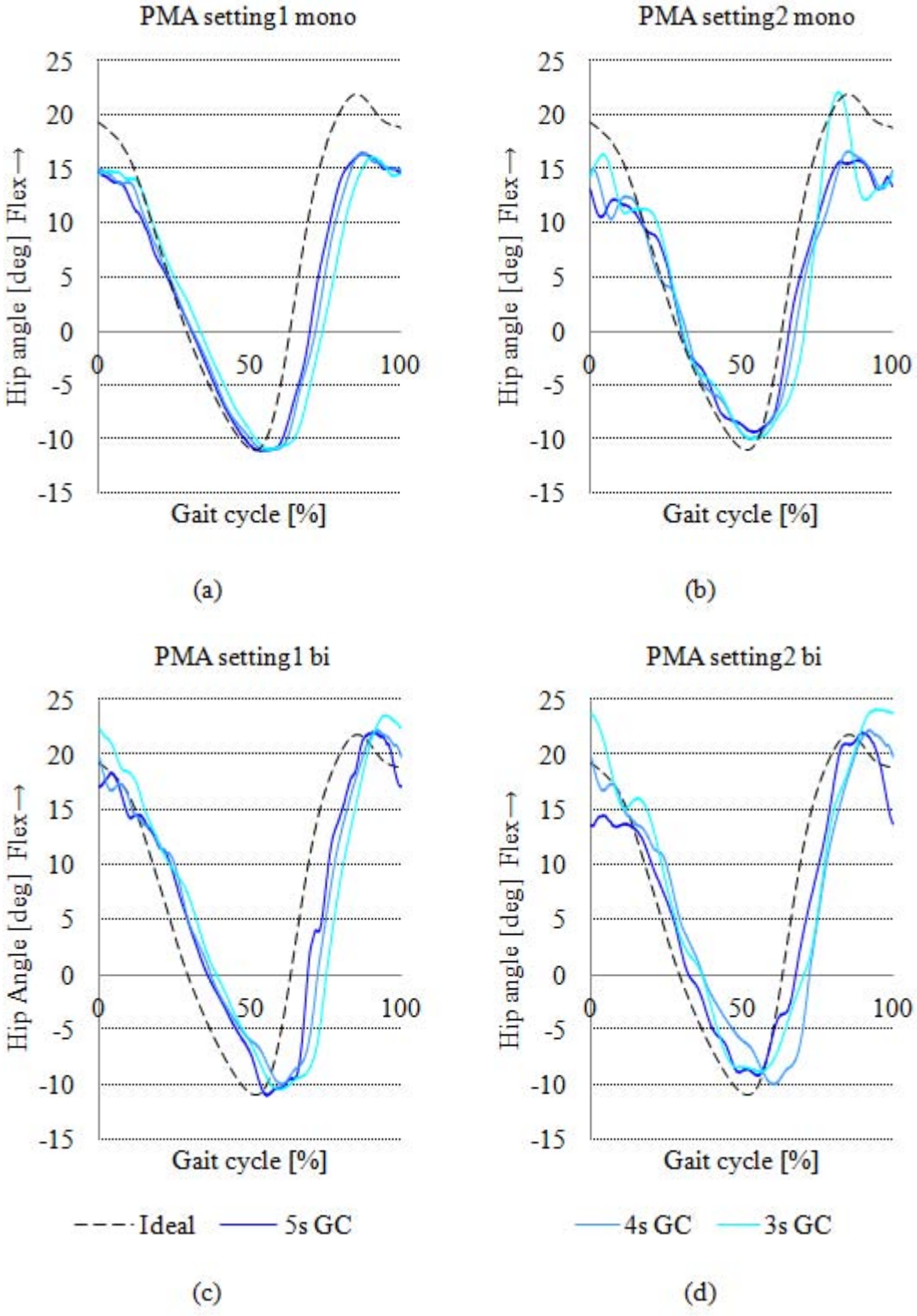

FIGURE 50 Hip joint excursions for co-contraction model controller scheme based P controller using MATLAB simulation.

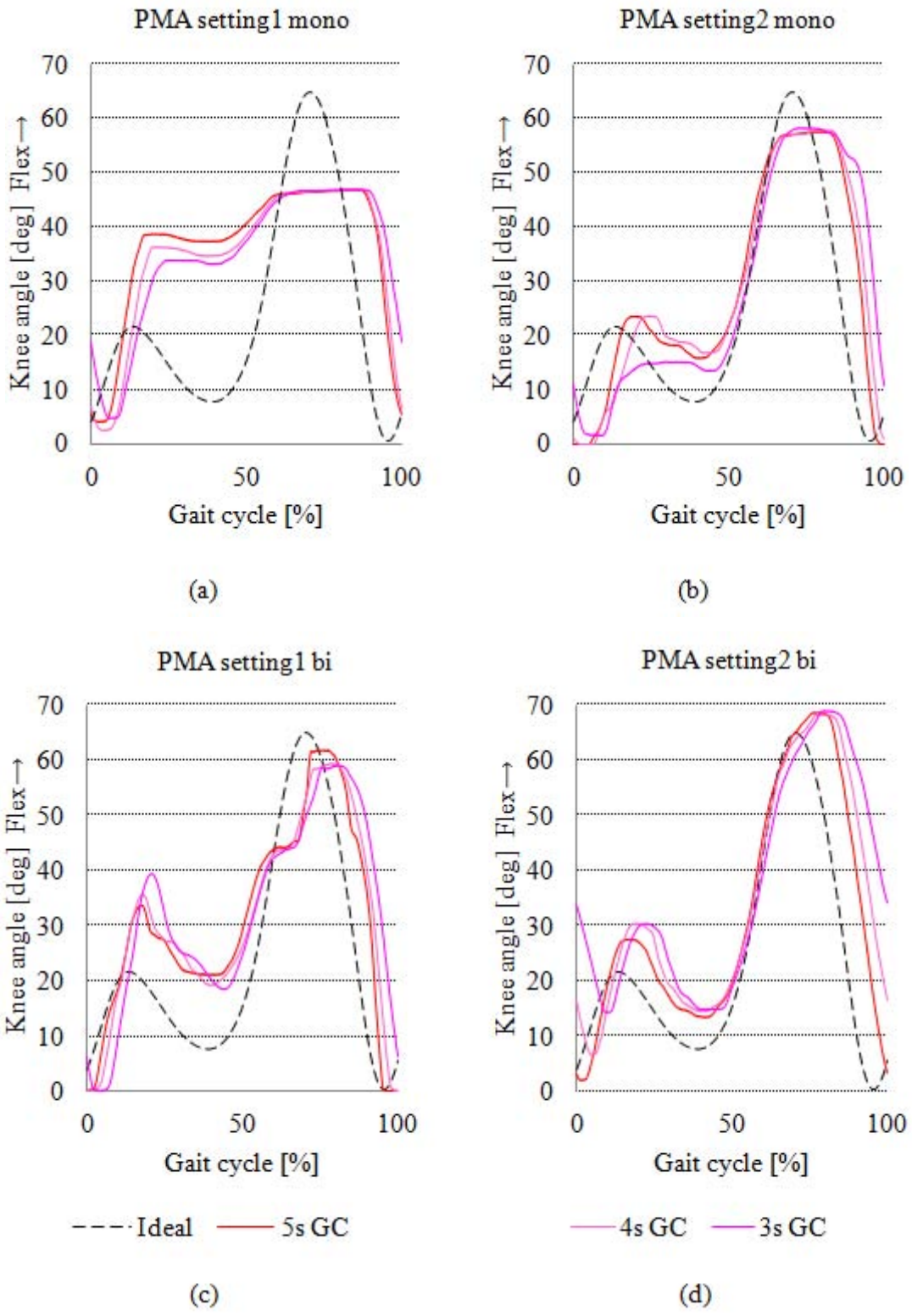

FIGURE 51 Knee joint excursions for co-contraction model controller scheme based P controller using MATLAB simulation.

6.3 Control of the Leg Orthosis WO/S: Evaluation between the Simulated and Derived Co-Contraction Model Control Scheme

The focus of this third assessment is on the evaluation of co-contraction model using the MATLAB simulation and the derived mathematical formulation to control the mono- and bi-articular actuators of the leg orthosis. It was conducted to determine the performances of the derived mathematical model when compared to the simulated model. Two tests were conducted, and both tests were using all six antagonistic actuators. The first was the controls of leg orthosis using simulated co-contraction model tested WO/S; and the second was the controls of leg orthosis using derived co-contraction model WO/S. These tests were evaluated at three GC speeds of 5 seconds, 4 seconds, and 3 second. Data related to the joints' trajectory of the leg orthosis were then gathered. The average GC for each GC speed was measured and represented in a graph.

Figures 52 (a) and 52 (b) show the hip and knee joint's trajectory for the controls of AIRGAIT exoskeleton's leg orthosis using simulated co-contraction model and derived co-contraction model control schemes. The results showed that both simulated and derived mathematical models were able to generate sufficient co-contraction and pressure patterns to manipulate the antagonistic mono- and bi-articular actuators at all evaluated GC speed of 5 seconds, 4 seconds, and 3 seconds. Based on the hip and joint excursions performance evaluation, it showed that the derived co-contraction model was proved to be much better in tackling the nonlinearity behaviour of the pneumatic muscle compared to the simulated co-contraction model. This could be explained because; the simulated co-contraction model control scheme was directly controlling the antagonistic actuators' input pressure of the leg orthosis. However, in the derived co-contraction model control scheme, the feedback control was purposely design to control the muscle activation level parameters (β and α) which manipulate the contraction patterns of the antagonistic actuators before the pressure patterns were determined. This shows that, the manipulation of the co-contraction model plays a significant role in the control strategy implementation for the controller scheme. Therefore, it can be concluded that, the co-contraction control strategy was able to adapt and reduce the nonlinearity effect of the pneumatic muscle such as hysteresis and time variance. In addition, the stiffness and the stability of the leg orthosis was also improved.

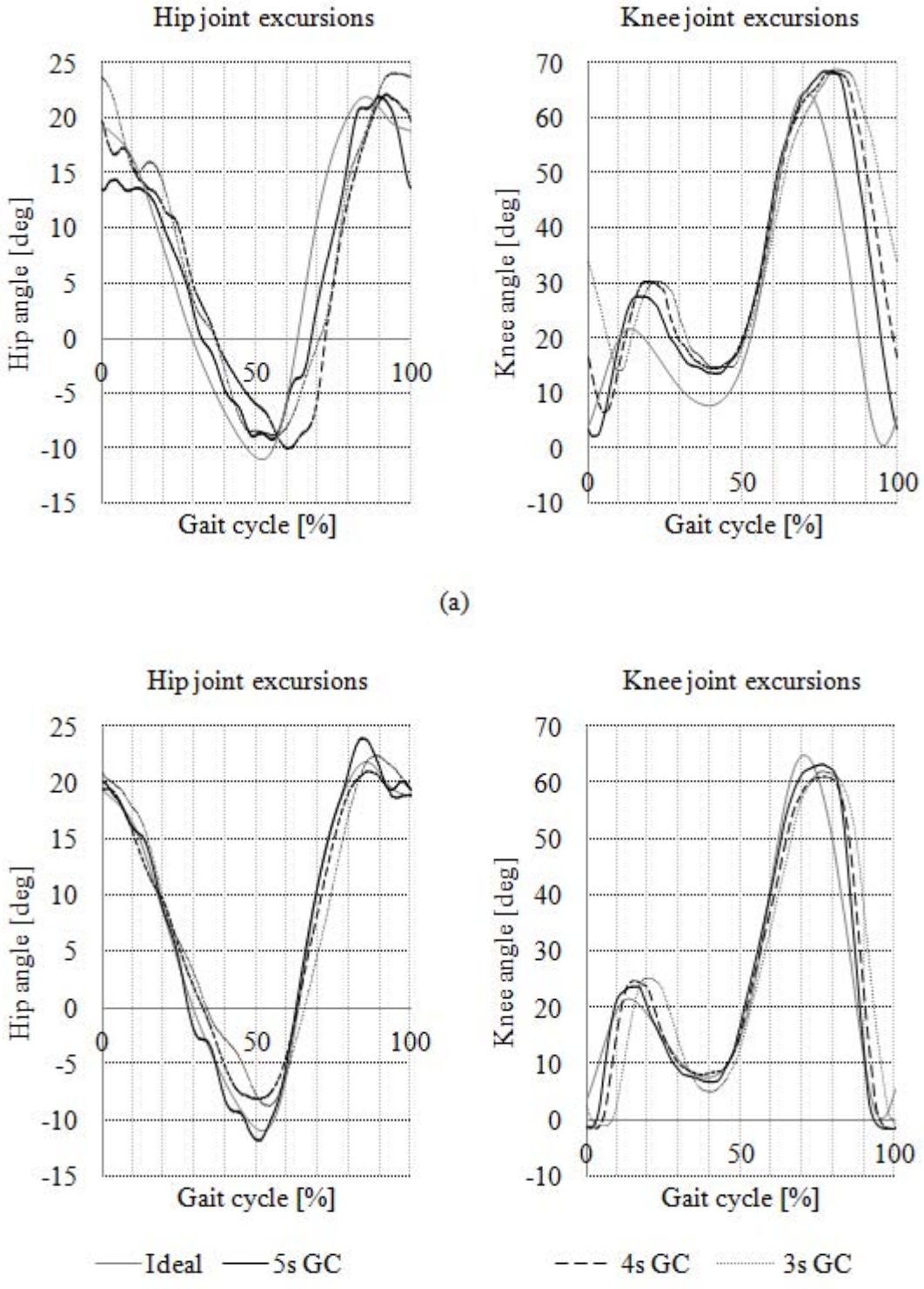

FIGURE 52 Hip and knee joint excursions for co-contraction model controller scheme based on; (a) simulated, and (b) derived co-contraction model control scheme.

6.4 Control of the Leg Orthosis WO/S: Evaluation on Antagonistic Mono- and Bi-Articular Actuators using Co-Contraction Model Control Scheme

The focus of this fourth assessment is on the implementation of co-contraction input patterns to control the mono- and bi-articular actuators of the exoskeleton of the AIRGAIT leg orthosis. It was conducted to determine the limitations when using mono-articular actuators alone and the advantages to be gained with the inclusion of bi-articular actuators. Two tests were conducted. The first using the mono-articular actuators only (i.e., hip and knee joints) tested WO/S; and the second with the addition of bi-articular actuators tested WO/S. These tests were evaluated at four GC speeds of 4 seconds, 3 seconds, 2 seconds, and 1 second so as to raise the stakes of the design controller and the appraisal of the strategy by increasing the GC speed. A total of 25 GCs were performed for each GC speed including the initial position cycle and data related to the trajectory of the joints were then gathered. The average GC for each GC speed was measured and represented in a graph.

Figure 53 and 54 show the trajectories evaluation of the joints of the leg orthosis controls between two settings (i.e. mono-articular actuators only, and with the inclusion of bi-articular actuators) tested WO/S using a co-contraction model control scheme. Based on the four GC speeds evaluation, it is evident that the leg orthosis was able to perform the gait motion smoothly up to a GC speed of 2 seconds. For the GC speeds of 4 seconds, 3 seconds, and 2 seconds, the orthosis displayed the complete gait motion (i.e., heel strike, foot flat, middle swing, and wide swing) by implementing the designed controller scheme. With the increments in GC speed, the time allocated for completing one GC will be reduced as the graph shifted forward. However, even with the forward shifting of the graph, the time delay in the system was only approximately 0.2 seconds for each GC speed.

For the control of leg orthosis using mono-articular actuators alone, it was expected that the trajectory of the joints will be slightly coarse due to the nonlinearity behaviour (i.e. compressible and hysteresis) of the PMA. Although this result may suggest that mono-articular actuators alone are able to support the orthosis, it must be noted that this evaluation was conducted WO/S. The situation changes during implementation W/S as the weight attributed to the actuators is increased. When the inertia and gravitational effect are included in the equation, the limitations of mono-articular actuators acting alone become evident as each actuator is only capable of

sustaining a pressure level of 5 [bars]. Moreover, due to the position of the antagonistic actuators, the length of mono-articular actuators is much shorter than those of bi-articular actuators. This reduces the maximum angle extension the joints can achieve especially at the knee where a much wider movement (63 degree) is required compared to the hip. This maximum angle extension is the maximum value of reference angle of the hip and knee joints, both the anterior and posterior sides. This value can be referred from David A. Winter, "Biomechanics and motor control of human movement", fourth edition, John Wiley & Sons, Inc., 2009 [118]. However, with the introduction of the bi-articular actuators, the coarse movement was reduced and the stiffness at the joints was improved due to the significant force exerted by these actuators. Manipulators that equipped with bi-articular actuators have been proved to have numerous advantages such as (1) dramatically increase in range of end effectors, (2) improvement of balance control, (3) efficiency increase of output force production, and (4) an arm that equipped with bi-articular actuators have the ability to produce a maximum output force at the end effectors in a more homogenously distributed way [93 - 95].

Even though the sources of the actuation system were different, the fundamental function of these bi-articular actuators (PMA) should be similar. With a stable force been assisting the movement of the leg orthosis, it reduces the coarse movement and improved the joints when compared to the leg orthosis actuated by the mono-articular actuators alone. The movement of the antagonistic bi-articular actuators was able to balance the coarse movement of the antagonistic mono-articular actuators at the joints thus reducing the effect of the hysteresis which was significant when implementing the mono-articular actuators alone WO/S. This is also due to the fact that the contraction of the PMA is in accordance with the hysteresis model. However, as the expansion of the PMA did not follow that of the hysteresis model, the co-contractive movements between the antagonistic mono- and bi-articular actuators were realized. At the GC speed of 1 second, the orthosis was not able to perform the gait motion completely with the heel strike stance. However, it was still able to demonstrate the 'foot flat up to swing stance' which provides the feel of a gait motion. By implementing the derived co-contraction model, all the six antagonistic mono- and bi-articular actuators were able to operate simultaneously and co-contractively. In overall, the derivation of co-contraction model was not only able to be effectively manipulated the antagonistic mono-articular actuators (i.e., hip and

knee joints). However, it is also could be implemented to generate sufficient input data of contraction and pressure patterns for manipulating the antagonistic bi-articular actuators.

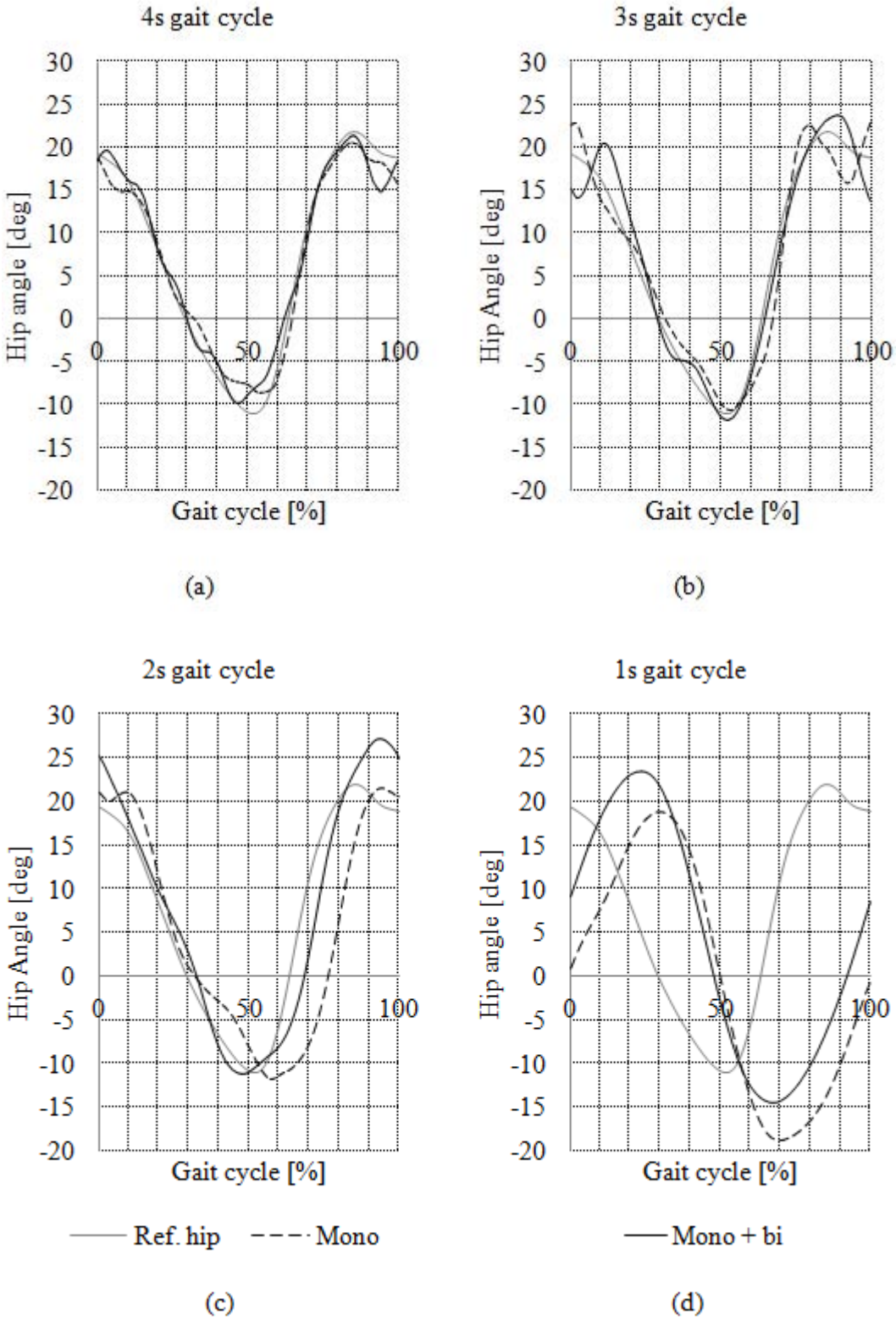

FIGURE 53 Hip joint trajectories for the control of the leg orthosis WO/S using a co-contraction model control scheme.

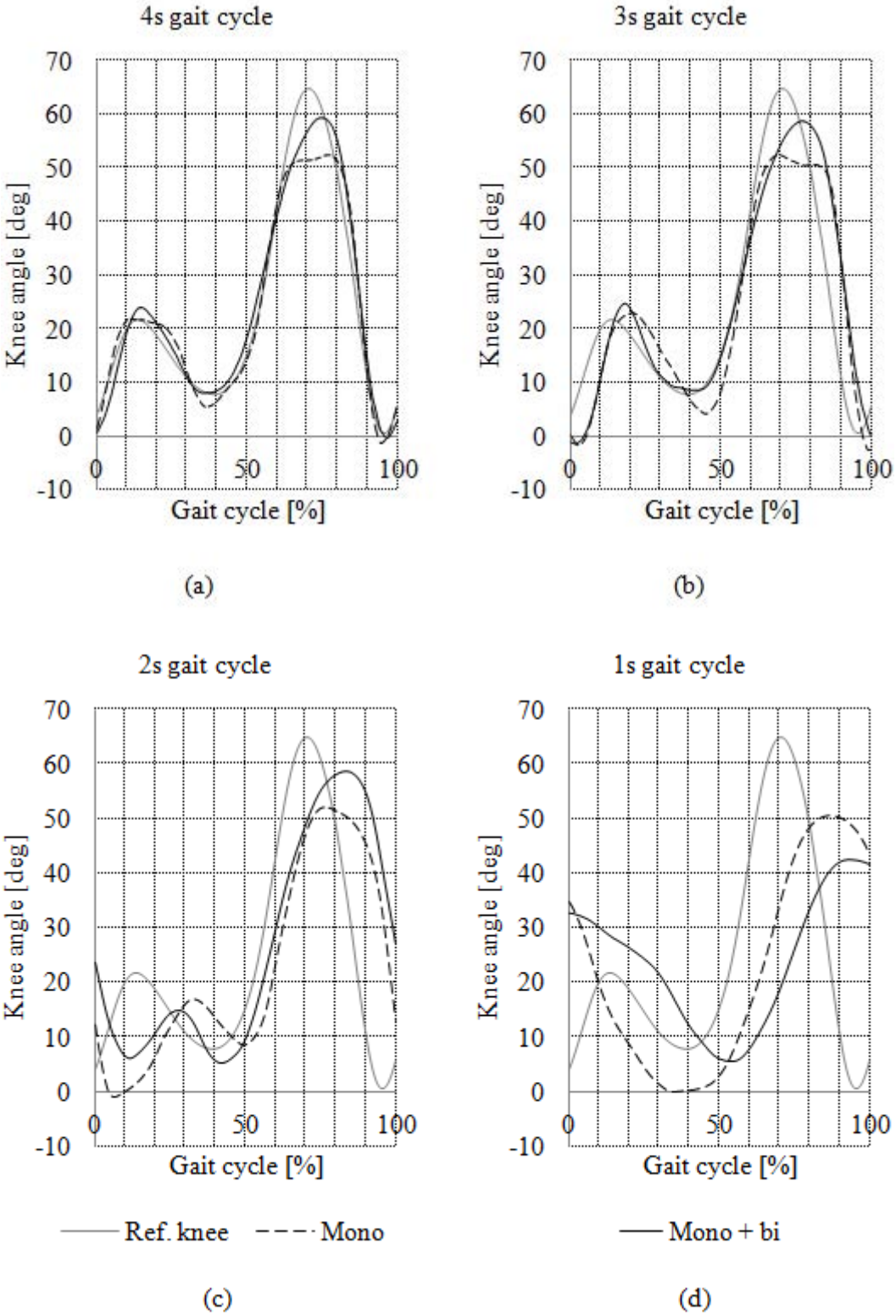

FIGURE 54 Knee joint trajectories for the control of the leg orthosis WO/S using a co-contraction model control scheme.

TABLE 12 Pearson coefficient of determination (r^2) for mono-articular actuators alone and with addition of bi-articular actuators.

Pearson coefficient of determination (r^2) for mono-articular and bi-articular actuators								
Joint actuators	Hip angle				Knee angle			
	4s GC	3s GC	2s GC	1s GC	4s GC	3s GC	2s GC	1s GC
Mono-articular actuators	0.8834	0.7921	0.3969	0.2500	0.7569	0.4761	0.1764	0.0225
Mono- and Bi-articular actuators	0.9025	0.8281	0.7744	0.0576	0.7569	0.4900	0.1444	0.1296

Table 12 shows the Pearson coefficient of determination (r^2) for the first assessment where the control tests with mono-articular actuators (hip and knee joints) alone and with addition of bi-articular actuators WO/S were evaluated. This r^2 value indicates how well the data fits the reference joints' trajectory. The result shows that the addition of the bi-articular actuators produce much higher r^2 coefficient values at most GC speeds as compared to mono-articular actuators alone.

6.5 Control of the Leg Orthosis W/S: Attributes in Implementing Antagonistic Mono-Articular with an Addition of Bi-Articular Actuators

In the previous study of AIRGAIT exoskeleton, the proportional directional control valve was used to actuate the antagonistic mono-articular actuators and applied a constant pressure to the bi-articular actuators. The operating condition for the valve will regulate the air pressure between its two ports. Due to the limitation of this mechanical system, they did not able to actuate the antagonistic mono and bi-articular actuators in a co-contraction movement, but simply alternating it between anterior and posterior actuators. The resulting performance was rather poor. However, in this research, one regulator for each actuator is used to replace the previous control system, which makes it possible to control the antagonistic muscle actuators in a co-contraction movement. When implementing the formed equations, it shows that the position of PMAs to the joints (r) and initial length (l_o) does not affect the muscle contraction pattern of the antagonistic mono- and bi-articular actuators. The study shows that the muscle contraction pattern of posterior and anterior PMAs follows the pattern of the positional data itself but only differs in gain value based on the posterior and anterior muscle activation levels (β and α).

The focus of this fifth assessment is to evaluate the actuators' limitation when operating the leg orthosis W/S using the mono-articular actuators alone, and with addition of bi-articular actuators. It was conducted to determine the maximum GC speed the leg orthosis will be able to operate when using mono-articular actuators alone and the advantages to be gained with the inclusion of bi-articular actuators. Two tests were conducted; the first using the mono-articular actuators only (i.e., hip and knee joints) tested W/S; and the second with the addition of bi-articular actuators tested W/S. These tests were evaluated at five GC speeds of 5 seconds, 4 seconds, 3

seconds, 2 seconds, and 1 second in increasing GC speed order as to consistently raise the stakes of the evaluation.

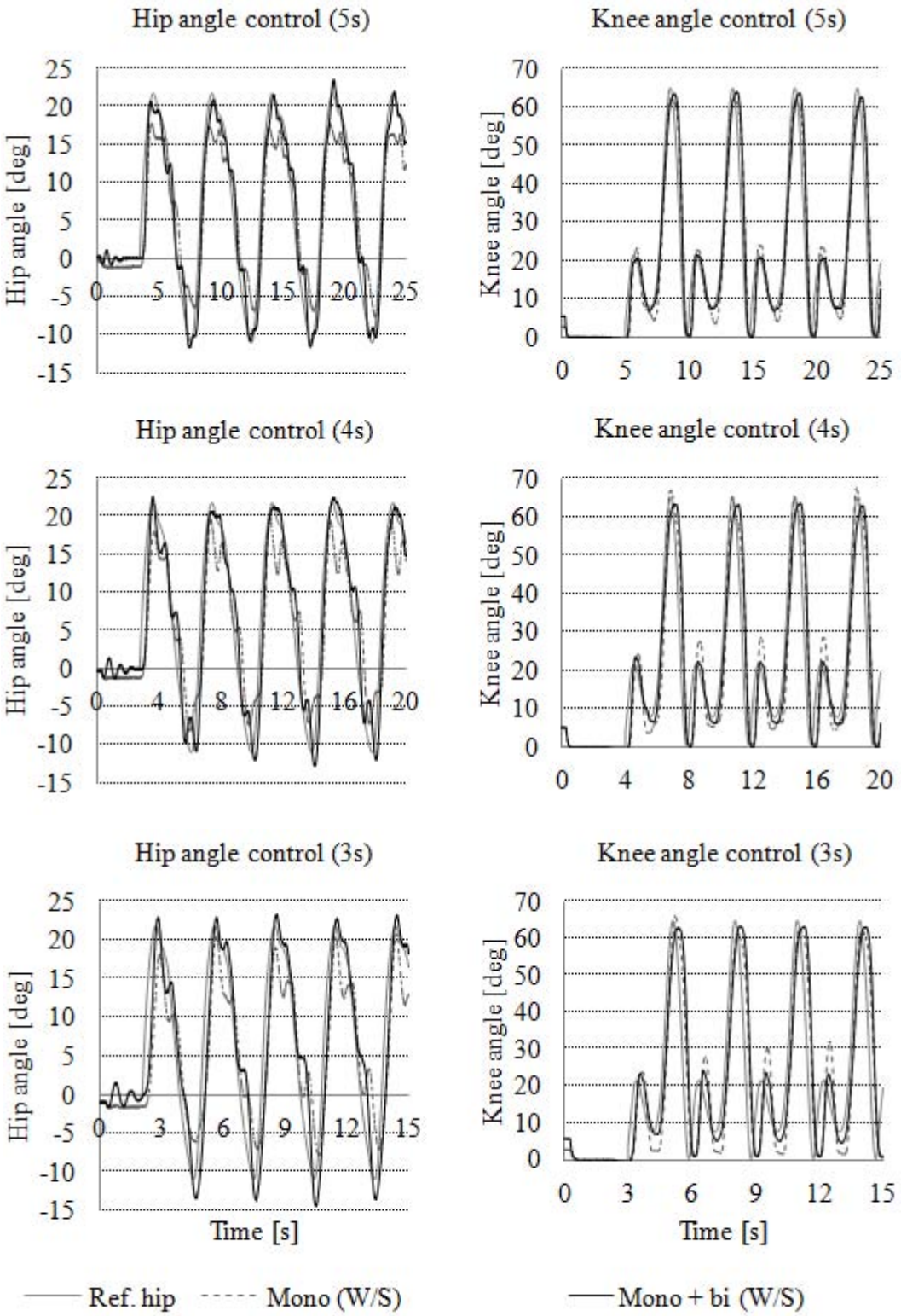

FIGURE 55 Hip and knee joint trajectories at different GC speeds of 5s, 4s, and 3s for the tests with W/S using mono-articular alone and with addition of bi-articular actuators.

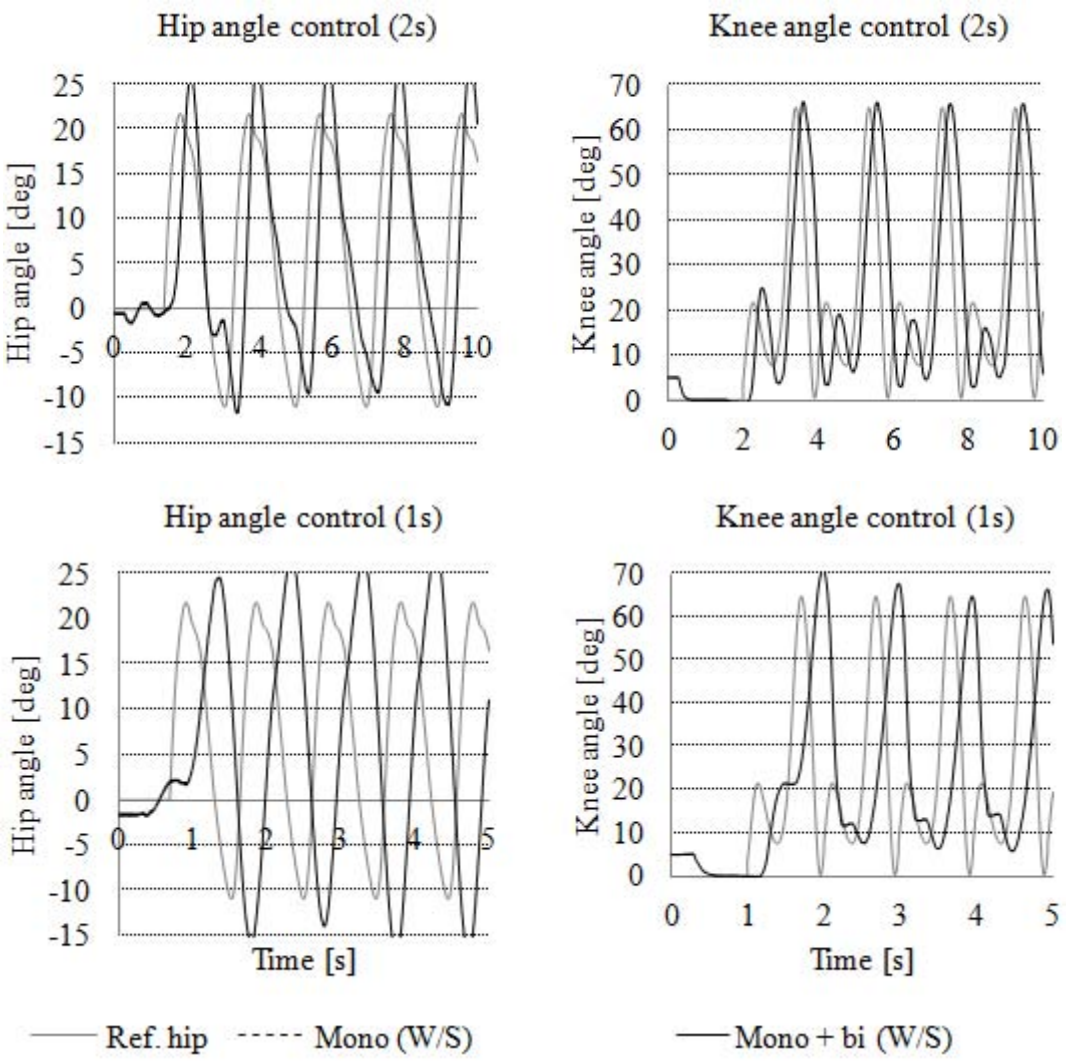

FIGURE 56 Hip and knee joint trajectories at different GC speeds of 2s, and 1s for the tests with W/S using mono-articular alone and with addition of bi-articular actuators.

Figure 55 and 56 show the results for the hip and knee joint angles control on different gait cycles for the tests using mono-articular actuators alone, and with the addition of bi-articular actuators. For the gait cycle time of 5 seconds, 4 seconds, and 3 seconds, both control tests are conducted on a healthy test subject, (W/S). The gait training system was able to perform good motion without much time delay and was able to follow the hip and knee angle patterns by using the developed contraction model. However, by implementing the mono-articular actuators alone, the system was not able to perform a smooth motion at the hip joint and heel contact positions (knee joint) due to lack of actuation power and inertia. To resolve the lack of actuation power from the mono-articular actuators, greater force from a PMA can be obtained by increasing its diameter size. However, this will affects its compressibility which is reduced with the increment of the PMA diameter size due to the McKibben

muscle actuator's limitation. On the contrary, with the addition of bi-articular actuators to the system, we were able to get a smooth motion at the hip joint and heel contact positions as well as achieving maximum muscle moment (flexion and extension) at hip and knee joints. By implementing these bi-articular actuators into the system, we managed to improve the lack of actuation power at the hip joint, and solving the problems caused by inertia. This result shows that the introduction of bi-articular PMA into a mono-articular PMA model was able to give good control performance and smooth motion at the hip and knee joints respectively. The contraction model which enables the antagonistic mono-articular and bi-articular actuators to move in a co-contraction movement in the control system also plays a major role in ensuring the precise motion at the hip and knee joints.

Based on the result, it shows that the lapse at the hip joint for the test using mono-articular actuators is around ±5º. This requires a bigger diameter antagonistic mono-articular PMA at the hip joint for better results. However, by implementing bi-articular actuators into the mono-articular actuators model, maximum muscle flexion and extension required at the hip joint were achieved with a lapse of ±1º up to 3s gait cycle. Furthermore, when the controller is tested for faster gait cycle of 2s and 1s, the mono-articular actuators alone were not able to withstand the external force generated from the AIRGAIT's inertia, and caused the PMA to break loose from the clamp before the 3 second mark. With the addition of bi-articular actuators, the system was able to distribute the external force generated from the inertia effect equally to the mono- and bi-articular actuators which enables the system to operate at a much faster gait cycle up to 1 second. However, it is at the cost of little time delay and extended movement of the hip and knee joints' excursion due to inertia.

6.6 Control of the Leg Orthosis WO/S: Evaluation on Designed Controllers using Derived Co-Contraction Model Control Scheme

The focus in this sixth assessment is on the evaluation of the designed controllers using derived co-contraction model control scheme. It was conducted to determine the limitations of the position (P) based control when acting on its own, and the superiority of the combined position-pressure (PP) based controls. Two experiments were conducted. In the first, the co-contraction model based P controller scheme was

tested WO/S, and in the second, the co-contraction model based PP controller scheme was tested WO/S. Both tests were performed with the presence of mono- and bi-articular actuators and evaluated at different GC speeds of 4 seconds, 3 seconds, 2 seconds, and 1 second. Five trials were performed for each GC speed, and each trial consisted of five cycles including the initial cycle position. Thus, a total of 25 GCs were obtained for each GC speed. The average GC for each GC speed was then determined and illustrated in a graph.

Figure 57 shows the trajectory evaluation of the joints of the leg orthosis controls between two designed control schemes (i.e. P control based co-contraction model and PP controls based co-contraction model) tested WO/S. From the results, it is evident that both designed controller schemes were able to wholly achieve the gait motion smoothly up to a GC speed of 2 seconds. However, failure to perform a complete gait motion was experienced at a higher GC speed of 1 second. These results reveal that PMA muscle activities (i.e., contraction, expansion, and response time) were curtailed at a GC speed above 2 seconds as the time allocated for completing the GC was drastically reduced. However, the results illustrate that the time response of the PMA muscle activity was much better with the implementation of the PP controller scheme compared to only the P controller scheme. Furthermore, the PP controller scheme was able to maintain the maximum angle extension achieved at the posterior side of the hip joint trajectory for all GC speeds compared to the P controller scheme (reduced with increase in GC speed) as can be seen in Figure 57 (a) of hip joint trajectories. PMA controls were insufficient with the P controller scheme alone as the dynamic characteristics of PMA include pressure activity. Table 13 shows the Pearson coefficient of determination (r^2) for the second assessment where the control tests for P and PP controllers of leg orthosis with mono- and bi-articular actuators WO/S were evaluated. The result shows that the addition of the pressure controller (PP) produces much higher r^2 coefficient values at all GC speeds as compared to position controller alone (P).

Through the introduction of a co-contraction model based PP controller scheme with modified design architecture, the maximum angle extension and time response of the system were improved at most GC speeds. This indicates that the addition of the pressure controller was able to improve the response time of the system as the pressure increased exponentially with the contraction of PMA consequently increasing the speed of PMA muscle activity during contraction mode.

Based on the results, the trajectory of the joints was slightly coarse at slower GC speeds (i.e. 4 seconds, and 3 seconds) as unlike the extension of the joint, the leg orthosis goes against the gravitational effect during the flexion of the hip joint. However, this effect was reduced with an increase in GC speed at the cost of insignificant angle extension. Conversely, only slight effects were detected in the knee trajectory for both controller schemes as the high muscle moment was larger at the hip joint compared to the knee joint.

When implementing the PP controller scheme, the maximum angle extension at the posterior side of the knee joint trajectory was slightly reduced with the improvement in PMA muscle activity response time. This is due to the maximum contraction achievable by each PMA (30% of its original length) which results in a limitation of orthosis movements. The speed of PMA muscle activity will reduce considerably with the approach of its maximum contraction. This affects the trajectory performance of the joints especially at the posterior side of the knee joint which requires a larger angle extension (63 degree).

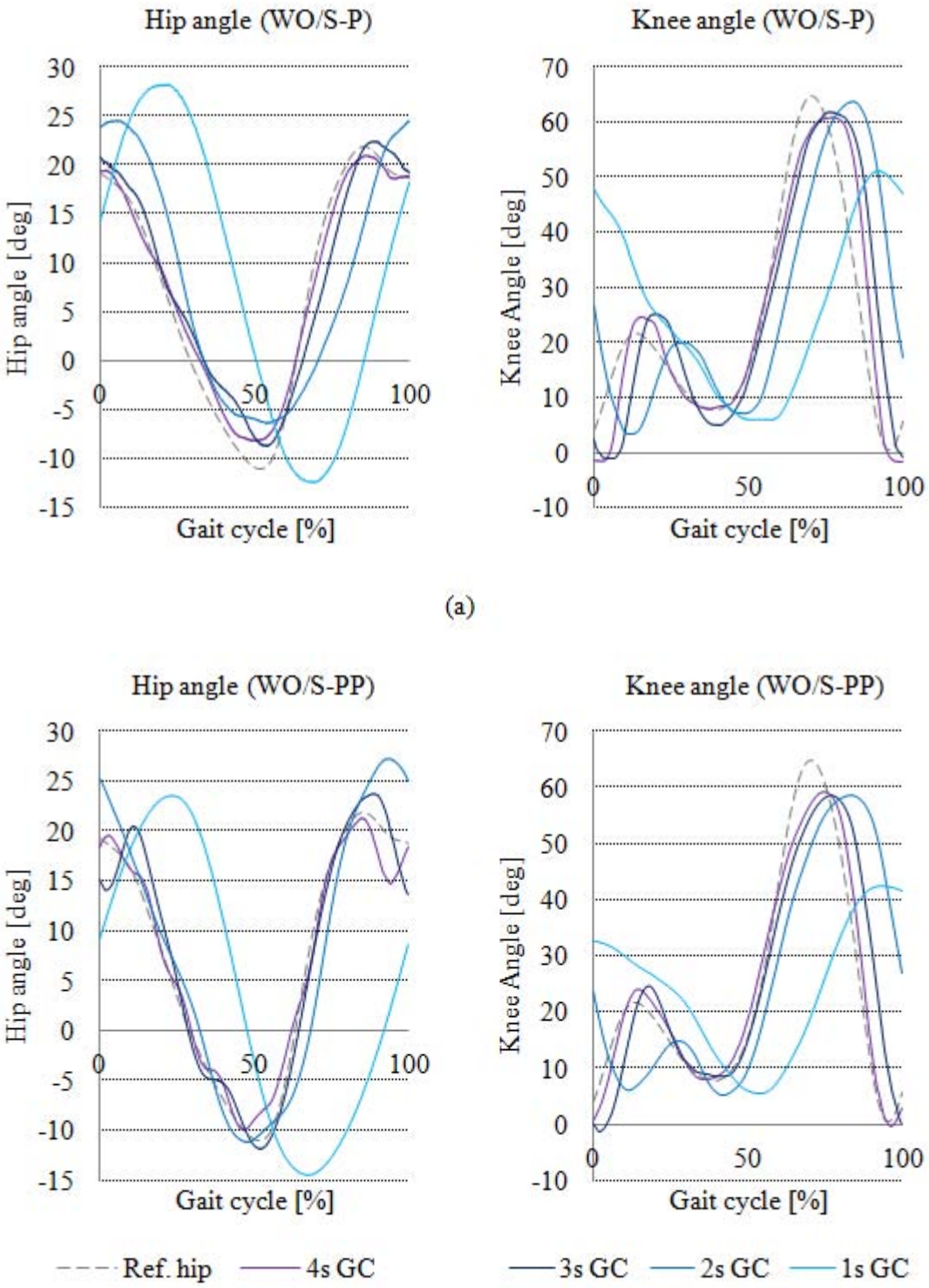

FIGURE 57 Joint trajectories of the leg orthosis controls between two designed control schemes tested WO/S; (a) P controller, and (b) PP controller.

TABLE 13 Pearson coefficient of determination (r^2) for co-contraction model based P and PP controllers.

Pearson coefficient of determination (r^2) for P and PP controllers								
Co-contraction model based	Hip angle				Knee angle			
	4s GC	3s GC	2s GC	1s GC	4s GC	3s GC	2s GC	1s GC
P controller	0.9139	0.7921	0.4761	0.0196	0.6241	0.4356	0.0900	0.1444
PP controller	0.9274	0.8649	0.7744	0.0625	0.7744	0.5184	0.1600	0.1681

6.7 Control of the leg Orthosis W/S: Evaluation on Designed Controllers using Derived Co-Contraction Model Control Scheme

The focus in this seventh assessment is on the evaluation of the co-contraction model based P and PP controller schemes at the end point (EP) of the leg orthosis. It was conducted to determine the reliability of the designed controller schemes when implemented on leg orthosis and tested both WO/S and W/S. Two tests were conducted. The first involved leg orthosis controls WO/S and the second, leg orthosis W/S. Both tests were performed with the presence of mono- and bi-articular actuators. Similar to previous assessments, the design controller scheme was evaluated at four GC speeds of 4 seconds, 3 seconds, 2 seconds, and 1 second. The normal GC speed of 1.25 seconds was not as necessary in the early stages of the gait rehabilitation therapy as it might not be able to furnish adequate afferent input to stimulate locomotor centres. However, during the later stages of rehabilitation therapy, gait training at the normal GC speed might be required. From the viewpoint of control architects, it is important to determine the system's maximum operating GC speed for the performance evaluation. Where, the limitation of the proposed control system could be analysed. A total of 25 GCs for each GC speed was collected, and the average GC was represented in a graph.

Figure 58 and 63 display the EP trajectories evaluation of the leg orthosis controls. This evaluation was carried out using the co-contraction model based P and PP controller scheme for tests WO/S and W/S. Figure 59 - 62 shows the gait velocities of each GC speeds for test WO/S. The results revealed that both designed controller schemes were able achieve a good EP trajectory for all GC speeds of 4 seconds, 3 seconds, 2 seconds, and 1 second. Although the performance level dipped at a slower GC speed due to the inertia, good gait motion was displayed especially during the stance phase of GC for both tests up to GC speed of 1 second. The coarse movement during the swing phase might be due to the increased load supported by the mono- and bi-articular actuators which forced the actuators into contraction mode to sustain the load much longer at a slower GC speed. This created an unbalanced state which disturbed the pressure activity of the antagonistic muscle actuators. Since the time allocated for completing one cycle was reduced with increases in GC speed, the posterior mono- and bi-articular actuators that contracted were unable to receive the control information fast enough to initiate the swing phase at the knee joint. This

reduced the response time at the mid-swing phase (60 ~ 80% GC) due to the slowing down of PMA muscle activity as it approached maximum contraction.

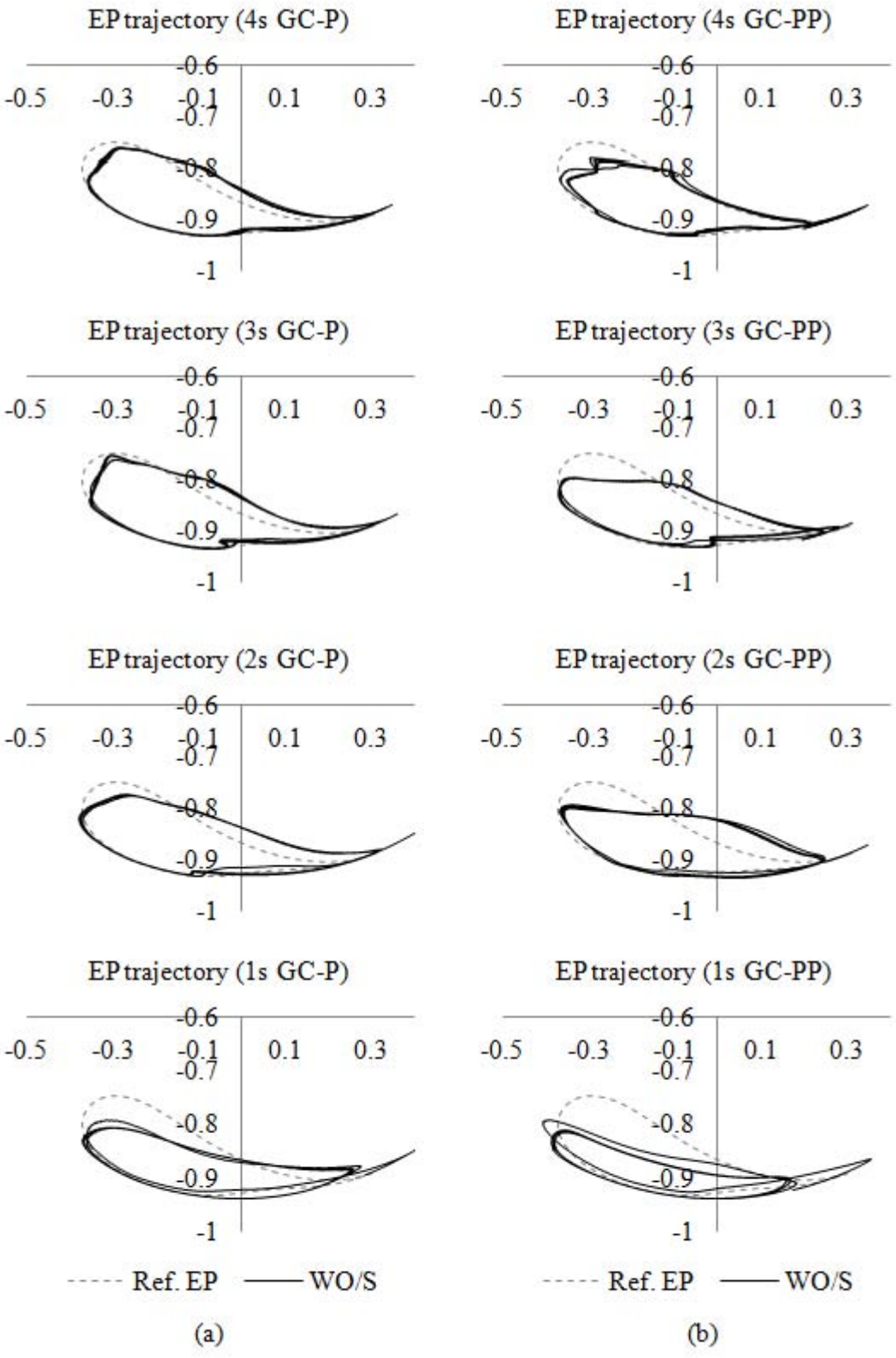

FIGURE 58 End point trajectories for the leg orthosis WO/S using co-contraction model based P and PP controllers.

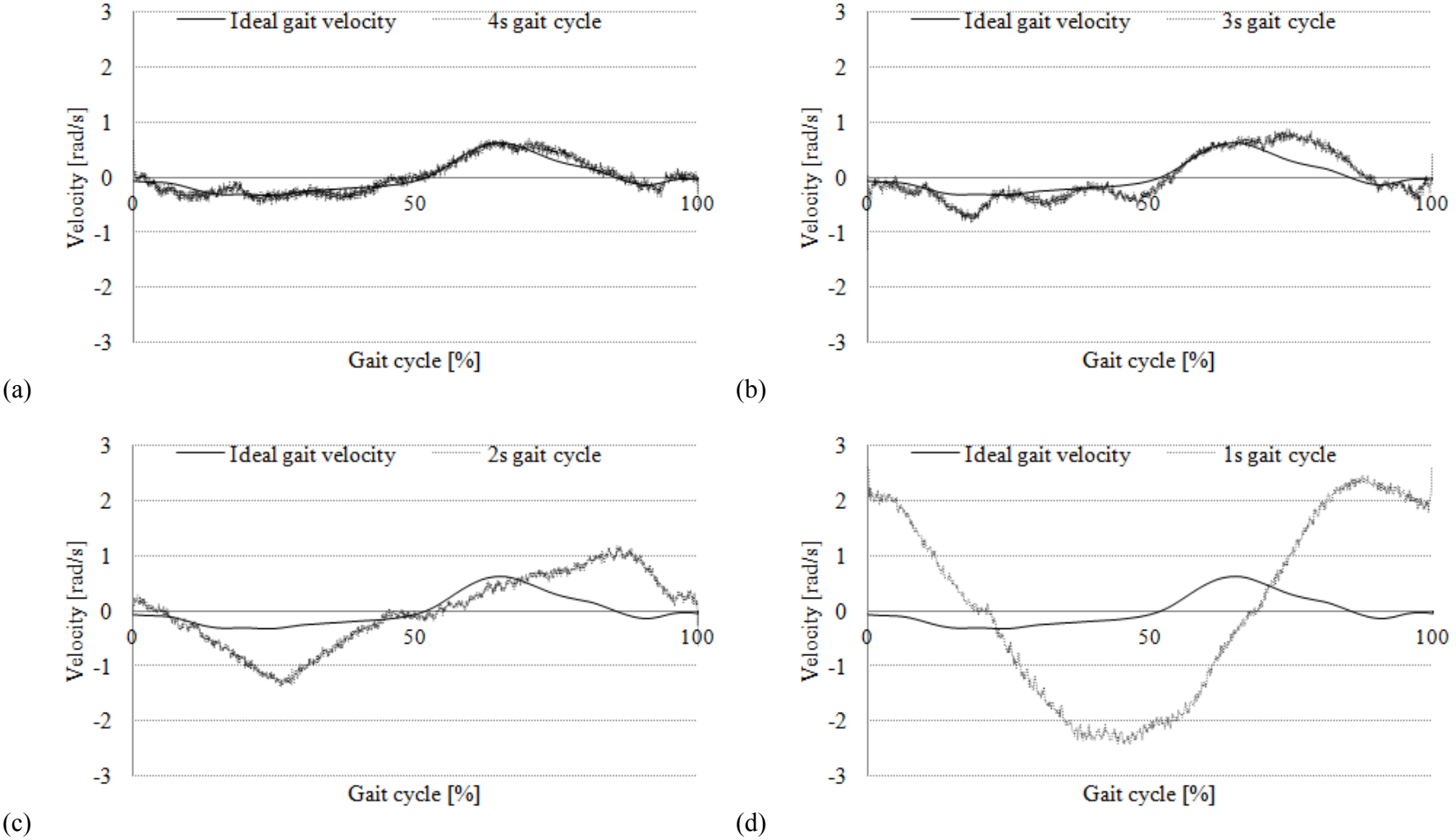

Figure 59 Gait velocity of the hip joint for the Position (P) control tests WOS at different GC speeds of 4, 3, 2, and 1 second.

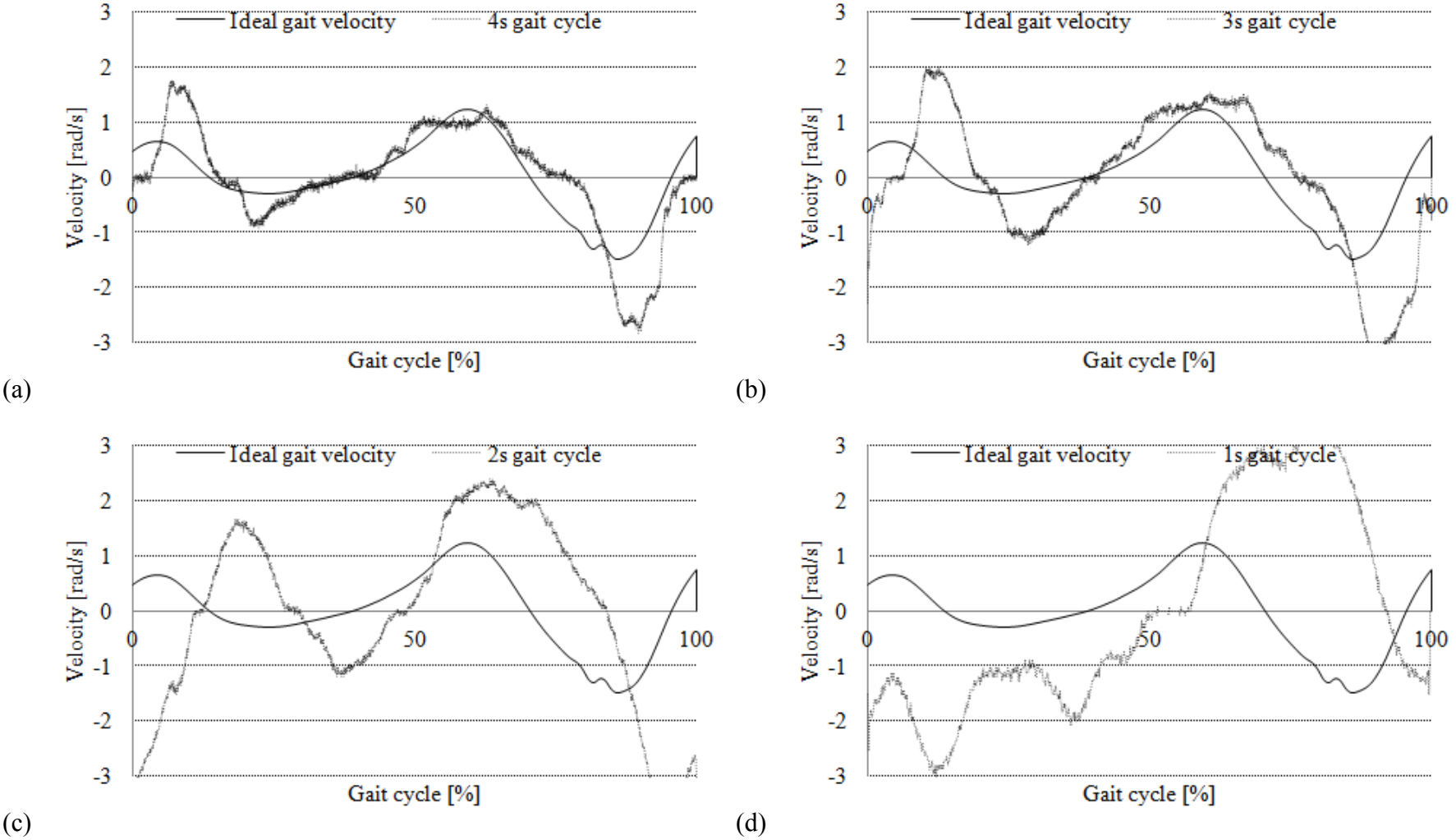

Figure 60 Gait velocity of the knee joint for the Position (P) control tests WOS at different GC speeds of 4, 3, 2, and 1 second.

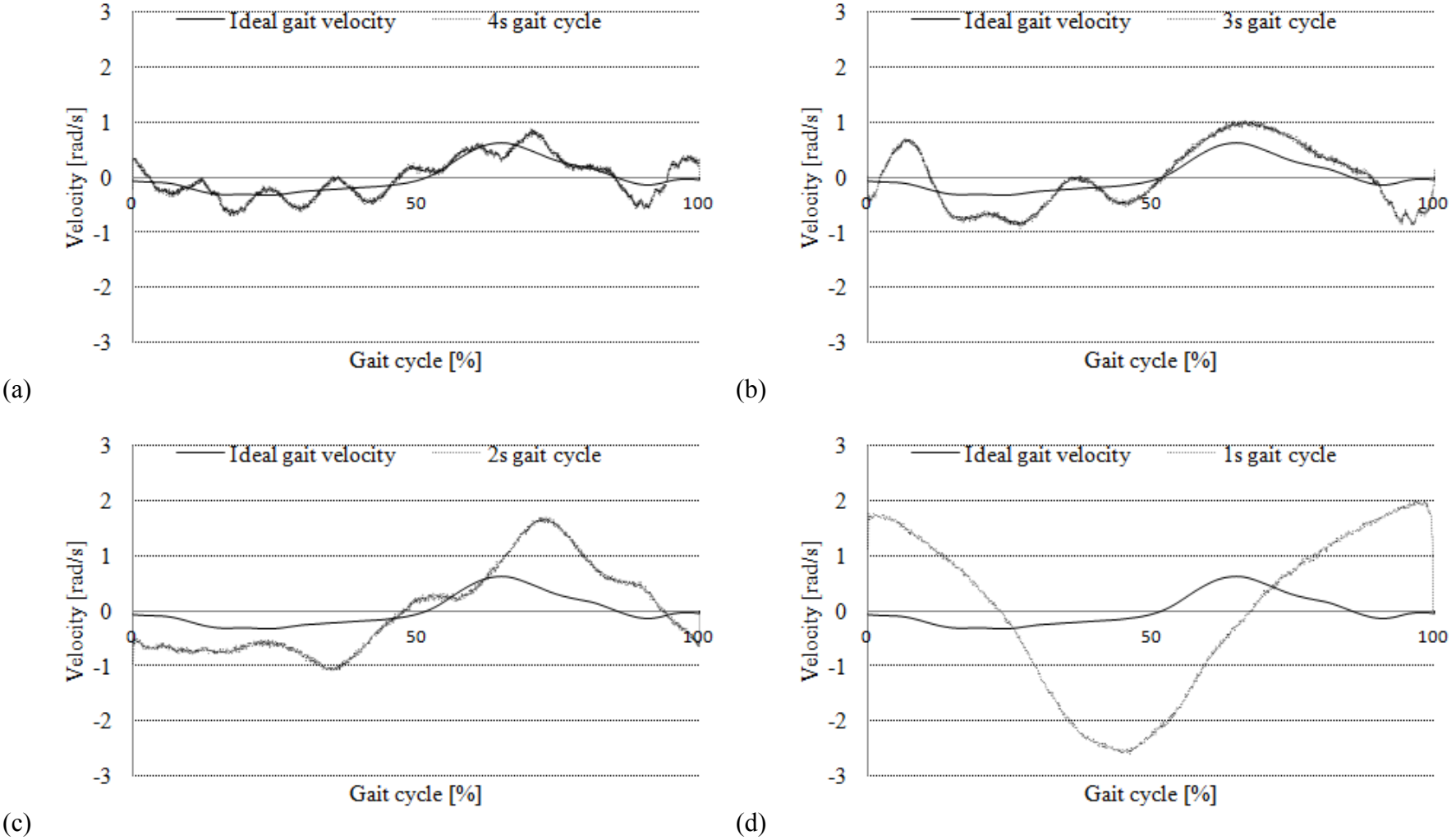

Figure 61 Gait velocity of the hip joint for the Position-Pressure (PP) control tests WOS at different GC speeds of 4, 3, 2, and 1 second.

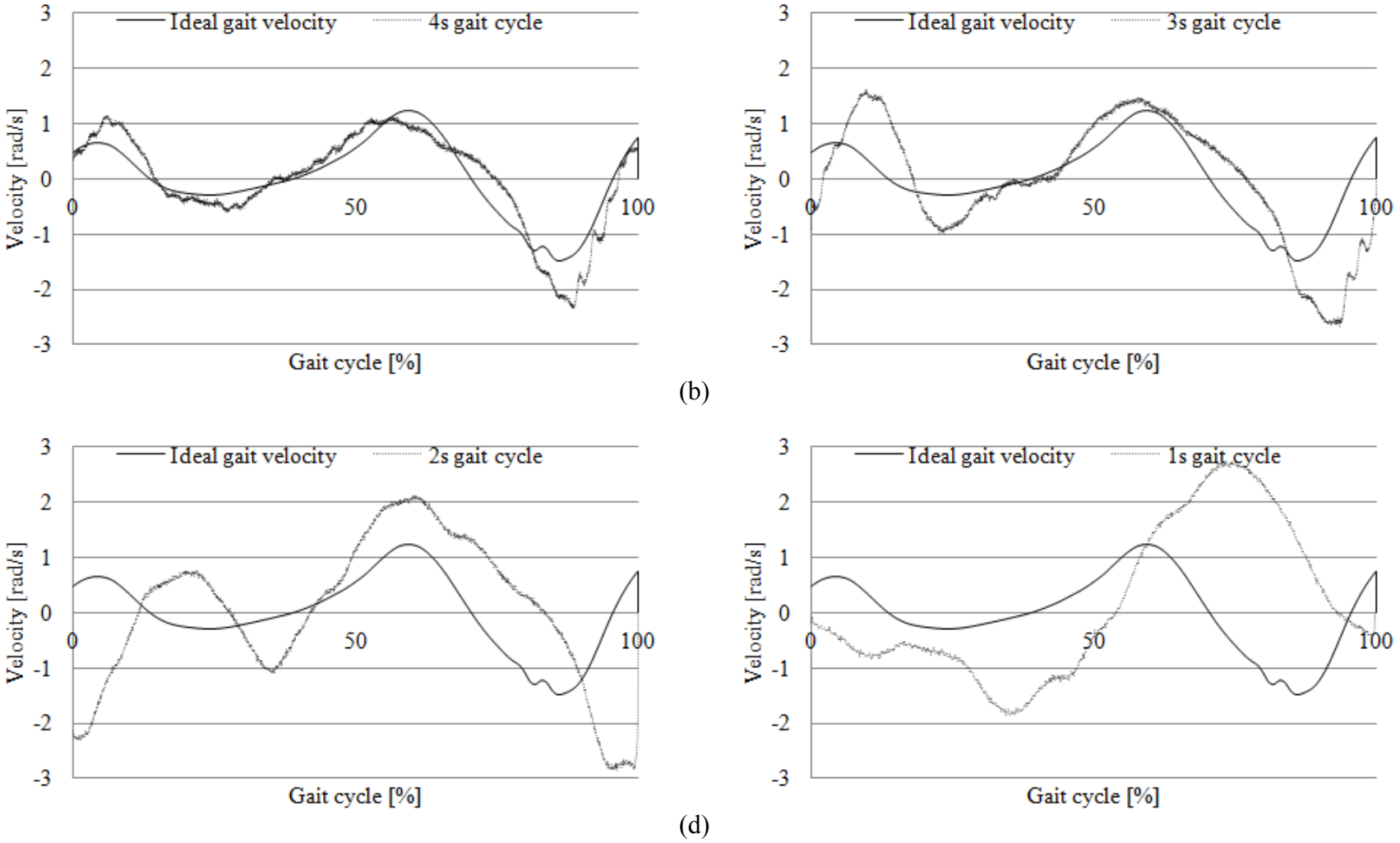

Figure 62 Gait velocity of the knee joint for the Position-Pressure (PP) control tests WOS at different GC speeds of 4, 3, 2, and 1 second.

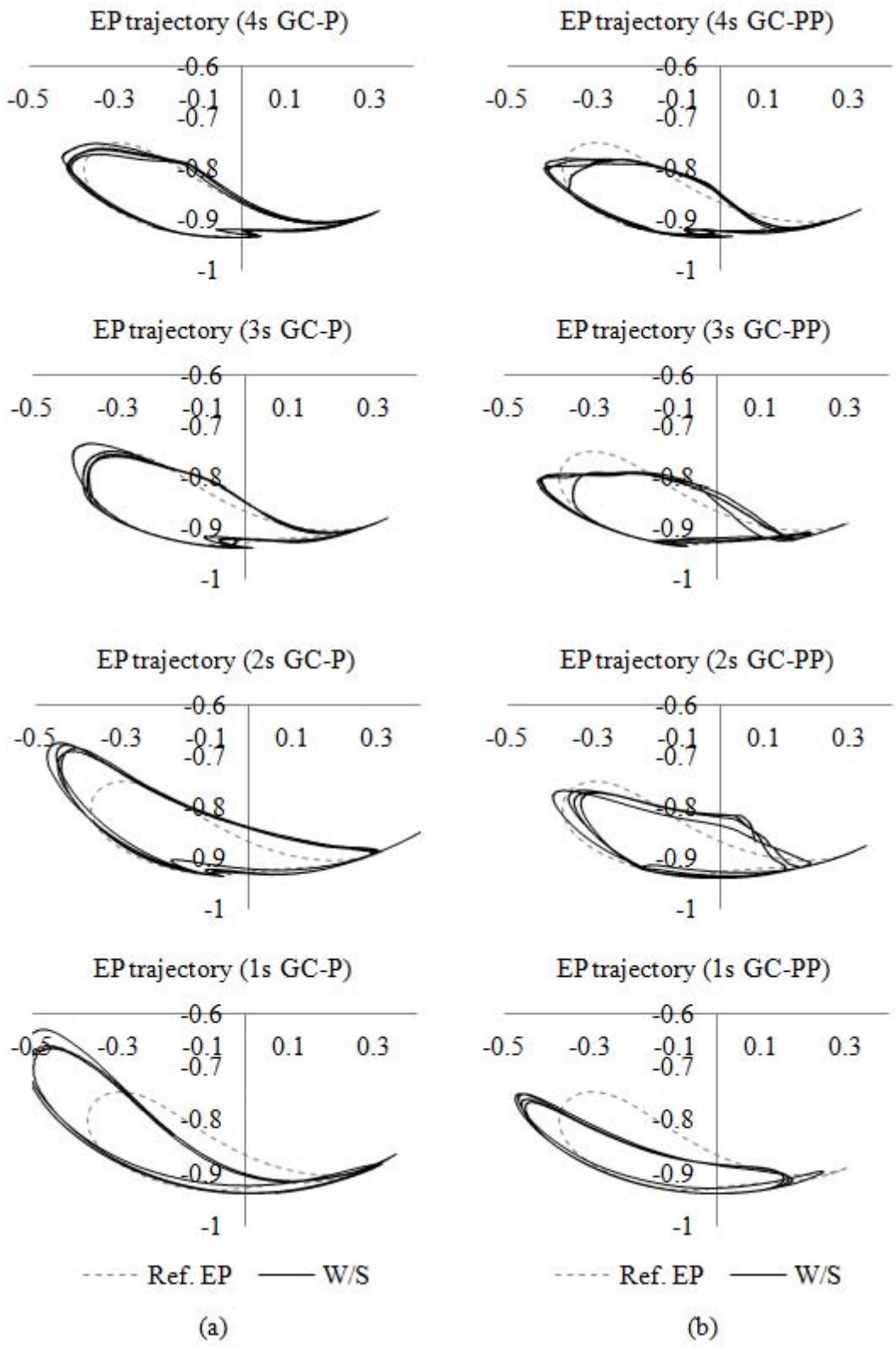

FIGURE 63 End point trajectories for the leg orthosis W/S using co-contraction model based P and PP controllers.

In addition, to increase the response time of the design controller scheme at faster GC speeds, especially during the maximum angle extension of the knee joint, the constraints related to the actuator need to be reduced. These constraints include the inability of the system's operating pressure to withstand more than 5 [bars] of maximum load. The gravitational effect also affected the gait motion performance at the hip joint during the muscle flexion (0 ~ 50% GC) as the anterior mono-articular actuators and anterior bi-articular actuators were working against gravity during the leg expansion. This "leg expansion" is the gait motion from the heel strike stance up to toe off stance. It is an observed fact that the performance of the PMA controls faltered in the face of the gravitational effect. Therefore, it might be practical to lower the muscle activation level of the actuators in expansion mode so as to reduce the gravitational effect on the orthosis. Additionally, the effect can also be reduced by increasing the PMA muscle activity and the GC speed.

To determine the performance of the design controller schemes for both WO/S and W/S tests, the evaluation will be based on the effective work and the inertia produced by the EP trajectory of the leg orthosis controls. Figure 64 shows the effective work and inertia for the control of leg orthosis for both WO/S and W/S tests using co-contraction model based P and PP controllers. It is illustrated using mean value and standard deviation. Based on the researches carried out by Sai K. Banala et al., to quantitatively determine the amount of adaptation, they implement a measure called "footpath deviation area". This area is the geometric area included between the swing phases of given foot trajectory and prescribed trajectory. The amount of area is the deviation of given trajectory from prescribed trajectory in the template [17 - 18]. By using the same principle, the effective work is defined as the area covered by the EP trajectory within the reference trajectory (inside area), while inertia is defined as the area covered by the EP trajectory outside the reference trajectory (outside area). These data (i.e. effective work and inertia) was measured as ratio of the covered area with the total reference trajectory area. It is inevitable that the inertia will eventually occurs as we tried to increase the GC speed from 4s GC (0.35m/s) up to 1s GC (1.40m/s), in which similar patterns can also be observed in [17]. Therefore, the over 60% of effective work performance was then considered as the minimum requirement to determine whether the leg orthosis was able or not to follow the reference foot trajectory. However, the total work done by the orthosis is defined as the sum of the effective work and inertia.

For the tests WO/S, both controller schemes produced nearly comparable effective work at the evaluated GC speeds of 4 seconds, 3 seconds, 2 seconds, and 1 second with 60% up to 89% of the ideal value. This effective work was reduced with the increases in the GC speed as the maximum knee angle extension achieved was reduced. However, with over 60% effective work achieved at all GC speeds; both designed controller schemes can be presumed to work properly. On the other hand, the inertia was also occurred as the EP trajectory deviated outward from the reference trajectory. This inertia will always present at every GC speeds due to the deviation. However, this inertia magnitude will varies with the increase of GC speed. Based on Figure 64 (a), it can be seen that the co-contraction model based P controller was generating much higher inertia during the controls of leg orthosis with -13% up to -54% inertia as compared to -11% up to -43% inertia using co-contraction model based PP controller at all GC speeds. With these data, the leg orthosis was then tested W/S to determine the reliability of the designed P and PP controllers using co-contraction model control scheme.

For the tests W/S, both controller schemes also produced nearly comparable effective work at the evaluated GC speeds of 4 seconds, 3 seconds, 2 seconds, and 1 second with 63% up to 85% of the ideal value as can be seen in Figure 64 (b). Moreover, this effective work was maintained with over 60% effective work achieved at all GC speed when compared to the test WO/S. On the other hand, based on the generated inertia evaluation; the inertia produced when using the co-contraction model based P controller was increasing with the increase of the GC speed, especially at the faster GC speeds of 2 seconds and 1 second. This indicates that the P controller alone was not enough to control the EP trajectory of the leg orthosis in the presence of inertia effect. However, when using the co-contraction model based PP controller, it was able to maintain the inertia produced at all evaluated GC speeds when tested both WO/S and W/S as illustrated in Figure 64 (a) and 64 (b). The generated inertia was around -13% up to -45% inertia (almost similar to the test WO/S with -11% up to -43% inertia) as compared to -15% up to -79% inertia when using P based controller scheme. This concludes that the PP controller scheme was able to correspond to the inertia effect, and thus give a more stable EP trajectory of the leg orthosis at the evaluated GC speeds. In addition, the implementation of the co-contraction model also improved the balance control of the leg orthosis between the antagonistic mono- and bi-articular actuators.

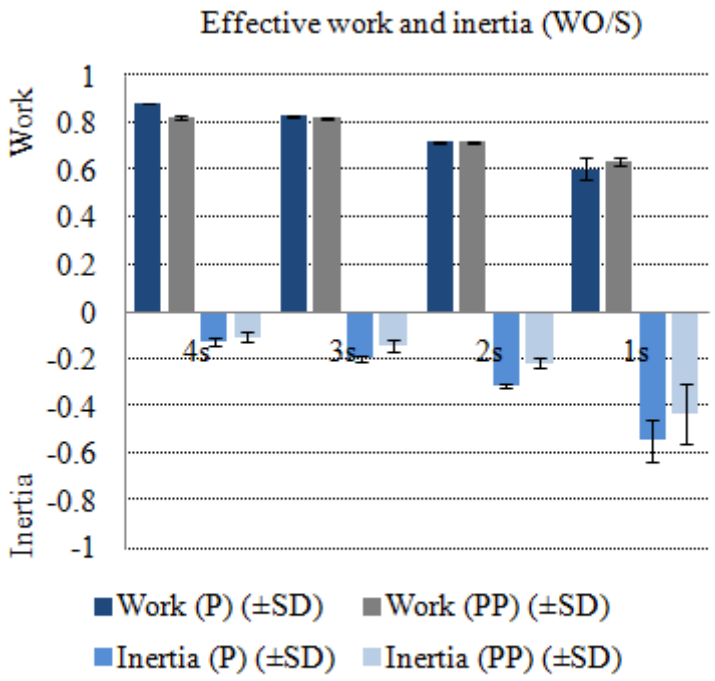

(a)

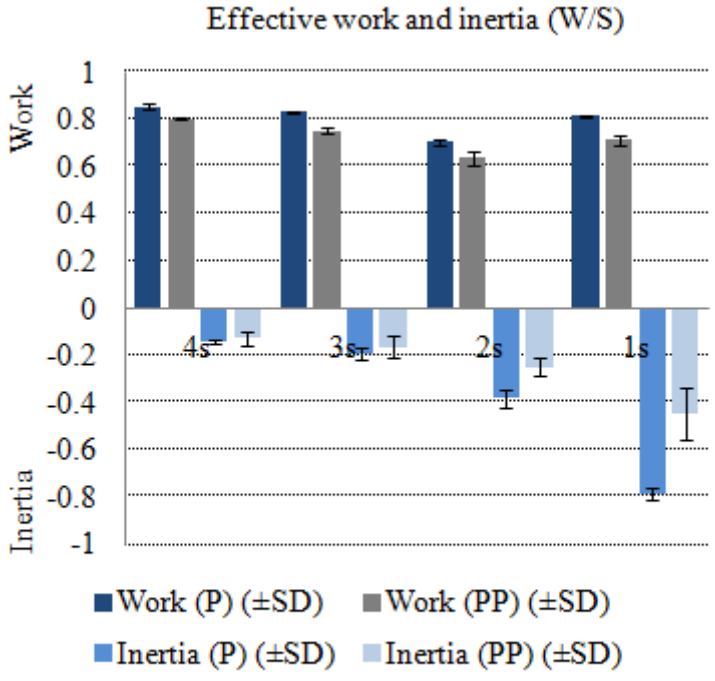

(b)

FIGURE 64 Effective works and inertia for the control of leg orthosis for both WO/S and W/S tests using co-contraction model based P and PP controllers.

6.8 Control of the Leg Orthosis WO/S: Evaluation on Antagonistic Bi-Articular Actuators Reliability Without the Presence of Knee Joint's Antagonistic Mono-Articular Actuators

The focus in this eighth assessment is on the evaluation of the improved AIRGAIT exoskeleton's leg orthosis using the L-shaped bar to replace the parallel bar at the knee joint. The test control system used was the design PP controller scheme based con-contraction model. It was conducted to determine the reliability of co-contraction model control scheme to manipulate the leg orthosis by using the bi-articular actuators without the presence of the knee joint's antagonistic mono-articular actuators to manipulate the leg orthosis and tested WO/S. This test was also performed to reduce the numbers of operating actuators. Only four actuators will be used in this experiment; where the antagonistic mono-articular actuators for knee joint were emitted from the leg orthosis to increase the evaluation on the bi-articular actuators. The new design orthosis was purposely designed as to increase the accuracy of the leg orthosis movements at the knee joint without the presence of the mono articular actuators as shown in Figure 65. The leg orthosis was evaluated at four GC speeds of 0.28m/s, 0.35m/s, 0.47m/s, and 0.70m/s. A total of 25 GCs for each GC speed was collected. Then, an average GC was measured and compared with the previous design leg orthosis controls at different GC speeds.

Figure 66 shows the hip and knee joint trajectories for the leg orthosis controls tested WO/S using developed PP controller scheme based co-contraction model. The results explained that during the test WO/S, the controls of antagonistic mono-articular actuators for hip joint and bi-articular actuators were able to demonstrate a good gait motion at all evaluated GC speeds at both hip and knee joints even when the mono-articular actuators for knee joint was emitted. This proved that, the co-contractively control of the antagonistic actuators using the designed controller scheme, was a noble ways of controlling the antagonistic bi-articular actuators. Moreover, the knee joint angle extension was also improved when compared to the previous design leg orthosis which unable to reach the maximum excursion of 63º during the middle swing motion. Figure 67 shows the end point foot trajectory for the previous and improved design leg orthosis WO/S using co-contraction model based PP controller. Based on this result, it shows that the introduction of the improved design leg orthosis which implemented only mono-

articular actuators for hip joint and bi-articular actuators was able to improve the footpath area covered during the stance and swing phases of the gait motion at all evaluated GC speeds. The effective work done by the leg orthosis was improved with over 80% of the ideal values as compared to over 60% of effective work from the previous orthosis system. However, there is still an amount of inertia that occurred due to the increases in operating GC speed. This could be improved with the improvement in the designed controller scheme either by introducing inertia model or moment model into the control system.

Table 14 shows the Pearson coefficient of determination (r^2) evaluation between the hip and knee joint trajectories for the leg orthosis controls at different GC speeds. The results showed that the r^2 coefficient values at most of the GC speeds were above 89% for both hip and knee joints angle. This is could be explained because of the smooth motion produced at the knee joint reduces the unnecessary movements generated by the antagonistic bi-articular actuators. The design improvement also increased the accuracy of the antagonistic bi-articular actuators' movement, and then enabled the knee joint's trajectory to be managed by antagonistic bi-articular actuators alone. This result might indicated that the redundancy of the actuation system could also be resolved if the controls of the AIRGAIT exoskeleton's leg orthosis can be managed using only by these four antagonistic actuators. The key to realize this would be the accurate control strategy of the antagonistic bi-articular actuators.

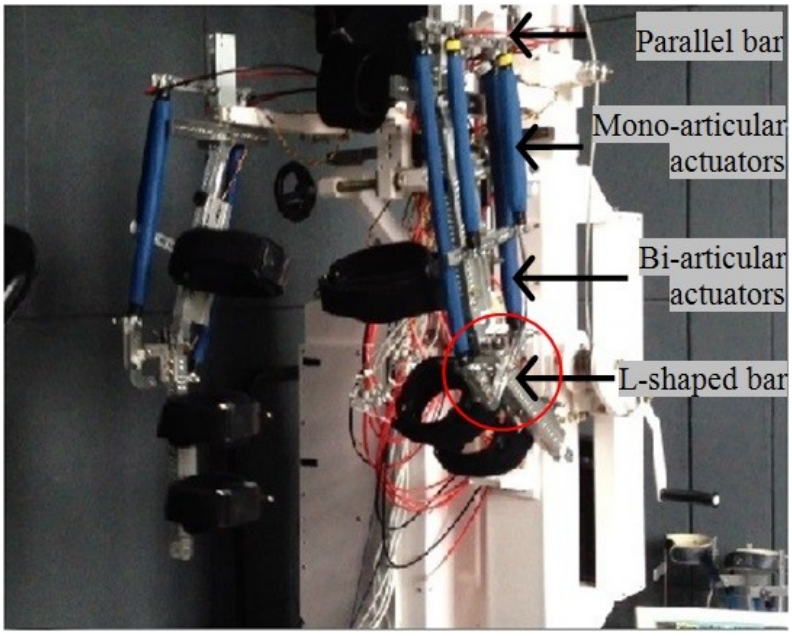

Figure 65 Leg orthosis with L-shaped bar at knee joint

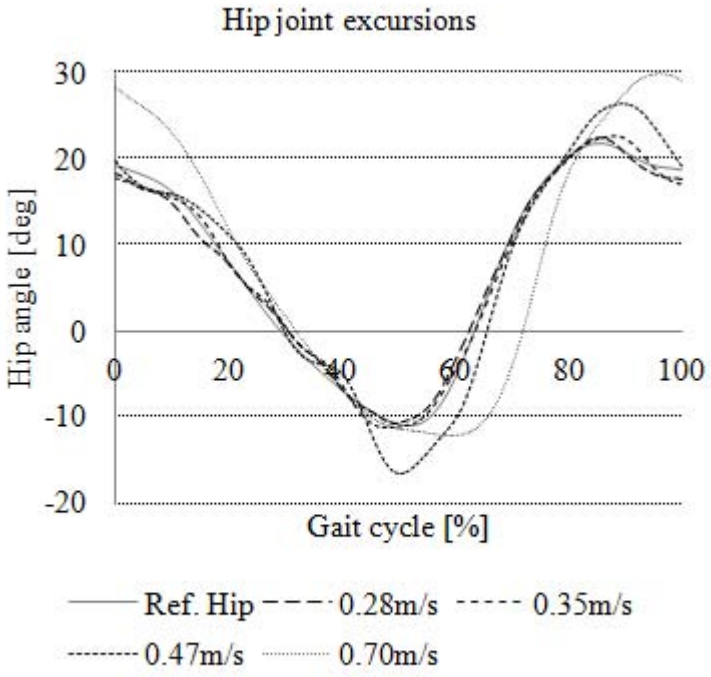

(a)

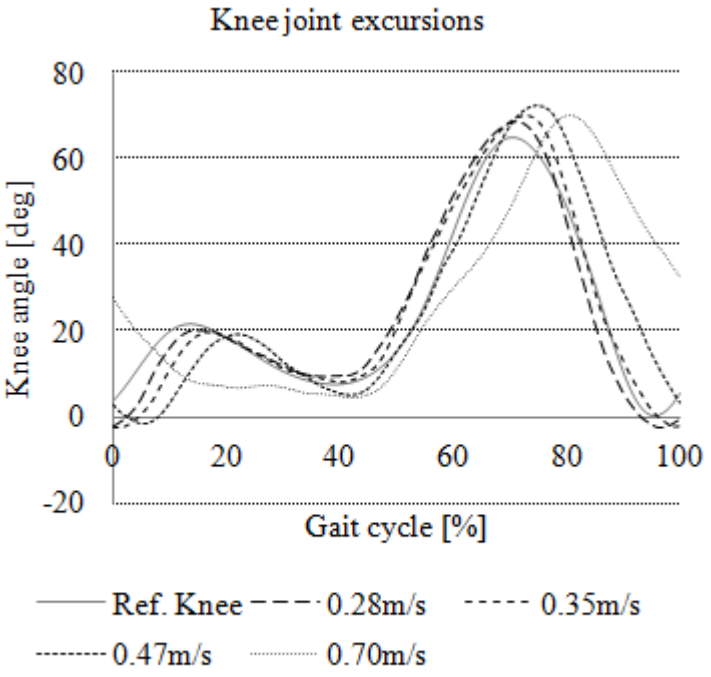

(b)

FIGURE 66 Hip and knee joints trajectories for leg orthosis controls tested WO/S using developed PP controller based co-contraction model control scheme.

TABLE 14 Pearson coefficient of determination (r^2) values for the improved leg orthosis at hip and knee joints.

Pearson coefficient of determination (r^2)				
GC speeds	0.28m/s	0.35m/s	0.47m/s	0.70m/s
Hip angle	0.9950	0.9757	0.9815	0.9107
Knee angle	0.9485	0.9343	0.8968	0.4541

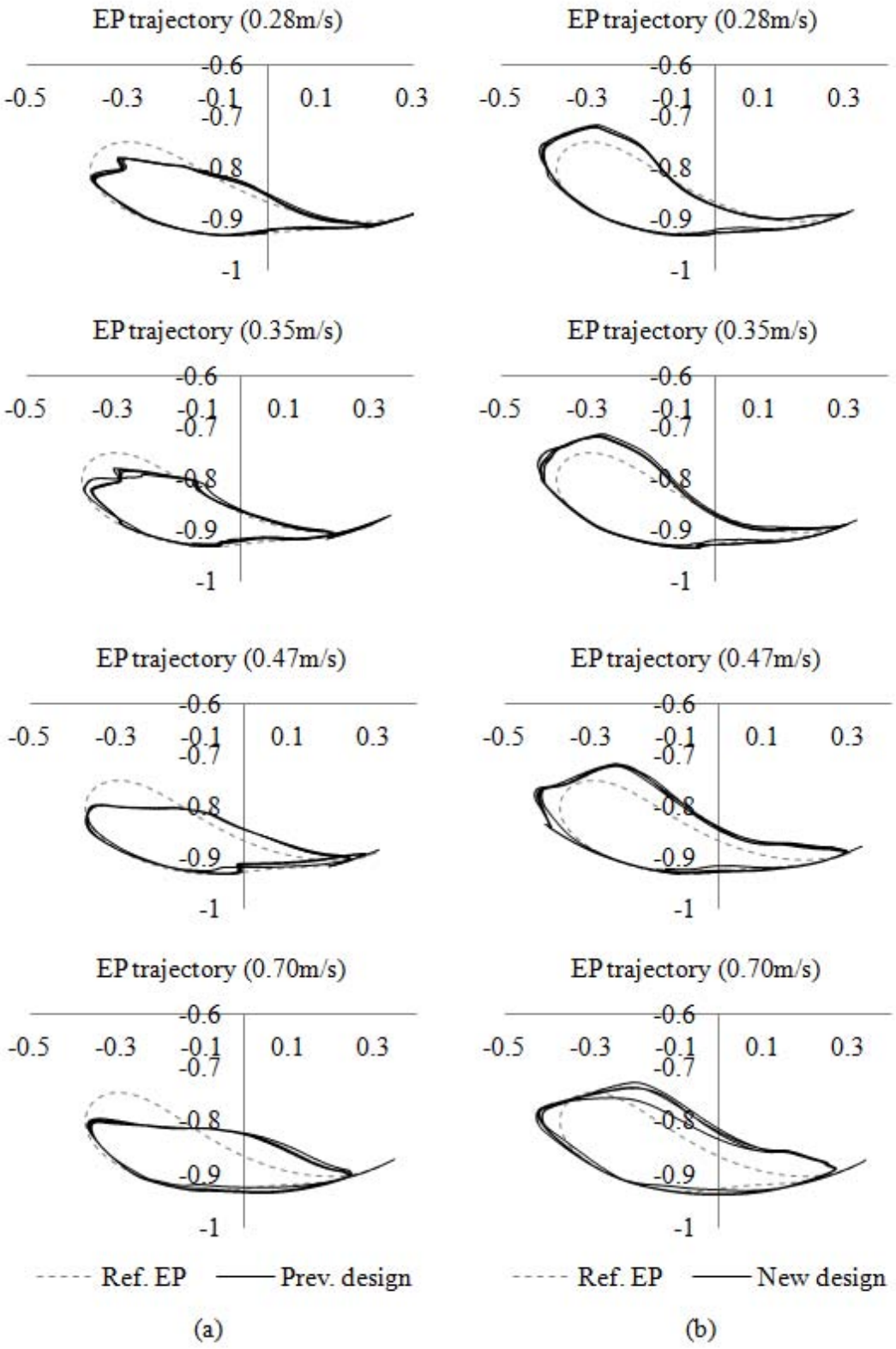

FIGURE 67 End point trajectories for the previous and improved design leg orthosis WO/S using PP controller scheme based co-contraction model.

6.9 Control of the Leg Orthosis WO/S: Evaluation on the Internal Pressure and Resultant Torque Generated from the Antagonistic Actuators

The focus in this assessment is on the evaluation of the internal pressure and resultant torque generated from the antagonistic mono-articular actuators for hip joint and bi-articular actuators. It was conducted to determine the functionality and reliability of the designed co-contraction model controller scheme's strategy in realizing the simultaneous movement of the antagonistic actuators in co-contractively movements. The antagonistic mono- and bi-articular actuators should be able to support each other during the control of the leg orthosis. The tests were evaluated at four different GC speeds of 0.28m/s, 0.35m/s, 0.47m/s, and 0.70m/s.

Figure 68 and 69 show the distributed internal pressures from the antagonistic mono- and bi-actuators at different GC speeds for tests WO/S. Figure 68 (a) and 68 (b) illustrate the internal pressure of the mono-articular actuators (i.e., anterior and posterior) for the hip joint. Figure 69 (a) and 69 (b) illustrate the internal pressure of the bi-articular actuators (i.e., anterior and posterior). Based on the results, it showed that the internal pressure of the antagonistic actuators were consistent at the slower GC speed of 0.28m/s and 0.35m/s. This shows that the antagonistic mono- and bi-articular actuators were operating at a normal situation where there is no sign of antagonistic actuators' irregular movements occurred during the gait motion. However, at the faster GC speed of 0.47m/s and 0.70m/s, it seems that the antagonistic bi-articular actuators were unable to achieve maximum operating pressure due to its slower contraction as it reaching maximum which can be see Figures 69 (a) and 69 (b). These antagonistic bi-articular actuators were then supported by the mono-articular actuators; where the sudden increased in its internal pressure can be observed in Figures 68 (a) and 68 (b).

Figure 70 shows the resultant torque generated from the antagonistic mono- and bi-articular actuators at different GC speeds for tests WO/S. Based on the result, it showed that the antagonistic bi-articular actuators were able to generate a strong moment arm at the joint when compared to those generated from the antagonistic mono-articular actuators. Therefore, it is important to introduce the antagonistic bi-articular actuators as its play a major role in achieving sufficient moment arm at the hip and knee joints. In addition, it also can be concluded that the antagonistic mono-

and bi-articular actuators were able to support each other when implementing the designed co-contraction model control scheme and strategy.

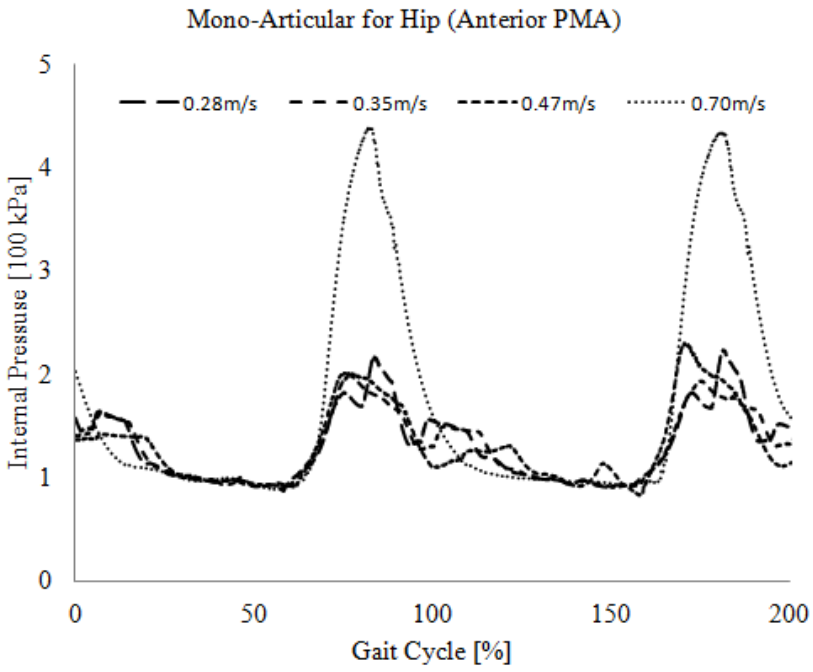

(a)

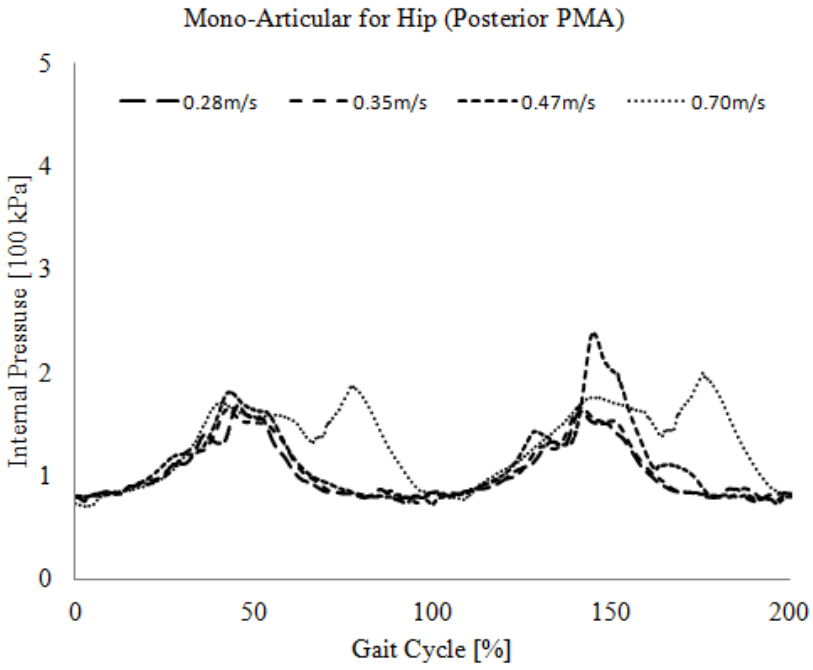

(b)

Figure 68 Internal pressures for antagonistic mono-articular actuators (hip joint) at different GC speeds

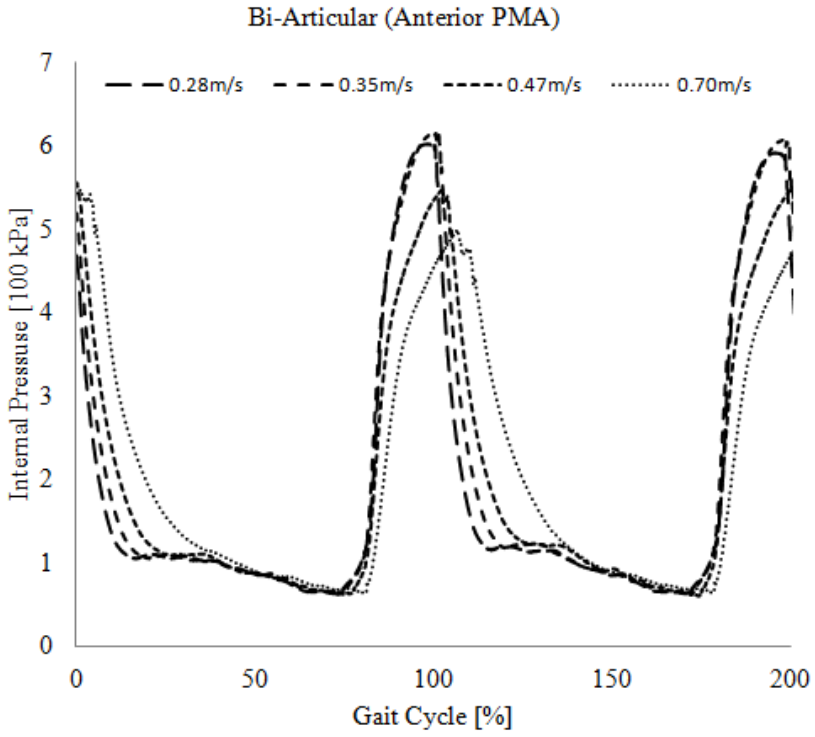

(a)

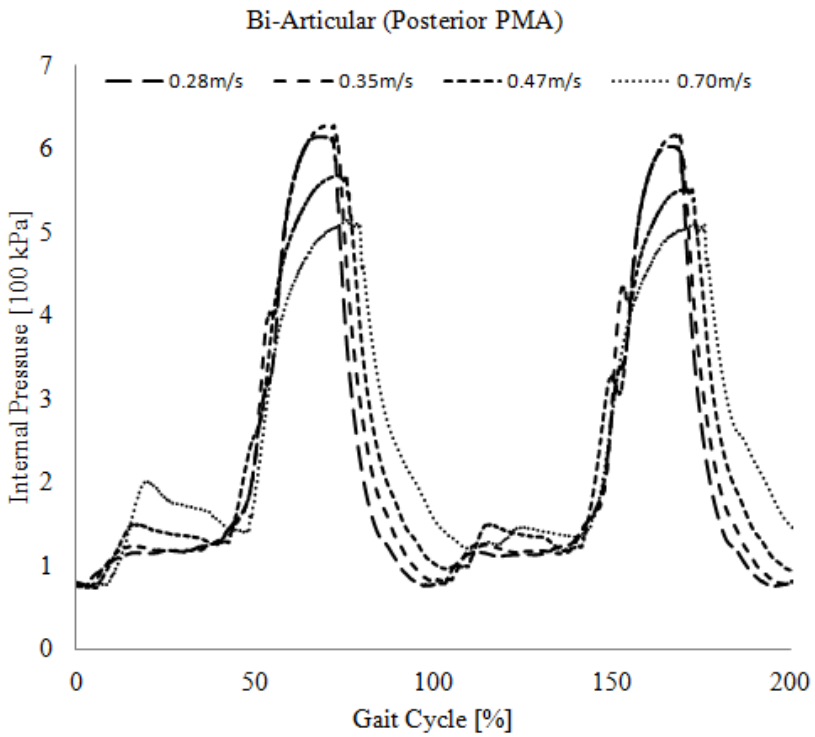

(b)

Figure 69 Internal pressures for the antagonistic mono-articular actuators (hip joint) at different GC speeds

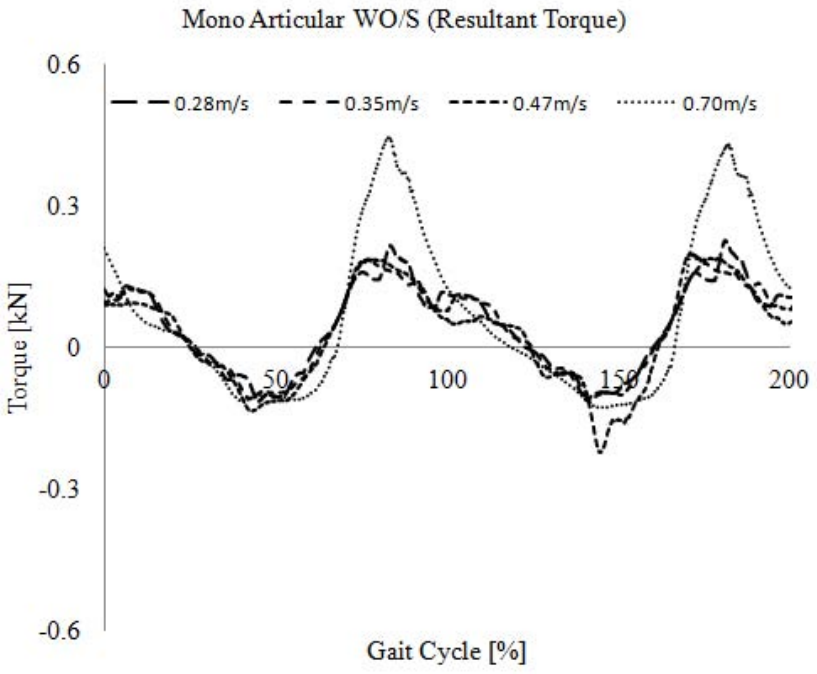

(a)

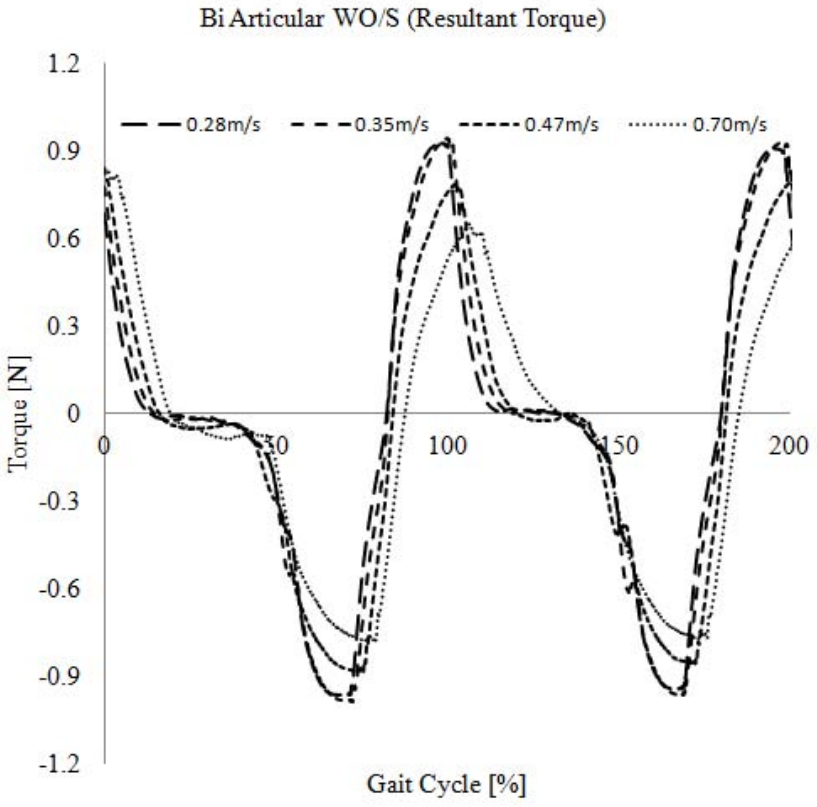

(b)

Figure 70 Resultant torques generated for the antagonistic mono- and bi-articular actuators at different GC speeds

6.10 Control of the Leg Orthosis WO/S: Evaluation between the Conventional PID and Co-Contraction Model Control Scheme's Controllers

The focus in this tenth assessment is on the evaluation of the proposed co-contraction controls with the conventional PID controls. Two tests were carried out; the first test is with mono-articular actuators, and the second test is with addition of bi-articular actuators. The actuators were arranged antagonistically (i.e., anterior and posterior) and simultaneously drive the leg orthosis. Six different control schemes based on conventional PID and co-contraction controls were tested at gait cycle (GC) speed of 0.28m/s for five cycles including the initial position cycle. The ideal joint trajectories (i.e., hip and knee angles) used for the leg orthosis control were obtained from Winter (2009) and verified throughout experimental setup. The result is then evaluated based on mean value of the Pearson coefficient of determination (r^2) for the hip and knee joint excursions.

The control system for this research delves into two parts; the first part employs the use of proportional directional control valve to enable the implementation of conventional PID controls of the antagonistic actuators; and, the second part employ the use of one regulator for each actuator to enable the implementation of co-contraction controls of the antagonistic actuators using derived mathematical model. Derivation of the co-contraction model has been recorded earlier and can be referred to [108]. The PID parameters were tuned using heuristic method. Real time control system was realized by using the MATLAB Simulink and xPC Target toolbox. The rotary potentiometer and compact pressure sensor were used to measure the required joint trajectories from the AIRGAIT exoskeleton's leg orthosis for the execution of closed loop control system. Figure 71 shows a simple schematic diagram for the control schemes.

Based on the review suggestions, control system evaluation is performed on the leg orthosis of the developed body weight support gait training system known as AIRGAIT. The design and evaluation of the AIRGAIT orthosis system have been recorded earlier and can be referred to [110]. Both control systems were first performed with only mono-articular actuators driven the leg orthosis. However, only the co-contraction controls were further tested with both mono- and bi-articular actuators. This is because the control of bi-articular actuators requires an additional model for generating its input patterns. Figure 72 and 73 show the hip and knee joint

excursions of the leg orthosis control for all evaluated control schemes. The result shows that by implementing conventional PID alone, it was not enough to achieve good joint trajectories either with pressure control or both pressure-position controls. The outcome was rather poor due to the insufficient joint stiffness and stability. However, it could be seen that with the implementation of additional model (co-contraction model) which enable the antagonistic actuators to be controlled co-contractively resulted in a much better gait trajectories. This could be explained due to the outcome of the co-contraction controls, with both anterior and posterior pneumatic muscles co-contractively contract and expands, it will resulted to an increase in the joint's stiffness and stability of the leg orthosis. In addition, by introducing this control scheme and strategy, the gravitational and hysteresis effects could also be reduced.

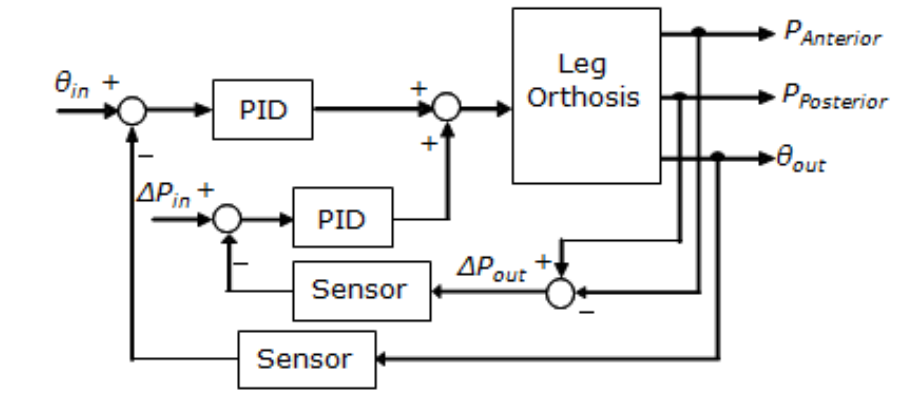

(a)

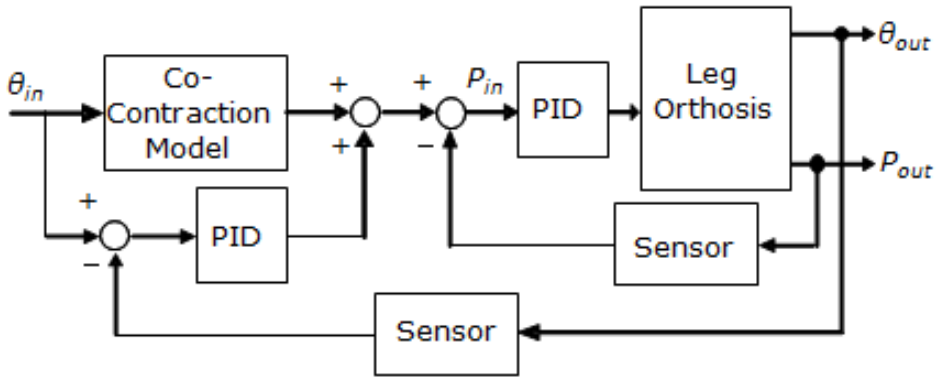

(b)

Figure 71 Simple schematic diagrams for pressure and position-pressure controls using conventional PID and co-contraction model

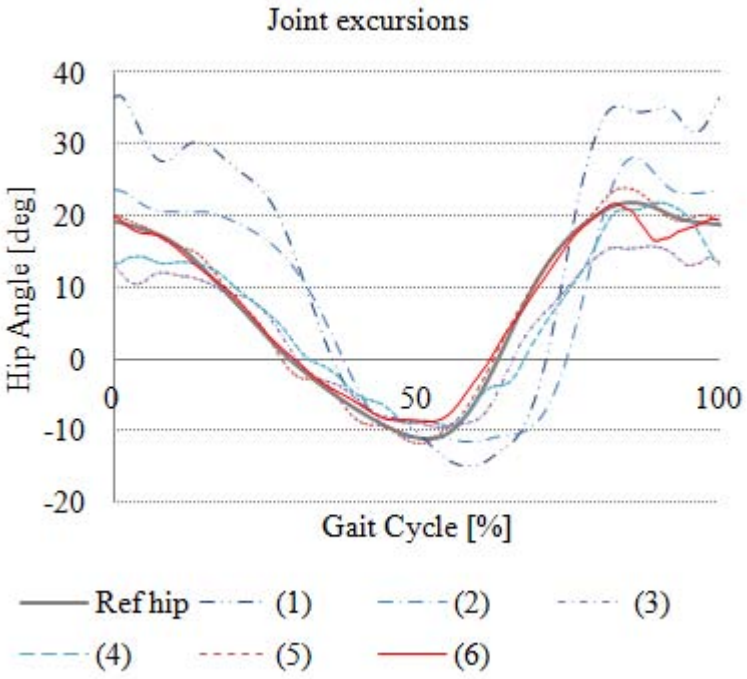

FIGURE 72 Hip joint excursions for all evaluated control schemes.

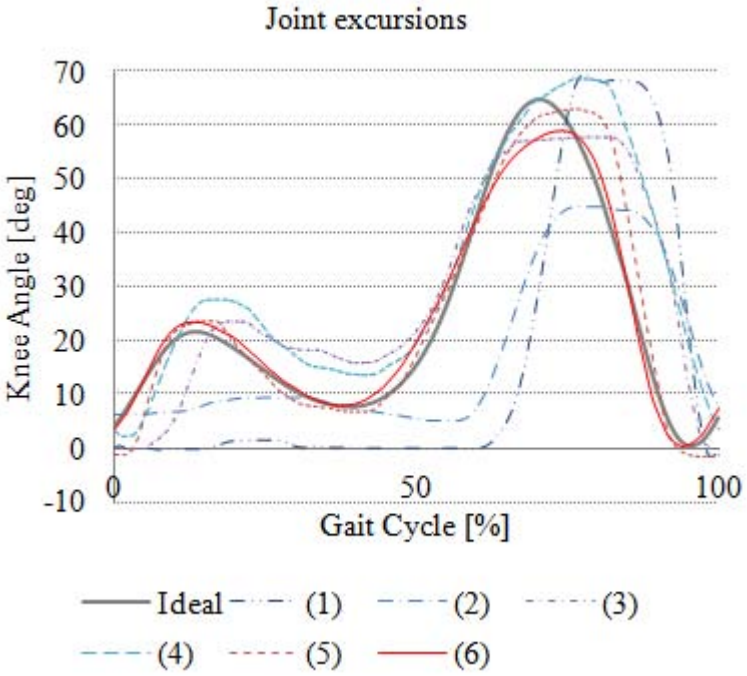

FIGURE 73 Knee joint excursions for all evaluated control schemes.

TABLE 15 Correlation coefficient (CC) and Pearson coefficient of determination (r^2) values for all evaluated control schemes.

Controller scheme	CC			r^2		
	Hip angle	Knee angle	Mean CC	Hip angle	Knee angle	Mean r^2
(1) Conventional PID - Pressure control (mono)	0.861	0.428	0.644	0.741	0.183	0.462
(2) Conventional PID - Position and pressure control (mono)	0.786	0.574	0.680	0.617	0.329	0.473
(3) Simulation model - Pressure control (mono)	0.975	0.855	0.915	0.950	0.730	0.840
(4) Simulation model -Pressure control (mono and bi)	0.955	0.897	0.926	0.913	0.805	0.859
(5) Co-contraction model - Position control (mono and bi)	0.998	0.975	0.987	0.996	0.951	0.974
(6) Co-contraction model - Position and pressure control (mono and bi)	0.996	0.990	0.993	0.992	0.980	0.986

The performance evaluation of the tested control schemes based on conventional PID and co-contraction controls were properly evaluated using the Pearson coefficient of determination as can be seen in Table 15. The table shows that mean r^2 value for pressure and pressure-position controls based on conventional PID were less than 0.5 (50%) which is rather low compared to the pressure control based on co-contraction model control scheme with mean r^2 value of 0.84 (84%). This shows that the co-contraction controls was able to precisely maneuver the joints orthosis according to the desired trajectories. Then, the gait motion was improved with the addition of bi-articular actuators, where the mean r^2 value indicated a measure of 0.859 (85.9%). This is because the bi-articular actuators were able to improvise the balance control of the leg orthosis and ability to produce maximum output force in a much more homogenously distributed ways. Subsequently, the joint excursions were much better using the position and pressure-position based on co-contraction controls with high mean r^2 values of 0.974 (97.4%) and 0.986 (98.6%) compared to the pressure control. This is because the designed pressure control only manages the pressure data based on the input patterns generated by co-contraction model. However, the addition of position control was controlling the muscle activation levels of the co-contraction model itself, which enables much precise co-contraction data to be generated. It is realized that the controls of the pressure and position based co-contraction controls was able to produce much better joint's stiffness and stability of the AIRGAIT exoskeleton's leg orthosis.

6.11 Human Muscle Activation Based on Electromyography (EMG) Signals

In this section the results of the EMG signal of the human muscle (i.e., rectus femoris (RF), bicep femoris (BF), soleus (SOL), medial gastrocnemius (MGAS), and tibialis anterior (TA)) were shown to analyze the contraction pattern of the human antagonistic muscles. It is strongly believed that the human antagonistic muscles activate simultaneously, when one muscle (i.e., anterior or posterior) is in contraction the other muscle (i.e., posterior or anterior) will be in expansion and vise versa. We define this as muscle co-contraction or muscle synergy. Muscle co-contraction refers to when any movement occurs which involved two sets of muscles working around joint. Normally, the muscles on one side of the joint must relax so that the muscles

on the other side can contract. However, in co-contraction is defined as both sets of muscles contract. Additionally, we also defined the co-contraction as both muscles were simultaneously contract. When the muscles on one side of the joint are in contraction, the opposite muscles will not be in completely relaxed. However, they are still in contraction but less than the opposite muscles. The muscle synergy refers to the interaction of two or more sets of muscles to produce a combined effect greater than the sum of their separate effects.

Three tests were conducted; the first is normal walking on the treadmill, the second is normal walking on the treadmill with attached orthosis, and the third is normal walking on the treadmill with assisted orthosis. Figure 74 and 75 shows the results of the EMG signals of the normal walking on the treadmill without orthosis and with attached orthosis. The EMG signal activities were much higher when we applied some load to the subject (with attached orthosis). With this, the patterns of the human muscle activities could be explained better. Based on the EMG signals of the without and with attached orthosis, it could be seen that the human antagonistic muscles were in co-contractively like movements. When the muscles on one side of the joint were active, the other side of muscle is not completely inactive. However, it could be seen that there is still some activity involved by the other muscles. This indicates the co-contraction movements applied by the human muscles to manipulate the joints. Figure 76 shows the EMG signals of the normal waking on the treadmill with an assistance of the orthosis using the co-contraction model control scheme. The result shows that, we were able to apply the antagonistic mono-and bi-articular actuators a co-contractively movements and drive the leg orthosis. Then, activate the human antagonistic muscles accordingly.

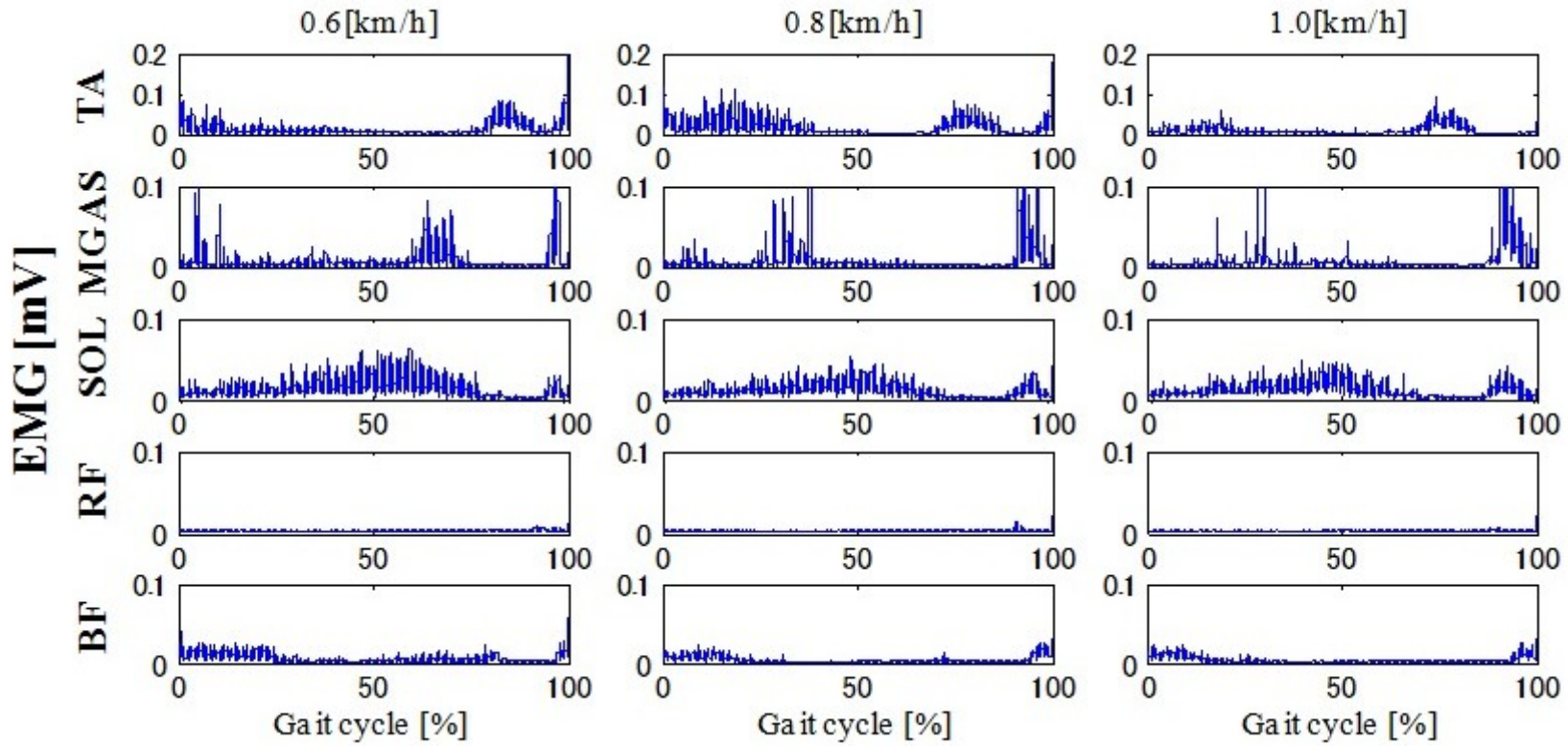

Figure 74 EMG signals of the normal walking on the treadmill.

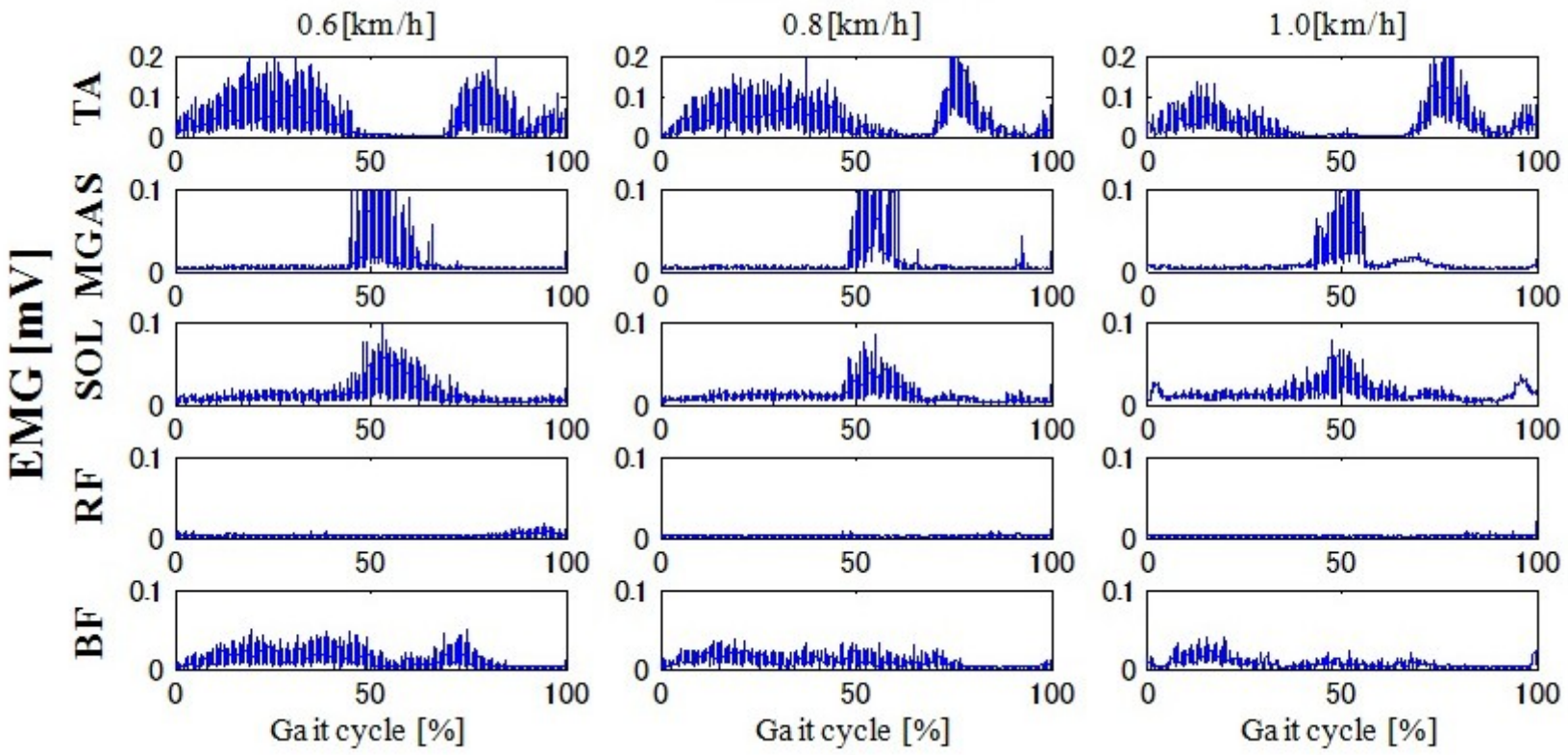

Figure 75 EMG signals of the normal walking on the treadmill with attached orthosis.

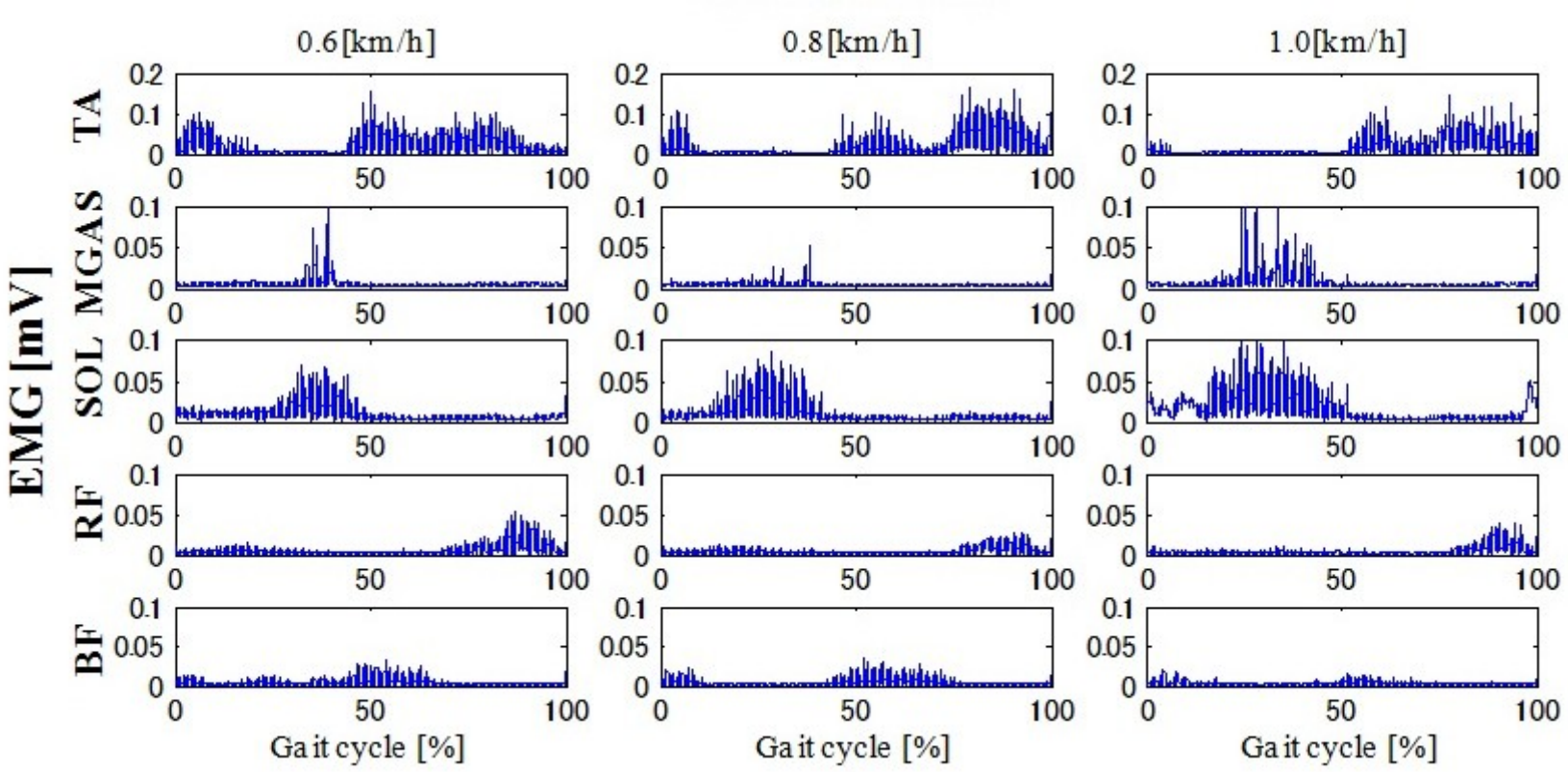

Figure 76 EMG signals of the normal walking on the treadmill with assisted orthosis.

6.12 Couple control model: Sine Signal and Real Trajectory Tests

In this final assessment, the validations test results of the orthosis controlled by the proposed model were shown. We give, as first test, a sinusoidal trajectory to both angles and varying its frequency. For the hip joint, the sine trajectory has a mean value and amplitude respectively equal to 1.57 and 0.4 rad. Instead, the sine wave, sent to the knee joint, has amplitude and a mean value both equal to 0.4 rad. In Figure 77 and 78 are shown the four cases that can be distinguish by the different frequencies of the sine wave that vary from 0.05 to 1 Hz. Particularly here we show the cases of 0.05, 0.1, 0.5 and 1 Hz that corresponds to periods of 20, 10, 2 and 1 second. It is also noticed that, in the worst case of a frequency of 1 Hz the system presents a delay but continues to follow almost well the sine wave, with respect to the minimum and maximum values. Moreover, the frequency of 1 Hz corresponds a walking speed of 1.40 m/s that is the speed of a healthy person [133]. Instead, for a person that needs of rehabilitation we can consider a speed less or equal to 0.7 m/s at which corresponds a frequency of 0.5 Hz.

Figure 79 (a) and 79 (b) show the control tests with a subject at frequencies of 0.5 Hz and 1 Hz to determine the reliability of the designed control system. The results show no significant differences for the tests without and with a subject. However, the maximum angle extension achieved at the hip joint was reduced. This suggested for the implementation of closed loop control system. Another important test is made by sending squared signals to both joints. The parameters of the squared trajectories, in terms of mean value and amplitude, are the same of those sinusoidal. Here we just show the case of 0.5 Hz. The main scope of stressing the system with a squared wave is to see the response speed. We show this test in Figure 80, and it can be noticed that the system is very quick to follow the squared trajectory. Particularly the mean time, considering both the loading and unloading parts, to reach the references is equal to 0.1 second. The last validation test is conducted by recording the hip and knee angles for a random walk and uses them as input for the system. By varying the time between the samples we can set easily the cycle speed. Here we show the worst case with a time period of 2 seconds. We can see, from Figure 81 that the input signals were well followed according to the previous validation tests. The angles showed in Figure 81 are used in Figure 82 in order to verify if the system is able to follow a specific path with the end effectors, in our case the ankle. We find

the position of the ankle just using the equations of the double pendulum, giving the angles of the random walk. We can see in the Figure 82 that the ankle position path is well followed compared to the reference trajectory.

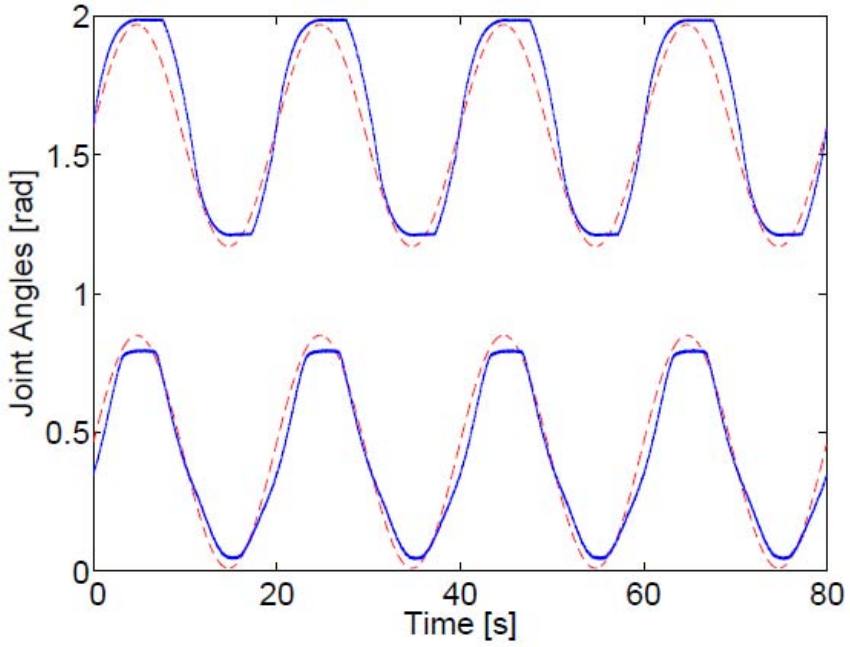

(a)

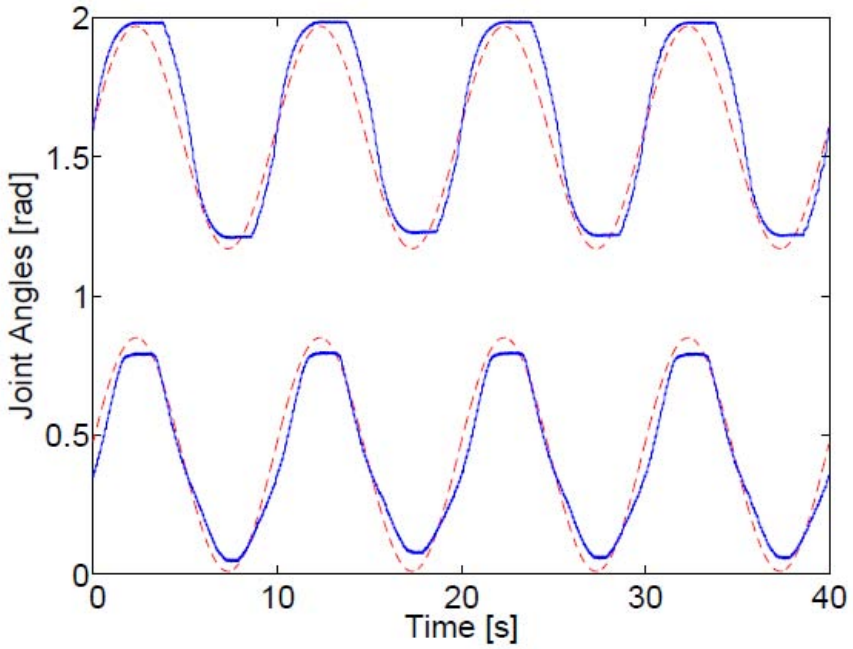

(b)

FIGURE 77 Sine trajectories test without a subject (WO/S) for different frequencies (a) 0.05 Hz, and (b) 0.1 Hz. The red dashed line is the input signal and the blue continuous line is the measured angles assumed by the orthosis.

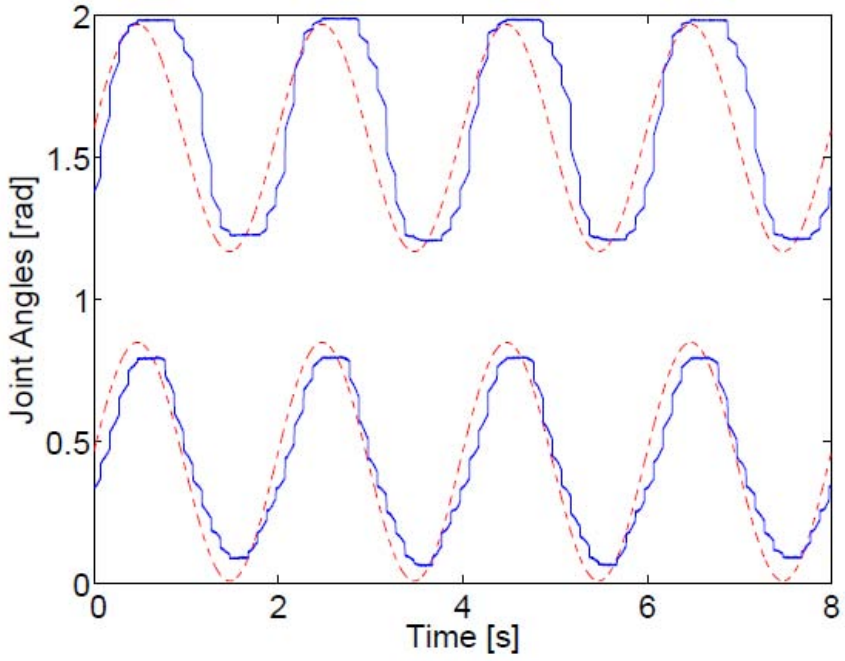

(a)

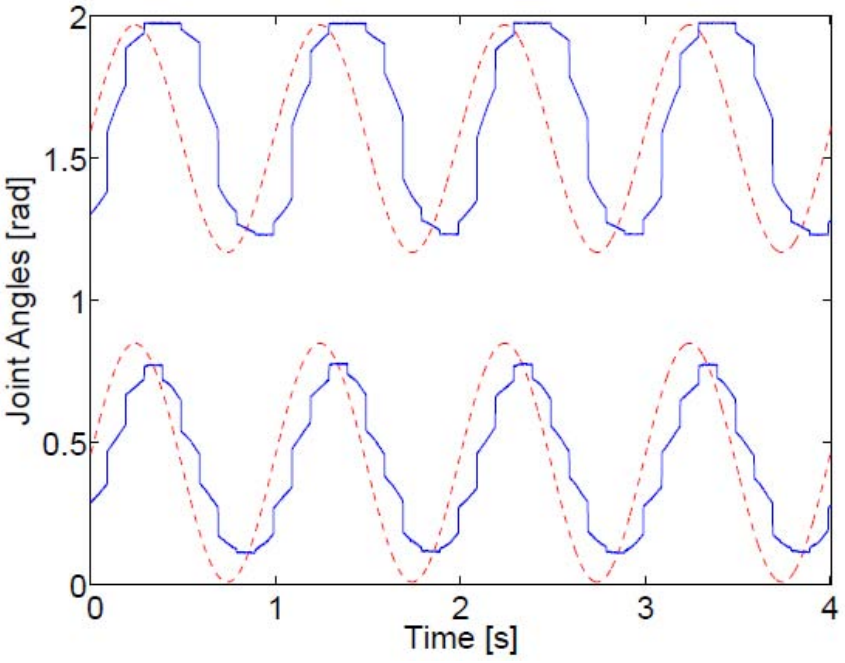

(b)

FIGURE 78 Sine trajectories test without a subject (WO/S) for different frequencies (a) 0.5 Hz, and (b) 1.0 Hz. The red dashed line is the input signal and the blue continuous line is the measured angles assumed by the orthosis.

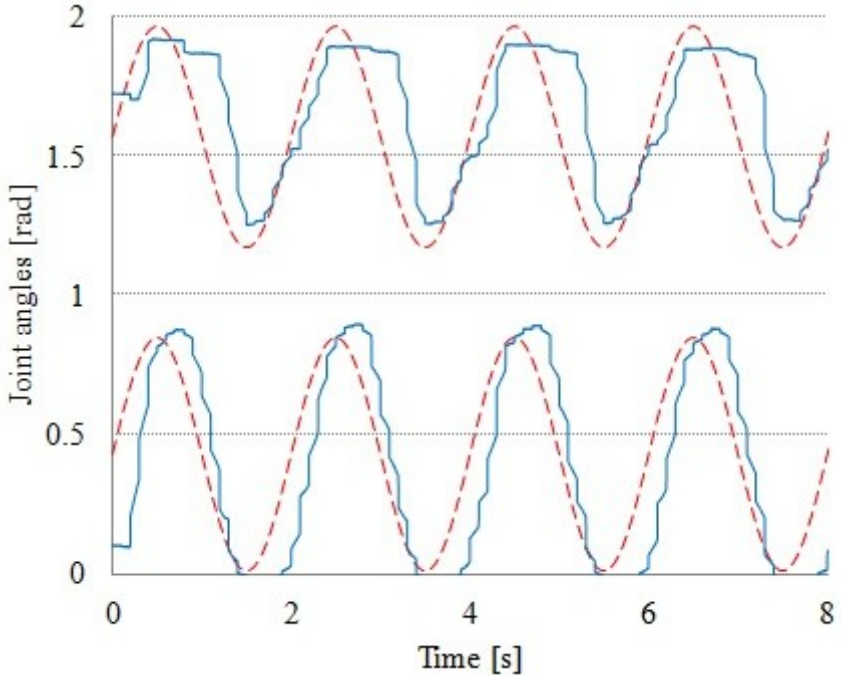

(a)

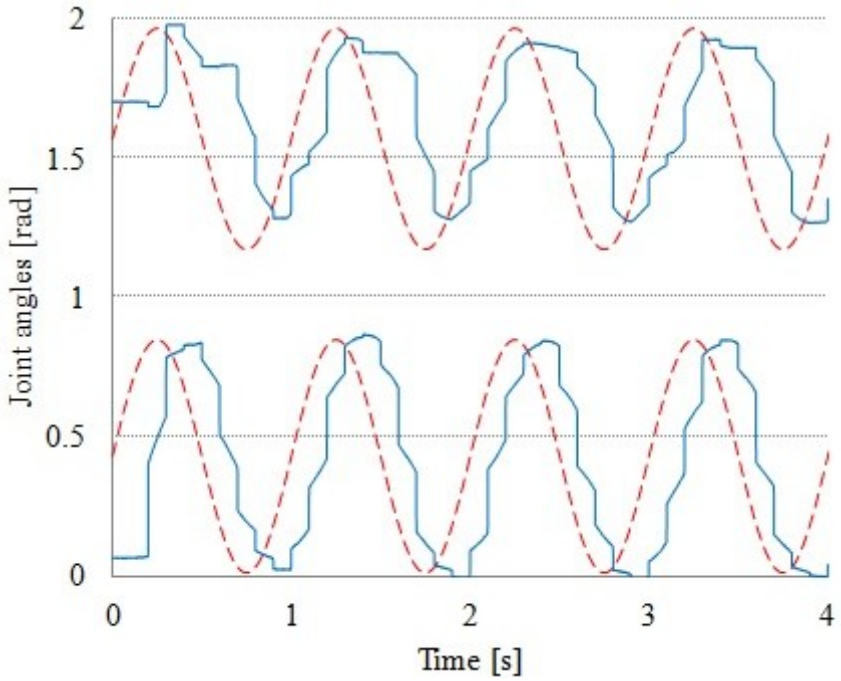

(b)

FIGURE 79 Sine trajectories test with a subject (W/S) for different frequencies (a) 0.5 Hz, and (b) 1.0 Hz. The red dashed line is the input signal and the blue continuous line is the measured angles assumed by the orthosis.

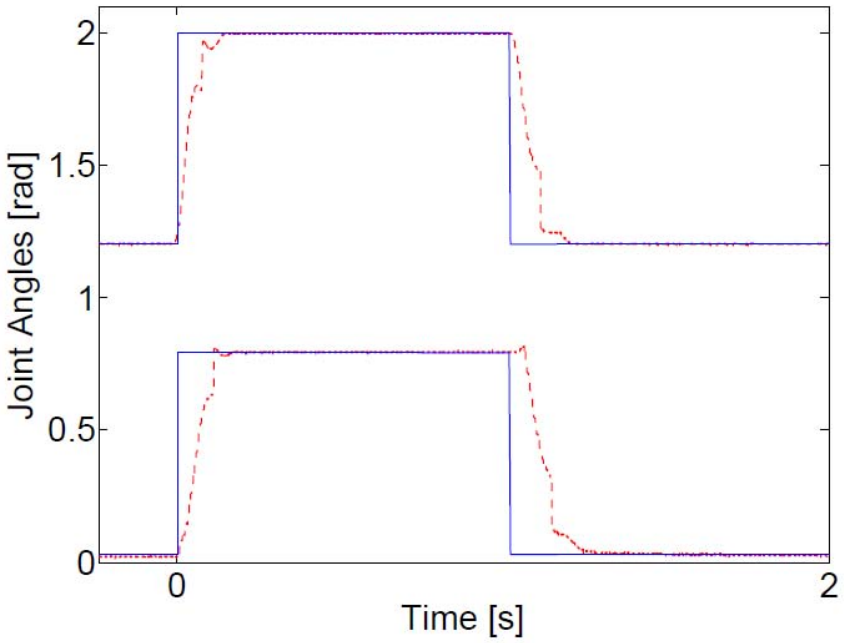

FIGURE 80 Squared trajectory tests with a frequency of 0.5 Hz. The red dashed line is the input signal and the blue continuous line is the measured angles assumed by the orthosis.

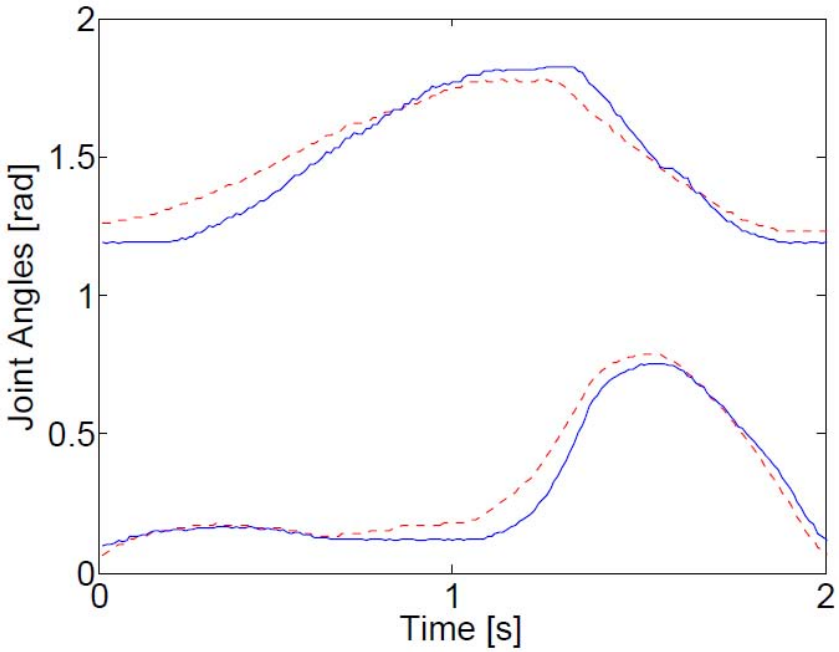

FIGURE 81 Real trajectories for the hip and knee angles for a random walk. The red dashed line is the input signal and the blue continuous line is the measured angles assumed by the orthosis.

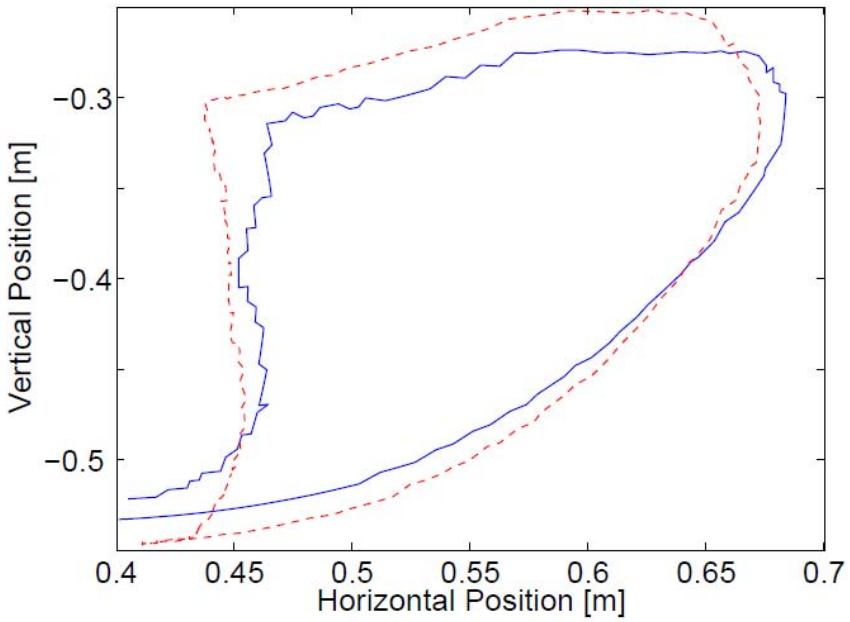

FIGURE 82 Ankle position paths for a random walk. The red dashed line is the input signal and the blue continuous line is the real position assumed by the orthosis.

In this research we continue the improvement of the control system for our AIRGAIT exoskeleton's leg orthosis. We introduce, with respect to the previous works, the effect of the dynamic components of the system by computing the couples of the joints with the use of the Newton-Euler equations. Moreover, we conducted different validation tests using sine, squared and true random walk trajectories. We show that for the specific purposes for what the orthosis is designed, the PMAs and the proposed control model catch the aim of our work. To the best of our knowledge we are the first on applying the computed-torque method on the control of a two degree of freedom orthosis actuated by PMAs. We show also that, even there is no managing on the feedback; the proposed model has the advantage to able the system to follow a given trajectory in a quick and best way.

CHAPTER 7

CONCLUSIONS AND RECOMMENDATIONS

Throughout the literature reviews (i.e., journals and conference papers) on existing research studies of the rehabilitation orthosis systems, the evaluation and comparison of the developed lower-limb rehabilitation orthosis using pneumatic muscle type of actuators including its control algorithms and strategies intended to provide stiffness and stability during the control system were thoroughly reviewed. Even though a considerable amount of work has now been employed, it could be said that the field is still rapidly evolving. Based on the review findings, it is understood that the issues of which are the most effective control algorithms is still wide open. However, the randomized controlled trials are still necessary for identifying the suitable control algorithms even though it is expensive and time-consuming. In conclusion, a few remarks were suggested for the future research of pneumatic muscle actuated gait trainers system; the first is, the pneumatic muscles arrangement for actuating the lower-limb orthosis should be antagonistically (i.e., agonist and antagonist); the second is, the co-contractive movement of the antagonistic pneumatic muscles can provide a good stiffness and stability for the leg orthosis system; the third is, a model paradigm is essential to generate adequate co-contractive input data for manipulating the antagonistic muscle actuators; and finally, the develop model should be manage by controllers to deal with the presence of dynamic properties and nonlinearity behavior of the system.

This research introduces the designed controller scheme and strategy to optimize the control of bi-articular actuators in co-contractive movements with the presence of mono-articular actuators. The approach strategy for this designed

controller scheme is the derivation of a co-contraction model which facilitates the implementation of position and pressure based controllers. The proposed co-contraction model based P and PP controller scheme correlates information on the joints with the dynamic characteristics (i.e., contraction and pressure) of the PMA. Input patterns are then generated for the antagonistic mono- and bi-articular actuators compared to the other control algorithms for PMA that predict or measure the required torque for the joints.

Generally, three tests were performed on the AIRGAIT exoskeleton's leg orthosis with the first using antagonistic mono-articular actuators alone tested WO/S; the second with the addition of antagonistic bi-articular actuators tested WO/S; and the third with the addition of antagonistic bi-articular actuators tested W/S. Total of tenth assessments were evaluated to determine the performance of the proposed co-contraction model control scheme.

The first assessment concluded that by implementing the conventional PID based control scheme, the control of the leg orthosis due to the nonlinearity behaviors of the antagonistic mono- and bi-articular actuators using pneumatic muscle could not be solved. This will be required for the implementation of a suitable control system to deal with the dynamic characteristics of the pneumatic muscle. In addition, a better control strategy will also be needed in controlling the antagonistic actuators (i.e., anterior and posterior) precisely and simultaneously. Therefore the co-contraction model control scheme was proposed.

In the second assessment, the implementation of the simulated co-contraction model control scheme was evaluated. The results showed the performance of leg orthosis controls based on simulated co-contraction model was far exceeded the performance of leg orthosis controls using conventional PID. This could be concluded that, the execution of co-contraction control scheme and strategy was effective in handling the nonlinearity of the system.

The third assessment concluded that by introducing the muscle activation level parameters (β and α) into the designed co-contraction model control scheme, a much precise control system could be achieved. This muscle activation levels were able to manipulate the contraction patterns of the antagonistic actuators before the pressure patterns were determined. This shows that, the manipulation of the co-contraction model plays a significant role in the control strategy implementation for the designed controller schemes.

The fourth assessment summarized that the addition of bi-articular actuators improved the joint stiffness of both the hip and knee. In addition, the bi-articular actuators also stabilized the coarse movements created by the mono-articular actuators during flexion of the joints and improved the maximum angle extension achieved at the knee joint.

The limitation of implementing antagonistic mono-articular actuators alone to control the leg orthosis was evaluated in the fifth assessment. The result showed that, it was able to withstand up until GC speed of 3 seconds when tested W/S. However, when the controller is tested at a much faster gait cycle of 2s and 1s, the mono-articular actuators alone were not able to withstand the external force generated from the AIRGAIT's inertia, and caused the pneumatic muscle to break loose from the clamp. With the addition of bi-articular actuators, the system was able to distribute the external force generated from the inertia effect equally to the mono- and bi-articular actuators which enables the system to operate at a much faster GC speed up to 1 second. This result concluded the importance and essence of the antagonistic bi-articular actuators implementation.

The sixth assessment concluded that compared to using the position based controller alone, the inclusion of the pressure based controller improved the response time of PMA muscle activities due to the effects of contraction and expansion. The designed controller scheme was able to achieve complete gait motion of leg orthosis (i.e., hip and knee joints) until a GC speed of 2 seconds with a slight time shift of approximately only 0.2 seconds.

The seventh assessment concluded that the co-contraction model based PP controller schemes was able to achieve a good EP trajectory of the leg orthosis up until GC speed of 1 second. The effective work achieved was over 60% of ideal value at all GC speeds of 4 seconds, 3 seconds, 2 seconds, and 1 second. Moreover, the generated inertia was also maintained at all GC speed. This concludes that the PP controller scheme was able to correspond to the inertia effect and then optimize the controls of leg orthosis. The modified control scheme will be introduced in the next assessment to consider the gravitational effect on the antagonistic actuators as to improve controls of the EP trajectory of the leg orthosis.

The eighth assessment concluded that by using the co-contraction model control scheme, the leg orthosis could be manipulated precisely even without the knee joint's antagonistic mono-articular actuators. It emphasized on the control of

antagonistic bi-articular actuators to efficiently maneuvers the hip and knee joint excursions. This concluded the reliability of the design co-contraction model control scheme and its strategy in handling both antagonistic mono- and bi-articular actuators simultaneously and co-contractively.

The ninth assessment concluded that the antagonistic bi-articular actuators were able to generate a strong moment arm at the joint when compared to those generated from the antagonistic mono-articular actuators. It is important to introduce the antagonistic bi-articular actuators as its play a major role in achieving sufficient moment arm at the hip and knee joints. In addition, it also can be concluded that the antagonistic mono- and bi-articular actuators were able to support each other when implementing the designed co-contraction model control scheme and strategy.

The tenth assessment concluded that the pressure and position based co-contraction model control scheme was able to produce much better joint's stiffness and stability of the AIRGAIT exoskeleton's leg orthosis when compared to other control schemes. The designed pressure control only able to manipulate the pressure data based on the input patterns generated by co-contraction model. However, an addition of position control enables the manipulation of the introduced muscle activation levels. Thus, an adaptable co-contraction input data and control scheme could be performed. This lead to a much precise leg orthosis controls.

The eleventh assessment concluded that human antagonistic muscles (i.e., agonist and antagonist muscles) exhibited muscle co-contraction movements in order to move the joints. This was one of the main factors that which why decided to propose the co-contraction model control scheme to control the antagonistic mono- and bi-articular actuators of the AIRGAIT exoskeleton's leg orthosis. The result shows that, we were able to apply the antagonistic mono-and bi-articular actuators with a co-contractively movements and drive the leg orthosis. Then, activate the human antagonistic muscles accordingly.

The last assessment concluded on the implementation of the couple control model to drive the leg orthosis. The result shows that, the system is very quick to follow the squared trajectory. Particularly the mean time, considering both the loading and unloading parts, to reach the references is equal to 0.1 second. In addition, the result also showed that it was able to operate up until frequency of 1 Hz (1.40m/s) of the human normal walking speed. However, we choose to operate at frequency of 0.5 Hz (0.70m/s), which is suitable for the rehabilitation training.

REFERENCES

[1] A. Wernig, S. Muller, A. Nanassy, and E. Cagol, "Laufband therapy based on 'rules of spinal locomotion' is effective in spinal cord injured persons", Eur J Neurosci, vol. 7, pp. 823-829, 1995.

[2] A. Wernig, A. Nanassy, and S. Muller, "Maintenance of locomotor abilities following laufband (treadmill) therapy in para- and tetraplegic persons: follow-up studies", Spinal Cord, vol. 36, pp. 744-749, 1998.

[3] V. Dietz, R. Muller and G. Colombo, "Locomotor activity in spinal man: significance of afferent input from joint and load receptors", Brain, vol. 125, pp. 2626-2634, 2002.

[4] V. Dietz, and Susan J. Harkema, "Locomotor activity in spinal cord-injured persons". Journal of Applied Physiology", vol. 96, pp. 1954-1960, 2004.

[5] Iñaki Díaz, Jorge Juan Gil, and Emilio Sánchez, "Lower-Limb Robotic Rehabilitation: Literature Review and Challenges", Journal of Robotics, vol. 2011, Article ID 759764, 11 pages, 2011.

[6] Laura Marchal-Crespo, and David J. Reinkensmeyer, "Review of control strategies for robotic movement training after neurologic injury", Journal of Neuro-Engineering and Rehabilitation, vol. 6, 15 pages, 2009.

[7] Andrew Pennycott, Dorio Wyss, Heike Vallery, Verena Klamroth-Marganska, and Robert Riener, "Towards more effective robotic gait training for stroke rehabilitation: a review", Journal of Neuro-Engineering and Rehabilitation, vol. 9, 13 pages, 2012.

[8] Aaron M. Dollar, and Hugh Herr, "Lower extremity exoskeletons and active orthoses: challenges and state-of-the-art", IEEE Transactions on Robotics, vol. 24, no. 1, 2008.

[9] G. Colombo, M. Wirz, and V. Dietz, “Driven gait orthosis for improvement of locomotor training in paraplegics patients”, International Medical Society of Paraplegia, Spinal Cord, Vol. 39, pp. 252-255, 2001.

[10] S. Jazernik, G. Colombo, and M. Morari, “Automatic gait pattern adaptation algorithms for rehabilitation with a 4-DOF robotic orthosis”, IEEE Transactions on Robotics and Automation, Vol. 20, No. 3, 2004.

[11] L. Lunenburger, G. Colombo, and R. Riener, “Biofeedback for robotic gait rehabilitation”, Journal of Neuro-Engineering and Rehabilitation, vol. 4, 11 pages, 2007.

[12] Susanna Freivogel, Dieter Schmalohr, MD, and Jan Mehrholz, “Improved walking ability and reduced therapeutic stress with an electromechanical gait device”, J Rehabil Med, vol. 41, pp. 734-739, 2009.

[13] Stanley Fisher, MD, Leah Lucas, and T. Adam Thrasher, “Robot-assisted gait training for patients with hemiparesis due to stroke”, Top Stroke Rehabil, vol. 18(3), pp. 269-276, 2011.

[14] R. Gary West, “Powered gait orthosis and method of utilizing SAME”, Patent Application Publication, US 2004/0019304 A1, 2004.

[15] J. Veneman, R. Kruidhof, E. Hekman, R. Ekkelenkamp, E. Van Asseldonk, and H.Van Der Kooij, “Design and evaluation of the LOPES exoskeleton robot for interactive gait rehabilitation”, IEEE Transactions on Neural Systems and Rehabilitation Engineering, vol. 15, no. 3, 2007.

[16] H. Vallery, J. Veneman, E. Van Asseldonk, R. Ekkelenkamp, M. Buss, and H. Van Der Kooij, “Compliant actuation of rehabilitation robots”, IEEE Robotics and Automation Magazine, 10 pages, 2008.

[17] S.K. Banala, S. Hun Kim, S.K. Agrawal, and J.P.Scholz, “Robot assisted gait training with active leg exoskeleton (ALEX) ”, IEEE Transactions on Neural Systems and Rehabilitation Engineering, vol. 17, no. 1, 2009.

[18] S.K. Banala, S.K. Agrawal, S. Hun Kim, and J.P. Scholz, “Novel gait adaptation and neuromotor training results using an active leg exoskeleton”, IEEE/ASME Transactions on Mechatronics, vol. 15, no. 2, 2010.

[19] V. Monaco, G. Galardi, M. Coscia, D. Martelli, and S. Micera, “Design and evaluation of NEUROBike: a neuro-rehabilitative platform for bedridden post-strike patients”, IEEE Transactions on Neural Systems and Rehabilitation Engineering, vol. 20, no. 6, 2012.

[20] A. Taherifar, M. Mousavi, A. Rassaf, F. Ghiasi, and M.R. Hadian, “LOKOIRAN - a novel robot for rehabilitation of spinal cord injury sand stroke patients”, RSI/ISM International Conference on Robotics and Mechatronics, Tehran, Iran, 2013.

[21] M. Pietrusinski, I. Cajigas, G. Severini, P. Bonato, and C. Mavroidis, “Robotic gait rehabilitation trainer”, IEEE/ASME Transactions on Mechatronics, 10 pages, 2013.

[22] B. Tondu, and P. Lopez, “Modelling and control of McKibben artificial muscle robot actuators”, IEEE Control Systems Magazine, 24 pages, 2000.

[23] D. G. Caldwell, A. Razak, and M. Goodwin, “Braided artificial muscle actuators”, in Proc. IFAC Intell. Auton. Veh., Southampton, U.K., 1993, pp. 507–512.

[24] D. G. Caldwell, G. A. Medrano-Cerda, andM. Goodwin, “Characteristics and adaptive control of pneumatic muscle actuators for a robotic elbow”, in Proc. Int. Conf. Robot. Autom., San Diego, CA, 1994, vol. 4, pp. 3558–3563.

[25] D. G. Caldwell, G. A. Medrano-Cerda, and M. Goodwin, “Control of pneumatic muscle actuators”, IEEE Control Syst. Mag., vol. 15, no. 1, pp. 40–48, Feb. 1995.

[26] D. G. Caldwell, N. Tsagarakis, and G. A. Medrano-Cerda, “Biomimetic actuators: Polymeric pseudo muscular actuators and pneumatic muscle actuators for biological emulation”, Mechatronics, vol. 10, pp. 499–530, 2000.

[27] S. Davis, N. Tsagarakis, J. Canderle, and D. G. Caldwell, “Enhanced modeling and performance in braided pneumatic muscle actuators”, Int. J. Robot. Res., vol. 22, no. 3–4, pp. 213–227, 2003.

[28] S. Davis and D. G. Caldwell, “Braid effects on contractile range and friction modeling in pneumatic muscle actuators”, Int. J. Robot. Res., vol. 25, no. 4, pp. 359–369, 2006.

[29] C. P. Chou and B. Hannaford, “Static and dynamic characteristics of McKibben pneumatic artificial muscles”, in Proc. IEEE Int. Conf. Robot. Autom., San Diego, CA, May 1994, vol. 1, pp. 281–286.

[30] C. P. Chou and B. Hannaford, “Measurement and modeling of McKibben pneumatic artificial muscles”, IEEE Trans. Robot. Autom., vol. 12, no. 1, pp. 90–102, Feb. 1996.

[31] Breno G. Nascimento, Claysson B. Vimieiro, Danilo A. Nagem, and Marcos

Pinotti., “Hip orthosis powered by pneumatic artificial muscle: voluntary activation in absence of myoelectrical signal”, Artificial Organs, vol. 32(4), pp. 317-322, 2008.

[32] Claysson B. Vimieiro, Breno G. Nascimento, Danilo A. Nagem, and Marcos Pinotti., “Development of a hip orthosis using pneumatic artificial muscles”, Proceeding of TMSi, 2005.

[33] Kartik Bharadwaj, and Thomas G. Sugar, “Kinematics of a robotic gait trainer for stroke rehabilitation”, IEEE International Conference on Robotics and Automation, 2006.

[34] Daniel P. Ferris, Keith E. Gordon, Gregory S. Sawicki, and Ammanath Peethambaran, “An improved powered ankle-foot orthosis using proportional myoelectric control”, Gait and Posture, vol. 23, pp. 425-428, 2006.

[35] Daniel P. Ferris, Joseph M. Czerniecki, and Blake Hannaford, “An ankle-foot orthosis powered by artificial pneumatic muscles”, J Appl Biomech, vol. 21(2), pp. 189-197, 2005.

[36] Keith E. Gordon, Gregory S. Sawicki, and Daniel P. Fessis, “Mechanical performance of artificial pneumatic muscles to power an ankle-foot orthosis”, Journal of Biomechanics, vol. 39, pp. 1832-1841, 2006.

[37] Nelson Costa, Milan Bezdicek, Michael Brown, John O. Gray, and Darwin G. Caldwell, “Joint motion control of a powered lower limb orthosis for rehabilitation”, International Journal of Automation and Computing, vol. 3, pp. 271-281, 2006.

[38] T. Miyoshi, K. Hiramatsu, S.I. Yamamoto, K. Nakazawa, and M. Akai, “Robotic gait trainer in water: development of an underwater gait-training orthosis”, Disability and Rehabilitation, vol. 30(2), pp. 81-87, 2008.

[39] P. Malcom, P. Fiers, V. Segers, I. Van Caekenberghe, M. Lenoir, and D. De Clercq, “Experimental study on the role of the ankle push off in the walk-to-run transition by means of a powered ankle-foot-exoskeleton”, Gait and Posture, vol. 30, pp. 322-327, 2009.

[40] P. Malcom, V. Segers, I. Van Caekenberghe, and D. De Clercq, “Experimental study of the influence of the m. tibialis anterior on the walk-to-run transition by means of a powered ankle-foot-exoskeleton”, Gait and Posture, vol. 29, pp. 6-10, 2009.

[41] S. Galle, P. Malcom, W. Derave, and D. De Clercq, “Adaptation to walking with an exoskeleton that assists ankle extension”, Gait and Posture, vol. 38, pp. 495-499, 2013.

[42] P. Malcom, W. Derave, S. Galle, and D. De Clercq, “A simple exoskeleton that assist plantarflexion can reduce the metabolic cost of human walking”, Plos One, vol. 8(2), 7 pages, 2013.

[43] Gregory S. Sawicki, and Daniel P. Fessis, “A pneumatically powered knee-ankle-foot orthosis (KAFO) with myoelectric activation and inhibition”, Journal of Neuro-Engineering and Rehabilitation, vol. 6, 16 pages, 2009.

[44] Tudor T. Deaconescu, and Andrea I. Deaconescu, “Pneumatic muscle actuated equipment for continuous passive motion”, IAENG Transactions on Engineering Technologies, vol. 3, 12 pages, 2009.

[45] T. J. Yeh, Meng Je Wu, Ting Jiang Lu, Feng Kuang Wu, and Chih Ren Huang, “ Control of McKibben pneumatic muscles for a power-assist, lower-limb orthosis”, Mechatronics, vol. 20, pp. 686-697, 2010.

[46] J. Carberry, G. Hinchly, J. Buckerfield, E. Taylor, T. Burton, S. Madgwick, and R. Vaidyanathan, “Parametric design of an active ankle foot orthosis with passive compliance”, Computer-Based Medical System (CBMS), 2011.

[47] Yong-lae Park, Bor-rong Chen, Diana Young, Leia Stirling, Rob Wood, Eugene Goldfield, Radhika Nagpal, “Bio-inspired Active Soft Orthotic Device for Ankle Foot Pathologies”, Intl. Conference on Robots and Systems (IROS), 2011.

[48] Yong-Lae Park, Bor-rong Chen, Carmel Majidi, Rob Wood, Radhika Nagpal, and Eugene Goldfield, “Active Modular Elastomer Sleeve for Soft Wearable Assistance Robots”, IEEE Intl. Conference on Robots and Systems (IROS), 2012.

[49] Chun M. Teng, Zhen Y. Wong, Wey Y. The, and Yu Z. Chong, “Design and development of inexpensive pneumatically-powered assisted knee-ankle-foot orthosis for gait rehabilitation-preliminary finding”, International Conference on Biomedical Engineering (ICoBE), 2012.

[50] T. Kawamura, and K. Takanaka, “Development of an orthosis for walking assistance using pneumatic artificial muscle-a quantitative assessment of the effect of assistance”, International Conference on Rehabilitation Robotics, 2013.

[51] S. Hussain, S.Q. Xie, and P.K. Jamwal, Adaptive impedance control of a robotic orthosis for gait rehabilitation, IEEE Transactions on Cybernetics, vol. 43, no. 3, 2013.

[52] S. Hussain, S.Q. Xie, P.K. Jamwal, Robust nonlinear control of an intrinsically compliant robotic gait training orthosis, IEEE Transactions on Systems, Man, and Cybernetics: Systems, vol. 43, no. 3, 2013.

[53] D.G. Caldwell, G.A. Medrano-Cerda, and M.J. Goodwin, "Braided pneumatic actuator control of a multi jointed manipulator", International Conference on Systems, Man and Cybernetics, 1993.

[54] D.G. Caldwell, G.A. Medrano-Cerda, and Mike Goodwin, "Characteristics and adaptive control of pneumatic muscle actuators for a robotic elbow", International Conference on Robotics and Automation, 1994.

[55] D.G. Caldwell, G.A. Medrano-Cerda, and Mike Goodwin, "Control of a pneumatic muscle actuators", IEEE Transactions on Control Systems, vol. 15(1), pp. 40-48, 1995.

[56] G.A. Medrano-Cerda, C.J. Bowler, and D.G. Caldwell, "Adaptive position control of antagonistic pneumatic muscle actuators", International Conference on Intelligent Robots and Systems", vol. 1, pp. 378-383, 1995.

[57] M. Hamerlain, "An anthropomorphic robot arm driven by artificial muscles using a variable structure control", International Conference on Intelligent Robots and Systems, vol. 1, pp. 550-555, 1995.

[58] Moenes Iskarous, and Kazuhiko Kawamura, "Intelligent control using a neuro-fuzzy network", International Conference on Intelligent Robots and Systems, vol. 3, pp. 350-355, 1995.

[59] P. van der Smagt, F. Groen, and K. Schulten, "Analysis and control of a rubbertuator arm", Biological Cybernetics, vol. 75, pp. 433-440, 1996.

[60] Dawei Cai, and Hiroo Yamaura, "A robust controller for manipulator driven by artificial muscle actuator", IEEE International Conference on Control Applications, 1996.

[61] C.J. Bowler, D.G. Caldwell, and G.A. Medrano-Cerda, "Pneumatic muscle actuators: musculature for an anthropomorphic robot arm", IEEE Colloquium on Actuator Technology, vol. 8, pp. 1-6, 1996.

[62] D.W. Repperger, K.R. Johnson, and C.A. Phillips, “Nonlinear feedback controller design of a pneumatic muscle actuator system”, Proceedings of American Control Conference, 1999.

[63] P. Carbonell, Z.P. Jiang, and D.W. Repperger, “Nonlinear control of a pneumatic muscle actuator: backstepping vs. Sliding-mode”, IEEE International Conference on Control Applications, 2001.

[64] P. Carbonell, Z.P. Jiang, and D.W. Repperger, “A fuzzy backstepping controller for a pneumatic muscle actuator system”, IEEE International Symposium on Intelligent Control, pp. 353-358, 2001.

[65] M. Folgheraiter, Guiseppina Gini, M. Perkowski, and M. Pivtoraiko, “Adaptive reflex control for an artificial hand”, Proceeding SYROCO, 2003.

[66] K. Balasubramanian, and Kuldip S. Rattan, “Feedforward control of a non-linear pneumatic muscle system using fuzzy logic”, IEEE International Conference on Fuzzy Systems, vol. 1, pp. 272-277, 2003.

[67] K.K. Ahn, and TuDiep Cong Thanh, “Improvement of the control performance of pneumatic artificial muscle manipulators using an intelligent switching control method”, KSME International Journal, vol. 18, no. 8, pp. 1388-1400, 2004.

[68] K.K. Ahn, and TuDiep Cong Thanh, “Nonlinear PID control to improve the control performance of the pneumatic artificial muscle manipulator using neural network”, Journal of Mechanical Science and Technology, vol. 19, no. 1, pp. 106-116, 2005.

[69] Harald Aschemann, and Dominik Schindele, “Sliding-mode control of a high-speed linear axis driven by pneumatic muscle actuators”, IEEE Transactions on Industrial Electronics, vol. 55, no. 11, 2008.

[70] Seung Ho Cho, “Trajectory tracking control of a pneumatic c-y table using neural network based PID control”, International Journal of Precision Engineering and Manufacturing, vol. 10, no. 5, pp. 37-44, 2009.

[71] K. Xing, J. Huang, Y. Wang, J. Wu, Q. Xu, and J. He, “Tracking control of pneumatic artificial muscle actuators based on sliding mode and non-linear disturbance observer”, IET Control Theory and Applications, vol. 4, issue 10, pp. 2058-2070, 2010.

[72] Neville Hogan, "Adaptive control of mechanical impedance by coactivation of antagonist muscles", IEEE Transactions on Automatic Control, vol. 29, no. 8, 1984.

[73] William R. Murray, "Modelling elbow equilibrium in the presence of co-contraction". Proceedings of the Bioengineering Conference, pp. 190-193, 1988.

[74] William R. Murray, and Neville Hogan, "Co-contraction of antagonist muscles: Prediction and observation". Joint Dynamics and Control, IEEE International Conference on Engineering in Medicine and Biology Society (EMBS), vol. 4, pp. 1926-1927, 1988.

[75] Shane A. Migliore, Edgar A. Brown, and Stephen P. De Weerth, "Novel nonlinear elastic actuators for passively controlling robotic joint compliance", Transactions of ASME, vol. 129, pp. 406-412, 2007.

[76] Alexander Schepelmann, M.D. Taylor, and Hartmut Geyer, "Development of a testbed for robotic neuromuscular controllers", Robotics: Science and Systems VIII, 2013.

[77] M. Laffranchi, N.G. Tsagarakis, F. Cannella, and D.G. Caldwell, "Antagonistic and series elastic actuators: a comparative analysis on the energy consumption", IEEE/RSJ International Conference on Intelligent Robots and Systems, 2009.

[78] Christian Klauer, Jorg Raisch, and Thomas Schauer, "Advanced control strategies for neuro-prosthetic systems", Technically Assisted Rehabilitation (TAR), 2013.

[79] D. Mitrovic, S. Klanke, R. Osu, M. Kawato, and S. Vijayakumar, "A computational model of limb impedance control based on principles of internal model uncertainty", Plos One, vol. 5, issue 10, 2010.

[80] F. Dierick, C. Domicent, and C. Detrembleur, "Relationship between antagonistic leg muscles co-contraction and body centre of gravity mechanics in different level gait disorders", Journal of Electromyography and Kinesiology, vol. 12, pp. 59-66, 2002.

[81] Theodore E. Milner, and Caroline Cloutier, "The effect of antagonist muscle co-contraction on damping of the wrist joint during voluntary movement", IEEE 17th Annual Conference on Engineering in Medicine and Biology Society, vol. 2, pp. 1247-1248, 1995.

[82] Karin Hollerbach, C.F. Ramos, and H. Kazerooni, “Destabilizing effects of muscular co-contraction in human-machine interaction”, Proceedings of the American Control Conference, 1993.

[83] Chunjiang Fu, and Rubun Wang, “The influence of co-contraction to the arm impedance during free planar movement”, International Conference on Bioinformatics and Biomedical Engineering (ICBBE), pp. 1-3, 2009.

[84] Cheryl L. Lynch, Dimitry Sayenko, and Milos R. Popovic, “Co-contraction of antagonist muscles during knee extension against gravity: insights for functional electrical simulation control design”, IEEE International Conference on Engineering in Medicine and Biology Society (EMBS), 2012.

[85] Lael Odhner, and Harry Asada, “Equilibrium point control of artificial muscles using recruitment of many motor units”, IEEE/RAS International Conference on Biomedical Robotics and Biomechatronics, 2008.

[86] Olivier Missenard, Denis Mottet, and Stephane Perrey, “The role of cocontraction in the impairment of movement accuracy with fatigue”, Exp Brain Res, vol. 185, issue 1, pp. 151-156, 2008.

[87] Christian Klauer, Jorg Raisch, and Thomas Schauer, “Nonlinear joint-angle feedback control of electrically simulated and λ-controlled antagonistic muscle pairs”, European Control Conference (ECC), 2013.

[88] P. Spagnol, C. Klauer, F. Previdi, J. Raisch, and T. Schauer, “Modelling and online-identification of electrically stimulated antagonistic muscles for horizontal shoulder abduction and adduction”, European Control Conference (ECC), 2013.

[89] Daniel P. Ferris, and Cara L. Lewis, “Robotic lower limb exoskeletons using proportional myoelectric control”, IEEE International Conference on Engineering in Medicine and Biology Society (EMBS), 2009.

[90] Kalyan K. Mankala, Sai K. Banala, Sunil K. Agrawal, “Passive swing assistive exoskeletons for motor-incomplete spinal cord injury patients”, IEEE International Conference on Robotics and Automation, 2007.

[91] M. Kumamoto, T. Oshima, and T. Fujukawa, “Control properties of a two-joint link mechanism equipped with mono- and bi-articular actuators”, IEEE International Workshop on Robot and Human Interactive Communication, 2000.

[92] S. Shimizu, N. Momose, T. Oshima, and K. Koyanagi, Development of robot leg which provided with the bi-articular actuator for training techniques of rehabilitation, IEEE International Symposium on Robot and Human Interactive Communication, 2009.

[93] V. Salvucci, S. Oh, and Y. Hori, "Infinity norm approach for precise force control of manipulators driven by bi-articular actuators", Annual Conference on IEEE Industrial Electronics Society, pp. 1908-1913, 2010.

[94] V. Salvucci, S. Oh, Y. Hori, and Y. Kimura, "Disturbance rejection improvement in non-redundant robot arms using bi-articular actuators", Industrial Electronics (ISIE), IEEE Symposium, pp. 2159-2164, 2011.

[95] V. Salvucci, Y. Kimura, Y. Oh, and Y. Hori, "Experimental verification of infinity norm approach for force maximization of manipulators driven by bi-articular actuators", American Control Conference on O'Farrell Street, 2011.

[96] Luc P.J. Selen, Peter J. Beek, and Jaap H. van Dieen, "Can co-activation reduce kinematics variability? a simulation study", Biological Cybernetics, 2005.

[97] William K. Durfee, "Task-based methods for evaluating electrically stimulated antagonist muscle controllers", IEEE Transactions on Biomedical Engineering, vol. 36, no. 3, pp. 309-321, 1989.

[98] Samer Mohammed, Philippe Fraisse, David Guiraud, Philippe Poignet, Hassan El Makssoud, "Towards a co-contraction muscle control strategy for paraplegics", 44th IEEE Conference on Decision and Control, pp. 7428-7433, 2005.

[99] Samer Mohammed, Philippe Poignet, Philippe Fraisse, David Guiraud, "Optimal stimulation patterns for knee joint movement restoration during co-contraction of antagonist muscles", International Conference on Biomedical Robotics and Biomechatronics, pp. 678-692, 2010.

[100] Stewart Heitmann, Norm Ferns, and Michael Breakspear, "Muscle co-contraction modulates damping and joint stability in a three-link biomechanical limb", Frontiers in Neurorobotics, vol. 5, article 5, 14 pages, 2012.

[101] H. Kawai, T. Murao, R. Sato, and M. Fujita, "Passivity-based control for 2DOF robot manipulators with antagonistic bi-articular muscles", IEEE International Conference on Control Applications (CCA), pp. 1451-1456, 2011.

[102] K. Sano. H. Kawai, T. Murao, and M. Fujita, "Open-loop control for 2DOF robot manipulators with antagonistic bi-articular muscles", IEEE International Conference on Control Applications (CCA), pp. 1346-1351, 2012.

[103] Y. Kawai, H. Kawai, and M. Fujita, "RISE control for 2DOF human lower limb with antagonistic bi-articular muscles", IEEE International Conference on Control Applications (CCA), pp. 109-114, 2013.

[104] Y. Kawai, Ryan J. Downey, H. Kawai, and Warren E. Dixon, "Co-contraction of antagonist bi-articular muscles for tracking control of human limb", CDC, 2013.

[105] Y. Kawai, "A design of co-contraction level of antagonist muscles with muscle contraction dynamics for tracking control of human limb", SICE, 2013.

[106] Y. Shibata, S. Imai, T. Nobutomo, T. Miyoshi, and S.I. Yamamoto, Development of body weight support gait training system using antagonistic bi-articular muscle model, 32nd Annual International Conference of the IEEE EMBS, Buenos Aires, Argentina, 2010.

[107] S.I. Yamamoto, Y. Shibata, S. Imai, T. Nobutomo, and T. Miyoshi, Development of gait training system powered by pneumatic actuator like human musculoskeletal system, IEEE International Conference on Rehabilitation Robotics, ETH Zurich Science City, Switzerland, 2011.

[108] M.A. Mat Dzahir, T. Nobutomo, and S.I. Yamamoto, "Antagonistic mono- and bi-articular pneumatic muscle actuator control for gait training system using contraction model", IEEE International Conference on Bio-Science and Bio-Robotics, Rio de Janeiro, Brazil, 2013.

[109] M.A. Mat Dzahir, T. Nobutomo, and S.I. Yamamoto, "Development of body weight support gait training system using pneumatic McKibben actuators: control of lower extremity orthosis", International Conference of the IEEE EMBS, Osaka, Japan, 2013.

[110] Mohd Azuwan Mat Dzahir and Shin-Ichiroh Yamamoto, "Design and Evaluation of the AIRGAIT Exoskeleton: Leg Orthosis Control for Assistive Gait Rehabilitation", Journal of Robotics, vol. 2013, Article ID 535106, 20 pages, 2013. doi:10.1155/2013/535106.

[111] Mohd Azuwan Mat Dzahir, Tatsuya Nobutomo, and Shin-Ichiroh Yamamoto, "Development of Gait Training System Powered by Antagonistic Mono-and Bi-Articular Actuators Using Contraction Model Control Scheme", Applied

Mechanics and Materials, vol. 393 (2013), pp 525-531, Trans Tech Publications, Switzerland. doi:10.4028/www.scientific.net/AMM.393.525

[112] S. Balasubramanian, J. Ward, T. Sugar, and J. He, "Characterization of the dynamic properties of pneumatic muscle actuators", IEEE International Conference on Rehabilitation Robotics, Noordwijk, Netherlands, 2007.

[113] M. Frey, G. Colombo, M. Vaglio, R. Bucher, M. Jorg, and R. Riener, "A novel mechatronic body weight support system", IEEE Transactions on Neural Systems and Rehabilitation Engineering, vol. 14, no. 3, 2006.

[114] J. Von Zitzewitz, M. Bernhardt, and R. Reiner, "A novel method for automation treadmill speed adaptation", IEEE Transactions on Neural Systems and Rehabilitation Engineering, vol. 15, no. 3, 2007.

[115] H. Van Hedel, L. Tomatis, and R. Muller, "Modulation of leg muscle activity and gait kinematics by walking speed and bodyweight unloading", Gait and Posture, vol. 24, pp. 35-45, 2006.

[116] J. Bae, and M. Tomizuka, "A gait rehabilitation strategy inspired by iterative learning algorithm", Journal of Mechatronics, vol. 22, pp. 213-221, 2012.

[117] TuDiep Cong Thanh, and K.K. Ahn, "Nonlinear PID control to improve the control performance of 2 axes pneumatic artificial muscle manipulator using neural network", Mechatronics, vol. 16, pp. 577-587, 2006.

[118] David A. Winter, "Biomechanics and motor control of human movement", Fourth Edition, John Wiley & Sons, Inc., 2009.

[119] C. E. Carr and D. J. Newman, "Characterization of a lower-body exoskeleton for simulation of space-suited locomotion", Acta Astronautica, 62(4):308-323, 2008.

[120] K. Kiguchi, M. H. Rahman, M. Sasaki, and K. Teramoto, "Development of a 3dof mobile exoskeleton robot for human upper-limb motion assist", Robotics and Autonomous Systems, 56(8):678-691, 2008.

[121] J.-F. Zhang, C.-J. Yang, Y. Chen, Y. Zhang, and Y.-M. Dong, "Modeling and control of a curved pneumatic muscle actuator for wearable elbow exoskeleton", Mechatronics, 18(8):448-457, 2008.

[122] F. Amato, D. Colacino, C. Cosentino, and A. Merola, "Robust and optimal tracking control for manipulator arm driven by pneumatic muscle actuators", In Mechatronics (ICM), 2013 IEEE International Conference on, pages 827-834. IEEE, 2013.

[123] T. Thanh and K. K. Ahn, “Nonlinear PID control to improve the control performance of 2 axes pneumatic artificial muscle manipulator using neural network”, Mechatronics, 16(9):577-587, 2006.

[124] Y. Ariga, H. T. Pham, M. Uemura, H. Hirai, and F. Miyazaki, “Novel equilibrium-point control of agonist-antagonist system with pneumatic artificial muscles”, In Robotics and Automation (ICRA), 2012 IEEE International Conference on, pages 1470-1475. IEEE, 2012.

[125] T.-Y. Choi, B.-S. Choi, and K.-H. Seo, “Position and compliance control of a pneumatic muscle actuated manipulator for enhanced safety”, Control Systems Technology, IEEE Transactions on, 19(4):832-842, 2011.

[126] Z. Situm and S. Herceg, “Design and control of a manipulator arm driven by pneumatic muscle actuators”, In Control and Automation, 2008 16th Mediterranean Conference on, pages 926-931. IEEE, 2008.

[127] M.-K. Chang, “An adaptive self-organizing fuzzy sliding mode controller for a 2-dof rehabilitation robot actuated by pneumatic muscle actuators”, Control Engineering Practice, 18(1):13-22, 2010.

[128] F. Prattico, M. A. M. Dzahir, and S.-i. Yamamoto, “Couple control model implementation on antagonistic mono-and bi-articular actuators”, arXiv preprint arXiv:1404.2983, 2014.

[129] A. Ho_sovsk_y and M. Havran, “Dynamic modelling of one degree of freedom pneumatic muscle-based actuator for industrial applications”, Tehnicki vjesnik, 19(3):673-681, 2012.

[130] P. Fisette and J.-C. Samin, “Symbolic generation of large multibody system dynamic equations using a new semi-explicit newton/euler recursive scheme”, Archive of applied mechanics, 66(3):187-199, 1996.

[131] D. B. Marghitu, “Mechanisms and robots analysis with MATLAB”, Springer, 2009.

[132] M. Grebenstein and P. van der Smagt, “Antagonism for a highly anthropomorphic hand-arm system”, Advanced Robotics, 22(1):39-55, 2008.

[133] F. Prattico, C. Cera, and F. Petroni, “A new hybrid infrared-ultrasonic electronic travel aids for blind people”, Sensors and Actuators A: Physical, 201:363-370, 2013.

APPENDIX

PUBLICATION
PAPER 1

PUBLICATION
PAPER 2

PUBLICATION
PAPER 3

PUBLICATION
PAPER 4

PUBLICATION
PAPER 5

PUBLICATION
PAPER 6

PUBLICATION
PAPER 7

PUBLICATION
PAPER 8

PUBLICATION
PAPER 9

PUBLICATION
PAPER 10

PUBLICATION
PAPER 11

PUBLICATION
PAPER 12

Robotics **2014**, *3*, 120-148; doi:10.3390/robotics3020120

OPEN ACCESS

robotics

ISSN 2218-6581

www.mdpi.com/journal/robotics

Review

Recent Trends in Lower-Limb Robotic Rehabilitation Orthosis: Control Scheme and Strategy for Pneumatic Muscle Actuated Gait Trainers

Mohd Azuwan Mat Dzahir [1,2,*] and Shin-ichiroh Yamamoto [1]

[1] Shibaura Institute of Technology, Department of Bio-Science Engineering, 307 Fukasaku, Minuma-ku, Saitama City, Saitama 337-8570, Japan; E-Mail: yamashin@se.shibaura-it.ac.jp

[2] Universiti Teknologi Malaysia, Faculty of Mechanical Engineering, UTM Skudai, Johor Bahru 81310, Malaysia

***** Author to whom correspondence should be addressed; E-Mail: nb11503@shibaura-it.ac.jp or azuwan@fkm.utm.my; Tel.: +80-80-4094-8009.

Received: 10 January 2014; in revised form: 17 March 2014 / Accepted: 21 March 2014 / Published: 14 April 2014

Abstract: It is a general assumption that pneumatic muscle-type actuators will play an important role in the development of an assistive rehabilitation robotics system. In the last decade, the development of a pneumatic muscle actuated lower-limb leg orthosis has been rather slow compared to other types of actuated leg orthoses that use AC motors, DC motors, pneumatic cylinders, linear actuators, series elastic actuators (SEA) and brushless servomotors. However, recent years have shown that the interest in this field has grown exponentially, mainly due to the demand for a more compliant and interactive human-robotics system. This paper presents a survey of existing lower-limb leg orthoses for rehabilitation, which implement pneumatic muscle-type actuators, such as McKibben artificial muscles, rubbertuators, air muscles, pneumatic artificial muscles (PAM) or pneumatic muscle actuators (PMA). It reviews all the currently existing lower-limb rehabilitation orthosis systems in terms of comparison and evaluation of the design, as well as the control scheme and strategy, with the aim of clarifying the current and on-going research in the lower-limb robotic rehabilitation field.

Keywords: pneumatic muscle-type actuators; co-contraction strategy of antagonistic actuators

---

1. Introduction

The outcomes of rehabilitation therapy that implements body weight support treadmill training for incomplete spinal cord injuries (SCIs) and stroke patients have been reported in several previous studies since the 1990s. SCI involves damage to any component of the nerves or spinal cord located at the end of the spinal canal, which is either complete or incomplete. However, it often causes permanent changes in strength, sensation and other body functions below the site of the injury. The symptoms vary widely, beginning with pain to paralysis and, then, to incontinence. The paralysis may be identified as a weakness, which might occur with abnormal tone (e.g., spasticity or rigidity). During the stance phase, leg instability (*i.e.*, hyperextension or knee buckling) may result in unsafe walking, pain and inefficient energy. Moreover, inadequate limb clearance, impaired balance, sensory deficits and pain during the swing phase may contribute to falls, loss of balance and increased nervousness associated with walking. Furthermore, the loss of motor control prevents a patient from performing a precise movement in coordination with the timing and intensity of the muscle action.

Previously, a patient's paralyzed legs were physically operated by two therapists in manual training. In accordance with treadmill training therapy, based on the rules of spinal locomotion, research carried out by Wernig *et al.* for the incomplete paralysation of paraplegic and tetraplegic patients confirmed that the training was able to improve most of the patients' walking capability [1,2]. The patients involved in this training were provided with motor-driven treadmill training therapy, along with a body weight support (BWS) and assisted limb movements by therapists, for daily upright walking training. Based on the rehabilitation sessions, nearly 80% of patients with incomplete spinal cord injuries (a total of 33 individuals) were capable of walking independently after the treadmill training, with partial body weight support. However, this training procedure was physically difficult for therapists to execute for long durations of time. Recently, robot-assisted therapy devices have become increasingly used in SCI rehabilitation therapy. This assistive robot either compensates for the functionalities that a patient does not have or tries to recover the impaired functionalities. Even though it may not be able to fully compensate for impairments, or even provide a cure, it should be able to enhance or extend certain impaired functions, consequentially increasing the quality of life, encouraging independent living, as well as supporting the need for social interactions and communication. Depending on the degree and location of the injury, the actual rehabilitation or treatment can vary widely. In many cases, substantial rehabilitation and physical therapy are required for spinal cord injuries, particularly if the patient's injuries interfere with the activities of daily life.

Since SCI patients frequently have difficulties with daily functional movements and activities, it is possible to decrease their loss of function through rehabilitation therapy during the critical stage. This rehabilitation therapy engages carefully designed repetitive exercises, which are either passive or active. In a passive exercise, the therapist or a robot will actively assist the patient with moving the affected lower-limb repetitively, as prescribed. In an active exercise, the patients themselves will put effort into moving their legs, with no physical assistance. With the contribution of therapists, assistive robotic technology has had a significant ability to provide novel means for motivating, monitoring and coaching. In addition, many lower-limb leg orthoses for rehabilitation have been developed to assist in human locomotion training; they can be used for a long time and for varying degrees of spasticity or paresis [1–14]. According to Dietz *et al.*, who performed lower-limb-assisted gait training using a

developed orthosis system with BWS and treadmill training on patients with incomplete SCI, advocated that the afferent participation from the lower limb and hip joint movements are essential for the activation of the central pattern generator for locomotion rehabilitation training in SCI patients [3,4].

Consequently, the interest in this field has grown exponentially in recent years, mainly due to the demand for a much more compliant and interactive human-robotics system. Therefore, this work will appraise all of the current existing lower-limb rehabilitation orthoses, based on compliant actuator systems, in terms of their evaluation, design, control scheme and strategy. They will then be compared to each another, with the intent of clarifying current and on-going research in the lower-limb robotics rehabilitation field.

2. Existing Lower-Limb Orthoses for Gait Rehabilitations and Evaluations

Numerous assistive orthosis systems for gait rehabilitation have been developed that delve into several types of lower-limb rehabilitation, such as treadmill gait trainers, over-ground gait trainers, stationary gait and ankle trainers, foot-plate-based gait trainers and active foot orthoses for the neurologically impaired (including stroke and spinal cord injury (SCI) patients) [5–8]. These systems implement very unique mechanical structures, designs, actuators, methods, control schemes and rehabilitation strategies, as well as various procedures to ensure the reliability and robustness of the systems when compared to others. The rapid development of rehabilitation robotics over the last decade is working toward fully restoring or improving the mobility of affected limb functions and helping patients achieve a better quality of life.

2.1. Motorized Lower-Limb Orthosis Systems for Rehabilitation

The driven gait orthosis (DGO), also known as LOKOMAT (Hocoma AG, Volketswill Switzerland), is currently available on the market and has been extensively researched in many rehabilitation centers as one of the best examples for a gait orthosis that can be used for lower-limb disabilities [9–11]. This orthosis system is shown in Figure 1a. It consists of three main parts: body weight support, treadmill and powered leg orthosis. A direct current (DC) motor, with helical gears, was used for the actuation power of the system to precisely control the trajectory of the hip and knee joints. Considerable control algorithms have been implemented in this system to improve its performance, such as position, adaptability, impedance controllers, *etc.* To stimulate the locomotor function of the spinal cord and to activate leg muscles that have lost the capacity to actuate voluntary movement, it is important to provide adequate afferent input to the affected lower limb. It could be anticipated that the afferent input produced using automatic-based training is at least as efficient as that generated using manual training.

Figure 1b shows the treadmill gait trainer system, which incorporated an electromechanical gait device with the treadmill/gait training, known as the LokoHelp (LokoHelp Group, Germany). The LokoHelp used a different mechanical system compared to the LOKOMAT, which implemented a powered leg orthosis. The foot-powered orthosis, known as “Pedago”, uses an electromechanical gait device that was designed to provide a gait motion during the training session [12]. The control device helps to move the patients’ foot trajectory with a fixed step length of 400 mm, in which the gait cycle

(GC) speed can be varied from zero up to 5 km/h. Based on the research findings, it was proven that walking ability could be improved by incorporating task-oriented gait training with mechanical gait training devices or with treadmill training.

Figure 1. (**a**) LOKOMAT [10]; (**b**) LokoHelp (picture courtesy of LokoHelp group); and (**c**) ReoAmbulator (picture courtesy of Motorika Ltd.).

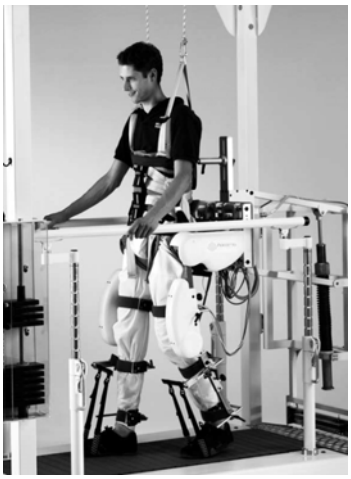

(**a**)

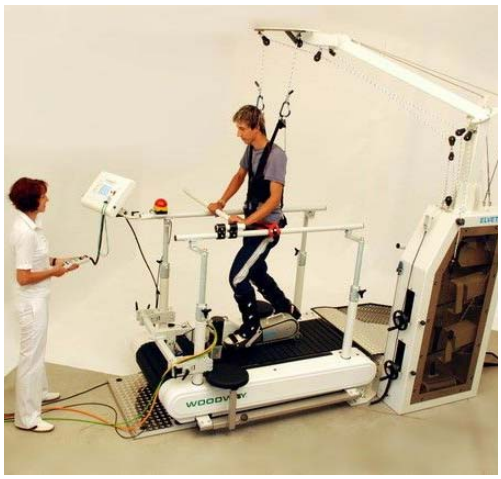

(**b**)

(**c**)

The ReoAmbulator robotic system (Motorika Ltd., Mount Laurel, NJ, USA), which is also known as "AutoAmbulator", is another example of existing treadmill gait trainers for lower-limb rehabilitation therapy, as shown in Figure 1c. This system has been used in research centers and medical hospitals for rehabilitation therapies and educational research studies [13,14]. This system also implements a powered leg orthosis, "robotic arms", which enables patients to contribute during the gait motion, but also provides the remaining force necessary for walking. The robotic arms are attached to the thigh and ankle of the patient's leg before a stepping pattern is performed using the implemented control scheme and strategy. In previous research on this system, it was concluded that robot-assisted gait training was able to provide improvements in balance and gait that are comparable to conventional/ manual physical rehabilitation therapies.

Apart from the available commercialized rehabilitation orthosis systems, the growth of the ReoAmbulator system has been rather immense with the development of different prototypes. The development of LOPES increased researchers' interest in developing a humanlike musculoskeletal assistive orthosis system. This gait rehabilitation orthosis employs the Bowden-cable driven series of elastic actuators (SEA), with the servomotors as the actuation system, to implement low weight (pure) force sources at both the posterior and anterior sides of the leg orthosis, as illustrated in Figure 2a [15,16]. It implemented impedance control (as opposed to admittance control), which is based on a combination of position sensing with force actuation to operate the lower-limb leg orthosis. The training effect of this orthosis was enhanced by emphasizing the implementation of an assist as needed (AAN) control algorithm. This enabled an increment of the active voluntary participation of the patients. Moreover, it is also possible to imply unhindered walking practice in the orthosis device, where the required forces/torques for imposing a gait pattern are determine based on the system's evaluation.

Figure 2. (**a**) LOPES [15]; (**b**) active leg exoskeleton (ALEX) [17]; and (**c**) NEUROBike [20].

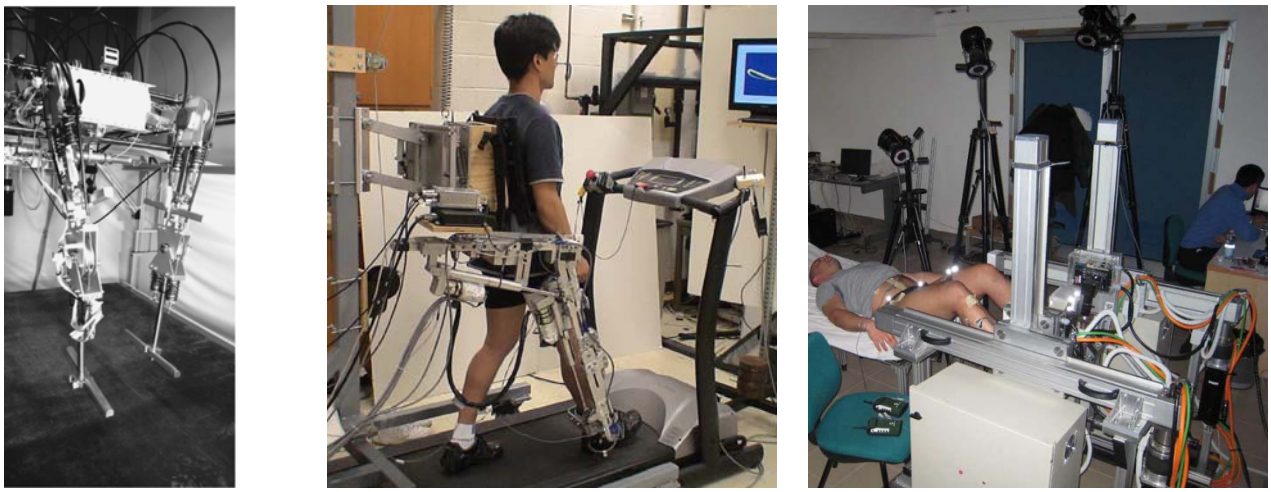

(**a**) (**b**) (**c**)

In the following years, a robot-assisted gait training (RAGT) was developed with an active leg exoskeleton (ALEX), also integrating the AAN rehabilitation strategy into the orthosis system. Compared to other existing robotic training methods, this strategy allows the patient to actively contribute during the retraining process of gait locomotion. This gait rehabilitation device is shown in Figure 2b. It implemented the use of linear actuators to actuate the hip joint thigh device and knee joint shank device of the leg orthosis [17,18]. It has been proven that an intensive gait retraining process has great potential to significantly provide benefits for the patients, including chronic stroke survivors. This can be achieved by effectively applying enough forces on the ankle of the subject through actuators placed at the hip and knee joints of the exoskeleton's leg orthosis, by means of a force-field controller.

Later, a stationary gait and ankle trainer system was developed to provide neural-rehabilitative treatments aimed at recovering walking abilities in post-stroke patients. This orthosis system employed the use of brushless servomotors and pulleys to actively control the angular excursions of the gait orthosis, known as the neural-rehabilitative platform for bedridden post-stroke patients (NEUROBike) [19]. The prototype of this system is shown in Figure 2c. The passive and active exercises were emphasized in this system by implementing the kinematic models of leg-joint angular excursions during both "sit-to-stand" and "walking" in the control algorithms. To summarize, providing a number of exercises at an early phase based on the intensity and the severity of the pathology is required by the programmed therapy. In addition, customized treatment adapted by this system may facilitate patients by increasing their flexibility in lower-limb control, which leads to significant improvements in motor control performance during locomotion.

In addition, a robotic gait rehabilitation (RGR) trainer prototype was also invented within the same year as the NEUROBike system, to assist treadmill gait retraining for patients with unusual gait patterns that were associated with exaggerated pelvis obliquity, illustrated in Figure 3a. This orthosis is composed of three subsystems: stationary frame, human-robot interface (HRI) and treadmill training. Servo-tube linear electromagnetic actuators were used to generate the power source for the exoskeleton [20]. Based on a hypothesis, the correction of a stiff-legged gait pattern entails addressing both the primary and secondary gait deviations to restore a physiological gait pattern. Therefore,

an expanded impedance control strategy was used to generate the corrective moments, only when the leg was in swing motion, by switching the force field that affects the obliquity of the pelvis. It has been demonstrated that this system can be effective in guiding the pelvis to the frontal plane via force fields used for altering pelvic obliquity.

Figure 3. (**a**) Robotic gait rehabilitation (RGR) trainer [20]; and (**b**) LOKOIRAN [21].

(**a**) (**b**)

Recently, a new gait training robotic device (LOKOIRAN) was designed to be suitable for patients with various diagnoses, such as SCI, stroke, multiple sclerosis (MS) and sport injury cases, aging and people with balance and locomotion disorders. Figure 3b illustrates the system's prototype. This gait training device delves into several subsystems, consisting of body weight support, a leg exoskeleton, a driving system and a transmission system. It employs alternating current (AC) motors connected to a slide-crank mechanism via belts and pulleys to provide the energy for the system [21]. The implemented control system enables flexibility in motion and permits subjects to change the speed of the foot plates by engaging the speed control mode and the admittance control mode.

The evaluated motorized lower-limb gait rehabilitation orthosis systems mentioned are only a fraction of the currently existing rehabilitation orthoses. However, it could be summarized from these examples that their development has reached an advanced level; whereby, many of the lower-limb gait rehabilitation orthoses, based on electrical motors, have already been commercialized. With the speed of growth in their mechanical design, as well as, the implementation of advanced control schemes and strategies, the space available for enhancements might soon reach its peak.

2.2. Attributes of Pneumatic Muscle Actuators (PMA)

The implementation of pneumatic muscles enables pneumatic power to be transferred into mechanical power. This actuator will be shortened in the longitudinal direction and enlarged in the radial direction during the contraction stage, when it is being inflated; when being deflated, it will turn back to its original form. The pneumatic muscle is able to employ a tensile force to an attached load during the contraction stage. This force is unidirectional, whereby the original length of a certain designed diameter and the internal pressure will determine its value. Moreover, this actuator also

inhibits nonlinear behaviors, such as hysteresis, compressibility and time variance. However, in exchange, this pneumatic muscle also has an inherently compliant attribute, which is suitable for a human-robotics system. This type of actuator is similar to the human muscle principle; a shorter muscle length produces a smaller contracting force and *vice versa*. Furthermore, it is comparable to electric actuators, due to the direct coupling to the load, the structural optimization and the power/weight ratio.

In addition to the abovementioned attributes, there exist two main weaknesses that limit the application of pneumatic muscles. The first weakness is the nonlinear behavior of pressure build-up, and the second weakness is the hysteresis effect, due to its geometric structure. These drawbacks cause complexity when scheming high-performance control systems. Therefore, this research is dedicated to solving these problems, using a simple paradigm and control strategy for handling the sudden increase in pressure and the hysteresis behavior of the PMA. Based on the proposed empirical-based static force mathematical model, which consist of a correction factor caused by the effect of the end caps, it showed an inconsistency of the high contracting ratios derived by the famous researcher, Tondu *et al.*, [22]. The extreme difficulty in constructing an accurate mathematical model was established by the fact that nearly all of the present models proposed were approximations. This model was later modified through various methods, used by other researches, to further improve the mathematical model [23–30].

2.3. Pneumatic Muscle Actuated Lower-Limb Rehabilitation Orthosis System

Compared to the motorized lower-limb rehabilitation orthosis systems (*i.e.*, DC motors, AC motors, linear actuators, SEA, servomotors, brushless motors and pneumatic cylinders), the growth of pneumatic muscle-actuated rehabilitation orthosis systems has been rather poor. This is also the description of the development of the control system for pneumatic muscles. However, numerous research studies in the last 10 years have tried to introduce these types of actuation systems into the lower-limb rehabilitation robotics field. This may indicate a significant shift of researchers' interests towards the implementation of a pneumatic muscle-actuated lower-limb rehabilitation orthosis.

A hip orthosis exoskeleton powered by pneumatic artificial muscle (PAM) was invented by Vimieiro *et al.*, at the Bioengineering Laboratory in 2004, as shown in Figure 4a [31,32]. This exoskeleton system was designed and modeled for patients with a motor deficit, a result of poliomyelitis. It consists of two main parts: the first is a polyethylene pelvic brace to provide the stability for the orthosis system, and the second is a polyethylene support for the thigh. This orthosis system implements position control using potentiometers for activating the control valves, either to pressurize the PAM or to return it to neutral status. Based on clinical tests, it was proven that this rehabilitation engineering was able to provide equipment and devices for aiding patients in recovering their movements or to improve their quality of life. A better gait pattern and an improvement of the left step transposition in the toe-off phase were reported by patients.

Later came the robotic gait trainer (RGT) for stroke rehabilitation, which is an ankle rehabilitation device powered by lightweight springs over muscle (SOM), proposed by Kartik *et al.* It was developed in 2006, as shown in Figure 4b [33]. The design is structurally based on a tripod mechanism with one fixed link. This orthosis device is able to provide the dorsiflexion and

plantar-flexion, as well as the inversion and eversion when moving the foot about the ankle joint. It implements an angular position for the control system and uses two types of sensors (*i.e.*, potentiometer and pressure sensor). In this study, Kartik *et al.* suggested that the range and position of motion (ROM) is necessary for safe dorsiflexion/plantar-flexion and inversion/eversion movements. This was proven by the results from their analysis, which demonstrated that the tripod structure was able to generate a ROM that matches the safe anatomical range of the ankle joint during the gait cycle.

Figure 4. (**a**) Hip orthosis [32]; (**b**) robotic gait trainer (RGT) [33]; and (**c**) ankle-foot orthosis (AFO). SOM, springs over muscle [36].

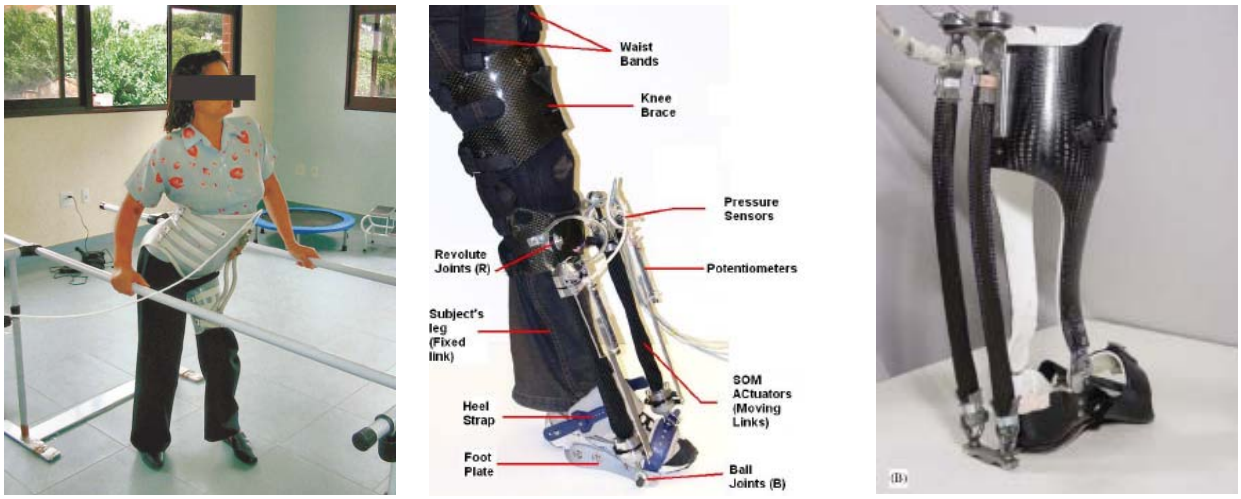

(**a**) (**b**) (**c**)

In contrast, the prototype of an ankle-foot orthosis (AFO) powered by artificial pneumatic muscle was also introduced by Ferris *et al.* in 2006. The prototype was of the human lower-limb that could comfortably provide dorsiflexion and plantar flexion torque during walking motion training, as illustrated in Figure 4 [34–36]. This orthosis is composed of a hinge joint, a carbon fiber shell and two pneumatic artificial muscles. The proportional myoelectric control, using a PC-based controller (real-time control), had been implemented in the control system. The performance of the novel controller enables naive wearers to promptly become accustomed to the orthosis, without the pneumatic muscle co-contraction. It is believed that this orthosis design will be useful in learning human walking biomechanics and in providing assistance of patients with neurological injuries during rehabilitation training.

Conversely, by focusing on the development of “human friendly” exoskeleton orthosis systems, Costa *et al.* in 2006 proposed a powered lower-limb orthosis, which can produce powerful, yet naturally safe, operations for paraplegic patients, as illustrated in Figure 5a [37]. This was realized by combining a highly compliant actuator (PMA) with an embedded intelligent control system (a three level PID joint torque control scheme) to manipulate the antagonistic actuators of the exoskeleton. It is difficult to provide a system with dependability and inherent safety, while utilizing a highly compliant actuator, using conventional designs alone. However, the design philosophy of this system may provide a significant insight into the development of rehabilitation orthosis systems and improve rehabilitative procedures for paraplegic patients.

Figure 5. (**a**) Powered lower-limb orthosis [37]; (**b**) Robotic Gait Trainer in Water (RGTW) [38]; and (**c**) powered ankle-foot exoskeleton [39].

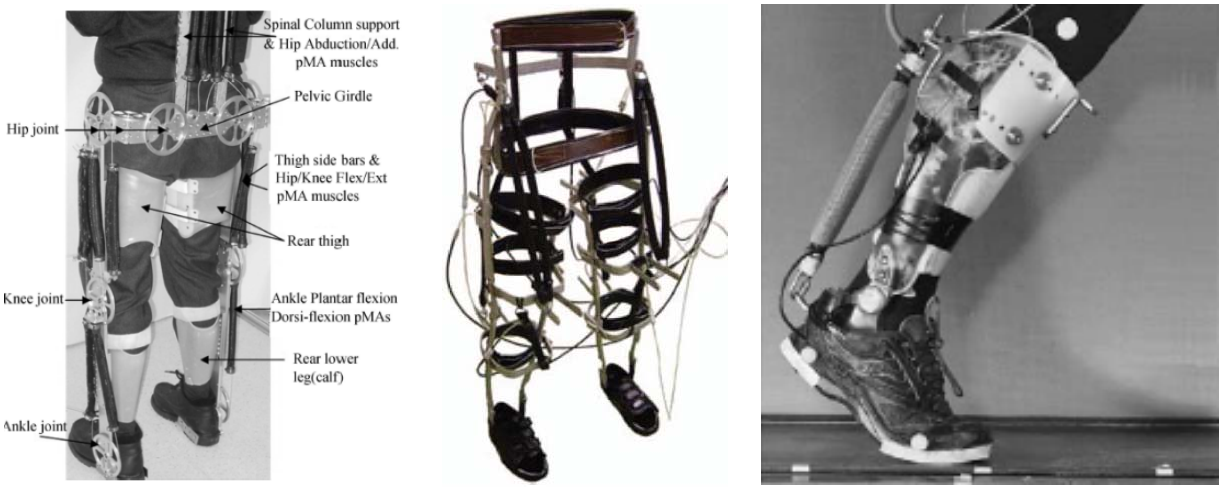

(**a**) (**b**) (**c**)

Contrastingly, Figure 5b shows the Robotic Gait Trainer in Water (RGTW). This system was designed for the development of an underwater gait training orthosis by Miyoshi *et al.* in 2008 [38]. The RGTW is a hip-knee-ankle-foot orthosis with pneumatic McKibben actuators as the actuation system. The basis of the angular motion for the control system was determined by a healthy subject walking under water. The aim for this study was to achieve repetitive physiological gait patterns to improve movement dysfunctions. By implementing this orthosis system device, not only the effect of hydrotherapy should be expected, but standard treadmill training is also included. This could also be sufficiently effective for patients undergoing hip-joint movement dysfunction treatments.

In 2009, Malcom *et al.* developed a powered ankle-foot exoskeleton, which investigated the role of the tibialis anterior (TA) in the walk-to-run condition, as shown in Figure 5c [39–42]. The pneumatic muscles are used to provide the dorsiflexion and plantar-flexion torques through the assisting orthosis for incomplete SCI patients during assist and resist conditions. This orthosis device implements an electromyography (EMG) control with a feed-forward algorithm; whereby, a set of rotary encoders and load cells are used to measure the treadmill belt speed, ankle angle and the dorsiflexion and plantar-flexion torques. Through a hypothesis developed from gait transitions and research evaluations, it was demonstrated that the powered exoskeleton had great potential in fundamental gait studies.

After the introduction of AFO by Ferris *et al.*, the development of this system was later continued by Sawicki *et al.*, a few years later. In 2009, the pneumatically powered knee-ankle-foot orthosis (KAFO) was proposed through the study of human motor adaptation, gait rehabilitation and locomotion energetics; as shown in Figure 6a [43]. Compared to the AFO control system, this system implements a physiologically-inspired controller that utilized the patient's muscle information, which is determined using electromyography to measure the timing and amount of the artificial muscle forces. Based on several research findings, it is believed that powered knee-ankle-foot orthoses are promising for basic science and clinical applications, since they have successfully assisted individuals with incomplete SCI during locomotor training, metabolic energy consumption and neural adaptation for neurologically intact human walkers.

Figure 6. (**a**) Knee-ankle-foot orthosis (KAFO) [43]; (**b**) continuous passive motion (CPM) [44]; and (**c**) power-assist lower-limb orthosis [45].

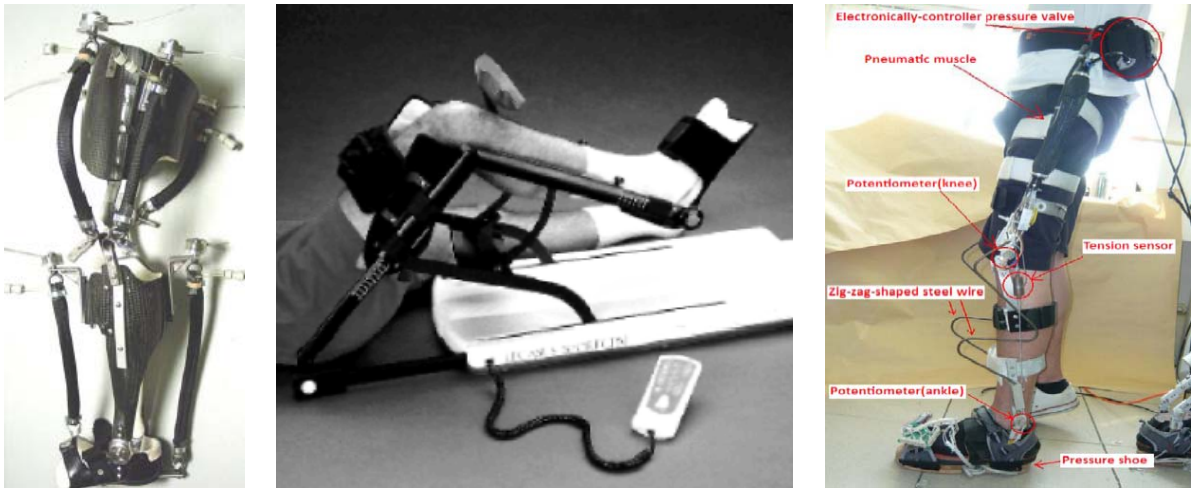

(**a**) (**b**) (**c**)

New high performance devices are required for applying continuous passive rehabilitation training for post-traumatic disabilities regarding the bearing joints of the inferior limbs; therefore, the introduction of a stationary gait and ankle trainer, known as continuous passive motion (CPM), was based on the rehabilitation system illustrated in Figure 6b [44]. This system was invented by Tudor *et al.* in 2009, using pneumatic muscles as the actuation system for providing a low-cost rehabilitation system. With the lower limb being immobilized during the rehabilitation (patient lying on a bed), it allows for the hip and knee joints to perform recovery exercises. When compared to the electro-mechanically-actuated rehabilitation system, which causes discomfort for the users, due to the introduction of shocks upon the reversion of the sensing of motion, this system utilizes a source of energy, namely air, which enables the shocks that occur to be completely absorbed.

Figure 6c shows a power-assist lower-limb orthosis, proposed by Yeh *et al.* in 2010, for assisting the elderly and individuals suffering from sport injuries with walking or climbing stairs using McKibben pneumatic muscles as the actuation system [45]. For achieving better tracking performance, an inverse control for the feed-forward compensation is constructed using the hysteresis model, which is then combined with loop transfer recovery (LTR) feedback control. In addition to ensuring smooth switching between different phases during operation, bump-less switching compensators are implemented in the combined control system. Based on the research findings, it was demonstrated that the orthosis was able to effectively accomplish the assistive function of human locomotion during walking and climbing stairs.

Moreover, the two-degrees of freedom active ankle-foot orthosis (AAFO) was designed and manufactured in 2011 by Carberry *et al.* for post stroke rehabilitation, exemplified in Figure 7a [46]. By implementing a novel actuator linkage using air muscles, a lightweight and discrete orthosis system was achieved. This design enables the entire actuation system to be placed behind the leg of the orthosis. A feedback control that utilizes a fuzzy logic gait phase detection system is implemented with the use of two types of sensory devices: the first is force sensitive resistors (FSRs), located under the insole of the shoe; the second is the rotary encoder for measuring the angular displacement of the ankle joint. However, it is unlikely that suitable methods of supplying air pressure to the device can be found,

even though this system exhibits many desirable features. This system may well be beneficial to after-stroke patients, as it allows a more complete rehabilitation of the ankle joint.

Figure 7. (**a**) Active ankle-foot orthosis (AAFO) [46]; (**b**) bio-inspired active soft orthotic for ankle-foot pathologies [47]; and (**c**) active modular elastomer for soft wearable assistance robots [48].

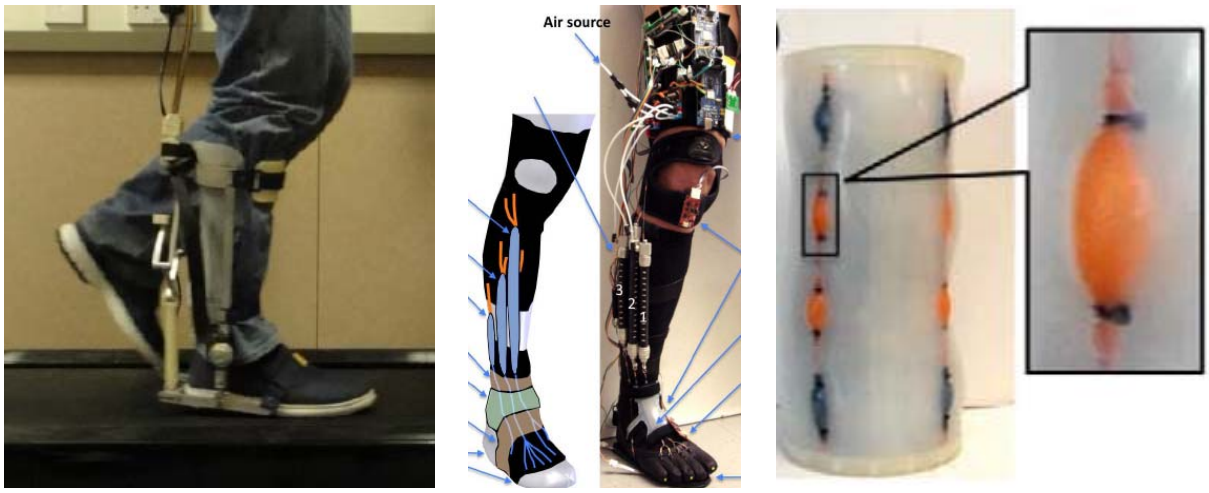

(**a**) (**b**) (**c**)

In 2011, a bio-inspired active soft orthotic device for ankle foot pathology was developed by Park *et al.* for treating gait pathologies associated with neuromuscular disorders, as shown in Figure 7b [47]. By utilizing the advantages of the pneumatic artificial muscle actuators, an inspired biological musculoskeletal system with a muscle-tendon-ligament structure was introduced as the design of this orthosis system. Three types of sensors are used for the control system: the first is a strain sensor for measuring ankle joint angle changes; the second is an internal measurement unit (IMU) to measure the orientations of the lower leg and the foot; and the third is a pressure sensor to identify the foot ground contacts and gait cycle events. The implemented feed-forward and feedback controllers were able to demonstrate a good repeatability of the ankle joint angle control. Based on the outcomes of the result, this research is believed to be capable of providing rich spaces for growth for rehabilitation techniques for ankle pathologies in the near future.

Furthermore, in 2012, Park *et al.* also developed another lower-limb rehabilitation orthosis, known as the active modular elastomer sleeve for soft wearable assistance robots, to support and monitor human joint motions, as illustrated in Figure 7c [48]. With a different system design proposal, this orthosis device implements a series of miniaturized pneumatically-powered McKibben-type actuators. These actuators are wrapped in between monolithic elastomer sheets, so as to exert tension. Through shape and rigidity control, simultaneous motion sensing and active force response are allowed by wrapping the material around the joint. The muscle contractions for the actuators are measured by placing the hyper-elastic strain sensor perpendicularly to the axial direction of each corresponding actuator. This strain sensor will detect the radial expansion of each actuator, which is then transformed to the contraction length of the muscle actuator. Based on the preliminary study of this device system, a few improvements should still be made within the design structure and control system.

Figure 8a presents a developed, inexpensive, pneumatically-powered assisted knee-ankle-foot orthosis (KAFO), using McKibben actuators, for providing assistance during gait training; proposed by Teng *et al.* in 2012 [49]. To determine the relationship between the inclination angles of each joint with pneumatic muscle displacement, the equation is expressed by using a trigonometry method; employed in the control system algorithm and strategy. However, this lower-limb orthosis system is still in the early development stage of design improvement; therefore, further evaluation on system performance has yet to be concluded.

Figure 8. (**a**) Inexpensive KAFO [49]; (**b**) orthosis for walking assistant [50]; and (**c**) a six degrees of freedom (DOF) robotic orthosis for rehabilitation [52].

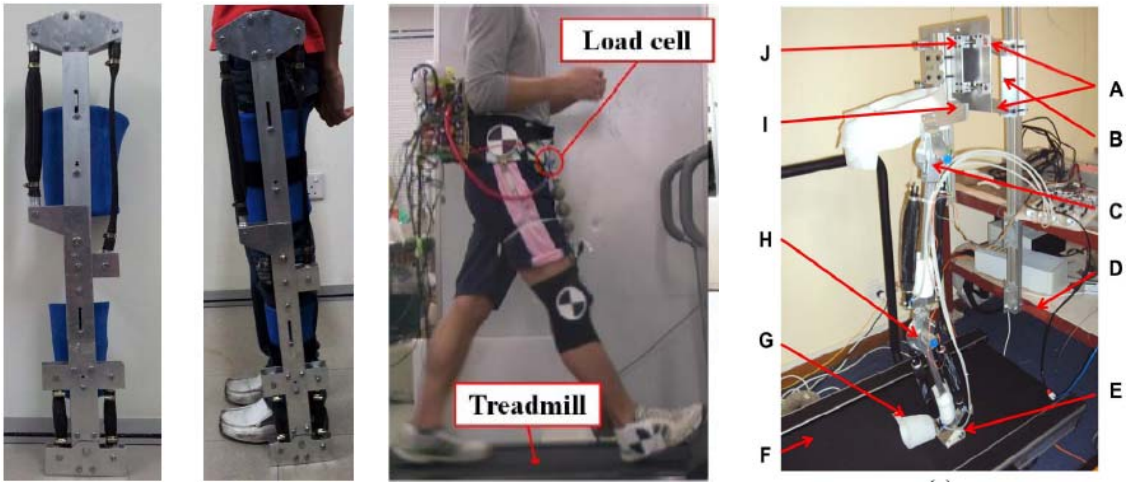

(**a**) (**b**) (**c**)

In 2013, Kawamura *et al.* initiated the development of an orthosis for walking assistance. It is designed using straight fiber pneumatic artificial muscles in assisting the forward swing of the leg and increasing the step length to further recuperate patients' walking abilities, as illustrated in Figure 8b [50]. The pressure control unit is implemented using the developed dual pneumatic control system (DPCS) by manipulating the pulse-width modulation (PWM) signal to control the valve. This orthosis system has yet to reach its completion and requires further improvements in its control scheme and strategy when handling the nonlinearity behavior of the actuator. The assistant force generated by the orthosis system is not adequate enough for driving the intended task.

Recently, in 2013, Hussain *et al.*, invented a six degree of freedom robotic orthosis for gait rehabilitation to encourage patients' voluntary contribution in the robotic gait training process, as shown in Figure 8c [51,52]. It implements four pneumatic muscle actuators, which are arranged as two pairs of antagonistic mono-articular muscles at the hip and knee joint angles. This system integrates the AAN gait training algorithm based on the adaptive impedance control, employing a boundary-layer-augmented sliding mode control (BASMC)-based position controller, to afford an interactive robotic gait training system. It was proven that the implementation of the adaptive impedance control scheme is able to provide gait motion training that is comparable to the one provided by physical therapists. Additionally, the result findings demonstrated that an increase/decrease in the human's voluntary participation during gait training will result in a decrease/increase of robotic assistance.

Table 1. Comparison of existing pneumatic muscle-actuated lower-limb rehabilitation orthosis systems.

Comparison of Existing Pneumatic Muscle Actuated Lower-Limb Rehabilitation Orthosis Systems						
Orthosis System	**Time Scale**	**Robotic System Types**	**Actuators**	**Antagonistic Actuators**	**Control System**	**References**
Hip orthosis exoskeleton	2004	Hip orthoses	McKibben pneumatic muscle	Mono-articular for hip joint (flexion)	Position control using the potentiometers for activating the control valves	[31,32]
Robotic gait trainer (RGT)	2006	Foot orthoses	Lightweight spring over muscle (SOM)	Mono-articular for ankle joint (dorsiflexion)	Angular position control system	[33]
Ankle-foot orthosis (AFO)	2006	Foot orthoses	McKibben pneumatic muscle	Mono-articular for ankle joint (dorsiflexion and plantar-flexion)	Proportional myoelectric control using a PC-based controller	[34–36]
Powered lower-limb orthosis	2006	Treadmill gait trainers	Pneumatic muscle actuators (PMA)	Mono-articular for hip joint (flexion, extension, abduction and adduction), knee joint (flexion and extension) and ankle joint (dorsiflexion and plantar-flexion)	Intelligent embedded control mechanism (a three-level PID joint torque control scheme)	[37]
Robotic gait trainer in water (RGTW)	2008	Over-ground gait trainers with orthosis	McKibben pneumatic muscle	Mono-articular for hip joint (flexion and extension) and knee joint (flexion and extension)	Position control system	[38]
Powered ankle-foot exoskeleton	2009	Foot orthoses	Pneumatic artificial muscle (PAM)	Mono-articular for ankle joint (dorsiflexion and plantar-flexion)	Electromyography (EMG) control with feed-forward algorithm	[39–42]
Powered knee-ankle-foot orthosis (KAFO)	2009	Knee and foot orthoses	McKibben pneumatic muscle	Mono-articular for knee joint (flexion and extension) and ankle joint (dorsiflexion and plantar-flexion)	Physiological-inspired controller using electromyography	[43]
Continuous passive motion (CPM)	2009	Stationary gait and ankle trainers	Pneumatic artificial muscle (PAM)	–	–	[44]

Table 1. *Cont.*

Comparison of Existing Pneumatic Muscle Actuated Lower-Limb Rehabilitation Orthosis Systems						
Orthosis system	**Time Scale**	**Robotic System Types**	**Actuators**	**Antagonistic Actuators**	**Control System**	**References**
Power-assist lower-limb orthosis	2010	Over-ground gait trainers (mobile)	McKibben pneumatic muscle	Mono-articular for knee joint (extension)	Inverse control and loop transfer recovery (LTR) feedback control	[45]
Active ankle-foot orthosis (AAFO)	2011	Foot orthoses	McKibben pneumatic muscle	Mono-articular for ankle joint (plantar-flexion)	Feedback control that utilizes a fuzzy logic gait phase detection system	[46]
Bio-inspired active soft orthotic device	2011	Foot orthoses	Pneumatic artificial muscle (PAM)	Mono-articular for ankle joint (dorsiflexion, inversion and eversion)	Feed-forward and feedback controllers	[47]
Active modular elastomer sleeve for soft wearable assistance robots	2012	Knee orthoses	Miniaturized McKibben pneumatic muscle	Mono-articular for knee joint (flexion and extension)	Through shape and rigidity control	[48]
Knee-ankle-foot orthosis (KAFO)	2012	Knee and foot orthoses	Pneumatic artificial muscle (PAM)	Mono-articular for hip joint (flexion and extension) and knee joint (flexion and extension)	_	[49]
Orthosis for walking assistant	2013	Hip orthoses	Straight fiber pneumatic artificial muscle (PMA)	Mono-articular for hip joint (flexion)	Dual pneumatic control system (DPCS) with a pulse-width modulation (PWM) signal	[50]
Six degree of freedom robotic orthosis for gait rehabilitation	2013	Treadmill gait trainers	McKibben pneumatic muscle	Mono-articular for hip joint (flexion and extension) and knee joint (flexion and extension)	Adaptive impedance control using boundary-layer-augmented sliding mode control (BASMC)	[51,52]

Table 1 shows the comparison of existing pneumatic muscle actuated lower-limb rehabilitation orthosis systems. Based on the evaluations of these systems for the past 10 years, it can be concluded that researchers' interests shifted to the implementation of the natural compliant-type actuators (*i.e.*, McKibben muscle, rubbertuators, air muscle, PAM, PMA, *etc.*). This was proven by the development of different types of assistive gait rehabilitation orthosis system prototypes, including foot orthoses, hip orthoses, knee-foot orthoses, stationary gait and ankle trainers, over-ground gait trainers with orthoses, mobile over-ground gait trainers and treadmill gait trainers [31–52]. In addition, the improvement of the control system implementation, since the year 2004 up until 2013, showed that researchers were gradually trying to improve the control of pneumatic muscle-actuated lower-limb orthoses, as illustrated in Table 1. In the beginning, only a simple angular position control was proposed to activate the control valves. Later, it was shifted to the implementation of proportional myoelectric control, intelligent embedded control, inverse control, feedback control (which utilized a fuzzy logic), rigidity control and, subsequently, adaptive impedance control. The exponential growth of these systems might also be due to the advantageous attributes of the pneumatic muscle actuator, as well as its nonlinear dynamic behavior. However, according to the evaluations of currently existing systems, it could be understood that suitable control schemes and strategies have yet to be found. Regardless, this only suggests that the space available for orthosis device improvements and enhancements, in either mechanical design or control scheme and strategy, is still boundless. This opportunity will attract researchers' interest in devising distinctive ideas and strategies to rectify previous methods or to discover new methods for the control system. Even though many different robotic system types for lower-limb rehabilitation orthoses have been developed, each prototype only implements the use of mono-articular muscles alone, either for hip, knee or ankle joints (*i.e.*, flexion, extension, abduction, adduction, plantar-flexion, dorsiflexion, inversion, eversion, *etc.*). However, no attempt has been made to introduce the implementation of bi-articular muscles, either to compensate for the lack of force/torque at the joints or to improve the control scheme and strategy performance.

3. Control Scheme and Strategy

The need for improved control strategies in handling the antagonistic actuator of pneumatic muscles will determine the progression of growth in lower-limb rehabilitation orthosis systems. Based on previous research, it is possible to utilize a standard PID controller in a feedback loop to control the joint angle of the assistive robotics within desired values. Nevertheless, without additional model paradigms or integrated controllers, it may not be able to accurately control a compliant robotic system, due to the complex and highly nonlinear dynamics of the pneumatic muscle. Thus, the resulting position control would be rather poor. For that reason, the implementation of conventional PID controllers should come with additional control strategies, such as additional model paradigms, auto-tuning, a nonlinear system, adaptive control, intelligent control (*i.e.*, neural network, fuzzy logic, genetic algorithm, *etc.*), robust control and stochastic control. A control scheme and strategy that enables a much simpler approach for the control system implementation in orthotic rehabilitation robotics is strongly desired. Therefore, in this review article, the implementation of co-contraction controls in manipulating the antagonistic actuators and the advantages will be discussed and elaborated thoroughly.

3.1. Pneumatic Muscle Actuators' Control System

Even though numerous control systems have been established for pneumatic actuators, especially pneumatic cylinders, only a fraction have been for artificial pneumatic muscles. From 1993 to 1995, some examples of well-known controllers that could be implemented, adopted by Caldwell *et al.*, were tested on a feed-forward PID regulator to develop an adaptive controller for a pneumatic artificial muscle (PAM) manipulator [53–55]. Likewise, in 1995, Gustavo *et al.* developed an adaptive position control for antagonistic pneumatic muscle actuators via adaptive pole-placement [56]. Furthermore, in 1995, Hamerlain *et al.* introduced a variable structure control that included a high robust performance, with respect to model errors, parameter variations and quick responses [57]. Within the same year, Iskarous *et al.* proposed intelligent control using a neuro-fuzzy network to control the complex dynamic properties of muscle actuators [58]. In 1996, van der Smagt *et al.*, introduced a neural network-based controller to a pneumatic robot arm; with complex, highly nonlinear dynamics that change over time, due to internal influences [59]. Additionally, in 1996, Cai and Yamaura presented a robust tracking control approach by implementing a sliding mode controller [60]. Within the same year, Colin *et al.* proposed position and PID controllers for force manipulation using adaptive pole-placement techniques [61].

Afterwards, in 1999, Repperger *et al.* handled the nonlinear factor with a nonlinear feedback controller, using a gain scheduling method [62]. Tondu and Lopez also employed a sliding-mode control approach in the year 2000 [22]. Contrarily, Carbonell *et al.* introduced nonlinear control of a pneumatic muscle actuator by using adaptive back-stepping and sliding-mode tracking controllers in 2001 [63,64]. In 2003, Folgheraiter *et al.* developed an adaptive controller based on a neural network for an artificial hand [65]. In the same year, Balasubramanian and Rattan proposed the feed-forward control of a nonlinear pneumatic muscle system using fuzzy logic [66]. From 2004 to 2006, Ahn and Tu proposed an intelligent switching control scheme by utilizing a learning vector quantization neural network and a nonlinear PID control to improve the control performance of a PAM manipulator using a neural network (NN) [67,68]. In 2008, Harald *et al.*, developed the cascade sliding mode (SM) control scheme for a high-speed linear axis pneumatic muscle [69]. Moreover, Seung *et al.* proposed a trajectory tracking control using a neural network based on PID control in 2009 [70]. In 2010, Xing *et al.* introduced the tracking control of pneumatic artificial muscle actuators based on a sliding-mode and non-linear disturbance observer (SMCBNDO) in order to improve the robustness and performance of the trajectory tracking control [71].

Unfortunately, applying a complicated control algorithm does not always indicate the best solution used to control pneumatic muscles. There is an argument in the field of rehabilitation robotics regarding what is the best control system of the orthotic problem for rehabilitation. It is preferred that control systems be simplified as much as possible; multiple sensors and impedances only increase the complexity of control systems. Rather than using a very complicated algorithm for a system, a much simpler approach may be proposed.

3.2. Co-Contraction of Antagonistic Muscle Control

An early study of the co-contraction of antagonist muscle control was carried out by Neville Hogan in 1984, which introduced the adaptive control of mechanical impedance by co-activation of antagonist muscles [72]. This research study focused on biomechanical modeling and the analysis of simultaneous co-activation of antagonist muscles by controlling the mechanical impedance. A dynamic optimization theory was used to obtain a prediction of antagonist co-activation, thus enabling a criterion function minimization, which represented the task of maintaining an upright posture. Based on the research findings, it was concluded that under normal psychological conditions, significant levels of the simultaneous activation of antagonist muscles were observed. In addition, the levels of antagonist muscles co-activation were also increased with the increment of gravitational torques. The modeled isometric muscle torque is represented in the following:

$$T_{biceps} = \left(T_o - K_{QS}\theta\right)u_{biceps} \tag{1}$$

$$T_{triceps} = -(T_o + K_{QS}\theta)u_{triceps} \tag{2}$$

$$(u) \text{ is the neural control } \begin{cases} 0 \le u_{biceps} \le 1 \\ 0 \le u_{triceps} \le 1 \end{cases} \tag{3}$$

Joint stiffness at maximum activation is:

$$\left(0 \le K_{QS} \le {}^{2T_o}/_{\pi}\right) \tag{4}$$

where (T_o) is the maximum isometric muscle torque.

Subsequently, in 1988, William R. Murray *et al.* carried on this research by implementing a simple model demonstrating the quasi-static behavior of skeletal muscles, in which the force generated by the muscle was the neural activation of the muscle and the bilinear function of the muscle length [73,74]. This muscle activation could be defined as the synchronized activation of agonist and antagonist muscle groups, acting in the same plane and crossing at the same joint. It was verified that the relationship between antagonistic actuators (*i.e.*, agonist and antagonist) could be linearly related in the occurrence of various fixed levels of co-contractions. In other words, the plane of agonist and antagonist muscle activity, the "equilibrium line" or the locus of all feasible levels of muscular activation, will be a straight line for which a particular equilibrium position is sustained. In addition, the intercepts and slopes of these equilibrium lines are such that the expected levels of muscular activation are counterintuitive. This explained why the anterior activation levels were higher than the posterior activation levels for all, regardless of how low the levels of muscular activity were.

Since then, numerous research studies have been implemented on the co-contraction of antagonistic muscle control, which have proven its ability to increase the stiffness and stability at the joints during volitional movements [75–86]. Based on these research studies, it was shown that by utilizing information from the antagonistic muscle co-contraction, muscular activation levels could be manipulated to control the movements of the joints. Recently, in 2013, Klauer *et al.* introduced the nonlinear joint-angle feedback control of electrical stimulated and λ-controlled antagonistic muscle pairs, in order to control the human limb movements in neural-prosthetic systems [87,88]. The desired recruitment levels, λ, of both muscles were estimated using the electrical stimulation-evoked

electromyography (EMG) measurements. The proposed controller enabled the tracking of reference joint torques and predefined muscular co-contraction using exact linearization methods. Based on the outcomes of the result, the control system was able to rapidly compensate for muscle fatigue and then change the muscular thresholds. It could be said that this is a prerequisite for a neural-prosthetic system's practical application within clinical environments. The asymptotically stable system for the torques is depicted in the following:

$$T_i(k) = k_{s,i}\left(\theta_{max,i} - \theta(k)\right)\left(\frac{q^{-2}(1-a)}{1-aq^{-1}}\right)\left(\frac{1-b_i}{1-b_i q^{-1}}\right) r_{\lambda_i} \quad (5)$$

where (λ_i) is the muscular recruitment level, (r_{λ_i}) is the desired recruitment level, (q^{-1}) is the backward shift operator, (q^{-2}) is the delay of two sampling steps and (k) is the sampling index.

$$\theta \in \left[\theta_{max,1}, \theta_{max,2}\right] \quad (6)$$

$$a \in [0,1] \quad (7)$$

$$b_i \in [0,1] \quad (8)$$

3.3. Simulation of the Co-Contraction Model for Antagonistic Muscles

In recent years, plenty of research studies have been carried out on assistive robotics for rehabilitation, either using motors or pneumatic muscle actuators for the robotic system's source of power [5–8]. Consequently, these studies have become the basis for many findings. Famous researchers in this field, such as Daniel Ferris, have mentioned that powered orthoses could assist the task-specific practicing of the gait, with the long-term goal of improving patient's inherent locomotor capabilities [89]. According to Kalyan K. Mankala and Sunil K. Agrawal *et al.*, passive swing assistance was able to assist patients, with less than ordinary muscle strength, to attain better gait trajectories [90]. Furthermore, analyses on the implementation of mono- and bi-articular actuators for achieving the high muscle moment required at the joints and better gait trajectories were also taken into consideration in real practice [91–95]. The study of antagonistic muscle co-contraction suggested that the control of the orthosis, which implements these mono- and bi-articular actuators, could achieve good joint stiffness and stability [75–86]. The design was biologically inspired (by human muscles), as it employed two compliant elements to manipulate the joints. Usually, this type of orthosis system, implemented antagonistically, actuated joints using the pneumatic-type muscle actuators. In addition, the co-contraction activations were also able to reduce the kinematic variability; whereby, through the increment of co-contraction activations, the kinematic variability could be reduced with the exception of the low co-contraction activation levels [96]. Therefore, it could be concluded that the modeling of co-contraction to represent the movement of antagonistic actuators may be beneficial.

An early study of the co-contraction model was proposed by William K. Durfee *et al.* in 1989. They developed task-based methods for evaluating electrically-simulated antagonist muscle controllers in a novel animal model [97]. The stimulus activation levels of two antagonist muscles, which manipulated an anesthetized cat's intact ankle joint, were determined by the controller output. In this study, three types of controllers were evaluated: the first was open loop reciprocal control; the second was P-D closed loop reciprocal control; and the third was open loop co-contraction control (Figure 9). Based on

the results of the analysis, it was shown that in the visual feedback, the performance of the open loop co-contraction control was comparable to the performance of the P-D closed loop control. This suggested that, in some cases of clinical neural prosthesis implementation, the feedback controller may not be required for good control system performance. In addition, these results also suggested the importance of co-contraction for position control tasks in neural prostheses. However, the disadvantage of this control scheme was that it required more than one input command for each degree of freedom of motion, which could cause premature muscle fatigue.

Figure 9. (**a**) Open loop reciprocal control; (**b**) P-D closed loop reciprocal control; and (**c**) open loop co-contraction control [97].

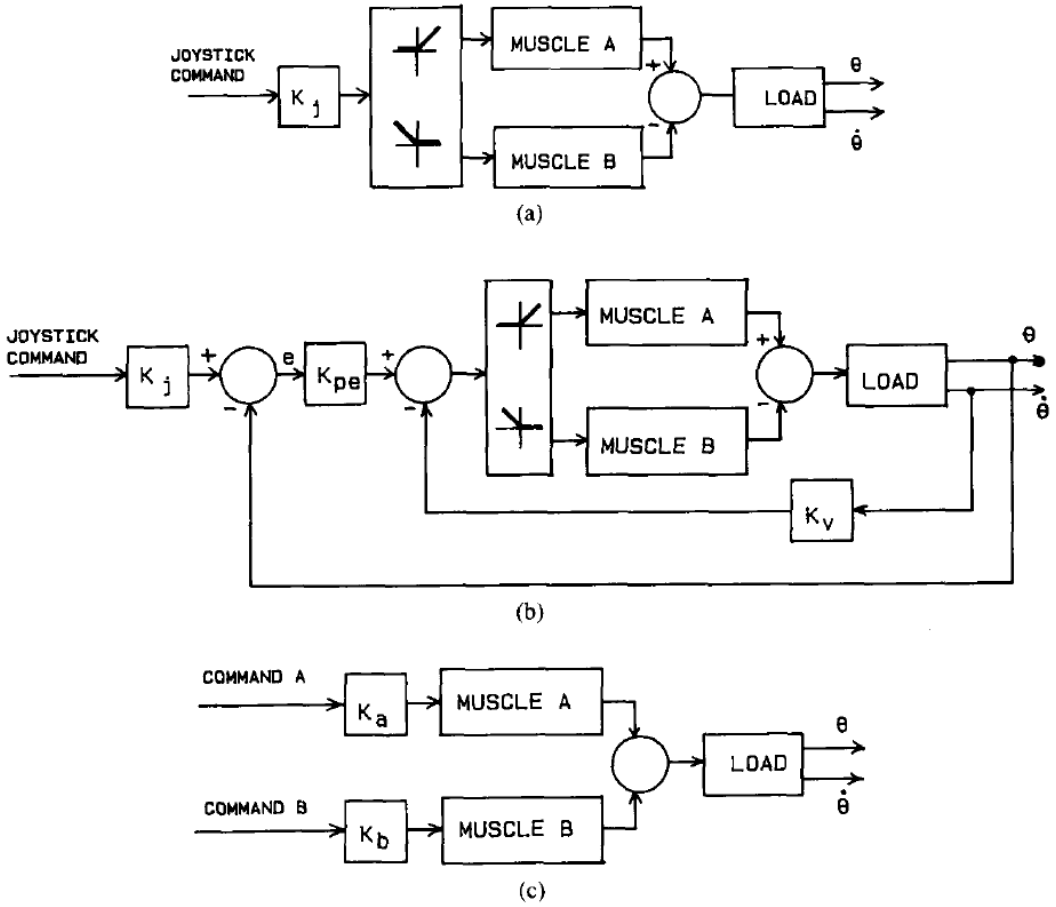

A simulation study of the co-contraction model control scheme for simultaneously manipulating antagonistic actuators was reinitiated by Mohammed *et al.* in 2005. It was mentioned in their study of a co-contraction muscle control strategy for paraplegics that the co-contraction of antagonistic muscle functions (basically, quadriceps and hamstrings) is not necessarily restricted to opposing motion, but may yield to increasing joint stiffness and stable movements [98]. The magnitude of antagonistic muscle co-contractions was first determined based on the optimization of the static linear constraints of muscle forces acting on the joint; whereby, the redundancy of two muscles in co-contraction (*i.e.*, agonist and antagonist) spanning the joint was resolved using the linear minimization of the total stress in the antagonistic muscles. Afterwards, the relationship between the amounts of muscle co-contractions and the maximum force for the antagonistic muscle actuators was computed by

implementing weight factors. However, to ensure the robustness and the safe movement of the orthosis, due to the nonlinearity and the presence of a second order system, a high order sliding mode (HOSM) controller was implemented. In addition, Mohammed *et al.* continued their research in 2010 by introducing an inverse model that considered the muscular dynamic contraction of muscle actuators [99]. This dynamic contraction consisted of two main components: the first was activation dynamics, and the second was contraction dynamics (*i.e.*, force-length and force-velocity relationships). However, the activation dynamics was neglected, as its role was assumed to not be essential during the optimization. The inability of most optimization models to compute muscle co-contractions may be caused by the utilization of monotonous increment objective functions that penalize every additional increment of muscle force. The amount of co-contraction muscle forces (*i.e.*, quadriceps and hamstrings) was derived as follows:

$$F_q = \xi_q F_{max,q} + r_q F^2{}_{max,q} \left(\frac{M - \xi_q \sum_q (r_q F_{max,q})}{\sum_q (r_q F_{max,q})^2} \right) \tag{9}$$

$$F_h = \xi_h F_{max,h} + r_h F^2{}_{max,h} \left(\frac{M - \xi_h \sum_h (r_h F_{max,h})}{\sum_h (r_h F_{max,h})^2} \right) \tag{10}$$

The constraints are:

$$\begin{cases} 0 \le F_i \le F_{max,i} \\ \sum_i r_i F_i = M \end{cases} (i = q, h) \tag{10}$$

(ξ_q) and (ξ_h) are the weight factors;

(F_{max}) is the maximum isometric muscle force;

(r) is the radius.

Subsequently, a simulation research study was instigated by Heitmann *et al.* in 2012 on the muscle co-contraction of a three-link biomechanical limb that modulates the damping and stability of the joints. This study was conducted to replicate the natural relationship, without information on anatomical detail, between the muscle activation and joint dynamics [100]. It was proven that the muscle co-contraction was able to alter the damping and the stiffness of the limb joint without altering the net joint torque, and its effect was incorporated into the model by attaching each manipulator joint with a pair of antagonist muscles. These muscles could be activated individually with each other using ideal mathematical forms of muscle co-contraction. This mathematical equation was derived from natural force-length-velocity relationships of contractile muscle tissue. From the simulation result and numerical stability analysis, it was proven that the damping in the biomechanical limb had increased consistently with the human motor control observation. Moreover, it was also revealed that under identical levels of muscle co-contraction, the bi-stable equilibrium positions could co-exist when the opponent muscles were configured with asymmetric contractile element force-length properties. There were two implications of these findings: the first was the practical implication for the nonlinear bio-mimetic actuator design; and the second was the theoretical implication of the biological motor control, which presumes that antagonist muscle systems are universally mono-stable.

In 2011, Kawai *et al.* had also instigated a simulation study for manipulating antagonistic mono- and bi-articular muscle actuators using a co-contraction-based model [101]. The purpose of this simulation study was to verify the proposed passivity-based control for two degrees of freedom (2 DOF) for human arm manipulators. The bi-articular manipulator dynamics for three muscle torques (*i.e.*, two pairs of mono-articular and a pair of bi-articular actuators) was constructed in order to design the control inputs for the system. The important property of passivity was used to examine the stability analysis of the proposed control law, even though the bi-articular manipulator dynamics passivity could not be determined based on the antagonistic bi-articular muscles. Afterwards, in 2012, Sano, K.; Kawai, H. *et al.* proposed a simulation study of the same 2 DOF manipulator systems using open loop control [102]. Compared to their previous simulation study, the Lyapunov method was used to examine the stability analysis of the proposed control law. However, the anticipated approach did not coincide with the bi-articular manipulator dynamic's uncertainties. This simulation study was then extended to a robust control method that enabled semi-global asymptotic tracking, using RISE control, due to an uncertain nonlinear model of the lower limb of the human body, in 2013 [103]. The results showed that the lower limb was able to be positioned in the desired trajectories in the presence of un-modeled bounded disturbances. However, the torque generated at the knee joint was less when compared to their previous method, due to the antagonistic bi-articular muscles. The contractile force of the flexor muscle (u_{fi}) and extensor muscle (u_{ei}) was derived as follows:

$$T_i = (u_{ei} - u_{fi})l_p - (u_{ei} + u_{fi})k_i {l_p}^2 q_i + (u_{e3} - u_{f3})l_p - (u_{e3} + u_{f3})k_3 {l_p}^2 (q_1 + q_2) \quad (11)$$

where ($i = 1, 2$), (l_p) and (k_i) are the radius of the joints;

(q_1) and (q_2) are the hip and knee joint angles;
(u_{e1}) and (u_{f1}) are the antagonistic mono-articular muscles for the hip joint;
(u_{e2}) and (u_{f2}) are the antagonistic mono-articular muscles for the knee joint;
(u_{e3}) and (u_{f3}) are the antagonistic bi-articular muscles.

Within the same year (2013), Kawai *et al.* also proposed a design of the co-contraction level of antagonistic muscles with muscle contraction dynamics for tracking the control of human lower limbs [104,105]. The manipulation of the antagonistic muscle co-contraction level was dependent on the angular velocity of human lower limbs. Based on the research findings, it could be verified that the co-contraction of antagonist muscles played an important role in the joint's stiffness and stability. In addition, the muscle co-contraction was not only useful for compensating for the joint's stiffness and stability, it was also able to maneuver the direction of the output force.

3.4. Co-Contraction Model for Antagonistic Actuators

Numerous studies have been investigated regarding the co-contraction movements of human antagonistic muscles. However, their model implementations in controlling the antagonistic muscle actuators of lower-limb orthoses have not been completely discovered. In addition, any research paper that focuses on the implementation of mono-articular and bi-articular muscle actuators using pneumatic muscles for the lower-limb rehabilitation orthosis has yet to be extensively investigated; thus, simply actuating the actuators may not give a good result for the joint's stiffness and the stability of the lower-limb leg orthosis and its position trajectory. Therefore, based on the evaluation and

suggestion of the related research findings, the simultaneous co-contraction movements between the agonist and antagonist muscle actuators should be considered with respect to the control system.

4. Conclusions

In this review article, the evaluation and comparison of the developed lower-limb rehabilitation orthoses using the pneumatic muscle-type actuators, including the control algorithms and strategies intended to provide stiffness and stability with respect to the control system, were reviewed. Although a considerable amount of work is now complete, the field is still rapidly evolving. The issue of which is the most effective control algorithm is still widely open. However, randomized controlled trials are necessary for identifying suitable control algorithms, even though this is expensive and time consuming. In conclusion, a few remarks about suggestions for future research of pneumatic muscle-actuated gait trainer system are as follows: firstly, the pneumatic muscle actuators' arrangement in the lower-limb orthosis should be antagonistic; secondly, the co-contractive movement of the antagonistic pneumatic muscles should provide good stiffness and stability for the leg orthosis system; thirdly, a model paradigm is essential for generating adequate co-contractive input data for manipulating the antagonistic muscle actuators; and finally, the developed model should be managed by controllers to deal with the presence of dynamic properties and the nonlinearity behavior of the system.

Acknowledgments

This work was supported by KAKENHI: Grant-in-Aid for Scientific Research (B) 21300202.

Author Contributions

Mohd Azuwan Mat Dzahir reviewed the related journal and conference papers, summarized the literature reviews and prepared the manuscript; Shin-ichiroh Yamamoto re-evaluated the manuscript.

Conflicts of Interest

The authors declare no conflict of interests.

References

1. Wernig, A.; Muller, S.; Nanassy, A.; Cagol, E. Laufband therapy based on "rules of spinal locomotion" is effective in spinal cord injured persons. *Eur. J. Neurosci.* **1995**, *7*, 823–829.
2. Wernig, A.; Nanassy, A.; Muller, S. Maintenance of locomotor abilities following laufband (treadmill) therapy in para- and tetraplegic persons: Follow-up studies. *Spinal Cord* **1998**, *36*, 744–749.
3. Dietz, V.; Muller, R.; Colombo, G. Locomotor activity in spinal man: Significance of afferent input from joint and load receptors. *Brain* **2002**, *125*, 2626–2634.
4. Dietz, V.; Harkema, S.J. Locomotor activity in spinal cord-injured persons. *J. Appl. Physiol.* **2004**, *96*, 1954–1960.
5. Díaz, I.; Gil, J.J.; Sánchez, E. Lower-limb robotic rehabilitation: Literature review and challenges.

J. Robot. **2011**, *2011*, 759764:1–759764:11.
6. Marchal-Crespo, L.; Reinkensmeyer, D.J. Review of control strategies for robotic movement training after neurologic injury. *J. Neuro-Eng. Rehabil.* **2009**, *6*, 20:1–20:15.
7. Pennycott, A.; Wyss, D.; Vallery, H.; Klamroth-Marganska, V.; Riener, R. Towards more effective robotic gait training for stroke rehabilitation: A review. *J. Neuro-Eng. Rehabil.* **2012**, *9*, 1–13.
8. Dollar, A.M.; Herr, H. Lower extremity exoskeletons and active orthoses: Challenges and state-of-the-art. *IEEE Transact. Robot.* **2008**, *24*, 144–158.
9. Colombo, G.; Wirz, M.; Dietz, V. Driven gait orthosis for improvement of locomotor training in paraplegics patients. International Medical Society of Paraplegia. *Spinal Cord* **2001**, *39*, 252–255.
10. Jazernik, S.; Colombo, G.; Morari, M. Automatic gait pattern adaptation algorithms for rehabilitation with a 4-DOF robotic orthosis. *IEEE Transact. Robot. Autom.* **2004**, *20*, 574–582.
11. Lunenburger, L.; Colombo, G.; Riener, R. Biofeedback for robotic gait rehabilitation. *J. Neuro-Eng. Rehabil.* **2007**, *4*, 1:1–1:11.
12. Freivogel, S.; Schmalohr, D.; Mehrholz, J. Improved walking ability and reduced therapeutic stress with an electromechanical gait device. *J. Rehabil. Med.* **2009**, *41*, 734–739.
13. Fisher, S.; Lucas, L.; Thrasher, T.A. Robot-assisted gait training for patients with hemiparesis due to stroke. *Top Stroke Rehabil.* **2011**, *18*, 269–276.
14. West, R.G. Powered Gait Orthosis and Method of Utilizing SAME. U.S. Patent 6689075, 29 January 2004.
15. Veneman, J.; Kruidhof, R.; Hekman, E.; Ekkelenkamp, R.; van Asseldonk, E.; van der Kooij, H. Design and evaluation of the LOPES exoskeleton robot for interactive gait rehabilitation. *IEEE Trans. Neural Syst. Rehabil. Eng.* **2007**, *15*, 379–386.
16. Vallery, H.; Veneman, J.; van Asseldonk, E.; Ekkelenkamp, R.; Buss, M.; van der Kooij, H. Compliant actuation of rehabilitation robots. *IEEE Robot. Autom. Mag.* **2008**, *15*, 60–69.
17. Banala, S.K.; Kim, S.H.; Agrawal, S.K.; Scholz, J.P. Robot assisted gait training with active leg exoskeleton (ALEX). *IEEE Trans. Neural Syst. Rehabil. Eng.* **2009**, *17*, 2–8.
18. Banala, S.K.; Agrawal, S.K.; Kim, S.H.; Scholz, J.P. Novel gait adaptation and neuromotor training results using an active leg exoskeleton. *IEEE/ASME Trans. Mechatron.* **2010**, *15*, 216–225.
19. Monaco, V.; Galardi, G.; Coscia, M.; Martelli, D.; Micera, S. Design and evaluation of NEUROBike: A neuro-rehabilitative platform for bedridden post-strike patients. *IEEE Trans. Neural Syst. Rehabil. Eng.* **2012**, *20*, 845–852.
20. Taherifar, A.; Mousavi, M.; Rassaf, A.; Ghiasi, F.; Hadian, M.R. LOKOIRAN—A novel robot for rehabilitation of spinal cord injury sand stroke patients. In Proceedings of the RSI/ISM International Conference on Robotics and Mechatronics, Tehran, Iran, 12–14 February 2013.
21. Pietrusinski, M.; Cajigas, I.; Severini, G.; Bonato, P.; Mavroidis, C. Robotic gait rehabilitation trainer. *IEEE/ASME Trans. Mechatron.* **2014**, *19*, 490–499.
22. Tondu, B.; Lopez, P. Modelling and control of McKibben artificial muscle robot actuators. *IEEE Control Syst. Mag.* **2000**, *20*, 15–38.
23. Caldwell, D.G.; Razak, A.; Goodwin, M. Braided artificial muscle actuators. In Proceedings of the IFAC, Southampton, UK, 18–21 April 1993; pp. 507–512.
24. Caldwell, D.G.; Medrano-Cerda, G.A.; Goodwin, M. Characteristics and adaptive control of pneumatic muscle actuators for a robotic elbow. In Proceedings of the International Conference

Robotics Automation, San Diego, CA, USA, 8–13 May 1994; Volume 4, pp. 3558–3563.
25. Caldwell, D.G.; Medrano-Cerda, G.A.; Goodwin, M. Control of pneumatic muscle actuators. *IEEE Control Syst. Mag.* **1995**, *15*, 40–48.
26. Caldwell, D.G.; Tsagarakis, N.; Medrano-Cerda, G.A. Biomimetic actuators: Polymeric pseudo muscular actuators and pneumatic muscle actuators for biological emulation. *Mechatronics* **2000**, *10*, 499–530.
27. Davis, S.; Tsagarakis, N.; Canderle, J.; Caldwell, D.G. Enhanced modeling and performance in braided pneumatic muscle actuators. *Int. J. Robot. Res.* **2003**, *22*, 213–227.
28. Davis, S.; Caldwell, D.G. Braid effects on contractile range and friction modeling in pneumatic muscle actuators. *Int. J. Robot. Res.* **2006**, *25*, 359–369.
29. Chou, C.P.; Hannaford, B. Static and dynamic characteristics of McKibben pneumatic artificial muscles. In Proceedings of the IEEE International Conference Robotics Automation, San Diego, CA, USA, 8–13 May 1994; Volume 1, pp. 281–286.
30. Chou, C.P.; Hannaford, B. Measurement and modeling of McKibben pneumatic artificial muscles. *IEEE Trans. Robot. Autom.* **1996**, *12*, 90–102.
31. Nascimento, B.G.; Vimieiro, C.B.; Nagem, D.A.; Pinotti, M. Hip orthosis powered by pneumatic artificial muscle: Voluntary activation in absence of myoelectrical signal. *Artif. Organs* **2008**, *32*, 317–322.
32. Vimieiro, C.B.S.; do Nascimento, B.G.; Nagem, D.A.P.; Pinotti, M. Development of a hip orthosis using pneumatic artificial muscles. In Proceeding of TMSi, São Paulo, Spain, 18–19 July 2005.
33. Bharadwaj, K.; Sugar, T.G. Kinematics of a robotic gait trainer for stroke rehabilitation. In Proceedings of the IEEE International Conference on Robotics and Automation, Orlando, FL, USA, 15–19 May 2006.
34. Ferris, D.P.; Gordon, K.E.; Sawicki, G.S.; Peethambaran, A. An improved powered ankle-foot orthosis using proportional myoelectric control. *Gait Posture* **2006**, *23*, 425–428.
35. Ferris, D.P.; Czerniecki, J.M.; Hannaford, B. An ankle-foot orthosis powered by artificial pneumatic muscles. *J. Appl. Biomech.* **2005**, *21*, 189–197.
36. Gordon, K.E.; Sawicki, G.S.; Fessis, D.P. Mechanical performance of artificial pneumatic muscles to power an ankle-foot orthosis. *J. Biomech.* **2006**, *39*, 1832–1841.
37. Costa, N.; Bezdicek, M.; Brown, M.; Gray, J.O.; Caldwell, D.G. Joint motion control of a powered lower limb orthosis for rehabilitation. *Int. J. Autom. Comput.* **2006**, *3*, 271–281.
38. Miyoshi, T.; Hiramatsu, K.; Yamamoto, S.I.; Nakazawa, K.; Akai, M. Robotic gait trainer in water: Development of an underwater gait-training orthosis. *Disabil. Rehabil.* **2008**, *30*, 81–87.
39. Malcom, P.; Fiers, P.; Segers, V.; van Caekenberghe, I.; Lenoir, M.; de Clercq, D. Experimental study on the role of the ankle push off in the walk-to-run transition by means of a powered ankle-foot-exoskeleton. *Gait Posture* **2009**, *30*, 322–327.
40. Malcom, P.; Segers, V.; van Caekenberghe, I.; de Clercq, D. Experimental study of the influence of the m. tibialis anterior on the walk-to-run transition by means of a powered ankle-foot-exoskeleton. *Gait Posture* **2009**, *29*, 6–10.

41. Galle, S.; Malcom, P.; Derave, W.; de Clercq, D. Adaptation to walking with an exoskeleton that assists ankle extension. *Gait Posture* **2013**, *38*, 495–499.
42. Malcom, P.; Derave, W.; Galle, S.; de Clercq, D. A simple exoskeleton that assist plantarflexion can reduce the metabolic cost of human walking. *PLoS One* **2013**, *8*, 0056137.
43. Sawicki, G.S.; Fessis, D.P. A pneumatically powered knee-ankle-foot orthosis (KAFO) with myoelectric activation and inhibition. *J. Neuro-Eng. Rehabil.* **2009**, *6*, 23:1–23:16.
44. Deaconescu, T.T.; Deaconescu, A.I. Pneumatic muscle actuated equipment for continuous passive motion. *IAENG Trans. Eng. Technol.* **2009**, doi:10.1063/1.3256258.
45. Yeh, T.J.; Wu, M.J.; Lu, T.J.; Wu, F.K.; Huang, C.R. Control of McKibben pneumatic muscles for a power-assist, lower-limb orthosis. *Mechatronics* **2010**, *20*, 686–697.
46. Carberry, J.; Hinchly, G.; Buckerfield, J.; Taylor, E.; Burton, T.; Madgwick, S.; Vaidyanathan, R. Parametric design of an active ankle foot orthosis with passive compliance. In Proceedings of the Computer-Based Medical System (CBMS), Bristol, UK, 27–30 June 2011.
47. Park, Y.; Chen, B.; Young, D.; Stirling, L.; Wood, R.; Goldfield, E.; Nagpal, R. Bio-inspired Active Soft Orthotic Device for Ankle Foot Pathologies. In Proceedings of the International Conference on Robots and Systems (IROS), San Francisco, CA, USA, 25–30 September 2011.
48. Park, Y.; Chen, B.; Majidi, C.; Wood, R.; Nagpal, R.; Goldfield, E. Active Modular Elastomer Sleeve for Soft Wearable Assistance Robots. In Proceedings of the IEEE International Conference on Robots and Systems (IROS), Vilamoura, Portugal, 7–12 October 2012.
49. Teng, C.M.; Wong, Z.Y.; The, W.Y.; Chong, Y.Z. Design and development of inexpensive pneumatically-powered assisted knee-ankle-foot orthosis for gait rehabilitation-preliminary finding. In Proceedings of the International Conference on Biomedical Engineering (ICoBE), Penang, Malaysia, 27–28 February 2012.
50. Kawamura, T.; Takanaka, K. Development of an orthosis for walking assistance using pneumatic artificial muscle-a quantitative assessment of the effect of assistance. In Proceedings of the International Conference on Rehabilitation Robotics, Seattle, WA, USA, 24–26 June 2013.
51. Hussain, S.; Xie, S.Q.; Jamwal, P.K. Adaptive impedance control of a robotic orthosis for gait rehabilitation. *IEEE Trans. Cybern.* **2013**, *43*, 1025–1034
52. Hussain, S.; Xie, S.Q.; Jamwal, P.K. Robust nonlinear control of an intrinsically compliant robotic gait training orthosis. *IEEE Trans. Syst. Man Cybern.: Syst.* **2013**, *43*, 655–665.
53. Caldwell, D.G.; Medrano-Cerda, G.A.; Goodwin, M.J. Braided pneumatic actuator control of a multi jointed manipulator. In Proceedings of the International Conference on Systems, Man and Cybernetics, Le Touquet, France, 17–20 October 1993.
54. Caldwell, D.G.; Medrano-Cerda, G.A.; Goodwin, M. Characteristics and adaptive control of pneumatic muscle actuators for a robotic elbow. In Proceedings of the International Conference on Robotics and Automation, San Diego, CA, USA, 8–13 May 1994.
55. Caldwell, D.G.; Medrano-Cerda, G.A.; Goodwin, M. Control of a pneumatic muscle actuators. *IEEE Trans. Control Syst.* **1995**, *15*, 40–48.
56. Medrano-Cerda, G.A.; Bowler, C.J.; Caldwell, D.G. Adaptive position control of antagonistic pneumatic muscle actuators. In Proceedings of the International Conference on Intelligent Robots and Systems, Pittsburgh, PA, USA, 5–9 August 1995; Volume 1, pp. 378–383.

57. Hamerlain, M. An anthropomorphic robot arm driven by artificial muscles using a variable structure control. In Proceedings of the International Conference on Intelligent Robots and Systems, Pittsburgh, PA, USA, 5–9 August1995; Volume 1, pp. 550–555.
58. Iskarous, M.; Kawamura, K. Intelligent control using a neuro-fuzzy network. In Proceedings of the International Conference on Intelligent Robots and Systems, Pittsburgh, PA, USA, 5–9 August1995; Volume 3, pp. 350–355.
59. Van der Smagt, P.; Groen, F.; Schulten, K. Analysis and control of a rubbertuator arm. *Biol. Cybern.* **1996**, *75*, 433–440.
60. Cai, D.; Yamaura, H. A robust controller for manipulator driven by artificial muscle actuator. In Proceedings of the IEEE International Conference on Control Applications, Dearborn, MI, USA, 15–18 September 1996.
61. Bowler, C.J.; Caldwell, D.G.; Medrano-Cerda, G.A. Pneumatic muscle actuators: Musculature for an anthropomorphic robot arm. *IEEE Colloq. Actuator Technol.* **1996**, *8*, 1–6.
62. Repperger, D.W.; Johnson, K.R.; Phillips, C.A. Nonlinear feedback controller design of a pneumatic muscle actuator system. In Proceedings of the American Control Conference, San Diego, CA, USA, 2–4 June 1999.
63. Carbonell, P.; Jiang, Z.P.; Repperger, D.W. Nonlinear control of a pneumatic muscle actuator: Backstepping *vs.* Sliding-mode. In Proceedings of the IEEE International Conference on Control Applications, Mexico City, Mexico, 5–7 September 2001.
64. Carbonell, P.; Jiang, Z.P.; Repperger, D.W. A fuzzy backstepping controller for a pneumatic muscle actuator system. In Proceedings of the IEEE International Symposium on Intelligent Control, Mexico City, Mexico, 5–7 September 2001; pp. 353–358.
65. Folgheraiter, M.; Gini, G.; Perkowski, M.; Pivtoraiko, M. Adaptive reflex control for an artificial hand. In Proceedings of the SYROCO, Wrocław, Poland, 1–3 September 2003.
66. Balasubramanian, K.; Rattan, K.S. Feedforward control of a non-linear pneumatic muscle system using fuzzy logic. In Proceedings of the IEEE International Conference on Fuzzy Systems, St. Louis, MO, USA, 25–28 May 2003; Volume 1, pp. 272–277.
67. Ahn, K.K.; Thanh, T.C. Improvement of the control performance of pneumatic artificial muscle manipulators using an intelligent switching control method. *KSME Int. J.* **2004**, *18*, 1388–1400.
68. Ahn, K.K.; Thanh, T.C. Nonlinear PID control to improve the control performance of the pneumatic artificial muscle manipulator using neural network. *J. Mech. Sci. Technol.* **2005**, *19*, 106–116.
69. Aschemann, H.; Schindele, D. Sliding-mode control of a high-speed linear axis driven by pneumatic muscle actuators. *IEEE Trans. Ind. Electron.* **2008**, *55*, 3855–3864
70. Cho, S.H. Trajectory tracking control of a pneumatic c-y table using neural network based PID control. *Int. J. Precis. Eng. Manuf.* **2009**, *10*, 37–44.
71. Xing, K.; Huang, J.; Wang, Y.; Wu, J.; Xu, Q.; He, J. Tracking control of pneumatic artificial muscle actuators based on sliding mode and non-linear disturbance observer. *IET Control Theory Appl.* **2010**, *10*, 2058–2070.
72. Hogan, N. Adaptive control of mechanical impedance by coactivation of antagonist muscles. *IEEE Trans. Autom. Control* **1984**, *29*, 681–690.

73. Murray, W.R. Modelling elbow equilibrium in the presence of co-contraction. In Proceedings of the Bioengineering Conference, Durham, NH, USA, 10–11 March 1988; pp. 190–193.
74. Murray, W.R.; Hogan, N. Co-contraction of antagonist muscles: Prediction and observation. In Proceedings of the Joint Dynamics and Control, IEEE International Conference on Engineering in Medicine and Biology Society (EMBS), New Orleans, LA, USA, 4–7 November 1988; Voluem 4, 1926–1927.
75. Migliore, S.A.; Brown, E.A.; de Weerth, S.P. Novel nonlinear elastic actuators for passively controlling robotic joint compliance. *Trans. ASME* **2007**, *129*, 406–412.
76. Schepelmann, A.; Taylor, M.D.; Geyer, H. Development of a testbed for robotic neuromuscular controllers. In *Robotics: Science and Systems VIII*; University of Sydney: Sydney, Australia, 2013.
77. Laffranchi, M.; Tsagarakis, N.G.; Cannella, F.; Caldwell, D.G. Antagonistic and series elastic actuators: A comparative analysis on the energy consumption. In Proceedings of the IEEE/RSJ International Conference on Intelligent Robots and Systems, St. Louis, MO, USA, 10–15 October 2009.
78. Klauer, C.; Raisch, J.; Schauer, T. Advanced control strategies for neuro-prosthetic systems. In Proceedings of the Technically Assisted Rehabilitation (TAR), Berlin, Germany, 14–15 March 2013.
79. Mitrovic, D.; Klanke, S.; Osu, R.; Kawato, M.; Vijayakumar, S. A computational model of limb impedance control based on principles of internal model uncertainty. *PLoS One* **2010**, doi:10.1371/journal.pone.0013601.
80. Dierick, F.; Domicent, C.; Detrembleur, C. Relationship between antagonistic leg muscles co-contraction and body centre of gravity mechanics in different level gait disorders. *J. Electromyogr. Kinesiol.* **2002**, *12*, 59–66.
81. Milner, T.E.; Cloutier, C. The effect of antagonist muscle co-contraction on damping of the wrist joint during voluntary movement. In Proceedings of the IEEE 17th Annual Conference on Engineering in Medicine and Biology Society, Montreal, Canada, 20–23 September 1995; Volume 2, 1247–1248.
82. Hollerbach, K.; Ramos, C.F.; Kazerooni, H. Destabilizing effects of muscular co-contraction in human-machine interaction. In Proceedings of the American Control Conference, San Francisco, CA, USA, 2–4 June 1993.
83. Fu, C.; Wang, R. The influence of co-contraction to the arm impedance during free planar movement. In Proceedings of the International Conference on Bioinformatics and Biomedical Engineering (ICBBE), Beijing, China, 11–13 June 2009; pp. 1–3.
84. Lynch, C.L.; Sayenko, D.; Popovic, M.R. Co-contraction of antagonist muscles during knee extension against gravity: Insights for functional electrical simulation control design. In Proceedings of the IEEE International Conference on Engineering in Medicine and Biology Society (EMBS), San Diego, California, USA, 28 August–1 September 2012.
85. Odhner, L.; Asada, H. Equilibrium point control of artificial muscles using recruitment of many motor units. In Proceedings of the IEEE/RAS International Conference on Biomedical Robotics and Biomechatronics, Scottsdale, AZ, USA 19–22 October 2008.

86. Missenard, O.; Mottet, D.; Perrey, S. The role of cocontraction in the impairment of movement accuracy with fatigue. *Exp. Brain Res.* **2008**, *185*, 151–156.
87. Klauer, C.; Raisch, J.; Schauer, T. Nonlinear joint-angle feedback control of electrically simulated and λ-controlled antagonistic muscle pairs. In Proceedings of the European Control Conference (ECC), Zurich, Switzerland, 17–19 July 2013.
88. Spagnol, P.; Klauer, C.; Previdi, F.; Raisch, J.; Schauer, T. Modelling and online-identification of electrically stimulated antagonistic muscles for horizontal shoulder abduction and adduction. In Proceedings of the European Control Conference (ECC), Zurich, Switzerland, 17–19 July 2013.
89. Ferris, D.P.; Lewis, C.L. Robotic lower limb exoskeletons using proportional myoelectric control. In Proceedings of the IEEE International Conference on Engineering in Medicine and Biology Society (EMBS), Minneapolis, MN, USA, 2–6 September 2009.
90. Mankala, K.K.; Banala, S.K.; Agrawal, S.K. Passive swing assistive exoskeletons for motor-incomplete spinal cord injury patients. In Proceedings of the IEEE International Conference on Robotics and Automation, Roma, Italy, 10–14 April 2007.
91. Kumamoto, M.; Oshima, T.; Fujukawa, T. Control properties of a two-joint link mechanism equipped with mono- and bi-articular actuators. In Proceedings of the IEEE International Workshop on Robot and Human Interactive Communication, Osaka, Japan, 27–29 September 2000.
92. Shimizu, S.; Momose, N.; Oshima, T.; Koyanagi, K. Development of robot leg which provided with the bi-articular actuator for training techniques of rehabilitation. In Proceedings of the IEEE International Symposium on Robot and Human Interactive Communication, Toyama, Japan, 27 September–2 October 2009.
93. Salvucci, V.; Oh, S.; Hori, Y. Infinity norm approach for precise force control of manipulators driven by bi-articular actuators. In Proceedings of the Annual Conference on IEEE Industrial Electronics Society, Glendale, AZ, USA, 7–10 November 2010; pp. 1908–1913.
94. Salvucci, V.; Oh, S.; Hori, Y.; Kimura, Y. Disturbance rejection improvement in non-redundant robot arms using bi-articular actuators. In Proceedings of the Industrial Electronics (ISIE), Gdańsk, Poland, 27–30 June 2011; pp. 2159–2164.
95. Salvucci, V.; Kimura, Y.; Oh, Y.; Hori, Y. Experimental verification of infinity norm approach for force maximization of manipulators driven by bi-articular actuators. In Proceedings of the American Control Conference on O'Farrell Street, San Francisco, CA, USA, 29 June–1 July 2011.
96. Selen, L.P.J.; Beek, P.J.; van Dieen, J.H. Can co-activation reduce kinematics variability? A simulation study. *Biol. Cybern.* **2005**, *93*, 373–381.
97. Durfee, W.K. Task-based methods for evaluating electrically stimulated antagonist muscle controllers. *IEEE Trans. Biomed. Eng.* **1989**, *36*, 309–321.
98. Mohammed, S.; Fraisse, P.; Guiraud, D.; Poignet, P.; el Makssoud, H. Towards a co-contraction muscle control strategy for paraplegics. In Proceedings of the 44th IEEE Conference on Decision and Control, Seville, Spain, 12–15 December 2005; pp. 7428–7433.

99. Mohammed, S.; Poignet, P.; Fraisse, P.; Guiraud, D. Optimal stimulation patterns for knee joint movement restoration during co-contraction of antagonist muscles. In Proceedings of the International Conference on Biomedical Robotics and Biomechatronics, Tokyo, Japan, 26–29 September 2010; pp. 678–692.
100. Heitmann, S.; Ferns, N.; Breakspear, M. Muscle co-contraction modulates damping and joint stability in a three-link biomechanical limb. *Front. Neurorobot.* **2012**, *5*, 5:1–5:14.
101. Kawai, H.; Murao, T.; Sato, R.; Fujita, M. Passivity-based control for 2DOF robot manipulators with antagonistic bi-articular muscles. In Proceedings of the IEEE International Conference on Control Applications (CCA), Denver, CO, USA, 28–30 September 2011; pp. 1451–1456.
102. Kawai, K.S.H.; Murao, T.; Fujita, M. Open-loop control for 2DOF robot manipulators with antagonistic bi-articular muscles. In Proceedings of the IEEE International Conference on Control Applications (CCA), Dubrovnik, Croatia, 3–5 October 2012; pp. 1346–1351.
103. Kawai, Y.; Kawai, H.; Fujita, M. RISE control for 2DOF human lower limb with antagonistic bi-articular muscles. In Proceedings of the IEEE International Conference on Control Applications (CCA), Hyderabad, India, 28–30 August 2013; pp. 109–114.
104. Kawai, Y.; Downey, R.J.; Kawai, H.; Dixon, W.E. Co-Contraction of Antagonist Bi-Articular Muscles for Tracking Control of Human Limb. Available online: http://wwwr.kanazawa-it.ac.jp/kawai/research/2013/CDC13KaDoKaDi.pdf (accessed on 12 March 2014).
105. Kawai, Y. A Design of Co-Contraction Level of Antagonist Muscles with Muscle Contraction Dynamics for Tracking Control of Human Limb. Available online: http://k-lab.e.ishikawa-nct.ac.jp/paper/2013/SICE13_0447_FI.pdf (accessed on 12 March 2014).

Hindawi Publishing Corporation
Journal of Robotics
Volume 2013, Article ID 535106, 20 pages
http://dx.doi.org/10.1155/2013/535106

Research Article

Design and Evaluation of the AIRGAIT Exoskeleton: Leg Orthosis Control for Assistive Gait Rehabilitation

Mohd Azuwan Mat Dzahir[1,2] and Shin-Ichiroh Yamamoto[1]

[1] *Shibaura Institute of Technology, Department of Bio-Science Engineering, 307 Fukasaku, Minuma-ku, Saitama City, Saitama 337-8570, Japan*
[2] *Universiti Teknologi Malaysia, Faculty of Mechanical Engineering, 81310 UTM Skudai, Johor Bahru, Malaysia*

Correspondence should be addressed to Mohd Azuwan Mat Dzahir; azuwan@fkm.utm.my

Received 18 July 2013; Accepted 21 September 2013

Academic Editor: Kazuhiko Terashima

This paper introduces the body weight support gait training system known as the AIRGAIT exoskeleton and delves into the design and evaluation of its leg orthosis control algorithm. The implementation of the mono- and biarticular pneumatic muscle actuators (PMAs) as the actuation system was initiated to generate more power and precisely control the leg orthosis. This research proposes a simple paradigm for controlling the mono- and bi-articular actuator movements cocontractively by introducing a cocontraction model. Three tests were performed. The first test involved control of the orthosis with monoarticular actuators alone without a subject (WO/S); the second involved control of the orthosis with mono- and bi-articular actuators tested WO/S; and the third test involved control of the orthosis with mono- and bi-articular actuators tested with a subject (W/S). Full body weight support (BWS) was implemented in this study during the test W/S as the load supported by the orthosis was at its maximum capacity. This assessment will optimize the control system strategy so that the system operates to its full capacity. The results revealed that the proposed control strategy was able to co-contractively actuate the mono- and bi-articular actuators simultaneously and increase stiffness at both hip and knee joints.

1. Introduction

Considerable assistive gait rehabilitation training methods for the neurologically impaired (including stroke and spinal cord injury (SCI) patients) have been developed using a variety of actuation systems to generate the necessary force to operate the leg orthosis. One of the best examples of gait rehabilitation orthosis is the LOKOMAT (Hocoma AG, Volketswill, Switzerland) or driven gait orthosis (DGO) which is commercially available and extensively researched in many rehabilitation centres [1–3]. This orthosis uses a DC motor for the actuation power to control trajectory at the hip and knee joints. Initially, this DGO implemented the position controller for the control system. However, with further research, this method was improved with the addition of the adaptive and impedance controllers. Emphasis is placed on providing adequate afferent input to stimulate the locomotor function of the spinal cord and activate leg muscles that have lost the capacity to actuate voluntary movement. On the other hand, The Lower Extremity Powered Exoskeleton (LOPES) is a gait rehabilitation orthosis that employs the Bowden-cable driven series elastic actuator (SEA) with the servo-motors as the actuation system to implement low-weight (pure) force sources [4, 5]. This orthosis uses impedance control as opposed to admittance control and is based on position sensing combined with force actuation to operate the lower limb extremity orthosis. This orthosis emphasises on incorporating the Assist as Needed (AAN) algorithm into the system to enhance the training effect by increasing the active participation of patients.

Conversely, robot-assisted gait training (RAGT) with an active leg exoskeleton (ALEX) implemented linear actuators to manipulate the thigh device (hip joint) and shank device (knee joint) [6, 7]. This exoskeleton uses a force-field controller by effectively applying forces on the ankle of the subject through actuators located at the hip and knee joints. They

also incorporate the AAN paradigm for rehabilitation into the system which allows patients to participate more actively in the retraining process compared to other currently available robotic training methods. There is also a neurorehabilitative platform for bedridden poststroke patients (NEUROBike) that employs the use of brushless servomotors and pulleys to actively control the angular excursions of the gait orthosis [8]. This system implements the kinematic models of leg-joint angular excursions during both walking and "sit-to-stand" into the control algorithms to carry out passive and active exercises. The aim of this system is to provide several exercises at an early stage according to the severity of the pathology and the intensity required by the programmed therapy.

The pneumatically operated gait orthosis (POGO) which utilizes pneumatic cylinders as an actuation system is another development [9]. This system incorporated the force and position controller to conform to the pelvis and legs of the subject to desired patterns. Due to the importance of generating normal sensory input during gait training, the POGO developed a device that can accommodate and control the naturalistic motion of the pelvis. In contrast, the robotic gait rehabilitation (RGR) trainer uses servotube linear electromagnetic actuators to generate the power source for the exoskeleton [10]. This system uses an expanded impedance control strategy by switching the force field that affects the obliquity of the pelvis to generate the corrective moments only when the leg is in swing motion. This system was based on the hypothesis that correction of a stiff-legged gait pattern requires addressing both the primary and secondary gait deviations to restore a physiological gait pattern. A newly developed gait training robotic device is LOKOIRAN which employs AC motors connected to a slide-crank mechanism via belts and pulleys to provide the energy for the system [11]. This system engages the speed control mode and the admittance control mode to manage trajectory of the joints in the robotic device. The objective of this system is to develop a passive orthosis to fully support the patient and provide joint angle data during training.

Recently, a robotic orthosis for gait rehabilitation utilising PMAs was developed [12, 13]. This system incorporated the AAN gait training algorithm based on the adaptive impedance control which uses a boundary-layer-augmented sliding mode control- (BASMC-) based position controller to provide interactive robotic gait training. However, it only implemented the use of monoarticular actuators at the hip and knee joints to actuate the leg orthosis without considering the implementation and control of bi-articular actuators. Previous research on the AIRGAIT exoskeleton suggests that the cocontraction of pneumatic McKibben actuators which set up an antagonistic arrangement of bi-articular muscles is able to increase stiffness of both hip and knee joints of the orthosis [14, 15]. However, these antagonistic bi-articular actuators only exerted a constant input pressure of 2.5 (bars) alternately at both sides. In view of this, this research introduces the designed controller scheme and strategy to optimize the control of bi-articular actuators and actuate them in co-contractive-like movements. The approach strategy for this designed controller scheme is the derivation of a cocontraction model which facilitates the implementation of position and pressure-based controllers which manage the antagonistic mono- and bi-articular actuators simultaneously. To the authors' best knowledge, assistive leg orthosis that emphasizes on the control of antagonistic bi-articular actuators using the PMA in the gait rehabilitation field is yet to be extensively investigated and made commercially available. This then provides the motivation and purpose for this research.

2. Design System of AIRGAIT Exoskeleton

Figure 1 shows the schematic diagram for the AIRGAIT exoskeleton. The design of this system and the mechanical structures involved were thoroughly evaluated in previously published papers [14, 15]. Currently, the AIRGAIT exoskeleton employs the PC-based control which utilizes the xPC-Target toolbox and MATLAB/Simulink software as the operating system. The input data is generated within the host-PC and then transferred to the target-PC using the D/A converter to operate the electropneumatic regulators. To realize the cocontraction movements between the antagonistic mono- and bi-articular actuators, one regulator for each actuator was used. Then, measurements by the system (i.e., joints' angle and PMAs' pressure) provide feedback to the host-PC through the A/D converter. The rotary potentiometer (contactless Hall-IC angle sensor CP-20H series, MIDORI PRECISIONS) was used to determine the trajectory of the hip and knee joints and then manage the PMAs' contraction parameters using a position controller. The compact pressure sensor for pneumatic actuators (PSE540-R06, SMC) was used to read the pressure level in each PMA, and the input patterns of the PMAs were managed with the utilisation of a pressure controller. This system will be converted to the Lab-View system for the implementation of real-time control of gait rehabilitation.

2.1. Mechanical Structure of the Leg Orthosis. The structure of the leg orthosis covers the thigh at the lower end of hip joint and shank at the lower end of the knee joint. The ankle joint orthosis was not included as the foot clearance during swing can be realized by implementing elastic straps, a passive foot lifter, or passive orthosis [1, 4]. However, for the implementation of the passive orthosis, the research on the ankle orthosis of the AIRGAIT exoskeleton was conducted separately. This leg orthosis was fixed in a sagittal plane at the pelvis rotation to facilitate gait motion training for the hip and knee joints [1, 4, 6, 10, 12]. The sagittal plane is a vertical plane which passes from ventral (front) to dorsal (rear) dividing the body into the right and left halves as shown in Figure 1(b). Weight compensation for leg orthosis is provided for by the parallel linkage and gas spring mechanisms. This limits vertical motion during the training session [1, 4, 6, 10, 12]. The upper and lower parts of the leg orthosis (i.e., thigh and shank) can be adjusted to agree with the height of the subject. Parallel bars were used to attach the end connectors of the mono- and bi-articular actuators (PMAs) at the anterior and posterior sides of the leg orthosis. By using the slider, these parallel bars can be adjusted accordingly to maximise the outcome of the joints angle trajectory.

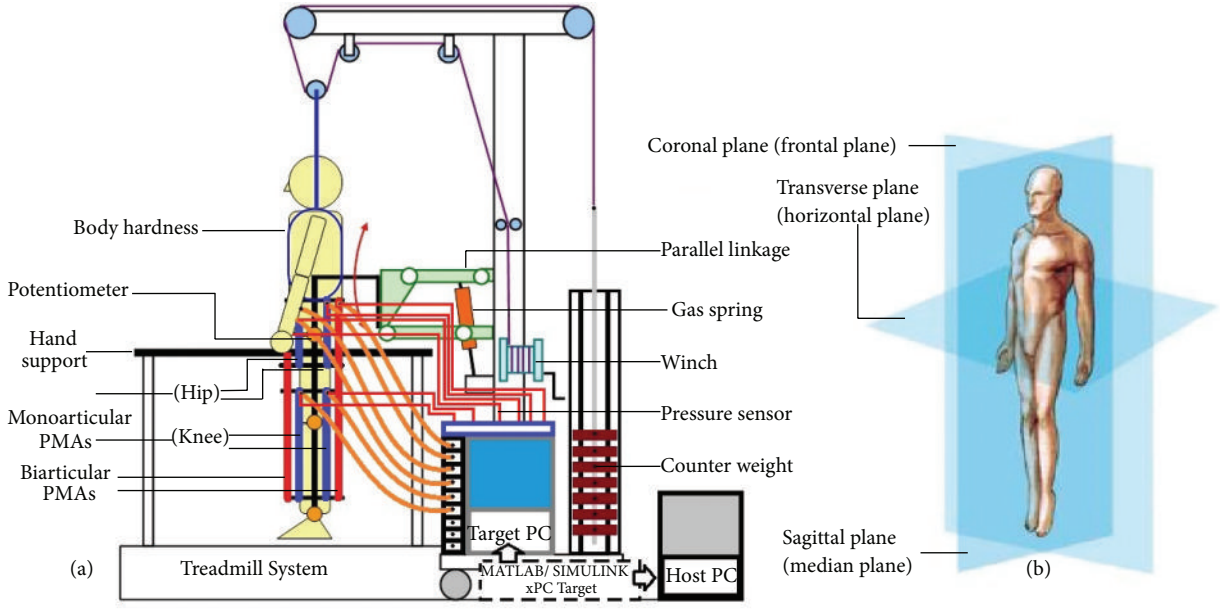

Figure 1: Schematic diagram for body weight support gait training system (AIRGAIT).

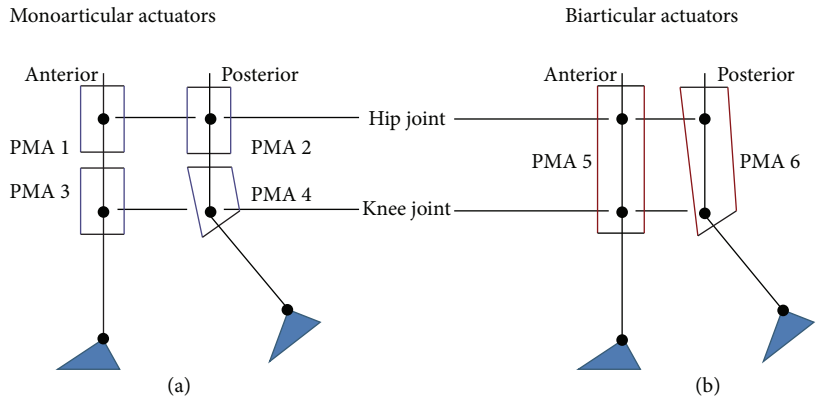

Figure 2: PMAs' setting; (a) antagonistic mono-articular (hip and knee joints) actuators and (b) bi-articular actuators.

2.2. Mono- and Biarticular Muscle Actuators. The implementation of mono- and bi-articular actuators to actuate the AIRGAIT exoskeleton leg orthosis is based on the McKibben muscle actuator. These actuators were fabricated within our laboratory using special tools which were designed to assemble the parts of the actuator (i.e., rubber tube, braided fabric, copper ring, end connector, and input connector). The implementation of these mono- and bi-articular actuators is based on the various human muscles (i.e., gluteus maximus, gluteus minimus, gluteus medius, vastus lateralis, gastrocnemius, rectus femoris, and hamstring) and antagonistically (i.e., anterior and posterior) attached to the leg orthosis. Compared to monoarticular actuators, bi-articular actuators require accurate input patterns to simultaneously actuate the antagonistic actuators which control two joint angles [14, 15]. Although the bi-articular actuators may be considered redundant in the actuation system, the strong force they generate will improve the maximum angle extension, provide precise movements, and ensure balance between antagonistic actuators and stiffness at the joints [16–20].

The position setting of the antagonistic actuators is illustrated in the Figure 2, where the position of the antagonistic mono-articular actuators both for the hip and knee joints is placed in between the antagonistic bi-articular actuators. This then provides the antagonistic bi-articular actuators with an extra length which helps in achieving much wider movement at the joints. The details on the best setup determination of the antagonistic actuators were recorded earlier and can be referred to in [21].

2.3. AIRGAIT Prototype. The prototype of the AIRGAIT exoskeleton was developed in 2010 and extensively researched for improvement. However, it is yet to be commercialized. The research on gait training is progressing rapidly towards enhancement in design structures and control algorithms. A lone operator is sufficient for the running of this system. The

(a) (b)

Figure 3: Body weight support gait training system (AIRGAIT) prototype.

process involves providing the subject with information on the training procedures and experiment protocols, putting on of the body harness, attaching the assisted leg orthosis to the lower limb of the subject, and finally, proceeding with the gait training or experiment. Figure 3 shows the prototype of the AIRGAIT exoskeleton.

2.4. Mechanical System. The mechanical structure of the AIRGAIT exoskeleton is made up of three main parts which are (a) the BWS system which consists of the body harness and counter weight, (b) the treadmill training which involves the treadmill and hand support, and (c) the assistive gait training which comprises the lower limb powered orthosis, spring, and parallel linkage (parallelogram). The spring and parallel linkage were fixed in a sagittal plane so that the gait motion training at hip and knee joints can be realized. The sagittal plane also compensates for the vertical weight load from the system [1, 4, 10, 12]. The subject is provided with the BWS so that he/she will be able to maintain his/her balance during the gait training or experimental tests [11, 22, 23]. A variable speed treadmill is also provided for the assisted leg orthosis gait training and the body weight support gait training [23, 24].

2.5. Safety Features. To ensure the safety of the subject during the assisted gait rehabilitation and experimental tests, several safety features were included in the AIRGAIT exoskeleton design. The implementation of the PMA as the actuation system is in itself a safety feature due to its naturally compliant mechanism [25]. Also, the exclusion of the possibility of short circuits in the actuation system during operation makes it suitable for the human-robot interaction. Moreover, as the system involves compressed air and the expansion and contraction of the braided rubber tube, it is possible to perform the orthosis in an underwater rehabilitation training scenario. Our earlier laboratory study of the robotic gait trainer (RGTW) indicated that hydrotherapy may be particularly effective in the treatment of individuals with hip joint movement dysfunction [26]. Since the PMA characteristics are based on its model parameters such as dimension (i.e., length and contraction) and pressure, the maximum contraction of PMA will prevent the exoskeleton of the AIRGAIT leg orthosis from exceeding the limitation of the joints [27]. However, as a further precaution, a stopper was positioned at the hip and knee joints of the leg orthosis to avoid the unexpected and provide another safety feature. Additionally, the implementation of the BWS system ensures that the subject is able to maintain his/her balance and not fall over while on the treadmill [22, 23].

3. Materials and Methods

3.1. Procedures. The exoskeleton of the AIRGAIT leg orthosis is first adjusted to correspond with the position of the hip and knee joints of the subject to obtain precise data during the experimental tests. Then, the controller parameters for the antagonistic mono-articular actuators (i.e., hip and knee joints) are tuned until good joint trajectory is attained. This is followed by the tuning of antagonistic bi-articular actuator controller parameters. The control for the leg orthosis WO/S is then set for different gait cycle (GC) speeds, and data for the trajectory of the hip and knee joints are gathered. The steps taken for testing W/S are (a) the subject is provided with sufficient information regarding the tests and procedures, (b) the subject is fitted with a body harness and a passive foot lifter was secured at the ankle joint before the leg orthosis was attached to the subject, and (c) the subject is provided with the full BWS before the control of leg orthosis was performed at different GC speeds including that of an average human. Table 1 below shows the existing lower limb gait rehabilitation orthosis systems such as LOKOMAT, LOPES, ALEX, Robotic Orthosis for Gait Rehabilitation, and our research AIRGAIT in terms of (1) type of actuator used as the actuation system; (2) number of joint manipulators; (3) plane of actuated DOFs; and (4) GC operating speed.

3.2. Experimental Tests. Three tests were conducted for the experimental study. These tests were performed on one side of the exoskeleton of the AIRGAIT leg orthosis. The first test was conducted using two sets of antagonistic mono-articular

Table 1: Existing lower limb gait rehabilitation orthosis systems comparison.

Comparison between existing lower limb gait rehabilitation orthosis systems					
Orthosis system	Type of actuator	Number of joints	Actuated DOFs	Operating speed	References
LOKOMAT	DC motors	Hip and knee joints, passive foot lifter was applied at ankle Joint	Sagittal plane	0.56 m/s	[1–3]
Lower Extremity Powered Exoskeleton (LOPES)	Bowden cable series elastic actuators (SEA) and servomotors	Hip and knee joints, elastic straps was applied at ankle joint	Sagittal plane	0.75 m/s	[4, 5]
Active Leg Exoskeleton (ALEX)	Linear actuators	Hip, knee, and ankle joints	Sagittal plane	0.40 m/s up to 0.85 m/s	[6, 7]
Robotic Orthosis for Gait Rehabilitation	Pneumatic muscle actuators (monoarticular actuators)	Hip and knee joints, foot lifter was used at ankle joint	Sagittal plane	0.60 m/s	[12, 13]
Body Weight Support Gait Training System (AIRGAIT)	Pneumatic muscle actuators (mono- and biarticular actuators)	Hip and knee joints, foot lifter was used at ankle joint	Sagittal plane	0.35 m/s (4s GC), 0.47 m/s (3s GC), 0.70 m/s (2s GC), and 1.40 m/s (1s GC)	

actuators (i.e., hip and knee joints) tested WO/S; the second with the addition of one set of antagonistic bi-articular actuators tested WO/S; and the third with the addition of one set of antagonistic bi-articular actuators tested W/S. Full BWS was implemented in this study during the test W/S as the load supported by the orthosis was at its maximum capacity. This assessment will optimize the control system strategy so that it operates at its maximum capability. The options for the subject were not really critical as the focus of the research is on the design controller. As such, the subject chosen was young, healthy, and not bearing any neurological disorder. With this, we were able to instruct the subject to be passive during the experimental tests. To achieve the natural posture of gait motion during training, the passive foot lifter was used to ensure enough foot clearance during the swing phase [1, 4].

The control of the leg orthosis WO/S and W/S is displayed in Figures 4 and 5. For the first and second tests (WO/S), GC speeds of 4 seconds, 3 seconds, 2 seconds, and 1 second were evaluated for the design controller scheme. Four GC speeds were also evaluated for the third test (W/S). Five trials were performed for each GC speed, and each trial consisted of five cycles including the initial cycle position. The total GCs performed for each GC speed was around 25 cycles. The average GC was then calculated and represented in a graph. Based on these data, three comparative evaluations were analysed to determine the design controller scheme and strategy performance. These were (a) between the mono-articular actuators alone (i.e., hip and knee joints) and with bi-articular actuators, (b) between the cocontraction model based position (P) controller scheme and the cocontraction model based position-pressure (PP) controller scheme tested WO/S, and (c) between the cocontraction model based P controller scheme and the cocontraction model based PP controller scheme tested W/S. The design controller scheme and strategy performance were evaluated based on the GC, movement of hip and knee joints trajectory, maximum joint angle extension, inertia, gravitational effect, and time shift.

4. Control System

4.1. Controller Algorithm. Figure 6 shows the schematic diagram of the exoskeleton of the AIRGAIT leg orthosis controller schemes. Figure 6(a) shows the cocontraction model based P controller, and Figure 6(b) shows the cocontraction model based PP controller. Unlike other control algorithms for PMA, the designed controller scheme does not predict or measure the required torque at the joints [25, 28–30]. Rather, it correlates the angle information of the joints with the dynamic characteristics of the PMA (i.e., contraction and pressure) and then realizes the position and pressure controls. In order to implement this controller scheme, the cocontraction model was developed. The control strategy was to execute the cocontraction model based position-pressure controller scheme. The position controller was used to tune the cocontraction model parameters (activation levels) while the pressure controller was used to control the input patterns of the antagonistic mono- and bi-articular actuators. The derived cocontraction model provides the input patterns for the mono- and bi-articular actuators and simultaneously actuates the antagonistic actuators cocontractively, while the PMA model was determined in order to consider the characteristics of the PMA that were to be introduced into the controller design. This dynamic model was evaluated in an experimental study and represented in an equation. The proposed controller scheme was specifically designed for simplifying the control of antagonistic bi-articular actuators so as to enhance the stiffness at both hip and knee joints. It is an arduous task to construct the plant model of leg orthosis (with antagonistic mono- and bi-articular PMAs) for the implementation of the Stochastic Optimization method to determine the control parameters of the design controller. As such, the heuristic method was implemented.

4.2. Cocontraction Model. The cocontraction model generates the input patterns for the antagonistic mono- and

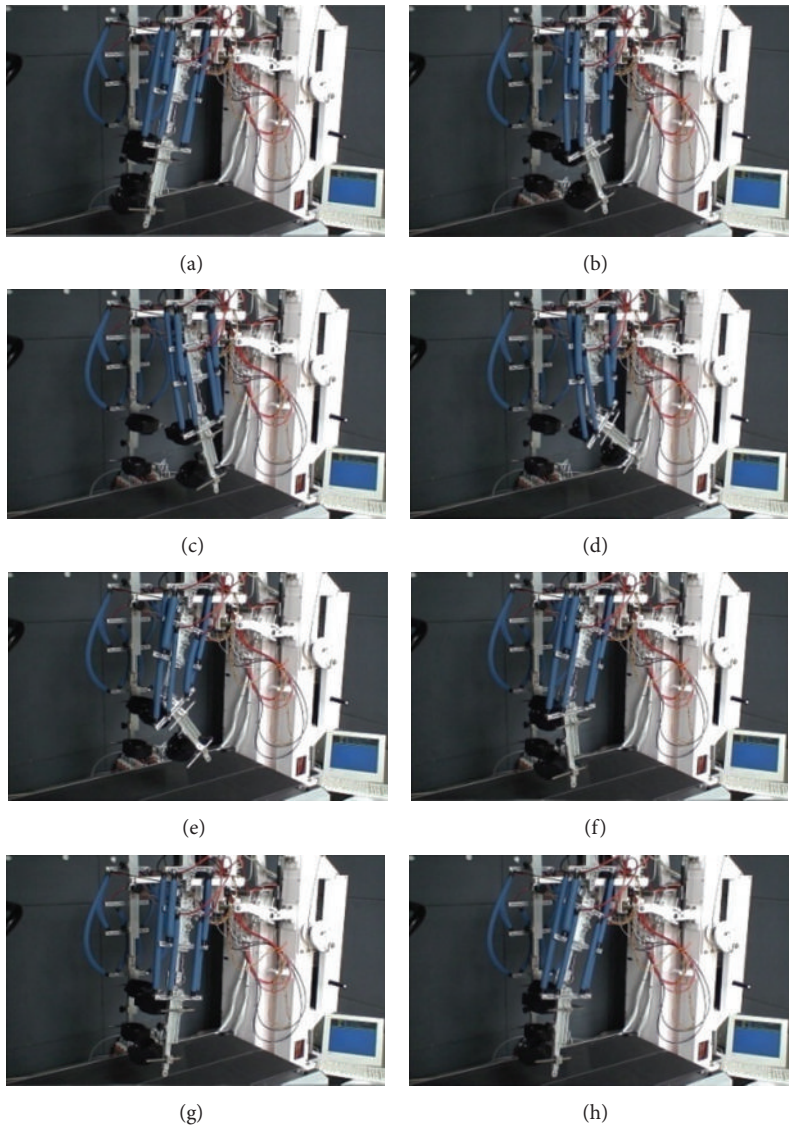

Figure 4: Control of the leg orthosis without a subject (WO/S).

bi-articular actuators (i.e., anterior and posterior) in order to realize the method for implementing the position-pressure controller scheme. This model correlates information on the joints with the dynamic characteristics of the PMA (i.e., contraction and pressure). Based on the derived mathematical model, the contraction of antagonistic mono-articular actuators can be characterized as proportional and inversely proportional (1st-order system) to the angle of the joint. As for the bi-articular actuators, a much higher-order system is required to enable these actuators to manage two joints simultaneously. To control these joints effectively, the input patterns for the antagonistic bi-articular actuators should be sufficiently accurate as this will ensure the efficient performance of the antagonistic mono-articular actuators and facilitate co-contractive movements between the antagonistic actuators. Determination of the co-contractive input for the bi-articular actuators is insufficient to achieve complete gait motion of the leg orthosis without the inclusion of mono-articular actuators. Thus, the role played by the control of the mono-articular actuators is crucial in the successful implementation of the bi-articular actuators.

Figure 7 shows the process of measuring the reference signal (input patterns) for the antagonistic mono- and bi-articular actuators. Figure 7(a) shows the reference angle of hip and knee joints. Point (A) shows the maximum contraction input pattern for the anterior actuators and minimum contraction input pattern for the posterior actuators as shown in Figure 7(b). Point (B) shows the maximum contraction input pattern for the posterior actuators and minimum contraction input pattern for the anterior actuators as shown in Figure 7(c). Based on this positional data information, the contraction patterns (i.e., $C1$–$C6$) of the mono- and bi-articular actuators were then determined using the mathematical derivation as follows.

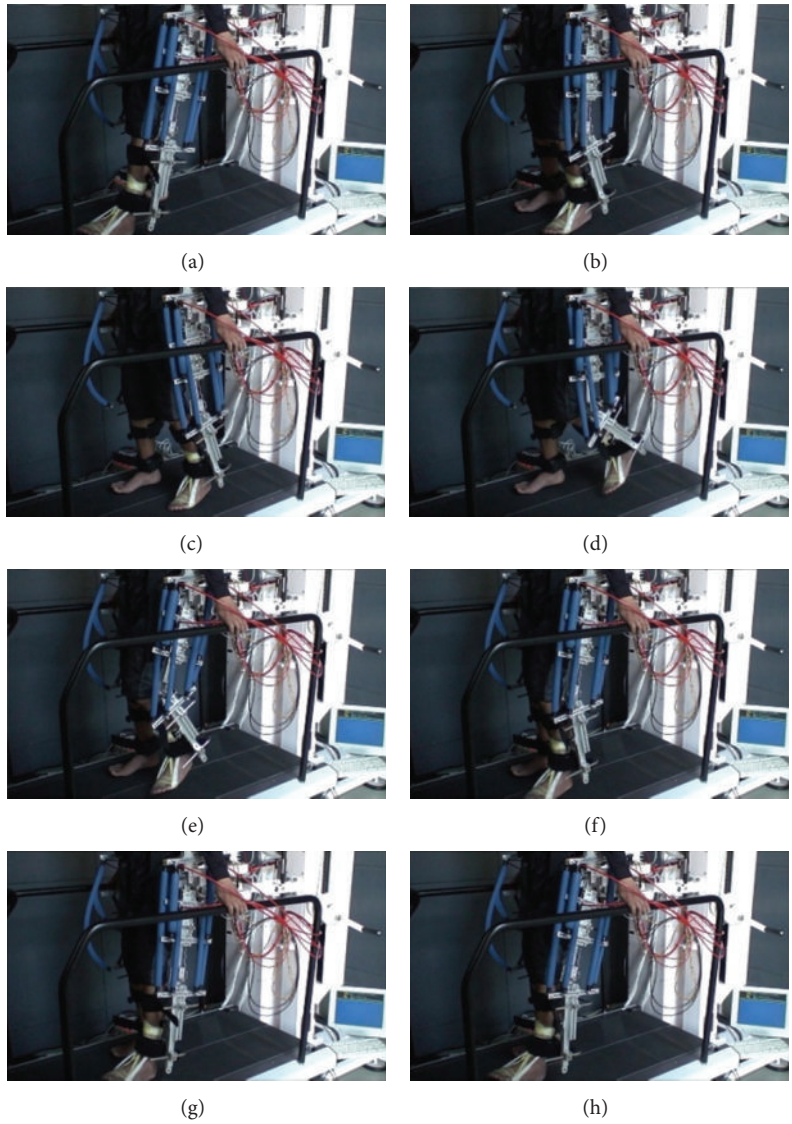

Figure 5: Control of the leg orthosis with a subject (W/S).

Mono-articular actuators for the hip joint:

$$C1 = \varepsilon_{ha}(t) = \left(\frac{r_h}{l_{o_{\text{hip}}}}\right) \cdot \alpha_h \cdot \theta_{ha}(t) \leq 0.3,$$
$$C2 = \varepsilon_{hp}(t) = \left(\frac{r_h}{l_{o_{\text{hip}}}}\right) \cdot \beta_h \cdot \theta_{hp}(t) \leq 0.3. \quad (1)$$

Mono-articular actuators for the knee joint:

$$C3 = \varepsilon_{ka}(t) = \left(\frac{r_k}{l_{o_{\text{knee}}}}\right) \cdot \alpha_k \cdot \theta_{ka}(t) \leq 0.3,$$
$$C4 = \varepsilon_{kp}(t) = \left(\frac{r_k}{l_{o_{\text{knee}}}}\right) \cdot \beta_k \cdot \theta_{kp}(t) \leq 0.3. \quad (2)$$

Bi-articular actuators for hip and knee joints:

$$C5 = \varepsilon_{ba}(t) = \left(\frac{r_{\text{bi}}}{l_{o_{\text{bi}}}}\right) \cdot \alpha_{\text{bi}} \cdot \left(\theta_h(t) + \theta_k(t)\right)_a \leq 0.3,$$
$$C6 = \varepsilon_{bp}(t) = \left(\frac{r_{\text{bi}}}{l_{o_{\text{bi}}}}\right) \cdot \beta_{\text{bi}} \cdot \left(\theta_h(t) + \theta_k(t)\right)_p \leq 0.3, \quad (3)$$

where ε is the contraction patterns; r is the PMAs distance from the joints; l_o is the PMA initial length; α and β are the anterior and posterior muscle activation levels; and 0.3 value is the PMAs' maximum contraction. The derivation of this cocontraction model for the mono- and bi-articular actuators was recorded earlier and can be referred to in [31].

This model was first verified by using the least squares (LS) and recursive least squares (RLS) prediction methods between the inputs patterns and the joint angles as can be seen in Table 2. The coding was programmed in MATLAB

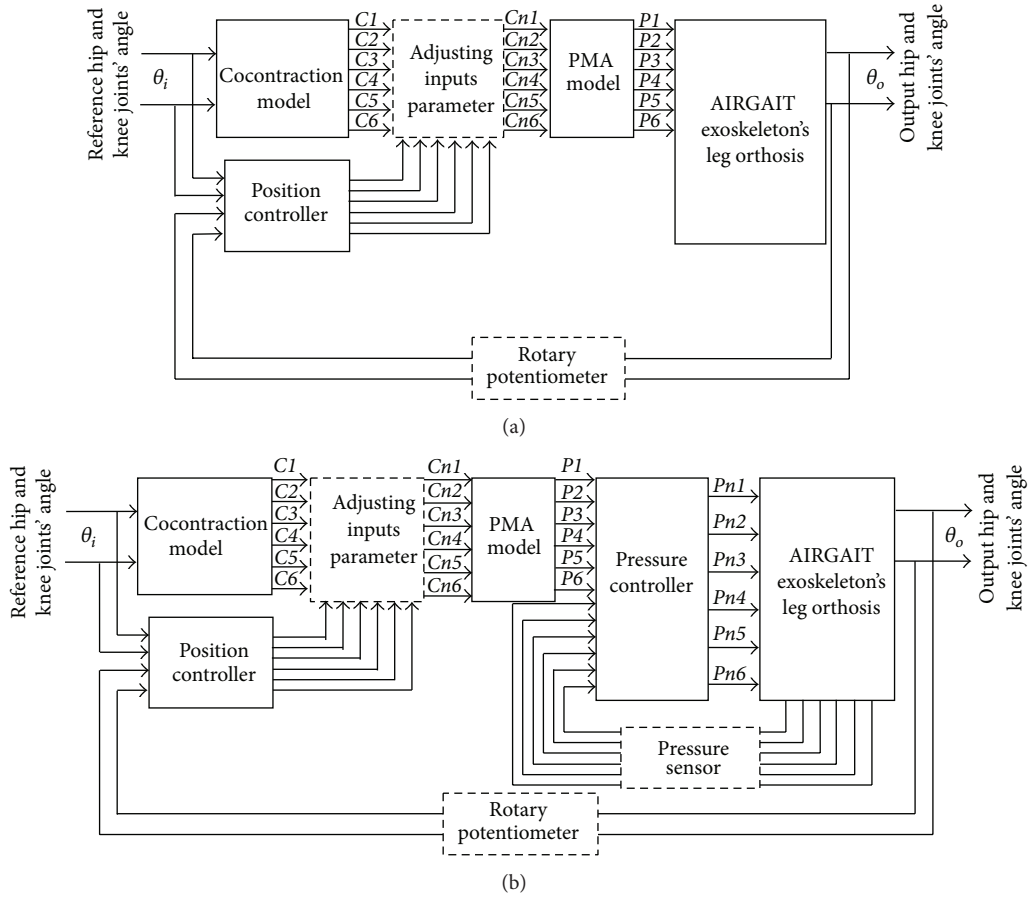

Figure 6: Schematic diagram of the exoskeleton of the AIRGAIT leg orthosis controller schemes. (a) Cocontraction model based P controller and (b) cocontraction model based PP controller, where ($C1$–$C6$) are the contraction input patterns, ($Cn1$–$Cn6$) are the corrected contraction input patterns, ($P1$–$P6$) are the pressure input patterns, and ($Pn1$–$Pn6$) are the corrected pressure input patterns.

Table 2: Input patterns model verification using LS and RLS prediction methods.

PMA actuators	LS and RLS prediction between the input patterns and the joint angles			
	LS method		RLS method	
	1st order	nth order	1st order	nth order
Monoarticular (hip)-Anterior PMA	Yes (proportional)	—	Yes (proportional)	—
Monoarticular (hip)-Posterior PMA	Yes (inversely proportional)	—	Yes (inversely proportional)	—
Monoarticular (knee)-Anterior PMA	Yes (proportional)	—	Yes (proportional)	—
Monoarticular (knee)-Posterior PMA	Yes (inversely proportional)	—	Yes (inversely proportional)	—
Biarticular (hip)-Anterior PMA	No	No	No	No
Biarticular (hip)-Posterior PMA	No	No	No	No

language. Based on the predetermine Transfer Function (TF), the contraction of antagonistic mono-articular actuators can be differentiated as proportional and inversely proportional (1st-order system) to the angle of the joint. However, the model for the antagonistic bi-articular actuators cannot be verified by using the LS and RLS prediction methods, as it requires much higher-order and complex system. This could be verified by using nonlinear ARX model or genetic algorithm (GA).

4.3. PMA Model. The development of the PMA model is for the purpose of increasing the effectiveness of the cocontraction model. While the cocontraction model provides the antagonistic actuators with the contractive data, this model translated that data into pressure patterns [in Volts] for activating the electropneumatic regulators. The dynamic characteristics of the PMA such as dimension (i.e., length and muscle contraction), pressure, and force data were determined in an experimental study. A model equation was

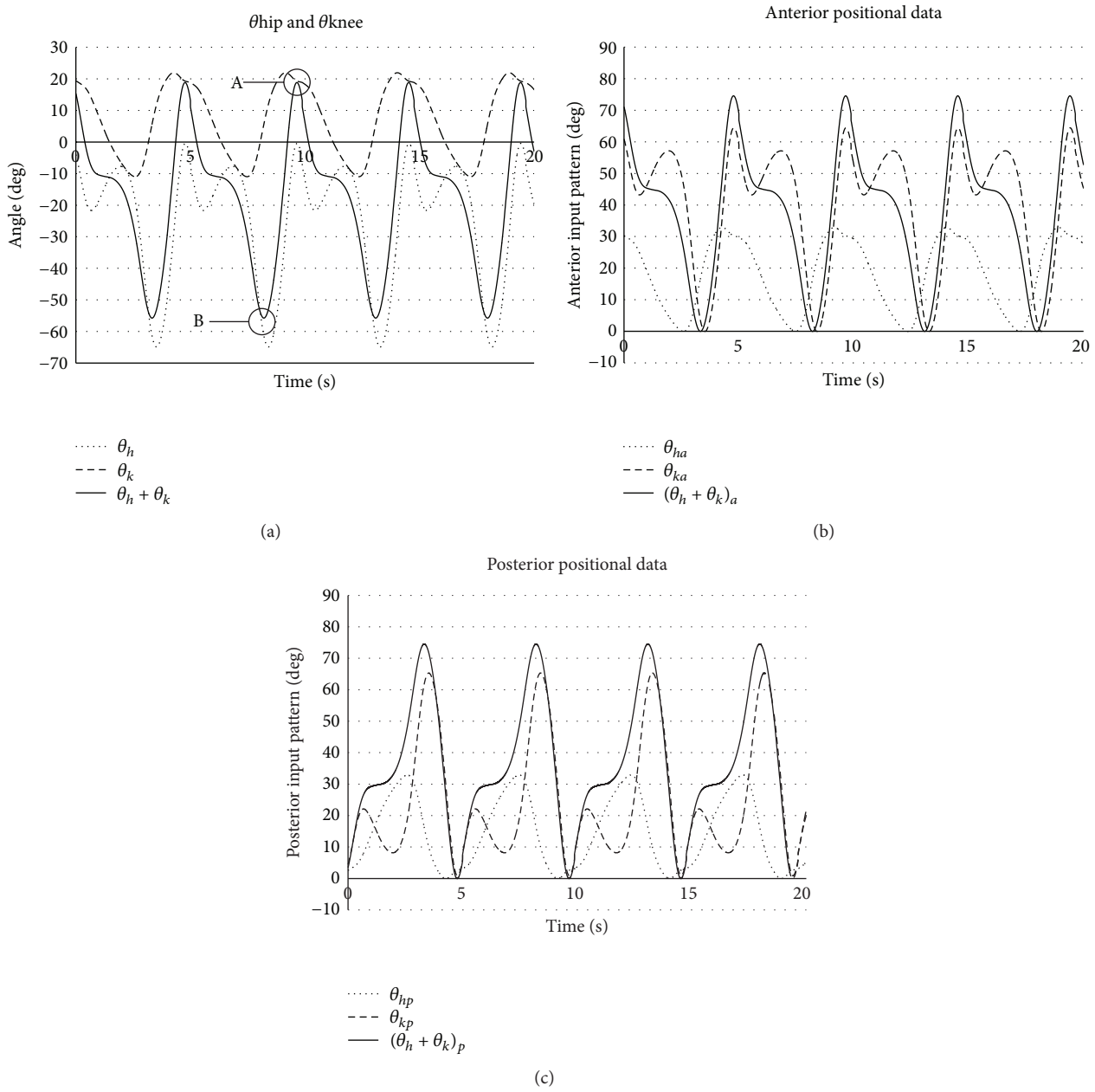

FIGURE 7: Input patterns of the antagonistic mono- and bi-articular actuators. θ_h is the hip joint angle; θ_k is the knee joint angle; θ_{ha}, θ_{ka}, and $(\theta_h + \theta_k)_a$ are the positional data for the anterior actuators; and θ_{hp}, θ_{kp}, and $(\theta_h + \theta_k)_p$ are the positional data for the posterior actuators.

then formulated to represent the PMA characteristics data with the high accuracy of 6th-order polynomial. This will be used as the reference model for the control strategy as can be seen in Figure 8. The cocontraction model control scheme considers the nonlinearity behaviour of the PMA by controlling the muscle activation level of the PMA. The PMA static model at zero load condition was defined as the minimum boundary to determine the nonlinearity area of the PMA. As the critical muscle activity with regard to the PMA is during its contraction, only the contraction mode was considered to realize the cocontraction movements between the antagonistic mono- and bi-articular actuators. The evaluation and derivation of this PMA model have been recorded earlier and can be observed in [21].

5. Results and Discussion

In this section, findings for the designed controller scheme tests and strategy were evaluated and discussed. The modus operandi from the early stage until the final stage was appropriately modelled to optimize the flow of this research. The discussion and evaluation of the findings were divided into three parts to explain each stage of the study. It comprises three assessments for evaluating the performance of the

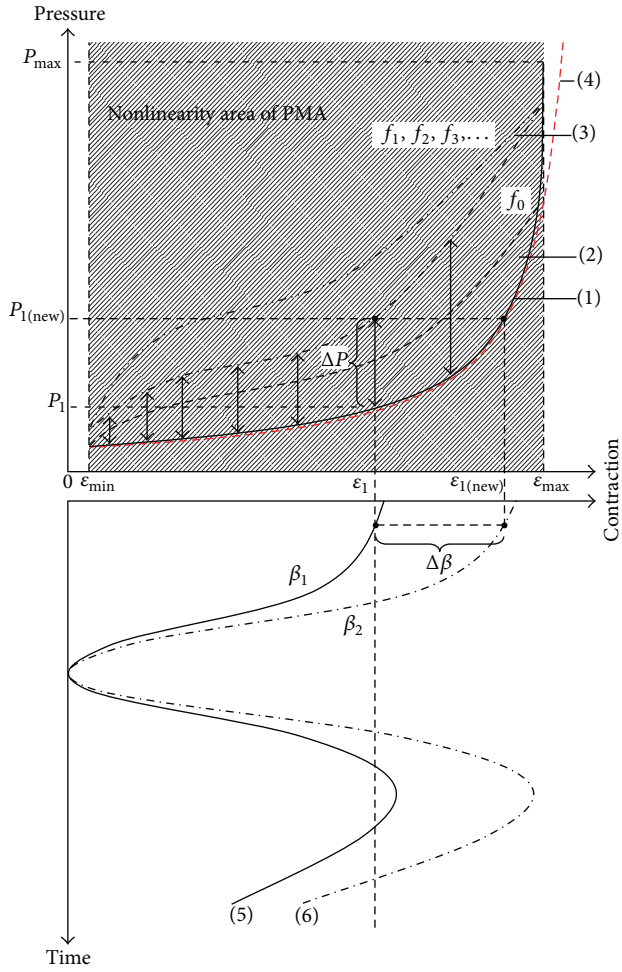

Figure 8: Cocontraction model control scheme's strategy, where (1) PMA static model of pressure versus contraction at zero load condition; (2) PMA hysteresis model at zero load (f_0) condition; (3) PMA hysteresis model at load ($f_1, f_2, f_3, \ldots$) condition; (4) PMA model using 6th-order polynomial equation; (5) contraction input pattern for the antagonistic mono- and bi-articular actuators; (6) controlled contraction input patterns after the controls of the muscle activation level (β); ΔP is the sudden increase in pressure due to the PMA nonlinearity; and $\Delta\beta$ is the increase in muscle activation level.

design controller scheme. These assessments are (a) comparison between the mono-articular actuators acting on their own (i.e., hip and knee joints) and with the addition of bi-articular actuators, (b) comparison between the cocontraction model based position (P) controller and the cocontraction model based position-pressure (PP) controller, and (c) comparison between the control of the leg orthosis WO/S and control of the leg orthosis W/S. The evaluation was based on the GC, movement of the trajectory of the hip and knee joints, maximum angle extension of the joints, inertia, gravitational effect, and time shift.

5.1. Control of the Leg Orthosis WO/S: Evaluation on Antagonistic Actuators. The focus of this assessment is on the implementation of cocontraction input patterns to control the mono- and bi-articular actuators of the exoskeleton of the AIRGAIT leg orthosis. It was conducted to determine the limitations when using mono-articular actuators alone and the advantages to be gained with the inclusion of bi-articular actuators. Two tests were conducted. The first using the mono-articular actuators only (i.e., hip and knee joints) tested WO/S and the second with the addition of bi-articular actuators tested WO/S. These tests were evaluated at four GC speeds of 4 seconds, 3 seconds, 2 seconds, and 1 second so as to raise the stakes of the design controller and the appraisal of the strategy by increasing the GC speed. A total of 25 GCs were performed for each GC speed including the initial position cycle, and data related to the trajectory of the joints were then gathered. The average GC for each GC speed was measured and represented in a graph.

Figures 9 and 10 show the trajectory evaluation of the joints of the leg orthosis controls between two settings (i.e., mono-articular actuators only and with the inclusion of bi-articular actuators) tested WO/S using a cocontraction model based PP controller. Based on the four GC speeds evaluation, it is evident that the leg orthosis was able to perform the gait motion smoothly up to a GC speed of 2 seconds. For the GC speeds of 4 seconds, 3 seconds, and 2 seconds, the orthosis displayed the complete gait motion (i.e., heel strike, foot flat, middle swing, and wide swing) by implementing the designed controller scheme. With the increments in GC speed, the time allocated for completing one GC will be reduced as the graph shifted forward. However, even with the forward shifting of the graph, the time delay in the system was only approximately 0.2 seconds for each GC speed. For the control of leg orthosis using mono-articular actuators alone, it was expected that the trajectory of the joints will be slightly coarse due to the nonlinearity behaviour (i.e., compressible and hysteresis) of the PMA. Although this result may suggest that mono-articular actuators alone are able to support the orthosis, it must be noted that this evaluation was conducted WO/S. The situation changes during implementation W/S as the weight attributed to the actuators is increased. When the inertia and gravitational effect are included in the equation, the limitations of mono-articular actuators acting alone become evident as each actuator is only capable of sustaining a pressure level of 5 (bars). Moreover, due to the position of the antagonistic actuators, the length of mono-articular actuators is much shorter than those of bi-articular actuators. This reduces the maximum angle extension the joints can achieve especially at the knee where a much wider movement (63 degrees) is required compared to the hip. This maximum angle extension is the maximum value of reference angle of the hip and knee joints, both the anterior and posterior sides. This value can be inferred from Winter [32].

However, with the introduction of the bi-articular actuators, the coarse movement was reduced and the stiffness at the joints was improved due to the significant force exerted by these actuators. Manipulators that, equipped with bi-articular actuators have been proved to have numerous advantages such as (1) dramatically increase in range of end effectors, (2) improvement of balance control, (3) efficiency increase of output force production, and (4) an arm that is equipped with bi-articular actuators having the ability to produce a maximum output force at the end effectors

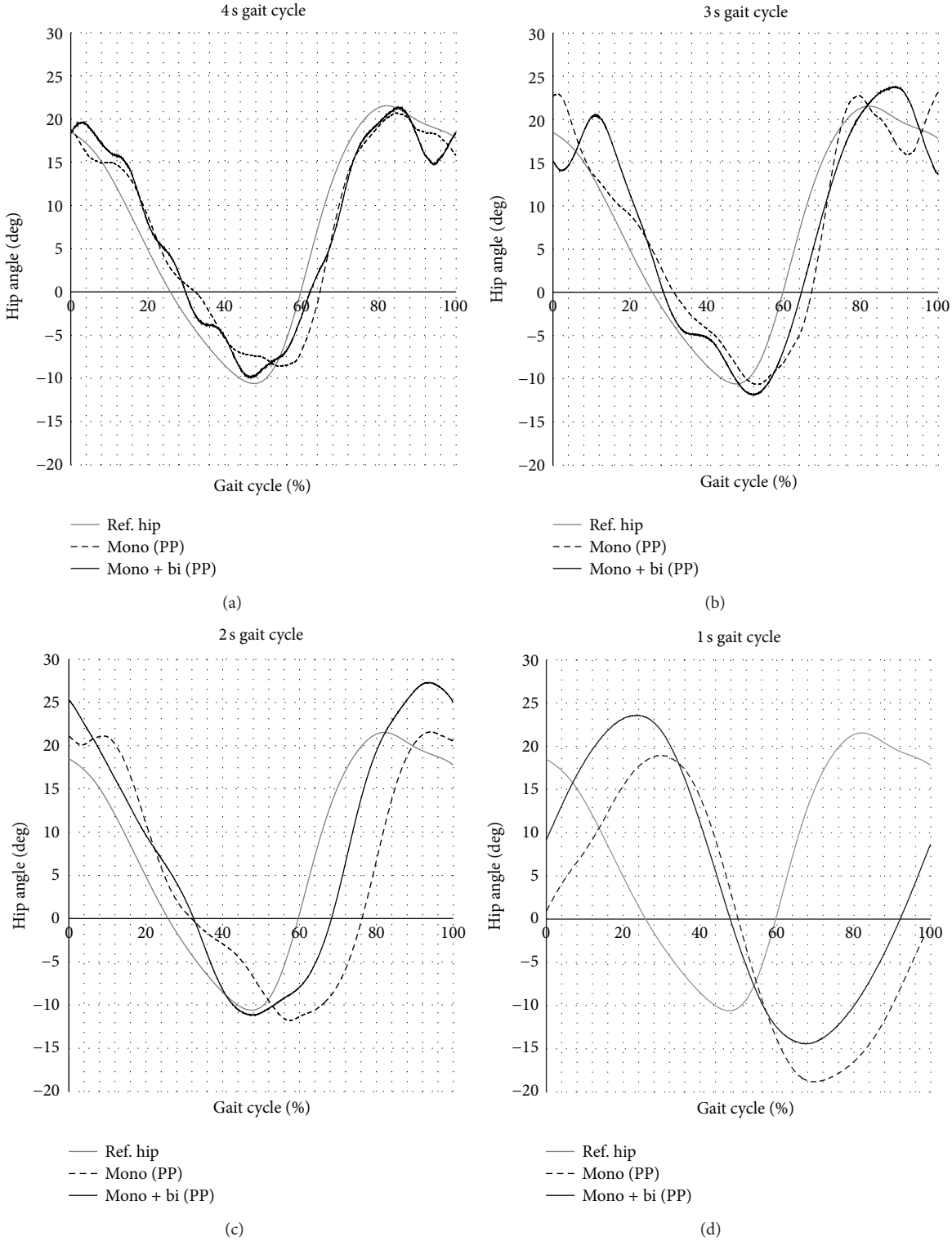

Figure 9: Hip joint trajectory for the control of the leg orthosis WO/S using a cocontraction model based PP controller.

in a more homogenously distributed way [18–20]. Even though the sources of the actuation system were different, the fundamental functions of these bi-articular actuators (PMA) should be similar. With a stable force assisting the movement of the leg orthosis, it reduces the coarse movement and improves the joints when compared to the leg orthosis actuated by the mono-articular actuators alone. The movement of the antagonistic bi-articular actuators was able to balance the coarse movement of the antagonistic mono-articular actuators at the joints, thus reducing the effect of the

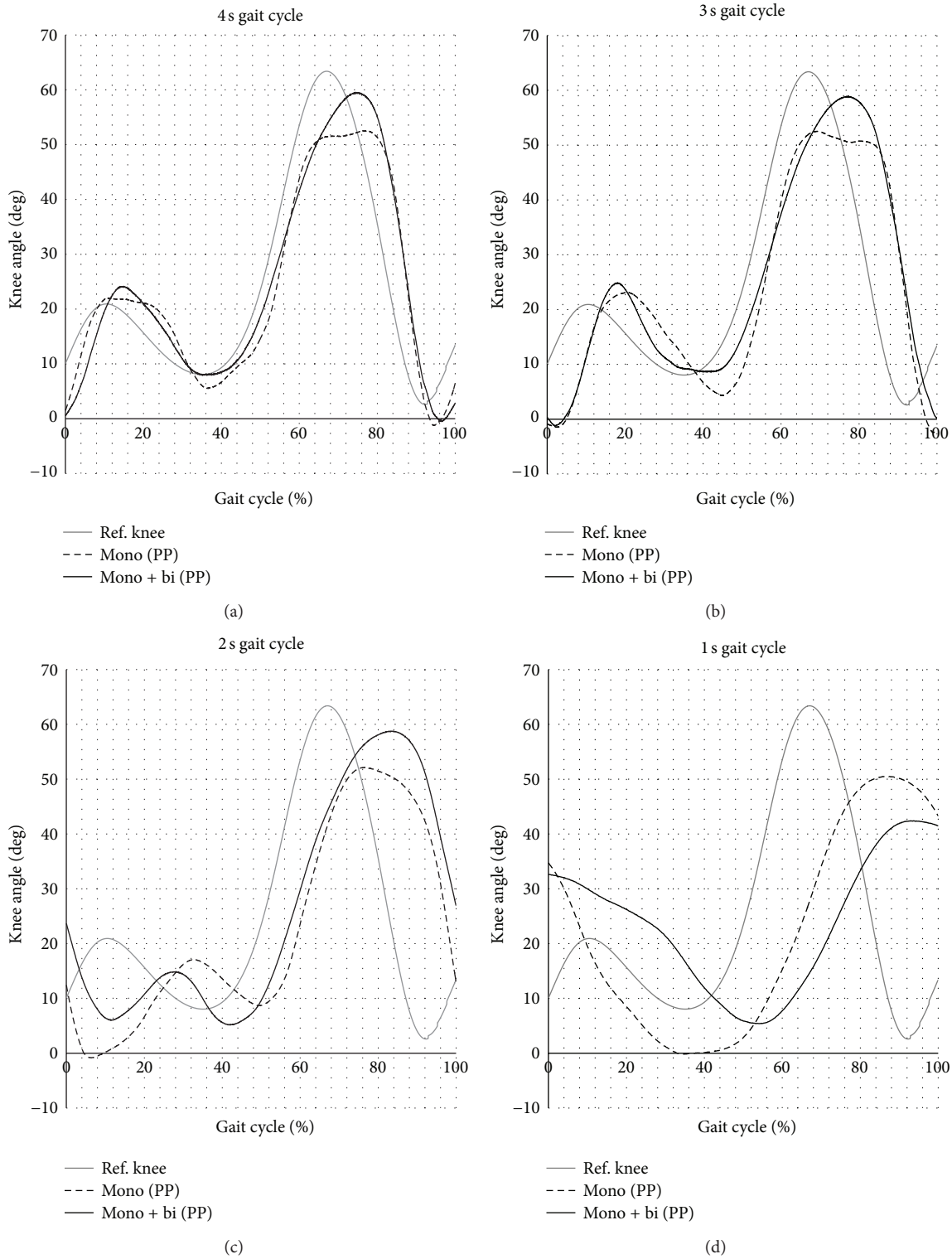

Figure 10: Knee joint trajectory for the control of the leg orthosis WO/S using a cocontraction model based PP controller.

hysteresis which was significant when implementing the mono-articular actuators alone WO/S. This is also due to the fact that the contraction of the PMA is in accordance with the hysteresis model. However, as the expansion of the PMA did not follow that of the hysteresis model, the co-contractive movements between the antagonistic mono- and bi-articular actuators were realized. At the GC speed of 1 second, the orthosis was not able to perform the gait motion completely with the heel strike stance. However, it was still able to demonstrate the "foot flat up to swing stance"

Table 3: Pearson coefficient of determination (r^2) for mono-articular (alone) and with addition of bi-articular actuators.

Joint actuators	Pearson coefficient of determination (r^2) for monoarticular and Biarticular actuators							
	Hip angle CC value				Knee angle CC value			
	4 s GC	3 s GC	2 s GC	1 s GC	4 s GC	3 s GC	2 s GC	1 s GC
Monoarticular actuators	0.8834	0.7921	0.3969	0.25	0.7569	0.4761	0.1764	0.0225
Mono- and Biarticular actuators	0.9025	0.8281	0.7744	0.0576	0.7569	0.49	0.1444	0.1296

Table 4: Pearson coefficient of determination (r^2) for co-contraction model based P and PP controllers.

Cocontraction model based	Pearson coefficient of determination (r^2) for P and PP Controllers							
	Hip angle CC value				Knee angle CC value			
	4 s GC	3 s GC	2 s GC	1 s GC	4 s GC	3 s GC	2 s GC	1 s GC
P controller	0.9139	0.7921	0.4761	0.0196	0.6241	0.4356	0.09	0.1444
PP controller	0.9274	0.8649	0.7744	0.0625	0.7744	0.5184	0.16	0.1681

which provides the feel of a gait motion. By implementing the derived cocontraction model, all the six antagonistic mono- and bi-articular actuators were able to operate simultaneously and co-contractively. Table 3 shows the Pearson coefficient of determination (r^2) for the first assessment where the control tests with mono-articular actuators (hip and knee joints) alone and with addition of bi-articular actuators WO/S were evaluated. This r^2 value indicates how well the data fits the reference joints' trajectory. The result shows that the addition of the bi-articular actuators produce much higher r^2 coefficient values at most GC speeds as compared to mono-articular actuators alone.

5.2. Control of the Leg Orthosis WO/S: Evaluation of Designed Controller Schemes. The focus in this second assessment is on the evaluation of the designed controller schemes and strategy. It was conducted to determine the limitations of the position-based controller when acting on its own, and the superiority of the combined position-pressure-based controller. Two experiments were conducted. In the first, the cocontraction model based P controller scheme was tested WO/S, and in the second, the cocontraction model based PP controller scheme was tested WO/S. Both tests were performed with the presence of mono- and bi-articular actuators and evaluated at different GC speeds of 4 seconds, 3 seconds, 2 seconds, and 1 second. Five trials were performed for each GC speed, and each trial consisted of five cycles including the initial cycle position. Thus, a total of 25 GCs were obtained for each GC speed. The average GC for each GC speed was then determined and illustrated in a graph. Table 4 shows the Pearson coefficient of determination (r^2) for the second assessment where the control tests for P and PP controllers of leg orthosis with mono- and bi-articular actuators WO/S were evaluated. The result shows that the addition of the pressure controller (PP) produces much higher r^2 coefficient values at all GC speeds as compared to position controller alone (P).

Figure 11 shows the trajectory evaluation of the joints of the leg orthosis controls between two designed controller schemes (i.e., cocontraction model based P controller and cocontraction model based PP controller) tested WO/S. From the results, it is evident that both designed controller schemes were able to wholly achieve the gait motion smoothly up to a GC speed of 2 seconds. However, failure to perform a complete gait motion was experienced at a higher GC speed of 1 second. These results reveal that PMA muscle activities (i.e., contraction, expansion, and response time) were curtailed at a GC speed above 2 seconds as the time allocated for completing the GC was drastically reduced. However, the results illustrate that the time response of the PMA muscle activity was much better with the implementation of the PP controller scheme compared to only the P controller scheme. Furthermore, the PP controller scheme was able to maintain the maximum angle extension achieved at the posterior side of the hip joint trajectory for all GC speeds compared to the P controller scheme (reduced with increase in GC speed) as can be seen in Figures 11(a) and 11(b) of hip joint trajectories. PMA control was insufficient with the P controller scheme alone as the dynamic characteristics of PMA include pressure activity. Through the introduction of a cocontraction model based PP controller scheme with modified design architecture, the maximum angle extension and time response of the system were improved at most GC speeds. This indicates that the addition of the pressure controller was able to improve the response time of the system as the pressure increased exponentially with the contraction of PMA, consequently increasing the speed of PMA muscle activity during contraction mode.

Based on the results, the trajectory of the joints was slightly coarse at slower GC speeds (i.e., 4 seconds and 3 seconds), as unlike the extension of the joint, the leg orthosis goes against the gravitational effect during the flexion of the hip joint. However, this effect was reduced with an increase in GC speed at the cost of insignificant angle extension. Conversely, only slight effects were detected in the knee trajectory for both controller schemes as the high muscle moment was larger at the hip joint compared to the knee joint. When implementing the PP controller scheme, the maximum angle extension at the posterior side of the knee joint trajectory was slightly reduced with the improvement in PMA muscle activity response time. This is due to the maximum contraction achievable by each PMA (30% of its original length) which results in a limitation of orthosis movements. The speed of PMA muscle activity will reduce considerably with

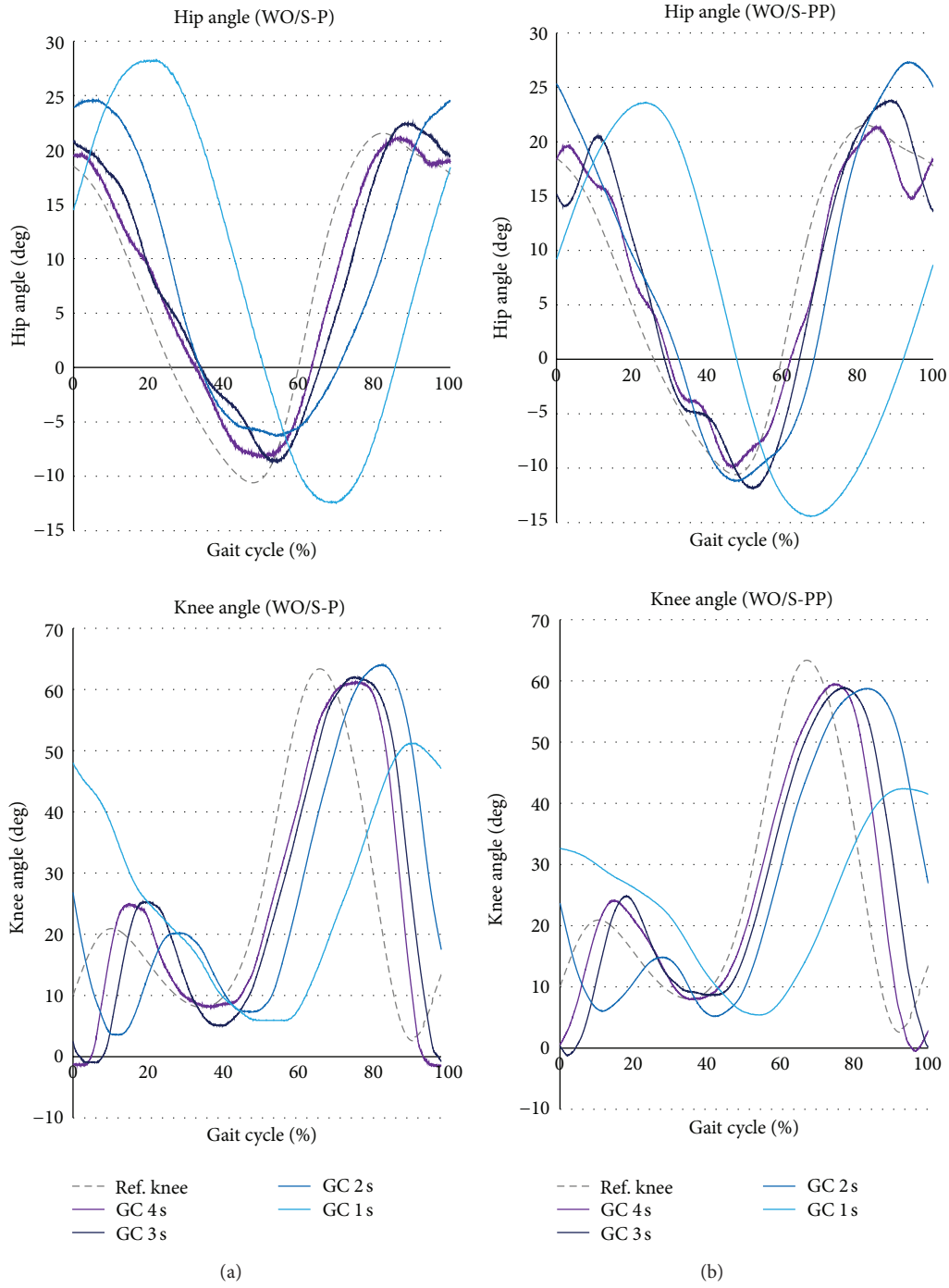

Figure 11: Hip and knee joints' trajectory evaluation of the leg orthosis controls between two designed controller schemes (i.e., P controller and PP controller) tested WO/S.

the approach of its maximum contraction. This affects the trajectory performance of the joints especially at the posterior side of the knee joint which requires a larger angle extension (63 degrees).

5.3. Control of the Leg Orthosis W/S. The focus in this third assessment is on the evaluation of the cocontraction model based P and PP controller scheme at the end point (EP) of the leg orthosis. It was conducted to determine the reliability of the designed controller scheme when implemented on leg orthosis and tested both WO/S and W/S. Two tests were conducted. The first involved leg orthosis controls WO/S and the second, leg orthosis W/S. Both tests were performed with the presence of mono- and bi-articular actuators. Similar to

previous assessments, the design controller scheme was evaluated at four GC speeds of 4 seconds, 3 seconds, 2 seconds, and 1 second. The normal GC speed of 1.25 seconds was not as necessary in the early stages of the gait rehabilitation therapy as it might not be able to furnish adequate afferent input to stimulate locomotor centres. However, during the later stages of rehabilitation therapy, gait training at the normal GC speed might be required. From the viewpoint of control architects, it is important to determine the system's maximum operating GC speed for the performance evaluation. A total of 25 GCs for each GC speed were collected, and the average GC was represented in a graph.

Figures 12 and 13 display the EP trajectory evaluation of the leg orthosis controls. This evaluation was carried out using the cocontraction model based P and PP controller scheme for tests WO/S and W/S. The results revealed that both designed controller schemes were able to achieve a good EP trajectory for all GC speeds of 4 seconds, 3 seconds, 2 seconds, and 1 second. Although the performance level dipped at a slower GC speed due to the inertia, good gait motion was displayed especially during the stance phase of GC both WO/S and W/S tests up to GC speed of 1 second. The coarse movement during the swing phase might be due to the increased load supported by the mono- and bi-articular actuators which forced the actuators into contraction mode to sustain the load much longer at a slower GC speed. This created an unbalanced state which disturbed the pressure activity of the antagonistic muscle actuators. Since the time allocated for completing one cycle was reduced with increases in GC speed, the posterior mono- and bi-articular actuators that contracted were unable to receive the control information fast enough to initiate the swing phase at the knee joint. This reduced the response time at the mid-swing phase (60~80% GC) due to the slowing down of PMA muscle activity as it approached maximum contraction.

To increase the response time of the design controller scheme at faster GC speeds, especially during the maximum angle extension of the knee joint, the constraints related to the actuator need to be reduced. These constraints include the inability of the system's operating pressure to withstand more than 5 (bars) of maximum load. The gravitational effect also affected the gait motion performance at the hip joint during the muscle flexion (0~50% GC) as the anterior mono-articular actuators and anterior bi-articular actuators were working against gravity during the leg expansion. This "leg expansion" is the gait motion from the heel strike stance up to toe off stance. It is an observed fact that the performance of the PMA controls faltered in the face of the gravitational effect. Therefore, it might be practical to lower the muscle activation level of the actuators in expansion mode so as to reduce the gravitational effect on the orthosis. Additionally, the effect can also be reduced by increasing the PMA muscle activity and the GC speed.

To determine the performance of the design controller schemes for both WO/S and W/S tests, the evaluation will be based on the effective work and the inertia produced by the EP trajectory of the leg orthosis controls. Figure 14 shows the effective work and inertia for the control of leg orthosis for both WO/S and W/S tests using cocontraction model based P and PP controllers. It is illustrated using mean value and standard deviation. Based on the researches carried out by Banala et al., to quantitatively determine the amount of adaptation, they implement a measure called "footpath deviation area." This area is the geometric area included between the swing phases of given foot trajectory and prescribed trajectory. The amount of area is the deviation of given trajectory from prescribed trajectory in the template [6, 7]. By using the same principle, the effective work is defined as the area covered by the EP trajectory within the reference trajectory (inside area), while inertia is defined as the area covered by the EP trajectory outside the reference trajectory (outside area). These data (i.e., effective work and inertia) were measured as ratio of the covered area to the total reference trajectory area. It is inevitable that the inertia will eventually occur as we tried to increase the GC speed from 4 s GC (0.35 m/s) up to 1 s GC (1.40 m/s), in which similar patterns can also be observed in [6]. Therefore, over 60% of effective work was judged as the minimum requirement to determine whether the leg orthosis was able or not to follow the reference foot trajectory. However, the total work done by the orthosis is defined as the sum of the effective work and inertia.

For the tests WO/S, both controller schemes produced nearly comparable effective work at the evaluated GC speeds of 4 seconds, 3 seconds, 2 seconds, and 1 second with 60% up to 89% of the ideal value. This effective work was reduced with the increases in the GC speed as the maximum knee angle extension achieved was reduced. However, with over 60% effective work achieved at all GC speeds; both designed controller schemes can be presumed to work properly. On the other hand, the inertia also occurred as the EP trajectory deviated outward from the reference trajectory. This inertia will always present at every GC speed due to the deviation. However, this inertia magnitude will vary with the increase of GC speed. Based on Figure 14(a), it can be seen that the cocontraction model based P controller was generating much higher inertia during the controls of leg orthosis with −13% up to −54% inertia as compared to −11% up to −43% inertia using cocontraction model based PP controller at all GC speeds. With these data, the leg orthosis was then tested W/S to determine the reliability of the designed controller schemes.

For the tests W/S, both controller schemes also produced nearly comparable effective work at the evaluated GC speeds of 4 seconds, 3 seconds, 2 seconds, and 1 second with 63% up to 85% of the ideal value. This effective work was maintained with over 60% effective work achieved at all GC speeds when compared to the test WO/S. On the other hand, based on the generated inertia evaluation, the inertia produced when using the cocontraction model based P controller was increasing with the increase of the GC speed, especially at the faster GC speeds of 2 seconds and 1 second. This indicates that the P controller alone was not enough to control the EP trajectory of the leg orthosis in the presence of inertia effect. However, when using the cocontraction model based PP controller, it was able to maintain the inertia produced at all evaluated GC speeds when tested both WO/S and W/S as illustrated in Figures 14(a) and 14(b). The generated inertia was around −13% up to −45% inertia (almost similar to the test WO/S with −11% up to −43% inertia) as compared to

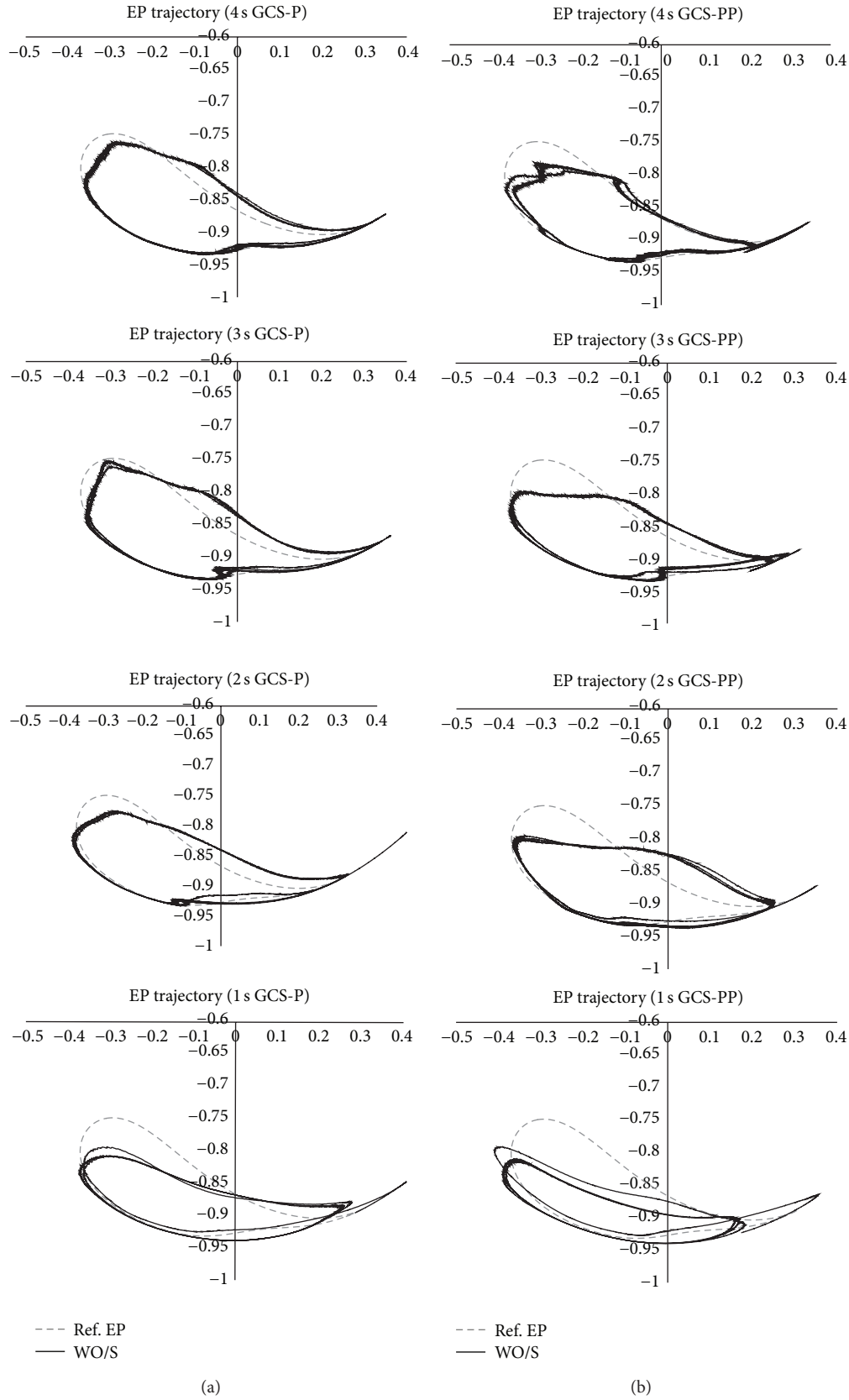

Figure 12: End point trajectory for the leg orthosis WO/S using cocontraction model based P and PP controllers.

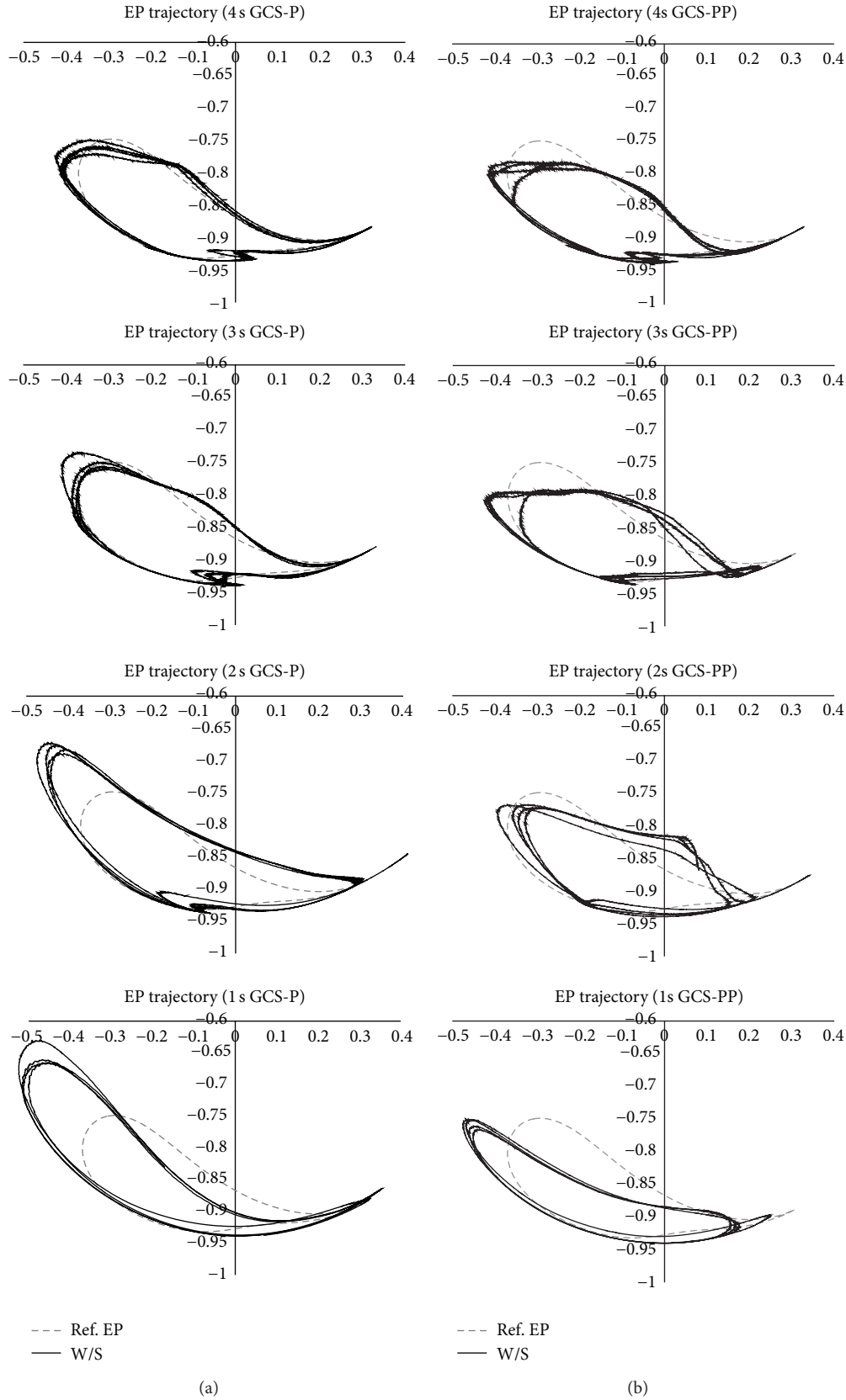

Figure 13: End point trajectory for the leg orthosis W/S using cocontraction model based P and PP controllers.

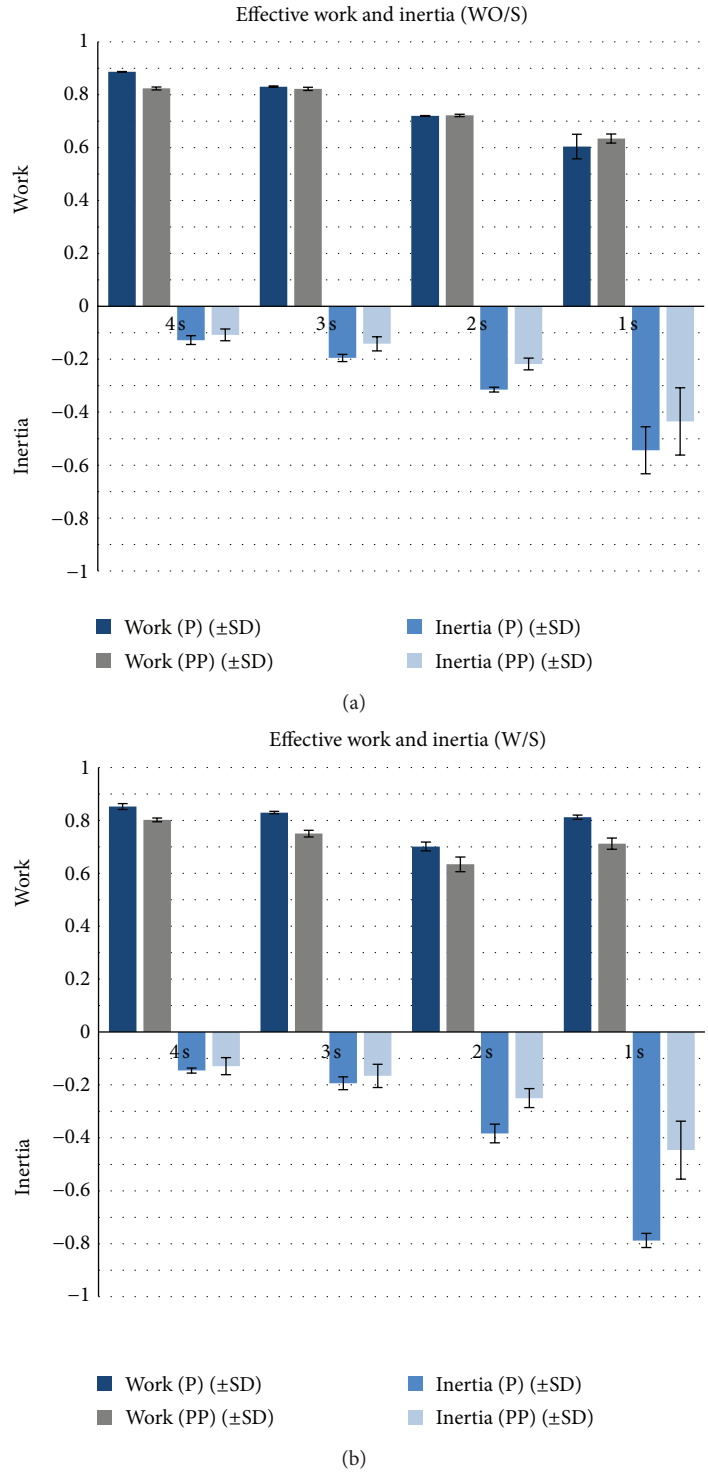

Figure 14: Effective work and inertia for the control of leg orthosis for both WO/S and W/S tests using cocontraction model based P and PP controllers.

−15% up to −79% inertia when using P based controller scheme. This concludes that the PP controller scheme was able to correspond to the inertia effect and thus gave a more stable EP trajectory of the leg orthosis at the evaluated GC speeds.

6. Conclusions

This research introduces the designed controller scheme and strategy to optimize the control of bi-articular actuators in co-contractive movements with the presence of mono-articular

actuators. The approach strategy for this designed controller scheme is the derivation of a cocontraction model which facilitates the implementation of position and pressure-based controllers. The proposed cocontraction model based PP controller scheme correlates information on the joints with the dynamic characteristics (i.e., contraction and pressure) of the PMA. Input patterns are then generated for the antagonistic mono- and bi-articular actuators compared to the other control algorithms for PMA that predict or measure the required torque for the joints.

Three tests were performed on the leg orthosis with the first using mono-articular actuators alone tested WO/S; the second with the addition of bi-articular actuators tested WO/S; and the third with the addition of bi-articular actuators tested W/S. Three assessments were evaluated to determine the performance of the designed controller scheme. The first assessment summarized that the addition of bi-articular actuators improved the joint stiffness of both the hip and knee. The bi-articular actuators also stabilized the coarse movements created by the mono-articular actuators during flexion of the joints and improved the maximum angle extension achieved at the knee joint. The second assessment concluded that compared to using the position based controller alone, the inclusion of the pressure-based controller improved the response time of PMA muscle activities due to the effects of contraction and expansion. The designed controller scheme was able to achieve complete gait motion of leg orthosis (i.e., hip and knee joints) until a GC speed of 2 seconds with a slight time shift of approximately only 0.2 seconds. The third assessment concluded that the cocontraction model based PP controller scheme was able to achieve a good EP trajectory of the leg orthosis up to GC speed of 1 second. The effective work achieved was over 60% of ideal value at all GC speeds of 4 seconds, 3 seconds, 2 seconds, and 1 second. Moreover, the generated inertia was also maintained at all GC speeds. This concludes that the PP controller scheme was able to correspond to the inertia effect and then optimize the controls of leg orthosis. The modified control scheme will be introduced in the next assessment to consider the gravitational effect on the antagonistic actuators as to improve control of the EP trajectory of the leg orthosis.

Conflict of Interests

The authors declare that they have no conflict of interests.

Acknowledgment

This work was supported by KAKENHI: Grant-in-Aid for Scientific Research (B) 21300202.

References

[1] G. Colombo, M. Wirz, and V. Dietz, "Driven gait orthosis for improvement of locomotor training in paraplegic patients," *Spinal Cord*, vol. 39, no. 5, pp. 252–255, 2001.

[2] S. Jezernik, G. Colombo, and M. Morari, "Automatic gait-pattern adaptation algorithms for rehabilitation with a 4-DOF robotic orthosis," *IEEE Transactions on Robotics and Automation*, vol. 20, no. 3, pp. 574–582, 2004.

[3] L. Lünenburger, G. Colombo, and R. Riener, "Biofeedback for robotic gait rehabilitation," *Journal of NeuroEngineering and Rehabilitation*, vol. 4, article 1, 2007.

[4] J. F. Veneman, R. Kruidhof, E. E. G. Hekman, R. Ekkelenkamp, E. H. F. Van Asseldonk, and H. Van Der Kooij, "Design and evaluation of the LOPES exoskeleton robot for interactive gait rehabilitation," *IEEE Transactions on Neural Systems and Rehabilitation Engineering*, vol. 15, no. 3, pp. 379–386, 2007.

[5] H. Vallery, J. Veneman, E. van Asseldonk, R. Ekkelenkamp, M. Buss, and H. van Der Kooij, "Compliant actuation of rehabilitation robots," *IEEE Robotics and Automation Magazine*, vol. 15, no. 3, pp. 60–69, 2008.

[6] S. K. Banala, S. H. Kim, S. K. Agrawal, and J. P. Scholz, "Robot assisted gait training with active leg exoskeleton (ALEX)," *IEEE Transactions on Neural Systems and Rehabilitation Engineering*, vol. 17, no. 1, pp. 2–8, 2009.

[7] S. K. Banala, S. K. Agrawal, S. H. Kim, and J. P. Scholz, "Novel gait adaptation and neuromotor training results using an active leg exoskeleton," *IEEE/ASME Transactions on Mechatronics*, vol. 15, no. 2, pp. 216–225, 2010.

[8] V. Monaco, G. Galardi, M. Coscia, D. Martelli, and S. Micera, "Design and evaluation of NEUROBike: a neuro-rehabilitative platform for bedridden post-strike patients," *IEEE Transactions on Neural Systems and Rehabilitation Engineering*, vol. 20, no. 6, 2012.

[9] D. J. Reinkensmeyer, D. Aoyagi, J. L. Emken et al., "Tools for understanding and optimizing robotic gait training," *Journal of Rehabilitation Research and Development*, vol. 43, no. 5, pp. 657–670, 2006.

[10] M. Pietrusinski, I. Cajigas, G. Severini, P. Bonato, and C. Mavroidis, "Robotic gait rehabilitation trainer," *IEEE/ASME Transactions on Mechatronics*, no. 99, pp. 1–10, 2013.

[11] A. Taherifar, M. Mousavi, A. Rassaf, F. Ghiasi, and M. R. Hadian, "LOKOIRAN—a novel robot for rehabilitation of spinal cord injury sand stroke patients," in *Proceedings of the RSI/ISM International Conference on Robotics and Mechatronics*, Tehran, Iran, 2013.

[12] S. Hussain, S. Q. Xie, and P. K. Jamwal, "Adaptive impedance control of a robotic orthosis for gait rehabilitation," *IEEE Transactions on Cybernetics*, vol. 43, no. 3, 2013.

[13] S. Hussain, S. Q. Xie, and P. K. Jamwal, "Robust nonlinear control of an intrinsically compliant robotic gait training orthosis," *IEEE Transactions on Systems, Man, and Cybernetics*, vol. 43, no. 3, 2013.

[14] Y. Shibata, S. Imai, T. Nobutomo, T. Miyoshi, and S.-I. Yamamoto, "Development of body weight support gait training system using antagonistic bi-articular muscle model," in *Proceedings of the 32nd Annual International Conference of the IEEE Engineering in Medicine and Biology Society (EMBC '10)*, pp. 4468–4471, Buenos Aires, Argentina, September 2010.

[15] S.-I. Yamamoto, Y. Shibata, S. Imai, T. Nobutomo, and T. Miyoshi, "Development of gait training system powered by pneumatic actuator like human musculoskeletal system," in *Proceedings of the IEEE International Conference on Rehabilitation Robotics (ICORR '11)*, Zurich, Switzerland, July 2011.

[16] M. Kumamoto, T. Oshima, and T. Fujikawa, "Control properties of a two-joint link mechanism equipped with mono- and bi-articular actuators," in *Proceedings of the 9th IEEE International Workshop on Robot and Human Interactive Communication (RO-MAN '00)*, pp. 400–404, Osaka, Japan, September 2000.

[17] S. Shimizu, N. Momose, T. Oshima, and K. Koyanagi, "Development of robot leg which provided with the bi-articular actuator for training techniques of rehabilitation," in *Proceedings of the 18th IEEE International Symposium on Robot and Human Interactive (RO-MAN '09)*, pp. 921–926, Toyama, Japan, October 2009.

[18] V. Salvucci, S. Oh, and Y. Hori, "Infinity norm approach for precise force control of manipulators driven by Bi-articular actuators," in *Proceedings of the 36th Annual Conference of the IEEE Industrial Electronics Society (IECON '10)*, pp. 1908–1913, November 2010.

[19] V. Salvucci, S. Oh, Y. Hori, and Y. Kimura, "Disturbance rejection improvement in non-redundant robot arms using bi-articular actuators," in *Proceedings of the IEEE International Symposium on Industrial Electronics (ISIE '11)*, pp. 2159–2164, June 2011.

[20] V. Salvucci, Y. Kimura, S. Oh, and Y. Hori, "Experimental verification of infinity norm approach for force maximization of manipulators driven by bi-articular actuators," in *Proceedings of the American Control Conference (ACC '11)*, pp. 4105–4110, San Francisco, Calif, USA, July 2011.

[21] M. A. Mat Dzahir, T. Nobutomo, and S. I. Yamamoto, "Development of body weight support gait training system using pneumatic McKibben actuators: control of lower extremity orthosis," in *Proceeding of the International Conference of the IEEE EMBS*, Osaka, Japan, 2013.

[22] M. Frey, G. Colombo, M. Vaglio, R. Bucher, M. Jörg, and R. Riener, "A novel mechatronic body weight support system," *IEEE Transactions on Neural Systems and Rehabilitation Engineering*, vol. 14, no. 3, pp. 311–321, 2006.

[23] H. J. A. van Hedel, L. Tomatis, and R. Müller, "Modulation of leg muscle activity and gait kinematics by walking speed and bodyweight unloading," *Gait and Posture*, vol. 24, no. 1, pp. 35–45, 2006.

[24] J. Von Zitzewitz, M. Bernhardt, and R. Riener, "A novel method for automatic treadmill speed adaptation," *IEEE Transactions on Neural Systems and Rehabilitation Engineering*, vol. 15, no. 3, pp. 401–409, 2007.

[25] B. Tondu and P. Lopez, "Modeling and control of McKibben artificial muscle robot actuators," *IEEE Control Systems Magazine*, vol. 20, no. 2, pp. 15–38, 2000.

[26] T. Miyoshi, K. Hiramatsu, S.-I. Yamamoto, K. Nakazawa, and M. Akai, "Robotic gait trainer in water: development of an underwater gait-training orthosis," *Disability and Rehabilitation*, vol. 30, no. 2, pp. 81–87, 2008.

[27] S. Balasubramanian, J. Ward, T. Sugar, and J. He, "Characterization of the dynamic properties of pneumatic muscle actuators," in *Proceedings of the IEEE 10th International Conference on Rehabilitation Robotics (ICORR '07)*, pp. 764–770, Noordwijk, The Netherlands, June 2007.

[28] J. Bae and M. Tomizuka, "A gait rehabilitation strategy inspired by an iterative learning algorithm," *Mechatronics*, vol. 22, no. 2, pp. 213–221, 2012.

[29] K. K. Ahn and D. C. T. Tu, "Improvement of the control performance of Pneumatic Artificial Muscle Manipulators using an intelligent switching control method," *KSME International Journal*, vol. 18, no. 8, pp. 1388–1400, 2004.

[30] T. D. C. Thanh and K. K. Ahn, "Nonlinear PID control to improve the control performance of 2 axes pneumatic artificial muscle manipulator using neural network," *Mechatronics*, vol. 16, no. 9, pp. 577–587, 2006.

[31] M. A. Mat Dzahir, T. Nobutomo, and S. I. Yamamoto, "Antagonistic mono- and bi-articular pneumatic muscle actuator control from gait training system using contraction model," in *Proceedings of the IEEE International Conference on Bio-Science and Bio-Robotics*, Rio de Janeiro, Brazil, 2013.

[32] D. A. Winter, *Winter, Biomechanics and Motor Control of Human Movement*, John Wiley & Sons, 4th edition, 2009.

Applied Mechanics and Materials Vol. 393 (2013) pp 525-531
Online available since 2013/Sep/03 at www.scientific.net

doi:10.4028/www.scientific.net/AMM.393.525

Development of Gait Training System Powered by Antagonistic Mono- and Bi-Articular Actuators using Contraction Model Control Scheme

Mohd Azuwan Mat Dzahir[1, 2, a], Tatsuya Nobutomo[1, b],
Shin-ichiroh Yamamoto[1, c]

[1]Bio-Science and Engineering Department, Shibaura Institute of Technology, Japan

[2]Faculty of Mechanical Engineering, Universiti Teknologi Malaysia, Malaysia

[a]azuwan@fkm.utm.my, [b]t.nobutomo@bpe.se.shibaura-it.ac.jp, [c]yamashin@se.shibaura-it.ac.jp

Keywords: PMA, contraction model, mono- and bi-articular actuators, control system.

Abstract. The use of Pneumatic Muscle Actuator (PMA) in medical robots for rehabilitation has changed due to the requirements for a compliant, light weight and user-friendly robotic system. In this paper, a control system for controlling the bi-articular actuators (PMA) is proposed. Based on the information obtained from the positional input data (hip and knee joint angles), a contraction model is derived using mathematical equations to determine the contraction patterns of antagonistic mono- and bi-articular actuators, and then implemented it into the control system. Anterior and posterior muscle activation levels are introduced into the model to manipulate its magnitude. There are two tests for the control system; first is with antagonistic mono-articular actuators alone; second is along with antagonistic bi-articular actuators. The contraction model control scheme was tested on a healthy subject in a robot assisted walk test, and satisfactory performance was obtained. The result showed that, the cycle time of the gait training system is improved up to 3 seconds gait cycle compared to 5 seconds gait cycle used in previous research. However, a little time shift and inertia occurred when the controller is tested at faster gait cycle time of 2 seconds and 1 second. Thus, the potential field and iterative learning control are suggested to improve the gait cycle of the system.

Introduction

In neuro-rehabilitation robotic view, the robot should be compliant to movement of impaired subjects often seen in neurologically impaired patients, such as spinal cord injury (SCI) and stroke patients [1, 2, 3]. Recent trends in rehabilitation robotics try to implement the use of natural compliant actuator (PMA) which has many advantages such as high power to weight ratio, inherent safety, easy maintenance, low cost, cheap power source and readily available.

This introduces the Body Weight Support Gait Training System (AIRGAIT) for lower extremity orthotic patients [4]. In their previous study, they were not able to achieve high stiffness on the hip and knee joints by using only mono-articular actuators. However, they were able to improve the system by implementing antagonistic bi-articular actuators with constant pressure input of 0.025[MPa] which resolves the problem that occurred during the use of mono-articular actuators alone. This shows that the implementation of antagonistic bi-articular actuators with addition of mono-articular actuators was a key to achieve high muscle moment (flexion and extension) at hip joint and wider range of motion (flexion) at knee joint. In this research, we try to improved the gait cycle up to normal gait cycle of human motion ($T \approx 1.25$s/cycle) compared to 5 seconds gait cycle used in the previous research [4] and control the bi-articular actuators in a co-contraction movement.

Based on previous researches, its show that the performances of two-joint link mechanism such as differences in characteristics of the output force, stiffness at endpoint of the leg and humanlike control properties at the endpoint depend on the presence or absence of bi-articular actuators when its present along with mono-articular actuators. According to V. Salvucci et al., the performance of bi-articular actuator can be seen when it works in the presence of mono-articular actuator [5]. While, M. Kumamoto et al. stated that when a two-joint link mechanism was installed with an antagonistic pair of bi-articular actuators in addition to antagonistic pairs of mono-articular actuators, the two-

joint link mechanism could demonstrates humanlike control properties at the endpoint [6]. In addition to this, S. Shimizu et al. also stated that the differences in characteristics of the output force and the stiffness at endpoint of the leg depend on the presence or absence of bi-articular muscles [7]. Most of the previous researches on the bi-articular actuators were focused on the DC motor compared to the PMA. However, in this study, a control system for controlling the bi-articular actuators (PMA) is proposed to obtain a greater force and precise movement from the system.

The main goal in doing this research is to derive a concrete model equation for controlling the bi-articular actuators which involve both hip and knee joints with co-contraction movement. The known fact is that it is difficult to control the bi-articular actuators using both hip and knee angle controls without complex algorithm and equations. Albeit that, if there is a model which correlates the PMA properties with the positional data, we might be able to control the orthosis mechanism precisely with co-contraction movement as well as simplifying the control algorithm and equations.

PMA Model. A PMA model for contraction vs. input pressure is determined using the average value of the data and then converted into an equation. The PMA used in this study is McKibben type of actuator. The data for changes in length, pressure and force of the McKibben actuators were collected in an experiment. Load cell and linear motion potentiometer were used to measure the increment value of the contraction and force of the PMA. This experiment uses 3 samples of McKibben actuators with different initial length (l_o), 300mm, 450mm, and 600mm. A regulator is used to control the input pressure into the PMA. The pressure is regulated from 0.0[MPa] to 0.5[MPa]. Figure 1 shows the model for the PMA's contraction under pressure influence for different initial lengths of PMA. From the data obtained, it can be concluded that the values of maximum contraction (ε_{max}) of the PMAs are similar with 0.3[30%] contraction.

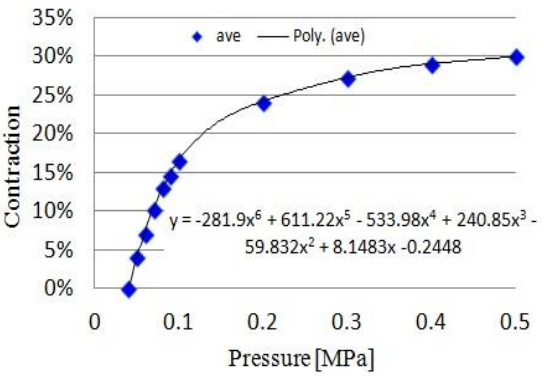

Fig. 1: PMA contraction model

Body Weight Support Gait Training System. The experimental test, mathematical model, and control system measurements for this research were based on the AIRGAIT system. Figure 2 illustrates the schematic diagram of an AIRGAIT orthosis system hardware and software. This model consists of a pair of anterior and posterior bi-articular actuators and two pairs of anterior and posterior mono-articular actuators which move in a co-contraction movement. The PMA operates similarly as a human muscle which is able to expand and contract by regulating air pressure from 0.0[MPa] to 0.5[MPa] using a mechanical regulator. The potentiometer is used for the feedback control system. A control program is applied to the AIRGAIT system with the aid of the xPC target toolbox and Simulink. Host PC and target PC are used to transfer the data to the AIRGAIT system.

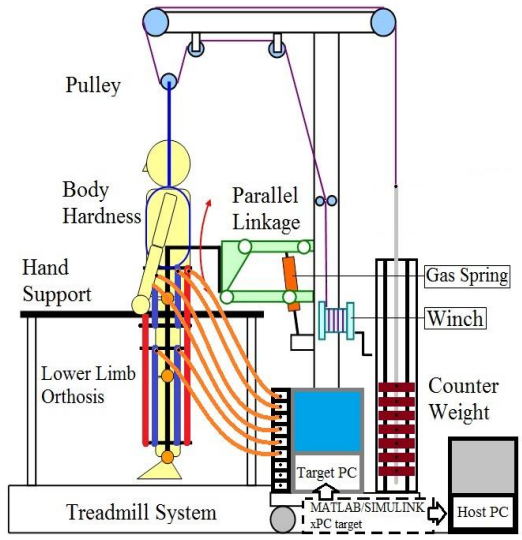

Fig. 2: AIRGAIT orthosis system.

Methods

A contraction model to determine the contraction patterns of antagonistic mono- and bi-articular actuators from positional data is derived and implemented into the control system. Reference input data (hip and knee angles) for the control system was obtained from [8]. Two tests for the control system using antagonistic mono-articular actuators alone and with the addition of antagonistic bi-articular actuators were conducted. The controller is tested for different gait cycle times (T = 5s, 4s,

3s, 2s and 1s) for five cycles including the initial position cycle. The contraction model control scheme was performed on a healthy subject with full body weight support (BWS) during robot assisted walk and from that the performance is obtained. The result is evaluated based on maximum flexion and extension of hip and knee joints, output pattern, time shift, and inertia.

Mathematical Design for Contraction Model. Figure 3 shows the model for leg orthosis system which consists of antagonistic mono-articular PMA model for hip joint (*h_p* and *h_a*), antagonistic mono-articular PMA model for knee joint (*k_p* and *k_a*) and antagonistic bi-articular PMA model (*bi_p* and *bi_a*). According to S. Balasubramanian et al., it is defined that PMAs are based on its model parameters such as relative muscle contraction and rise natural frequency which are affected more by PMA dimensions [9]. In this study, we focus on the mathematical design for contraction model (change in length) of the PMA that is to be implemented into the control system. The general idea for this mathematical model was formed based on the information gained from the reference input data analysis. From the positional input data of hip and knee angles, the locations of minimum (ε_{min}) and maximum (ε_{max}) value for the PMA contractions were determined. For example, point (a) in Figure 4 shows minimum value for posterior muscle contraction (PMA), but maximum value for anterior muscle contraction (PMA). On the contrary, point (b) shows minimum value for anterior muscle contraction (PMA), but maximum value for posterior muscle contraction (PMA).

For a better representation of maximum and minimum antagonistic PMA contractions, these data were illustrated as positive values to represent the muscle contraction patterns as can be seen in Figure 4(b), 4(c), 5(b) and 5(c). These figures show PMA contraction patterns of antagonistic mono-articular actuators for hip and knee joints. In this mathematical model, a condition for maximum muscle contraction was set, where; $\varepsilon_{p(max)} = \varepsilon_{a(max)} \leq 0.3$.

By referring to Figure 3, the change in arc length (ΔS) at the hip and knee joints are defined based on the change in the length (Δl) of PMA to correlate the PMA's contraction with the positional data. Antagonistic mono-articular actuator contractions for hip joint are:

$$\Delta l = \Delta S = \theta . r \quad (1)$$

Posterior: $\Delta l_{h\_p} = \theta_{hp} . r$

$$\varepsilon_{hp} = \frac{\Delta l_{h\_p}}{l_o} = \beta_h . \left(\frac{\theta_{hp} . r}{l_o}\right) \quad (2)$$

Anterior: $\Delta l_{h\_a} = \theta_{ha} . r$

$$\varepsilon_{ha} = \frac{\Delta l_{h\_a}}{l_o} = \alpha_h . \left(\frac{\theta_{ha} . r}{l_o}\right) \quad (3)$$

Equation (2) and (3) can be defined as a time function as follows:

Posterior: $\varepsilon_{hp}(t) = \left(\frac{r}{l_o}\right) . \beta_h . \theta_{hp}(t) \leq 0.3 \quad (4)$

$$\varepsilon_{hp(\max)} = \left(\frac{r}{l_o}\right) \beta_{h(max)} . |\theta_{hp}(t)|_{max} = 0.3$$

Anterior: $\varepsilon_{ha}(t) = \left(\frac{r}{l_o}\right) . \alpha_h . \theta_{ha}(t) \leq 0.3 \quad (5)$

$$\varepsilon_{ha(max)} = \left(\frac{r}{l_o}\right) \alpha_{h(max)} . |\theta_{ha}(t)|_{max} = 0.3$$

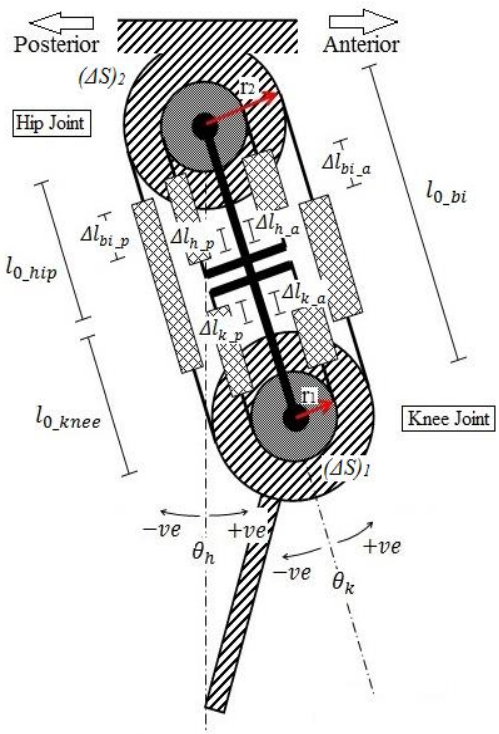

Fig. 3: Powered orthosis design.

These equations are similar to the antagonistic mono-articular actuators for the knee joint:

$$\varepsilon_{hp}(t) = \left(\frac{r}{l_o}\right) . \beta_h . \theta_{hp}(t) \leq 0.3 \quad (6)$$

$$\varepsilon_{ha}(t) = \left(\frac{r}{l_o}\right).\alpha_h.\theta_{ha}(t) \leq 0.3 \quad (7)$$

For the mathematical design's implementation into the system, another condition was set; when the anterior side is in a contraction mode, both the anterior mono- and bi-articular actuators will be in a contraction mode. On the contrary, when the posterior side is in an expansion mode, both the posterior mono- and bi-articular actuators will be in an expansion mode, and, vise versa.

Noted that θ_{hp} (hip posterior) and θ_{ha} (hip anterior) have the same magnitude but different signs between muscle contraction (+) or expansion (-). These variables were determined as pattern (positional based data) with a positive value to measure the contraction of the antagonistic mono- and bi-articular actuators, which is also applied for the θ_{kp} (knee posterior) and θ_{ka} (knee anterior). Where; l_o is the initial length for PMA, r is the distance from the PMA endpoint to the attached joint, ε_{hp} is the posterior muscle contraction of mono-articular PMA for hip joint, ε_{ha} is the anterior muscle contraction of mono-articular PMA for hip joint, β_h is the activation level of posterior muscle contraction for hip joint, and α_h is the activation level of anterior muscle contraction for hip joint. Maximum contraction for the posterior and anterior PMAs are $\varepsilon_{p(max)} = \varepsilon_{a(max)} \leq 0.3$.

The posterior and anterior muscle activation levels (β and α) are introduced to manipulate the gain of the antagonistic mono- and bi-articular actuator contractions, where the muscle activation level is ranged from ($0 < \beta \leq \beta_{max}$ and $0 < \alpha \leq \alpha_{max}$). These parameters are similar for the antagonistic mono-articular actuators for knee joint and bi-articular actuators.

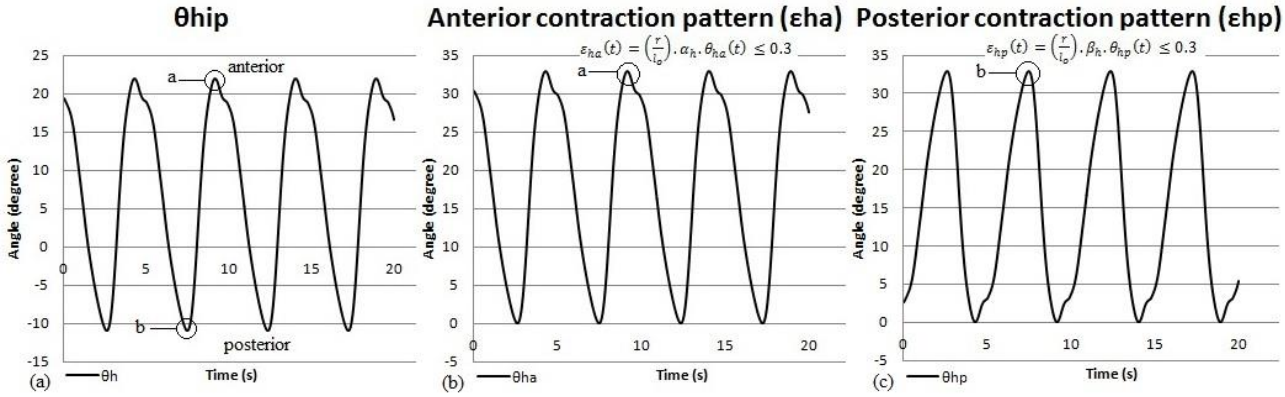

Fig. 4: Antagonistic mono-articular actuator contraction patterns for the hip joint.

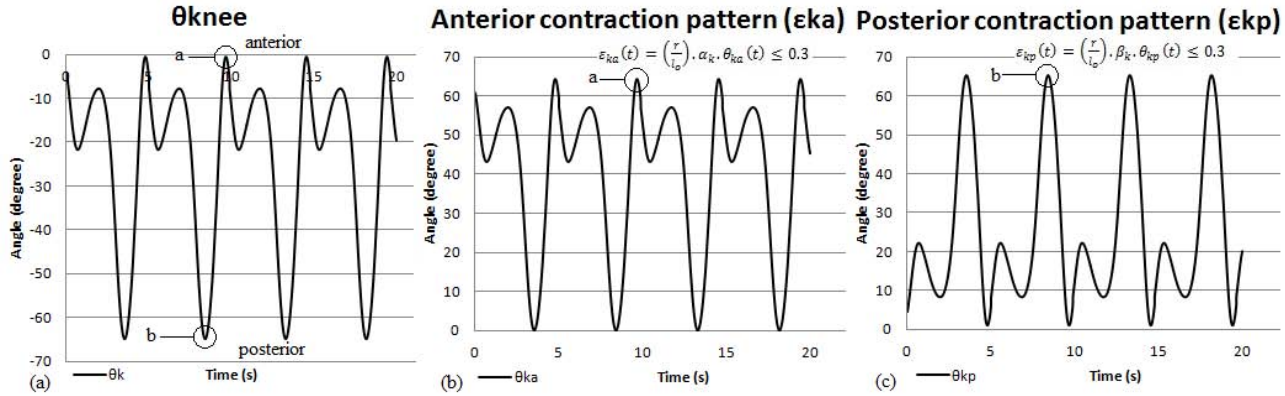

Fig. 5: Antagonistic mono-articular actuator contraction patterns for the knee joint.

The interesting part that found in this study was on the bi-articular actuator contraction patterns. It can be defined that, the muscle contraction pattern for the antagonistic bi-articular actuators can be represent as a pattern of the total hip and knee joint angles. Figure 6(a) shows the positional based data for bi-articular actuators which is defined as a pattern of the total hip and knee angles ($\theta_h + \theta_k$). The activation levels for bi-articular actuator muscle contractions are defined as (β_{bi} and α_{bi}). Antagonistic bi-articular actuator muscle contractions (ε_p and $\varepsilon_{a)}$ are:

Posterior: $\Delta l_{bi\_p} = (\Delta l_h + \Delta l_k)_p = r.(\theta_h + \theta_k)_p \rightarrow \varepsilon_p = \frac{\Delta l_{bi\_p}}{l_o} = \beta_{bi}.\left[\frac{r.(\theta_h+\theta_k)_p}{l_o}\right]$

$$\varepsilon_p(t) = \left(\frac{r}{l_o}\right).\beta_{bi}.(\theta_h(t) + \theta_k(t))_p \leq 0.3 \quad (8)$$

Anterior: $\Delta l_{bi_a} = (\Delta l_h + \Delta l_k)_a = r.(\theta_h + \theta_k)_a \rightarrow \varepsilon_a = \frac{\Delta l_{bi\_a}}{l_o} = \alpha_{bi}.\left[\frac{r.(\theta_h+\theta_k)_a}{l_o}\right]$

$$\varepsilon_a(t) = \left(\frac{r}{l_o}\right).\alpha_{bi}.(\theta_h(t) + \theta_k(t))_a \leq 0.3 \quad (9)$$

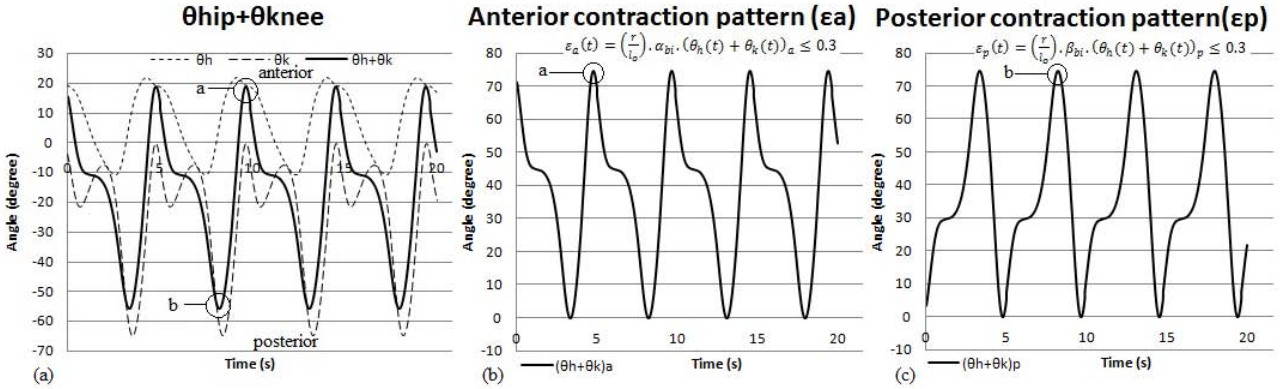

Fig. 6: Antagonistic bi-articular actuator contraction patterns (positional based data).

Control System. Figure 7 explains the schematic diagram of the proposed control system based on the contraction model. In this control system, the normal gait trajectory (hip and knee angles) data are converted to six input patterns for controlling the mono- and bi-articular actuators. Then, the orthosis system is tested using a proposed control system. The Proportional + Integral (PI) controller is implemented to control the gain value of the input patterns. The PI controller is applied because of its robustness and easy implementation into the control system. Heuristic method is used to tune the PI gain parameters. Where θ is hip and knee angles as well as total of hip and knee angles (θ_h+ θ_k), θ_o is output data, v_i is pressure input, ev_i is correction for gain value, and v_p is input pressure after the correction due to the PMA nonlinearity.

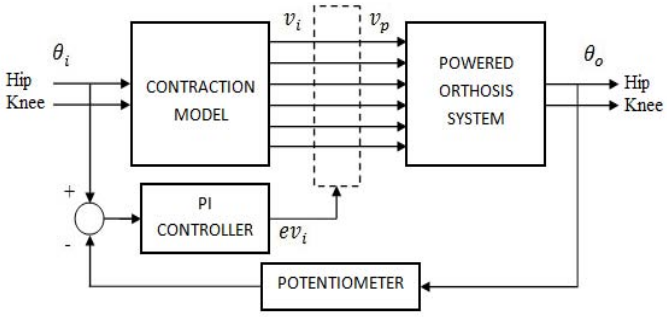

Figure 7: Schematic diagram.

Results and Discussions

In the previous study of AIRGAIT [4], they used proportional directional control valve to actuate the antagonistic mono-articular actuators and applied a constant pressure to the bi-articular actuators. The operating condition for the valve will regulate the air pressure between its two ports. Due to the limitation of this mechanical system, they did not able to actuate the antagonistic mono and bi-articular actuators in a co-contraction movement, but simply alternating it between anterior and posterior actuators. The resulting performance was rather poor. However, in this research, one regulator for each actuator is used to replace the previous control system, which makes it possible to control the antagonistic muscle actuators in a co-contraction movement.

When implementing the formed equations, it shows that the position of PMAs to the joints (r) and initial length (l_o) does not affect the muscle contraction pattern of the antagonistic mono- and bi-articular actuators. The study shows that the muscle contraction pattern of posterior and anterior

PMAs follows the pattern of the positional data itself but only differs in gain value based on the posterior and anterior muscle activation levels (β and α).

Figure 8 shows the result for the hip and knee joint angles control on different gait cycles for the tests using mono-articular actuators alone, and with the addition of bi-articular actuators. For the gait cycle time of 5 seconds, 4 seconds, and 3 seconds, both control tests are conducted on a healthy test subject, (W/S). The gait training system was able to perform good motion without much time delay and was able to follow the hip and knee angle patterns by using the developed contraction model. However, by implementing the mono-articular actuators alone, the system was not able to perform a smooth motion at the hip joint and heel contact positions (knee joint) due to lack of actuation power and inertia. To resolve the lack of actuation power from the mono-articular actuators, greater force from a PMA can be obtained by increasing its diameter size. However, this will affects its compressibility which is reduced with the increment of the PMA diameter size due to the McKibben muscle actuator's limitation. On the contrary, with the addition of bi-articular actuators to the system, we were able to get a smooth motion at the hip joint and heel contact positions as well as achieving maximum muscle moment (flexion and extension) at hip and knee joints. By implementing these bi-articular actuators into the system, we managed to improve the lack of actuation power at the hip joint, and solving the problems caused by inertia. This result shows that the introduction of bi-articular PMA into a mono-articular PMA model was able to give good control performance and smooth motion at the hip and knee joints respectively. The contraction model which enables the antagonistic mono-articular and bi-articular actuators to move in a co-contraction movement in the control system also plays a major role in ensuring the precise motion at the hip and knee joints.

Based on the result, it shows that the lapse at the hip joint for the test using mono-articular actuators is around ±5º. This requires a bigger diameter antagonistic mono-articular PMA at the hip joint for better results. However, by implementing bi-articular actuators into the mono-articular actuators model, maximum muscle flexion and extension required at the hip joint were achieved with a lapse of ±1º up to 3 seconds gait cycle. Furthermore, when the controller is tested for faster gait cycle times (T = 2 seconds and 1 second), mono-articular actuators alone were not able to withstand the external force generated from the AIRGAIT's inertia, and caused the PMA to break loose from the clamp before the 3 second mark. With the addition of bi-articular actuators, the system was able to distribute the external force generated from the inertia effect equally to the mono- and bi-articular actuators which enables the system to operate at a much faster gait cycle up to 1 second. However, it is at the cost of little time delay and extended movement of the hip and knee joints due to inertia.

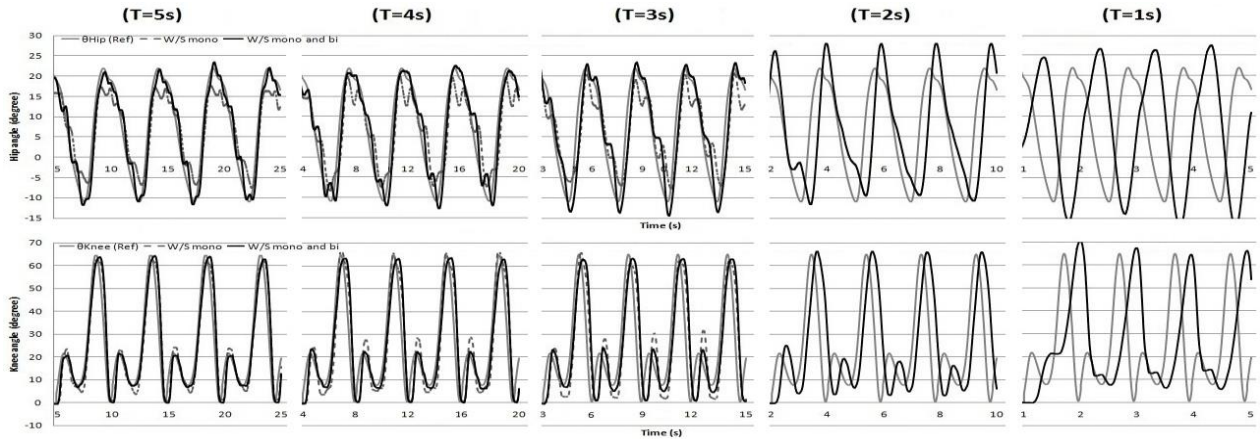

Fig. 8: Hip and knee joint angles control on different gait cycles.

Conclusion and Future Work

It is important in gait rehabilitation therapy to achieve a gait cycle of the same or similar to the natural state of human walking motion so that the patient can experience natural sensation and emotion of walking again. Thus, if the controller is able to simulate the normal walking speed of a

healthy human being (gait cycle, T ≈ 1.25s/cycle), better results in rehabilitation therapies can be obtained. It shows that the introduction of bi-articular actuators in the presence of mono-articular actuators was able to give good control performance and smooth motion at the knee joint. Moreover, the developed contraction model also enables the anterior and posterior actuators to move in a co-contraction movement in the control system which plays a major role in ensuring precise movement at the joints. These factors also apply for the performance at the hip joint, which was able to achieve maximum muscle moment (flexion and extension) due to lack of actuation power when compared to mono-articular actuators alone and problems caused due to inertia. For the test with full BWS subject, we were able to achieve maximum muscle flexion and extension required at the hip joint with a lapse of ±1° for up to 3 seconds gait cycle. The gait cycle time was improved to 3 seconds gait cycle compared to 5 seconds gait cycle in the previous research. The result was still acceptable for faster gait cycle of 2 seconds and 1 second. However, the angle extension was increased due to inertia and a little time shift occurred. Moreover, the PI controller used for tackling the PMA's nonlinearity by manipulating the contraction's gain value also might be improved by using the optimization methods. If an intelligent controller were to be added to the system, such as potential field and iterative learning control, the gait training's control system could be improved further.

Acknowledgement

This work was supported by KAKENHI: Grant-in-Aid for Scientific Research (B) 21300202.

References

[1] A. Wernig, S. Muller, A. Nanassy, and E. Cagol, "Laufband therapy based on 'rules of spinal locomotion' is effective in spinal cord injured persons". Eur J Neurosci vol. 7, pp823-829, 1995.

[2] V. Dietz, R. MuEller and G. Colombo, "Locomotor activity in spinal man: significance of afferent input from joint and load receptors". Brain, 125, pp2626-2634, 2002.

[3] G. Colombo, M. Wirz, and V. Dietz, "Driven gait orthosis for improvement of locomotor training in paraplegic patients". International medical society of paraplegia, Spinal Cord, 39, 252-255, 2001.

[4] Y. Shibata, S. Imai, T. Nobutomo, T. Miyoshi, and S.I Yamamoto, "Development of body weight support gait training system using antagonistic bi-articualar muscle model". 32nd Annual International Conference of the IEEE EMBS, Buenos Aires, Argentina, 2010.

[5] V. Salvucci, Oh Sehoon, Y. Hori, and Y. Kimura, "Disturbance rejection improvement in non-redundant robot arms using bi-articular actuators". Industrial Electronics (ISIE). IEEE Symp. pp. 2159~2164, 2011.

[6] M. Kumamoto, T. Oshima, and T. Fujikawa, "Control properties of two joint link mechanism equipped with mono and bi-articular actuators". Robot & Human Interactive Com., IEEE Proc. pp. 400~404, 2010.

[7] S. Shimizu, N. Momose, T. Oshima, and K. Koyanagi, "Development of robot leg which provided with the bi-articular actuator for training techniques of rehabilitation". Robot and Human Interactive Communication, IEEE Symp. pp. 921~926, 2009.

[8] David A. Winter, "Biomechanics and motor control of human movement". Fourth Edition, John Wiley & Sons, Inc., 2009.

[9] S. Balasubramanian, J. Ward, T. Sugar, and J. He, "Characterization of the dynamic properties of pneumatic muscle actuators". Proceedings of the 2007 IEEE 10th International Conferences on Rehabilitaion Robotics, June 12-15, Noordwijk, The Netherlands.

Advances in Manufacturing and Mechanical Engineering
10.4028/www.scientific.net/AMM.393

Development of Gait Training System Powered by Antagonistic Mono-and Bi-Articular Actuators Using Contraction Model Control Scheme
10.4028/www.scientific.net/AMM.393.525

Computed-torque method for the control of a 2 DOF orthosis actuated through pneumatic artificial muscles: a specific case for the rehabilitation of the lower limb.

Flavio Prattico*

Dipartimento di Ingegneria Industriale e dell'Informazione e di Economia, Università degli studi dell'Aquila, Italy

**Corresponding Author, flavioprattico@gmail.com, via G. Gronchi 18, 67100, L'Aquila, Italy*

Mohd Azuwan Mat Dzahir

Bio-Science and Engineering Department, Shibaura Institute of Technology, Japan

Shin-ichiroh Yamamoto

Bio-Science and Engineering Department, Shibaura Institute of Technology, Japan

Abstract

In this paper we give a new control model based on the so called computed-torque method for the control of a 2 degrees of freedom orthosis for the rehabilitation of the lower limb, the AIRGAIT exoskeleton's leg orthosis. The actuation of the AIRGAIT is made through self-made pneumatic muscles. For this reason this work starts with the static and dynamic characterization of our pneumatic muscles. The followed approach is based on the analytical description of the system. For this, we describe the pneumatic muscles behaviour with an easy-invertible polynomial fit function in order to model its non-linear trend. We give a geometrical model of the mechanical system to compute the length between the attachments of the pneumatic muscles to the structure for every angles assumed by the two joints. We evaluate through Newton-Euler equation the couples at the joints for each values of the angles. At last we show some validation tests in order to characterize the functioning of the proposed control model on the actuation of the orthosis.

Keywords: Computed-torque method, Pneumatic muscles, Newton-Euler, Lower limb rehabilitation system

1. Introduction

Pneumatic artificial muscles (PAMs) are often used for the actuation of rehabilitation devices or, more generally, in most application where there is the interaction between machines and humans [**?** **?** **?**]. In these devices, when the motion is not managed by a human, a control model is needed. In literature there are a lot of models for this purpose and applied to PMAs based actuations. The different approaches can be divided into two main groups: feedback linearization and computed-torque method [**?**]. In the first class can be group all the control models that work on the feedback of the measured control variable such as fuzzy [**?**], PID, Neural Network [**?**] or other models [**?** **?**]. Many of these control models were tested on 1 degree of freedom systems ([**?** **?**]) but recently many authors are working on more complex systems that can simulate well the human morphology of the arms or of the legs, then with 2 degrees of freedom, see [**?** **?** **?**].

The computed-torque method, instead, requires a complete description of the system and, if it has a high number of degrees of freedom, the formulation of the couple joint expression appears to be very difficult to solve. On the contrary, if the analytical description of the system is well-made, it will be faster to follow the inputs with respect to the other main control model class. In this paper we propose and use a model control based on the computed-torque method for the managing of our AIRGAIT orthosis for the rehabilitation of the lower limb [**?** **?** **?**].

The paper is organized as follow. In section 2 we give an overview on the AIRGAIT system. In section 3 we show the main characterization of our self-made PAMs. The control model with all its parts is described in section 4. Section 5 contains all the validation tests made on the system in order to verify the goodness of the control model. At last, in section 6 we give some concluding remarks.

2. Overview of AIRGAIT exoskeleton's leg orthosis

Figure 1 shows the AIRGAIT exoskeletons leg orthosis of the developed body weight support gait training system used for this research. The leg orthosis system implemented six PAM which antagonistically arranged based on the human musculoskeletal system (i.e., mono- and bi-articular muscles).

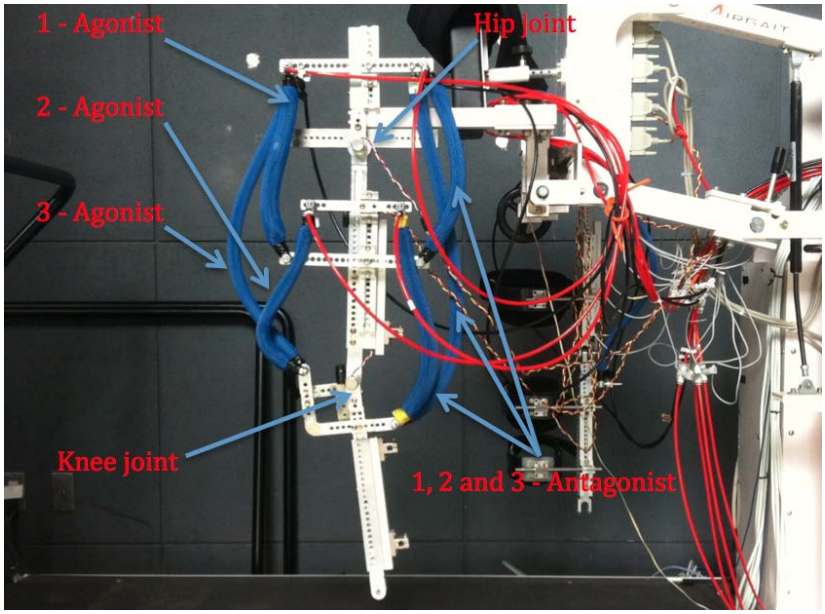

Figure 1: AIRGAIT exoskeletons leg orthosis

The PAM used in this research is a self fabricated McKibben artificial muscle actuator. The input pressure of the PAM is regulated by electro-pneumatic regulator separately for each actuator. The special characteristic of PAM will cause it to contract when the air pressure is supplied, and expand when the air pressure is removed. In other words, the PAM is able to emulate the force and muscle contraction of humans muscle. In addition, it is also might be able to perform similar contractions and expansions, where their movement is almost similar to the movements of the humans muscles. The measurement of the joint excursions (i.e., hip and knee) is made using potentiometer. This system uses the Lab-View software and RIO module to provide the input signals and to read the output data of the leg orthosis.

3. Pneumatic muscle characterization

The Mckibben PAM used for this study are built in our laboratory using commercial parts. For this reason we have to characterize them in order to understand and fix their properties and behaviours. We conduce two main kind of characterizations, one static and another dynamic. With the data collected by the first one we are able to model the non-linearity of the

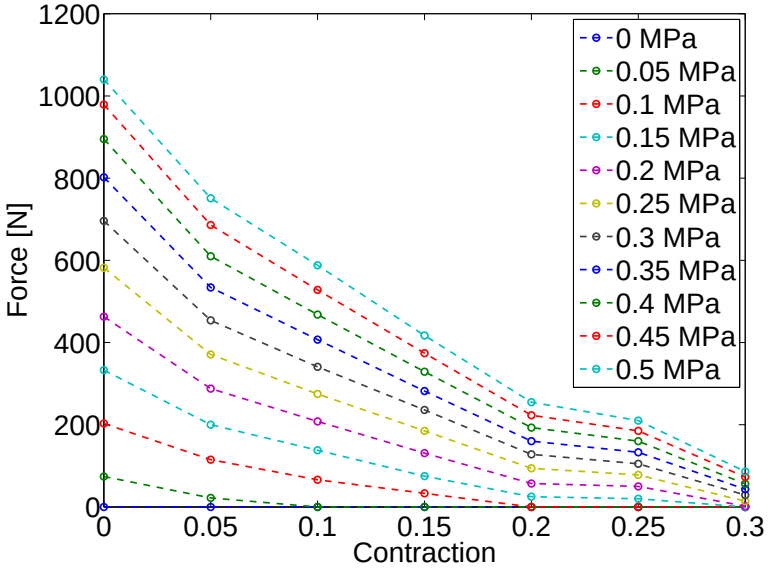

Figure 2: Static characterization of the PAM

PAM by fitting the data with a polynomial function. With the dynamic characterization instead, we can estimate *a priori* the error in position due to the hysteresis. The static characterization is conduced by setting the ends of the PAM at given positions in order to have a variation from 0 to the 30% of the contraction. This parameter is defined as the difference between the length of the muscle and the given position, divided by the length of the muscle, then:

$$k = \frac{l_m - l}{l_m} \tag{1}$$

Once the distance between the ends is fixed, we vary the pressure supply inside the PAM from 0 to 0.5 MPa and we record, through a load cell, the reaction force. The results of the described experiment are show in figure 2. It is possible to note in this figure that the main static properties of the PAM are very similar to those of the commercial PAM.

The dynamic characterization allow us to check the ability of the artificial muscle to follow dynamic signals. We conduce two dynamic experiments one with and one without loads. To conduce these experiments we fix the PAM only on one side, maintaining the other free or putting on a weight. We supply the muscle with a pressure signal going from zero to a setted value

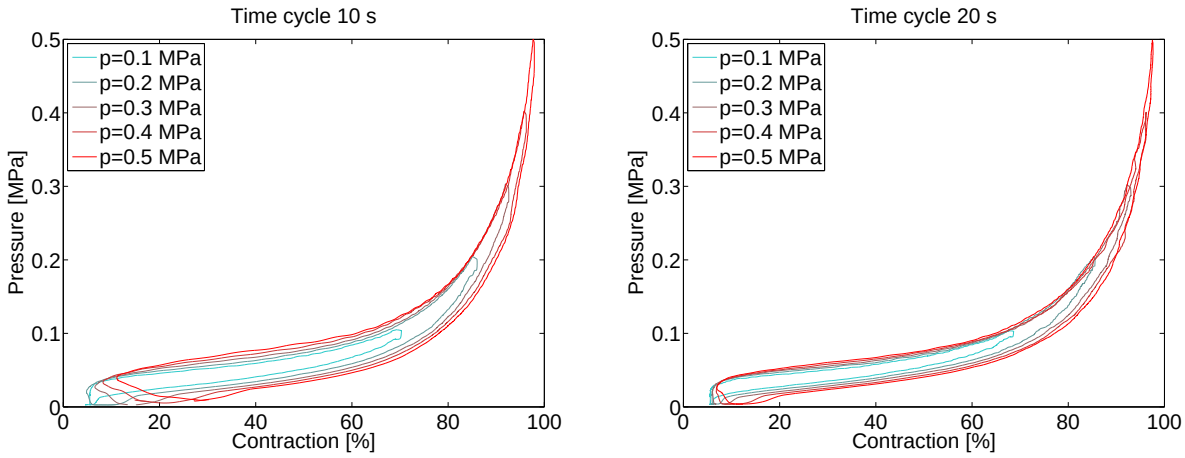

(a) (b)

Figure 3: Hysteresis characterization with different time cycle: 10 s (panel a) and 20 s (panel b).

and once again to zero. The setted we use for the experiments are 0.1, 0.2, 0.3, 0.4 and 0.5 MPa. The results of the experiment without loads is presented in figure 3. The left panel shows the hysteresis behaviour with a time cycle of 10 s. As it is possible to notice, for high values of the pressure 10 s are not enough to complete the loading-unloading cycle. On the right panel, instead, there are the hysteresis trends with a time cycle of 20 s. In this case, with all the values of the pressure, the cycle is completed.

Fixing the time cycle to 20 s, we conduce the same hysteresis characterization, then loading and unloading cycle, with different maximum pressures, but including a load on the muscle. We test it with 10 and 20 kg, that can be considered very high in comparison with the real loads that the system could be stressed. In figure 4, panel a there is the hysteresis behaviour with a load of 10 kg instead, in panel b that with 20 kg. The main interesting consideration can be made by comparing the results of figure 3 with those of figure 4 in terms of distance between the loading and unloading curves. Also with the presence of great load this distance remain almost constant confirming the goodness of these kind of actuation.

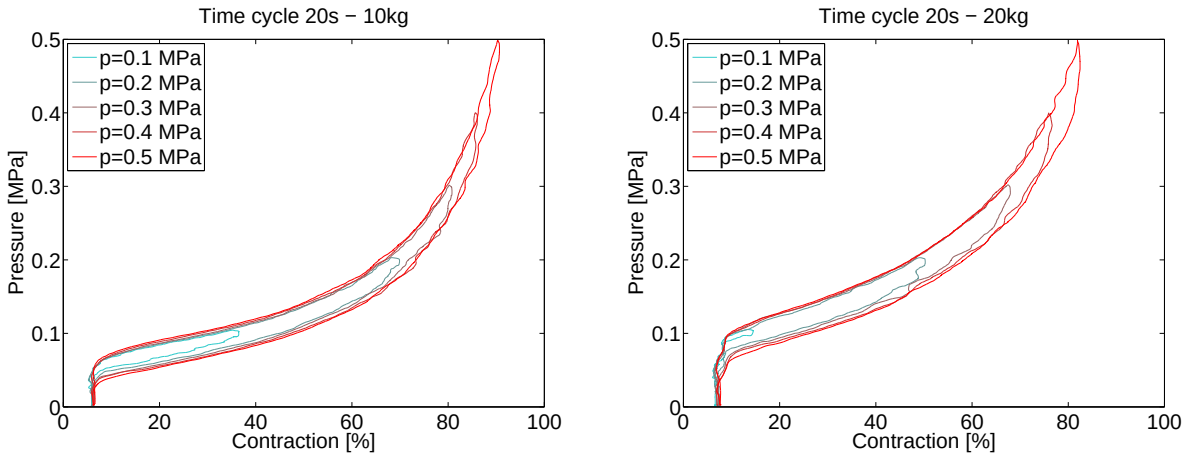

(a) (b)

Figure 4: Hysteresis characterization with a time cycle of 20 s and different loads: 10 kg (panel a) and 20 kg (panel b).

4. Control model and application to the orthosis

The control model, proposed in this paper, is based on the analytical description of the system and on the use of the so called computed-torque method. In this section we will show all the main components of the entire control model and the main idea at its basis.

4.1. Fitting model of the non-linear behaviour of the PAM

One of the most difficult problems to solve when we work with PAMs is the non-linear behaviour of the PAMs. The main task is to find, as made by [**?**], the force that the PAM can apply as a function of the supply pressure and of its contraction.

The data collected into the static characterization (see figure 2) will be here fit with a surface. We choose to fit the surface with a two variables polynomial function. We need to express the supply pressure as a function of the force and the contraction. To do this, the fitting equation must be solvable in the term of the pressure, then the term of the pressure must have a degree equal or less to two (different approach used in [**?**] in which the equation is fifth degree in both variables, then needs to solve numerically with long computing time). We then conduce a sensibility analysis on the degree of the fitting equation. Particularly we compute the Root Mean Square Error

Degree of x	Degree of y	RMSE [N]
1	1	116
2	1	53
2	2	31
2	3	21
2	4	19
1	2	43
1	3	32
1	4	29

Table 1: Sensibility analysis of the fitting curve of the experimental data as a function of the degrees of the polynomial surface

(RMSE) between the experimental point of Figure 2 and the fitting surface and we express the results as a function of the degrees of the two variables x and y (pressure and contraction). The results are summarized in the Table 1. As it is possible to notice we have a great reduction of the RMSE from first to second degree in x and, at the same time, we choose to have third degree in y. This choice is due to the fact that we do not have a great reduction of the RMSE between third and fourth degree in y and then we decide to reduce the number of the parameters to increase the computational speed.

The resulting fitting equation is the follow:

$$f(x,y) = a_1 + a_2x + a_3y + a_4x^2 + a_5xy + a_6y^2 + a_7x^2y + a_8xy^2 + a_9y^3 \quad (2)$$

where, as mentioned before, x represents the supply pressure, y is the contraction and $f(x,y)$ is the force. The numeric values of the parameters of this equation are shown in the Table 2.

At last, we show in figure 5 the equivalent polynomial surface with the experimental points coming from the characterization. As it is possible to notice from this figure, the equation fits well the real data.

4.2. Newton-Euler equation model

The crucial part of the proposed model is based on the computation of the couples for every angles assumed by the two joints. Here we follow the Newton-Euler approach in order to obtain an analytical formulation of the

Parameter	Value
a_1	-7
a_2	2384
a_3	-1135
a_4	-467
a_5	-12480
a_6	8682
a_7	4160
a_8	13290
a_9	-15960

Table 2: Numeric values of the parameters of the fitting polynomial equation

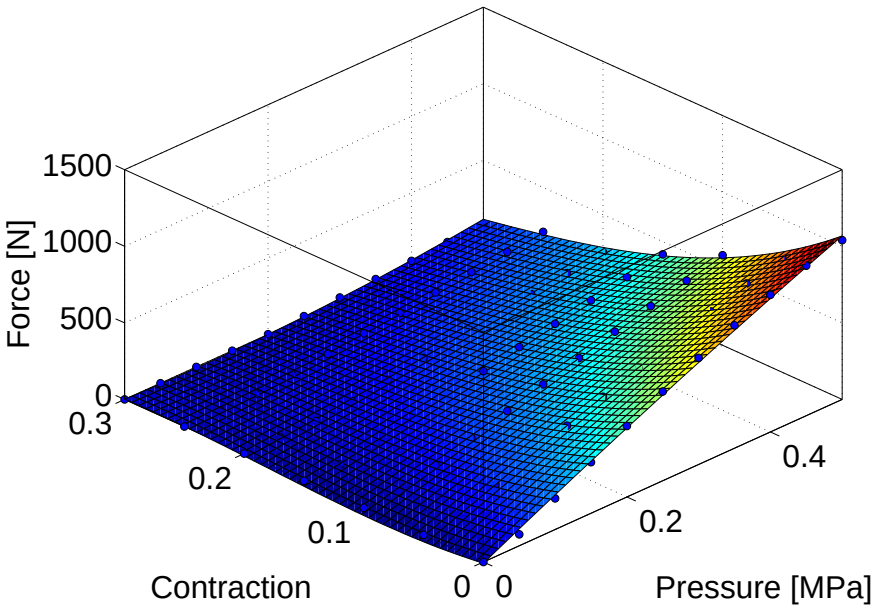

Figure 5: Graphic visualization of the fitting polynomial equation.The blue dot are the experimental points

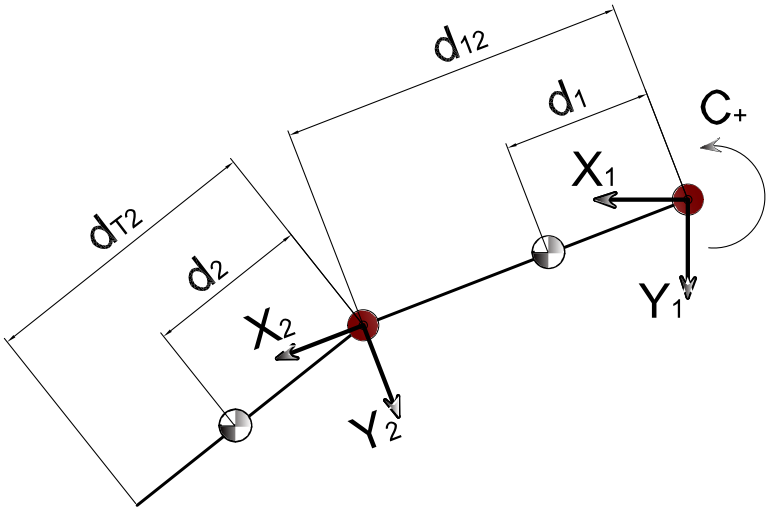

Figure 6

two couples. Just to remind and using a simplified formulation, we can model the dynamics of a robot with revolution joints by the follow equation:

$$M(q)\ddot{q} + C(q,\dot{q}) + g(q) = \tau \tag{3}$$

where $\ddot{q}$, $\dot{q}$ and q are respectively the vectors of joint positions, velocities and acceleration, $M(q)$ is the articulated robot inertia matrix, $C(q,\dot{q})$ is the vector of centripetal and Coriolis force, $g(q)$ is the vector of gravitational forces and τ is the vector of joint torque [**?**]. In figure 6 we give a schematic representation of the orthosis. In this figure d_1 and d_2 denote the distances between the joints and the centers of mass of the two links instead, d_{12} and d_{T2} are the lengths of the two links. Referring to figure 6, we can solve the equation 3, in order to find the couples of the two joints:

$$\begin{aligned} C_1 \;=\; & I_{11}\ddot{\theta}_1 + I_{22}\ddot{\theta}_1 + I_{22}\ddot{\theta}_2 + \ddot{\theta}_1 d_1^2 m_1 + \ddot{\theta}_1 d_2^2 m_2 + \ddot{\theta}_2 d_2^2 m_2 + \ddot{\theta}_1 d_{21}^2 m_2 + \\ & d_2\, g\, m_2 cos(\theta_1+\theta_2) + d_1\, g\, m_1 cos(\theta_1) + d_{21}\, g\, m_2 cos(\theta_1) - \\ & \dot{\theta}_2{}^2 d_2 d_{21} m_2 sin(\theta_2) + 2\ddot{\theta}_1 d_2 d_{21} m_2 cos(\theta_2) + \ddot{\theta}_2 d_2 d_{21} m_2 cos(\theta_2) - \\ & 2\dot{\theta}_1\dot{\theta}_2 d_2 d_{21} m_2 sin(\theta_2) \end{aligned}$$

$$\begin{aligned} C_2 \;=\; & I_{22}(\ddot{\theta}_1 + \ddot{\theta}_2) + d_2 m_2 (d_{21} sin(\theta_2)\dot{\theta}_1{}^2 + g\, cos(\theta_1+\theta_2) + d_2(\ddot{\theta}_1 + \ddot{\theta}_2) + \\ & \ddot{\theta}_1 d_{21} cos(\theta_2)) \end{aligned}$$

Parameter	Value
I_{11}	0.052 kgm^2
I_{22}	0.032 kgm^2
m_1	1.34 kg
m_2	0.97 kg
d_1	0.2 m
d_2	0.15 m
d_{21}	0.4 m
d_{T2}	0.37 m

Table 3: Numerical data of the orthosis geometry

where I is the inertia, m is the mass and g is the gravity acceleration. The equations of the two couples are obtained by a symbolic generation of large multibody system dynamic equations proposed in [**?**] and in [**?**].

In the table 3 are summarized the numerical data of the orthosis geometry.

4.3. Geometric description model

In this section we give the geometric model of the system. We have to describe the variation of the lengths between the ends of the PAMs during the functioning of the orthosis in order to derive the contraction through equation 1. Then, we have to find a relation between these lengths l_i, related to the muscle i, and the joints angles. As the system is made, we have to discern the two cases separately: mono- and bi-articular actuation. These are schematized in figure 7, mono-articular in panel a and bi-articular in panel b. Another distinction will be made for the two kind of muscle configurations (agonist and antagonist), these due just to the angles coordinate system.

For what concerns the mono-articular configuration (figure 7, panel a) we can describe the variation of the length of the muscle, defined as $\overline{AB}$, through the use of the law of cosine. Here we show the implementation for the mono-articular hip joint as a function of the angle θ_1, but the same formulation can be derived for the knee joint as a function of the angle θ_2.

$$\overline{AB} = \sqrt{\overline{AC}^2 + \overline{BC}^2 - 2\overline{AC} \cdot \overline{BC} cos(\alpha)} \tag{4}$$

where α, as mentioned before, will have different value for the two cases of

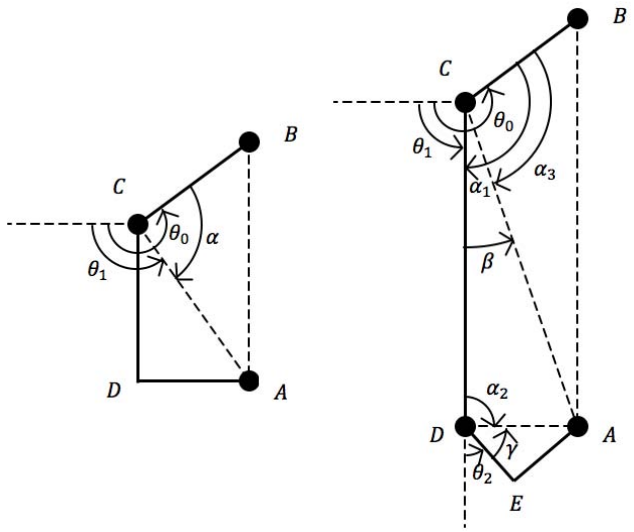

(a) (b)

Figure 7: Geometric scheme of the actuation. Panel a mono-articular, panel b bi-articular.

muscle configuration, then:

$$Agonist: \qquad \alpha = \theta_1 + \theta_0$$

$$Antagonist: \qquad \alpha = \theta_1 - \theta_0$$

where

$$\theta_0 = \alpha|_{\theta_1=0}$$

with these positions we can explicit, through the equation 1, the variation of the contraction as a function of the joint angle:

$$k(\theta_1) = k^{ag} = k^{ant} = \frac{l_m - \overline{AB}}{l_m} \tag{5}$$

where k^{ag} and k^{ant} are respectively the contraction of the agonist and antagonist muscles.

The formulation of the contraction of the muscles in the bi-articular actuation, instead, will be related to both angles. Referring to figure 7, panel b, we can explicit

$$\overline{AC} = \sqrt{\overline{AD}^2 + \overline{CD}^2 - 2\overline{AD} \cdot \overline{CD} cos(\alpha_2)} \tag{6}$$

where

$$\alpha_2 = \pi - \gamma - \theta_2$$

and γ is a static angle that can be measure manually on the orthosis. It is equal to 1.89 rad for the agonist side and 0.68 rad for the antagonist one.

$$\overline{AB} = \sqrt{\overline{AC}^2 + \overline{CB}^2 - 2\overline{AC} \cdot \overline{CB} cos(\alpha_3)} \tag{7}$$

where

$$\alpha_3 = \alpha_1 - \beta$$

with

$$\beta = acos\left(\frac{\overline{CD}^2 + \overline{AC}^2 - \overline{DA}^2}{2\overline{CD} \cdot \overline{AC}}\right) \tag{8}$$

and distinguishing for the two cases of muscle configurations, α_1 is equal to

$$Agonist: \qquad \alpha_1 = \theta_1 + \theta_0$$

$$Antagonist: \qquad \alpha_1 = \theta_1 - \theta_0$$

The contraction for the muscles in the bi-articular actuation can be now evaluated as

$$k(\theta_1, \theta_2) = k^{ag} = k^{ant} = \frac{l_m - \overline{AB}}{l_m} \tag{9}$$

4.4. Control Model

First of all, we can define the stiffness of a system as the measure of the resistance to the deformations. For our system this concept of stiffness translates itself into the level of the force of the antagonist muscle that we can call the "base force" (following a similar nomenclature proposed by [**?**]). In order to describe the control model we can set and define, as $R = cost$, the stiffness of the system that represents the force of the PAM that is working against the motion.

From the geometrical model we can find the contraction of the three pairs of muscles as a function of the angle θ_1 and/or θ_2, then:

$$k_1^{ag} = f(\theta_1) \quad and \quad k_1^{ant} = f(\theta_1) \tag{10}$$

$$k_2^{ag} = f(\theta_2) \quad and \quad k_2^{ant} = f(\theta_2) \tag{11}$$

$$k_3^{ag} = f(\theta_1, \theta_2) \quad and \quad k_3^{ant} = f(\theta_1, \theta_2) \tag{12}$$

where k_1^{ag} represents the contraction of the agonist muscle of the joint 1, instead k_2^{ant} is the contraction of the antagonist muscle of the joint 2. From the NE equations we can compute the couples C_1 and C_2 as follow:

$$C_1 = f(m_1, m_2, I_{11}, I_{22}, \theta_1, \theta_2, \dot{\theta}_1, \dot{\theta}_2, \ddot{\theta}_1, \ddot{\theta}_2) \tag{13}$$

$$C_2 = f(m_2, I_{22}, \theta_1, \theta_2, \dot{\theta}_1, \dot{\theta}_2, \ddot{\theta}_1, \ddot{\theta}_2) \tag{14}$$

but geometrically the couples C_1 and C_2 can be also computed as:

$$C_1 = (F_1^{ag} - F_1^{ant}) \cdot l_i \tag{15}$$

$$C_2 = (F_2^{ag} - F_2^{ant}) \cdot l_i \tag{16}$$

where l_i is the distance between the $i-th$ muscle force and the joint. When the orthosis is working, the couples could be both negative and positive. The two cases allow us to distinguish when the agonist or antagonist muscle has to work against the motion and be equal to R. For the negative couple case, for example, we can compute the two forces from the equations 15 and 16 as follow:

$$F_1^{ag} = \frac{C_1}{l} + R \tag{17}$$

$$F_2^{ag} = \frac{C_2}{l} + R \tag{18}$$

The last step of the model consists into solving the fit function of the PAM characterization. Then, using the follow positions

$$A = a_4 + a_7 y$$

$$B = a_2 + a_5 y + a_8 y^2$$

$$C = a_1 + a_3 y + a_6 y^2 + a_9 y^3 - f(x, y)$$

we can easily solve the equation 2, as

$$x = \frac{-B \pm \sqrt{B^2 - 4AC}}{2A} \tag{19}$$

and considering the physical meaning of x, y and $f(x, y)$, the equation can be summarize as $P = f(F, K)$. Then, known the force and the contraction of the muscle we can compute the required pressure.

In the figure 8 we give the schematic idea of the proposed control model.

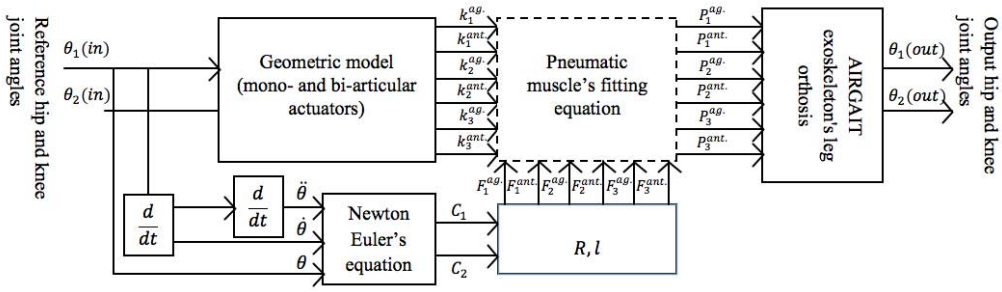

Figure 8: Block diagram of the proposed control model

5. Validation tests

In this section we show the results of the validation tests made on the orthosis controlled by the proposed model. We give, as first test, a sinusoidal trajectory to both angles varying its frequency. For the hip joint the sine trajectory has a mean value and an amplitude respectively equal to 1.57 and 0.4 rad. Instead, the sine wave, sent to the knee joint, has an amplitude and a mean value both equal to 0.4 rad. In figure 9 are shown the four cases that can be distinguish by the different frequencies of the sine wave that we vary from 0.05 to 1 Hz. Particularly here we show the cases of 0.05, 0.1, 0.5 and 1 Hz that corresponds to periods of 20, 10, 2 and 1 s. It can be noticed that also in the worst case of a frequency of 1 Hz the system presents a delay but continues to follow almost well the sine wave, with respect to the minimum and maximum values. Moreover we can say that at the frequency of 1 Hz corresponds a walking speed of 1.40 m/s that is the speed of a healthy person [**?**]. Instead for a person that needs of rehabilitation we can consider a speed less or equal to 0.7 m/s at which corresponds a frequency of 0.5 Hz.

Another important test is made by sending a squared signals to both joints. The parameters of the squared trajectories, in terms of mean value and amplitude, are the same of those sinusoidal. Here we just show the case of 0.5 Hz. The main scope of stressing the system with a squared wave is to see the response speed. In figure 10 we show this test and we can noticed that the system is very quick to follow the squared trajectory. Particularly the mean time, considering both the loading and unloading parts, to reach the input signal is equal to 0.1 s.

The last validation test is conduced by recording the hip and knee angles for a random walk and use them as input for the system. By varying the

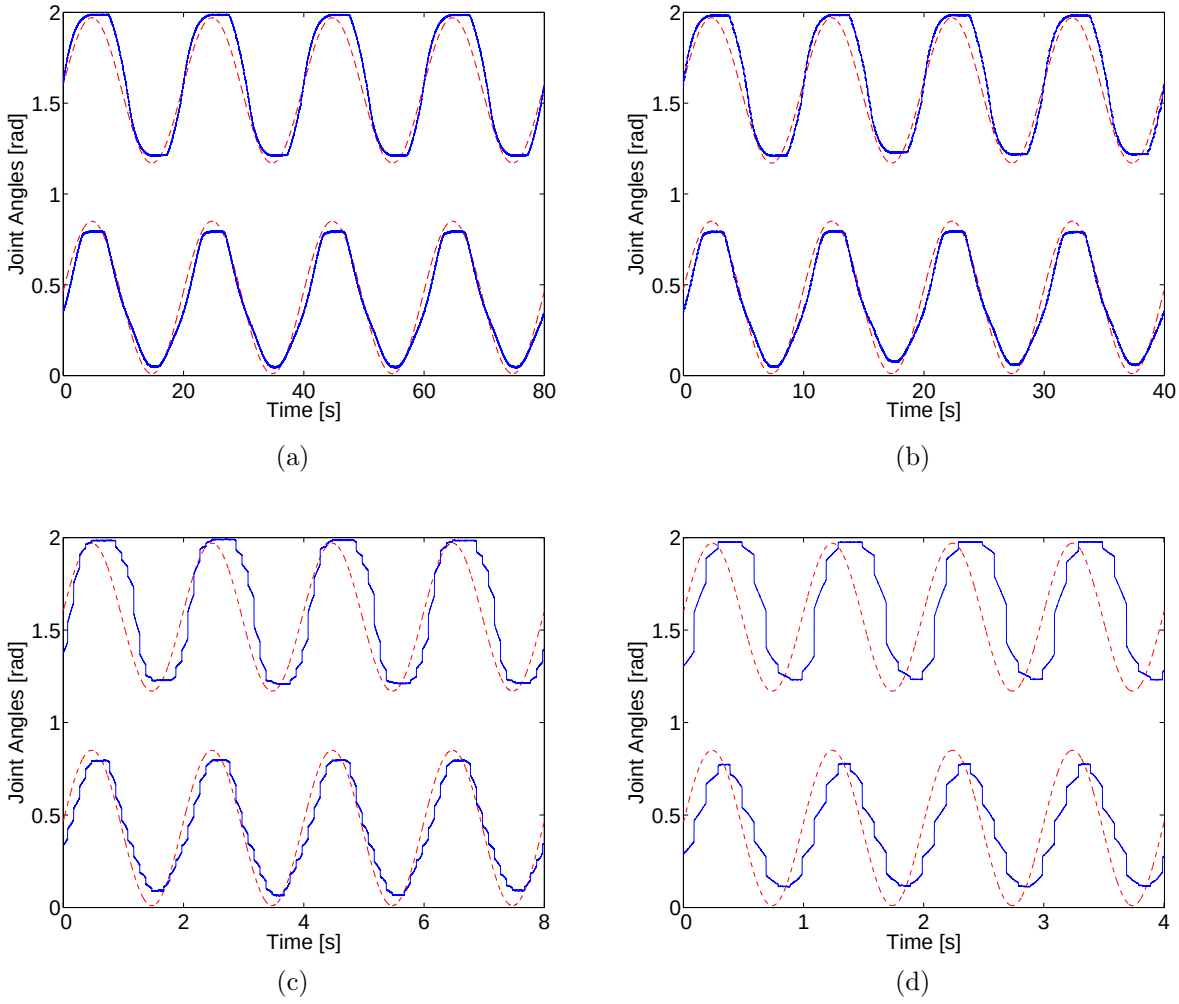

Figure 9: Sine trajectories test for different frequencies. Panel a - 0.05 Hz, panel b - 0.1 Hz, panel c - 0.5 Hz, panel d - 1 Hz. The red dashed line is the input signal and the blue continuous line is the measured angles assumed by the orthosis.

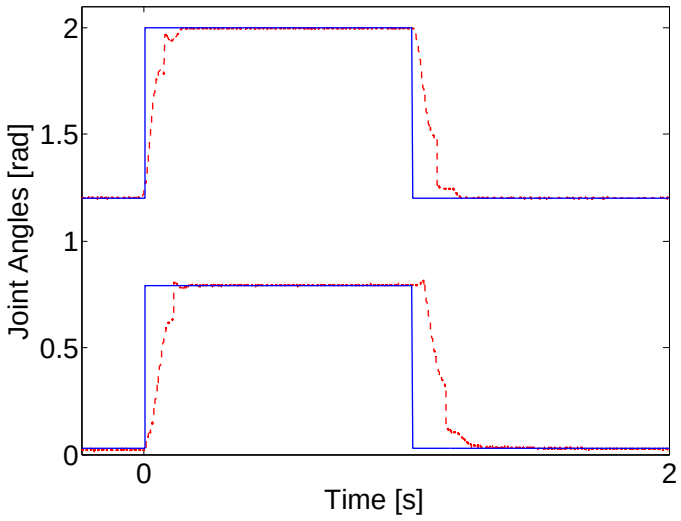

Figure 10: Squared trajectory test with a frequency of 0.5 Hz. The red dashed line is the input signal and the blue continuous line is the measured angles assumed by the orthosis.

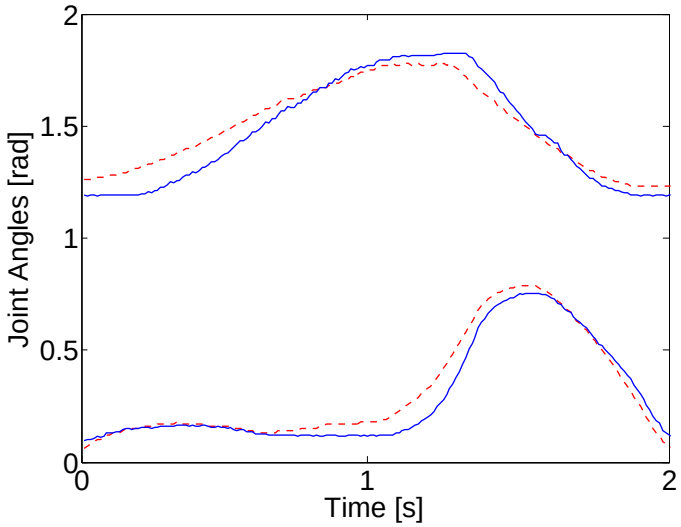

Figure 11: Real trajectories for the hip and knee angles for a random walk. The red dashed line is the input signal and the blue continuous line is the measured angles assumed by the orthosis.

time between the samples we can set easily the cycle speed. Here we show the worst case with a time period of 2 s. We can see, from figure 11 that the input signals are followed with a good accuracy, according to the previous validation tests.

The angles showed in figure 11 are used in figure 12 in order to verify if the system is able to follow a specific path with the end effector, in our case the ankle. We find the position of the ankle just using the equations of the double pendulum, giving the angles of the random walk. We can see in figure 12 that the path is well followed.

6. Discussion and conclusion

In this paper we continue the improvement of the control system for our AIRGAIT exoskeleton's leg orthosis. We introduce, with respect to the previous works, the effect of the dynamic components of the system by computing the couples of the joints with the use of the Newto-Euler equations. Moreover, we conduce different validation tests using sine, squared and true

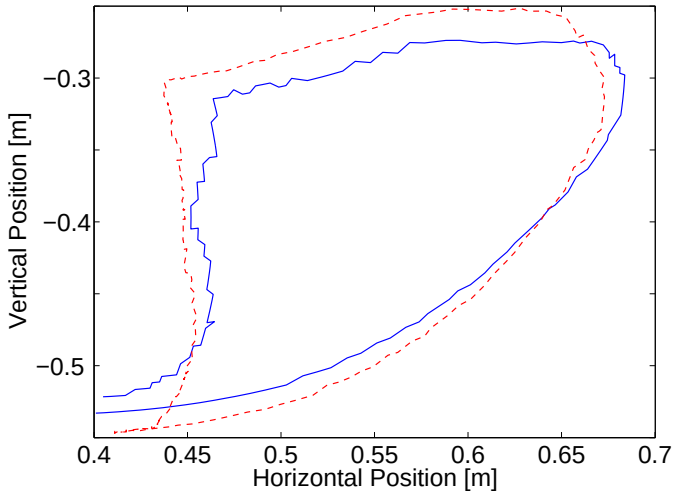

Figure 12: Ankle position path for a random walk. The red dashed line is the input signal and the blue continuous line is the real position assumed by the orthosis.

random walk trajectories. We show that for the specific purposes for what the orthosis is designed, the PAMs and the proposed control model catch the aim of our work. To the best of our knowledge we are the first on applying the computed-torque method on the control of a two degree of freedom orthosis actuated by PAMs. We show also that, even if there is no managing on the feedback, the proposed model has the advantage to allow the system to follow a given trajectory in a very quickly and with a great accuracy.

7. Acknowledgement

This work was supported by KAKENHI: Grant-in-Aid for Scientific Research (B) 21300202.

BRC2013 1569689277

Antagonistic Mono- and Bi-Articular Pneumatic Muscle Actuator Control for Gait Training System using Contraction Model

M.A. Mat Dzahir[a,b], T. Nobutomo[a], S.I. Yamamoto[a]

a) Bio-Science and Engineering
Shibaura Institute of Technology
Saitama, Japan
azuwan@fkm.utm.my

b) Faculty of Mechanical Engineering
Universiti Teknologi Malaysia
Johor, Malaysia
azuwan@fkm.utm.my

***Abstract*—in recent years, the use of the pneumatic muscle actuator (PMA) to acquire greater power from the actuation system especially for the development of medical rehabilitation robotic for gait training system has increased. Usually, the bi-articular actuators are treated as a redundancy in actuation since the number of actuators is greater than the number of joints. However, these actuators are able to generate a strong force due to wider range of motion compared to the mono-articular actuators and it is thought to generate instantaneous force. In the case of lower orthotic gait training system, the implementation of antagonistic bi-articular actuators along with mono-articular actuators plays a major role to achieve the required afferent input for the lower limb and hip joint as well as smooth and precise movements at the endpoint. One of the important characteristics of PMA is based on its muscle contraction. In this study, we modelled mathematical equations to determine the muscle contraction pattern for the antagonistic mono- and bi-articular PMAs as a function of the hip and knee angles in which its magnitude is influenced by the anterior and posterior muscle activation levels. From this model, we are able to determine the input pressure for each of the antagonistic mono- and bi-articular PMAs and then control the system using a feedback controller.**

Keywords—Mono-articular actuator, bi-articular actuator, pneumatic muscle actuator, contraction model, control system.

I. INTRODUCTION

The effect of body weight support treadmill training for incomplete spinal cord injured (SCI) patients has been reported in several previous studies since the 1990s. In those trainings, however, therapists must manually move both of the patient's paralyzed legs. Wernig et al. studied the manual training which is assisted by two physical therapy instructors to start with the training operation [1]. From the rehabilitation sessions, around 76% of patients with incomplete spinal cord injuries (total of 33 persons) were able to walk independently after the treadmill training with partial body weight support. For the therapists, this training process is physically difficult to be done for long periods of time. In the field of neuro-rehabilitation robotics, a driven gait orthosis (DGO) that can be used on patients with varying degrees of paresis or spasticity for a long time had been developed [3]. Dietz, et al. (2002) used this DGO on patients with incomplete SCI and suggested that the afferent input from lower limb and hip joints' movement are important for the activation of central pattern generator for locomotion training in SCI patients [2]. The newly developed Body Weight Support Gait Training System (AIRGAIT) for lower extremity orthotic patients which implemented McKibben pneumatic actuators (PMA) is a complex and non-linear system [7] [8]. In the previous study of AIRGAIT, it was not able to achieve high stiffness on the hip and knee joints by using mono-articular actuators alone. Those results were improved when they implemented antagonistic bi-articular actuators with constant pressure input of 0.025MPa. This suggest that the antagonistic bi-articular actuators plays a major role in achieving high muscle moment (flexion and extension) at hip joint and wide range of motion (flexion) at knee joint. V. Salvucci et al. mentioned that the performance of bi-articular actuators can be seen when it works in the presence of mono-articular actuators [11]. While, M. Kumamoto et al. stated that when a two-joint link mechanism was installed with an antagonistic pair of bi-articular actuators in addition to antagonistic pairs of mono-articular actuators, the two-joint link mechanism could demonstrate humanlike control properties at the endpoint [10]. In addition to this, S. Shimizu et al. also stated that the differences in characteristics of the output force and the stiffness at the endpoint of the leg depends on the presence or absence of bi-articular muscles [13]. The purpose of this study is to control the bi-articular actuators which involve both hip and knee joints. It is hard to control the bi-articular actuators using both hip and knee angles positional data. However, if we were able to find a concrete model which correlates the actuators with the positional data, we might be able to implement the bi-articular actuators with co-contraction movement into the system and simplify the control algorithm.

II. SYSTEM DESIGN

All the measurements for this study were based on the developed AIRGAIT system. Figure 1 shows the design of AIRGAIT's powered orthosis for SCI patients' rehabilitation. This model is controlled using a pair of anterior and posterior bi-articular actuators and two pairs of anterior and posterior mono-articular actuators which move in co-contraction movement. This muscle actuator works by using compressed air to expand and contract similar to the human muscle

principle. Air pressure is regulated from 0MPa to under 0.5MPa by six mechanical regulators. The pressure sensor and potentiometer is used for the feedback control system. With the aid of xPC target toolbox and Simulink, we applied a control program to the AIRGAIT system. A host PC and target PC is used to transfer the data to the AIRGAIT system.

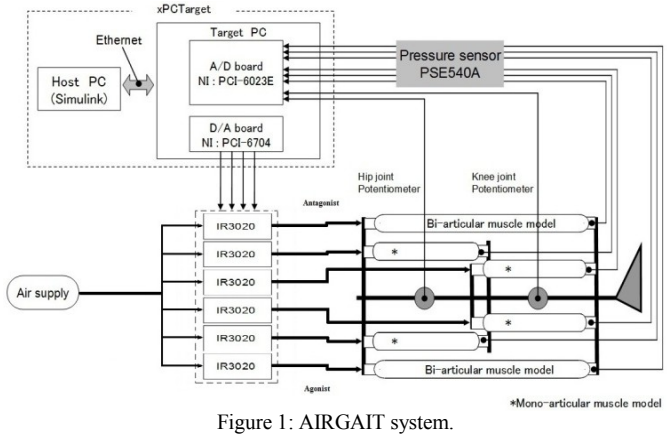

Figure 1: AIRGAIT system.

III. METHODS

We developed a contraction model using mathematical calculations to determine the contraction patterns of antagonistic mono- and bi-articular actuators from the positional data, then implementing it into the control system. Subject for the test is a healthy adult of 26 years old, weighs 65kg, and 173cm in height. Input for the control system is the hip and knee angles for walking motion [6]. The controller is tested for different gait cycle times (T = 5s, 4s, 3s, 2s, and 1s) for five cycles including the initial position cycle. The data is collected for a controller without a subject and with full body weight support (BWS) subject. Results were evaluated based on the maximum muscle moment (flexion and extension), output pattern, inertia, and time delay. For the test setup, an xPC target system and MATLAB Simulink are used for the control system software. The PMA used for this gait training system is a McKibben type muscle actuator with initial diameter of 25mm and initial length of 300mm, 450mm and 600mm. Six regulators are used to control the input pressure into the antagonistic mono- and bi-articular actuators, and the pressure is regulated from 0MPa to 0.5MPa.

IV. MATHEMATICAL MODELLING FOR CONTRACTION PATTERN

Mathematical model for the contraction patterns of antagonistic mono- and bi-articular actuators was developed based on the one link and two link leg manipulator models as can be seen in figure 2. Figure 2(a) shows the antagonistic mono-articular PMA model for hip joint, and 2(b) shows the antagonistic mono-articular PMA model for knee joint. One of the important characteristics of PMA is based on its muscle contraction (change in length). Based on the characteristics of muscle contraction for antagonistic mono- and bi-articular muscle actuators, we were able to determine the required input pressure for the actuators which enabled the system to move in a co-contraction movement. For the mathematical model, we consider the correlation between the change in length of the antagonistic actuators ($\Delta l_{ha}, \Delta l_{hp}, \Delta l_{ka}, \Delta l_{kp}$) and the change in arc length at the joints ($\Delta S_{hip}, \Delta S_{knee}$). Then we came up with one mathematical expression which correlates the antagonistic actuators contraction with positional data of hip angle (θ_h) and knee angle (θ_k), both for mono- and bi-articular actuators. Initial length for the actuators is defined as (l_o), and distance from the PMA joint to the joint (hip and knee) is r.

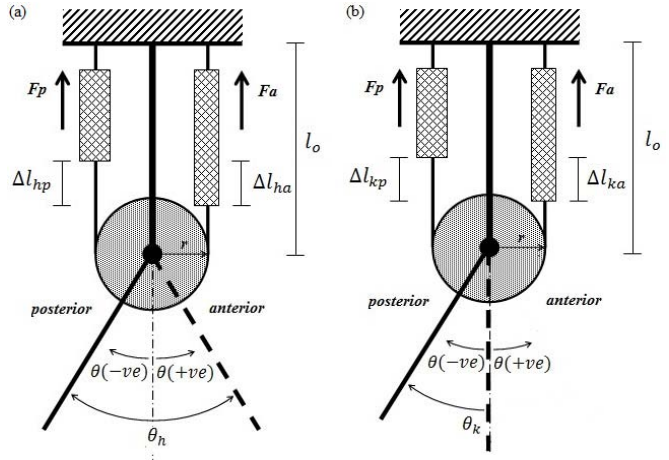

Figure 2: Antagonistic mono-articular PMA model for (a) hip joint, and (b) knee joint.

From the positional input data of hip and knee angles (see figure 3, 5 and 8), we can determine the locations of zero point value for anterior PMA muscle contraction at point (a), zero point value for posterior PMA muscle contraction at point (b) and zero point value for positional data of hip and knee angle at point (c). Point (a) shows the maximum muscle contraction for the anterior PMA and minimum muscle contraction for the posterior PMA. Point (b) shows the maximum muscle contraction for the posterior PMA and minimum muscle contraction for the anterior PMA. The activation levels for the posterior and anterior PMA (β and α) will determine its maximum muscle contraction, while the measurement of muscle contraction is based on its correlation with the positional input data (hip and knee angles).

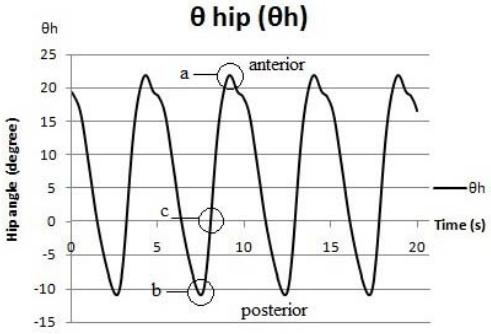

Figure 3: Positional input data of hip angle.

For a better understanding on the muscle contraction of antagonistic mono-articular PMA, the positional based data for the posterior and anterior is set to a positive value which can be seen in figure 4 and figure 6. These figures show the muscle contraction pattern for the antagonistic mono-articular PMA (posterior and anterior) with the maximum muscle contraction is less than 0.3 ($\varepsilon_{max} = 0.3$). From the kinematic analysis, it can be proved that the muscle contraction pattern for posterior $\varepsilon_p(t)$ and anterior $\varepsilon_a(t)$ follows the pattern of the positional data itself

but only differs according to the posterior and anterior muscle activation levels (β and α).

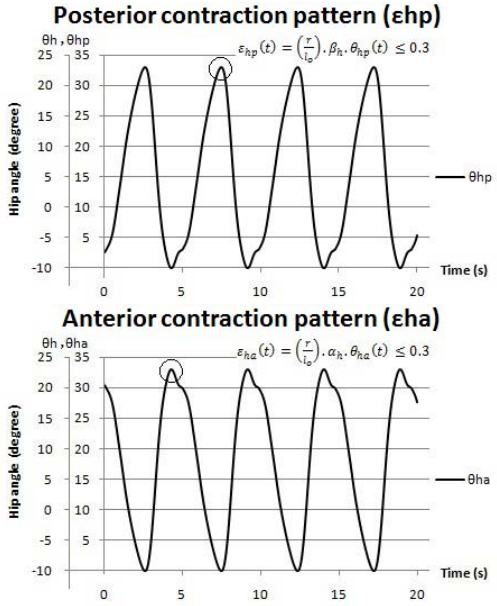

Figure 4: Muscle contraction pattern for the antagonistic mono-articular PMA (hip joint).

From the definition of the arc length (ΔS), the change in length (Δl) for a PMA is:

$$\Delta l = \Delta S = \theta . r \quad (1)$$

The muscle contractions of the antagonistic mono-articular actuators (ε_{hp} and ε_{ha}) for hip joint are defined using (1)

$$\Delta l_{hp} = \theta_{hp} . r$$
$$\varepsilon_{hp} = \frac{\Delta l_{hp}}{l_o} = \beta_h . \left(\frac{\theta_{hp} . r}{l_o}\right) \quad (2)$$
$$\Delta l_{ha} = \theta_{ha} . r$$
$$\varepsilon_{ha} = \frac{\Delta l_{ha}}{l_o} = \alpha_h . \left(\frac{\theta_{ha} . r}{l_o}\right) \quad (3)$$

Where θ_{hp} is the posterior PMA positional based data of hip joint, and θ_{ha} is for the anterior PMA as can be seen in figure 4. The muscle activation levels (β and α) are introduced to manipulate the gain of muscle actuators' contractions. We can determine the value of maximum activation level for actuators at maximum contraction point ($0 < \beta_h < \beta_{h(max)}$) and ($0 < \alpha_h < \alpha_{h(max)}$). The maximum contraction for posterior and anterior actuators are ($\varepsilon_{hp(max)} \leq 0.3$) and ($\varepsilon_{ha(max)} \leq 0.3$). Equation (2) and (3) can be defined as a time function as follows

$$\varepsilon_{hp}(t) = \left(\frac{r}{l_o}\right) . \beta_h . \theta_{hp}(t) \leq 0.3 \quad (4)$$
$$\varepsilon_{hp(\max)} = \left(\frac{r}{l_o}\right) \beta_{h(max)} . \left|\theta_{hp}(t)\right|_{max} = 0.3$$
$$\beta_{h(max)} = 0.3 \left[\frac{l_o}{r . \left|\theta_{hp}(t)\right|_{max}}\right]$$
$$\varepsilon_{ha}(t) = \left(\frac{r}{l_o}\right) . \alpha_h . \theta_{ha}(t) \leq 0.3 \quad (5)$$
$$\varepsilon_{ha(max)} = \left(\frac{r}{l_o}\right) \alpha_{h(max)} . \left|\theta_{ha}(t)\right|_{max} = 0.3$$
$$\alpha_{h(max)} = 0.3 \left[\frac{l_o}{r . \left|\theta_{ha}(t)\right|_{max}}\right]$$

Where: ε_{hp} is the posterior muscle contraction of mono-articular PMA for hip joint, ε_{ha} is the anterior muscle contraction of mono-articular PMA for hip joint, β_h is the activation level of posterior muscle contraction ε_{hp} for hip joint, α_h is the activation level of anterior muscle contraction ε_{ha} for hip joint.

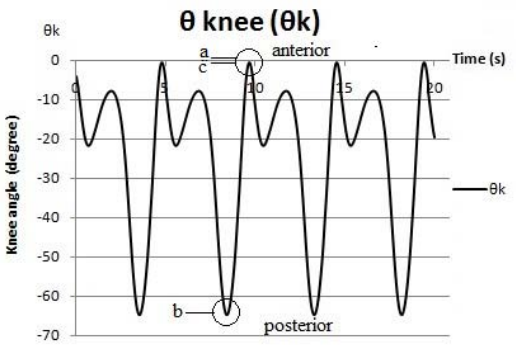

Figure 5: Positional input data of knee angle.

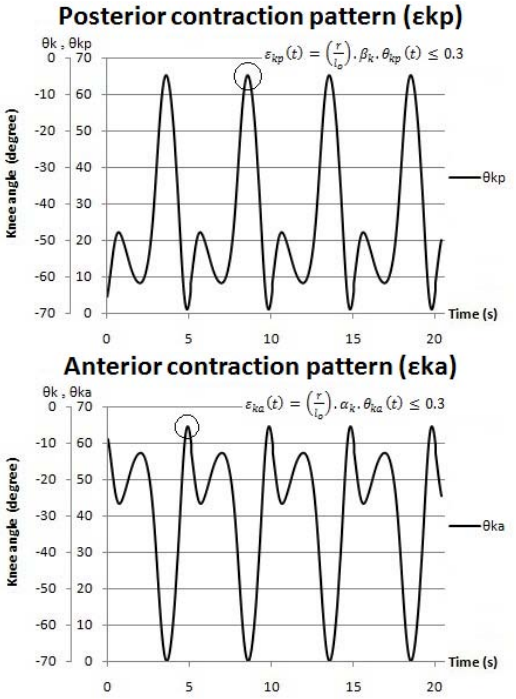

Figure 6: Muscle contraction pattern for the antagonistic mono-articular PMA (knee joint).

The muscle contractions of the antagonistic mono-articular (posterior and anterior) PMAs for knee joint are

$$\Delta l_{kp} = \theta_{kp} . r$$
$$\varepsilon_{kp} = \frac{\Delta l_{kp}}{l_o} = \beta_k . \left(\frac{\theta_{kp} . r}{l_o}\right) \quad (6)$$
$$\Delta l_{ka} = \theta_{ka} . r$$
$$\varepsilon_{ka} = \frac{\Delta l_{ka}}{l_o} = \alpha_k . \left(\frac{\theta_{ka} . r}{l_o}\right) \quad (7)$$

Where θ_{kp} is the posterior PMA positional based data of knee joint, and θ_{ka} is for the anterior PMA as can be seen in figure 6. Maximum muscle activation levels for antagonistic mono-articular actuators of knee joint is ranged from ($0 < \beta_k < \beta_{k(max)}$) and ($0 < \alpha_k < \alpha_{k(max)}$). While, the maximum contractions it can achieve are ($\varepsilon_{kp(max)} \leq 0.3$) and ($\varepsilon_{ka(max)} \leq$

0.3). Equation (6) and (7) can be defined as a time function as follows

$$\varepsilon_{kp}(t) = \left(\frac{r}{l_o}\right).\beta_k.\theta_{kp}(t) \le 0.3 \quad (8)$$

$$\varepsilon_{kp(\max)} = \left(\frac{r}{l_o}\right)\beta_{k(max)}.\left|\theta_{kp}(t)\right|_{max} = 0.3$$

$$\beta_{k(max)} = 0.3\left[\frac{l_o}{r.\left|\theta_{kp}(t)\right|_{max}}\right]$$

$$\varepsilon_{ka}(t) = \left(\frac{r}{l_o}\right).\alpha_k.\theta_{ka}(t) \le 0.3 \quad (9)$$

$$\varepsilon_{ka(max)} = \left(\frac{r}{l_o}\right)\alpha_{k(max)}.\left|\theta_{ka}(t)\right|_{max} = 0.3$$

$$\alpha_{k(max)} = 0.3\left[\frac{l_o}{r.\left|\theta_{ka}(t)\right|_{max}}\right]$$

Where: ε_{kp} is the posterior muscle contraction of mono-articular PMA for knee joint, ε_{ka} is the anterior muscle contraction of mono-articular PMA for knee joint, β_k is the activation level of posterior muscle contraction ε_{kp} for knee joint, α_k is the activation level of anterior muscle contraction ε_{ka} for knee joint.

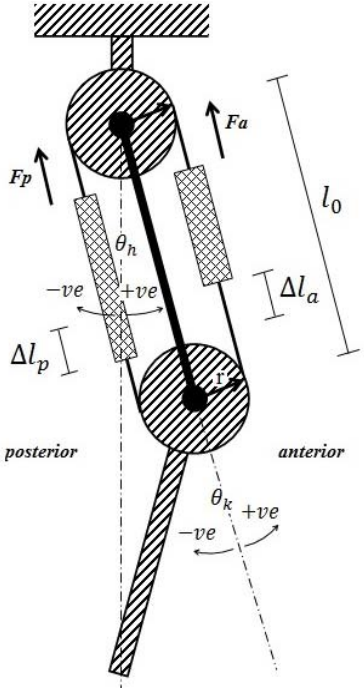

Figure 7: Antagonistic bi-articular PMA model for two link leg manipulators.

Figure 7 shows the antagonistic bi-articular PMA model for two-link manipulators. Similar with the mono-articular PMA models, we can also determine the locations of the zero point value as well as the maximum and minimum muscle contraction points for the posterior and anterior bi-articular PMAs (see figure 8). The positional based data for bi-articular PMAs are defined as a pattern of total hip and knee angles ($\theta_h + \theta_k$). Point (a) shows the maximum muscle contraction for the anterior PMA and minimum muscle contraction for the posterior PMA, while point (b) shows the maximum muscle contraction for the posterior PMA and minimum muscle contraction for the anterior PMA. The activation levels for the posterior and anterior PMAs, (β_{bi} and α_{bi}) determines the bi-articular PMAs' muscle contractions, while the measurement of muscle contractions are based on its correlation with the positional input data (hip and knee angles).

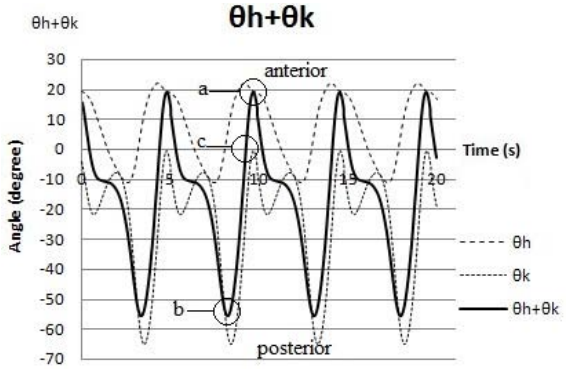

Figure 8: Positional based data for bi-articular PMA (pattern of total hip and knee angles).

For a better understanding of the muscle contraction for antagonistic bi-articular actuators, the positional based data for the posterior and anterior are set to a positive value as can be seen in figure 9. This figure shows the muscle contraction pattern for the antagonistic bi-articular actuators with the maximum muscle contractions are less than 0.3 ($\varepsilon_{max} = 0.3$).

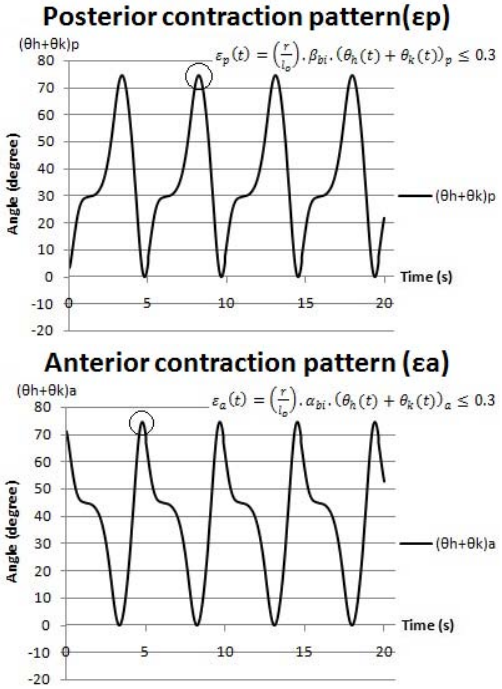

Figure 9: Muscle contraction pattern for the antagonistic bi-articular PMA.

Relative muscle contractions for the antagonistic bi-articular (posterior and anterior) PMAs of two link leg manipulators are

$$\Delta l_p = (\Delta l_h + \Delta l_k)_p$$

$$\Delta l_p = (\theta_h.r + \theta_k.r)_p$$

$$\varepsilon_p = \frac{\Delta l_p}{l_o} = \beta_{bi}.\left[\frac{(\theta_h.r+\theta_k.r)_p}{l_o}\right] \quad (10)$$

$$\Delta l_a = (\Delta l_h + \Delta l_k)_a$$

$$\Delta l_a = (\theta_h.r + \theta_k.r)_a$$

$$\varepsilon_a = \frac{\Delta l_a}{l_o} = \alpha_{bi}.\left[\frac{(\theta_h.r+\theta_k.r)_a}{l_o}\right] \quad (11)$$

Maximum muscle contraction condition also can be applied for the antagonistic bi-articular actuators, with maximum

activation levels of ($0 < \beta_{bi} < \beta_{bi(max)}$) and ($0 < \alpha_{bi} < \alpha_{bi(max)}$). The maximum contractions they can achieve are ($\varepsilon_{p(max)} \leq 0.3$) and ($\varepsilon_{a(max)} \leq 0.3$). Equation (10) and (11) can be defined as a time function as follows

$$\varepsilon_p(t) = \left(\frac{r}{l_o}\right).\beta_{bi}.(\theta_h(t) + \theta_k(t))_p \leq 0.3 \quad (12)$$

$$\varepsilon_{p(max)} = \left(\frac{r}{l_o}\right).\beta_{bi(max)}.\left|(\theta_h(t) + \theta_k(t))_p\right|_{max} = 0.3$$

$$\beta_{bi(max)} = 0.3\left[\frac{l_o}{r.\left|(\theta_h(t)+\theta_k(t))_p\right|_{max}}\right]$$

$$\varepsilon_a(t) = \left(\frac{r}{l_o}\right).\alpha_{bi}.(\theta_h(t) + \theta_k(t))_a \leq 0.3 \quad (13)$$

$$\varepsilon_{a(max)} = \left(\frac{r}{l_o}\right).\alpha_{bi(max)}.\left|(\theta_h(t) + \theta_k(t))_a\right|_{max} = 0.3$$

$$\alpha_{bi(max)} = 0.3\left[\frac{l_o}{r.\left|(\theta_h(t)+\theta_k(t))_a\right|_{max}}\right]$$

Where: ε_p is the posterior muscle contraction of bi-articular PMA for knee joint, ε_a is the anterior muscle contraction of bi-articular PMA for knee joint, β_{bi} is the activation level of posterior muscle contraction (ε_p), α_{bi} is the activation level of anterior muscle contraction (ε_a).

V. CONTROL SYSTEM

The reference input used for this system is the positional data of hip and knee angles which is referred from (Winter, 2009) and validated in the test [6]. The output we want to obtain from the system are the positional output data of hip and knee angles. However, the input data required for the antagonistic mono and bi-articular actuators of hip and knee joints are not the positional data, but it is the pressure input data which is in a correlation of hip and knee angles. Based on the control system, an error from the positional data is different with an error from the posterior and anterior actuators' input data (pressure). This positional error contributes in manipulating the gain of the input pressure due to the PMA's nonlinearity, not the correction of the input pressure pattern. Therefore, we implement the developed contraction model into the system to measure the required input pressure based on the estimated contraction pattern. The value of the muscle activation levels for posterior (β) and anterior (α) is determined using the heuristic method. For this controller scheme, we are controlling the contraction pattern of the antagonistic mono- and bi-articular actuators which are in correlation of hip and knee angles instead of controlling the hip and knee angles' values. Then, the PI feedback controller is used to manipulate the gain of the contraction model due to the PMA nonlinearity. Figure 10 shows the schematic diagram for the developed controller based on the contraction model. An angle of θ represents the positional input data which is the hip angle (θ_h), knee angle (θ_k), and the total of hip and knee angles ($\theta_h + \theta_k$). The positional output data is defined as (θ_o). The angle $\theta(+)$ represents the contraction patterns for the antagonistic mono- and bi-articular PMAs which is defined as a positive value of the positional data. The equation to change the positional data into the contraction model with a positive value is defined as G_a and G_b. A PI controller is used to manipulate the correction value for the input pressure (ev_i) using the positional error data. Input pressure is defined as (v_i), while (v_p) is the input pressure after the correction due to the PMA nonlinearity.

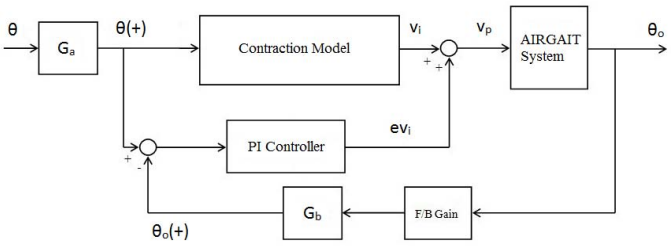

Figure 10: Schematic diagram of controller based on contraction model.

VI. RESULTS AND DISCUSSIONS

Based on the developed equations, it shows that the position of actuators to the joints, (r) and initial length, (l_o) does not affect the muscle contraction patterns. The study shows that the muscle contraction patterns of posterior and anterior actuators follows the pattern given by the positional data itself which only differs in gain value based on the posterior and anterior muscle activation levels (β and α). Figure 11 shows the results for the hip and knee angle controls with different gait cycle (T = 5s, 4s, 3s, 2s, and 1s) using the contraction model controller scheme. From the results, it shows that for gait cycle of 5 and 4 seconds, the gait training system were able to perform smooth movement without extended movement and time delay, both with and without full BWS subject tests. For the knee angle control, the controller was able to follow the heel contact position accurately and was able to achieve maximum angle extension of 60˚ at knee joint. However, due to an error of -3º, maximum angle for anterior and posterior of hip angle control was not achieved. For the 3 seconds gait cycle, inertia effect occurred during the test without subject at the hip joint and heel contact position of the knee joint. However, the system still was able to follow the pattern given by the hip and knee angle without time delay. It managed to perform good control at the knee joint both with and without full BWS subject, but maintains the -3º error at the posterior side of hip joint. For the 2 seconds gait cycle, the system managed to perform hip and knee angle patterns, but with extended the movement (due to inertia effect) of +3º and 0.15 seconds time delay on the anterior side of the hip joint. Even with the 0.15 seconds time delay, the system was able to perform the heel contact position at the knee joint. As for the 1 second gait cycle, the result shows that there is inertia effect which caused the anterior side of hip joint to extend to +5º, 0.2 seconds time delay, and the system was not able to perform heel contact movement perfectly due to the time delay. However, it was able to imitate the walking motion. This result shows that, the addition of bi-articular PMA in the presence of mono-articular PMA was able to give good control performance and smooth movement at the knee joint. The contraction model which enables the anterior and posterior PMAs to move in a co-contraction movement in the control system also plays a major role in ensuring the precise movement at the knee joint. These factors also apply for the performance at the hip joint, which gave good control performance for the test without subject. However, for the test with full BWS subject, we are not able to achieve the maximum angle extension due to the high moment required at the hip joint with an error of ±3º. This requires for a much bigger PMA for the mono-articular actuators at the hip joint.

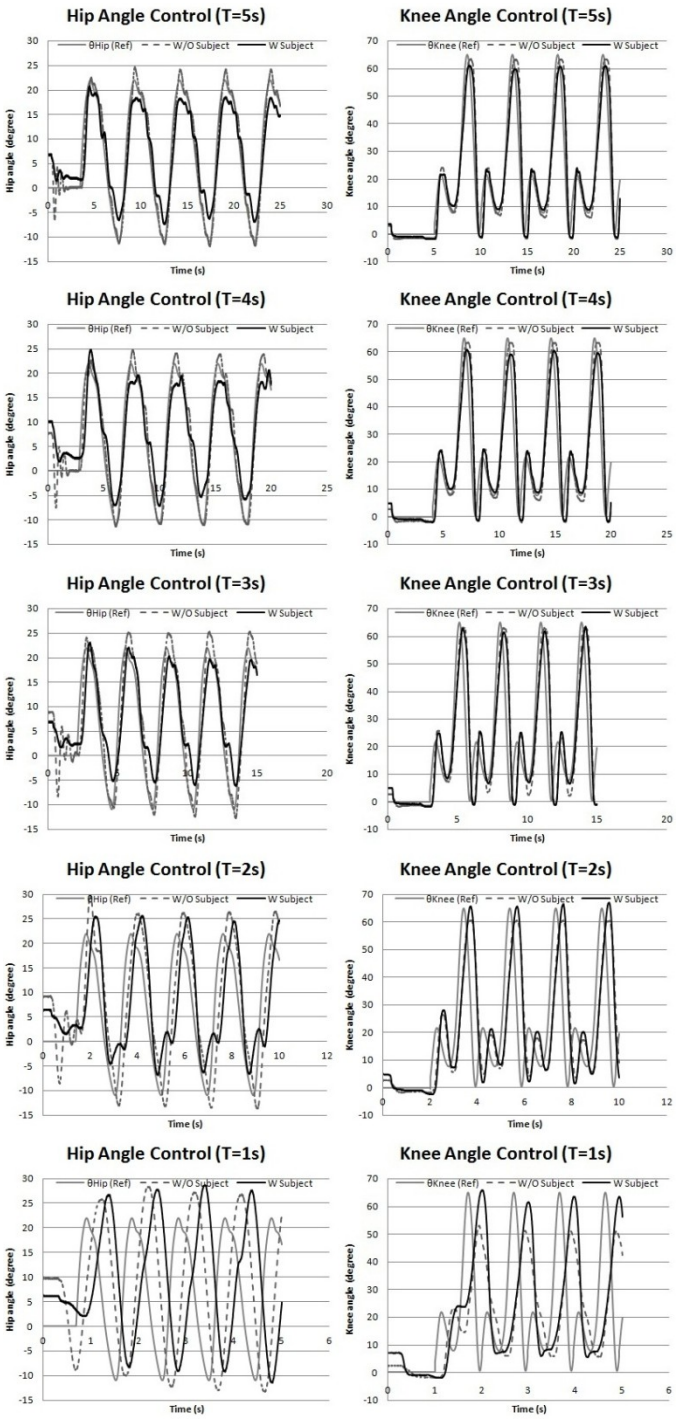

Figure 11: Hip and knee angle controls with different gait cycle.

VII. CONCLUSION

In a rehabilitation exercise, we try to perform the natural walking speed of a human being which is a gait cycle of (T ≈ 1.25s/cycle) to obtain a better result. This requires a good control system. By implementing this controller based contraction model, the gait training system was able to follow the human walking motion with little inertia effect and time delay up to 2 seconds gait cycle time. From the results, it shows that the addition of bi-articular PMAs in the presence of mono-articular PMAs was able to give good control performance and smooth movement at the knee joint. The developed contraction model also enables the anterior and posterior PMAs to move in a co-contraction movement in the control system which plays a major role in ensuring the precise movement at the joints. These factors also apply for the performance at the hip joint, which gave good control performance for the test without the subject. However, for the test with full BWS subject, we are not able to achieve maximum angle extension due to the high moment required at the hip joint with an error of ±3º. For the improvement of the gait training system, the addition of intelligent controllers such as adaptive and neural network controller is needed. This study will contribute to the control system for the PMA as well as the gait training system for rehabilitation.

ACKNOWLEDGMENT

This work was supported by KAKENHI: Grant-in-Aid for Scientific Research (B) 21300202

REFERENCES

[1] A. Wernig, S. Muller, A. Nanassy, and E. Cagol, “Laufband therapy based on 'rules of spinal locomotion' is effective in spinal cord injured persons”. Eur J Neurosci vol. 7, pp823-829, 1995.

[2] V. Dietz, R. MuEller and G. Colombo, “Locomotor activity in spinal man: significance of afferent input from joint and load receptors”. Brain, 125, pp2626-2634, 2002.

[3] G. Colombo, M. Wirz, and V. Dietz, “Driven gait orthosis for improvement of locomotor training in paraplegic patients”. International medical society of paraplegia, Spinal Cord, 39, 252-255, 2001.

[4] Varonov A.V, “the roles of mono-articular and bi-articular muscles of the lower limbs in terrestrial locomotion”. Human Physiology, Vol. 30, No. 4, pp. 476-484, 2003.

[5] Renato Grasso, Y.P. Ivanenko, Myrka Zago, M. Molinari, and G. Scivoletto, “Distributed plasticity of locomotors pattern generators in spinal cord injury patients”. Brain, 127, pp. 1019~1034, 2004.

[6] David A. Winter, “Biomechanics and motor control of human movement”. Fourth Edition, John Wiley & Sons, Inc., 2009.

[7] Y. Shibata, S. Imai, T. Nobutomo, T. Miyoshi, and S.I Yamamoto, “Development of body weight support gait training system using antagonistic bi-articualar muscle model”. 32nd Annual International Conference of the IEEE EMBS, Buenos Aires, Argentina, 2010.

[8] S.I Yamamoto, Y. Shibata, S. Imai, T. Nobutomo, and T. Miyoshi, “Development of gait training system powered by pneumatic actuator like human musculoskeletal system”. IEEE International Conference on Rehabilitation Robotics, Rehab Week Zurich, ETH Zurich Science City, Switzerland, 2011.

[9] M. Kumamoto, T. Oshima, and T. Fujikawa, “Bi-articular muscle as a principle keyword for Biomimetric motor link system”. Microtechnologies in Medicine & Biology 2nd Annual International IEEE-EMB Special Topic Conference on, pp 346–351, 2002.

[10] M. Kumamoto, T. Oshima, and T. Fujikawa, “Control properties of two joint link mechanism equipped with mono and bi-articular actuators”. Robot & Human Interactive Com., IEEE Proc. pp. 400~404, 2010.

[11] V. Salvucci, Oh Sehoon, Y. Hori, and Y. Kimura, “Disturbance rejection improvement in non-redundant robot arms using bi-articular actuators”. Industrial Electronics (ISIE). IEEE Symp. pp. 2159~2164, 2011.

[12] V. Salvucci, Oh Sehoon, and Y. Hori, “Infinity norm approach for precise force control of manipulators driven by bi-articular actuators”. IECON, IEEE Proc. pp. 1908~1913, 2010.

[13] S. Shimizu, N. Momose, T. Oshima, and K. Koyanagi, “Development of robot leg which provided with the bi-articular actuator for training techniques of rehabilitation”. Robot and Human Interactive Communication, IEEE Symp. pp. 921~926, 2009.

35th Annual International Conference of the IEEE EMBS
Osaka, Japan, 3 - 7 July, 2013

Development of Body Weight Support Gait Training System using Pneumatic McKibben Actuators ~Control of Lower Extremity Orthosis~ *

M.A. Mat Dzahir, T. Nobutomo, and S.I. Yamamoto, *Member, IEEE*

Abstract— **Recently, robot assisted therapy devices are increasingly used for spinal cord injury (SCI) rehabilitation in assisting handicapped patients to regain their impaired movements. Assistive robotic systems may not be able to cure or fully compensate impairments, but it should be able to assist certain impaired functions and ease movements. In this study, the control system of lower extremity orthosis for the body weight support gait training system which implements pneumatic artificial muscle (PAM) is proposed. The hip and knee joint angles of the gait orthosis system are controlled based on the PAM coordinates information from the simulation. This information provides the contraction data for the mono- and bi-articular PAMs that are arranged as posterior and anterior actuators to simulate the human walking motion. The proposed control system estimates the actuators' contraction as a function of hip and knee joint angles. Based on the contraction model obtained, input pressures for each actuators are measured. The control system are performed at different gait cycles and two PMA settings for the mono- and bi-articular actuators are evaluated in this research. The results showed that the system was able to achieve the maximum muscle moment at the joints, and able to perform the heel contact movement. This explained that the antagonistic mono- and bi-articular actuators worked effectively.**

Keywords—Mono-articular actuators, bi-articular actuators, pneumatic artificial muscle, and contraction model based controller.

I. Introduction

The needs for the medical and rehabilitation technology were increased with the increase numbers of old people and decrease numbers of young labors. Furthermore, lack of people's welfare places also contribute for the needs of medical and rehabilitation technology. These facilities are essential to lessen the burdens for the doctors. Moreover, it's also eases the handicap people, old people and helpers physically and mentally. This research focuses on the control system for legs orthosis of the developed Body Weight Support Gait Training System [1, 2]. This system aims was the assistive rehabilitation gait training for the spinal cord injury (SCI) patient that suffer the lower limb disability either one side or both side of their legs. The developed system was implemented PAM actuators and has a complex and non-linear system. However, its control system which implemented proportional directional control valve was rather poor.

Based on the previous researches, it is possible to use a standard PID controller in a feedback loop to control the joints' angle of the assistive robotic towards their desired values. Nevertheless, without additional model or integrated controller, it is not able to control compliant robots accurately due to the complex and highly nonlinear dynamics of the PMA, thus the resulting position was rather poor. There are lots of established controller design which are used to control this muscle actuator such as; Caldwell (1993~1995), tested a feed forward PID regulator and developed an adaptive controller for the pneumatic artificial muscle (PAM) manipulator; Repperger (1999) handled the nonlinear factor with a nonlinear feedback controller using a gain scheduling method; Tondu, and Lopez (2000) employed sliding-mode control approach; Folgheraiter (2003) developed an adaptive controller based on the neural network for the artificial hand; Balasubramanian, and Rattan (2003) proposed feed forward control of a nonlinear pneumatic muscle system using fuzzy logic; Ahn, and Tu (2003~2005) proposed an intelligent switching control scheme using a learning vector quantization neural network and a nonlinear PID control to improve the control performance of PAM manipulator using neural network (NN). However, using a complicated control algorithm does not always indicates the best solution that can be used. Rather than using a very complicated algorithm for the system, a much simpler approach is to be proposed.

II. System Overview for the Lower Limb Orthosis

Figure 1 shows the developed Body Weight Support Gait Training system used for this research. This system used six PAM actuators which arranged as antagonistic (posterior and anterior) mono-articular and bi-articular actuators based on the human musculoskeletal system. The PAM used in this research is the McKibben artificial muscle actuator, which was assembled manually in our laboratory. It is constructed using a rubber tube which is braided with braiding strips. The input pressures of the PAMs are regulated by electro-pneumatic regulator. The increase in air pressure will cause the internal rubber tube to expand, but the outer layer which is the braiding will suppress the tube elongation. In other words, the PAM actuators can imitate the force and muscle

*Research supported by KAKENHI.

M.A. Mat Dzahir, He received master's degree (2011) in mechanical engineering from Faculty of Mechanical Engineering at Universiti Teknologi Malaysia; UTM. Since Sept. 2011, He has been a doctoral course at SIT. 307 Fukasaku, Minuma-ku, Saitama-City, Saitama, 337-8570 Japan. (phone:+080-4094-8009;e-mail: azuwan@fkm.utm.my).

T. Nobutomo, He received bachelor's degree (2010) in engineering from department of machinery & control system, SIT. Since Apr. 2011, He has been a master course at SIT.

S.I. Yamamoto, He received the Ph.D. (2000) degrees in science from the Department of Life Science, The University of Tokyo. He is a professor at SIT, Japan. (phone:+81-48-720-6024; e-mail: yamashin@se.shibaura-it.ac.jp).

contractions of humans' muscle. The PAM's movement principal is almost similar to the human muscles' principle and might be able to perform similar contractions and expansions. The hip and knee joint control angles are measured using potentiometers. This system uses the xPC-Target toolbox to exchange the information signals and output data between the host PC and the target PC. Control program is coded in the C language using the MATLAB/Simulink software.

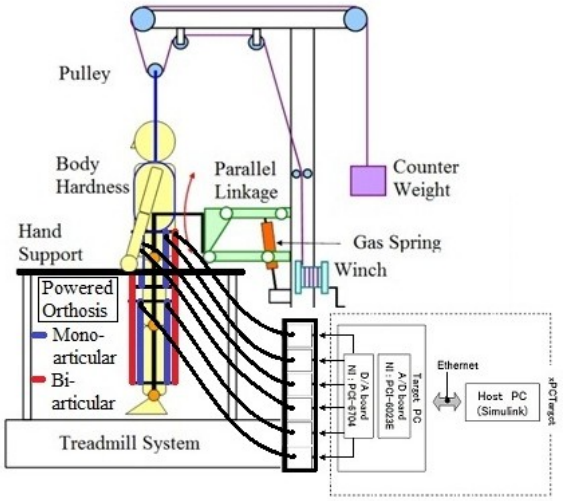

Figure 1: Overview of control system.

III. Methods

The antagonistic PAM actuators' contraction of the lower limb orthosis is determined using the coordinates system. Then, a control system which estimates the antagonistic PAM length (contraction) from the hip and knee joints' angle is constructed. Based on the PAM's contraction equation, the pressure input pattern for each actuators are determined. Two tests are performed in this experiment; first, with the antagonistic mono-articular PAMs alone; and second, is with the addition of antagonistic bi-articular PAMs. Each test is evaluated with different gait cycles of 3, 4, and 5 seconds for five cycles of the human's natural gait trajectory [11]. Moreover, two position settings of the PAMs are performed for both tests as can be seen in Figure 8. In total, we performed four tests for the control system; first, mono-articular setting (PAM setting 1); second, mono-articular setting (PAM setting 2); third, mono- and bi-articular setting (PAM setting 1); and fourth, mono- and bi-articular setting (PAM setting 2). The control system is evaluated using the percentage [%] of gait cycle.

IV. Pneumatic Artificial Muscle's Contraction Measurement

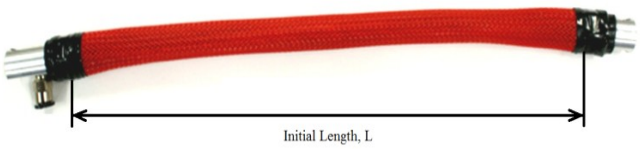

Figure 2: Pneumatic artificial muscle (PAM) - McKibben.

Figure 2 shows the pneumatic muscle actuator (McKibben) with diameter of 1.0 [inch] which is used as the sample to evaluate the PMA's contraction percentage with the input pressure as the variable. The behavior of PAM with regards to its shape, contraction and tensile force when inflated depends on the geometry of the inner elastic part and the braid at rest and on the materials used (Tondu 2000). Maximum force of approximately 800[N] at 0.5[MPa] can be generated from this muscle actuator without load condition. Figure 3 shows the experimental setup used for the measurements. Three samples of the PMAs with different initial lengths, L of 300, 450, and 600 [mm] are used for the measurements. These PMAs' actuator are evaluated at different pressure inputs of 0.1, 0.2, 0.3, 0.4, and 0.5[MPa] for the unloading condition to determine its' contraction characteristics. Further measurement is also conducted for a pressure under 0.1[MPa].

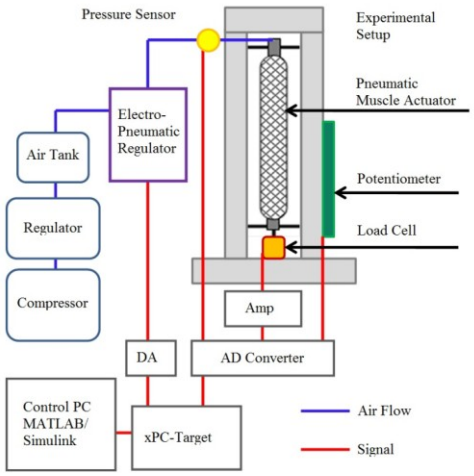

Figure 3: Experimental Setup.

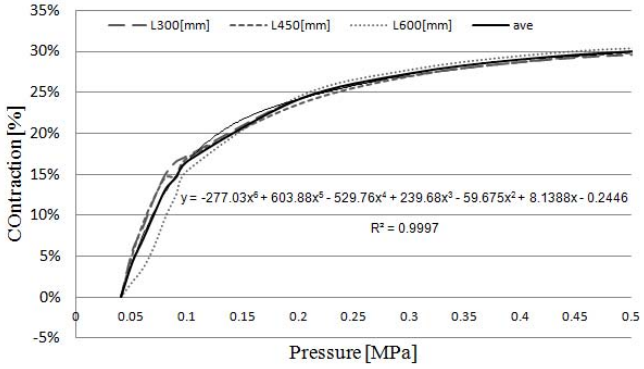

Figure 4: Contraction measurements.

Based on the results in Figure 4, it shows that the PAMs' contraction gives an approximately similar value, converging at 30% of muscle contraction. The result is represented using the average value of the PAMs contractions with 6th order-polynomial function and high approximation of (R^2=0.9997). This function is introduced into the control system to determine the input pressure for each of the mono- and bi-articular actuators.

V. Control System for the Lower Limb Orthosis

Figure 5 shows the antagonistic mono-articular and bi-articular PAM actuators maximum and minimum allowable range for its arrangement. In order to reduce the moment of inertia, the orthosis was set symmetrically in the longitudinal

direction. The PAM's location in the coordinate system is obtained from the model simulation which was programmed using the MATLAB/Simulink. This model is actuated based on the reference input angle of hip and knee joints. The changes in length of the PAMs from the simulation provide the co-contraction data for the mono- and bi-articular actuators. Then, these data is obtained using the coordinate's equation as can be seen in Figure 6.

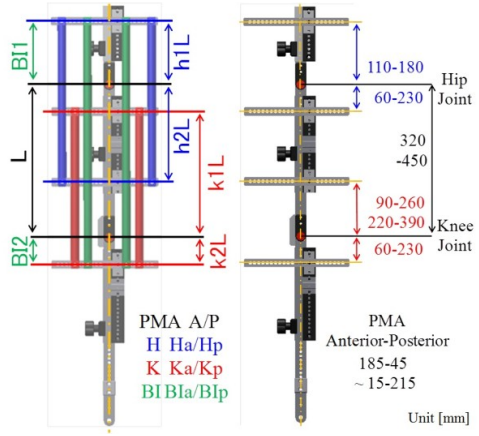

Figure 5: Range of position configuration for PAMs and orthosis system.

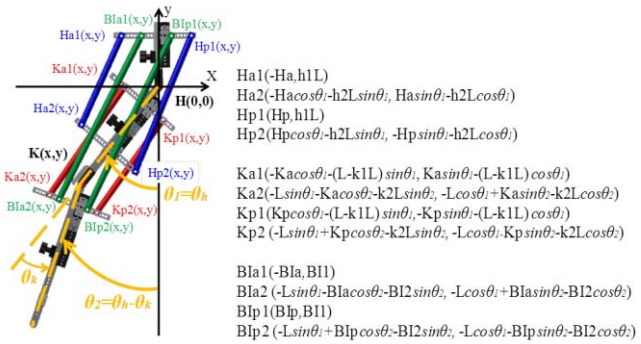

Figure 6: PAM's configuration coordinate system.

By using the equation obtained in Figure 4, the PAMs' contraction data are converted into input pressures for each of antagonistic mono- and bi-articular actuators. Based on this method, the inputs for actuating the lower extremity orthosis are determined. PID controller is used for correcting the required input pressure for each actuator. Output data is measured using potentiometers. Figure 7 shows the control system schematic diagram for the gait training system.

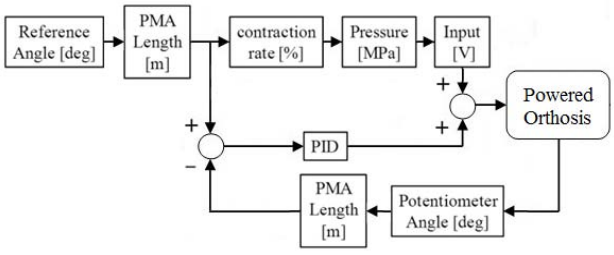

Figure 7: Control system schematic diagram.

VI. Experiment Setup

The required software and hardware for this gait training system experiment is showed in the previous section (see Figure 1). There are two tests for this experiment which is with the antagonistic mono-articular PAMs alone, and with the addition of antagonistic bi-articular PAMs. Each test is performed with gait cycles of 3, 4, and 5 seconds for five cycles of the human walking motion. The hip and knee joint angles data of the leg orthosis are collected for the performance analysis. There are two PAM position settings which are considered for the test as can be seen in Figure 8, and the best position setting is determined based on the gait cycle performance. We performed the tests using four different settings; first, mono-articular setting (PAM setting 1); second, mono-articular setting (PAM setting 2); third, mono- and bi-articular setting (PAM setting 1); and fourth, mono- and bi-articular setting (PAM setting 2).

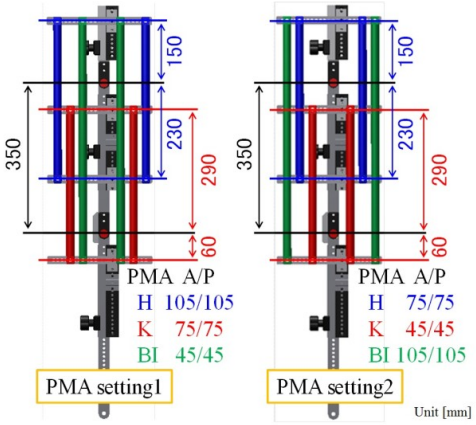

Figure 8: PAM's position for the orthosis system.

VII. Results and Discussions

In this study, the control system which implements the PAM's contraction model and equation (Figure 4) is proposed to control the input pressure of the antagonistic mono- and bi-articular actuators. This control system controls the hip and knee joints' angle of the leg orthosis in a co-contraction movement.

Figure 9 shows the hip angle control for the tests with mono-articular actuators alone, and with the addition of bi-articular actuators, both for PAM settings 1 and 2. In addition, Figure 10 shows the knee angle control with the same PAM settings. For the hip angle control performance (Figure 9), the result shows that, we are not able to achieve the maximum muscle moment (flexion) by using the mono-articular PAM actuators alone. However, when we tested the control system with the addition of bi-articular PAM actuators, there is an improvement in hip angle control for both of the tests with PAM settings 1 and 2. Moreover, the performance for the knee angle control also shows an improvement as can be seen in Figure 10. The result shows that we are not able to achieve the maximum muscle moment (flexion) and unable to get smooth heel contact movement at knee joint by using the mono-articular PAM actuators alone. However, when we implement the gait training system with the addition of bi-articular PAM actuators, we were able to achieve the maximum knee angle extension as well as smoother movement during the heel contact position for both PAM settings.

The comparison of mono-articular and bi-articular actuators' range of motion shows that, bi-articular PAMs has

wider range of motion and are able to generate a greater force. As a result, this enables the orthosis system to achieve the high muscle moment which cannot be obtained by using mono-articular actuators alone. The addition of bi-articular actuators works as a muscle support system that provides the orthosis system with greater actuation power and smoother movement at the joints including the heel contact position. When we consider the result of the hip and knee angles (with addition of bi-articular PAMs), its range of motion is sufficient to simulate the human's walking motion with little time delay. In the single support phase of the gait cycle 10-30 [%], sufficient bending at the knee joint was achieved during the heel contact movement which is difficult to obtain using mono-articular PAM actuators alone for both PAM settings. However, if we try to shorten the gait cycle and time delay, the inertia effect becomes evident.

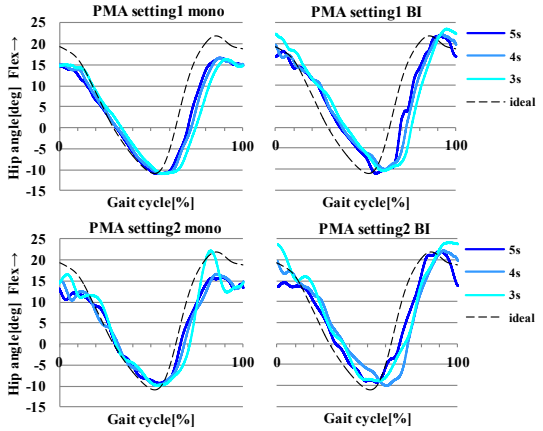

Figure 9: Hip joint angle.

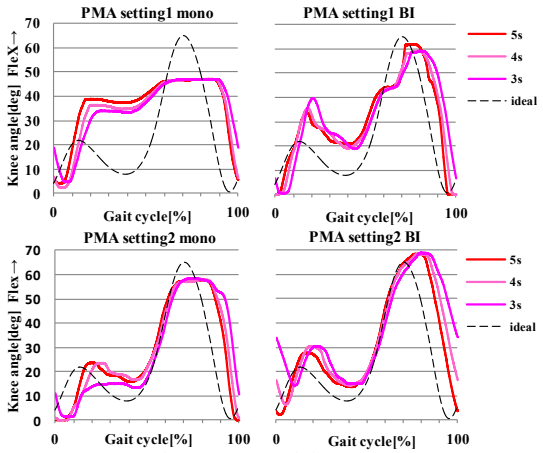

Figure 10: Knee joint angle.

VIII. Conclusion

In this paper, we determined the movements of the lower limb orthosis with the coordinates system and then constructed a control system which estimates antagonistic PAMs' length (contraction) from the hip and knee joint angles. Furthermore, we performed the controller tests for different gait cycles and PAM settings to see the performance of the lower extremity orthosis using the contraction model based controller. The results show that, the performance of the leg orthosis was satisfying. The system was able to achieve the maximum muscle moment at hip and knee joints, and was also able to perform the heel contact movement which could not be achieved by the use of mono-articular PAM actuators alone. This shows that the hip and knee joints' actuators worked effectively. However, if there is a load or subject on the orthosis system, the steady state error might occur within the system due to the nonlinearity behavior of the PAMs. The relationship between the contraction of a PAM and its pressure was measured without load. Thus, it is required to measure the PAM contraction's characteristics with load as there will be different test subjects and walking period (gait cycle). It is also necessary to consider the inertia effect and include the joints' moment measurement into the control system.

Acknowledgment

This work was supported by KAKENHI: Grant-in-Aid for Scientific Research (B) 21300202.

References

[1] Y. Shibata, S. Imai, T. Nobutomo, T. Miyoshi, and S.I Yamamoto, "Development of body weight support gait training system using antagonistic bi-articualar muscle model". 32nd Annual International Conference of the IEEE EMBS, Buenos Aires, Argentina, 2010.

[2] S.I Yamamoto, Y. Shibata, S. Imai, T. Nobutomo, and T. Miyoshi, "Development of gait training system powered by pneumatic actuator like human musculoskeletal system". IEEE International Conference on Rehabilitation Robotics, Rehab Week Zurich, ETH Zurich Science City, Switzerland, 2011.

[3] Caldwell, D.G., Medrano-Cerda, G. A., Goodwin, M. J. (1994) Characteristics and Adaptive Control of Pneumatic Muscle Actuators for a Robotic Elbow. Proc., IEEE Int., Conf., Robotics and Automation, Vol.4, pp. 3558 ~ 3563.

[4] Caldwell, D.G., Medrano-Cerda, G.A. and Goodwin, M.J. (1995) Control of Pneumatic Muscle Actuators. IEEE Contr., Syst., Mag., Vol. 15, No. 1, pp. 40~48.

[5] Repperger, D. W., Johnson, K. R. and Phillips, C.A. (1999) Nonlinear Feedback Controller Design of a Pneumatic Muscle Actuator System. Proc., American Control Conference, Vol. 3, pp. 1525~ 1529.

[6] Tondu B. and Lopex P. (2000) Modeling and Control of Mckbben Artificial Muscle Robot Actuators. IEEE Contr., Syst., Mag., Vol. 20, No. 1, pp. 15~38.

[7] Folgheraiter, M., Gini, G., Perkowski, M. and Pivtoraiko, M. (2003) Adaptive Reflex Control for an Artificial Hand. Proc., SYROCO 2003, Symposium on Robot Control, Holliday Inn, Wroclaw, Poland.

[8] Balasubramanian, V. and Rattan, K. S. (2003) Feedforward Control of a Non-linear Pneumatic Muscle System using Fuzzy Logic. IEEE Int., Conf., Fuzzy Systems, Vol. 1, pp. 272~277.

[9] Ahn K. K., Tu D. C. T. (2004) Improvement of the Control Performance of Pneumatic Artificial Manipulators using an Intelligent Switching Control Method. Int., Jour., Vol. 18, No. 8, pp. 1388~ 1400.

[10] Ahn K. K., Tu D. C. T (2005) Nonlinear PID Control to Improve the Control Performance of the Pneumatic Artificial Muscle Manipulator Using Neural Network. Journal of Mechanical Science and Technology, Vol. 19, No. 1, pp. 106--115.

[11] David A. Winter, "Biomechanics and motor control of human movement". Fourth Edition, John Wiley & Sons, Inc., 2009.

[12] A. Wernig, S. Muller, A. Nanassy, and E. Cagol, "Laufband therapy based on 'rules of spinal locomotion' is effective in spinal cord injured persons". Eur J Neurosci vol. 7, pp823-829, 1995.

[13] V. Dietz, R. MuEller and G. Colombo, "Locomotor activity in spinal man: significance of afferent input from joint and load receptors". Brain, 125, pp2626-2634, 2002.

[14] GVaronov A.V, "the roles of mono-articular and bi-articular muscles of the lower limbs in terrestrial locomotion". Human Physiology, Vol. 30, No. 4, pp. 476-484, 2003.

2014 CMBEC37 Conference
Vancouver, BC
May 21 – 23, 2014

RECENT TREND IN LOWER-LIMB ROBOTIC REHABILITATION ORTHOSIS: PNEUMATIC MUSCLE ACTUATED GAIT TRAINER SYSTEMS

Mohd Azuwan Mat Dzahir[1,2] and Shin-ichiroh Yamamoto[1]
[1]Department of Bi-Science and Engineering, Shibaura Institute of Technology, Japan. [2]Faculty of Mechanical Engineering, Universiti Teknologi Malaysia, Malaysia.

ABSTRACT

A review study was conducted on existing lower-limb orthosis systems for rehabilitation which implemented pneumatic muscle type of actuators with the aim to clarify the current and ongoing research in this field. It is a general assumption that pneumatic muscles will play an important role in the development of assistive rehabilitation robotics system. In the last decade, the development of this orthosis system was relatively slow compared to the motorized orthosis system. However, in recent years, the interest in this field had grown exponentially mainly due to the demand on a much compliant human-robotics system and advantageous attributes of the pneumatic muscles. Based on the review study, it could be understood that the suitable control schemes and strategies have yet to be found. In this research, a co-contraction controls scheme is proposed. Results were able to demonstrate the ability of the co-contraction controls to manoeuvre and improvise the joint's stiffness and stability of the leg orthosis.

INTRODUCTION

The existing pneumatic muscle actuated lower-limb rehabilitation orthosis systems comparison was shown in Table 1. Based on the development of different orthosis systems in last 10 years, it might be concluded that the researchers' interest has been shifted to the implementation of the natural type of compliant actuators [1 -14]. Although lots of researches have been investigated regarding the co-contraction movements of human antagonistic muscles. However, their model implementation in controlling the antagonistic muscle actuators of lower-limb orthosis has not been completely discovered. In addition, research study which focuses on the implementation of mono- and bi-articular actuators using pneumatic muscles for the lower-limb rehabilitation orthosis has yet to be extensively investigated; thus, simply actuating the actuators might not give a good result on the joint's stiffness and stability of the lower-limb leg orthosis and its joint trajectories. Therefore, based on the related research findings, the simultaneous co-contractively like movements between the anterior and posterior actuators could be considered within the control system strategy [15 – 17].

Table 1: Existing pneumatic muscle actuated gait trainer systems

Orthosis system	Types	Year
Hip orthosis exoskeleton [1]	Hip orthoses	2004
Robotic gait trainer (RGT) [2]	Foot orthoses	2006
Ankle-foot orthosis (AFO) [3]	Foot orthoses	2006
Powered lower-limb orthosis [4]	Treadmill gait trainers	2006
Robotic gait trainer in water (RGTW) [5]	Over-ground gait trainers	2008
Powered ankle-foot exoskeleton [6]	Foot orthoses	2009
Powered knee-ankle-foot orthosis (KAFO) [7]	Knee and foot orthoses	2009
Continuous passive motion (CPM) [8]	Stationary gait and ankle trainers	2009
Power-assist lower-limb orthosis [9]	Over-ground gait trainers	2010
Active ankle-foot orthosis (AAFO) [10]	Foot orthoses	2011
Bio-inspired active soft orthotic device [11]	Foot orthoses	2011
Active modular elastomer sleeve [12]	Knee orthoses	2012
Orthosis for walking assistant [13]	Hip orthoses	2013
6 DOF robotic orthosis [14]	Treadmill gait trainers	2013

Even though a considerable amount of work has now been done, the field is still rapidly evolving. The issue of which are the most effective control algorithms is still wide open. However, the randomized controlled trials are still necessary for identifying the suitable control algorithms even though it is expensive and time-consuming. A few remarks will be considered within this research; the first is antagonistic arrangement of the pneumatic muscles; the second is co-contractively like movement between the antagonistic actuators; the third is an additional model to generate adequate co-contractive input data; and finally, the controller scheme that can deal with the pneumatic muscle nonlinearities.

METHODOLOGY

Two tests were carried out; the first test is with mono-articular actuators, and the second test is with an addition of bi-articular actuators. The actuators were arranged antagonistically (i.e., anterior and posterior) and simultaneously drive the leg orthosis. Six different control schemes based on conventional PID and co-contraction controls were tested at gait cycle (GC) speed of 0.28m/s for five cycles including the initial position cycle. The ideal joint trajectories (i.e., hip and knee angles) used for the leg orthosis control were obtained from Winter (2009) and verified throughout experimental setup. The result is then evaluated based on mean value of the Pearson coefficient of determination (r^2) for the hip and knee joint excursions.

CO-CONTRACTION CONTROLS

Based on the research findings, it could be verified that the co-contraction of antagonist muscles were play an important role for the joints stiffness and stability. Moreover, muscle co-contraction is not only useful to compensate the joint's stiffness and stability. However, it is also able to manoeuvre the direction of output forces [15 - 17]. In addition, the co-contraction activations were able to reduce a kinematic variability where, through the increment of co-contraction activations, the kinematic variability could the reduced, except for the low co-contraction activation levels [18]. Therefore, it could be concluded that modelling of the co-contraction model to represent the movement of antagonistic actuators could be sufficiently beneficial. It is believed that, this is one of a crucial factor that will lead to a good control system performance.

CONTROL SYSTEM

The control system for this research delves into two parts; the first part employs the use of proportional directional control valve to enable the implementation of conventional PID controls of the antagonistic actuators; and, the second part employs the use of one regulator for each actuator to enable the implementation of co-contraction controls of the antagonistic actuators using derived mathematical model. Derivation of the co-contraction model has been recorded earlier and can be referred to [19]. The PID parameters were tuned using heuristic method. Real time control system was realized by using the MATLAB Simulink and xPC Target toolbox. The rotary potentiometer and compact pressure sensor were used to measure the required data information from the AIRGAIT exoskeleton's leg orthosis for the execution of closed loop control system. Figure 1 shows the schematic diagram for the control schemes.

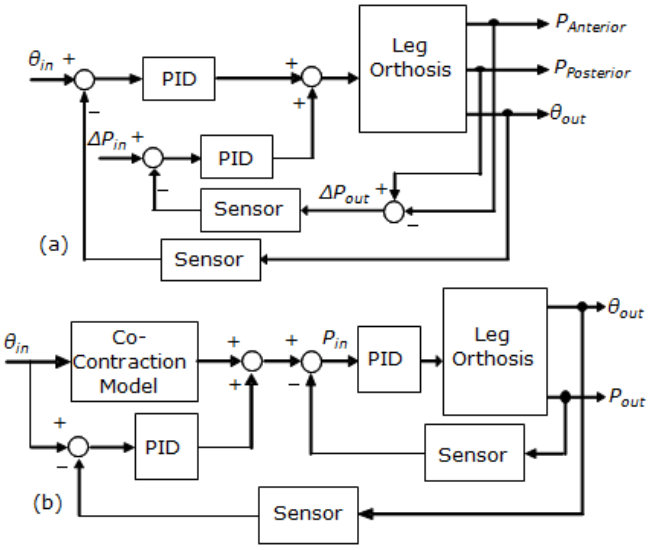

Figure 1: Conventional PID and co-contraction control scheme for pressure position controls

RESULTS AND DISCUSSION

Based on the review suggestions, control system evaluation is performed on the leg

orthosis of the developed body weight support gait training system known as AIRGAIT. The design and evaluation of the AIRGAIT orthosis system have been recorded earlier and can be referred to [19]. Both control systems were first performed with only mono-articular actuators driven the leg orthosis. However, only the co-contraction controls were further tested with both mono- and bi-articular actuators. This is because the control of bi-articular actuators requires an additional model for generating its input patterns. Figure 2 shows the hip and knee joint excursions of the leg orthosis control for all evaluated control schemes. The result showed that by implementing conventional PID alone, it was not enough to achieve good joint trajectories either with pressure control or both pressure-position controls. The outcome was rather poor due to the insufficient joint stiffness and stability. However, it could be seen that with the implementation of additional model (co-contraction model) which enable the antagonistic actuators to be controlled co-contractively resulted in a much better gait trajectories. This could be explained due to the outcome of the co-contraction controls, with both anterior and posterior pneumatic muscles co-contractively contract and expands. This action resulted to an increase in the joint's stiffness and stability of the leg orthosis. In addition, by introducing this control scheme and strategy, the gravitational and hysteresis effects could also be reduced.

The performance evaluation of the tested control schemes based on conventional PID and co-contraction controls were properly evaluated using the Pearson coefficient of determination as can be seen in Table 2. The table shows that mean r^2 value for pressure and pressure-position controls based on conventional PID were less than 0.5 (50%) which is rather low compared to the pressure control based on co-contraction model control scheme with mean r^2 value of 0.84 (84%). This shows that the co-contraction controls was able to precisely maneuver the joints orthosis according to the desired trajectories. Then, the gait motion was improved with the addition of bi-articular actuators, where the mean r^2 value indicated a measure of 0.859 (85.9%). This is because the bi-articular actuators were able to improvise the balance control of the leg orthosis and ability to produce maximum output force in a much more homogenously distributed ways. Subsequently, the joint excursions were much better using the position and pressure-position based on co-contraction controls with high mean r^2 values of 0.974 (97.4%) and 0.986 (98.6%) compared to the pressure control. This is because the designed pressure control only manages the pressure data based on the input patterns generated by co-contraction model. However, the addition of position control was controlling the muscle activation levels of the co-contraction model itself, which enables much precise co-contraction data to be generated. It is realized that the control of pressure and position based co-contraction controls produce much better joint's stiffness and stability.

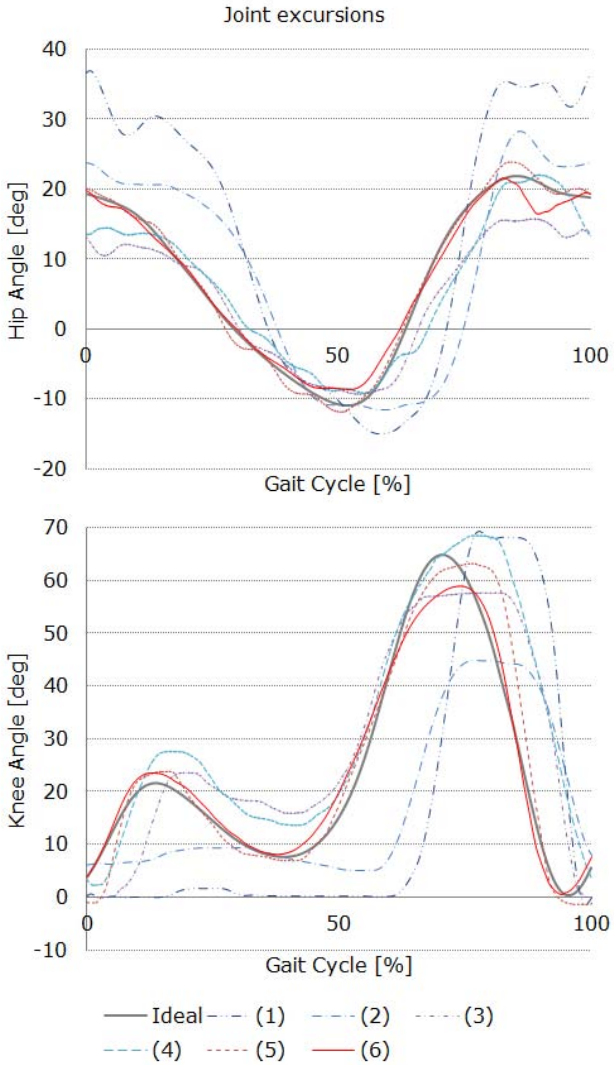

Figure 2: Hip and knee joint excursions

Table 2: Pearson coefficient of determination (r^2) comparison

Controller scheme	r^2 Hip angle	r^2 Knee angle	Mean r^2
(1) Conventional PID - Pressure control (mono)	0.741	0.183	0.462
(2) Conventional PID - Position and pressure control (mono)	0.617	0.329	0.473
(3) Co-contraction model - Pressure control (mono)	0.950	0.730	0.840
(4) Co-contraction model -Pressure control (mono and bi)	0.913	0.805	0.859
(5) Co-contraction model - Position control (mono and bi)	0.996	0.951	0.974
(6) Co-contraction model - Position and pressure control (mono and bi)	0.992	0.980	0.986

CONCLUSION

In conclusion, it is suggested that the pneumatic muscles arrangement for the leg orthosis should be antagonistically, and it is believed the co-contractively like movements of antagonistic actuators could provide a good joint's stiffness and stability of the leg orthosis. Besides, an additional model is essential to produce adequate co-contractive input data for manipulating the bi-articular actuators. Finally, the intelligent control scheme will be required to deal with the presence of dynamic properties and nonlinearity behavior of the system.

ACKNOWLEDGEMENTS

KAKENHI: Grant-in-Aid for Scientific Research (B) 21300202.

REFERENCES

[1] Breno G. Nascimento, Claysson B. Vimieiro, Danilo A. Nagem, and Marcos Pinotti., "Hip orthosis powered by pneumatic artificial muscle: voluntary activation in absence of myoelectrical signal", Artificial Organs, vol. 32(4), 2008.

[2] Kartik Bharadwaj, and Thomas G. Sugar, "Kinematics of a robotic gait trainer for stroke rehabilitation", IEEE Int. Conference on Robotics and Automation, 2006.

[3] Daniel P. Ferris, Keith E. Gordon, Gregory S. Sawicki, and Ammanath Peethambaran, "An improved powered ankle-foot orthosis using proportional myoelectric control", Gait and Posture, vol. 23, 2006.

[4] Nelson Costa, Milan Bezdicek, Michael Brown, John O. Gray, and Darwin G. Caldwell, "Joint motion control of a powered lower limb orthosis for rehabilitation", Int. Journal of Automation and Computing, vol. 3, 2006.

[5] T. Miyoshi, K. Hiramatsu, S.I. Yamamoto, K. Nakazawa, and M. Akai, Robotic gait trainer in water: development of an underwater gait-training orthosis, Disability and Rehabilitation, vol. 30(2), 2008.

[6] P. Malcom, P. Fiers, V. Segers, I. Van Caekenberghe, M. Lenoir, and D. De Clercq, "Experimental study on the role of the ankle push off in the walk-to-run transition by means of a powered ankle-foot-exoskeleton", Gait and Posture, vol. 30, 2009.

[7] Gregory S. Sawicki, and Daniel P. Fessis, "A pneumatically powered knee-ankle-foot orthosis (KAFO) with myoelectric activation and inhibition", Journal of Neuro-Engineering and Rehabilitation, 2009.

[8] 44. Tudor T. Deaconescu, and Andrea I. Deaconescu, "Pneumatic muscle actuated equipment for continuous passive motion", IAENG Transactions on Engineering Technologies, vol. 3, 12 pages, 2009.

[9] T. J. Yeh, Meng Je Wu, Ting Jiang Lu, Feng Kuang Wu, and Chih Ren Huang, " Control of McKibben pneumatic muscles for a power-assist, lower-limb orthosis", Mechatronics, vol. 20, pp. 686-697, 2010.

[10] J. Carberry, G. Hinchly, J. Buckerfield, E. Taylor, T. Burton, S. Madgwick, and R. Vaidyanathan, "Parametric design of an active ankle foot orthosis with passive compliance",CBMS, 2011.

[11] Yong-lae Park, Bor-rong Chen, Diana Young, Leia Stirling, Rob Wood, Eugene Goldfield, Radhika Nagpal, "Bio-inspired Active Soft Orthotic Device for Ankle Foot Pathologies", IEEE IROS, 2011.

[12] Yong-Lae Park, Bor-rong Chen, Carmel Majidi, Rob Wood, Radhika Nagpal, and Eugene Goldfield, "Active Modular Elastomer Sleeve for Soft Wearable Assistance Robots", IEEE IROS, 2012.

[13] T. Kawamura, and K. Takanaka, "Development of an orthosis for walking assistance using pneumatic artificial muscle-a quantitative assessment of the effect of assistance", Int. Conference on Rehabilitation Robotics, 2013.

[14] S. Hussain, S.Q. Xie, and P.K. Jamwal, Adaptive impedance control of a robotic orthosis for gait rehabilitation, IEEE Trans. on Cybernetics, vol. 43, no. 3, 2013.

[15] William K. Durfee, "Task-based methods for evaluating electrically stimulated antagonist muscle controllers", IEEE Trans. on Biomedical Engineering, vol. 36, 1989.

[16] Samer Mohammed, Philippe Fraisse, David Guiraud, Philippe Poignet, Hassan El Makssoud, "Towards a co-contraction muscle control strategy for paraplegics", 44th IEEE Conf. on Decision and Control, 2005.

[17] Stewart Heitmann, Norm Ferns, and Michael Breakspear, "Muscle co-contraction modulates damping and joint stability in a three-link biomechanical limb", Frontiers in Neurorobotics, vol. 5, 2012.

[18] Luc P.J. Selen, Peter J. Beek, and Jaap H. van Dieen, "Can co-activation reduce kinematics variability? a simulation study", Biological Cybernetics, 2005.

[19] M.A. Mat Dzahir, T. Nobutomo, and S.I. Yamamoto, "Antagonistic mono- and bi-articular pneumatic muscle actuator control for gait training system using contraction model", IEEE Int. Conference on Bio-Science and Bio-Robotics, 2013.

CONTROL OF LOWER LIMB ORTHOSIS: SIMPLE PARADIGM FOR THE CONTROL OF ANTAGONISTIC ACTUATORS

Mohd Azuwan Mat Dzahir and Shin-ichiroh Yamamoto

Department of Bio-Science and Engineering, Shibaura Institute of Technology

ABSTRACT

In this research paper, the evaluation of control paradigm and strategy of the AIRGAIT exoskeleton's leg orthosis were analyzed using the simulation model before implementing the derived mathematical model into real system. It was conducted to determine the performances of the derived mathematical model when compared between the simulation and real system test. The simulation model was evaluated using the particle swarm optimization (PSO) method. The development of the control paradigm and strategy should enable the antagonistic mono- and bi-articular actuators in supporting each other during the control system. Furthermore, the assessment on the bi-articular actuators control was increased by omitting the mono-articular actuators at the knee joint. During the real system tests, the leg orthosis was evaluated at four gait cycle (GC) speeds of 0.28m/s, 0.35m/s, 0.47m/s, and 0.70m/s. A total of 25 GCs for each GC speed was collected, and the average GC was measured and compared.

1. INTRODUCTION

In recent years, lots of researches had been carried out on assistive robotics for rehabilitation, either using motors or pneumatic muscle actuators (PMA) as the source of power [1]. Consequently, many findings had been based on these researches. Famous researchers in this field, such as Daniel Ferris et al., have mentioned that powered orthosis could assist the task specific practice of gait, with a long-term goal of improving patient's inherent locomotor capabilities [2]. According to Kalyan K. Mankala, Sunil K. Agrawal et al., passive swing assistance was able to help patients, with less than normal muscle strength, to achieve better gait trajectories [3]. Furthermore, research on the implementation of the mono- and bi-articular actuators for achieving the high muscle moment required at joints and better gait trajectories, was also taken into consideration [4 - 5]. A study on the co-contraction of antagonist muscles was carried out by William R. Murray et al., in 1988; which implemented a simple model representing the quasi-static behaviour of skeletal muscle, in which the force produced by the muscle was a bilinear function of muscle length and the neural activation of the muscle [6]. In 2005 and 2010, Samer Mohammed et al., mentioned in their study of co-contraction muscle control strategy for paraplegics, that co-contraction of antagonistic muscles (basically quadriceps and hamstrings) may yield an increasing joint stiffness and stable movement [7]. Other researches on co-contraction of antagonist muscle, such as by Cheryl L. Lynch et al., in 2012, showed that during the maximum velocity knee extension trial, the importance that the antagonist knee flexor muscle plays in damping knee dynamics; thereby preventing the knee from overshooting and experiencing a long settling time.

This research paper focuses on the implementation of mono- and bi-articular actuators using PMA; thus, simply actuating the actuators might not give a good result on the joint's stiffness of leg orthosis and its position trajectory. Therefore, the co-contraction movements between the anterior and posterior PMA, should be considered.

2. NEW DESIGN OF AIRGAIT EXOSKELETON

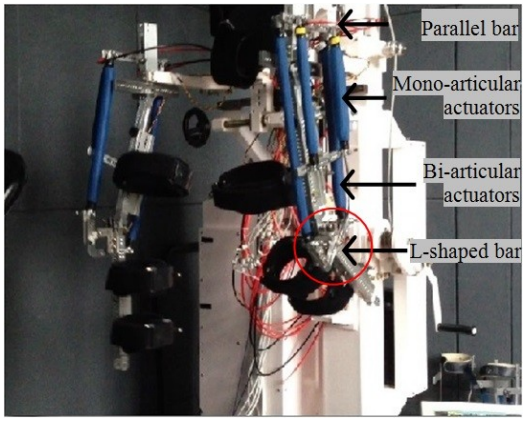

Figure 1 AIRGAIT exoskeleton's leg orthosis.

Figure 1 shows the prototype of AIRGAIT exoskeleton's leg orthosis for gait motion rehabilitation training. This model consists of a pair of antagonistic mono-articular actuators at hip joint, and a pair of bi-articular actuators. The concept used for this leg exoskeleton's design utilizes L-shaped bar at knee joint to optimize the length and movements of the antagonistic bi-articular actuators. Thus, unnecessary movements of antagonistic actuators at the knee joint are minimized compared to the previous design [8]. Moreover, previous model does not fully utilize the use of bi-articular muscle actuators which is the main objective of this study. The leg orthosis improvement at knee joint using L-shaped bar was enabled the leg orthosis to be actuated by the antagonistic mono-articular at hip joint and bi-articular actuators alone (six actuators used in previous design).

This reduction in the number of actuators at knee joint was considered as to increase the assessment on the antagonistic bi-articular actuators, and to reduce the redundancy in actuation system. All the simulation analysis and experimental tests are based on this system.

3. METHODS

In this research, the control system paradigm and strategy were first analysed using simulation model. The simulation was based on the PSO which were coded using MATLAB language and Simulink block to evaluate the reliability of the control system and determine the range of PID gains. The derivation of the co-contraction model control scheme and strategy was recorded earlier and can be referred to in [8]. After that real system controls of leg orthosis was performed at different GC speeds of 0.28m/s, 0.35m/s, 0.47m/s, and 0.70m/s to see the reliability of the control system at speed variability. The data for the hip and knee joint excursions were then recorded using the potentiometer. The Pearson coefficient of determination (r^2) was utilized to evaluate the performance of the control system paradigm and strategy.

4. ROTATIONAL DYNAMIC

The mass of the leg orthosis (m_1 and m_2) as well as the frictions (T_{f1} and T_{f2}) occurs during the gait motion were considered within the dynamics analysis by implementing equation of motion or Newton's second law of rotation. The torques (τ_1 and τ_2) were calculated using the equations below. Where the rotational dynamics was evaluated based on double pendulum model of two links leg manipulators as can be seen in Figure 2.

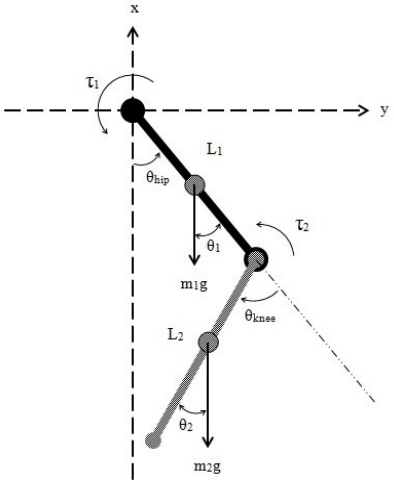

Figure 2 Simple two link leg manipulators model.

Implementing the Newton's second law of rotation:

$$\Sigma\tau_o = I_o\alpha \quad (1)$$

The mass of inertia (I_o) for the slender rod is assumed to be a constant thus neglecting the Coriolis terms.

$$I_o = \frac{1}{3}ml^2 \quad (2)$$

$$\tau_2 - m_2 g sin\theta_2 \left(\frac{l_2}{2}\right) - T_{f2} = I_2\ddot{\theta}_2 \quad (3)$$

$$\tau_2 - \left(\frac{m_2 g l_2}{2}\right) sin\theta_2 - T_{f2} = \frac{1}{3}m_2 {l_2}^2 s^2\theta_2$$

$$\left[\tau_2 - \left(\frac{m_2 g l_2}{2}\right) sin\theta_2 - T_{f2}\right]\frac{3}{m_2 {l_2}^2 s^2} = \theta_2 \quad (4)$$

$$\tau_1 - m_1 g sin\theta_1 \left(\frac{l_1}{2}\right) - m_2 g sin\theta_1 (l_1) - T_{f1} - \tau_2 = I_1\ddot{\theta}_1 \quad (5)$$

$$\tau_1 - m_1 g sin\theta_1 \left(\frac{l_1}{2}\right) - m_2 g sin\theta_1 (l_1) - T_{f1} - \tau_2$$

$$= \frac{1}{3}m_1 {l_1}^2 s^2\theta_1$$

$$\left[\tau_1 - m_1 g sin\theta_1 \left(\frac{l_1}{2}\right) - m_2 g sin\theta_1 (l_1) - T_{f1} - \tau_2\right]\frac{3}{m_1 {l_1}^2 s^2}$$

$$= \theta_1 \quad (6)$$

5. PSO OPTIMIZATION METHOD

The PSO optimization method was used to evaluate the developed control paradigm and strategy, and to verify the range of PID gains. The simulation was performed to determine the functionality and reliability of the designed controller scheme, where the simultaneous and co-contractively movements of the antagonistic actuators to be achieved. The antagonistic mono- and bi-articular actuators should be able to support each other during the control of the leg orthosis and tackling the nonlinearity behaviour of the muscle actuators. The control parameters for the PSO are shown in Table 1.

Table 1 PSO control parameters.

Control parameters		
Population size	NP	25
Acceleration constant	C1	2
	C2	2
Inertia weight	w	0.8
Random number	R1	Rand()
	R2	Rand()

Figure 3 shows the control paradigm's schematic diagram for the AIRGAIT exoskeleton's leg orthosis system. Based on the derived equation (4) and (6) of the two link leg manipulators rotational dynamics, the plan model for the AIRGAIT exoskeleton's leg orthosis was then modelled using MATLAB language and Simulink

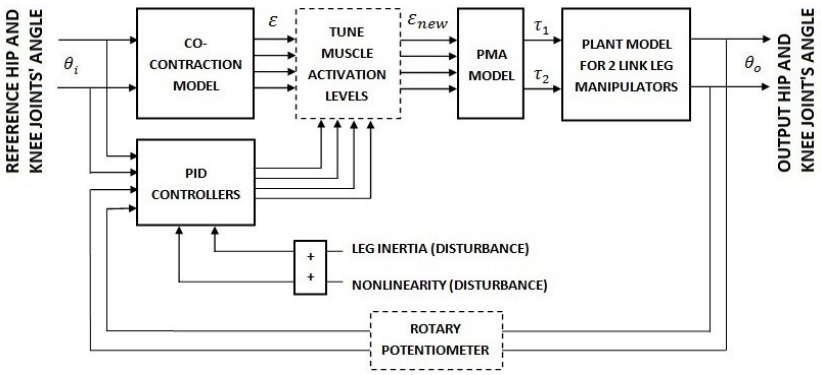

Figure 3 Control paradigm's schematic diagram for the system using PSO optimization method.

block. The system's nonlinearity was considered by implementing additional inertia and PMA nonlinearity disturbances.

6. RESULTS AND DICUSSIONS

The focus in this assessment is on the evaluation of the new design AIRGAIT exoskeleton's leg orthosis. To reduce the numbers of operating actuators, only four actuators will be used in this experiment (i.e., antagonistic mono-articular actuators at hip joint and bi-articular actuators). The antagonistic mono-articular actuators for knee joint were emitted from the leg orthosis to increase the evaluation on the bi-articular actuators. The new design orthosis was purposely designed as to increase the accuracy of the leg orthosis movements at the knee joint without the presence of the mono articular actuators. Figure 4 shows the simulation results for the control paradigm and strategy using PSO at different GC speeds. The simulation results show that the developed control system was able to adapt to the system's nonlinear behaviour and follows the reference trajectories. In the real system tests, the leg orthosis was evaluated at four GC speeds of 0.28m/s, 0.35m/s, 0.47m/s, and 0.70m/s. A total of 25 GCs for each GC speed was collected, and the average GC was then compared with

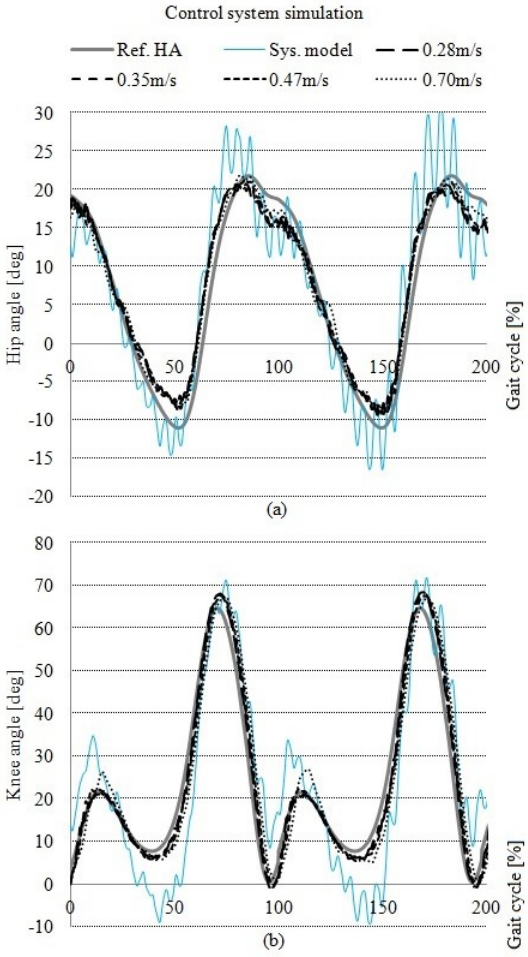

Figure 4 Simulation results for the control paradigm using PSO (a) hip joint excursion and (b) knee joint excursion.

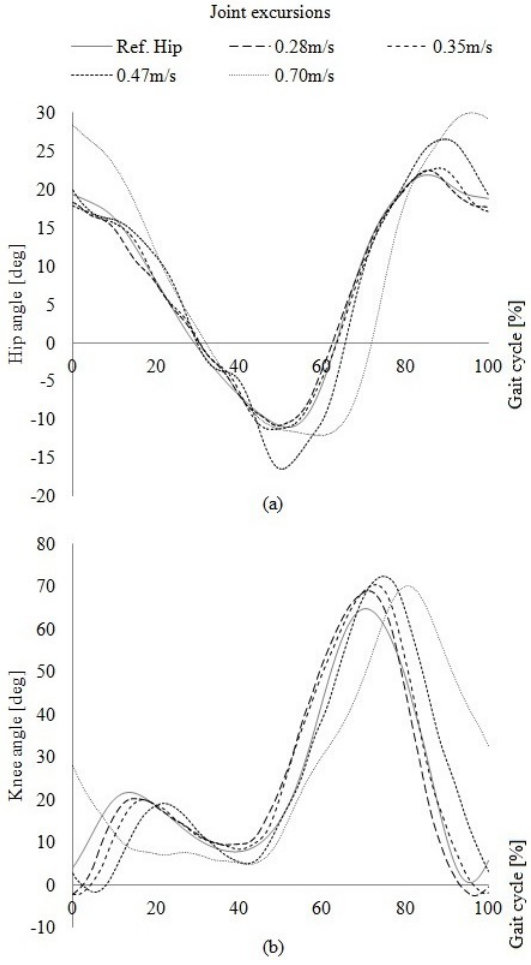

Figure 5 Experimental test results for control system at different GC speeds; (a) hip joint excursion and (b) knee joint excursion.

the reference trajectories. Figure 5 shows the hip and knee joints trajectory for the controls of leg orthosis using the developed control paradigm and strategy. The results explained that during the tests, the controls of antagonistic mono-articular actuators for hip joint and bi-articular actuators were able to demonstrate a good gait motion at all evaluated GC speeds for both hip and knee joints even when the mono-articular actuators for knee joint was emitted. This proved that, the co-contractively control of the antagonistic actuators using the designed controller scheme, was a noble ways of controlling the antagonistic bi-articular actuators. Moreover, the knee joint angle extension was also improved when compared to the previous design leg orthosis which unable to reach the maximum excursion of knee excursion (63º) during the middle swing motion.

Table 2 Pearson Coefficient of Determination (r^2) for hip and knee joint excursions.

Pearson coefficient of determination (r^2)				
GC speeds	0.28m/s	0.35m/s	0.47m/s	0.70m/s
Hip angle	0.9950	0.9757	0.9815	0.9107
Knee angle	0.9485	0.9343	0.8968	0.4541

Table 2 shows the Pearson coefficient of determination (r^2) for hip and knee joint excursions at different GC speeds of 0.28m/s, 0.35m/s, 0.47m/s, and 0.70m/s. The result shows that the r^2 coefficient values at most of the GC speeds were above 89% for both hip and knee joints angle. This illustrates that the design of the leg orthosis at the knee joint where L-shaped bar was introduced improves the antagonistic bi-articular actuators movements. Thus enables the knee excursion to be managed by antagonistic bi-articular actuators alone. However, the mono-articular actuators at hip joint are still needed to guide the trajectory of the leg orthosis throughout the process. This result might indicated that the redundancy of the actuation system could also be resolved if the controls of the AIRGAIT exoskeleton's leg orthosis can be managed using only by these four antagonistic actuators. The key to realize this would be the accurate control strategy of the antagonistic bi-articular actuators. However, it is necessary to evaluate this new design orthosis with a subject at different GC speeds before a further conclusion could be made.

CONCLUSION

In conclusion, the developed control system paradigm and strategy were able to co-contractively control the antagonistic actuators of the leg orthosis and performed good hip and knee joint excursions at different GC speeds. The simulation results show that the designed control scheme was able to handle the nonlinearity behaviours which were caused from the disturbances of the inertia and muscle actuator's nonlinearity. This shows that the manipulation of the muscle activation levels were able to cope with the muscle actuator's nonlinearity behaviours such as hysteresis effect and time variance. Furthermore, with performance of ($r^2 > 0.89$) based on the real system tests at different GC speeds of 0.28m/s, 0.35m/s, 0.47m/s, and 0.70m/s, it can be concluded that the control system was able to adapt with the change in speeds as well. Even with absence of antagonistic mono-articular actuators at knee joint, the joint trajectories was able to materialized by the antagonistic bi-articular actuators with the support of antagonistic mono-articular actuators at hip joint. These results explain the reliability and efficiency of the co-contractively movements control of the antagonistic actuators using the developed control paradigm and strategy.

REFERENCES

Iñaki Díaz, Jorge Juan Gil, and Emilio Sánchez, "Lower-Limb Robotic Rehabilitation: Literature Review and Challenges," Journal of Robotics, vol. 2011, 11 pages, Hindawi Publishing Corporation, 2011.

Daniel P. Ferris, Cara L. Lewis, "Robotic lower limb exoskeletons using proportional myoelectric control". 31st Annual Intl. Conference of the IEEE EMBS, 2009.

Kalyan K. Mankala, Sai K. Banala, Sunil K. Agrawal, "Passive swing assistive exoskeletons for motor incomplete spinal cord injury patients". IEEE Intl. Conference on Robotics and Automation, 2007.

M. Kumamoto, T. Oshima, and T. Fujikawa, "Control properties of two joint link mechanism equipped with mono and bi-articular actuators". Robot & Human Interactive Com., IEEE Proc. pp. 400~404, 2010.

V. Salvucci, Oh Sehoon, Y. Hori, and Y. Kimura, "Disturbance rejection improvement in non-redundant robot arms using bi-articular actuators". Industrial Electronics (ISIE). IEEE Symp. pp. 2159-2164, 2011.

William R. Murray, Neville Hogan, "Co-contraction of antagonist muscles: Prediction and observation". Joint Dynamics and Control, IEEE EMBS, 1988.

Samer Mohammed, Philippe Fraisse, David Guiraud, Philippe Poignet, Hassan El Makssoud, "Towards a co-contraction muscle control strategy for paraplegics". 44th IEEE Conference on Decision and Control, 2005.

Mohd Azuwan Mat Dzahir and Shin-Ichiroh Yamamoto, "Design and Evaluation of the AIRGAIT Exoskeleton: Leg Orthosis Control for Assistive Gait Rehabilitation," Journal of Robotics, vol. 2013, 20 pages, Hindawi Publishing Corporation, 2013.

Mohd Azuwan Mat Dzahir received M.E. (2011) degrees in mechanical engineering from Universiti Teknologi Malaysia (UTM). He is a PhD student at Shibaura Institute of Technology, Saitama, Japan.

Shin-Ichiroh YAMAMOTO received D.E. (2000) degree in science from the Department of Life Science from The University of Tokyo. He is a professor at Shibaura Institute of Technology, Saitama, Japan.

ANTAGONISTIC MONO- AND BI-ARTICULAR ACTUATORS CONTRACTION MODEL FOR BODY WEIGHT SUPPORT GAIT TRAINING SYSTEM

M. A. Mat Dzahir, T. Nobutomo, and S. I. Yamamoto

Department of Bio-Science and Engineering, Shibaura Institute of Technology

ABSTRACT

The challenge in developing a medical robotics for rehabilitation has significantly changed due to the requirement for a compliant, less weight and human-friendly robotics system which lead to the use of Pneumatic Muscle Actuator (PMA). In this study, we wrote contraction pattern's equation for the antagonistic mono- and bi-articular PMAs by using information from the positional input data. Then, control the system using PI controller. This contraction model is influenced by the anterior and posterior muscle activation levels which determine its magnitude. We tested the control system for hip and knee joints' angle control using antagonistic mono-articular actuators alone; and with presence of antagonistic bi-articular actuators. Result shows the control performance of hip and knee joints' angle for body weight support gait training system.

1. INTRODUCTION

From the neuro-rehabilitation robotic view, the robot should be compliant to spastic reactions which often seen in the neurologically impaired patients such as spinal cord injury (SCI) and stroke patients. Due to this issue, the recent trends in rehabilitation robotics try to implement the use of the natural compliant actuator which consist lots of advantages such as its high power to weight ratio, inherent safety, easy for maintenance, low cost, cheap power source and readily availability. This introduces the Body Weight Support Gait Training System (AIRGAIT) for lower extremity orthotic patient [2, 3]. In previous study, they were able to improve the system by implemented antagonistic bi-articular actuators with constant pressure input of 0.025MPa. However, the system was unable to achieve high stiffness on the hip and knee joints by using mono-articular actuators alone. This shows that, implementation of antagonistic bi-articular actuators with addition of mono-articular actuators was a key to achieve high muscle moment (flexion and extension) at hip joint and wider range of motion (flexion) at knee joint. From the study carried out by other researches, it shows that the performance of two-joint link mechanism such as differences in characteristics of the output force, stiffness at the endpoint of the leg and the perfect humanlike control properties at the endpoint depends on the presence or absence of bi-articular actuators when it works in the presence of mono-articular actuators [4, 5, 6]. In this study, we want to actuate the mono-articular and bi-articular actuators with co-contraction movement. Then, getting a smooth and precise movement at the hip and knee joints. Thus, we wrote mathematical model to measure the muscle contraction of the antagonistic mono- and bi-articular actuators using the information from the positional input data. Using this approach, we were able to develop a simple control algorithm for the system.

2. BODY WEIGHT SUPPORT GAIT TRAINING SYSTEM

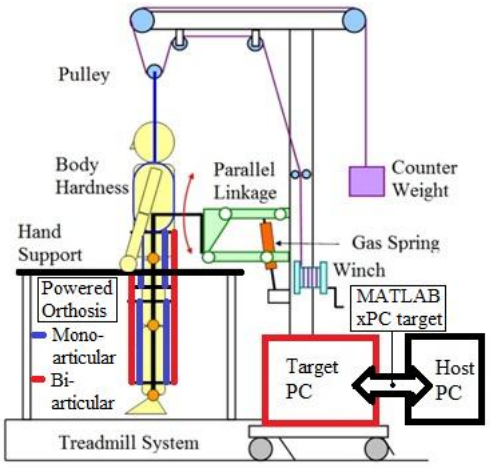

Figure 1 AIRGAIT system

Figure 1 shows the schematic diagram for the AIRGAIT system that is used in this study. This system is controlled by using a pair of anterior and posterior bi-articular actuators and two pairs of anterior and posterior mono-articular actuators which are moving in a co-contraction movement. MATLAB Simulink and xPC target tools were used to program the control system. The PMA used for this system is McKibben muscle type actuator with initial diameter of 25mm and initial length of 300mm, 450mm and 600mm. For controlling the input pressure to the antagonistic mono- and bi-articular PMAs, six regulators are used for each side, and the pressure is regulated from 0MPa to 0.5MPa.

3. METHODS

In this paper, we wrote mathematical equations using

a simple approach to determine the contraction patterns of antagonistic mono- and bi-articular actuators from the positional input data. Then, implemented it into the control system. There are two tests for the control system; first is using antagonistic mono-articular actuators alone; and second is with additional of antagonistic bi-articular actuators. Inputs for the control system are the hip and knee joints' angle for walking motion. The controller was tested for different gait cycle time (T = 5s, 4s, and 3s) for five cycles including the initial position cycle. The data was collected for a control system with a full body weight support (BWS) subject. Result is determined based on the maximum flexion and extension (hip and knee joints), output pattern, time shift, and inertia.

4. CONTRACTION MODEL

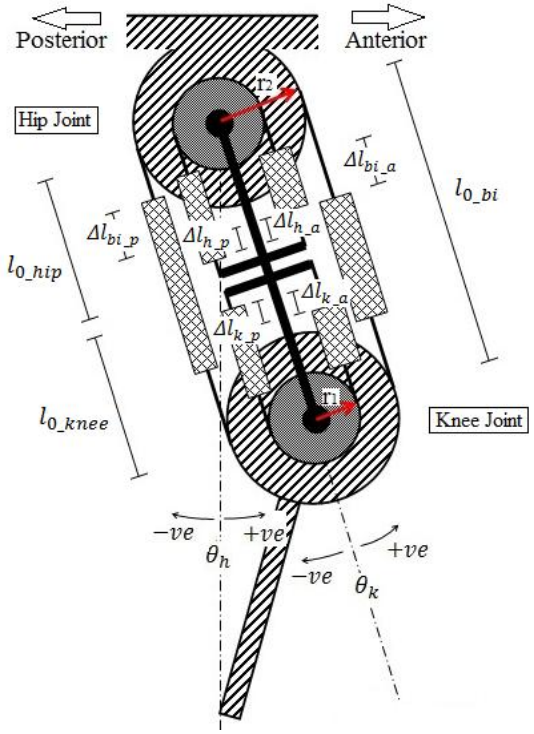

Figure 2 Mono-articular (hip), mono-articular (knee), and bi-articular actuators' model.

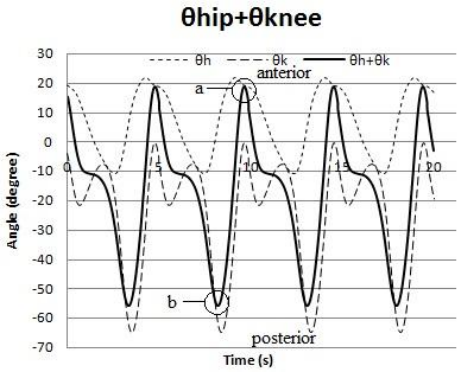

Figure 3 Hip, knee, and total angle input pattern

Figure 2 shows the mono-articular (hip and knee joints) and bi-articular actuators model for the powered orthosis system. Figure 3 shows the hip and knee angle as well as its' total angle which are used as an input data for the powered orthosis system. Where; hip angle (θ_h) is the input data for hip joint's mono-articular actuators; knee angle (θ_k) is the input data for knee joint's mono-articular actuators; and the total of hip and knee joint's angle (θ_h+ θ_k) represents input data for the antagonistic bi-articular actuators. From these data, we determined the locations of zero value for the muscle contractions (ε). For example, point (a) shows minimum value for posterior bi-articular PMA's muscle contraction, but maximum value for anterior PMA. Inversely, point (b) shows minimum value for anterior bi-articular PMA's muscle contraction, but maximum value for posterior PMA. Then, these data were illustrated as positive value to represent the muscle contraction patterns as can be seen in figure 4 below.

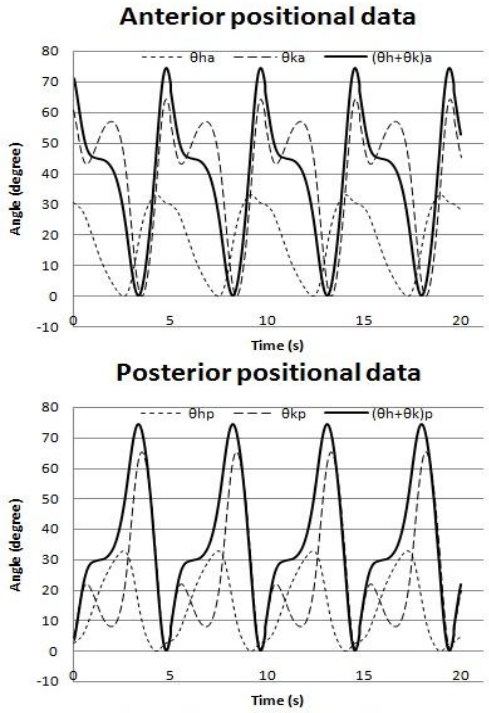

Figure 4 Anterior and posterior positional data

From the definition of the arc length (ΔS), the change in length (Δl) for antagonistic PMAs are;

$\Delta S = \theta . r$ ~where θ is in radian

$$\Delta l = \Delta S = \theta . r \quad (1)$$

The muscle contractions of antagonistic mono-articular PMAs for hip joint are defined using (1)

$$\Delta l_{hp} = \theta_{hp} . r$$

$$\varepsilon_{hp} = \frac{\Delta l_{hp}}{l_o} \approx \beta_h . \left(\frac{\theta_{hp} . r}{l_o}\right) \quad (2)$$

$$\Delta l_{ha} = \theta_{ha} . r$$

$$\varepsilon_{ha} = \frac{\Delta l_{ha}}{l_o} \approx \alpha_h . \left(\frac{\theta_{ha} . r}{l_o}\right) \quad (3)$$

Here, we introduces the posterior and anterior muscle activation levels (β and α) as a constant value for the actuator's muscle contraction. Maximum contraction that can be achieved by posterior and anterior actuators (McKibben muscle actuator) is ($\varepsilon_{p(max)} = \varepsilon_{a(max)} \approx 0.3$).

Then, equation (2) and (3) are illustrated as a time function as follows;

$$\varepsilon_{hp}(t) = \left(\frac{r}{l_o}\right).\beta_h.\theta_{hp}(t) \le 0.3 \quad (4)$$

$$\varepsilon_{hp(\max)} = \left(\frac{r}{l_o}\right)\beta_{h(max)}.\left|\theta_{hp}(t)\right|_{max} \approx 0.3$$

$$\beta_{h(max)} \approx 0.3\left[\frac{l_o}{r.\left|\theta_{hp}(t)\right|_{max}}\right]$$

$$\varepsilon_{ha}(t) = \left(\frac{r}{l_o}\right).\alpha_h.\theta_{ha}(t) \le 0.3 \quad (5)$$

$$\varepsilon_{ha(max)} = \left(\frac{r}{l_o}\right)\alpha_{h(max)}.\left|\theta_{ha}(t)\right|_{max} \approx 0.3$$

$$\alpha_{h(max)} \approx 0.3\left[\frac{l_o}{r.\left|\theta_{ha}(t)\right|_{max}}\right]$$

The muscle contractions for the knee joint antagonistic mono-articular PMAs are;

$$\varepsilon_{kp}(t) = \left(\frac{r}{l_o}\right).\beta_k.\theta_{kp}(t) \le 0.3 \quad (6)$$

$$\varepsilon_{kp(\max)} = \left(\frac{r}{l_o}\right)\beta_{k(max)}.\left|\theta_{kp}(t)\right|_{max} \approx 0.3$$

$$\beta_{k(max)} \approx 0.3\left[\frac{l_o}{r.\left|\theta_{kp}(t)\right|_{max}}\right]$$

$$\varepsilon_{ka}(t) = \left(\frac{r}{l_o}\right).\alpha_k.\theta_{ka}(t) \le 0.3 \quad (7)$$

$$\varepsilon_{ka(max)} = \left(\frac{r}{l_o}\right)\alpha_{k(max)}.\left|\theta_{ka}(t)\right|_{max} \approx 0.3$$

$$\alpha_{k(max)} \approx 0.3\left[\frac{l_o}{r.\left|\theta_{ka}(t)\right|_{max}}\right]$$

The muscle contractions for the antagonistic bi-articular PAMs are;

$$\varepsilon_p(t) = \left(\frac{r}{l_o}\right).\beta_{bi}.(\theta_h(t) + \theta_k(t))_p \le 0.3 \quad (8)$$

$$\varepsilon_{p(max)} = \left(\frac{r}{l_o}\right).\beta_{bi(max)}.\left|(\theta_h(t) + \theta_k(t))_p\right|_{max} \approx 0.3$$

$$\beta_{bi(max)} \approx 0.3\left[\frac{l_o}{r.\left|(\theta_h(t)+\theta_k(t))_p\right|_{max}}\right]$$

$$\varepsilon_a(t) = \left(\frac{r}{l_o}\right).\alpha_{bi}.(\theta_h(t) + \theta_k(t))_a \le 0.3 \quad (9)$$

$$\varepsilon_{a(max)} = \left(\frac{r}{l_o}\right).\alpha_{bi(max)}.\left|(\theta_h(t) + \theta_k(t))_a\right|_{max} \approx 0.3$$

$$\alpha_{bi(max)} \approx 0.3\left[\frac{l_o}{r.\left|(\theta_h(t)+\theta_k(t))_a\right|_{max}}\right]$$

Where ($0 < \beta \le \beta_{(max)}$) and ($0 < \alpha \le \alpha_{(max)}$). From the developed equations, it shows that the position of PMAs to the joints (r) and initial length (l_o) does not affect the muscle contraction patterns of the antagonistic mono- and bi-articular actuators. The study shows that the muscle contraction patterns of posterior and anterior PMAs follow the pattern given by the positional data itself. Moreover, these patterns only differ in gain based on the posterior and anterior muscle activation levels (β and α).

5. CONTROL SYSTEM

Figure 5 shows the schematic diagram for the developed controller based on contraction model. The angle (θ) is the positional input data which represent hip joint angle (θ_h); knee joint angle (θ_k); and positional data of bi-articular actuators ($\theta_h + \theta_k$). The angle (θ_o) is the positional output data. While, θ (+) represents the contraction patterns of antagonistic mono- and bi-articular actuators. These patterns are defined as positive value of the positional data. G_1 and G_2 are the function used to change the positional data into the positive value contraction patterns. Variable v_i is the input pressure, and v_p is the input pressure after the correction due to the PMA dynamic properties. Then, the controller (PI) is used to adjust the input pressure to the antagonistic mono- and bi-articular PMAs due to its nonlinearity.

6. RESULTS AND DICUSSIONS

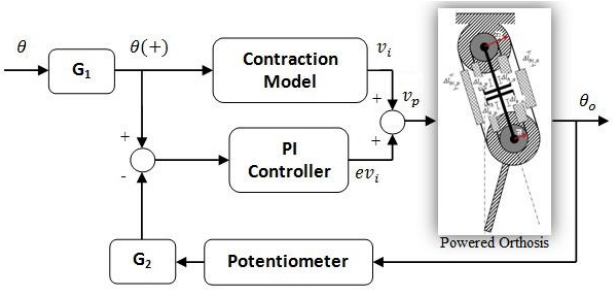

Figure 5 Schematic diagram

Figure 6 shows the result for the hip and knee joints' angle control with different gait cycles. The control system was performed using mono-articular actuators alone and with additional of bi-articular actuators. For gait cycles of 5 seconds, 4seconds, and 3 seconds using mono- and bi-articular actuators with subject (W/S) driven, the gait training system was able to perform a good movement without much time shift and able to follow the target hip and knee joints' angle. However, this cannot be achieved by implementing the mono-articular actuators alone. The system was not able to get a smooth motion at the hip joint and heel contact position (knee joint) due to lack of actuation power and inertia. On the other hand, with additional of bi-articular actuators to the system, we are able to get a smooth motion at hip joint and heel contact position. Moreover, maximum high muscle moment (flexion and extension) achieved at hip and knee joints also increased. By implementing the bi-articular actuators, we managed to improve the lack of actuation power at the hip joint, and tackling the errors from the inertia. This result shows that, additional of bi-articular PMAs with presence of mono-articular PMAs were able to give a good control performance and smooth movement at the hip and knee joints. The contraction model which enables the antagonistic mono-articular and bi articular actuators to move like a co-contraction during the control system also plays a major role in ensuring the precise movement at the hip and knee joints. By using this contraction model, the lapse at the hip joint for the test with subject using mono-articular actuators alone is ±5°. This requires a bigger (diameter) antagonistic mono-articular PMAs at hip joint for a better result.

However, by implementing bi-articular actuators in presence of mono-articular actuators, we were able to achieve the maximum muscle flexion and extension required at the hip and knee joints with a lapse of ±1º for different gait cycles.

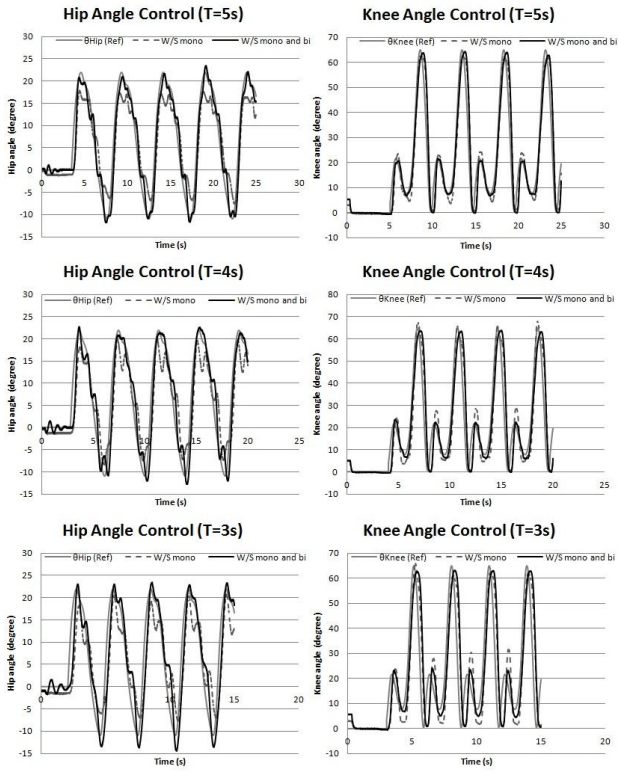

Figure 6 Hip and knee angle controls.

CONCLUSION

From the result, it shows that additional of bi-articular actuators with presence of mono-articular actuators were able to give a good control performance and smooth movement at the knee joint with a lapse of ±1º. Furthermore, we were able to achieve high muscle moment (flexion and extension) at the hip joint which cannot be obtained using mono-articular actuators alone. This is because, the force generated from mono-articular actuators alone is not enough to actuate the powered orthosis at hip joint. In addition, we were able to achieve the maximum muscle flexion and extension required at the hip joint with a lapse of ±1º for different gait cycles of 5, 4, and 3 seconds. Moreover, the developed contraction model also enables the anterior and posterior actuators to contract and expand in a co-contraction movement, thus, ensuring precise movement at the hip and knee joints. For the improvements of gait training system, an additional of intelligent controller such as auto tuning and neural network controllers will be required.

REFERENCES

A. Wernig, S. Muller, A. Nanassy, and E. Cagol, “Laufband therapy based on 'rules of spinal locomotion' is effective in spinal cord injured persons”. Eur J Neurosci vol. 7, pp823-829, 1995.

Y. Shibata, S. Imai, T. Nobutomo, T. Miyoshi, and S.I Yamamoto, “Development of body weight support gait training system using antagonistic bi-articualar muscle model”. IEEE Int. Conf. EMBS, Buenos Aires, Argentina, 2010.

S.I. Yamamoto, Y. Shibata, S. Imai, T. Nobutomo, and T. Miyoshi, “Dev. of gait training system powered by pneumatic actuator like human musculoskeletal system”. IEEE Int. Conf. on Rehabilitation Robotics, Switzerland, 2011.

M. Kumamoto, T. Oshima, and T. Fujikawa, “Control properties of two joint link mechanism equipped with mono and bi-articular actuators”. Robot & Human Interactive Com., IEEE Proc. pp. 400~404, 2010.

V. Salvucci, Oh Sehoon, Y. Hori, and Y. Kimura, “Disturbance rejection improvement in non-redundant robot arms using bi-articular actuators”. Industrial Electronics (ISIE). IEEE Symp. pp. 2159~2164, 2011.

S. Shimizu, N. Momose, T. Oshima, and K. Koyanagi, “Dev. of robot leg which provided with the bi-articular actuator for training techniques of rehabilitation”. Robot and Human Interactive Communication, IEEE Symp. pp. 921~926, 2009.

M. Kumamoto, T. Oshima, and T. Fujikawa, “Bi-articular muscle as a principle keyword for Biomimetric motor link system”. Microtechnologies in Medicine & Biology 2nd Annual International IEEE-EMB Special Topic Conference on, pp 346–351, 2002.

V. Salvucci, Oh Sehoon, and Y. Hori, “Infinity norm approach for precise force control of manipulators driven by bi-articular actuators”. IECON, IEEE Proc. pp. 1908~1913, 2010.

Mohd Azuwan Mat Dzahir received M.E. (2011) degrees in mechanical engineering from Universiti Teknologi Malaysia (UTM). He is a PhD student at Shibaura Institute of Technology, Saitama, Japan.

Shin-Ichiroh YAMAMOTO received D.E. (2000) degree in science from the Department of Life Science from The University of Tokyo. He is a professor at Shibaura Institute of Technology, Saitama, Japan.

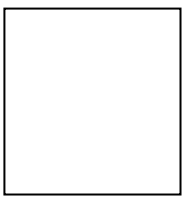

Tatsuya Nobutomo received B.E. (2010) degrees from Shibaura Institute of Technology, SIT. He is a Master student at SIT, Saitama, Japan.

ニューロリハビリテーションロボティクスの現状と課題

Trends and Issues in Neuro-Rehabilitation Robotics

○ 山本紳一郎，Mohd Azuwan bin Mat Dzahir，信友達哉(芝浦工大)，柴田芳幸(産技高専)

Shin-ichiroh Yamamoto, Mohd Azuwan bin Mat Dzahir, Tatsuya Nobutomo, Shibaura Institute of Technology
Yoshiyuki Shibata, Tokyo Metropolitan College of Industrial Technology

Abstract: The effect of body weight support treadmill training for incomplete spinal cord injured (SCI) patient has been reported in several previous studies since 1990s. In those training process, however, therapists must manually move both the patient's paralyzed legs. For the therapist, this training process is physically hard to continue for a long period. From the viewpoint of neuro-rehabilitation robotics, Colombo, et al. (2000) developed a driven gait orthosis (DGO) that can be used on patients with varying degrees of paresis or spasticity for a long time. Dietz, et al. (2002) used this DGO on patients with incomplete SCI and suggested that the afferent input from lower limb and hip joints movement are important for the activation of central pattern generator for locomotion training in SCI patients. In recent clinical assessment, however, there are some papers questioned its effectiveness. On the other hands, there are many papers suggested the feasibility of robotic rehabilitation for several patients. Thus, I report and introduce the recent trends and issues in neuro-rehabilitation robotics, especially for gait training.

Key Words: Motor dysfunction, Stroke, Spinal cord injury, Robotic Gait training

1. はじめに

1980 年代後半から脊髄損傷者のリハビリテーションには世界的に大きな変容が起こっている．脊髄神経回路網のセントラルパターンジェネレータがヒトにも存在し，かつ可塑性があることがわかってきており，その概念をもとにした脊髄損傷者のリハビリテーションプログラムとして，免荷式トレッドミル歩行訓練が欧米の多くのリハビリテーション病院で導入されてきた．しかしながら，マニュアルアシストによる歩行訓練では，セラピストの労力が必要であり，長時間の訓練ができないことから，LOKOMAT に代表されるようなロボット型歩行訓練システムに期待が寄せられ，事実多くの欧米のリハビリテーション病院で試験的に導入されてきた [1)2)]. しかしながら, 最近の臨床報告では, そのようなロボット歩行リハビリテーションの効果を疑問視するような内容の論文がいくつか報告されている．一方では，ロボット歩行リハビリテーションの様々な運動機能障がいに対する効果の可能性を報告する論文も多くみられる．

本講演では，これらの最近のニューロリハビリテーションの概念をもとにしたロボット歩行リハビリテーションの最近の報告を解説するとともに，筆者らの研究室で開発している歩行訓練システム(AirGait)を紹介する．

2. 最近のニューロリハビリテーションの報告について

ロボットを用いた脊髄損傷者に関する臨床事例報告では, リハビリテーションとしての効果があるという報告も多くあるが，2 名のセラピストが手動で実施するマニュアルアシスト訓練と比べて有意な効果の差がないとする報告や逆にマニュアルアシスト訓練のほうが有効であったとする報告もあり，統一した見解が得られていない．

また，脳卒中片麻痺者に対するアプローチもあり，多くの臨床事例報告があるが，ロボットリハビリテーションによる著しい効果を示唆している報告よりも，効果が同等であるか，逆に疑問視する内容の報告が多い傾向にある．

近年では小児麻痺を対象とするロボットリハビリテーションに関する臨床事例報告も多くあり，そのほとんどはロボットリハビリテーションの有用性，可能性を提案する内容の報告が多い．

近年のロボット歩行リハビリテーション研究では，いずれの機能障がいに対するアプローチでも，患者のモチベーションをどのように維持するかが課題である．ロボット型訓練システムの開発者らは，患者のモチベーションをあげるため，様々な改良を始めている．一つには，バーチャルリアリティシステムを導入することによって，視覚から入力されるバイオフィードバックを強化して訓練を実施する方法が多くの開発研究で導入され始めている．また，これまで再現される歩容が重要視されすぎたため，位置制御を中心としたアシストを行うロボットが多かったが，近年では患者の随意運動する意志をより増大させるような適応制御を導入している研究もみられる [3)].

本講演では，上述した以外の先行研究も紹介するとともに，今後のロボット歩行リハビリテーションの課題について提案したい．

3. 免荷式歩行訓練システム AirGait の開発

筆者の研究室では，これまで免荷式歩行訓練システム AirGait の開発を進めてきた．AirGait は空気圧人工筋をアクチュエータとして用いて，ヒトの骨格筋配置と同様に各筋に対して力をアシストできるよう設計した．本システムでは, 各患者に適した最小限の筋力アシストをすることで, 最大限のリハビリテーション効果を上げられるのでないかというコンセプトのもと開発を進めている．すなわち，各筋の麻痺の程度に合わせた力アシスト制御が可能であり，逆に麻痺していない筋には力アシストしないことも可能である．

本講演では, AirGait 開発の詳細な内容とその進捗報告を行う．

参考文献

1) G. Colombo et al: Research and Development 37,6, 693-700, 2000.
2) V. Dietz et al: Brain,125, 2626-2634, 2002.
3) R. Riener et al: IEEE Trans Neural Sys Rehab Eng, 13, 3, 380-394, 2005

Bi-Articular Muscle Actuators Kinematics Analysis for Gait Training System

M. Azuwan Mat Dzahir, Y. Shibata, M. Azwarie Mat Dzahir, and S. Yamamoto

IN their previous study, Shibata et. al. state that when the gait training system (AIRGAIT) for orthosis with subject driven using a mono-articular muscle model only, the kinematics of powered orthosis result shows that range of motion for the hip joint greatly decreased when compared to the human natural gait angle pattern [1]. This shows that the generated flexion and extension forces of the hip joint were not satisfactory. By applying both the mono-articular and bi-articular muscle models, the result is not as decreased as compared just using the mono articular muscle model. This indicates that the range of motion by the high muscle moment especially at hip joint moment can be achieved with addition of the bi-articular muscle model.

I. Methods

This study investigates two design aspects of the AIRGAIT system, which is the possibility of using bi-articular muscle actuators instead of or in addition to mono-articular actuators, and the use of L-shape rod at the knee joint. A sample data of ideal hip and knee angle from (Winter 2009) is used as an input for the analysis. A sampling time (frequency) uses for the analysis is 0.001seconds for approximately 5.0 seconds to complete one cycle of human walking motion. The bi-articular muscle actuators model kinematic analysis was done by measuring the muscle actuators length and contraction cycle as a function of hip and knee angle. In other words, by plotting the distance of muscle actuator end points in a graph, the actuators length and contraction for one complete cycle of walking motion can be measure. The actuators contraction data will be used as an input value for the Inverse Dynamics Analysis, to measure the input pressure required for each muscle actuators.

II. Bi-Articular Muscle Actuators Kinematics Analysis

From figure (a), the blue circle represents the antagonist actuator's kinematics, and green circle for agonist actuator's kinematics. These two circles are used to determine the actuators contraction for each muscle actuators. Figure (b) represents 3 parameters, which is hip angle, knee angle, and length for the muscle actuator. The black lines pattern is the graph of the muscle actuators length as a function of knee angle for a set of given hip angles, with an accuracy of 0.1 degree. The blue line shows the actuator's length for one complete cycle. From this data, maximum muscle actuator's length required for each muscle actuators were determined. Figure (c) shows an improvement for muscle actuators contraction of a new design with maximum actuator's contraction less than 16% of its original length, while the previous design model required less than 20%.

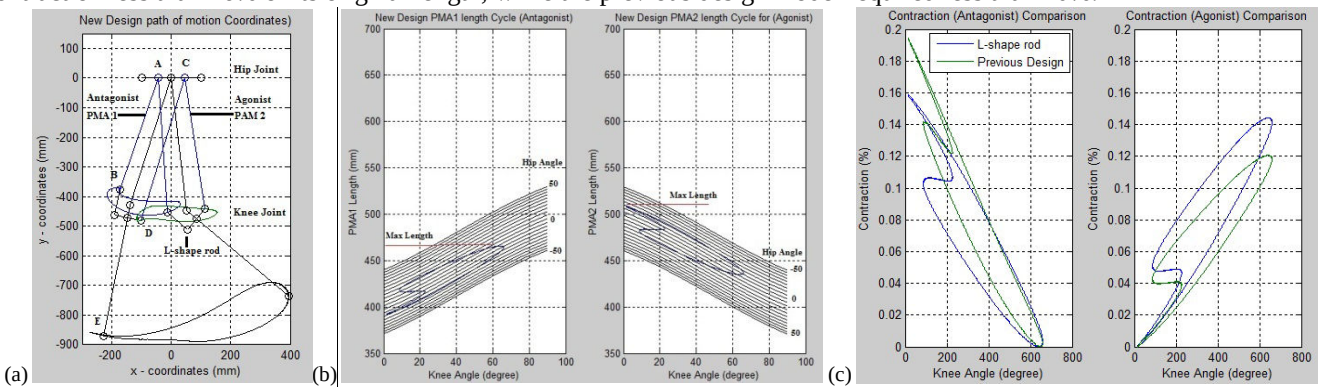

References

[1] Y. Shibata, S. Imai, T. Nobutomo, T. Miyoshi, S.I Yamamoto (2010) Development of body weight support gait training system using antagonistic bi-articular muscle model. 32nd Annual International Conference of the IEEE EMBS, Buenos Aires, Argentina.

[2] A. Wernig, S. Muller, A. Nanassy, E. Cagol. Laufband therapy based on 'rules of spinal locomotion' is effective in spinal cord injured persons. Eur J Neurosci vol. 7, pp823-829, 1995.

[3] V. Dietz, R. MuEller and G. Colombo, Locomotor activity in spinal man: significance of afferent input from joint and load receptors, Brain, 125, pp2626-2634, 2002.

This work was supported by KAKENHI: Grant-in-Aid for Scientific Research (B) 21300202.

OS Number 04

DEVELOPMENT OF BODY WEIGHT SUPPORT GAIT TRAINING SYSTEM USING PNEUMATIC MCKIBBEN ACTUATOR
~DEVELOPMENT OF MEASUREMENT AND CONTROL SYSTEM~

Taiga Seya, Mohd Azuwan Mat Dzahir, Yoshiyuki Shibata, Shin-Ichiroh Yamamoto

Dept. of Biological and Engineering Science, Shibaura Institute of Technology

Abstract

The purpose of this research is to develop body weight support gait training system for stroke and the spinal cord injury (SCI) patients. This bodyweight support gait training system consists of an orthosis powered by pneumatic McKibben actuators (PMA), double belt treadmill with force sensor, and equipment of body weight support. We develop the program to measure subject condition for new assistive control system. In this study, we experimented to evaluate the program. This system corresponds with the subject condition such as change in treadmill speed or BWS level. This program is useful to measure the gait parameters when treadmill speed is changed. BWS level is low; it can analyze the gait parameter. However BWS level is high; It can't support to analyze the gait parameter.

1. INTRODUCTION

Based on the information gathered on assistive rehabilitation robotics, many research suggested that the body weight support treadmill training is effective for the patient with SCI. Wernig, et al. (1995) also mentioned about effectiveness of the gait ability recovery which operated by physical therapist[1]. However, this manual training is difficult and implies a burden to the therapists. On the other hand, Colombo et al. (2000) was developed a driven gait orthosis (DGO) [2]. This system was able to automatically move subject's lower limb. In addition to this, Dietz et al. (2002) were implemented the DGO and reported its efficiency for the patient with SCI [3].

In our previous study, we developed body weight support gait training system using PMA which was arranged antagonistically (i.e., two pairs of mono articular actuators, and a pair of bi-articular actuators) [4 5]. PMA yield muscle-like mechanical actuation with high force to weight ratio, soft and flexible structure [6]. In recent researches, robotic orthosis which implemented electric motors are developed [3 7 8]. However, electric motor only drives joint of the orthosis, not muscle. Therefore, it is impossible to support only the paralyzed muscle. Our system aims for the improvement of the muscles which were paralyzed using PMA like a human musculoskeletal system. The developed powered orthosis is controlled by the input data of joint angles. Then the feedback signals are measured by the joint angle sensors which are used for the position control system. Nevertheless, this control system is not suitable for the movement of each particular subject, because it replays healthy subject's gait cycle and it doesn't refer subject data, for example height, weight, gait speed and so on.

The last aim of this study is to measure gait parameters (i.e., cadence, joint angle, step length and so on.) for each individual subject in real time. The data is utilized to build an assistive system for the subject's gait training and also to use for the input signal of the control system when training of locomotion.

2. MECHANICAL SETUP

The system consisted of a three main parts which is body weight support system (BWS), powered orthosis, and twin belt treadmill (Bertec Co.). The electric pneumatic regulators (SMC Co.) were used to allocate the required input pressure to the antagonistic actuators. The control/measure PC was used to perform the Graphical user interface (GUI) for the measurement and control system program which was coded in LabVIEW (NI Co) software.

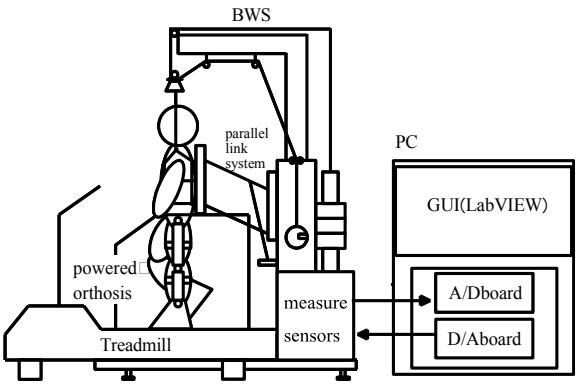

Fig.1 Body Weight Support Gait Training System and Powered Orthosis

2.1 MEASUREMENT SYSTEM

There are three types of measurement sensors that were used in this system; the first is position sensor which measures the powered orthosis hip and knee joint angles; the second is pressure sensor that measures the antagonistic actuators output pressure; and, the thirds is the ground reaction force (GRF) sensors which located at the four corners of the treadmill. The center of pressure (COP) of the subject can be determined by implementing equation (1), (2). These equations determined the right and left COP positions (i.e., x-axis and y-axis) on the treadmill.

$$COPx = -My / GRF \ldots(1)$$

$$COPy = Mx / GRF \ldots(2)$$

2.2 CONTROL SYSTEM

Figure 2 shows the measurement and control system's signal flow. The information data to be transferred to the electric pneumatic regulators are measured by control PC using which was programmed in MATLAB (MathWorks CO) and LabVIEW (NI CO) software.

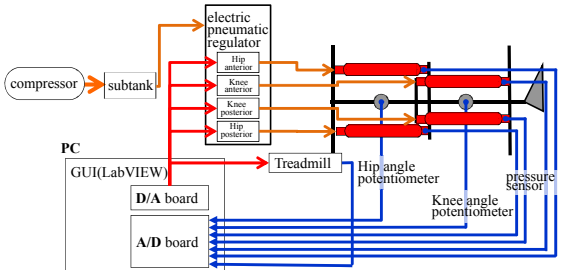

Fig. 2 measurement & control system

3. MEASUREMENT PROGRAM

It is important to determine heel contact for analyzing the human's gait motion and patterns. In this study, a program to measure the heel contacts from GRF was developed, in which the different of heel contacts would be focused on the COP trajectory. Equation (3) determines the average COP for the heel contact as well as sides (i.e., left or right) of the leg on the treadmill, while, equation (4) determines the timing of the heel contact. The COPy trajectory shifted to the front on the treadmill during the heel contact. These equations are the threshold for measuring the heel contact.

$$COPx < average(COPx) \ldots(3)$$

$$COPy' > average(COPy') + 2 * stdev(COPy') \ldots(4)$$

4. EXPERIMENT

Experimental tests were performed to evaluate the functionality of the developed measurement system. This system has to correspond with the subject condition such as change in treadmill speed or BWS level.

4.1 THE FIRST EXPERIMENT: SPEED CHANGE

This assessment is evaluated at different speed and it is able to support a change in speed. Six subjects participate this experiment (age: 22.83± 1.17 [year], height: 174.57 ± 4.69 [cm], weight: 64.46±5.87 [kg]). We instructed patients to walk on the treadmill for one minute. Then the treadmill speeds of 1.0km/h, 1.5km/h, 2.0km/h and 2.5km/h were tested. Figure 3 shows the GRF [kg] and COP trajectory per one gait cycle, while figure 4 shows the gait parameters.

The results show that 98.6% of the heel contacts's position which is measured by program was matching with the reference heel contacts. This shows that subject's cadences between all treadmill speeds are significant. However, there was no significant difference on the step lengths among all treadmill speeds. It proves that, the subject continues to increase the step length and raises the cadence when treadmill speed was increased. The increase in the cadence was the result of higher GRF. This result suggested that this program is useful to measure the gait parameters in this experiment protocol.

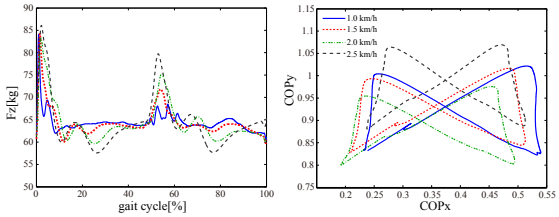

Fig.3 Fz & COP position while gait cycle

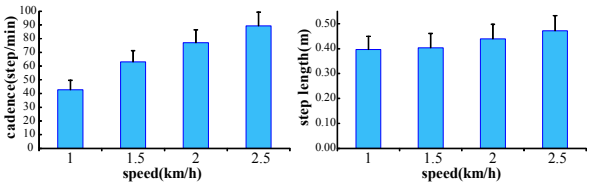

Fig.4 gait parameters

Table1. The program accuracy of heel contact

body weight support rate	without orthosis			with orthosis		
	a	b	c	a	b	c
0%	100%	89%	100%	100%	100%	100%
30%	97%	100%	94%	97%	100%	92%
50%	92%	88%	59%	83%	92%	96%
70%	94%	68%	98%	64%	85%	86%

4.2 THE SECOUND EXPERIMENT: BWS CHANGE

This assessment is evaluated at different body weight support. Three subjects were participate in this experiment (age: 22.33 ± 0.58 [year], height: 175.30 ± 4.68[cm], weight: 65.83±1.78 [kg]). We instructed subjects to walk on the treadmill at 1km/h. Then, eight different combinations of BWS (0%, 30%, 50% and 70%) without and with orthosis were performed. The measurement parameters are treadmill speeds, strides and corresponding program at sampling frequency of 1 kHz.

Table 1 illustrated the real heel contact position which was measured by footswitch and measurement system in case without and with orthosis. Figure 5 illustrates the COP trajectory at 8 different conditions. The program accuracy in the second experiment is lower than the accuracy of the first experiment (98.6%). The average of accuracy is over 95% at 0% and 30% of BWS level. However the program at 50% and 70% BWS levels did not work. The GRF signals were too weak at 50% and 70% BWS level; the program could not distinguish the heel contact position. Therefore it can't analysis gait parameters because the program depends on the heel contact measurements. It is necessary for the program to distinguish method the heel contact. For the solution, we consider two methods. The first is using orthosis knee angle sensor. Which shows the heel contact of the orthosis when the knee angle shows 0 degree. We think that we can incorporate orthosis angle to the program to use second threshold. Second is to use laser sensors, but this method would be expensive, so we chose the first method.

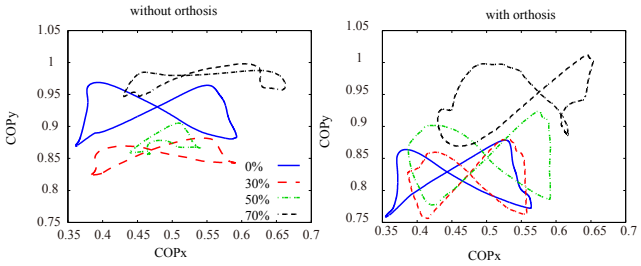

Fig.5 COP trajectory each 8 different combinations

6 FUTURE STUDIES

In this report, we made the program which based on assistive control system for the subject's gait training. However it is not perfect. If the developed measurement program is able to measure the heel contact precisely, the gait parameters such as step lengths, cadences, GRF, heel contacts and the COP trajectory could be determined. The obtained data will be used in the control program. We try to control the orthosis using COP data. It is possibility to control, we will execute assistive control.

REFERENCES

[1] A. Wernig, S. Muller, A. Nanassy, and E. Cagol, "Laufband therapy based on 'rules of spinal locomotion' is effective in spinal cord injured persons". Eur J Neurosci vol. 7, pp823-829, 1995.

[2] G. Colombo, M. Joerg, R. Schreier, and V. Dietz, Treadmill training of paraplegic patients using a robotic orthosis, Journal of Rehabilitation Research and Development Vol. 37 No. 6, pp.693-700, 2000.

[3] V. Dietz, R. MuÈller and G. Colombo, Locomotor activity in spinal man: significance of afferent input from joint and load receptors, Brain, 125, pp2626-2634, 2002.

[4] Y. Shibata, S. Imai, T.Nobutomo, T. Miyoshi, S. Yamamoto "Development of Body Weight Support Gait Training System usingAntagonistic Bi-articular Muscle Model", EMBC, 32, 4468-4471, 2010

[5] M.A.Mat Dzahir, S.Yamamoto "Design and Evaluation of the AIRGAIT Exoskeleton: Leg Orthosis Control for Assistive Gait Rehabilitation" Journal of Robotics,

[6] Kanchana Crishan Wickramatunge, Thananchai Leephakpreeda "Study on mechanical behaviors of pneumatic artificial muscle" International Journal of Engineering Science 48, 188-198, 2010

[7] S Hesse, C Werner, and A Bardeleben, "Electromechanical gait training with functional electrical stimulation: case studies in spinal cord injury". Spinal Cord, 42, pp346-352, 2004

[8] Zhang Jia-fan, Dong Yi-ming, Yang Can-jun, Geng Yu , Chen Ying , Yang Yin, "5-Link model based gait trajectory adaption control strategies of the gait rehabilitation exoskeleton for post-stroke patients" Mechatronics, 20, 368-376, 2010

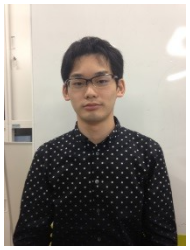

Taiga Seya received the B.E. (2012), degrees in Biological and Engineering Science mechanical engineering from Shibaura institute technology. He is a Master student at Shibaura Institute of Technology, Saitama, Japan.

Mohd Azuwan Mat Dzahir received M.E. (2011) degrees in mechanical engineering from Universiti Teknologi Malaysia (UTM). He is a PhD student at Shibaura Institute of Technology, Saitama, Japan.

Yoshiyuki Shibata received D.E. (2011) degrees in mechanical engineering from Shibaura institute technology. He is a professor at Tokyo Metropolitan College of Industrial Technology, Tokyo, Japan.

Shin-Ichiroh YAMAMOTO received D.E. (2000) degree in science from the Department of Life Science from The University of Tokyo. He is a professor at Shibaura Institute of Technology, Saitama, Japan.